An Examination of the Measurement and Extent of Atmospheric Microplastic Pollution in Urban and Remote Spaces

Declaration of Authenticity and Author's Rights

This thesis is the result of the author's original research. It has been composed by the author and has not been previously submitted for examination which has led to the award of a degree.

The copyright of this thesis belongs to the author under the terms of the United Kingdom Copyright Acts as qualified by the University of Strathclyde Regulation 3.50. Due acknowledgment must always be made of the use of any material contained in, or derived from, this thesis.

Signed: 

Date: 14th of September 2025

Statement of Co-authorship

The following people and institutions contributed to this thesis:

Candidate: Anna MacDonald, University of Strathclyde

Supervisor 1: Dr Christopher J. White , University of Strathclyde (Primary Supervisor)

Supervisor 2: Prof Vernon Phoenix, University of Strathclyde (Second Supervisor)

Supervisor 3: Dr Deonie Castle, University of Waikato (Third Supervisor)

Peer-reviewed publications featured in this thesis, including co-author contributions:

Paper 1 (presented as Chapter 5 in this thesis)

Citation: 'Polar Particles: Atmospheric Microplastic Pollution in the Arctic Region – an examination of deposited and suspended microplastics in Ny-Ålesund, Svalbard'

Status: Submitted to *Nature: Communications Earth & Environment* on the 5th of September 2025, pending peer-review.

Authors and contributions:

Anna MacDonald (85%): Conceptualisation, field work, data analysis, writing – original draft, editing

Nikolaos Evangeliou (5%): Conceptualisation of FLEXPART modelling, data analysis, modelling, writing of dispersion modelling section, reviewing and editing

Sabine Eckhardt (1%): Assistance with FLEXPART particle modelling

Deonie Castle (2%): Conceptualisation, reviewing & editing

Christopher J. White (2%): Review & editing

Vernon R. Phoenix (2%): Review & editing

Dušan Materić (3%): Help with data analysis, review & editing, facilitated access to μRaman spectrometer used for data analysis

Paper 2 (presented as Appendix II in this thesis)

Citation: 'Investigating Current Analytical Methods for the Identification of Airborne Microplastics'

Status: About to be submitted for second round of peer-review.

Authors and contributions:

Alex Aves (80%): Conceptualisation, writing of original draft, carried out field experiments and data analysis (FTIR, Nile Red, Py-GC/MS, TD-PTR-MS)

Anna MacDonald (5%): Carried out data analysis (μRaman), writing, reviewing, editing

Sebastian Naeher (2%): Assisted with data analysis (Py-GC/MS), writing, reviewing

Dusan Materic (2%): Assisted with data analysis (TD-PTR-MS), writing, reviewing

Deonie Castle (2%): Writing, reviewing, assisted with data analysis (μRaman), writing reviewing

Sally Gaw1(1%): Conceptualisation, writing, reviewing, editing

Laura Revell (1%): Conceptualisation, writing, reviewing, editing

Paper 3 (presented as Appendix III in this thesis)

Citation: 'People, plastic and behaviour change – a comment on drivers of plastic pollution, barriers to change and targeted behaviour change intervention'

Status: Published in *Environmental Science: Advances* on the 20th of February 2023

Authors and contributions:

Anna MacDonald (85%): Data analysis, writing of original draft, reviewing, editing

Deonie Allen (5%): Conceptualisation, data collection, writing, reviewing editing

Lynn Williams (5%): Conceptualisation, reviewing, editing

Paul Flowers (2%): Reviewing, editing

Tony R. Walker (2%): Reviewing, editing

Acknowledgements

I would first like to thank Dr Deonie Allen for her help and support during my PhD. Without her assistance and input, this thesis would not have been possible. I am grateful for the opportunity to have worked and learned from her. Thank you also to my supervisors Dr. Chris White and Prof Vernon Pheonix for their support, guidance and encouragement throughout the PhD.

To my family I cannot express my gratitude enough. Their unwavering support and encouragement during this process has been a lifeline and I will be forever grateful. A special thanks goes to my mother, Ishbel, her help, support and wise words have been vital during this process. I will be repaying her in chocolate and cups of tea until I die. To my sister Màiri, I thank you for encouraging me to push on and for being a constant source of laughter. To my dad, David, your sarcasm and poor jokes have been a huge help.

To my friends within the department, I owe you my deepest gratitude. The comradery, support and laughter have been central in getting me to the finish line. I am indebted to Elena Dafoniti, Ryan Lee, Archie Rudman, Lou Brett, Katherine Deeming, Sally Jack, Jason Erikson, Chris McMahon and Sara Drais, for their friendship and encouragement during this time. To my friends I have met whilst doing research in other institutes I am also incredibly thankful and grateful. Justine Ammendolia and Alex Aves have been a constant support and I am grateful to have met such inspiring women. My friends outwith the department have been a constant support and I extend a special thanks to Linnea Hay for being my rock throughout this process.

I would like to thank the staff within and outwith the university that have helped me navigate the nuances of microplastics. Firstly, Dr Liam Kellecher at the University of Birmingham for his support and knowledge. Dr Martin Ward in CMAC, for all his help and patience using the Raman spectrometer. Similarly Dr Matthias Schmidt at the Helmholtz Association for his support using the Raman and for his knowledge on analytical chemistry (and everything else). Finally, Dr Dusan Materic (Matt) for his support, helping me access a functioning Raman, his scientific input and advice.

For the staff within the University of Strathclyde, I would like to extend my thanks and gratitude. A special thanks goes to Darren Grant and Matthew Mclean for their consistent IT support over the years and especially for rescuing my external hard drive when I thought all was lost. Without your help this thesis would not exist and I am eternally grateful. Another special thanks goes to Mara Knapp for her support, help and for being a source of laughter when lab work got too much.

Contents

Declaration of Authenticity and Author's Rights i

Acknowledgements iv

List of Figures x

List of Tables xviii

List of Boxes xix

List of Abbreviations xx

Abstract 1

Chapter 1. Introduction 3

1.2 Research Questions 5

1.3 Thesis Structure 7

Chapter 2. Literature Review 7

2.1 Microplastics and Atmospheric Microplastics 10

2.1.1 Emergence of Microplastics as an Environmental Concern 10

2.1.2 Atmospheric Microplastics as an Emerging Field 12

2.2 Atmospheric Microplastic Sources and Transport Mechanisms 12

2.2.1 Sources of Microplastics – Primary and Secondary Microplastics 14

2.2.2 Microplastic Transport – The 'Plastic Cycle' 16

2.2.3 Atmospheric transport - mechanisms of transport, atmospheric dispersion and deposition 17

2.3 Methods of Sampling, Pre-Treatment, and Characterisation Techniques 25

2.3.1 Methods for Sample Collection – Passive and Active Sampling 25

2.3.2 Methods for Sample Treatment – Digestion and Density Separation 27

2.3.3 Microplastic Characterisation and Quantification – 'Race to the Bottom', The Pursuit of Smaller Particle Identification 28

2.3.4 Contamination Protocols QA/CC – Minimising the Inevitable 43

2.4 How bad is it? – Environmental and Human Health Risks 43

2.4.1 Interaction with biota and ecosystems and implications for climate change 43

2.4.3 Microplastics and Human Health 45

2.5 Plastic Pollution Mitigation and Policy Implications 50

2.5.1 Current policies to reduce microplastic pollution 50

2.5.2 Systemic and Individual Level Approaches – Behaviour Change 55

2.6 Gaps in Knowledge and Research - Critical gaps in understanding and key issues for development of the field – method development, accessibility, and awareness 55
Chapter 3. General Overview of Methods 58
3.1 Methods used to Sample Atmospheric Microplastics 58
3.1.1 Active Sampling Techniques 58
3.1.1 Passive Sampling Techniques 60
3.1.3 Filters used for Atmospheric MP collection and analysis 62
3.2 Method of Polymer Identification - µRaman Spectroscopy 63
3.2.1 Raman Spectrometry for Dummies 63
3.2.2 The Tale of Two Ramans 67
3.2.3 Spectral Correction and Multivariate Analysis 71
3.3 Nile Red Staining and Fluorescence Microscopy 72
3.3.1 Nile Red Staining and Optimisation 72
3.3.2 Microscope Imaging and Fluorescence 75
3.3.3 Image Processing and Particle Analysis 76
3.4 QA Contamination Control – Minimising the Inevitable 77
3.5 Calculating MP Concentrations and Statistics 79
Chapter 4 - Pilot Study: Examination of Active Air Sampling Efficiencies 79
4.1 Introduction 82
4.2 Methods and materials 84
4.2.1 Field Experiment – Sample Collection and Experimental Parameters 84
4.2.2 Micro-Raman (µRaman) spectroscopy 89
4.2.3 Nile Red staining 90
4.2.4 Microplastic contamination prevention 91
4.2.5 Statistical analysis 92
4.3 Results and Discussion 93
4.3.1 MP content for Pumping Rate and Sampling Duration 93
4.6.1 MP Size Distribution for Pumping Rate and Sampling Duration 97
4.3.3 MP Shape Characteristics for Pumping Rate and Sampling Duration 98
4.3.4 Polymer Composition for Pumping Rate and Sampling Duration 101
4.3.5 Thresholds and Recommendation for Future Research 103
4.6 Conclusions 107
Chapter 5 – Remote Atmospheric Microplastic Pollution – Svalbard, Norway 109

5.1 Introduction 109
5.2 Methods 111
5.2.1 Sample location and collection 111
5.2.2 Micro-Raman (μRaman) spectroscopy 113
5.2.3 Nile Red staining 113
5.2.4 Microplastic contamination prevention 115
5.2.5 Statistical analysis 116
5.2.6 Relationship with Weather Parameters 116
5.2.7 Atmospheric dispersion modelling 118
5.3 Results 119
5.3.1 Microplastic Concentrations: Suspended and Deposited Particulates 119
5.3.2 Microplastic Characteristics 123
5.3.3 Polymer composition (μRaman) 125
5.3.4 Atmospheric MP pollution and weather parameters at Ny-Ålesund, Svalbard .. 127
5.3.5 Potential contributing sources of MP in Svalbard 128
5.4 Discussion 131
5.4.1 Comparison of deposited and suspended particulates 131
5.4.2 Potential Relationships with Weather Parameters 132
5.4.3 Potential transport of Atmospheric MP pollution in Svalbard 132
5.4.3 Microplastic pollution in the Arctic region 134
5.5 Conclusions 139
Chapter 6 – Urban Atmospheric Microplastic Pollution – Glasgow 139
6.1 Introduction 141
6.2 Methods 143
6.2.1 Field Sampling 143
6.2.2 μRaman and Nile Red Staining with Fluorescence Microscopy 145
6.2.3 Microplastic contamination prevention 147
6.2.4 Statistical analysis 148
6.2.3 Meteorological Data 149
6.2.5 Air Quality Data 149
6.2.6 Particle Modelling – HYSPLIT Trajectory Analysis 151
6.3 Results and Discussion 153
6.3.1 Particle Concentration, Shape and Size 153

6.3.2 Polymer Composition ... 158
6.3.3 Relationship with Meteorological Variables ... 160
6.3.4 Relationship between Air Pollutants at Urban Location ... 161
6.3.5 Results of HYSPLIT Backward Trajectory Modelling and Possible Sources ... 161
6.3.7 Results of HYSPLIT Back Trajectory Particle Modelling – Influence of Particle Size and Polymer Density ... 165
6.3.7 Results of HYSPLIT Forward Trajectory Modelling and Potential End Point ... 179
6.3.8 Results of HYSPLIT Forward Trajectory Particle Modelling – Influence of Particle Size and Polymer Density ... 179
6.4 Conclusion ... 194
Chapter 7 – Discussion of Urban and Remote Atmospheric Microplastic Pollution ... 199
7.1 Summary and Discussion of Key Findings ... 199
7.1.1 Guidance for Active Sampling Measurements of Atmospheric Microplastics ... 199
7.1.2 Remote Atmospheric Microplastic Pollution: Svalbard, Norway ... 200
7.1.2 Urban Atmospheric Microplastic Pollution: Glasgow, Scotland ... 202
7.2 Comparison of Urban and Remote Atmospheric Microplastics ... 202
7.3 Recommendations for Future Research and Policy ... 208
7.3.1 Recommendations for Future Research ... 208
7.3.2 Recommendations for Future Policy ... 208
Chapter 8 – Conclusion ... 214
References ... 214
Appendices ... 249
Appendix I. Table Summary of Atmospheric Microplastics Studies (published up to 22nd of November 2024) ... 250
Appendix II. Draft copy of manuscript comparing analytical methods used in microplastic research ... 279
Appendix III. Manuscript published in Environmental Science: Advances ... 298
Appendix IV. Standard Operating Procedure for creating particle mapping 'mask' for use on µRaman at Helmholtz Association Leipzig ... 311
Appendix V. Supplementary Tables for Research Chapter 4 ... 316
Appendix VI. Manuscript version of research Chapter 5 on Svalbard Atmospheric MP Pollution ... 342
Appendix VII. Supplementary Data and Figures for Research Chapter 5 ... 373
Appendix VII. Supplementary Data used in Research Chapter 6 on Glasgow Atmospheric MP Pollution ... 389

Appendix IX. Results of Individual HYSPLIT Scenarios Forward and Backward Trajectory 394

List of Figures

Figure 2. 1 A) Bar graph showing distribution of MP publications across research topics from studies published up to 31/12/2021 (Allen et al., 2022) (B) Line graph showing MP research topic trends from 2011-2021 (Allen et al., 2022) 11
Figure 2. 2 (A) Newspaper Article from British Newspaper, 'The Guardian' (Mains, 2024); (B) Newspaper from U.S Newspaper, 'The New York Times', published same year as thesis, showing media attention to MP pollution (Sloat, 2024) 12
Figure 2. 3 Visual Representation of the 'Plastic Cycle' (Horton and Dixon, 2018). 17
Figure 2. 4 Figure from Allen et al., (2022) study using HYSPLIT to model global atmospheric transport of MP and NP at 10m above ground level (Allen et al., 2022) 21
Figure 2. 5 Figure from Evangeliou et al (2020) study modelling TWP and BWP transport in the atmosphere using FLEXPART model; both wet and dry deposition for both types of MP particulates are displayed using data from 2014 and with the assistance of GAINS model (Greenhouse gas-Air pollution Interactions and Synergies) (Evangeliou et al., 2020) 22
Figure 2. 6 (A) Passive (Left) and Active (Right) Air Sampling Equipment in the Field, Svalbard, Norway; (B) Different Methods of Passive/Deposition Sampling used in Atmospheric MP Research (Knobloch et al., 2024) 25
Figure 2. 7(A) Active Sampling Equipment in the Field (Active Air Filter Sampler – Left; 'Nano-tank Sampler - Right'; Svalbard, Norway); (B) Middle Flow Air Sampler (Munro Instruments, 2024); (C) TISCH High Volume Air Sampler (TISCH, 2024) 26
Figure 2. 8 Microplastics in their different morphological forms and colours – spheres, fibres, fragments and films – all <1mm in size, identified from samples from the Caspian Sea (D'Hont et al., 2021) 30
Figure 2. 9 SEM images of MPs identified from atmospheric samples from Beijing and Shanghai (Liu et al., 2024b) 31
Figure 2. 10 Raman spectra used to identify polymer 'fingerprint' for common polymers including PS, PC, PP, PE, PET, PVC, PA, PTFE, PMMA, PLA (Anger et al., 2018) 34
Figure 2. 11 LDIR chemical imaging and spectra of 8 polymers identified in Svalbard water samples including PE, PET, PE, PU, PP, PVC and PS (Bao et al., 2021) 35
Figure 2. 12 Pyrolysis products (pyrograms) used to identify three polymers from surface water samples at Osaka Bay including, PS, PE, PP, using Py-GC-MS (Frontier Laboratories Ltd., 2024) 36

Figure 2. 13 Figure from Materic et al., (2020) displaying indicator ions to identify common polymer types using TD-PTR-MS for the first time including HDPE, LDPE, PET, PP, PPC, PS, and PVC (Materic et al., 2020) 40
Figure 2. 14 Figure from Iannilli et al. (2020) showing MP particles fluorescing green with the assistance of Nile Red dye, with normal microscopic images for comparison, from freshwaters samples taken in Italy (<50µm) (Iannilli et al. 2020) 42
Figure 2. 15 Short-term and long-term health effects of MP on humans (Adapted by Akanyange et al., 2021from, Karbalei et al., 2018) 48
Figure 2. 16 Butterfly diagram showing Circular Economy Model (Ellen Macarthur Foundation. 2023) 51

Figure 3. 1 (A)Image of Direct Air Filtration System as set up in the field (Svalbard, Norway); 3.1(B) Diagram of Direct Air Filtration Sampling System (Active Sampling) 59
Figure 3. 2 (A) Image of Nanotank System in the field (Svalbard, Norway); 3.2B) Diagram of Nanotank Sampling System (Active Sampling; the orange arrows indicate air being drawn throw the chamber assisted by the pump and the green arrows indicate the movement of air into the chamber with the collected particulates 60
Figure 3. 3 (A)An Image of deposition chamber in the field (with lid, Svalbard, Norway); (B) image of deposition sample being vacuum filtered on to QMA filter with filtration kit 61
Figure 3. 4 Diagram of filtration kit used to vacuum filter liquid samples (nanotank and deposition samples) 61
Figure 3. 5 Microscope image of trapped microplastic in QMA filter; image taken during Nile Red staining and imaging atmospheric from Glasgow, Scotland, taken in 2021; objective x10; see also Chapter 3.3 63
Figure 3. 6 Principles of Rayleigh and Raman Scattering (Horiba Scientific, 2023) 64
Figure 3. 7 Raman Spectral Signals of Fingerprints for common polymer types ((a) PE, polyethylene; (b) iPP, isotactic polypropylene; (c) PS, polystyrene; (d) PET, polyethylene terephthalate; (e) PA, NY66, polyamide; (f) PVC, polyvinyl chloride) (Nava et al., 2021) 65
Figure 3. 8 Chemical structure of commonly used polymers (Iowa State University, 2025) 66
Figure 3. 9(A) Image of µRaman Spectrometer at the Technology and Innovation Centre at University of Strathclyde; (B) Image of Sample Under µRaman microscope (Active Air Sample on QMA Filter, taken from Glasgow 2021) before points map is

added; (C) Image of Sample Under µRaman microscope with points map added (same Active Air Sample on QMA Filter, taken from Glasgow 2021) 68
Figure 3. 10(A) Image of µRaman Spectrometer at the Helmholtz Association, Leipzig; 3.6(B) Image of Laser used, Helmholtz Association, Leipzig; 3.6(C) Series of images showing the process of creating a points map to be fed back into the µRaman spectrometer to mimic particle mapping function; first image shows the original image of Filter (Deposition Filter Svalbard (QMA Whatmann (25mm, 1.6µm))under µRaman 70
Figure 3. 11 Diagram showing filtering of Nile Red solution via vacuum filtration. 74
Figure 3. 12(A) An Image of Stereomicroscope used in this thesis, with foil to cover sample during microscope imaging; (B) Brightfield image of atmospheric sample taken from Glasgow, Scotland (2021); (C) Fluorescence mode image of same atmospheric sample taken from Glasgow, Scotland (2021) 76
Figure 3. 13 (A) Image of Scale taken with stereomicroscope using x10 objective; 3.9(B) Image of atmospheric sample taken from Glasgow, Scotland (2021) with ImageJ processing (brightness and contrast enhanced, threshold (30+255) for particle analysis 76

Figure 4. 1 Map of Glasgow and Rutherglen, red dot indicating the sampling location (Arc GIS, 2025) 85
Figure 4. 2 Image of Experimental Set-Up in Glasgow, the nanotank samplers can be seen in the red box; the daily sampling duration direct air filtration samplers are in the yellow box; the weekly sampling duration direct air filtration samplers are in the green box; the monthly sampling duration direct air filtration samplers are pictured in the blue box 85
Figure 4. 3 Diagram of the two active air sampling systems used, (A) Direct Air Filtration System; (B) Nanotank System 86
Figure 4. 4 Experimental Set Up- Pumping Rate and Sampling Duration values 88
Figure 4.5 (A) Bar Chart displaying normalised results for each sampling duration and pumping rate expressed as total MP count per filter; (B) Bar Chart displaying normalised data for each sampling duration and pumping rate particles per m^3; (C) Bar Graph displaying nanotank daily sampling frequency particle counts expressed as total MP count per filter (*NB: 40 L/min was the maximum limit for the nanotank sampling but is presented as 50 L/min here) (D) Bar Graph displaying nanotank daily sampling frequency particle counts expressed as particles per m^3 96

Figure 5. 1 Black points indicate Ny-Ålesund and the location of the research. (A) indicates the sample location relative to the extreme latitudes, (B) highlights the sample location within the more detailed visualisation of the Arctic circle. (C) indicates that actual building location where the sampling was undertaken (D) building and balcony used for sampling 112

Figure 5. 2 (A) Passive (red box) and active equipment set-up on Veksthuset station roof; (B) Active equipment set-up at the Veksthuset station (air filter and nanotank samplers) 113
Figure 5. 3 MP concentrations for active direct air filtration samples (MP/m^3); b) MP concentrations for active nanotank samples MP/m^3 c) MP concentrations for passive (deposition) samples (MP/m^2); error bars indicate standard deviation. Nanotank and Deposition samples represent daily sampling, while each direct air filtration sample was collected for three days (Appendix Table VII.1). 120
Figure 5. 4 MP Concentrations for Active/Suspended Samples; Direct Air Filtration with Corresponding Nanotank Values (Appendix Table VII.I)..... 121
Figure 5. 5 Particle size distribution for suspended particulates (direct air filtration and nanotank samples) as a percentage of the total particle count; b) Particle size distribution for deposition particulates (deposition samples) as a percentage of the total particle count (Appendix Table VII.2-4)..... 124
Figure 5. 6 (A) Example Nile Red image of fibre found in a nanotank sample on 19 May 2021; (B) Example Nile Red image of fragment found in a deposition sample on 04 June 2021; (C) Example Nile Red image of fragments found in an air filter sample from 04-07 June 2021; (D) Bright field image of the same fragment (figure 6.c) from air filter sample 04-07 June 2021 (x10 objective for all microscope images); (E) Percentage of particles analysed that are fragments or fibres (<0.3m circularity; n=9229)..... 125
Figure 5. 7 (A) Polymer composition direct air filtration samples; (B) polymer composition of nanotank air filtration samples; (C) polymer composition of deposition samples; (all expressed as total percentage of polymers identified using µRaman); (D) Image of deposition filter from micro-Raman spectrometer (QMA Whatmann 25mm, 1.6µm; x10 objective)(see Appendix Table VII.5)..... 126
Figure 5. 8 Source contribution to modelled MP at Ny-Ålesund for (A) active and nanotank samples (surface concentrations and (B) passive samples (deposition rates). Five different emission sectors were considered, namely MP suspended from the ocean (sea-spray), agricultural activity (e.g., agricultural nets), soil (mineral dust), road dust (tire wear particles) and microfibers (releases from clothes of the

population), adopted from an updated version of the MP emission dataset from Evangeliou et al. (2022). (Figure created by Nikos Evangeliou)..... 130
Figure 5. 9 Average footprint emissions sensitivity for the (a) lowest (left) and the (b) highest 25% (right) measured surface concentration (active and nanotank samples) and deposition rates (passive samples) of MP in Ny-Ålesund. (Figure produced by Dr Nikos Evangeliou..... 132
Figure 6. 1 Map of Scotland with Sampling Location (Blue) (Google Earth, 2025) 144

Figure 6. 2Image of Experimental Set-Up in Glasgow, the nanotank samplers can be seen in the red box; the daily sampling duration direct air filtration samplers are in the yellow box; the weekly sampling duration direct air filtration samplers are in the green box; the monthly sampling duration direct air filtration samplers are pictured in the blue box..... 144
Figure 6. 3 (A) Bar Graph showing concentrations of atmospheric MPs via direct air filtration with a daily sampling frequency from 17th Nov-23rd Nov'21 (n=6, D6.10* presented as an average of other daily measurements due to data loss); (B) Bar Graph showing distribution of atmospheric MP concentrations of weekly measurements via direct air filtration from the 3rd Nov-1st Dec'21 (n=4); (C) Bar Graph showing distribution of atmospheric MP concentrations via nanotank sampling system with daily sampling frequency from the 17th-23rd Nov'21 (n=7) (Appendix Table V.1) . 154
Figure 6. 4 (A) Line Graph showing particle size distribution of daily direct air filtration samples 17th Nov-23rd Nov'21 (n=7); (B) Line Graph showing particle size distribution of weekly direct air filtration samples taken from 3rd Nov-1st Dec'21 (n=7), (C) Line Graph showing particle size distribution of daily nanotank samples taken from the 17th-23rd Nov'2 1(n-7) (Appendix Table V2-5)..... 158
Figure 6. 5 (A) Stacked Column Graph Showing Percentage of Polymers Identified by µRaman spectroscopy for Weekly Direct Air Filtration Samples (n=4); (B) Stacked Column Graph Showing Percentage of Polymers Identified by µRaman spectroscopy for Daily Nanotank Samples (n=7) (due to resource restraints daily direct air filtration samples were mostly analysed with Nile Red staining and there was not a consistent number of daily direct air filtration samples with polymer composition data in order to present consistent dataset)..... 159
Figure 6. 6 (A) Results from HYSPLIT Back and Forward Trajectory Modelling for the 17th Nov'21; (B) Results from HYSPLIT Back and Forward Trajectory Modelling for the 17^{8h} Nov'21; (C) Results from HYSPLIT Back and Forward Trajectory Modelling for the 19th Nov'21; (D) Results from HYSPLIT Back and Forward Trajectory Modelling for the 20th Nov'21 ; (E) Results from HYSPLIT Back

and Forward Trajectory Modelling for the 21st Nov'21; (F) Results from HYSPLIT Back and Forward Trajectory Modelling for the 22nd Nov'21; (G) Results from HYSPLIT Back and Forward Trajectory Modelling for the 23rd Nov'21; Different Elevations Depicted by Red – 10 m; Blue – 50 m; Green – 100 m (Google Earth, 2025) 164
Figure 6. 7 (A) Results from Backward Trajectory Modelling for 48hrs for 10 µm particles with 1 g density 17th of Nov'21; (B) Results from Backward Trajectory Modelling for 48hrs for 10 µm particles with 0.625 g density for the 17th of Nov Backward 0.625g density (Google Earth, 2025) 166
Figure 6. 8 (A) Results from Backward Trajectory Modelling for 48hrs for 10 µm particles with 1 g density 19th of Nov'21; (B) Results from Backward Trajectory Modelling for 48hrs for 10 µm particles with 0.625g density for the 19th of Nov Backward 0.625 g density (Google Earth, 2025) 167
Figure 6. 9 (A) Results from Backward Trajectory Modelling for 48hrs for 10 µm particles with 1 g density 22nd of Nov'21; (B) Results from Backward Trajectory Modelling for 48hrs for 10 µm particles with 0.625g density for the 22nd of Nov Backward 0.625g density (Google Earth, 2025) 168
Figure 6. 10 (A) Results from Backward Trajectory Modelling for 48hrs for 10 µm particles with 1 g density 23rd of Nov'21; (B) Results from Backward Trajectory Modelling for 48hrs for 10 µm particles with 0.625 g density for the 23rd of Nov Backward 0.625g density (Google Earth, 2025) 169
Figure 6. 11 (A) Results from Backward Trajectory Modelling for 48hrs for 20µm particles with 1 g density 23rd of Nov'21; (B) Results from Backward Trajectory Modelling for 48hrs for 20µm particles with 0.625g density for the 23rd of Nov Backward 0.625 g density (Google Earth, 2025) 170
Figure 6. 12 (A) Results from Backward Trajectory Modelling for 20µm particles, 1 g density, for the 19th of Nov' 21; (B) Results from Backward Trajectory Modelling for 20µm particles, 0.625 g density for the 19th of Nov'21 (Google Earth, 2025) .. 171
Figure 6. 13 (A) Results from Backward Trajectory Modelling for 20 µm particles, 1 g density, for the 22nd of Nov' 21; (B) Results from Backward Trajectory Modelling for 20 µm particles, 0.625 g density for the 22nd of Nov' 21 (Google Earth, 2025) 172
Figure 6. 14 (A) Results from Back Trajectory Modelling for 20 µm 1 g density for the 23rd of Nov'21; (B) Results from Back Trajectory Modelling for 20 µm 0.625 g density for the 23rd of Nov'21 (Google Earth, 2025) 173
Figure 6. 15 (A) Results from Back Trajectory Modelling for 100 µm 1 g density for 48hrs for the 17th of Nov' 21; (B) Results from Back Trajectory Modelling for 100 µm 0.625 g density for 48hrs for the 17th of Nov' 21 (Google Earth, 2025) 174

Figure 6. 16 (A) Results from Back Trajectory Modelling for 100 µm 1 g density for 48hrs for the 19th of Nov' 21; (B) Results from Back Trajectory Modelling for 100 µm 0.625 g density for 48hrs for the 19th of Nov' 21 (Google Earth, 2025) 175
Figure 6. 17 (A) Results from Back Trajectory Modelling for 10 0µm 1 g density for 48hrs for the 21st of Nov' 21;)B) Results from Back Trajectory Modelling for 10 0µm 0.625 g density for 48hrs for the 21st of Nov' 21(Google Earth, 2025)..... 177
Figure 6. 18 (A) Results from Back Trajectory Modelling for 100 µm 1 g density for 48hrs for the 23rd of Nov' 21; (B) Results from Back Trajectory Modelling for 100 µm 0.625 g density for 48hrs for the 23rd of Nov' 21 (Google Earth, 2025) 178
Figure 6. 19 (A) Results from Forward Trajectory Modelling of 10 µm 1 g density for 48hrs on the 17th of Nov'21; (B) Results from Forward Trajectory Modelling of 10 µm 0.625 g density for 48hrs on the 17th of Nov'21 (Google Earth, 2025)..... 181
Figure 6. 20 (A) Results from Forward Trajectory Modelling of 10 µm 1 g density for 48hrs on the 19th of Nov'21; (B) Results from Forward Trajectory Modelling of 10 µm 0.625 g density for 48hrs on the 19th of Nov'21 (Google Earth, 2025)..... 182
Figure 6. 21 (A) Results from Forward Trajectory Modelling of 10 µm 1 g density for 48hrs on the 22nd of Nov'21; (B) Results from Forward Trajectory Modelling of 10 µm 0.625 g density for 48hrs on the 22nd of Nov'21 (Google Earth, 2025)..... 183
Figure 6. 22 (A) Results from Forward Trajectory Modelling of 10 µm 1 g density for 48hrs on the 23rd of Nov'21; (B) Results from Forward Trajectory Modelling of 10 µm 0.625 g density for 48hrs on the 23rd of Nov'21 (Google Earth, 2025) 184
Figure 6. 23 (A) Results from Forward Trajectory Modelling of 20 µm 1 g density for 48hrs on the 17th of Nov'21; (B) Results from Forward Trajectory Modelling of 20 µm 0.625 g density for 48hrs on the 17th of Nov'21 (Google Earth, 2025)..... 185
Figure 6. 24 (A) Results from Forward Trajectory Modelling of 20 µm 1g density for 48hrs on the 19th of Nov'21; (B) Results from Forward Trajectory Modelling of 20 µm 0.625 g density for 48hrs on the 19th of Nov'21 (Google Earth, 2025)..... 186
Figure 6. 25 (A) Results from Forward Trajectory Modelling of 20 µm 1 g density for 48hrs on the 22nd of Nov'21; (B) Results from Forward Trajectory Modelling of 20 µm 0.625 g density for 48hrs on the 22nd of Nov'21 (Google Earth, 2025)..... 187
Figure 6. 26 (A) Results from Forward Trajectory Modelling of 20 µm 1 g density for 48hrs on the 23rd of Nov'21; (B) Results from Forward Trajectory Modelling of 20 µm 0.625 g density for 48hrs on the 23rd of Nov'21 (Google Earth, 2025) 188
Figure 6. 27 (A) Results from Forward Trajectory Modelling of 100 µm 1 g density for 48hrs on the 17th of Nov'21; (B) Results from Forward Trajectory Modelling of 100 µm 0.625 g density for 48hrs on the 17th of Nov'21 (Google Earth, 2025)..... 189

Figure 6. 28 (A) Results from Forward Trajectory Modelling of 100 µm 1g density for 48hrs on the 19th of Nov'21; (B) Results from Forward Trajectory Modelling of 100 µm 0.625g density for 48hrs on the 19th of Nov'21 (Google Earth, 2025)..... 190
Figure 6. 29 (A) Results from Forward Trajectory Modelling of 100 µm 1 g density for 48hrs on the 22nd of Nov'21; B. Results from Forward Trajectory Modelling of 100 µm 0.625 g density for 48hrs on the 22nd of Nov'21 (Google Earth, 2025)..... 191
Figure 6. 30 (A) Results from Forward Trajectory Modelling of 100 µm 1 g density for 48hrs on the 23rd of Nov'21; (B) Results from Forward Trajectory Modelling of 100 µm 0.625 g density for 48hrs on the 23rd of Nov'21 (Google Earth, 2025) 192

List of Tables

Table 4.1 Sampling Information from Research at time of research design (Environment; Quantity of Sampled Air; Duration; Sampling Rate; Sampler Type) (Syafei et al., 2019; Peller et al., 2019; Li et al., 2020; Dris et al., 2017; Gaston et al., 2020; Panko et al., 2019; Abbasi et al., 2019; Trainic et al., 2020; Asrin and Dipareza et al., 2019; Allen et al., 2020; Liu et al., 2019a; Liu et al., 2019b; Wang et al., 2020; Tunahan Kaya et al., 2018; Akhbarizadeh et al., 2020) 87
Table 4.2 MP Average Particle Counts Expressed as Total MP per Filter and Average Particle MP Counts Expressed per m^3 and MP (Appendix Table V.1) 94
Table 4.3 Particle Size Distribution of MP Particulates as Percentage of Particles Identified (Nile Red) (Appendix Table V.2-5) 97
Table 5. 1 Average MP for suspended and deposited particulates (μRaman)122

Table 5. 2 Size ranges of atmospheric MP as a percentage of particles identified for both suspended (air filter and nanotank) and deposited particulates (Appendix Table VII.2-4)..... 123
Table 5. 3 Comparison of MP studies in the Arctic, Antarctica, remote and urban regions (non-exhaustive)..... 136
Table 6. 1 Sample type and respective flow rate chosen for Glasgow Atmospheric MP content 145

Table 6. 2 Particle Characteristics and Parameters used to Calculate Velocity for HYSPLIT Model Inputs..... 152

List of Boxes

Box 1.1 Overarching Thesis Research Aim 5
Box 2.2 Summary of Initiatives that are included in the EU's Circular Economy Plan that address plastic pollution (European Commission, 2020)..... 51

List of Abbreviations

ABS	Acrylonitrile Butadiene Styrene
CE	Cellulose
CO^2	Carbon Dioxide
COVID-19	Coronavirus 2019
GHG	Greenhouse gases
LOD	Limit of detection
Milli-Q	Deionised Water
NO_x	Nitrogen oxides
NO2	Nitrogen dioxide
Nylon/PA	Nylon/Polyamide
PBL	Planetary Boundary Layer
PC	Polycarbonate
PE	Polyethylene
PES	Polyethersulfone
PET	Polyethylene terephthalate
PLS	Polysulfone
PLA	Polylactic acid
PLS	Polysulfone
PM_{10}	Particulate Matter (10µm fraction)
$PM_{2.5}$	Particulate Matter (2.5µm fraction)
PM_1	Particulate Matter (1µm fraction)
PMMA	Polymethyl methacrylate
PP	Polypropylene
PRF	Plastics Recycling Facility
PS	Polystyrene

PU	Polyurethane
PVA	Polyvinyl alcohol
PVC	Polyvinyl chloride
Rbr	Rubber
TWP	Tire wear particles

Abstract

Microplastics (MPs) defined as polymeric particles between 1μm and 5mm in size, have been reported in every environmental compartment (air, water, sediments). Their small size facilitates transport and ingestion by animals and humans, and raises environmental and climate concerns.

Since atmospheric MPs were first reported in 2015 research has grown rapidly, but significant knowledge gaps remain regarding their extent, transport and impacts. Inconsistent sampling and analytical methods limit comparison between studies, particularly between remote and urban environments.

This thesis addresses these gaps by **evaluating active atmospheric sampling parameters, comparing remote and urban environments, and investigating long-range transport.** For the first time, the influence of sampling duration and pumping rate on MP measurements is assessed. Results show that sampling parameters affect MP concentrations, particle size distribution and morphologies, but not polymer composition. Increasing sampled air volume did not proportionally increase MP concentrations (MP/m^3), while shorter sampling durations and lower pumping rates enhanced particle collection efficiency. Practical recommendations are provided to guide future atmospheric sampling strategies.

Atmospheric MPs were characterised in suspended and deposited atmospheric particles in the Artic region for the first time (Svalbard, Norway). The atmospheric MP content of the urban environment is also examined (Glasgow, Scotland). MPs were identified in all samples. In both locations, the majority of particles were below <20μm (~70%). Dispersion modelling indicates long-distance transport from the North Atlantic and continental Europe, highlighting marine-atmospheric and transboundary pathways. Urban concentrations were several orders of magnitude higher and included more fibres, consistent with textile sources. Acrylic, Polysulfone, and

Polyethersulfone were common polymers in both locations, indicating industrial and textile sources.

Overall this thesis that demonstrates that MP are ubiquitous in both remote and urban environments. Modelling confirms the significance of long-range and marine-atmospheric pathways and highlights the need for improving detection limits and the need for harmonised methods to report on polymer composition and particle characteristics.

Chapter 1. Introduction

1.1 Introduction to Atmospheric Microplastics and Research Focus

The term microplastic (MP) was first used in 2004 from a study examining marine water samples (Thomson et al., 2004). Since then, MPs have been reported in all environmental compartments (air, water, sediments, and biota) (Ali et al., 2021), from remote mountain catchments (Allen et al., 2019; Guo et al.,2024) and the Antarctic (Aves et al., 2022, Illuminati et al., 2024) to urban megacities (Li et al., 2020; Liu et al., 2019b; Jung et al., 2024; Jia et al., 2024). Understanding the extent of MP pollution, both in terms of its global distribution and concentration, and its impact on our ecosystems and human health, is one of the biggest environmental concerns of this generation and is an ongoing research challenge.

MPs can be defined as "any synthetic solid particle or polymeric matrix, with regular or irregular shape and within a size range from 1μm to 5mm, of either primary or secondary manufacturing origin, which are insoluble in water" (Frias and Nash, 2019: p.146). Primary MPs are plastics that are deliberately manufactured to be in MP form – e.g. for use in manufacturing or 'microbeads' (Jemec Kokalj et al., 2019). Secondary MPs are formed by the weathering and degradation of larger plastics or macroplastics (Zhang et al., 2020a). MPs are easily ingested by a wide range of animal species; can cause a range of issues including starvation and choking; and have been reported to be endocrine disruptors (Akdogan and Guven, 2019). MPs have been increasingly reported in the human body, most recently in human lung tissue (Jenner et al., 2022), brain tissue (Nihart et al., 2025) and blood (Leslie et al., 2022), emphasising the importance of understanding more about this inhalable pollutant. Given their small size they can easily be transported throughout the body and there is potential for further exposure to chemical additives used in their manufacture. Further to this, as MPs have a hydrophobic surface, it is thought MPs can absorb other organic contaminants and heavy metals, and act as vectors for these pollutants, which can cause further adverse effects to humans and animals (Wright and Kelly, 2017).

Atmospheric MP particulates were first reported in 2015 (Dris et al., 2016) and since then the field of research has increased rapidly (Zhang et al., 2020a). MPs are thought to be dispersed via atmospheric processes such as wind, precipitation and snow (Yao et al., 2022). Other weather parameters such as humidity and temperature may also impact MP transport (Nafea et al., 2024), but there is still a lack of consensus on the effects of weather parameters on MP dispersion and deposition (Liu et al., 2025). Despite this increase in research, large knowledge gaps exist in relation to their main sources, transport, and global extent. MP pollution is known to be transported between different environmental compartments via the 'Plastic Cycle' (Horton and Dixon, 2018). This refers to the transport and retention of MPs across environmental compartments, whereby particles can migrate between systems and accumulate in areas far from their original source. Due to the small particle size, atmospheric MP pollution is thought to be capable of covering large distances, over thousands of kilometres (Allen et al., 2021). MPs are thought to travel faster and further in the atmospheric compartment compared to other environmental matrices (Zhang et al., 2020a). This rapid and distal transport is concerning due to its potential to pollute environments and cause adverse effects in areas far from its original source. For example, MP contamination found on ice caps – far from their origin – can absorb light, reduce the albedo effect and accelerate the melting of polar ice (Revell et al., 2021). Given the associated risks of environmental toxicity and climate implications, the ability of MPs to be transported from urban areas with increased human activity and pollution, to remote areas is of increased interest. This is especially true in relation to fragile and unique ecosystems such as the Arctic. Scientific knowledge and the understanding of atmospheric MP transport is, however, in its infancy, requiring research to quantify the presence of atmospheric MPs in remote and urban areas and understand the potential long-range transport mechanisms.

The science is also evolving in relation to effective measurement and analysis of atmospheric MPs. There is demand within the field for the development of consistent methodologies to report concentrations accurately and facilitate comparison. Due to the variety of methods used, direct comparison of MP concentrations between studies

with different environmental characteristics remains challenging. As a result, there is limited information about how atmospheric MP pollution differs between urban and remote locations. Due to the transboundary nature of this pollutant, understanding these differences and possible transport mechanisms is crucial in adding to the knowledge on the global extent of this pollutant and how it could be impacting different environments.

To address these challenges, this thesis has the following aim:

Box 1.1 Overarching Thesis Research Aim

To improve understanding of atmospheric MP pollution by assessing their measurement, comparing their presence in remote and urban environments and exploring potential long-range transport pathways.

1.2 Research Questions

To achieve the stated aim, this thesis addresses four research questions (RQs), each with specific objectives, that focus on the methods used in the field to measure atmospheric MP pollution, variances of atmospheric MP pollution between remote and urban environments, and its global transport:

RQ(1) How do the parameters used in active atmospheric microplastic (MP) sampling influence measured particle concentrations relative to environmental conditions?

- To determine the appropriate pumping rate for optimal filter collection under field conditions.
- To establish the optimum duration for sampling intervals relative to field conditions.
- To evaluate the influence of pumping rate and sampling duration on the type of MP particles collected (polymer composition, shape (fragment/fibre) and size).

RQ(2) What are the concentrations and main characteristics (polymer composition, particle concentration, shape, and size) of atmospheric MPs in remote locations (using a case study of Svalbard, Norway), and how do these relate to weather conditions and potential transport pathways?

- To quantify the atmospheric MP content in the Svalbard planetary boundary layer (the lowest portion of the atmosphere), considering both suspended and deposited particulates.
- To characterise atmospheric MP pollution at this remote location in terms of particle size, shape, and polymer composition.
- To investigate the relationship between MP concentrations and weather parameters.
- To compare the characteristics of deposited versus suspended MP particulates.
- To identify the main transport pathways for atmospheric MP pollution at this remote location.

RQ(3) What are the concentrations and main characteristics (polymer composition, particle concentration, shape, and size) of atmospheric MPs in urban locations (based on a case study of Glasgow, Scotland), and how do these relate to weather conditions and potential transport pathways?

- To quantify the atmospheric MP content in the planetary boundary layer in Glasgow.
- To characterise atmospheric MP pollution at this urban location in terms of particle shape, size, and polymer composition.
- To investigate the relationship between MP concentration and weather parameters.
- To investigate the relationship between MP concentration and local air pollution.

- To identify the main transport pathways for atmospheric MP pollution at this urban location and examine the role of particle characteristics in atmospheric transport.

RQ(4) How do atmospheric MP concentrations, characteristics (polymer composition, particle concentration, shape, and size), transport pathways, and relationships with weather conditions differ between urban and remote environments?

- To compare the concentration of atmospheric MPs found in remote and urban locations.
- To compare the characteristics (polymer composition, particle concentration, shape and size) between remote and urban locations.
- To compare the respective relationships between atmospheric MP pollution and weather parameters between remote and urban locations.
- To compare the transport pathways of atmospheric MP pollution from urban and remote locations.

1.3 Thesis Structure

The thesis has been constructed through the following Chapters:

Chapter 2: Literature Review

The literature review gives an in-depth context of atmospheric MPs and the current state of research knowledge. This includes the current state of science on its measurement and methodologies, transport, and its risks to our environment, human health and climate. It also identifies the current research gaps and need for further research. In **Appendix I** there is a tabulated summary of the atmospheric MP studies published up to 22nd November 2024 and their respective methods and findings.

Chapter 3: Overview of Methods

This chapter gives an overview of the methods used within this thesis. This includes the methods used to collect, analyse and report on atmospheric MPs in remote and urban environments. Measures to minimise contamination are also explained which is an important aspect of quality control in MP research. In **Appendix II** there is a draft of a peer-reviewed paper comparing the various analytical methods used to analyse MP, which the candidate co-wrote in addition to this thesis.

Chapter 4: Examination of the Effect of Sampling Volume and Pumping Rate on Atmospheric Microplastic Particle Concentration and Representation

This chapter addresses RQ1 by examining the parameters used for active sampling of atmospheric MPs and their effect on the concentration and representativeness of the resulting sample. No technical guidance exists to date on how to adjust active sampling parameters to suit the research aim or research environment. To address this, a field experiment was designed to test various sampling volumes and pumping rates over the same time period, to assess their relative importance in terms of particle concentrations and representation in the same environment.

Chapter 5: Examination of the presence of atmospheric microplastics in the remote environment: Svalbard, Norway

Chapter 5 addresses RQ2 by examining atmospheric MP in both suspended and deposited particulates in the Arctic region. A 28-day field campaign with both active (suspended) and passive (deposited) measurements was conducted and the results are compared with local weather data to observe potential relationships. Dispersion modelling was used to observe potential atmospheric transport of MPs to this remote location.

Chapter 6: Examination of the presence of atmospheric microplastics in the urban environment: Glasgow, Scotland

RQ3 is addressed in Chapter 6 that presents an examination of suspended atmospheric MPs in the urban environment from a field study in Glasgow, Scotland. A 28-day field campaign of active measurements was conducted and the results are compared with local weather data and air pollution data to observe potential relationships. Particle modelling was used to observe potential transport and pathways of atmospheric MP pollution at this urban location. The effect of particle characteristics (polymer density and size) on the transport mechanisms of atmospheric MP are also examined.

Chapter 7: Discussion of findings, limitations and recommendations for future research

This chapter summarises the results presented and compares the presence of atmospheric MP pollution in remote and urban regions. This includes the differences in particle characteristics (size, shape, polymer composition), concentrations, and possible transport at both locations. The aims and objectives of this thesis are re-stated and answers presented, before recommendations for future research are explored.

Chapter 8: Conclusion

The final chapter addresses the answers to the research questions (RQ1-4) and the objectives of the thesis. It presents the key findings and recommendations for future work.

Chapter 2. Literature Review

This literature review explores the emergence of MPs research as an environmental concern; their sources and transport; the challenges facing their collection, treatment and measurement; risks to environmental and public health; policies for mitigation; and recommendations for future research and policy.

2.1 Microplastics and Atmospheric Microplastics

2.1.1 Emergence of Microplastics as an Environmental Concern

The plastic problem was originally documented on a larger size scale with research on macroplastics (>5mm) on beaches and in the digestive systems of marine animals (Schmid et al., 2021). But due to a study by Thomson and colleagues in 2004 where MPs were first reported, attention has become increasingly focused on MPs in the literature, but also public attention, and policy (Catarino et al., 2021). A MP is defined as any polymeric particle between 5mm and 1μm in size (Frias and Nash, 2019), and the term was first used to document the extent of plastic pollution from sea water and sediment samples taken from the northeast of Scotland to Iceland (Thomson et al., 2004). Since then, it has been reported in every environmental compartment, in urban and remote environments in locations all over the world (Hasan Anik et al., 2021). Due to the impact of MP pollution on ecosystems, human health, and climate processes (see **Chapter 2.4**), and due to its fast-travelling and transboundary nature (see **Chapter 2.2**), this emerging pollutant that is deserving of the growth in research and public, and policy attention.

So far, a significant amount of research focus in MPs is concentrated on marine systems. As much as 96% of MP research is focused in this area (Xu et al., 2020a). It was originally thought that all plastic originated on land and this was transported to the marine environment where it remained (Thomson et al., 2004). However, in recent years there has been a growth in studies reporting MP concentrations in other

environmental matrices, such as snow, soil, terrestrial biota, and the atmosphere; and the rate of publications on MP has increased significantly (Allen et al., 2022; **Figure 2.1**).

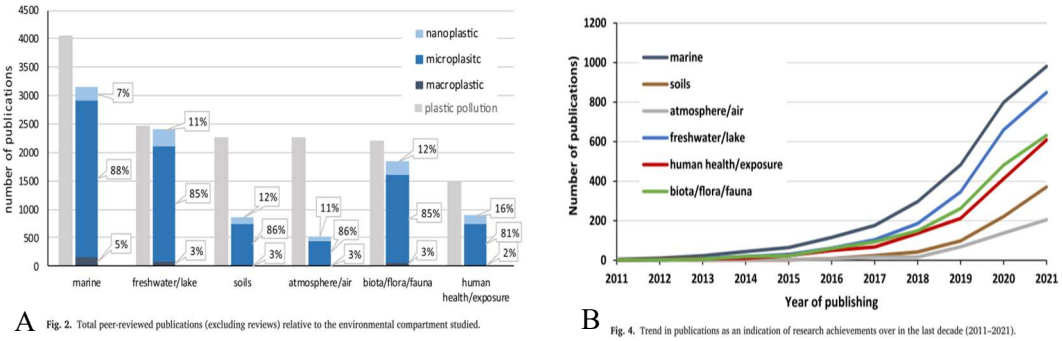


Figure 2. 1 A) Bar graph showing distribution of MP publications across research topics from studies published up to 31/12/2021 (Allen et al., 2022) (B) Line graph showing MP research topic trends from 2011-2021 (Allen et al., 2022)

As the field has developed, one of the main themes of MP research appears to be the '*race to the bottom'*, to observe and quantify the smallest sizes of MP present in the environment (Dong et al., 2023). This is due to the consideration that the majority of studies have reported that as particle size decreases, there is an increase in the number of MP particles identified. Reporting on MP concentrations with the inclusion of the smallest fraction, is important to report accurate quantifications, but also due to their small size, particles <10-20µm are more of a concern due to their efficient transport, and environmental and human health consequences (Ziani et al., 2023; Xu et al., 2024). Another theme of MP research is lack of standardisation in terms of methodology and reporting (Pérez-Guevara et al., 2022; see also **Chapter 2.3**). However, this lack of harmony in scientific reporting and communication, should not prevent more MP research taking place. Although there are still large knowledge gaps in MP research and its impact, the precautionary principle should be applied, and research should continue to examine and report on this pollutant. With global plastic production estimated to increase to 12,000Mt by 2050 (Geyer et al., 2017), and as waste continues to be mismanaged, MP pollution will become an increasing concern as more is learned about this pollutant. Therefore, research and resources are needed in this area. The

mainstream media has been increasingly reporting on this issue (see **Figure 2.2**), and it appears to have gathered policy attention (see **Chapter 2.5**), so research on this topic is both warranted and in demand.



Figure 2. 2 (A) Newspaper Article from British Newspaper, 'The Guardian' (Mains, 2024); (B) Newspaper from U.S Newspaper, 'The New York Times', published same year as thesis, showing media attention to MP pollution (Sloat, 2024)

This thesis focuses on MP pollution in the atmospheric compartment, how it is measured, and how it can differ from remote to urban locations. The following sections provide some context on the methods used to study this pollutant and its wider transport and environmental and human health implications.

2.1.2 Atmospheric Microplastics as an Emerging Field

The potential threat of atmospheric MP pollution is often overlooked (Wright et al., 2020), but there has been an increase in published papers in this field in recent years (Zhang et al., 2020a). However, there are still large gaps in the knowledge surrounding atmospheric MPs, this section will cover the research that has been conducted so far and highlight these gaps.

The first known atmospheric MP study was published by Dris and colleagues in 2016 reporting atmospheric deposition of MP in Paris, France (Dris et al., 2016). Since then, there have been studies conducted all over the world including cities such as Beijing (Li et al., 2020), London (Wright et al., 2020) and Mexico City (Shruti et al., 2022a), and remote locations such as Antarctica (Aves et al., 2022), the Pyrenees (Allen et al.,

2019), and the Himalayas (Ankit et al., 2024). These studies often report MP presence in all or the majority of samples, and studies to date have demonstrated that these MP particles can travel longer distances in the atmospheric compartment (Allen et al., 2022) than other matrices. **Appendix I** contains a table which summarises the atmospheric MP studies published up until the 22nd of November 2024, and highlights the location, type of environment (urban/remote), and main methodologies used for sample collection and analysis.

Currently, despite an increase in atmospheric MP studies, there are still large knowledge gaps in relation to the sources, transport dynamics, and environmental impacts of MP (Peterson & Hubbart, 2021). Also, one of the main threads of contention throughout atmospheric MP studies is the lack of standardisation in methodology in atmospheric MP analysis, the lack of harmony when reporting concentrations and the difficulty in analysing MPs (Zhang et al., 2020a). This is due to the type of equipment needed to analyse MP samples, and also the different types of samples that can be collected (**see Chapter 2.3**).

However, there are some consistencies across the research. Firstly, as particle size decreases, there is an increase in the number of particles found which is consistent with all MP research (Ding et al., 2021, Jenner et l., 2022, Allen et al., 2019; Fan et al., 2022); larger particles tend to be found in indoor air compared to outdoor air (Dris et al., 2017; Gaston et al. 2020; Choi et al., 2022); and most studies report MP in the majority, if not all samples (Wright et al., 2020; Chen et al., 2023; Sharaf Din, et al., 2024). This highlights that MP pollution in the atmosphere is extensive, that the size limit of the study can influence the number of particles reported, and that the environment in which the sample is taken can influence the size of particulates found. The following sections will cover the main aspects of atmospheric MP research including sources and transport, MP measurement, and the wider impact of this pollutant and current policy.

2.2 Atmospheric Microplastic Sources and Transport Mechanisms

2.2.1 Sources of Microplastics – Primary and Secondary Microplastics

MPs can be deliberately manufactured to be micro in size (<1mm), for example industrial applications or 'microbeads' often found in personal care products (Jemec Kokalj et al., 2019) and are referred to as 'primary' MPs. They are also formed by the degradation of larger plastic items and are referred to as 'secondary' MPs. These sources include the degradation of synthetic textiles, the breakdown of plastic via abrasive processes such as waste management and recycling, and the breakdown of marine plastic debris (GESAMP, 2016, in Zhang et al., 2020a); erosion of tyres, artificial turfs and mulching (Huang et al., 2020a); and the transport of particles from sewage sludge (Wang et al 2021). Both sources of MPs can find their way into our terrestrial, marine and atmospheric ecosystems due to their small size.

It is thought that MP particles enter the atmosphere via a plethora of avenues. To date the literature has cited multiple sources – textile production and the degradation of synthetic textile fibres (Dris et al., 2017; Gong and Xie, 2020; Wang et al., 2020a), clothes drying, plastic packaging (Liu et al., 2019a; Wang et al., 2020), recycling and waste management activities (Abbasi et al., 2019; Dehghani et al., 2017; Dris et al., 2016), and landfill leakage (Thinh et al., 2020a; Xu et al., 2020a). It is also known that the following activities cause MP pollution in aquatic systems but their contribution to atmospheric pollution is not yet known – for example wastewater treatment plants (Dris et al., 2016; Liu et al., 2019b), agricultural activities such as the use of sewage sludge (Mahon et al., 2017; Zhang et al., 2020a), plastic films and mulching (Huang et al., 2020a; Liu et al., 2019b), and finally the wear and tear of rubber tires, artificial turfs and road paints (Xu et al., 2020a). Therefore there is no doubt that human activity can be directly linked with the increase in atmospheric MP concentrations. Wang and colleagues (2024b) found a correlation with the air quality index in South Korea and the abundance of atmospheric MPs in total (TSP), and the PM_{10}, and $PM_{2.5}$, size fractions. Furthermore, Beaurepaire et al. (2024) found when

comparing pre- and post-lockdown atmospheric deposition in Paris, MP concentrations were significantly lower during the lockdown, highlighting the contribution of human activity to atmospheric MP pollution.

Source appointment of MPs is a complicated task and given that there is no openly available ingredient list for the production of polymers, tracking the origins of this pollution can be difficult. To date, studies have focused on conducting field sampling, and then making assumptions on possible sources based on based on morphology and polymer composition of the particles. For example, Kannankai and Devipriya (2024), who sampled urban locations in Kochi, India and used back trajectory modelling which indicated that the municipal landfill could be a major source of the atmospheric MP pollution there, and that this deposition could extend to the Arabian Sea with atmospheric transport (Kannankai and Devirpiya, 2024). To give more indication of what is being transported from the landfill itself, the study could have used an additional sampling site close to the landfill and compared this to their original location. Furthermore, due to the limitations of the back-trajectory models used, it was only possible to gain straight line wind parcels. There is not enough time within in the trajectories to deal with significant changes in wind direction or speed. As a result, the air mass paths are simplified and approximate rather than realistic representations of how air parcels move. Therefore, while these models are helpful at estimating where pollution could be originating, they cannot give a full picture of source appointment.

Some studies have carried out source monitoring, such as a study by Thinh and colleagues, which monitored atmospheric deposition at a landfill site in Ho Cho Minh city (Thinh et al., 2020). However, only deposition was measured and the limit of detection (LOD; the smallest particle identified as a polymer) was <100µm. This means the suspended particulates have not been measured, and the smaller MP size fraction is not known, therefore the MP concentration for this landfill site could be much higher. Brown and colleagues (2023) examined the MP pollution from wash water from mechanical recycling processes at a plastics recycling facility (PRF) and took atmospheric deposition samples from within the facility while the samples were

being collected. Their results showed high levels of atmospheric MP in the facility, with >61% of deposited particles being <10µm (Brown et al., 2023), which as highlighted above, may have more environmental and human health implications, and longer-range environmental transport. This study highlights the need for more research on MP pollution from recycling facilities and its contribution to atmospheric MP content.

A common approach to allocating the main sources of MPs is using computer models. The accuracy of computer models is also dependent on the use of correct assumptions, which can be subject to human bias, and models are only as valuable as the inputs and variables that are used. These models are discussed further in **Chapter 2.2.2.**

2.2.2 Microplastic Transport – The 'Plastic Cycle'

MP contamination has been reported as ubiquitous in all environmental compartments (Patil et al., 2021). These compartments are usually considered separately but due to the multiple transport pathways of MPs, they are interconnected (Horton and Dixon, 2018). The term 'Plastic Cycle' was introduced by Horton and Dixon (2018) and describes the processes that control the movement and retention of MPs between the many different environments affected by MP pollution (Horton and Dixon, 2018). As can be observed in **Figure 2.3**, MP sources (in grey) are assumed to originate on land; however this diagram is missing marine plastic from fishing and tourism (Shahul Hamid et al., 2018), which can be transported (in blue) to different sinks (in orange)) in the form of freshwater sediments, river waters and eventually marine waters (Horton and Dixon, 2018.

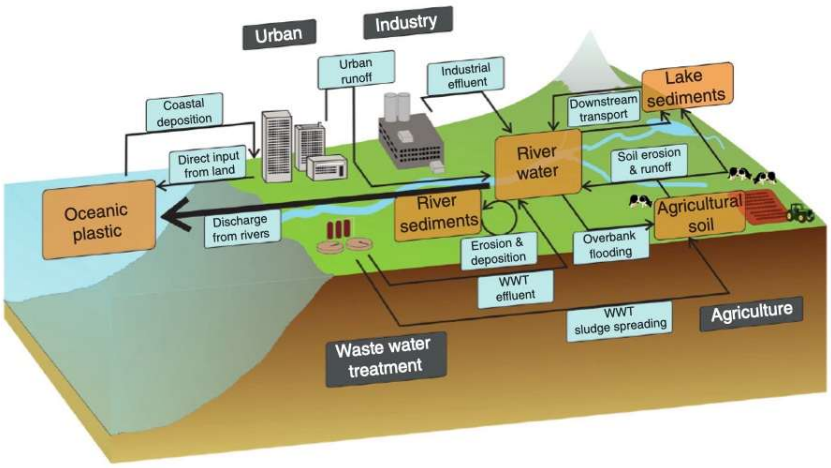


FIGURE 3 Conceptual model representing the "Plastic Cycle" concept (wastewater treatment, WWT). Orange boxes represent sinks, blue boxes represent transport mechanisms and arrows represent transport pathways. Atmospheric microplastics are not included within the model as they cannot be attributed to a specific compartment or route of transport

Figure 2. 3 Visual Representation of the 'Plastic Cycle' *(Horton and Dixon, 2018)*

In **Figure 2.3,** Horton and Dixon (2018) have omitted atmospheric MP as they cannot be attributed to a terrestrial or aquatic environmental compartment and their transport is unclear. However, although exact source appointment is difficult and there is not a great deal of consensus of the transport processes and conditions that influence atmospheric MP pollution (see previous sections), the addition of atmospheric transport is important to understand the extent of MP pollution across all environmental compartments. How these processes and mechanisms interact requires research attention and examining where atmospheric MP fits into the 'Plastics Cycle' is vital to understanding the importance of this new field of research. By examining the atmospheric MP content of urban and remote locations, and using particle modelling to observe their transport, this study hopes to contribute to the understanding of the atmospheric compartment of the 'Plastic Cycle'.

2.2.3 Atmospheric transport - mechanisms of transport, atmospheric dispersion and deposition

The movement of MPs in the atmosphere, like other atmospheric pollutants, is considered to be due to transport mechanisms called dispersion and deposition.

Dispersion is the process in which pollutants are spread due to local turbulence (Martina & Trini Castelli 2023). Deposition processes are precipitation, scavenging, and sedimentation. Particles are removed from the atmosphere by wet scavenging (snow, rain) or dry scavenging (particles settling from the atmosphere and depositing onto surfaces), which causes the vertical transport of pollutants toward the ground (Samson, 1988), including MPs (Nafea et al., 2024). Deposition is sometimes split into dry deposition and wet deposition. Dry deposition is when deposition happens during dry weather (non-precipitation events) and causes particles to settle slowly, with larger particles depositing faster (Giardina, M., & Buffa2018). Wet deposition occurs when there is precipitation (snow or rain) (Wu et al., 2017). It was originally thought that processes such as precipitation could increase deposition of particles, but studies have found both positive (Winijku et al., 2024; Jia et al., 2022; Wang et al., 2022 ; Wright et al., 2020a; Liu et al., 2019a) and negative (Szewc et al., 2021; Truong et al., 2021 Allen et al., 2019a,) correlations with deposition and precipitation. The effect of other weather parameters such as humidity and temperature have also been considered to impact MP transport (Nafea et al., 2024), and have been suggested to have negative (Chen et al., 2024, Zhang et al., 2023a) and positive (Klein et al., 2023, Jai et al., 2022) correlations with MP deposition. Therefore, more studies are needed to examine unique weather events.

The main known mechanism for atmospheric MPs transport is wind, which can transport particles laterally and vertically (Liu et al., 2019b). Vertical convection currents can transport particles to higher altitudes and over large distances, even to remote regions (Chen et al., 2023. The transport of MP is influenced by the characteristics of the particle such as size, shape, and density (Huang et al., 2024). Smaller particles are more easily transported by wind, and larger particles may deposit more quickly (Ward et al., 2024). Given the variability of this pollutant, and the multiple factors that can affect its transport, this is an area which still needs more consistent research to monitor transport over time. Atmospheric MP transport has also been found to be a source of marine MP pollution (Liu et al., 2020b) and conversely ocean spray is also said to be a mechanism of transport of MP to the atmosphere (Allen

et al., 2020a). It is thought that wind transport has the potential to move and deposit MPs from different terrestrial environments (Mbachu et al., 2020). Given the multiple pathways by which MPs can be transported, understanding their emission, transport and deposition is crucial to understand the extent of this pollutant globally.

As mentioned previously, models are often used to examine atmospheric transport of MPs (Allen et al., 2022);however, they are subject to bias and limitations due to the inputs and simplifications needed to make the model efficient. In other words, "All models are wrong, but some are useful" (UNEP, 2016: p.74). Due to the many parameters used in transport models, they will always have to be a "simplification of reality" (UNEP, 2016: p.74). The most commonly used models are LPDMs (Lagrangian Particle Dispersion Models) which model the movement of individual particles by simulating their transport within a moving air mass using their trajectories. The model then predicts how the particles are affected by wind, turbulence and settlement via deposition, and also consider other weather parameters such as temperature and humidity (Brioude et al., 2013). The two most commonly used LPDMs are FLEXPART (FLEXible PARTicle dispersion model) and HYSPLIT (Hybrid Single-Particle Lagrangian Integrated Trajectory) which both provide high-resolution results for understanding particle transport (Nafea et al., 2024).

2.2.3.1 HYSPLIT Back Trajectory Modelling

HYSPLIT was developed by the National Oceanic and Atmospheric Administration (NOAA) Air Resources Laboratory (NOAA, 2024a) and has been used in atmospheric MP research to compute backward air parcel trajectories to model MP transport and to track potential source appointment (Zhang et al., 2020a). The model uses meteorological data to track how individual particles may be transported by wind processes (Luo et al., 2022) and can provide detailed atmospheric dispersion modelling of MP transport over large distances (Nafea et al., 2024). The meteorological data is uploaded in gridded meteorological fields from weather prediction models (e.g. the National Oceanic and Atmospheric Administration (NOAA) or reanalysis data from

the Global Data Assimilation System (GDAS)), which allows the model to move and disperse particles through wind and turbulence, and remove them through processes like rain using a Langranian (stochastic) framework. This results in a simulation of how particles may be transported in the atmosphere (Draxler et al., 2025). It has been used in studies to suggest where concentrations of atmospheric MPs may have originated by estimating linear trajectories of MPs at sampling locations (Nafea et al., 24; Li et al., 2023; Kannankai and Devirpiya, 2024; Abbasi et al., 2022; Wang et al., 2020); Trainic et al., 2020). Although the model may not be able to include interactions between atmospheric chemistry and complex terrain (NOAA, 2024b), and its use can sometimes involve oversimplifications of parameters, it can provide suggestions on potential sources and the movement of particles in the atmosphere, where empirical data is lacking. For example, it has been used to understand the differences in transport between MP and smaller nanoplastic (NP) particles (see **Figure 2.4**). The modelling in the study found that NP particles could be transported further distances and had the potential to remain suspended in the atmosphere for up to 7 days (Allen et al., 2022). Another study using the HYSPLIT model found that fibres are deposited over a larger area compared to other particle shapes, and that particle shape should also be included as a parameter when using the model (Ward et al., 2024). The ease in which the model can be set up and operated (Stein et al., 2015) can also ensure that particle modelling is more accessible and replicable for other studies.

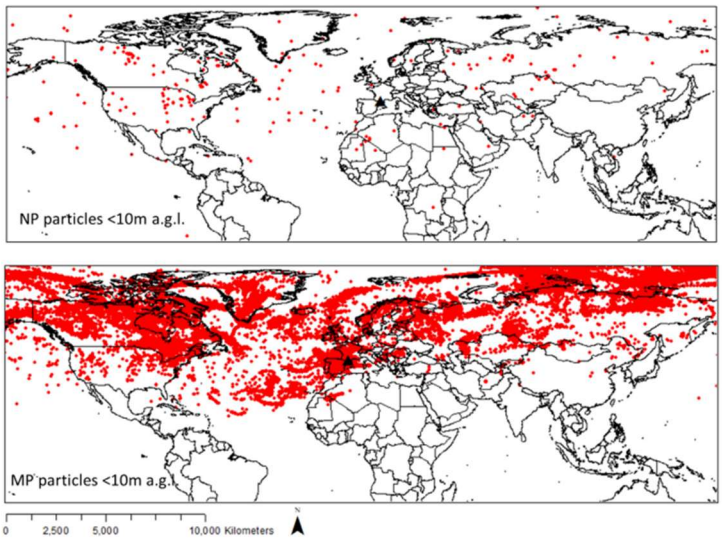


Fig. 4. Visualisation of particles at or below 10m a.g.l. during the backward trajectory particle modelling.

Figure 2. 4 Figure from Allen et al., (2022) study using HYSPLIT to model global atmospheric transport of MP and NP at 10m above ground level *(Allen et al., 2022)*

2.2.3.2 FLEXPART Back Trajectory Modelling

Another Lagrangian particle model commonly used is FLEXPART, and it again uses meteorological data and simulates the long-range transport of individual particles (Nafea et al., 2024) using a stochastic approach, and incorporating turbulence and mixing processes. This model can incorporate more detail compared to HYSPLIT as it simulates turbulent air motions using stochastic equations, which may represent vertical and horizontal transport more accurately (Evangeliou et al., 2022). HYSPLIT can use backward and forward simulations for source appointment and to examine transport. Evangeliou et al. (2020) used the FLEXPART model to simulate transport of MPs from road traffic, mainly tyre wear particles and brake wear particles (Evangeliou et al., 2020; see **Figure 2.5**).

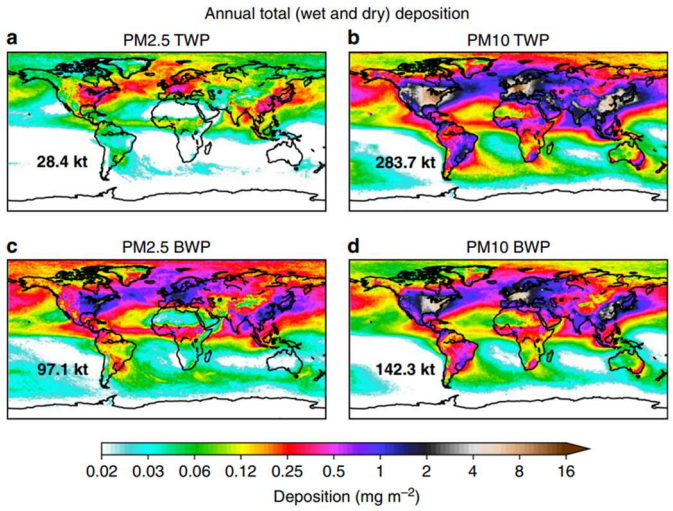


Figure 2. 5 Figure from Evangeliou et al (2020) study modelling TWP and BWP transport in the atmosphere using FLEXPART model; both wet and dry deposition for both types of MP particulates are displayed using data from 2014 and with the assistance of GAINS model (Greenhouse gas-Air pollution Interactions and Synergies) (Evangeliou et al., 2020)

Although data on tyre and brake wear particles was only available for Northern Europe, they did try to extrapolate the data and adjust for regional differences in vehicle use and emissions. Adjusting for regional variations and acknowledging differences in anthropogenic activities between different countries has allowed for a more accurate representation for the pollution and transport of atmospheric MPs. This study also suggested that MP from road traffic has high transport efficiencies and remote regions like the Arctic may receive a high proportion of this particulate matter, where it may cause accelerated warming of the cryosphere (Evangelou et al., 2020). This demonstrates the utility of the model when parameters are not over-simplified.

In a step further to this, in 2024 Evangeliou and colleagues, also studied the atmospheric MP resuspension from Bare Soil Regions which represent large sources of dust aerosols. Using an estimate of resuspensions, and the inclusion of two particle shapes – fibre and sphere; and by utilising a technique that varies input data (Evangeliou et al., 2024), it was possible for the study to create a more accurate

representation of MP particle resuspension and dispersion. The FLEXPART model indicated that fibres have higher concentrations in the atmosphere and are dispersed more widely than spheres (Evangeliou et al., 2024). This is consistent with Tatsii et al. (2023) which coupled novel laboratory experiments to investigate the gravitational settling of MP fibres and utilised FLEXPART to track their transport using this information. This study found that the settling velocities of fibres were 76% lower than spheres, and that this significantly increases the vertical and horizontal transport of fibres. This can result in the fibres reaching more remote regions of the globe, such as the Arctic, and their settling velocities results in transport higher into the stratosphere. Here, MP degradation by ultraviolet radiation could release chlorine and bromine and cause damage to this layer of the ozone (Tatsii et al., 2024). Bucci et al., (2024) used FLEXPART to investigate the ocean as a source of atmospheric MP pollution and found that models to date have underestimated MP concentrations. This study used a global oceanic model which utilised a size distribution estimate for MPs and a sea salt emission scheme, then used FLEXPART to model their transport. The model showed that MP particles can be transported swiftly across the globe and that they can remain in the stratosphere for months, consistent with Tatsii and colleagues (2023) findings. The ocean was confirmed as a source of atmospheric MP pollution, which is consistent with Trainic et al. (2020)'s similar study which used HYSPLIT. This highlights that both HYSPLIT and FLEXPART have indicated that marine MP transport to the atmosphere is crucial. The study by Tatsii et al. (2023) also demonstrated that by utilising more data variability, and complementing particle modelling with other datasets and models, can provide a more detailed picture of atmospheric MP transport. Although FLEXPART can provide a thorough investigation into atmospheric MP transport, it is more specialist than HYSPLIT and requires more resources to operate, and is said to not be as efficient for quick dispersion modelling (Bakels et al., 2024). Therefore, it might not be as accessible for more standardised particle modelling.

2.2.3.3 Community Earth System Model

The Community Earth System Model (CESM) has been used to model global atmospheric MP transport (Brahey et al., 2021). This is a grid-based model, designed for the modelling of large-scale atmospheric processes and interactions, within a fixed spatial or temporal resolution (Hurrell et al., 2013). Brahey and colleagues (2021) used the model to investigate the sources, movement and deposition of MP. However, the model relied on a set of assumptions that may be considered as over-simplifications. For example, the assumption that global deposition of MP particles is consistent with their emission estimate from roadside MP emissions in the United States (Brahey et al., 2021). This is not consistent with the literature, which despite the lack of standardised methodology, reports larger variances in atmospheric MP deposition across regions (see **Appendix I**). The study also assumed that as MP particle size decreases, there is a decrease in the number of particles (Brahey et al., 2021), which is contrary to the majority of results published in the literature (see **Chapter 2.1**). The study assumed that all MPs have the same density, which is not reported in the literature. These assumptions make it difficult to compare the results to the reality of atmospheric transport of MPs and their source appointment, and to other particle modelling studies. Although the multiple variables and parameters that are included in MP modelling are vast, future research should seek to avoid over-generalising data and assuming that MP pollution is the same globally. It is also true for all models - there is a general lack of understanding for the settling rates of all MP particles; their change in static charge in the atmosphere; and how they interact in the atmosphere (Revell et al., 2021). Therefore, there is space for more research and improvement for these models and the input data that is used.

Despite the limitations that can be experienced with using models, given the time-intensive nature of measuring atmospheric MP content, their small size and the large distances they can cover, computer models can fill in large knowledge gaps that empirical data cannot cover. Therefore, their accurate use and improvement will

hopefully answer more questions about atmospheric MP sources and their transport as the field progresses.

2.3 Methods of Sampling, Pre-Treatment, and Characterisation Techniques

2.3.1 Methods for Sample Collection – Passive and Active Sampling

The methods used for the collection of atmospheric MP samples, have been mostly adapted from the collection of samples for more traditional air pollutants, such as particulate matter (PM) and carbon. The simplest method used, is 'passive' or 'deposition' sampling, which samples deposited particulates. This can be either dry or wet deposition sampling - , or both can be measured at the same time (bulk deposition). This involves leaving a vessel – in this case normally made of stainless steel (see **Figure 2.6A**) – in the environment, either with some liquid or dry – for set period of time, to collect particles being deposited from the atmosphere. This can also be in the form of a funnel, or beaker, or deposition collected via adhesive (see **Figure 2.6B**), however the adhesive method is not recommended for atmospheric MP deposition collection (Knobloch et al., 2024).

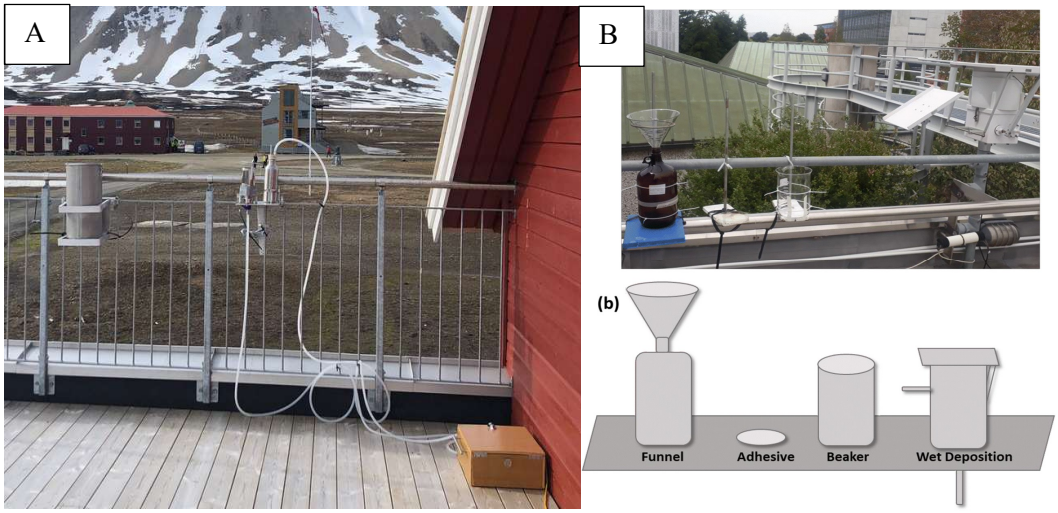


Figure 2. 6 (A) Passive (Left) and Active (Right) Air Sampling Equipment in the Field, Svalbard, Norway; (B) Different Methods of Passive/Deposition Sampling used in Atmospheric MP Research (Knobloch et al., 2024)

The other approach used is ‘active’ or ‘pumped’ sampling (Wright et al., 2019; Azari et al., 2023), which can take many different forms. In its simplest form, it involves using a calibrated pump to draw a known volume of air, through a chamber on to a filter, where the suspended atmospheric particulates can be collected, and later removed and analysed. More advanced models can use size diffraction to limit larger particles being collected, and direct deposition (Ashley and Connor, 2017). These devices also normally have a cover or ‘hat’ to prevent direct atmospheric deposition of particulates, so just the suspended particulates are collected (see **Figure 2.7**). Common devices used in this field include the active air filter sampler (**Figure 2.7A**); middle flow air samplers (e.g. Munro Instruments L10B – **Figure 2.7B**); and a high-volume air samplers (e.g. TISCH TSP **Figure 2.7C**). These measure suspended particulates by drawing the particulates suspended in the atmosphere into the sampler.

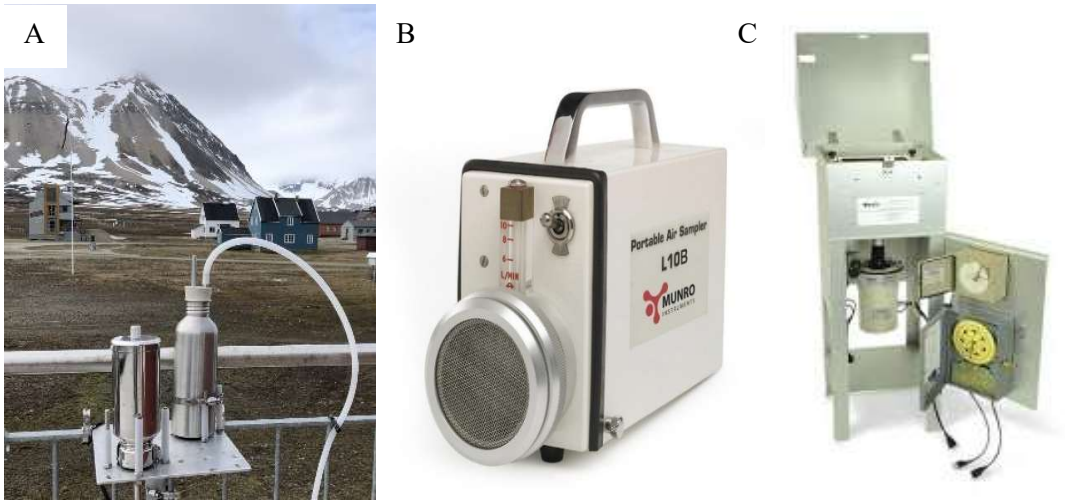


Figure 2. 7(A) Active Sampling Equipment in the Field (Active Air Filter Sampler – Left; ‘Nano-tank Sampler - Right’; Svalbard, Norway); (B) Middle Flow Air Sampler *(Munro Instruments, 2024)****; (C) TISCH High Volume Air Sampler*** *(TISCH, 2024)*

Passive deposition sampling is a convenient method for measuring atmospheric pollutants without expensive devices, power supply, or monitoring. However, both active and passive methods are recommended to gain samples of deposited and suspended particulates, and therefore gain a better understanding of the total picture of

atmospheric MP content (Zhang et al., 2020a). Another method that is utilised is snow sampling which normally produces a measurement of MP per unit of snow (usually litres of melted snow), which can make comparison to measurements of air normally reported as a concentration per metres.

Given the novelty of the field, there has not been significant advancements in the techniques and methods used to collect atmospheric MP samples. However, there has been some efforts made to develop the methods used to suit this emerging pollutant. One area that is still not fully understood, is the parameters used in sampling, and how they affect the collection of samples. As can be observed from **Appendix I,** the flow rate used to control the volume of air sampled, and the sampling duration, are different from study to study. However, there is no technical guidance on how to adjust these parameters to suit your study and its research objectives. In traditional air pollution research, it is known that the volume of air sampled can affect the sample greatly (Ashley and Connor, 2017), therefore one of the main aims of this thesis is to examine the efficiencies of different flow rates and sampling durations on MP concentration. It is hoped this can be used to evaluate, and provide guidance, on how to adjust these parameters to produce accurate and representative samples. This is covered in **Chapter 4**.

2.3.2 Methods for Sample Treatment – Digestion and Density Separation

Environmental samples can often contain organic and mineral material which can make the identification of MP particles more difficult (Song et al., 2015, In: Enyoh et al., 2019). Due to the delicate nature of MPs and their small size, treatment of samples to remove organics has to minimise particle damage and particle loss. There are many common methods used in the literature to do this in an effective manner, for example digestion using hydrogen peroxide (H_2O_2) usually at ≈30% concentration; or Fenton's reagent (H_2O_2 and Iron Sulphate (FeSO4)), is popular for the removal of organics without chemical damage to the polymers (Mbachu et al., 2020). Other solutions of

H_2O_2 and sulphuric acid (H_2SO_4) and nitric acid (HNO_3), and enzymic digestion have also been used (Huang et al., 2020b).

If some organic material remains, some studies use a density separation process to ensure the samples are suitable for further analysis. This involves separating the different materials by their relative density using a saturated solution. Materials that are lighter than the supernatant will float to the top, so a solution with a greater density that MP is needed (Thompson,et al., 2004). This is normally in the form of zinc chloride or calcium chloride (Huang et al., 2020b; Mbachu et al., 2020). The separated sample is treated again with H_2O_2 and transferred on to a filter for further analysis (Enyoh et al., 2019b). This step may not be necessary for samples with low levels of organic material, and every additional step can introduce opportunities for MP contamination. Given their environmental matrix, atmospheric samples can contain less organic material than marine or terrestrial MP samples (Allen et al., 2020), therefore sample pre-treatment may not always be needed.

2.3.3 Microplastic Characterisation and Quantification – 'Race to the Bottom', The Pursuit of Smaller Particle Identification

There are multiple options when it comes to analysing samples for microplastics. As mentioned previously there is no standard method for researching atmospheric microplastics and the technique used can be chosen based on the focus of the research. The techniques and equipment used are also typically expensive and time-consuming, so decisions are often made on an ad-hoc basis.

2.3.3.1 Microplastic Morphology: Shape, Colour and Size

One of the aims of atmospheric MP sample analysis is to characterise the morphology or physical characteristics of the particles found – this normally includes size; shape; and colour (**Figure 2.8**). Some suggest the size can indicate possible sources, as well as the age of the plastic. Furthermore, smaller particles could indicate more

degradation and more aging of the particle (Hebner, & Maurer-Jones, 2020). Size will also determine its transport in the atmosphere – both vertical and horizontal (Tatsii et al., 2024); and its environmental and human health impact (Ziani et al., 2023; Xu et al., 2024) as size is said to be crucial for toxicology (Thorton Hampton et al., 2022). In terms of shape, MP has been categorised as spheres, beads, fragments, foams, fibres, chips and films (Luo et al., 2024a). The type of plastic, surface properties, additives, and residency time in the environment can all influence degradation and shape of a MP particle (Chen et al., 2021). It has been reported that fibres are more easily transported through the atmospheric compartment and different particle shapes will have different settling velocities (Tatsii et al., 2024). Given the difficulty defining these different categories some studies focus primarily on identifying fibres and fragments (Borah et al., 2024; Allen et al., 2019). A fibre is normally defined as a MP particle having a 1:3 width to length ratio (Na et al., 2024; Li et al. 2020) and fragments counted as the particles remaining. It should be noted that a fibres can be the primary shape of a MP particle or can be formed via the degradation of a larger MP particle.

Colour is also identified in some studies (Zhang et al., 2020a), and it has been thought to suggest the potential origin of the MP but due to the many processes that can change the original colour of the plastic, such as abrasion and UV degradation of the plastic in the environment, and the digestion process for organic removal (Pfeiffer & Fischer, 2020).; Luo et al., 2024a); it is not always measured. Some studies have also suggested that colour is important in terms of the atmospheric transport of the particle and its subsequent influence on climate processes (Revell et al., 2021); as well as the degradation and environmental impact of that particle (Zhao et al., 2022). However, the choice of method used to analyse atmospheric samples can determine if this is reported in studies.

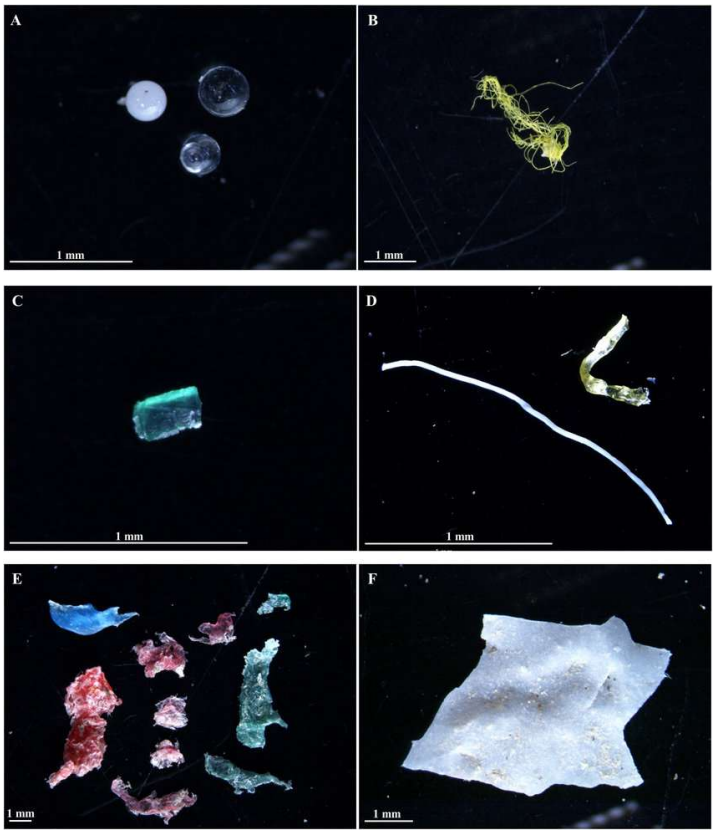


Figure 2. 8 Microplastics in their different morphological forms and colours – spheres, fibres, fragments and films – all <1mm in size, identified from samples from the Caspian Sea *(D'Hont et al., 2021)*

2.3.3.2 Microplastic Polymer Composition

The other main aim of identifying and characterising particulates is to measure the polymer composition. To be accurate, this has to be done via an analytical method which can identify the main chemical properties or origin of the plastic (Zhang et al., 2020b; Luo et al., 2024a). Previously microplastics research relied on visual inspection with a microscope and hot needle testing, but this is subject to human bias and has a limit of detection (LOD) of <500µm. Therefore, it is recommended that all research use a form non-visual spectroscopy (Zhang et al., 2020b) to improve the size range detectable and the accuracy of results. Polymer composition can give information about the potential origin of the MPs; and given that each polymer will have a different density, it can influence the behaviour of the particle in the

atmosphere in terms of suspension and deposition, and lower density polymers potentially being transported longer distances (Luo et al., 2024a).

2.3.3.3 Scanning Electron Microscopy

One method also used to identify the chemical composition of a MP particle is scanning electron microscopy (SEM) coupled with energy dispersive X-ray spectroscopy (EDS) or SEM-EDX (Li et al., 2020). SEM provides a clear high-resolution image (see **Figure 2.9**) and EDX identifies the chemical composition of the particles so that it is possible to discern if the particles are organic, plastic or otherwise. The EDS allows for plastics to be distinguished from organics by their unique elemental fingerprints. For example, PVC can easily be identified by SEM due to the distinct elemental signatures for chlorine and mineral species that may be misidentified as plastics can also be identified (Wang et al., 2017). However, colours cannot be identified with this method and it is described as expensive and time-consuming (Shim et al., 2017). This technique was used by a study in Beijing, China, with a reported a limit of detection of 5µm and its focus was to observe the type, size and concentration of MP particles in that area (Li et al., 2020). It can be observed from **Figure 2.9** that is possible to gain highly detailed images, and the use of SEM-EDX has grown in the past two years (Huang et al., 2024; Liu et al., 2024b; Wang et al., 2022; Shruti et al., 2022a). However, it is often used as a complimentary method of analysis alongside other analytical methods.

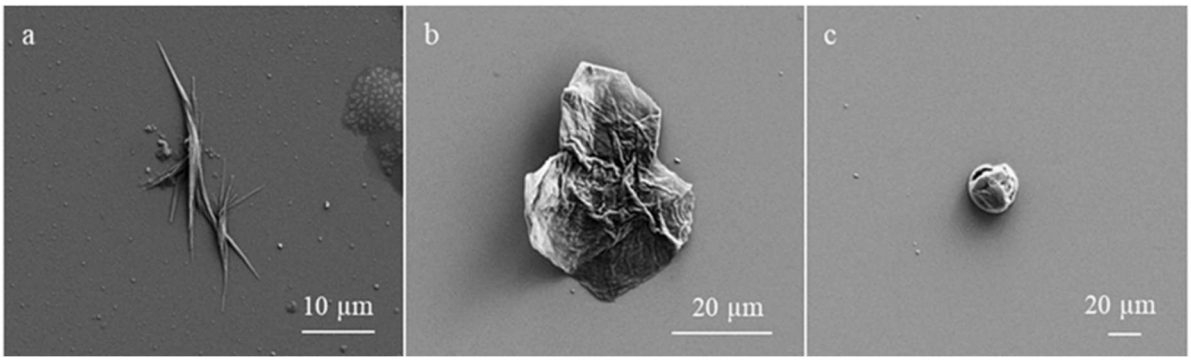


Figure 2. 9 SEM images of MPs identified from atmospheric samples from Beijing and Shanghai *(Liu et al., 2024b)*

SEM coupled with EDS or EDX can identify the elemental composition of MPs and produce high resolution images of particles down to the nano scale (<1µm), but it cannot identify the specific bonds that characterise the polymer type of a MP particle (Ivleva, 2021). Therefore it is beneficial to compliment this technique with another technique which can provide information on the polymer spectra.

2.3.3.4 Fourier Transform Infrared Spectroscopy

One of the more popular methods is Fourier transform infrared (FTIR) spectroscopy which uses infrared light to scan samples. The changes in the patterns of the light absorption indicate changes in material composition and bond types which are used to create a spectral fingerprint (Titus et al., 2019) which can be used to identify polymers. This is sometimes coupled with Attenuated Total Reflectance (ATR) which obtains the infrared spectrum of the sample by using a crystal (Thermo Fisher Scientific, 2018). Carbon-based polymers are easy to analyse with this technique as each bond creates a unique spectra. A reference library is then used to compare the spectra and allow for the polymer type to be discerned (Shim et al., 2017). FTIR can determine particle composition and is commonly used in MPs research due to the simplicity of the equipment, operation and common reference libraries. However, it's LOD is 20µm (Vianello et al., 2019) which means missing the smaller fraction of particulates. There is also micro-FTIR or µ-FTIR which has been found to identify particles down to 11µm (Gillibert et al., 2019) but with less confidence (Zhang et al., 2020a).

2.3.3.5 Raman and µRaman Spectroscopy

Raman is an increasingly popular technique and operates in a similar way to FTIR but at a higher frequency. The infrared laser in the Raman excites the sample to release photons (Zhang et al., 2020a) which causes Raman scattering (Titus et al., 2019). These signals can then be compared to reference library to identify the types of polymers present in the sample (see **Figure 2.10**). Although it is more resource expensive than FTIR, it is more accessible to operate and reduces the LOD (Zhang et al., 2020a). Similar to FTIR, there is micro-Raman (µRaman) which in theory has a LOD as low as 1µm (Thermo Fisher Scientific, 2018) but in atmospheric MP research the smallest particle size reported to date is 2µm (Allen et al., 2019a; Wright et al., 2019). Another disadvantage to Raman is that some samples produce fluorescence when exited with the laser which can interfere with the Raman signal, while fluorescence is not an issue with FTIR. However, this can be prevented by choosing an appropriate laser wavelength. There are also less reference libraries for Raman spectrometry and it is more expensive than FTIR. That being said, it is preferable to observe particles below 20µm, which is important given that as particle size decreases, there is an increase in the number of particles (Morioka et al., 2023l; Zhang et al., 2020a; Isobe et al., 2015). Therefore, it is vital that the smaller fraction of MP size ranges be included in analysis for accurate reporting of atmospheric MP concentrations. Furthermore, Raman and FTIR have the option to include an automated particle finder which would make analysis less subject to human error, less time-consuming and more effective (Thermo Fisher Scientific, 2018). Another caveat to using techniques like Raman and FTIR is the effect of weathering on the identification of MP. When MP have been subject to weathering in the environment it can lead to changes in the peaks in the spectra (Fernández-González et al., 2021; Phan et al., 2022) which are usually used to characterise polymers by comparing them to reference libraries.

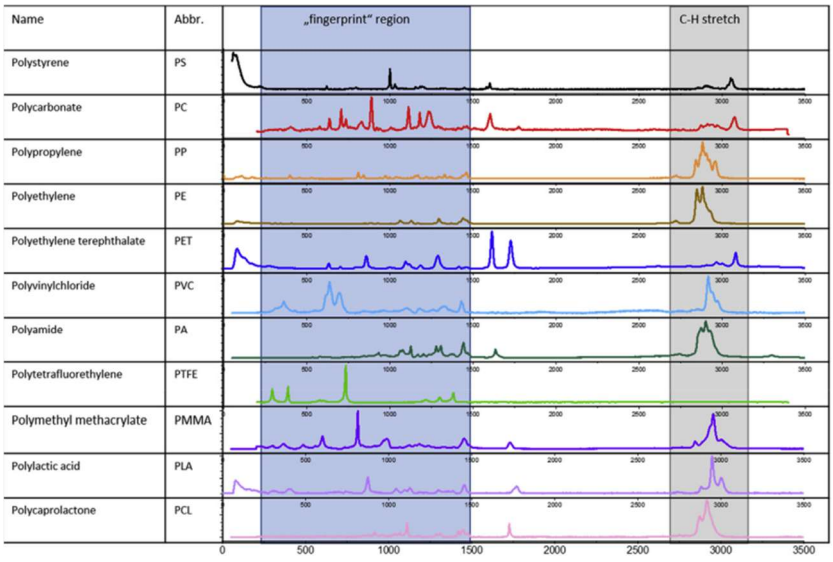


Figure 2. 10 Raman spectra used to identify polymer 'fingerprint' for common polymers including PS, PC, PP, PE, PET, PVC, PA, PTFE, PMMA, PLA *(Anger et al., 2018)*

2.3.3.6 Laser Direct Infrared Spectrometry

One method which is being reported more in the literature recently is Laser Direct Infrared Spectrometry, or LDIR. It utilises a laser which emits light in the mid- and far-infrared regions of the electromagnetic spectrum, called a 'quantum cascade laser' (Carruthers et al., 2022). It is said that this improves the speed and accuracy of identifying MPs (Luo et al., 2022; Dong et al., 2023). LDIR offers the opportunity to identify the polymers, count, size, aspect ratio, and circularity of MP particles with one method of analysis and it is possible to identity MP particles down to 10µm (Dong et al., 2023) (see **Figure 2.11**). However, it requires more pre-treatment of samples and it has been said that it is more susceptible to misidentifying particles compared to other methods (Tian et al., 2022).

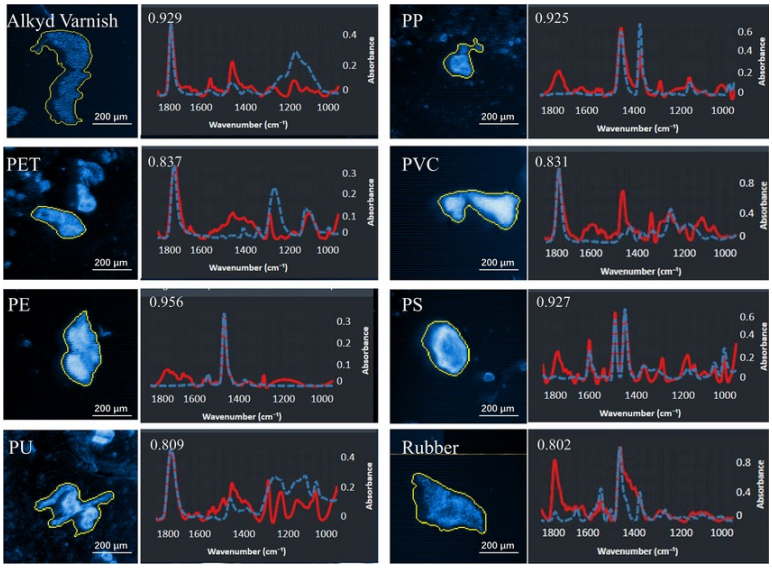


Figure 2. 11 LDIR chemical imaging and spectra of 8 polymers identified in Svalbard water samples including PE, PET, PE, PU, PP, PVC and PS *(Bao et al., 2021)*

2.3.3.7 Pyrolysis and Gas Chromatography

Another method is use of thermochemical techniques such as pyrolysis paired with gas chromatography and mass spectrometry (Py-/GC/MS). This is a relatively novel technique within atmospheric MP, with only a few studies to date using Py-GC/MS to analyse atmospheric samples (Fan et al., 2022; Mizguchi et al., 2023; Agullo et al., 2024; Gregoris et al., 2023), but it has been successfully used in other forms of MPs research (Okoffo et al., 2020; Okoffo et al., 2022; Picó & Barceló, 2020). Py/GC/MS involves heating the sample and using gas chromatography to separate the sample into its individual components before then using mass spectrometry to obtain the spectra of each component, which can be compared with a reference library to identify if polymers are present (Zhang et al., 2020a). With polymer characterisation certain indicator ions can be used to identify polymers (Picó & Barceló, 2020) (see **Figure 2.12**), but the calibration process and set-up can be complicated, and different factors can affect the identification of these ions (Torres-Agullo et al., 2024) which could subsequently result in an underestimation of particles. This method also produces a

mass concentration of particles, rather than giving information on individual particles, so it is not possible to gain information on colour or shape or particle numbers, which can make comparison with other studies difficult. This method is destructive as samples are burned, so it should be paired with another method that characterises the morphology of MP particles (Lee et al., 2023).

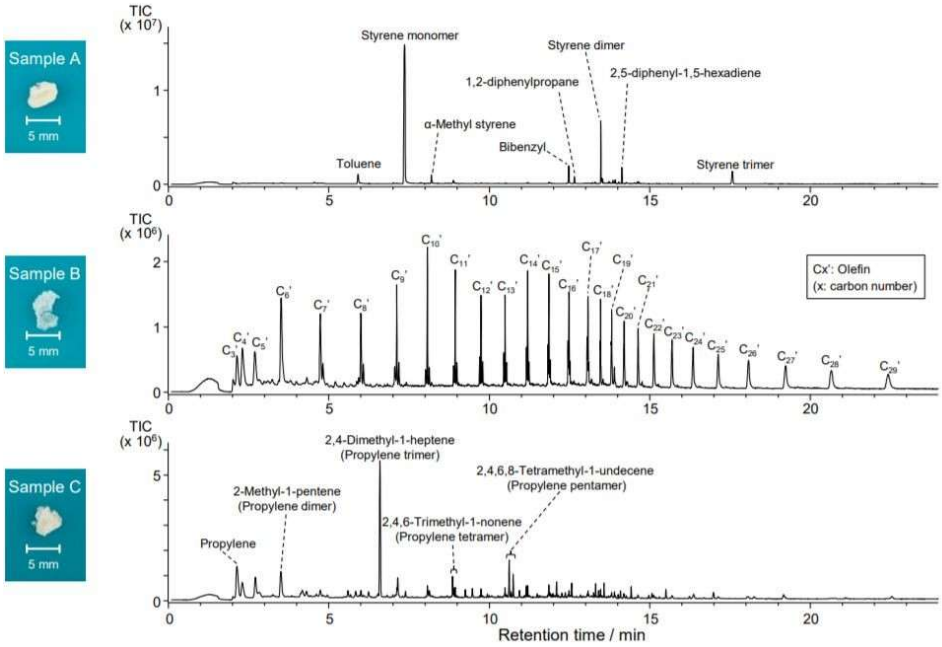


Figure 2. 12 Pyrolysis products (pyrograms) used to identify three polymers from surface water samples at Osaka Bay including, PS, PE, PP, using Py-GC-MS *(Frontier Laboratories Ltd., 2024)*

However, it can produce fast and reliable results, and the lack of pre-treatment (Lou et al., 2024a), can make it an attractive option for efficiency. Fan and colleagues (2022) was the first study to date that utilised Py-GC-MS for the analysis of atmospheric samples. After conducting deposition sampling in two locations in Auckland, New Zealand, the study used Py-GC-MS to analyse polymer composition, and Nile Red fluorescence to report particle size and shape. The study highlights the ability to study more particulates compared to other spectroscopic methods (Fan et al., 2022) as Py-

GC/MS can be automated and gives more rapid results. The study characterised 8 polymers, with PE, PC, and PET being the most commonly observed. Although some spectroscopic methods allow for the identification of a wider variety of polymers, this method was still effective given the difficulty of most methods to identify polymers efficiently. Furthermore, due to the use of complimentary methods, it is possible to gain information on particle shape, size and concentration, rather than just having a sole mass base concentration of polymers, which is usually presented with thermochemical methods. A study in Krakow, Poland, also used Py-GC/MS the same year to report concentrations of deposition samples (Jarosz et al., 2022). Again, the study used complimentary methods, in this case FTIR, and SEM-EDS, to allow for both the polymer composition, and shape and size of particles to be reported. From their methods they were able to identify six polymers (LDPE, Nylon, PE, PET, PP, PU), which is less than Fan and colleagues (2022), but they were able to use the other methods to identify other contaminations present on the MPs.

Gregoris and colleagues (2023) were able to identify three of the main polymers – PE, PP, PS; but also introduced an "aerosol organic baseline" (Gregoris et al., 2023: p.1), to estimate interference with polymer traces due to the organic matter present on samples. Mizuguchi and colleagues (2023), found that the identification of polymers was different based on the three size classifications used to collect deposition samples, and that by using a double shot method it was possible to detect phthalates from the samples (Mizuguchi et al., 2023). This method involves conducting two sets of gas chromatography (GC) analyses on one sample, and here it identified phthalates or 'plasticisers', which are the additives used to alter their behaviour – make them more flexible, durable, transparent – and have been linked to environmental and health concerns (Eales et al., 2022; Tuan Tran et al., 2022; see also **Chapter 2.4**). Another study used Py-GC/MS coupled with an Orbitrap-MS, which uses an ion trap mass analyser to separate ions and determine their mass to charge ratio (Hofman et al., 2020), for more accurate mass measurement of polymers for active samples from indoor air in Spain. The study developed and assessed the performance of the technique to identify 10 polymers - PMMA; nylon; PP; rubber; PVC; PET; acrylic;

PE; PC; PS - which is a larger variance in polymers than other studies to date. The study also reported that pyrolyzing conditions are crucial for getting a high response for the ions for each polymer and this will depend on the polymers and the matrix of the sample. It found that some polymers saturated at higher mass concentrations than others, which meant some polymers were not detected. They highlight that the choice of polymer standard can influence the indicator compounds during pyrolysis, the ramp temperature is also crucial for enhancing the sensitivity of the method for indicating polymers. Furthermore, that the presence of organic matter can influence the response of polymers (Torres-Agullo et al., 2024), which is contrary to previous studies which state there is no need for sample pre-treatment and organic removal. It can be said that Py-GC/MS offers a method for the fast characterisation of atmospheric MP samples and given that this equipment can be more accessible than spectroscopic methods, it can offer a more affordable and efficient method for polymer analysis. However, given the complexity of the set-up, and the intricacies of polymer ion identification, there are still some barriers to this method being accurately employed in the field. That being said, given the development in the past few years, it may be more commonplace in the field in years to come.

2.3.3.8 Thermal Desorption and Thermogrametric Analysis

There have been some advancements using thermal desorption and thermogrametric analysis (TGA) or TDS-GC/MS, could allow for smaller particles to be identified (Zhang et al., 2020a). One method that has been used more recently in the literature is TD-PTR-MS (Thermal Desorption-Proton Transfer Reaction Mass Spectrometry), which is based on the concept that different polymer types will have different melting points, and they will release volatile organic compounds (VOCs) when they are heated, and the signal from the VOCs can be used to indicate polymer type. By gradually increasing the temperature (in comparison to Py-GC/MS which involves a faster temperature ramp (Materic et al., 2020), and combining this with PTR-MS, it is possible to characterise atmospheric MP samples and provide a mass-based

concentration. This again relies on the indicator ions associated with the thermal products of polymers, but it is also a highly sensitive and challenging method (Materic et al., 2022a), which means its use is not widespread in the field to date.

However, it has been successfully applied to alpine snow to quantify MPs and nanoplastics (NP), down to the LOD of <1ng, which is reportedly 100 times more sensitive than other spectroscopic measures (Materic et al., 2020). By developing an algorithm to account for sensitivities in the system to organic material, the processing steps were reduced, and it was possible to identify eight common polymers from the remote location – PET, PVC, PC, HDPE, LDPE, PP, PS, PPC (Materic et al., 2020; see **Figure 2.13**). The same team also applied these techniques to samples from Sonnblick Observatory in Austria, where 6 polymers were identified, including tire wear particles, which cannot be identified with spectroscopic methods due to their inability to reflect light (Baensch-Baltruschat et al., 2020). The study found NP and MP concentrations in the region to be comparable to similar data at an urban location, highlighting the importance of studying the ultrafine fraction of MPs. TD-PTR-MS has also been applied to seawater samples (Materic et al., 2022b), indicating that this method could be applied in different matrixes, and might be more widely employed in the field as the method develops.

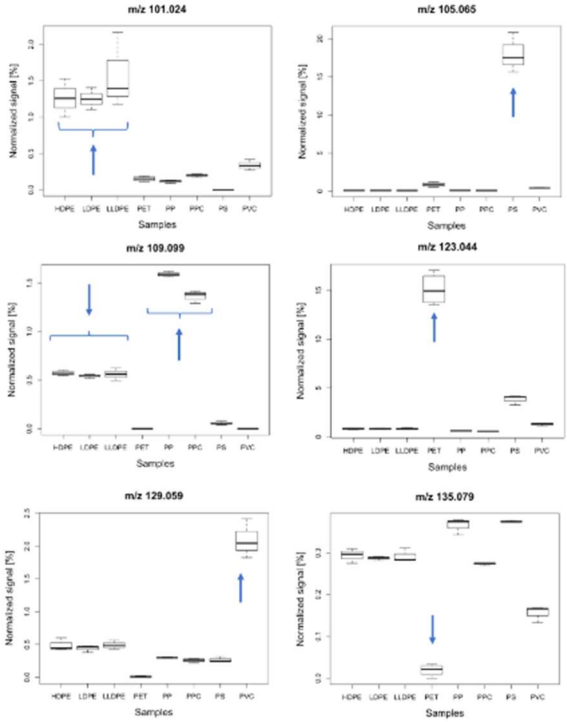


Figure 1. Example of ions obtained by the analysis of the pure polymer, which can be used to identify and distinguish the different types of plastics. HDPE, high-density polyethylene; LDPE, low-density polyethylene; LLDPE, linear low-density polyethylene; PET, polyethylene terephthalate; PP, polypropylene; PPC, polypropylene carbonate; PS, polystyrene; and PVC, polyvinyl chloride. The signal is normalized to the total concentration of all the ions. The arrows are added to highlight the differences between plastic types.

Figure 2. 13 Figure from Materic et al., (2020) displaying indicator ions to identify common polymer types using TD-PTR-MS for the first time including HDPE, LDPE, PET, PP, PPC, PS, and PVC (Materic et al., 2020)

2.3.3.9 Nile Red Staining and Fluorescence Microscopy

Another method used frequently in microplastics research is Nile Red and fluorescence microscopy. It is often used as it is less demanding in terms of equipment and cost compared to FTIR and Raman. Nile Red is a fluorescent dye which is added to samples to stain microplastics due to its hydrophobic properties (Shim et al., 2016). This dye causes plastic particles to fluoresce under specific wavelengths of light (see **Figure 2.14**) and with the assistance of a microscope it is possible to identify plastic particles down to a few micrometres in size (Maes et al., 2017). Alongside imaging software, it is possible to take the images captured and count the plastic particulates present in the sample and gain information on particle morphology (Maes et al., 2017). In theory, other particles in the sample such as other organic or inorganic particulates, should not

fluoresce to the same extent as plastic particles (Tamminga, Hengstmann & Fischer, 2017). Although it has been widely used in numerous atmospheric MP studies (Luo et al., 2024b; Yadav, Sethulekshmi and Shrivastav (2022); Liao et al., 2021) there are still some uncertainties in using method. Stanton et al. (2019), reported large over-estimations of MP particle counts by using Nile Red due to its ability to stain other organic and inorganic particles. The study discourages the use of this method on its own for MP analysis and particle counts (Stanton et al., 2017) due to the potential for Nile Red dye to stain organics and over-estimate MP particle counts. Nile Red also cannot accurately distinguish between polymer types (Prata et al., 2023). Although efforts have been made to identify the fluorescence thresholds for different polymers (Nel et al., 2021). It should also be noted that tyre wear particles do not fluoresce (Sturm et al., 2023a), therefore their presence is often underreported if this technique is used.

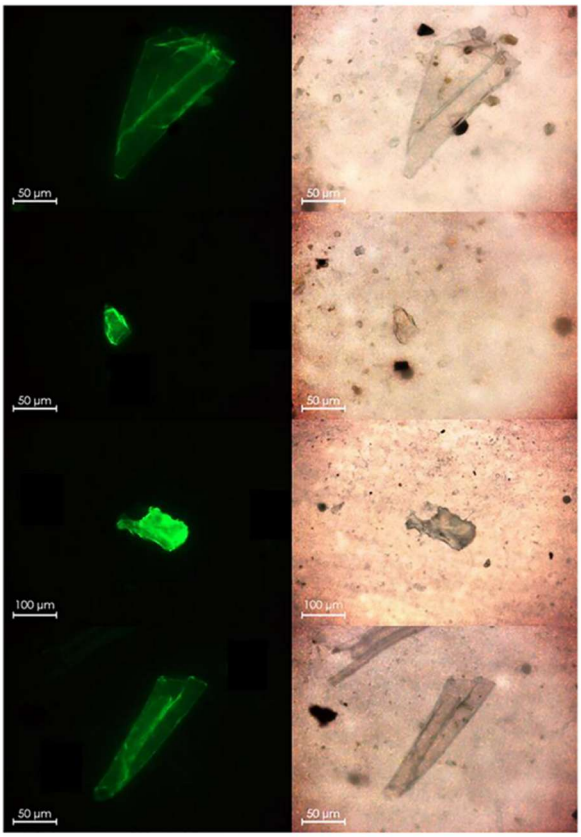


Figure 2. 14 Figure from Iannilli et al. (2020) showing MP particles fluorescing green with the assistance of Nile Red dye, with normal microscopic images for comparison, from freshwaters samples taken in Italy (<50µm) *(Iannilli et al. 2020)*

However, there is still room for Nile Red in microplastics research. It can be an effective method to confirm particle counts after the use of µFTIR or µRaman and remove the possibility of human bias with these methods (Shim et al., 2016). It was previously thought that Nile Red staining could interfere with spectroscopic methods such as FTIR and Raman, but recent research suggests this can be avoided by using lower concentrations of the dye (Maes et al., 2017). Furthermore, given its low cost and ability to examine a larger number of particles in a more time-efficient manner (Sturm et al., 2023b; Süssmann et al., 2024; Ho et al., 2024), it is an effective method for the identification of microplastics, in conjunction with another complimentary method of analysis, such as Raman, FTIR, or Py-GC/MS. This allows for a larger number of samples to be processed and both polymer characterisation, and particle morphology and concentration to be identified.

2.3.4 Contamination Protocols QA/CC – Minimising the Inevitable

When processing MP samples from all environmental matrices, there is a chance of contamination of MP from outwith the sample. This may take the form of MP on researchers' clothing, from laboratory materials or laboratory environments during sample processing, or from equipment. To minimise the risk or contamination or rule out any potential interference with results on polymer type, and particle concentrations and morphology, there are a number of steps that can be taken. Firstly, equipment used to collect or store samples can be cleaned and, in some cases, heat treated to destroy any contamination from manufacturing or storage. This is normally carried out by heating the material to ~400^{o}C for a set period of time to destroy any polymers present. To clean equipment, studies normally triple rinse with milli-Q purified water and in some cases ethanol. Another big step to minimising contamination is to reduce the possibility of MP from clothing coming into contact with the sample, so cotton lab-coats and natural fibre clothing is recommended (Prata et al., 2021). Some researchers will be able to keep clean rooms where plastic products, clothing, and outside contamination can be controlled. Studies should also carry out laboratory and/or procedural blanks to account for extra MP contamination from sample processing and analysis (Munno et al., 2023), and blanks are then analysed in the same manner as the samples. Procedural blanks can be taken during each step in sample processing to account for contamination during each stage of the characterisation process. The resulting MP characterisation data is subtracted from results to account for this, which means that particles are not overestimated or falsely reported.

2.4 How bad is it? – Environmental and Human Health Risks

2.4.1 Interaction with biota and ecosystems and implications for climate change

MPs have become a significant environmental concern due to their widespread occurrence and their impact on our ecosystems. They have been reported throughout the food chain (Pironti et al., 2021) and have detrimental effects on food webs. Due to

their small size they can easily be ingested by marine organisms and transferred throughout the food chain (Smith et al., 2018). Once ingested they can cause choking, digestive issues, starvation and have been reported as endocrine disruptors (Akdogan and Guven, 2019). MP ingestion is also thought to cause oxidative stress in cells, leading to cell damage and reduced cell growth. It is also reported to hinder neurological function and interfere with immune response in organisms (Mao et al., 2022). In marine ecosystems where they were first reported they can interact with other persistent organic pollutants (POPs) and increase the toxicity of the pollutants to organisms (Ali et al., 2024). In terrestrial systems, MPs have also been reported as vectors for other soil contaminants leading to co-toxicity. When present in soil they can change the structure of the soil and its ability to hold water; as well as affecting the soil's microbial properties which can disrupt the soil habitat (Zeb et al., 2024). Remote environments are more at risk to MP pollution due to the unique environmental characteristics and evolution (Horton and Barnes, 2020), which highlights the need for more research into MP occurrence in remote regions. Furthermore, the research on the impact of the chemicals used to alter the physical properties of plastics – phthalates or plasticisers – is also increasing. This has been linked to endocrine disruption, hormone disruption, and genetic changes in organisms (Net et al., 2024). The consequential effects this could have on biodiversity loss could be detrimental (de Souza Machado et al., 2018). The research on the implications of MP on ecosystems is vast and growing (Roy et al., 2022), and it is evident that there is a demand for research to understand accurate levels of MP concentrations across the globe, as this will indicate the level of risk to our ecosystem health and function. This thesis aims to contribute to the knowledge on the presence and extent of MP pollution in remote and urban regions.

It has also been reported that MP occurrence in our environmental matrices has implications for climate change. In marine systems, MP pollution has harmful effects on gas exchange and marine carbon cycling, leading to increased greenhouse gas (GHG) emissions from ocean environments (Li et al., 2024). In the cryosphere, it has been reported that MP contamination on ice caps could absorb light and accelerate the melting of polar ice (Revell et al., 2021). It has also thought to cause radiative effects

in the atmosphere by absorbing infrared radiation, which can contribute to greenhouse warming (Revell et al., 2021). Another study reported that MP could impact cloud formation processes, which could in turn, impact the Earth's radiation balance and climate (Aeschlimann et al., 2022). In the terrestrial environment, MP pollution in soil has been linked to increase in CO_2 emissions, causing changes in soil microbiome and carbon fluxes, and influencing climate feedbacks (Zhao et al., 2024). Given the nature of plastics being derived from fossil fuels, both their production and degradation is contributing to GHG emissions (Sharma et al., 2023) in an already fragile climate. It is estimated that by 2025 GHG emissions from plastic production, use and disposal will account for 15% of global emissions, which is under the current goal of limiting global warming to 1.5^{o}C (UNEP, 2021)

It is evident that not only is MP pollution affecting biodiversity and ecosystem function, it is also negatively impacting overall climate health. If the world is to meet the current Paris Agreement 2050 targets, and prevent potentially irreversible damage to our natural environment, MP pollution appears to be a pressing issue at the centre. By examining the extent of atmospheric MP pollution in remote and urban environments and examining the most effective way to measure this pollutant, it is hoped that this thesis can contribute to the field of MPs, and improve the understanding on the risk this pollutant poses.

2.4.3 Microplastics and Human Health

MPs have been increasingly reported in the human body, most recently in human lung tissue (Jenner et al., 2022), emphasising the importance of understanding more about this inhalable pollutant. It has also been reported in the placenta (Regusa et al., 2021), blood stream (Liddle et al., 2021), and it is a known threat to human health (Chen et al., 2020). Improved knowledge of MPs is important in relation to the wealth of research on the impact of air pollution on human health. It is a well-established public health threat with implications to respiratory health, cardiovascular health and beyond (Eljarrat et al., 2020). Although the relationship between air pollution and ill-health

has been established, researching the impact of this in isolation of other public health factors, is difficult (European Environment Agency, 2018). Correlations and relationships are made through long-term epidemiological studies and factors such as environment, lifestyle and occupation can be adjusted for but establishing strong links is complex. As a result of this air pollution can often be overlooked by the general public when discussing health. However, in 2020 air pollution was linked as a cause of death for the first time in the UK (PA Media, 2020) which emphasises the importance of understanding the impact of manmade activities to our surrounding environment and the human health impact for those who occupy those spaces.

Similar to traditional air pollutants, it is thought that atmospheric MP inhalation could cause respiratory and cardiovascular complications and possibly beyond (Prata, 2018). This is especially of concern for particles <10µm which due to their small size, which can be inhaled deep into the respiratory system and have the potential to pass through cell walls and travel further into the body (Wright and Kelly, 2017). Particles above 100µm are not usually of concern as they are not typically inhaled (US Environmental Protection Agency, 2011). Particles below 2.5µm and fibres, however, are of most concern due to their potential to cause damage to the gastrointestinal tract. It is thought that the inhalation of MP can cause oxidative stress (Wright and Kelly, 2017), dyspnoea (shortness of breath) and inflammation of the airway and lung tissue (Prata, 2018). Pauly et al., (1998) reported the presence of MP in human lung tissue, but it has been a considerable amount of time since this study was published (Pauly et al., 1998). As there has been an increase in plastic production and a shift in the polymer types and additives used (Geyer, 2020) in the past 20 years, a more recent study on microplastics in lung tissue is warranted. Studies have identified a possible link between inhalation of MP and interstitial lung disease (causes coughing, dyspnoea (shortness of breath) and reduced lung function (Wright and Kelly, 2017)) but further research is needed to identify the processes that cause this (Amato-Lourenço et al., 2020).

Within human health research it has been assumed environmental concentrations of atmospheric MPs are low (Prata, 2018). However, as discussed earlier, lower detection limits vary, therefore it is likely that concentrations have been underestimated. To date there have been no studies on the retention time of MP in the human body. Research has identified MP in human stool (Hartmann et al., 2024), urine (Pironti et al., 2022), and human tissue (Enyoh et al., 2023), suggesting intake, transport, and excretion mechanisms. However, a recently published article challenged the limited contamination controls in MP human exposure studies and lack of validation steps which could influence the accuracy of reported concentrations (Monikh et al., 2025). Therefore, there are still methodological challenges and gaps in empirical data when it comes to human MP exposure research.

There has been research on occupational exposure, as some jobs will cause individuals to be exposed to higher concentrations of MPs. Studies have been conducted on workers within the textile industry, the flock industry (compacting small fibres to produce fleece or velvet fabrics), and plastic production (Prata, 2018). Occupational studies such as Pimental et al., 1975, found that the risk of respiratory symptoms increased more than three-fold in flock workers working with polypropylene, compared to controls. They also conducted lung biopsies from workers exposed to synthetic fibres such as acrylic, polyester and nylons. They found varying degrees of inflammation, granulomas and interstitial fibrosis (Pimental et al., 1975, in: Amato-Lourenço et al., 2020). Despite the age of the initial study, it is consistent with recent literature (Prata, 2018; Wright and Kelly, 2017) and highlights the danger of increased exposure to inhalable MP particles.

Given that MPs are ubiquitous in the environment there are multiple exposure pathways for humans and animals (Deng et al., 2017). In humans the ingestion of MPs is also thought to cause numerous short-term and long-term effects. MP can be ingested via seafood, salt, bottled water and sugar to name a few (Karbalaei et al., 2018). These effects have been summarised by Karbalei et al., 2018 and Akanyange et al., 2021 in

Figure 2.15 and the potential effects range from respiratory stress, to cancer and obesity.

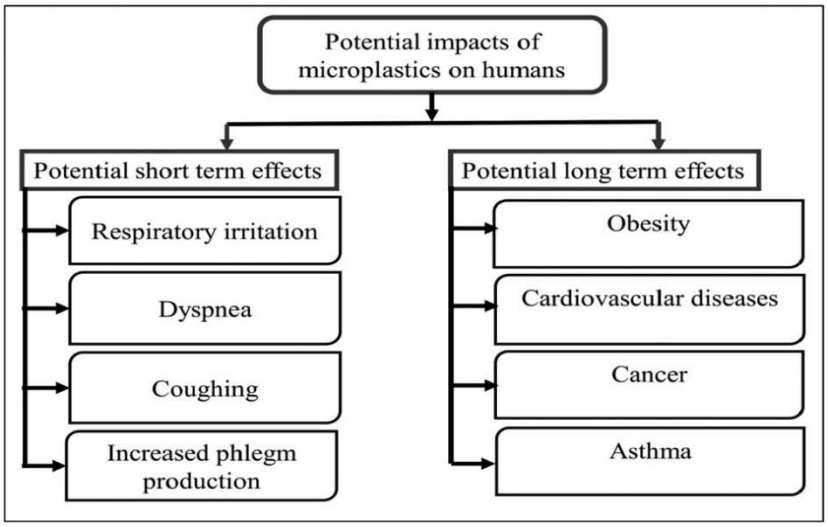


Figure 2. 15 Short-term and long-term health effects of MP on humans *(Adapted by Akanyange et al., 2021from, Karbalei et al., 2018)*

Senathirajah et al. (2021) estimated the mass of MPs ingested by the global population. They summarised data from available publications and found that on average humans may ingest 0.1-5g of MP weekly through exposure from drinking water, salt, beer and shellfish. This may vary depending on individual age, size, cultural heritage and demographics (Senathirajah et al. 2021). Although such an estimation has not been previously attempted and this study provides an initial assessment of knowledge in MP ingestion in humans, there were some assumptions made about MP pollution that are not environmentally representative or have been disputed in other studies. For example, the paper assumed that all MP are within the 0-1mm size range and are all spherical in shape which is known not to be the case (see **Chapter 2.3**). Also, the study did not include MP ingestion from fish as the MP would be removed during food preparation (e.g. removing the intestinal systems that contain the MP). However, a study performed on seabass, a commonly consumed fish, found that MP translocation from the gut to other parts of the fish was possible via the intestinal tract (Zeytin et al.,

2020). Therefore, it is possible that this could be an under-estimation of global average intake.

It is common to use pristine MP in exposure studies (Paul-Pont et al., 2018). Although it is useful to be sure of the polymer type when studying exposure, this is not an accurate representation of environmental MP exposure. MP will be exposed to mechanical abrasion, UV degradation changing their surface area which result in the sorption of other additives (Santos et al., 2021). The sorption of organic or inorganic compounds from the environment on to the MP, could cause further health implications (Wang et al., 2020). For example, the weathering and aging process have been found to encourage the sorption of pharmaceuticals to MP (Santos et al., 2021). Furthermore, additives such as phthalates or 'plasticisers' used in the production of plastic products have been found to have long-term human and environmental health implications (Gustafsson et al., 2020). For example, endocrine disruption, obesity and diabetes (Benjamin et al., 2017). Another group of additives called 'PFAS' (poly-fluorinated alkyl substances) or 'forever chemicals' due to their persistence in the environment (Fidra, 2021), have also been found to disrupt hormone production and have been found to affect endocrine function, and low birth weight (Eales et al., 2022).In addition to this, the concentrations in exposure studies are unlikely to be representative of realistic current environmental exposure (Paul-Pont et al., 2018). More research is needed to understand the realistic implications of MP exposure under realistic conditions and with the added risk of exposure to other organic and inorganic additives.

There is also little information about the presence of these plastic additives in relation to atmospheric MP concentrations. Conventional sample analysis methods such as FTIR and Raman can measure the size, shape and colour of MP but cannot tell us more about the additives present. Although it is not the focus of this thesis, in future research there is scope for the use of a technique such as Py/GC/MS to measure the presence of additional harmful

2.5 Plastic Pollution Mitigation and Policy Implications

2.5.1 Current policies to reduce microplastic pollution

As discussed previously, the dangers of plastic pollution are well established, so there have been efforts on many levels to introduce policies to try and reduce plastic pollution, with varying degrees of success. On the international level, in 2022 the UN 'Global Plastic Treaty' resolution was adopted into the UN Environment Assembly. This is the first legally binding treaty of its kind on plastic pollution which includes the marine environment (Ellen Macarthur Foundation, 2024). This document aims to address the whole life cycle of plastic, from production to disposal, and the goal is to reduce plastic production by 80% by 2040 through the circular economy approach (UNEP, 2024). This includes a ban of single-use plastics, promoting the reuse of plastic products, and improving recycling infrastructure (UNEP, 2022).

Circular economy (CE) frameworks tend to be the main mechanisms employed to help reduce plastic emissions (Ellen Macarthur Foundation, 2024). CE models involve extending the life cycle of materials and products by keeping them in the loop of production and consumption via processes such as reusing, repairing and eventually recycling (European Parliament, 2023; see also **Figure 2.16**). In the context of plastic pollution, this would mean moving away from the linear or linear+ systems currently in place whereby plastic is produced used and recycled or wasted, to a system which allow plastic to remain within our economy for longer. CE adoption would mean more reusable plastic items and systems and developing better collection and recycling infrastructure (Ellen Macarthur Foundation, 2025).

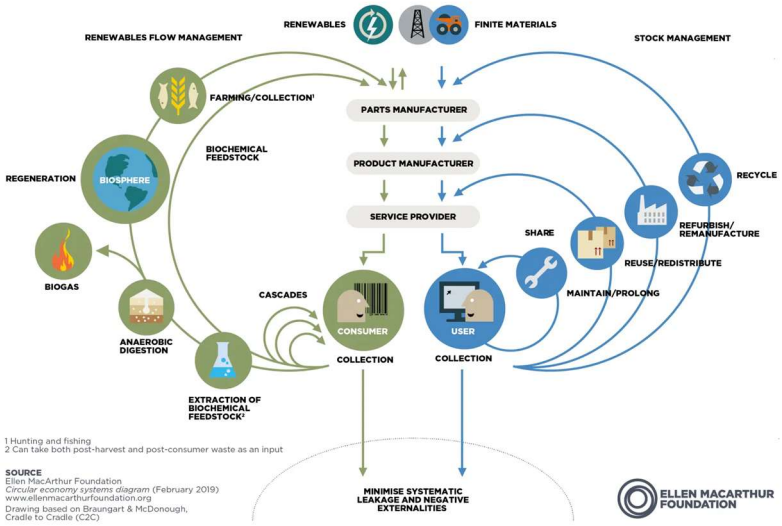


Figure 2. 16 Butterfly diagram showing Circular Economy Model *(Ellen Macarthur Foundation. 2023)*

The United Nations Environment Programme (UNEP) talks in April of 2024, held in Ottawa Canada, aimed to get as close as possible to the final text of the plastics treaty (UNEP, 2024). However, it is considered by some as a "failure" (Speed, 2024) and contains many contradictions and conflicting views. For example, the treaty aims to be as fair as possible considering the imbalances between developing and developed countries regarding their production, use, and waste management. This is due to the fact that developing countries produce the least amount of plastic waste but feel the impacts of plastic pollution disproportionally to developed countries. States that produce more fossil-fuels, and therefore make more money from plastic production, appear to be resistant to measures to limit the production of virgin plastic, and focus on circularity measures (Speed, 2024). This is related to the ongoing issue in plastics policy that virgin plastic is more profitable and cheaper to produce (House of Commons, 2022), which reduces the incentive for states to increase recycling and limit plastic production. The final stages of this treaty took place at the end of 2024 in Busan, in the Republic of Korea (UNEP, 2024), and concluded without a legally binding agreement to combat plastic pollution (European Commission, 2024) and the rescheduled talks in Geneva, Switzerland in 2025 also failed to reach an agreement.

This is due to the decisive issues surrounding whether the focus should be on producer responsibility for managing plastic pollution and the costs involved with pollution remediation (Stallard and Poynting, 2025). Due to the transboundary nature of plastic pollution, it requires a collective global effort to limit plastic production, manage waste effectively and prevent further environmental pollution.

On a European level the European Union (EU) and the European Commission have addressed measures to address plastic pollution. For example, the 'EU Directive on single-use plastics' which aims to tackle 10 of the most commonly used items such as plastic bags, cigarette butts, and cotton buds to name a few. These products are to be limited and if sustainable and affordable alternatives are available the items are not to be placed on the market of member states (European Commission, 2023). Furthermore, under the REACH Regulations (the Regulation on the registration, evaluation, authorisation, and restriction of chemicals) bans the use of intentionally-added MPs, such as those used in cosmetics (European Commission, 2023). The EU has also announced plans to move towards a Circular Economy and as part of that has included measures to address plastic pollution, a summary can be found in **Box 2.1**.

Box 2.1 Summary of Initiatives that are included in the EU's Circular Economy Plan that address plastic pollution *(European Commission, 2020)*

European Commission – '*A new Circular Economy Action Plan For a cleaner and more competitive Europe*' (2020)
EU Strategy for Plastics in the Circular Economy

- Set of initiatives to address plastic consumption, the sustainability challenge's posed by plastic and to tackle plastic pollution
- To increase plastic recycling and more sustainable use of plastic, EU Commission has proposed a set of **mandatory requirements for recycled content and waste reduction** measures for key issues such as packaging, construction materials and vehicles
- There is the inclusion of measures to address presence of MP in environment including
    - restriction of **intentionally added** MP (e.g. cosmetics)and tackling pre-production plastic pellets (nurdles)
    - developing "**labelling, standardisation**, certification and regulatory measures on unintentional release of microplastics in, including measures to increase capture of microplastics at all relevant stages of products' lifecycle" (p.10)
    - "further **developing and harmonising methods for measuring** unintentionally released MPs, especially from tyres and textiles and delivering harmonised data on microplastics concentrations in seawater"
    - Close the scientific gaps in relation to risk and occurrence of MP in the environment
- Aims to address emerging sustainability challenges to plastic by using **"bio-based plastics"** and **"biodegradable or compostable plastics**" (p.10)
- Also includes implementation of Directive **Single Use Plastic Products** and fishing gear to address marine plastic pollution

Textiles

- Proposes a **"comprehensive EU Strategy for Textiles"** – set of measures including:
    - Empowering businesses to choose more "**eco-design measures"**, to make sure textile production is more circular
    - Incentives for sustainable and circular materials and production processes
    - "boosting the sorting, re-use and recycling of textiles" (p.11)

It can be observed from the box that there are a few measures that are the focus of policy, including waste reduction and the increase of recycling. However, it should also be noted that there is a focus on harmonising, and standardising methods of measurement included in the policy wording. As highlighted previously in this review, this is a key theme in MPs research and the inclusion of this in policy shows how important it is to develop and standardise MP measurement. It should also be noted that there is a focus on bio-based, bio-degradable, and compostable plastics. This is controversial as it has been reported that compostable and bio-degradable plastics can actually be more toxic than conventional plastics due the chemicals needed to make

natural plastics durable (Zimmerman et al., 2020). It has also been reported that bio/bio-degradable/compostable plastics come with their own associated waste management issues and do not encourage other pro-environmental behaviours needed to reduce overall waste (MacDonald et al., 2021). Due to the harm already posed to the environment from plastics, policy should focus on the reduction of all plastic products, not just conventional plastics.

On a national level, in the UK intentionally added MPs in cosmetics were banned in 2017 (BBC, 2016), and in 2021 a plastic packaging tax was introduced (HM Revenue & Customs, 2021). In Scotland, a deposit return scheme to increase recycling and reduce plastic waste, which has been hugely successful in Mexico (Kutralam-Muniasamy et al., 2023) and Germany (Hailstone, 2022), was met with controversy due to potential impacts to small businesses and was due to be rolled out in 2025 (Watson, 2023), but has now been delayed until 2027 (Comerford, 2024). This highlights the contention which is often associated with plastic pollution. India brought in a ban on single-use plastics in 2022, and banned items such as straws, cutlery, and certain packaging, but this has had varying degrees of success, with implementation and enforcement differing across the country, and adverse socio-economic and environmental impacts reported (Nøklebye et al., 2023). France has committed to reducing microfibre pollution from clothing and clothes washing coming into force in 2025 (Hailstone, 2022) and have also introduced an anti-waste law to mandate reusable containers in supermarkets, and banning SUPs (European Union, 2020). Despite EU attempts at introducing legislation on plastic pollution, some countries felt this was not far enough and in April 2023 Germany, the Netherlands, France, Denmark, Luxembourg and Germany signed a joint paper to call for EU measures that go beyond voluntary actions. This paper also calls for a more a more uniform system for the monitoring of MP in air water and soil (Abnett, 2023), reflecting the sentiments of EU policy and the MP discipline itself. By evaluating the efficient measurement of atmospheric MPs, and the global extent of this pollutant, it is hoped this thesis can contribute to scientific knowledge which can, in turn, inform more effective policies to target plastic pollution.

2.5.2 Systemic and Individual Level Approaches – Behaviour Change

So far it can be noted that there have been attempts on an international and national systemic level to curb plastic pollution, but it can also be argued that plastic pollution is inherently tied up in human behaviour, especially in relation to its use and disposal. The current state of science on individual behaviour change and plastic use is limited, and it can be argued that understanding the behavioural elements of plastic use could identify key changes in guidance and policy to target behaviours related to plastic pollution. See **Appendix III** for a systematic literature review which highlights the need for more research into understanding individual motivation for plastic use in relation to behavioural psychology, and the need for policy that takes behavioural motivations into consideration.

2.6 Gaps in Knowledge and Research - Critical gaps in understanding and key issues for development of the field – method development, accessibility, and awareness

This chapter has covered the main topics associated with atmospheric MPs from their definition, origin, transport and analysis. Although the research has grown on MPs since they were first reported in the marine environment in 2004, there are still some considerable gaps in knowledge and some key themes that are associated with the research. In relation to atmospheric MP transport, there are still large unknowns when it comes to how particles behave in the atmosphere, their source appointment beyond particle modelling, and how these particles interact with meteorological variables. This is related to the 'Plastic Cycle' and how particles move between environmental compartments, and how little is known about what role atmospheric transport plays in this. Although there has been progress on examining waves as a method of marine MP transport into the atmosphere, there are still unknowns on how this pollutant interacts with each environmental compartment and how it is transported from one to another. Furthermore, once this pollutant is present in the environment, its true impacts are not fully known. Toxicity studies are often carried

out on pristine MP (Paul-Pont et al., 2018), rather than environmentally relevant ones therefore the interaction with additives and other environmental pollutants is unclear. Although it is useful to be sure of the polymer type when studying exposure, this is not accurate of environmental exposure. MPs will be exposed to mechanical abrasion, UV degradation changing their surface area which can mean it is more susceptible to the sorption of other additives (Santos et al., 2021). The sorption of organic or inorganic compounds from the environment on to the MP, could cause further health implications (Wang et al., 2020). For example, the weathering and aging processes have been found to encourage the sorption of pharmaceuticals to MP (Santos et al., 2021). It is also not known what is the safe limit for exposure to MP for both ecosystems and humans is, given the difficulty analysing MP and understanding their physiological impacts. Furthermore, the research on the relationship between MP and our overall climate health is still in the early stages.

Another consistent theme in the literature is the lack of harmony with the methods used to sample, and analyse MP particles. This is often due to the availability and accessibility of equipment as analysing MP samples is time and resource intensive. That being said, there is no technical guidance on the correct methods to use for each type of sample collected (active/passive), taking into consideration the research question and environment, and any information on margins for error when it comes to using different equipment or parameters. This can all affect the output of results especially in relation to reporting the smaller size fraction (<20µm), as mentioned previously, this can lead to under-reporting of concentrations. It has also been discussed that there is no standardisation when it comes to the reporting MP concentrations in the literature. This also makes comparison between different studies, and different countries difficult. This results in a poor understanding of regional variances of this pollutant and overall global burden. This thesis aims to add to the discussion of effective atmospheric MP sampling by comparing different parameters used while conducting active sampling and making recommendations for future research and policy. Furthermore, by using the same consistent methodology in both an urban, and a remote location, it is hoped that this thesis can make

comparisons between regions and environment more accurately. This can give an indication to how this pollutant differs regionally, and by utilising atmospheric MP modelling hint to transport of this pollutant globally. In **Appendix II** there is research that was conducted alongside this thesis which compares analytical methods of identifying atmospheric MP to add to the discussion surrounding the standardisation of methods.

It appears that although policy appears to have a circular economy approach, there is still the inclusion of 'bioplastics' and a focus on recycling. Our waste management practices do need attention, and plastic will always have a use in our society, especially in medical and food safety terms, however, both systemic and individual level behavioural change is needed to tackle this issue. In order for the system to be circular, waste needs to be avoided and reduced from the outset. Plastic alternatives that claim to be biodegradable or compostable, have been problematic in terms of waste management and can be more toxic than traditional plastics. More research and resources are needed to investigate materials that can provide the same benefits of plastic in terms of durability and anti-microbial properties, but without the toxicity that is associated with plastic of all forms to date. Furthermore, the policy attention should be focused on making waste and plastic reduction the most convenient option for industry and the individual (see **Appendix III**). Without considerable attention on the way in which our society uses plastic and manages it, it is unlikely the targets set out by the UN, EU, or individual states, will be met. As research on this topic grows and improves, the true extent of this pollutant and its impacts will become more tangible, and policy will be able to keep up with these developments.

Chapter 3. General Overview of Methods

The previous literature review chapter gave a brief summary of the various methods used in the field of atmospheric MPs to sample and characterise environmental samples. This chapter will provide an overview of the specific methods used in this thesis to report on environmental concentrations of atmospheric MP in remote and urban locations. This includes a section covering the contamination protocols used to minimise MP contamination during the sampling and analysis process and how this contamination is accounted for. **Appendix II** contains a draft of a peer-reviewed paper comparing the various analytical methods used to analyse MP, which the author co-wrote alongside this thesis.

3.1 Methods used to Sample Atmospheric Microplastics

The two main methods for the collection of atmospheric MP samples are active and passive. This section will cover the specific techniques used within this thesis to collect these types of samples.

3.1.1 Active Sampling Techniques

The simplest method for collecting active samples to measure suspended particulates is a direct air filtration system. This consists of using a calibrated pump to draw a known volume of air into a chamber, where particulates are collected on a filter. This filter is later removed for future analysis. This can be repeated, using sterilized new filters replaced in the filter holder at set intervals (Enyoh et al., 2019) (see **Figure 3.1**).

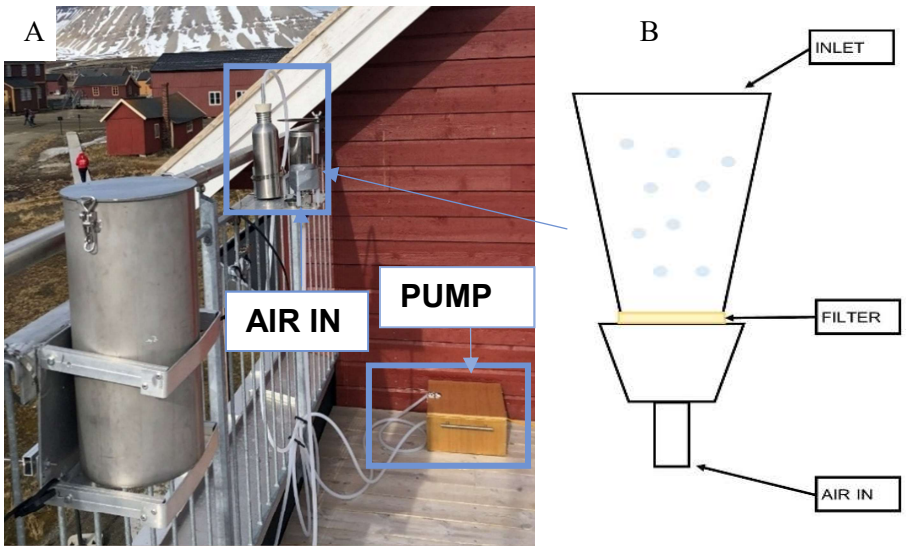


Figure 3. 1 (A)Image of Direct Air Filtration System as set up in the field (Svalbard, Norway); 3.1(B) Diagram of Direct Air Filtration Sampling System (Active Sampling)

A second technique used in this thesis is a novel technique that is still in development. This technique, termed the 'nanotank', also uses a pump to draw air into a chamber, but in this case the particulates are collected in milli-Q water within the sealed chamber (see **Figure 3.2**) attempting to prevent particles being re-entrained during sample collection. The liquid is removed and later vacuum filtered on to a filter (see **Chapter 3.1.3**) for analysis following the same processes as the air filter method.

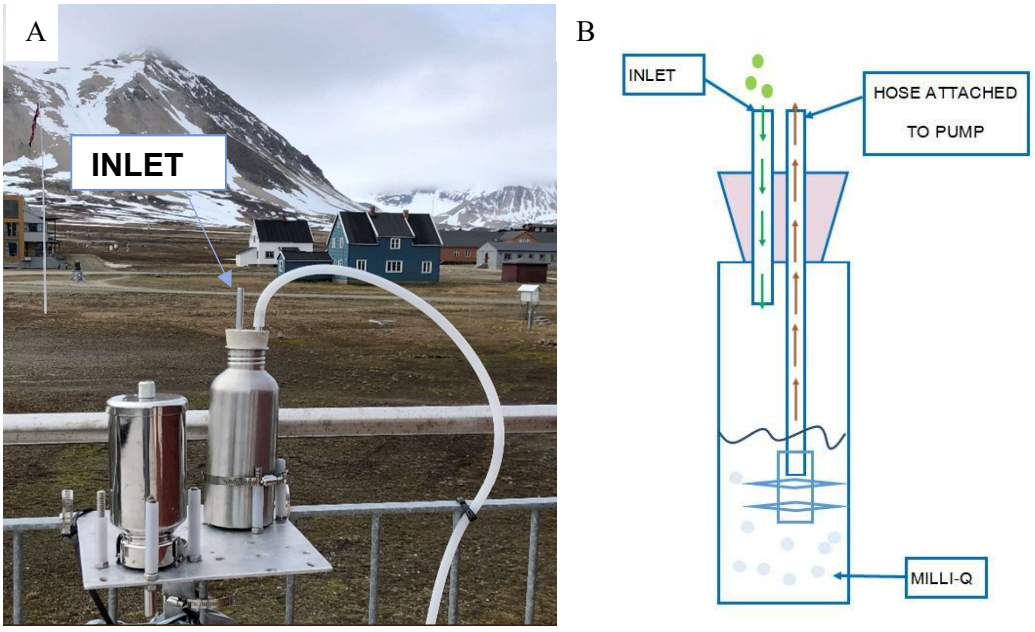


Figure 3. 2 (A) Image of Nanotank System in the field (Svalbard, Norway); 3.2B) Diagram of Nanotank Sampling System (Active Sampling; the orange arrows indicate air being drawn throw the chamber assisted by the pump and the green arrows indicate the movement of air into the chamber with the collected particulates

Both of these techniques were used to examine active air sampling efficiencies and examine atmospheric MP pollution in the Arctic and Glasgow.

3.1.1 Passive Sampling Techniques

Passive or deposition sampling collects deposited atmospheric particulates via deposition, and involves using a container which is left open in the environment (see Chapter 2). In this thesis, a stainless-steel chamber (a NILU deposition collector, 200mm diameter, height 400mm; NILU: Ecomeasure, 2022) (see **Figure 3.3**) filled with 500ml of milli-Q and left open at sampling locations for a period of 24hrs. This liquid sample was then vacuum filtered on to a filter (QMA Whatmann 1.6µm pore size, 25mm diameter) for later analysis (see **Figure 3.3**).

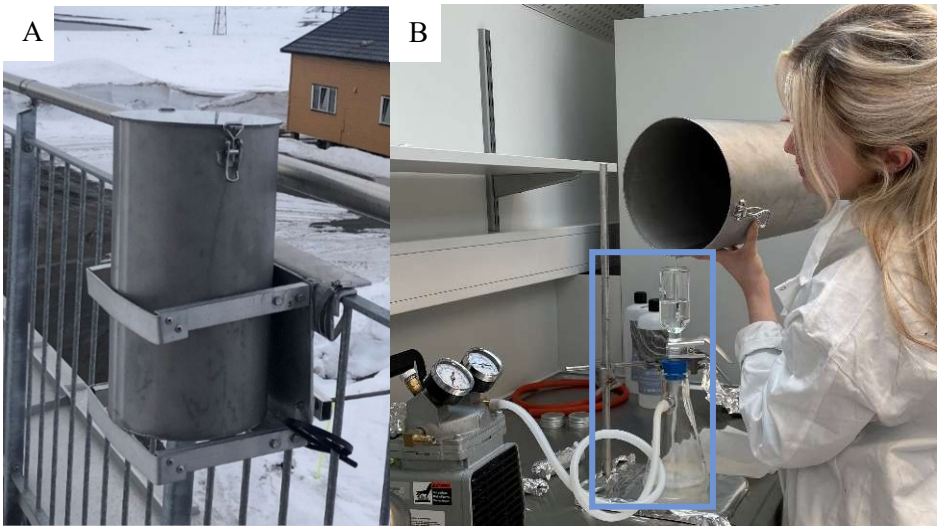


Figure 3. 3 (A)An Image of deposition chamber in the field (with lid, Svalbard, Norway); (B) image of deposition sample being vacuum filtered on to QMA filter with filtration kit

Liquid was added to the deposition chamber while sampling to aid particle retention by minimising resuspension of deposited material (Abbassi et al., 2023). In Svalbard, 50 mL of 20% ethanol was added to the milli-Q solution in order to prevent the liquid freezing in Arctic temperatures. This method was chosen given its simplicity and the recommendation of using open receptacles for the collection of deposited particulates (Knobloch et al., 2023).

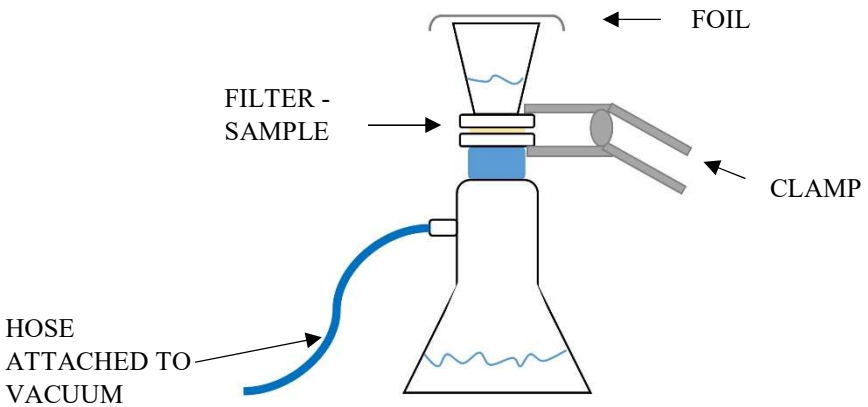


Figure 3. 4 Diagram of filtration kit used to vacuum filter liquid samples (nanotank and deposition samples)

The filtration of deposition samples (and nanotank samples) involves using a filtration system in a fume hood or pristine and controlled environment. The filter is placed in the filtration kit (see **Figure 3.4**) and the pump induced vacuum within the flask draws the liquid sample through the filter where the particulates are collected. The filter is then removed and stored in a covered, sterilized aluminium container until dry for later analysis. The filtered residual liquid is disposed of and the filtration system is cleaned thoroughly with milli-Q in triplicate in-between samples to avoid contamination between samples.

3.1.3 Filters used for Atmospheric MP collection and analysis

There are many different options for the filters used to collect atmospheric MPs and for filtration of MP samples for analysis. Cotton fibre-based filters have been found to have a low-retention of microplastics which can lead to an underestimation of particle count (Cai et al., 2020). Filters made of plastic – such as PFTE (Abbasi et al., 2019) or polycarbonate (Trainic et al., 2020) or Teflon (Peller et al., 2019) – have been used, but the contamination from these filters presents challenges when examining the presence of polymers and the filter material would need to be omitted from the plastic types investigated. Glass microfiber filters have also been utilised in atmospheric MP research (Gaston et al., 2020; Liu et al., 2019a, 2019b; Wang et al., 2020) and another popular filter material is quartz microfibre (QMA) (Akhbarizadeh et al., 2021; Allen et al., 2020a; Dris et al., 2017; Panko et al., 2019). QMA is advantageous in that it is not polymer-based so all polymers can be included in sample analysis. Quartz has previously been commonly used in atmospheric particle research (non-plastic focused studies) and is well studied and established as an atmospheric sampling collection material. Although, some particulates can become trapped in the QMA filter (Felsing et al., 2018). Due to the durability of QMA filters and due to the reduced chance of polymer contamination, they were deemed to be the most suitable for the research in this thesis, specifically Whatmann QMA filters with a 1.6µm pore size. This pore size was chosen to ensure that smaller particulates would not pass through the mesh. The

material itself was chosen due to its frequent use in atmospheric MP studies to date and to minimise contamination from polymer-based filters. Although some particles did become trapped on one occasion (see **Figure 3.5**), overall this filter was durable and effective during sample collection, treatment and analysis.

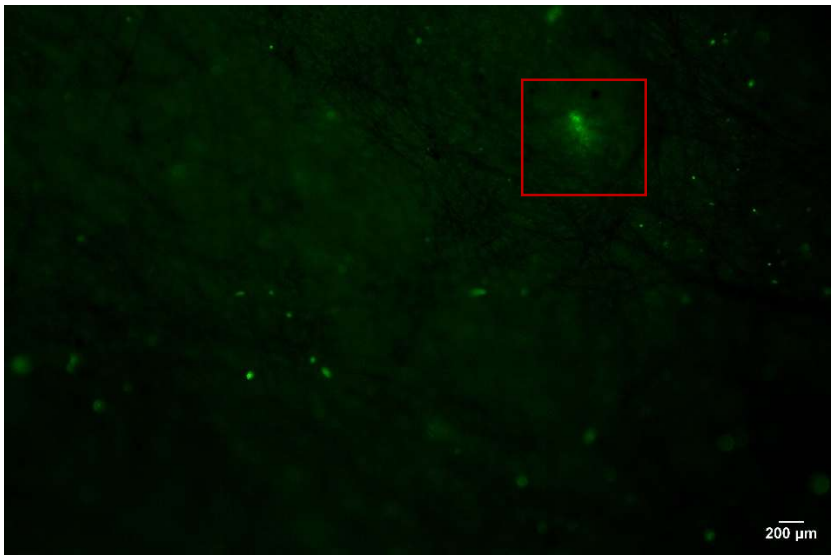


Figure 3. 5 Microscope image of trapped microplastic in QMA filter; image taken during Nile Red staining and imaging atmospheric from Glasgow, Scotland, taken in 2021; objective x10; see also Chapter 3.3

QMA filters (QMA Whatmann, 1.6µm) were used in the direct air filtration systems as well as the vacuum filtration of nanotank and deposition samples.

3.2 Method of Polymer Identification - µRaman Spectroscopy

3.2.1 Raman Spectrometry for Dummies

The two main aims when analysing MPs is polymer characterisation and determining the morphology (size and shape), in order to give an accurate overall picture of characteristics of the plastic within an environmental sample as well as concentration. In this thesis, the method of Raman spectroscopy was chosen, specifically micro-Raman (µRaman), to determine the polymer composition of atmospheric samples. This involves using an infrared laser to excite the sample causing it to release photons

(Zhang et al., 2020a). Most photons are elastically scattered, and the scattered photons have same energy and frequency as the incident photons (see **Figure 3.6)**. However, when there is inelastic scattering and the scattered photons have a different energy and frequency than the incident photons (see also **Figure 3.6**), this is termed 'Raman scattering' named after one of the inventors Sir Chandrasekhara Venkata Raman (Bumbrah & Sharma, 2016).

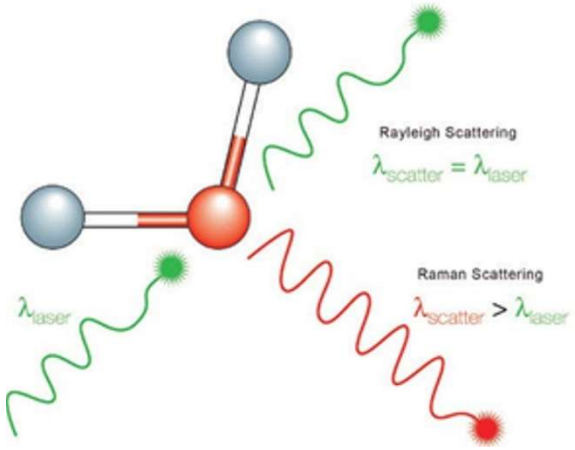


Figure 3. 6 Principles of Rayleigh and Raman Scattering *(Horiba Scientific, 2023)*

If the resulting scattered radiation has a higher frequency than that of the incident photons, 'Stoke lines' can be observed in the Raman spectrum, and if it is lower than the incident photons 'anti-stoke lines' can be observed. The Raman spectrum is then presented as an intensity versus wavelength shift (Bumbrah & Sharma, 2016). This shift creates a unique spectral fingerprint due to the vibrations from each bond type (see **Figure 3.7**) which will be different depending on each individual polymer. For example, part of the Raman spectral fingerprint of polyethylene (PE) is characterised by bands at 1062 and 1130 cm^{-1} which is due to vibrations of the C-C (carbon atom) bonds of the polymer (Nava et al., 2018) (see also **Figure 3.8**). This will differ depending on the carbon bonds and atoms that make up each long chain of atoms for each polymer type (Iowa State University, 2025). This unique fingerprint can then be compared to reference libraries to identify substances, and in the case of MPs there are

multiple polymer reference libraries available for comparison (Zhang et al., 2020a). This method of polymer identification was chosen given its non-destructive nature, and its ability to observe and identify particles down to 1µm and wider spectral coverage compared to FTIR (Araujo et al., 2018). This is necessary given the trend in MPs research that as the particle size decreases, the number of particles increase (Morioka et al., 2023l; Zhang et al., 2020a; Isobe et al., 2015), therefore gaining data on the smallest size fraction is desirable when reporting on MP contamination accurately.

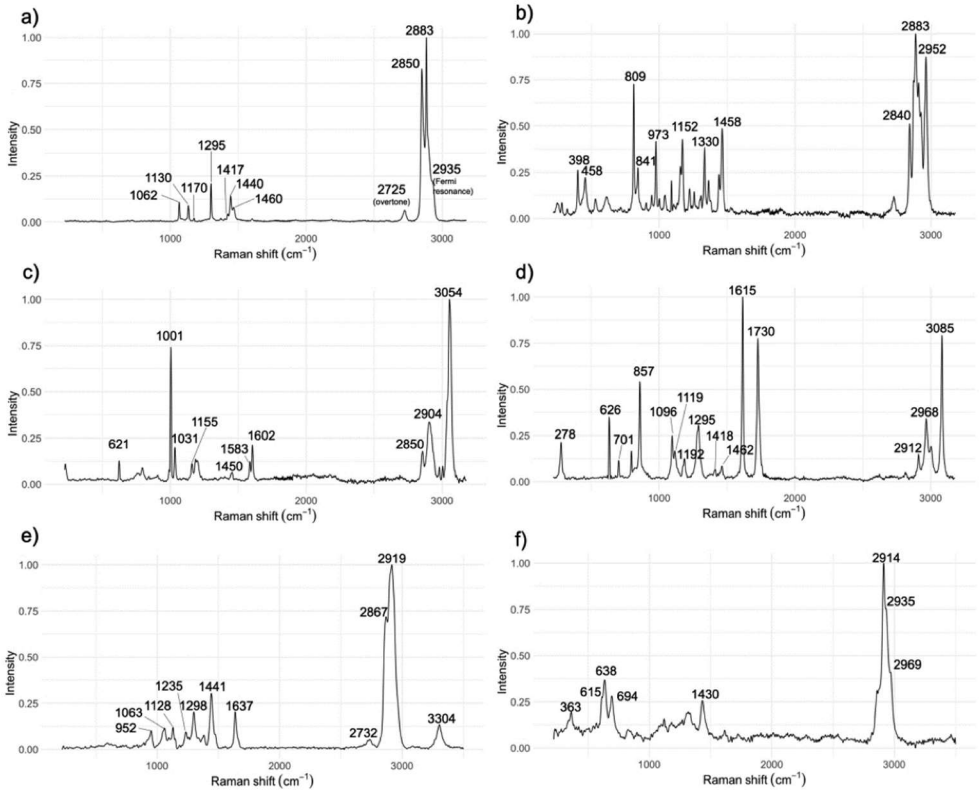


Figure 3. 7 Raman Spectral Signals of Fingerprints for common polymer types ((a) PE, polyethylene; (b) iPP, isotactic polypropylene; (c) PS, polystyrene; (d) PET, polyethylene terephthalate; (e) PA, NY66, polyamide; (f) PVC, polyvinyl chloride) *(Nava et al., 2021)*

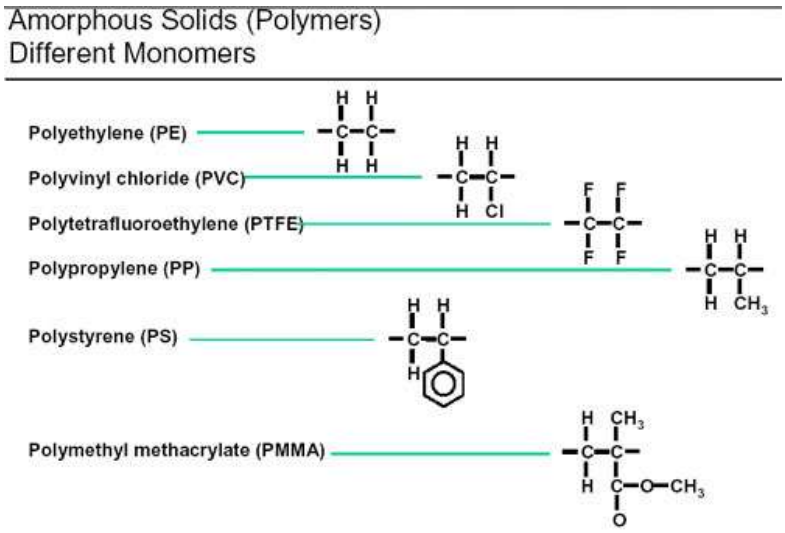


Figure 3. 8 Chemical structure of commonly used polymers *(Iowa State University, 2025)*

When collecting Raman spectra, there are multiple parameters that can be changed in order to suit the sample you are analysing and the research question you are trying to answer. Raman spectrometers can be equipped with different lasers but typically 532nm lasers and 785nm lasers are available. Shorter wavelengths from the 532nm laser can provide stronger Raman signals but can cause fluorescence of the plastic particles in a sample which can hinder MP identification (Nava et al., 2021). A longer wavelength laser can also be used – 785nm laser – which produces slightly weaker Raman signals and can require more time to acquire spectra, but can reduce fluorescence (Edinburgh Instruments, 2021a). This is a popular laser choice in MP research due to is fluorescence suppression, cost and overall performance in relation to MP identification (Nava et al., 2021). The power which the laser omits is also a variable that can affect your signal. Utilising a higher power output can improve your signal intensity but can result in burning and degrading your sample (Wieboldt, 2010). Using a lower laser power, shorter integration times and near infrared wavelengths (e.g. 785nm) have been shown to reduce the chance of thermal damage to the particles (Umurhan et al., 2025); therefore, there is a balance to be struck between signal strength and retaining the integrity of your sample.

There are also choices to be made for exposure time (the length of time the laser excites the sample for) and the number of accumulations (how many times the particle is scanned). By increasing the exposure time, the amount of noise compared to the laser signal – signal-to-noise ratio – can increase, but this can also encourage fluorescence or sample degradation (Wieboldt, 2020). Most studies utilise a 1 to 10 second scan depending on the sample and laser power. By utilising more accumulations or scans, it is possible to improve the signal quality and reduce background noise (Nava et al., 2021) and often 3-5 accumulations are used in MP research (Kappler et al., 2016) but this increases the scanning time which can already be a resource intensive process. In terms of spectral resolution, the higher the resolution the more accurately the peaks from the signal (e.g. the fingerprint of the signal) can be identified, but again this results in a longer scanning time and larger files (Cowger et al., 2020). Again, there is a trade-off to be made between the resolution needed and the time taken to analyse the sample, especially for larger datasets. The spectral range usually spans 200-4000cm^{-1} with polymer peaks often found between 400-1800cm^{-1} (Lenz et al., 2016). By choosing the correct spectral range it is possible to be more efficient in identifying peaks and refining data collection. Each Raman instrument will have different objective lenses, in the case of μRaman common choices range from x10 to x100 objectives (Nava et al., 2021). Higher magnifications can improve spatial resolution which can be helpful when analysing particles <10μm (Primpke et al., 2020). Lower magnifications – between 10x and 20x – allow for a broader field of view (Edinburgh Instruments, 2021b). which is beneficial for analysing a larger representative area of the filter. For this reason, the 10x objective was chosen for the analysis of samples in this thesis. The following section discusses the parameters chosen for μRaman spectrometry in this thesis.

3.2.2 The Tale of Two Ramans

Due to technical issues, the μRaman analysis for this thesis was completed using two different μRaman spectrometers but efforts have been made to keep results consistent.

After repeated mechanical failures with the µRaman at the University of Strathclyde, and in interest of time, another µRaman was used at the Helmholtz Association in Leipzig, Germany. Each machine behaved slightly differently with standard samples, providing a slight difference in signal to noise ratios and fluorescence. Both Polyethylene Terephthalate (PET, Sigma Aldrich, 429252, 1.68 g/mL) and Polyvinyl Chloride (PVC, Sigma Aldrich, 81388, 1.4 g/mL) that were filtered onto the same filter type used in the field in this thesis (as above, QMA Whatmann 1.6µm pore size, 25mm diameter), and used as µRaman analysis standards. These polymer standards were examined to observe how the spectra on each µRaman responded using different settings. Due to the differences in the spectrum created by each µRaman spectrometers different parameters were used (scan duration, repetition, energy).

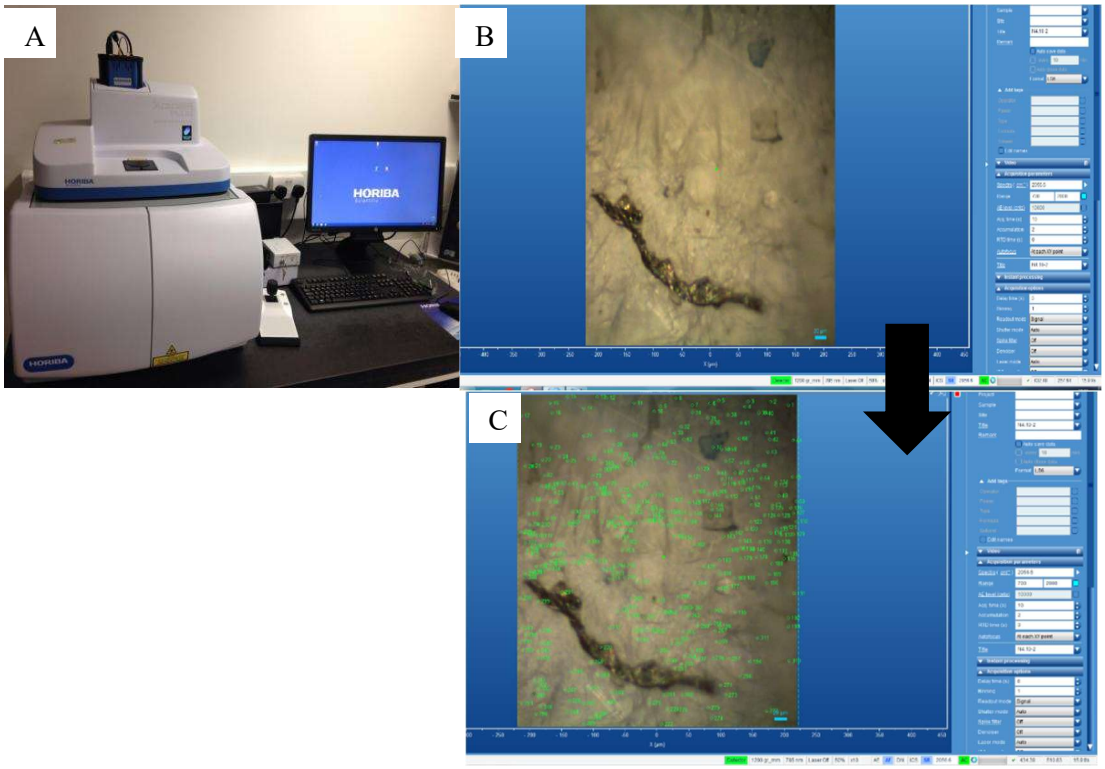


Figure 3. 9(A) Image of µRaman Spectrometer at the Technology and Innovation Centre at University of Strathclyde; (B) Image of Sample Under µRaman microscope (Active Air Sample on QMA Filter, taken from Glasgow 2021) before points map is added; (C) Image of Sample Under µRaman microscope with points map added (same Active Air Sample on QMA Filter, taken from Glasgow 2021)

The μRaman analysis for the Glasgow samples was completed using the Horiba Scientific Xplora PLUS (**Figure 3.9A**). This was conducted using a 785nm laser (red), using a x10 objective and 1200gr grating. The range was set at 700-2000cm^{-1} and the exposure time set to ten seconds, coupled with two sets of accumulations. The use and support of this machine was facilitated by Dr Martin Ward at the Continuous Manufacturing and Advanced Crystallisation (CMAC) Hub at the University of Strathclyde. This model did not have automated particle mapping; therefore particles were manually selected using a point map which allowed for multi-point analysis. The point map directed the laser to appropriate X and Y coordinates, and an automated Z-focus made sure the laser focused on the correct particle (see **Figure 3.9B**). This was beneficial as it allowed for multi-particle analysis in one scan rather than individual scans per particle, which made it possible to analyse ≈100-700 particles per scan if necessary. This allows for a more representative dataset as it is possible to analyse more particulates on a filter in a given timeframe. For both instruments, 3 areas were selected on the filter and the polymer composition and counts were averaged over the 3 scans, and multiplied based on the area of the filter (see **Chapter 3.5 for calculations**).

The μRaman located at the Helmholtz Association in Leipzig, Germany, was a WiTec Alpha 300 RA (see **Figure 3.10A and 3.10B**), using a 532nm laser and the same accumulations and exposure time were used. The use and support of this machine was facilitated by Dr Matthias Schmidt and Dr Dusan Materic at the Helmholtz Association. The 532nm laser produced a stronger signal with the plastic standard samples tested than the 785nm, therefore it was decided it was more optimal to choose this laser. This μRaman had a particle mapping function, but when tested with the plastic standard samples, it was found that the particle mapping software was missing lighter coloured particles (presented a particle colour bias). When particle finder settings were adjusted to focus on lighter particles, darker particles were then missed. The mapping function was also not as effective at identifying smaller particles. In order to analyse as many particles as possible in a short-time period, and gain a representative sample by ensuring as many particles as possible were analysed, Dr

Matthias Schmidt and the researcher created a method of creating a particle 'mask' which mapped out the particles manually, and the resulting file was uploaded to the Raman to mimic a particle mapping function (see **Figure 3.10C;** also SOP at **Appendix IV**). This allowed for accurate multi-point analysis, saving time and allowing for more particulates to be analysed. The one drawback to this solution is that the spectrum produced for the particulates cannot be exported as one file, instead each spectra was manually copy and pasted into its own file. This was time intensive but it was worth the time spared to gain detailed individual particle spectra.

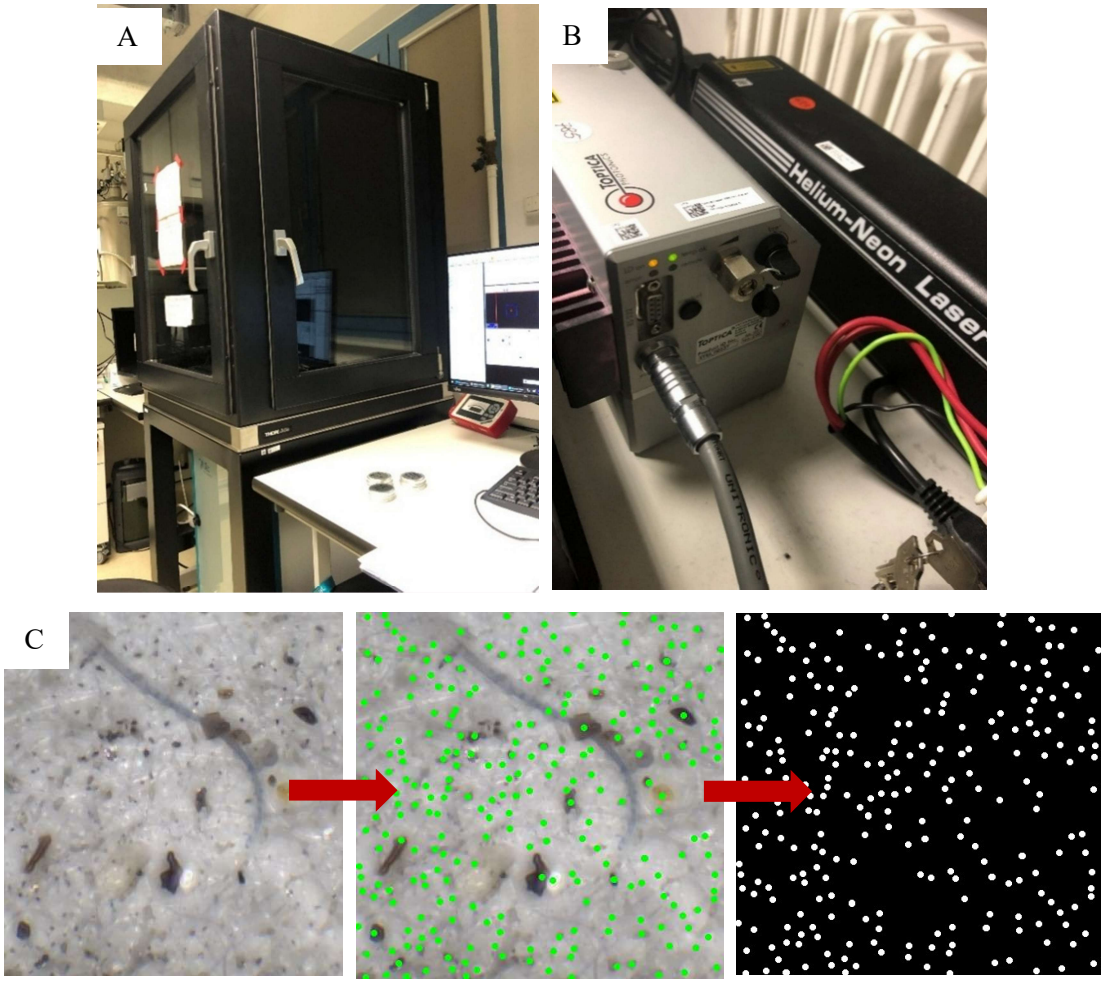


Figure 3. 10(A) Image of µRaman Spectrometer at the Helmholtz Association, Leipzig; 3.6(B) Image of Laser used, Helmholtz Association, Leipzig; 3.6(C) Series of images showing the process of creating a points map to be fed back into the µRaman spectrometer to mimic particle mapping function; first image shows the original image of Filter (Deposition Filter Svalbard (QMA Whatmann (25mm, 1.6µm))under µRaman

To ensure samples were analysed accurately, three areas on each sample/filter were picked at random to analyse particles for polymer composition and then the results are reported as an average of the triplicates.

3.2.3 Spectral Correction and Multivariate Analysis

Once the spectrum for particles are collected, they can be treated before they are compared to reference libraries in order to make them clearer and more identifiable. It is possible to remove baseline signals which removes interference with background material and make the spectra clearer. The spectra can also be smoothed in order to help justify for noise in the signal, a common method used is the Savitzky-Golay algorithm (Bai and Liu, 2020). This technique can reduce the noise in a spectrum and whilst maintaining spectral features (Barton, Ward & Kelly, 2018; Munno et al., 2023). It involves fitting the datapoints to a low-degree polynomial using least squares regression (Savitzky & Golay, 1964). In basic terms, the polynomials are simple curves which model the data without overfitting them (Smyth, 2014) so the Savitzky Golay filter smooths the spectra without overcorrecting the peaks. Similarly, the least squares regression is used to fit the polynomial to the data by using a best-fit line which minimises the distances from the data points on the curve, so the filter can minimise noise without losing detail. It is desirable to carefully balance treating the spectrum to make them clearer, but without over-correcting, as it is possible to lose detail in the peaks of the spectrum. These peaks are matched with the polymer libraries, therefore overcorrecting them can make identification more difficult and result in underestimation.

Both datasets were treated using Spectragryph software (version 1.2.15, Menges, 2022) and the spectrum treated with Savitzky Golay algorithm for smoothing and baseline correction was also applied. Both datasets were cut from 800 to 1800cm^{-1} (Raman shift), and after their respective treatment the peak data from each dataset was exported to Excel for multi-variate analysis to identify the peaks in each of the spectra.

The multi-variate analysis consisted of taking the data from the peaks identified via Spectragrpyh and using principal component analysis to split the peak data into categories based on the wavelength data and Raman shift to look for more detail amongst the peaks. This has been used by previous studies (Jin et al., 2022; Levermore et al., 2020; Xu et al., 2020b) and has been found to improve accuracy and increase sensitivity in order to improve the classification of polymers. Reference libraries were used to confirm polymer identification (SIMPLE, SLOPP and SLOPPE databases and the laboratory reference plastics spectral (Jin et al., 2022; Levermore et al., 2020; Xu et al., 2020b). Particles were only confirmed as plastic if a hit quality index (HIT) rate of ≥80% was achieved (Cowger et al., 2020; Levermore et al., 2020), and those below the <80% threshold discounted as non-plastic particles. This threshold has is considered best practice (Cowger et al., 2020) in order to avoid overestimating particles.

3.3 Nile Red Staining and Fluorescence Microscopy

3.3.1 Nile Red Staining and Optimisation

The other main aim of MP analysis, is to gain information on the characteristics of the MP particles – namely morphology or shape (fibre/fragment) and the size of the particle. Nile Red is a lipophilic dye used to identify MP in environmental samples (Shim et al., 2016). The Nile Red preferentially binds to plastic particles, which causes them to fluorescence under specific wavelengths of light. The multiple carbon-hydrogen bonds in polymers allow for the dye molecules to bond to the hydrophobic surfaces, which causes the fluorescence (Galvão et al., 2023). This allows for MP identification that is not economically or time intensive, and avoids extensive sample preparation (Maes et al., 2016). However, it has been found that Nile Red can stain organic matter, leading to false positives (Stanton et al., 2019). In order to avoid this, several steps can be taken.

To remove any excess organic material, some studies digest their samples with oxidising agents such as hydrogen peroxide (H_2O_2) or Fenton's reagent ((H_2O_2) and ferrous iron (Fe^2)), for a period of 24hrs-48hours (Mbachu et al., 2020; Huang et al., 2020). This is commonly used with environmental samples containing a heavy amount of organic material such as terrestrial or marine samples. But due to the nature of atmospheric samples containing less organic material (Allen et al., 2020), this thesis chose not to perform an organic digestion step, as the potential for MP contamination and the risk of losing MPs through this process was deemed more costly than the risk of false positives. Alternatively, further steps were taken to reduce this possibility.

The main approach to optimise staining conditions was to adjust the concentration of Nile Red and to incubate samples prior to microscope imaging to enhance the selective staining of MPs. In the literature it has been found that lower concentrations of Nile Red can reduce the formation of fluorescent aggregates that could be falsely identified as MPs (Hernandez et al., 2023). Chatterjee and colleagues (2023) found that with decreasing concentration, the presence of NR aggregates, which can be mistaken for MP, also decreases. However, with the decreasing concentration there can also be an underestimation of particles. A systematic review of the use of Nile Red dye recommends a concentration of 0.1 and 2 $\mu g\ ml^{-1}$ to avoid the dye clumping and false positives (Shruti et al., 2022b). After studying the staining properties of different polymer fibres, Galvão and colleagues recommend an incubation time for at least 30 minutes as an effective time for the dye to bond to the particles (Galvão et al., 2023). Furthermore, it is recommended that dye is carefully spread uniformly and without excessive use, in order to avoid missing particles that have not been stained, and again to avoid excessive staining (Shruti et al., 2022b). This thesis recognises that Nile Red staining is not recommended as a standalone MP quantification method (Shruti, et al., 2022b). Instead, Nile Red staining is used as a complementary method of analysis to benefit from rapidly and inexpensively quantifying MP concentration, shape and size alongside the polymer identification methods.

With these considerations and recommendations in mind, the following method for staining the atmospheric samples was taken. A Nile Red Solution was made by taking 1µg of Nile Red powder (Sigma Aldrich, 72485, 318.37amu), and 1L of methanol (Merick) (same concentration as previous studies examining effectiveness of Nile Red (Hernandez et al., 2023; Chatterjee et al., 2023; Galvão et al., 2023)), and dissolving the powder in the methanol in batches of 250mL and 0.25µg of the Nile Red Powder. This was then vacuum filtered in a fume hood, with the top of the vacuum covered with foil (see **Figure 3.11**). The solution was then stored in glass bottle that has been pre-rinsed in triplicate with milli-Q; this bottle was then covered in foil to prevent light degrading NR, and stored in the fridge to maintain its stability and effectiveness (Sigma Aldrich, 2024).

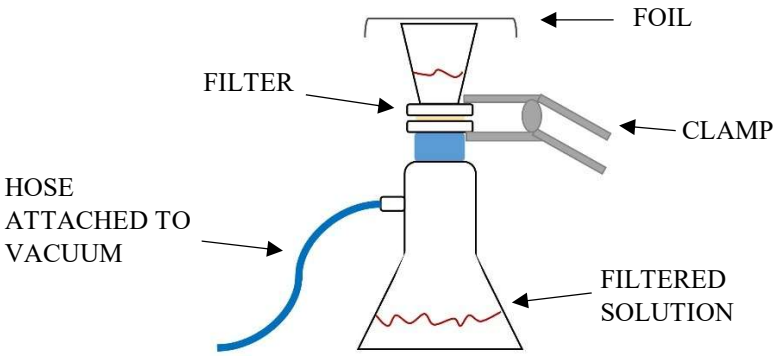


Figure 3. 11 Diagram showing filtering of Nile Red solution via vacuum filtration

Whilst the filter rested in its aluminium storage tin, a pipette was used to drop small droplets of the NR solution on filter (enough to wet the sample and filter but not enough to resuspend any particulates). This started lightly around the edges and was let spread across the filter, then if needed a couple more droplets were dropped in the middle of the filter. This was then covered as soon as solution is on the filter with the aluminium tin lid. With the lid covering the filter but not screwed on (to allow for the filter to dry), the sample was then wrapped carefully in aluminium foil and put in 50°C oven for 30 minutes to dry the filter out and increase fluorescence stability (Lv et al.,

2019). After cooling overnight, covered in aluminium foil and within a fume hood, the lids were then screwed back on tightly and samples were then moved to the fridge until ready for microscope imaging. Storing the samples in the fridge (4^{o}C) is also an important step as fluorescent dye can lose its signal faster when exposed to light and if kept at room temperature (Rumin et al., 2015) so this step can ensure a good fluorescent signal is maintained. To prevent contamination from using a shared fridge samples were stored in aluminium trays covered with more foil.

3.3.2 Microscope Imaging and Fluorescence

Samples analysed in this thesis were imaged using a stereomicroscope (Nikon Eclipse LV100ND Microscope) with NIS Elements software. A 10x objective was used, and images were taken with florescence mode coupled with 470nm wavelength light source. By utilising the 470nm light source, it can increase the fluorescence of stained MP particles making it easier to identify MP more clearly (Prata et al., 2019) and improve accuracy. It has also been found that some organic particles do not to fluoresce under 470nm excitation (Maes et al., 2017), reducing the possibility of false positives and again improving accuracy. Aluminium foil used to cover the sample whilst it is being viewed with the microscope. This blocks outside light sources and prevents contamination in share laboratory facilities (see **Figure 3.12A**).

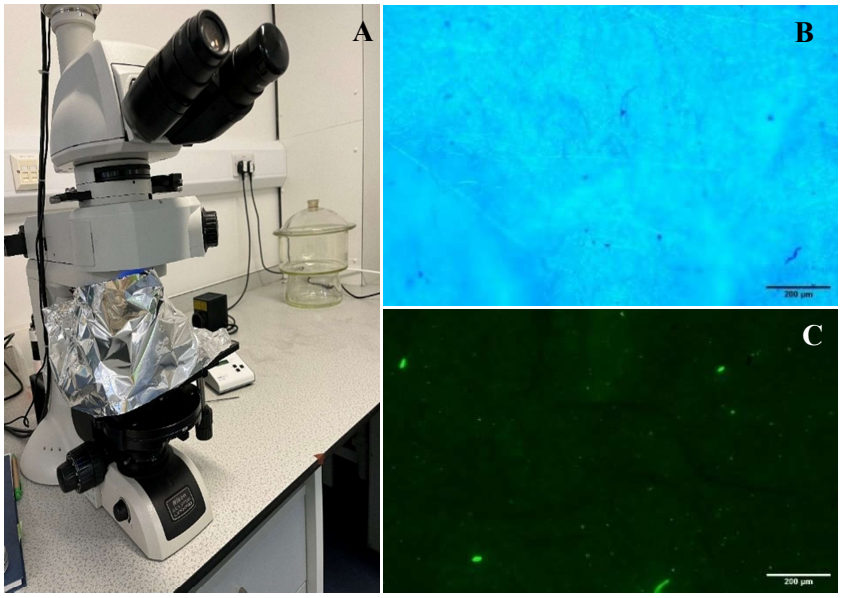


Figure 3. 12(A) An Image of Stereomicroscope used in this thesis, with foil to cover sample during microscope imaging; (B) Brightfield image of atmospheric sample taken from Glasgow, Scotland (2021); (C) Fluorescence mode image of same atmospheric sample taken from Glasgow, Scotland (2021)

Once the filter is under the microscope, the top of the filter is identified and particles are focused using the manual Z-focus and using the bright field (BF) view (see **Figure 3.12B**). Once the particles are in clear, the fluorescence mode was used (FL1), to examine the particles fluorescing (see **Figure 3.12C**). Images were then taken in a transect from the top of the filter to the bottom (1.4mm x 0.4mm images). The particles identified were then multiplied out based on the area of the filter (see **Chapter 3.5**) to gain a representative number of the whole sample. This method was chosen in order to examine a high number of samples and still gain a representative particle count.

3.3.3 Image Processing and Particle Analysis

To analyse the microscope images for MP particle count, and also gain information on shape (fibre or fragment) and size, images were analysed using Image J software (ImageJ-win64, Schneider, Rasband, & Eliceiri, 2012). The scale is set manually using

an image of a scale (see **Figure 3.13A**) taken with the same microscope objective (x10).

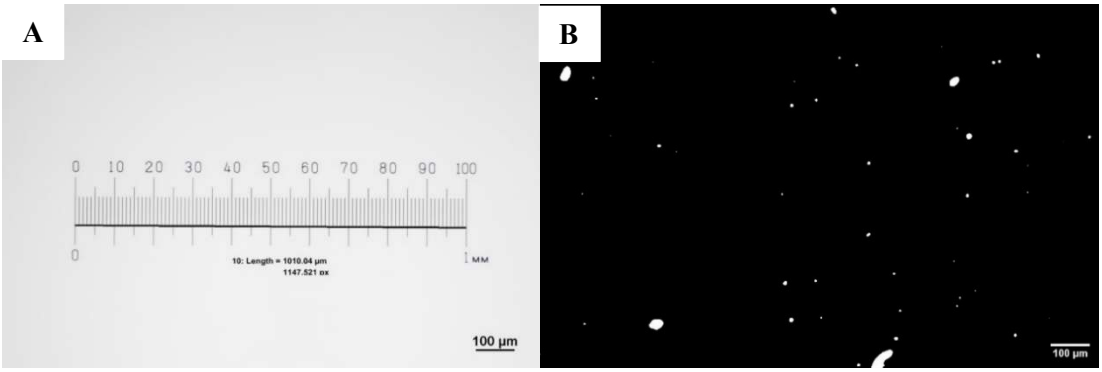


Figure 3. 13 (A) Image of Scale taken with stereomicroscope using x10 objective; 3.9(B) Image of atmospheric sample taken from Glasgow, Scotland (2021) with ImageJ processing (brightness and contrast enhanced, threshold (30+255) for particle analysis

The brightness and contrast are enhanced to make the particles more clearly and easily visible, and then smoothed to contour the particles. The image is then converted to an 8-bit image to make the background black and the particles white (see **Figure 3.13B**). The threshold was manually set for each image (range ≈12-30 and 255 (on a sliding scale of 0-255) depending on the brightness of the particles). ImageJ then provides particle information on the size, and shape descriptors (area, perimeter circularity, Feret diameter (longest distance between any two points along the selection boundary) to name a few). This information is then copied into an Excel sheet where the samples can be organised and a summary of the particle count, shape and particle size distribution can be created.

3.4 QA Contamination Control – Minimising the Inevitable

When collecting environmental samples to examine the presence of MP, the possibility of external MPs contaminating the sample is a main concern to ensure MP numbers are reported accurately. Due to the ubiquitous nature of MP in our environment, contamination can occur while collecting the sample, and when the sample is being

processed and analysed. There are many steps that can be taken to ensure that this contamination is kept to a minimum and to report for potential contamination accurately.

In this thesis, during field sampling campaigns the equipment was set up away from any potential interference or contamination from the public. In Svalbard, equipment was placed on the roof of a research station to prevent interference from visitors or staff present at the research base. In Glasgow, the equipment was placed at the end of a garden, away from the public and only the researcher collected samples and operated the equipment. In both locations, only natural materials (cotton, wool) were worn during sample collection and during sample processing (as recommended by Gao et al., 2023; Prata et al., 2018). The University of Strathclyde, where the samples were processed, provided a MP clean lab where entry was restricted, only natural materials are permitted to be worn, cotton lab coats were used, there was a HEPA air filer in operation (to filter and collect potential contamination). Surfaces in the laboratory were regularly cleaned with milli-Q and ethanol to ensure surfaces were clean from any contamination from MP deposition from the lab environment. The filters used to collect samples and the stainless-steel tins used to transport samples were heat treated before use (~450℃ oven for 15 minutes – temperature selected to burn off any potential polymer contamination (Gao et al., 2023)). Furthermore, any solutions used in sample preparation and processing were vacuum filtered before use (Whatmann QMA filters with 1.6µm pore size) and blanks of the milli-Q, ethanol and the milli-Q/ethanol solution were taken to account for potential contamination in reagents (Bai et al., 2023). Whilst samples were being processed they were covered with foil or the filter tin lids were left on, to minimise deposition from the lab environment. All equipment was plastic free (e.g. glass, stainless steel) and was triple rinsed with milli-Q in order to remove potential contamination, before and after use.

In addition, procedural blanks were taken during sample collection (field blanks) and during sample processing (filtering and staining) (as recommended by Brander et al., 2020; Gao et al., 2023; Prata et al., 2018). Field blanks consisted of leaving a clean

filter open to the air while samples were being changed over. Procedural blanks involved leaving a sterilised filter open to potential MP deposition in the laboratory while Nile Red staining took place. Procedural nanotank blanks consisted of filling the nanotank with 500 ml of milli-Q after it had been cleaned, which was then collected and vacuum filtered on to a filter (same QMA Whatmann, 1.6µm pore size) to examine if there was contamination between samples. All blanks were treated in the same way as the samples, with some being analysed with µRaman spectroscopy to gain an understanding of polymer contamination, and the rest stained and imaged with Nile Red to understand the particle size, shape and number of particulates from contamination. All results have been adjusted (blank corrected) to account for the contamination found in these field and procedural blanks, based on their particle size distribution from the Nile Red staining of blanks, and based on the polymers found in any procedural and field blanks.

3.5 Calculating MP Concentrations and Statistics

To calculate the amount of MPs in each deposited and suspended sample, the following sets of equations for used.

To calculate the number of MPs per sample (all samples):

$$\mu P = (P_s/A_s) \times A_f$$

μP = MP per total sample

P_s = MP particles in the subsampled area (count)

A_s = area subsampled (mm^2)

A_f = area of total filter (mm^2)

For individual suspended samples (direct air filter and nanotank), to calculate the volume of air per sample, following equation was used:

$$V = (t_s \text{ x } f_s)/1000$$

t_s = time (mins) for the total sample

f_s = flow rate (L/min) for the sample

V = air volume sampled (m^3)

For the suspended air samples (nanotank and direct active air samples), the total representative MP per m^3 is calculated as:

Total suspended MP = µP/V (MP/m^3) , which in long had is:

$$= ((P_s/A_s) \text{ x } A_f)/ ((t_s \text{ x } f_s)/1000)$$

Filters were generally 47mm diameter for direct air filtration samples, and 25mm diameter for nanotank samples.

One of the main research questions for examining both remote and urban atmospheric MP pollution, is their potential relationship with weather parameters. In relation to atmospheric MP pollution in Svalbard, weather data collected at the Ny-Ålesund research station was collated from the Norwegian Centre for Climate Change repository (Maturilli et al., 2022a, 2022b; Norwegian Centre for Climate Services, 2021) for the sampling period May-June 2022. The main variables of interest here were precipitation (mm), atmospheric pressure (hPa), snow depth (cm), snow cover (%), wind speed (m/s), and wind direction. To examine the relationship between weather variables and urban atmospheric MP pollution, weather data was taken from the Visual Crossing (Visual Crossing, 2011) for the period of November-December 2021. The same variables were of interest here but snow cover was not included due to the lack of snowfall in Glasgow from November 2021-December 2021 – when sampling took place. Due to higher atmospheric pollution levels at the urban location

(Glasgow), it was of interest to observe if there was a relationship between atmospheric MP pollution at the site, and other atmospheric pollutants. For this purpose, air quality was taken from the International Air Quality Index (AQI, 2021) database.

To examine potential relationships between atmospheric MP concentrations and weather parameters, and air pollution levels respectively, statistical correlation analysis was performed in Excel. The correlations between MP Concentration and weather and pollution data were completed using the Correlation function in Excel which produces a p-value. To examine the significance of this p-value, the r-value was calculated using Pearson correlation with the following equation:

$$r = \frac{\sum(x^i - \bar{x})(y_i - \bar{y})}{\sqrt{\sum((x^i - \bar{x})(y^i - \bar{y})^2}}$$

Where:

$\sum$ = sum

x^i and y_i = are the data points

$\bar{x}$ = mean of x values

$\bar{y}$ = mean of y values

The methods detailed in this section were used consistently throughout this thesis and research.

Chapter 4 - Pilot Study: Examination of Active Air Sampling Efficiencies

This chapter will cover the first research question (RQ1): How do the parameters used in active atmospheric MP sampling influence measured particle concentrations relative to environmental conditions?

4.1 Introduction

The field of atmospheric MPs is still considered novel, given the first study was published in 2016 (Dris et al., 2015), and only 124 studies published as of 2023 (O'Brien et al., 2023). Although the field is rapidly growing in interest and studies, there is still a lack of understanding and consensus on methods used to sample and analyse atmospheric MPs. Active sampling (also known as atmospheric concentration sampling for aerosol particles) is a method used in atmospheric science to collect particulates, relative to a known volume of air and collects mostly suspended particulates (those suspended in the air, rather than deposited). This can be carried out using a variety of instruments and methods, but for atmospheric MPs this mostly involves a calibrated pump drawing a known volume of air through a chamber on to a sample medium (filter) onto which particulates are retained (Zhang et al., 2020a). In atmospheric science, the elements of the sampling process can affect the results and validity of your study. There are many choices to make sure the methodology and sampling procedure used are: 1) best suited to your research question; 2) most effective for the sample you want to attain; and 3) best suited to the research environment. Factors such as the volume of air sampled, pumping rate, and the environment where the sampling is taking place are important in terms of representation and accuracy (Haig et al., 2016;). Sampling too much air, either with an excessive pumping rate or sampling duration could cause the filter to become overloaded (blinded). Overloading could result in inconsistencies in the pumping rate as the ability to draw air through the filter is reduced and could cause particle re-entrainment, leading to lower collection

efficiencies. Alternatively, if the pumping rate is low or the sample duration is too short, there could be a limited residence time between the sample and the filter, resulting in limited material being collected relative to background contamination, also causing lower collection efficiencies.

Although guidance exists for traditional air pollutants on how to plan and adjust for these parameters (McCammon, Woebkenberg, & Ashley (2016), limited literature exists on how this information can be adapted and applied to atmospheric MP sampling campaigns in areas with different levels of environmental contamination. As no guidance exists to date on how these parameters can affect MP sampling, this pilot study was designed to test each of the abovementioned parameters and examine its significance. It has been observed that there is a positive relationship between particulate matter (a more traditionally measured air pollutant) and atmospheric MP and it is considered that atmospheric MPs will contribute to ambient PM (Akhbarizadeh et al., 2021). It is therefore assumed that some of the principles that have been established for traditional air pollutants, can be applied to atmospheric MPs.

Air pollution is a long-established field and an international public health concern; therefore standards have been created to improve the efficiency of sampling. For example, the US Environment Protection Agency (EPA) and the Environment Agency in the UK have both published technical guidance on this (Environment Agency, 2011; US Environmental Protection Agency, 2011). Although this can provide helpful information on the various methods that are used, the advice on the limits of detection and reported uncertainty would need to be adapted to suit the differences with MP research. For example, the LOD of MP can vary from 2µm (Allen et al., 2019; Wright et al., 2019) to 5mm (Dris et al., 2017), which is a much larger range than considerations for PM which is normally measured in the range of 2.5µm, and 10µm ($PM_{2.5}$ and PM_{10}). Furthermore, despite an extensive literature search there appears to be little guidance on how to adjust sampling campaigns relative to the contamination in the surrounding environment. To address this, a pilot study was designed whereby

various sampling volumes and pumping rates were tested over the same time period, to assess their relative importance in terms of particle concentrations and representation in the same environment. The objectives of this study were to determine: 1) to determine the *pumping rate* is appropriate for optimal filter collection relative to field conditions; 2) to determine the optimum *duration* for sampling intervals relative to field conditions; 3) to examine if pumping rate and sampling duration influence the type of MP particles collected (polymer composition, shape (fibre/fragment) and size).

4.2 Methods and materials

4.2.1 Field Experiment – Sample Collection and Experimental Parameters

A single moderate density urban location in the city of Glasgow, UK, was used to ensure consistency in environmental conditions. Glasgow has the population of 633,100 (as of 2019) (Glasgow City Council, 2021), and is still known for its commercial and industrial economy (IFSDG, 2021). Sampling took place in Rutherglen which is a town ≈5 miles from the centre of Glasgow (see **Figure 4.1**), which is mostly residential with some urban and industrial activity and a population of ≈30,000 as of 2022 (South Lanarkshire Council, 2023). At the time of this research (Nov-Dec'21) there were still some COVID-19 restrictions in place, including government advice to work from home where possible. This meant a reduction in public transport and traffic, but as some activity had returned to the city, it was determined that a representative sample was still possible.



Figure 4. 1 Map of Glasgow and Rutherglen, red dot indicating the sampling location *(Arc GIS, 2025)*

All samples were taken over the same period and same location to ensure there were no spatial or temporal variances. Sixteen samplers were set up at ≈0.75m height, each with one stainless steel filter holder and a silicone hose attached to a calibrated pump to draw air through the chamber to the filter (QMA Whatmann 1.6µm pore size) (see **Figure 4.2**).



Figure 4. 2 Image of Experimental Set-Up in Glasgow, the nanotank samplers can be seen in the red box; the daily sampling duration direct air filtration samplers are in the yellow box; the weekly sampling duration direct air filtration samplers are in the green box; the monthly sampling duration direct air filtration samplers are pictured in the blue box

Direct air filtration sampling was used whereby the pump draws the particulates on to a filter (**Figure 4.3A**) The nanotank sampler operates by using a pump to draw air into a sealed chamber where the particulates are collected in milli-Q water (see **Figure 4.3B**), and the milli-Q is later removed and vacuum filtered onto a quartz fibre filter (QMA Whatmann 1.6µm pore size). The aim of using both samplers in parallel was to examine if one method was more effective at collecting particulates or collected different characteristics of MP than the other. The nanotank is a novel design attempting to prevent particle re-entrainment as particles are drawn into a liquid media rather than directly onto a filter. A discussion on the design and detail of the nanotank is provided in **Chapter 3**.

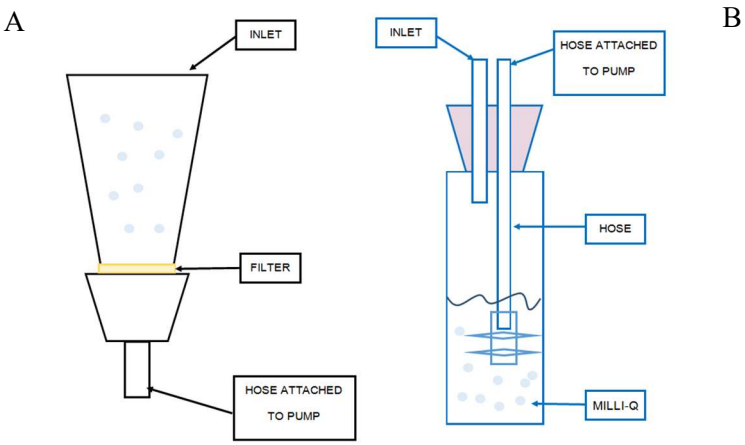


Figure 4. 3 Diagram of the two active air sampling systems used, (A) Direct Air Filtration System; (B) Nanotank System

When designing this research study, published atmospheric MP studies to date were examined to compare the active sampling parameters used across studies and locations. Seventeen published studies were identified as relevant (**Table 4.1**). These studies examined samples in a range of locations from coastal areas to densely populated cities and remote mountain catchments. No trend or correlation was apparent between the quantity of sampled air, duration of sampling periods, and pumping rates. All samples were collected via pump onto filter (active air sampling).

Sampling campaigns seemed to be designed on a needs basis; therefore, it would be advantageous to improve understanding on the limits of detection and improve the efficacy of sampling campaigns.

Table 4.1 Sampling Information from Research at time of research design (Environment; Quantity of Sampled Air; Duration; Sampling Rate; Sampler Type) *(Syafei et al., 2019; Peller et al., 2019; Li et al., 2020; Dris et al., 2017; Gaston et al., 2020; Panko et al., 2019; Abbasi et al., 2019; Trainic et al., 2020; Asrin and Dipareza et al., 2019; Allen et al., 2020; Liu et al., 2019a; Liu et al., 2019b; Wang et al., 2020; Tunahan Kaya et al., 2018; Akhbarizadeh et al., 2020)*

Reference	Environment	Quantity of Sampled Air (m^3/sample)	Duration of Deposition Sampled	Pumping rate (L/min) ($1m^3 = 1000L$)	Sampler Type
Syafei et al., 2019	City environment – outdoor	Period 1 = $0.9m^3$ Period 2 = $19m^3$	3 days	Period 1 = 0.2 L/min Period 2 = 0.4 L/min	Stainless steel 1000 mL funnels, and vacuum pumps (Vacuubrand pumps)
Peller et al., 2019	Lake environment – outdoor	8.64-12.96m^3	2-3 days	3 L/min	12V DC battery powered small pump and
Li et al., 2020	City environment – outdoor	1.8-2.4m^3	6-8 hrs	5 L/min	MiniVol samplers (Airmetrics, USA)
Dris et al., 2017	City environment – outdoor	2-5m^3	4-7hrs	8 L/min	Stand-alone sampling pump (GH300, Deltanova, France)
Gaston et al., 2020	City environment (coastal) – outdoor	4.6m^3? (4615L for 8 hours)	5 days	11.7 L/min	Simple vacuum filtration array and vacuum pump (Cole-Parmer Air Admiral)
Panko et al., 2019	City environments – outdoor	LA = $44m^3$ London = $75.3m^3$ Tokyo = $95.3m^3$	LA = 48hrs London = 72hrs Tokyo = 72hrs	LA = 16.5 L/min London = 17.4 L/min Tokyo = 16.7 L/min	LA = BGI PQ 200 samplers (Mesa Labs) – PM2.5 inlet London = Thermo Partisol 2025 samplers (ThermoFisher) Tokyo = - 2000 FRM samplers (ThermoFisher)
Abbassi et al., 2019	City environment – outdoor	24m^3	24 hrs	16.67 L /min	ECHO PM ambient filter sampler (TECORA, Italy)
Trainic et al., 2020	Ocean environment – outdoor	12-60m^3	10-50hrs	20 L/min	Inlet, positioned 15m above sea level, vacuum pump pumping on to a filter
Asrin and Dipareza, 2019	City environment – outdoor	24.7m^3	13 hrs	31.6 L/min	Stainless steel funnels, and vacuum pumps (Vacuubrand pumps).
Allen et al., 2020	Ocean environment – outdoor	72m^3	24hrs	50 L/min	Standard vacuum pump, Caltech Active Strand Cloudwater Collector (CASCC)
Liu et al., 2019a	City environment – outdoor	6m^3	1hr	100 L/min	KB-120F type intelligent middle flow total suspended particulate sampler (Jinshida, Qingdao)
Liu et al., 2019b	Ocean environment – outdoor	24-144m^3	4-12hrs	100 L/min	KB-120F type intelligent middle flow total suspended particulate sampler (Jinshida, Qingdao)

Reference	Environment	Quantity of Sampled Air (m^3/sample)	Duration of Deposition Sampled	Pumping rate (L/min) ($1m^3 = 1000L$)	Sampler Type
Wang et al., 2020	Ocean environment – outdoor	53-259m^3	10-48hrs	100 L/min	KB-120F type intelligent middle flow total suspended atmospheric particulate sampler (Jinshida, Qingdao)
Tunahan Kaya et al., 2018	City environment – outdoor	9m^3	1/2hr	300 L/min	Specially build air pump device
Akhbarizadeh et al., 2020	City environment – outdoor	12096m^3	6 days	1400-1600 L/min	Tisch high volume sampler (TE-6070D, USA)

To address this knowledge gap, the following methodology was devised. A matrix of pumping rates and sampling duration (and therefore air quantity) were tested. For both parameters, four values were be tested – one lower limit, two middle values and one upper limit (see **Figure 4.4**).

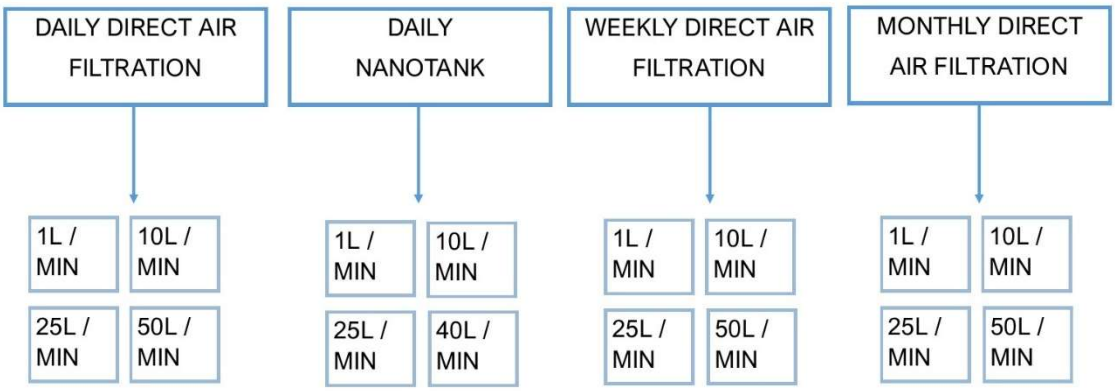


Figure 4. 4 Experimental Set Up- Pumping Rate and Sampling Duration values

The first parameter considered was pumping rate. The lower limit was constrained to 1 L/min, which was the lowest value reported in the literature (Syafei et al., 2019). The next parameter was 10 L/min which is another lower figure used (Dris et al., 2017; Gaston et al., 2020) and then 25 L/min. Finally, the upper limit to be tested was 50 L/min, used by Allen and colleagues (2020) in an ocean environment. This also was the upper limit of the direct air filtration sampling equipment used in this study.

The second parameter tested, sampling duration, followed the same framework. The lower limit of one day was chosen as this is the shortest period in which any sample is

thought to be valid in an urban location. This was also used by Abbassi and colleagues (2019) in an urban environment in Iran (see **Table 4.1**). This was not the lowest figure used in the literature (1 hour, **Table 4.1**); however, that study was for a much larger urban area and had much higher pumping rate (100L/min). It has also been argued that 24 hours is too little time for the detection limits of some air pollutants (Gaga et al., 2012). Hence a longer duration of 7 days was also chosen, which was the longest period reported for MPs in the literature (Akhbarizadeh et al., 2021). Finally, the upper limit chosen was 28 days. So far, no studies in atmospheric MPs have sampled for this long. We hypothesised that this limit could extend beyond the maximum limit for sampling durations. The selection of daily, weekly, and 28 days during a single 28-day period was to establish the failure point at which the system is no longer effectively collecting MPs and depositing them evenly across the filter in the pilot study location. Pump rate and duration were assessed to quantify the atmospheric MP sampling efficiency. The efficiency is based on the MP count found in each sample relative to negative controls (field blanks – see **Chapter 3**). The type of particle collected was also examined (polymer composition, shape and size). Based on this information recommendations on the ideal sampling duration and pumping rate, relative to field conditions, were made.

4.2.2 Micro-Raman (μRaman) spectroscopy

Micro-Raman (μRaman) spectroscopy was used to provide polymer characterisation, specifically identification of the types of plastic polymers within the different sample sets. This enables individual particles to be characterised through comparison of their μRaman spectra with established libraries of known plastic polymers (Enyoh et al., 2019).

A selection of the samples were analysed with μRaman spectroscopy (58% of samples, 46 unique individual samples completed in triplicate) to gain a picture of the polymer composition of the dataset. While it would be ideal to undertake analysis of the totality of all filters using μRaman, the resource (both financial and time) required to achieve

this with a sample set of 76 sample types and timesteps (n = 228 including triplicate assessments) make this unviable. Therefore, a selection of daily direct air filtration samples, nanotank daily samples, weekly and monthly direct air filtration samples, were selected for μRaman analysis. The μRaman spectrometer (Horiba Scientific, XPlora Plus, University of Strathclyde) employed a 785nm laser with a 1200mm^{-1} grating and 50μm split settings. The spectrometer was set to collect spectra between 200-2000 cm^{-1} Raman shift for all particles down to 1.6 μm, with an acquisition time of 10 seconds and 2 accumulations and with power at 35mW. Each sample was analysed in triplicate across three areas (≈1% of the filter in each sub-sample window, 1x1mm). There was no bias in the particle selection for analysis based on colour, shape, or size (all particles were analysed irrespective of appearance), and the filter was also analysed for background spectra analysis. There were >100 particles analysed per subsample. This sub-sample area selection was used to provide a representative sample (>100 particles) (Zhao, Dahal, & Marfil-Vega, 2020; Cowger et al., 2024) within a sensible and achievable time frame. The resulting spectra were saved as SPC files and analysed using Spectragryph (version 1.2.15) (Menges, 2022). Multivariate analysis of each spectra was completed and reference libraries were used to confirm polymer identification (SIMPLE, SLOPP and SLOPPE databases and the laboratory reference plastics spectral database (Jin et al., 2022; Levermore et al., 2020; Xu et al., 2020b)). Particles were only confirmed as plastic if a HIT (hit quality index) rate of ≥80% was achieved (Cowger et al., 2020; Levermore et al., 2020), and those below the <80% threshold discounted as non-plastic particles.

4.2.3 Nile Red staining

In order to gain information on the size and shape of the MP particles and a comprehensive particle count, samples were also analysed with Nile Red fluorescence microscopy. Fibres were identified using the standard 1:3 width ratio as used frequently within MP studies (Na et al., 2024; Li et al., 2020), and the rest are classified as fragments. A 1% (1μg mL^{-1}) Nile Red solution was used to stain the samples, which were then oven dried at 30°C overnight and then stored in a fridge 4ºC in sealed

aluminium containers to rest before they were imaged with the fluorescent microscope. This process of drying, cooling and de-energizing (in the dark) can aid with the MP staining and fluorescence efficiency as well as minimise staining and fluorescence of organics resulting in false-positives (Galvão et al., 2023). All samples that were not subject to µRaman analysis were imaged with a fluorescence microscope (Nikon Eclipse LV100ND), using a x10 objective and fluorescence mode (with QMA Whatmann with 1.6µm pore size), and a 470nm wavelength lamp. A transect of images (1.4 x 0.94 mm each) was taken from the top to the bottom of the filters resulting in 20% of the filter being analysed (taking into consideration the sub-sample method findings of (Huppertsberg and Knepper 2018). The software FIJI/ImageJ (Schindelin et al., 2012) enabled automated particle count, shape and size. Resulting MP counts were then calculated relative to the total area of the area analysed and extrapolated for the total area of the filter.

4.2.4 Microplastic contamination prevention

Multiple steps were taken to ensure that contamination of MPs was minimised at each step of the data collection and analysis process. In the field, the equipment was set-up away from any potential interference or contamination. In addition to this, only natural materials were worn during the collection of samples (wool, cotton) and blanks were taken during sample collection, in the processing laboratories in Glasgow. The University of Strathclyde, where sample preparation and all Nile Red staining and images were produced, has a MPs clean lab where only natural materials are permitted to be worn, cotton lab coats are used, there is an air filter used, cleaning with ethanol and milli-Q is conducted regularly and access is limited in order to minimise contamination. In addition, the filters used to collect samples and the stainless-steel containers used to store and transport the samples were heat treated before use (~450℃ oven for 15 minutes). The ethanol used for field sampling was vacuum filtered before use (Whatmann QMA filters with 1.6µm pore size) and blanks of the milli-Q, ethanol and the milli-Q/ethanol solution were taken. All blanks were treated in the same way

as the samples, with one field blank and one procedural blank (see **Chapter 3**) being analysed with μRaman spectroscopy to gain an understanding of polymer contamination, and the rest stained and imaged with Nile Red to understand the particle size, shape and number of particulates from contamination. All results have been adjusted to account for the contamination found in these field and procedural blanks based on their particle size distribution from the Nile Red staining of blanks, and all samples blank corrected based on the polymers presence in the field and procedural blanks. The polymers identified in both the procedural nanotank blank and the field blank taken, which have been subtracted from the particle counts.

4.2.5 Statistical analysis

To calculate the amount of MPs in each deposited and suspended sample, the following sets of equations for used.

To calculate the number of MPs per sample (all samples):

$$\mu P = (P_s/A_s) \times A_f$$

μP = MP per total sample

P_s = MP particles in the subsampled area (count)

A_s = area subsampled (mm^2)

A_f = area of total filter (mm^2)

For individual suspended samples (direct air filter and nanotank), to calculate the volume of air per sample, following equation was used:

$$V = (t_s \times f_s)/1000$$

t_s = time (mins) for the total sample

f_s = flow rate (L/min) for the sample

V = air volume sampled (m^3)

For the suspended air samples (nanotank and direct active air samples), the total representative MP per m^3 is calculated as:

Total suspended MP = µP/V (MP/m^3) , which in long had is:

$$= ((P_s/A_s) \times A_f)/ ((t_s \times f_s)/1000)$$

Filters were generally 47mm diameter for direct air filtration samples, and 25mm diameter for nanotank samples.

4.3 Results and Discussion

4.3.1 MP content for Pumping Rate and Sampling Duration

The particle counts for each pumping rate and sampling duration are reported as a result of both µRaman analysis and Nile Red staining (see **Appendix V** for supplementary data). Time weighted average MP for each parameter expressed as MP per total filter and MP per m^3 can be found in **Table 4.2.** Standard deviations are included to illustrate variability of daily (n=7) and weekly (n=4) sampling but not possible for the 28-day sampling (n=1). As the samples were taken on different days in an environmental setting, the concentrations of MP found on each day will be subject to daily variations. Therefore the standard deviation is representative of variability rather than error with the sampling system and parameters tested. Furthermore, the contamination measured with the field and procedural blanks has been subtracted from the concentrations reported here and is therefore not part of the variability found.

Table 4.2 MP Average Particle Counts Expressed as Total MP per Filter and Average Particle MP Counts Expressed per m^3 and MP (Appendix Table V.1)

MP Average Particle Counts Expressed as Total MP Count per Filter			
Sampling Duration	**Pumping Rate**	**Time Weighted Average**	**Standard Deviation**
Daily	**1L/min**	13700	12300
	10L/min	21400	7600
	25L/min	23200	39900
	50L/min	67200	63100
Nanotank	**1L/min**	2890	4650
	10L/min	3530	4620
	25L/min	3460	3360
	40L/min	1820	1650
Weekly	**1L/min**	12500	17200
	10L/min	57600	76300
	25L/min	15500	18600
	50L/min	59500	47100
Monthly	**1L/min**	1180	NA
MP Particle Counts Reported per m^3			
Sampling Duration	**Pumping Rate**	**Time Weighted Average**	**Standard Deviation**
Daily- Direct Air Filtration	**1 L/min**	9440	8740
	10 L/min	1500	533
	25 L/min	649	1120
	50 L/min	940	882
Daily - Nanotank	**1 L/min**	2010	3230
	10 L/min	247	3230
	25 L/min	96.8	93.9
	40 L/min	31.8	28.9
Weekly- Direct Air Filtration	**1 L/min**	1220	1730
	10 L/min	572	7590
	25 L/min	60.9	74.8
	50 L/min	118	94
Monthly- Direct Air Filtration	**1 L/min**	203	NA
	10 L/min	160	
	25 L/min	22.3	
	50 L/min	0.1	

MP counts per filter generally increase as pumping rate increases (**Table 4.2**), which is expected because of the increased air volume across the filter. Interestingly, the range of MPs recovered from the weekly and monthly samples is consistent with the daily samples, suggesting that filters from the weekly and monthly samples are becoming overloaded (blinded). If these results are converted to MP per m^3, as is often used in atmospheric MP studies, these results can be compared directly. Daily direct air filtration samples retained the largest amounts of MP particles compared to the

weekly and monthly sampling or the daily nanotank sampling system (**Table 4.2)**. Similarly, the slowest pumping rate (1 L/min) retained the most MPs per unit volume sampled and, as the pumping rate increased, the average particle collection decreased. The nanotank also displayed a similar trend with average particle collection per m^3 decreasing as the pumping rate increased.

Because sampling periods overlapped, the sum of the MP recovered in the daily samples were compared to the weekly samples that were collected during the same 7-day period across all four pumping rates (**Figure 4.5**). The sum of MP in the 7 daily samples exceeded the weekly samples across all pumping rates (**Figure 4.5A**). MP collected per filter increased with as pumping rate increased. Again, normalising to MP per m^3 sampled, the lowest pumping rate (L/min) collected the most MP (**Figure 4.5B**). The average particle collection decreases as the pumping rate increased from 1 L/min to 25 L/min. A small increase was observed as the pumping rate increased to 50L/min, but MP recovered per unit volume remained less than what was recovered by the 1 L/min and 10 L/min pumping rates. Based on these results, the 1 L/min daily sampling is the most effective set of conditions among those tested for this location; however, a lower pumping rate and/or more frequent sampling should be evaluated to determine optimal sampling conditions.

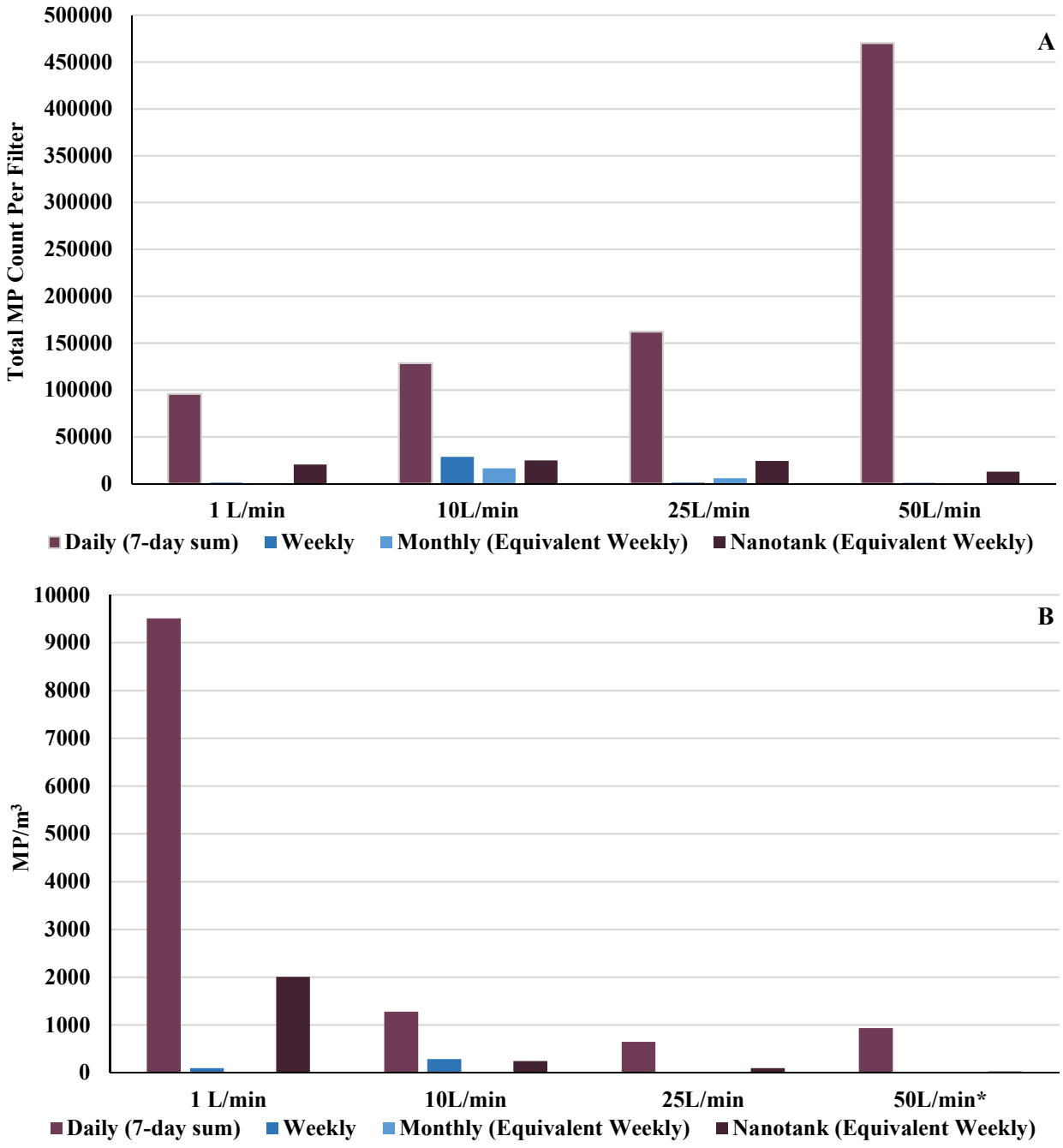


*Figure 4.5 (A) Bar Chart displaying normalised results for each sampling duration and pumping rate expressed as total MP count per filter; (B) Bar Chart displaying normalised data for each sampling duration and pumping rate particles per m^3; (C) Bar Graph displaying nanotank daily sampling frequency particle counts expressed as total MP count per filter (*NB: 40 L/min was the maximum limit for the nanotank sampling but is presented as 50 L/min here) (D) Bar Graph displaying nanotank daily sampling frequency particle counts expressed as particles per m^3*

4.6.1 MP Size Distribution for Pumping Rate and Sampling Duration

From the Nile Red analysis, it showed that the majority of particles were <250µm (53.7%) but there was variation in particle size between the sampling durations and pumping rates (**Table 4. 3**).

Table 3.3 Particle Size Distribution of MP Particulates as Percentage of Particles Identified (Nile Red) (Appendix Table V.2-5)

Size Range	Daily	Nanotank	Weekly	Monthly
1.6-10µm	92.6%	69.4%	83.1%	72.8%
10-20 µm	6.1%	22.4%	13.3%	20.0%
20-30 µm	1.0%	4.8%	1.7%	4.6%
30-40 µm	0.2%	1.6%	1.0%	1.1%
40-50µm	0.0%	0.9%	0.0%	0.5%
50-100µm	0.0%	0.7%	0.2%	0.6%
100-150µm	0.0%	0.1%	0.4%	0.2%
150-200µm	0.0%	0.0%	0.1%	0.1%
200-250µm	0.0%	0.0%	0.1%	0.1%

The daily sampling duration using direct air filtration collected particles with a smaller size distribution with 92% of particulates identified <1 0µm, followed by 6% in the 10-20 µm range. This indicates that daily sampling is more biased to collecting the smallest MP particulates compared to longer sampling durations. Within the different pumping rates tested within the daily sampling duration, the particle size distribution remains fairly similar with the majority of particulates <10 µm (see **Figure 4.6A**) but there is some variation between the different pumping rates. From **Figure 4.6A** it can be observed that the 25 L/min rate collected a wider range of particle sizes compared to the other pumping rates tested, which may be desirable in order to observe a wider range of particle characteristics. It is interesting to note that the 50 L/min rate collected the highest average MP/Filter but shows the smallest range in particle size distribution for daily direct air filtration.

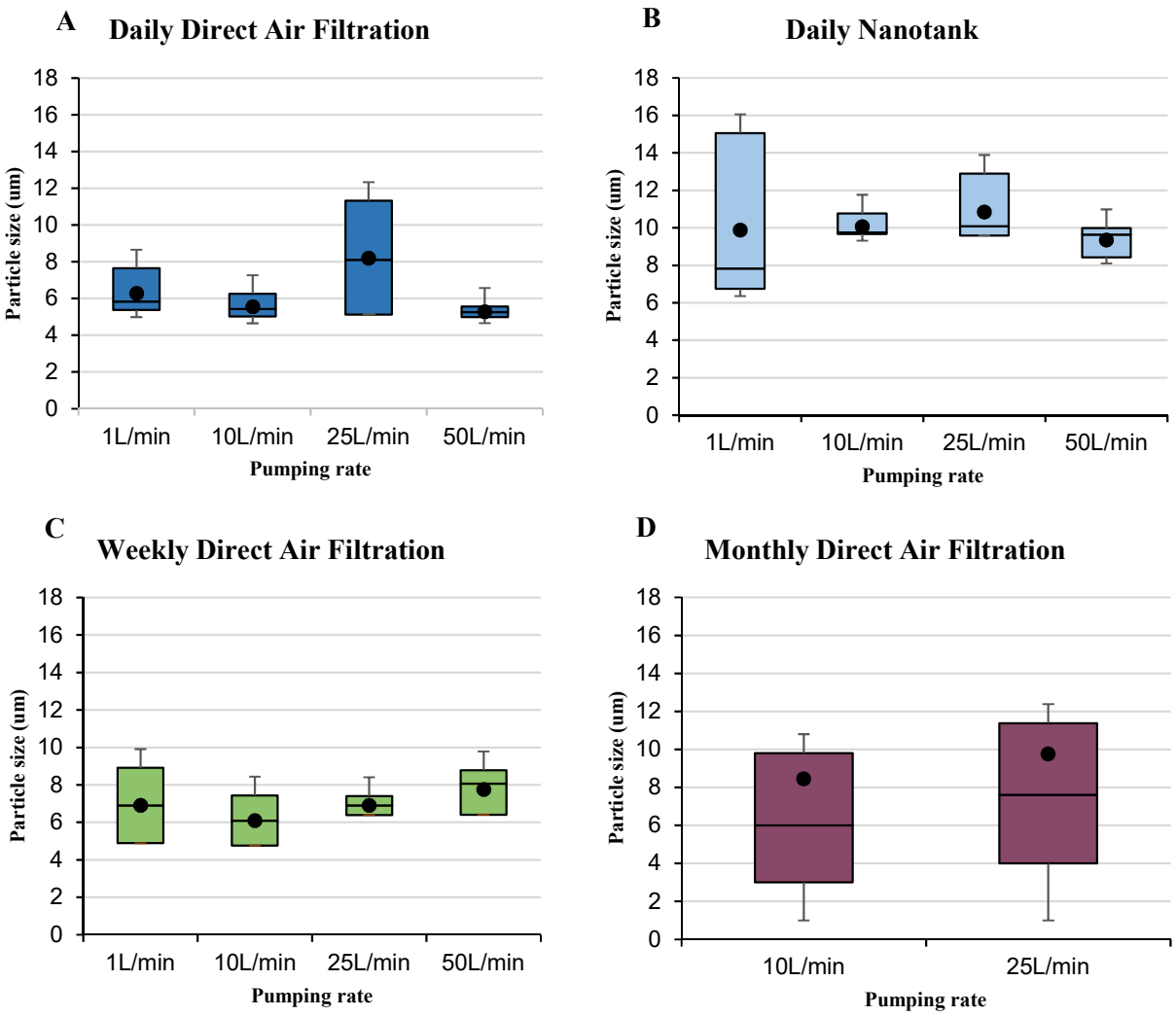


Figure 4. 6(A) Box Plot showing particle size distribution of identified MP particles using Nile Red staining, for samples using direct air filtration and daily sampling duration n = 21 ; (B) Box Plot showing particle size distribution of identified MP particles using Nile Red staining, for samples using a nanotank sampling system and daily sampling duration n= 15; (C) Box Plot showing particle size distribution of identified MP particles using Nile Red staining, for samples using direct air filtration and weekly sampling duration n = 9 ; (D) Box Plot showing particle size distribution of identified MP particles using Nile Red staining, for samples using direct air filtration and monthly sampling duration n= 2 (only two monthly samples analysed with Nile Red)(Appendix Table V.2-5)

The nanotank sampling system showed a more varied particle size distribution with 69.4% of identified MP particulates <10µm, followed by 10-20µm (22.4%), and then 20-30µm (4.8%). From **Figure 4.6B** it can be observed that the 1 L/min pumping rate displayed the largest range of particle size distribution of the pumping rates using this

system. The particle sizes across all four pumping rates in the nanotank were larger than particle sizes in the corresponding direct air filtration systems (**Figures 4.6A** and **B**), which suggests that direct air filtration may be more effective at collecting the smallest particles (1.6-11µm).

In terms of the weekly sampling duration, there is again a high proportion of particles identified <10µm (83.1%), again followed by 10-20µm. From **Figure 4.6C** and **Table 4.3**, it can be observed that the weekly sampling system collected more larger particle size ranges. It is clear there is a similar average particle size for reach pumping rate, with the median and mean at similar values. Again, there is not a corresponding increase in particle size ranges observed with the increase of average MP count per filter.

The monthly sampling duration shows the biggest range in particle size distribution. There is still a high proportion in the <10µm range (72.8%), but with a higher percentage in the >10µm size range compared to the other direct air filtration sampling durations (**Table 4.3**). In **Figure 4.6D** it can be observed that there is a bigger range in size distribution and the average particle size is higher than the other sampling durations rested. There is an increase in the average particle size as the pumping rate is increased to 25 L/min and there is a similar range in particle size distribution to the 10 L/min rate, but the range is more unevenly distributed in the lower quartile, with a larger lower outlier. As the 10 L/min pumping rate was the most effective rate at collecting MP particles within the monthly sampling duration (**Fig 4.6D**), it is promising that this rate could collect a range of particle sizes.

4.3.3 MP Shape Characteristics for Pumping Rate and Sampling Duration

In terms of shape, the MP particles identified were divided into two categories – fibre and fragment. Fibres were identified using the standard 1:3 width ratio as used frequently within MP studies (Na et al., 2024; Li et al., 2020). There was some variation in the proportion of fibre and fragment amongst the different sampling

durations and pumping rates. The daily sampling duration via direct air filtration (n=21) did not collect a high number of fibres overall with 98.82% of particles identified as fragments after blank correction. The 1 L/min pumping rate did not collect any fibres, but the 10 L/min collected the highest proportion of fibres (0.07%), followed by 25 L/min (0.04%). Then as the pumping rate increases to 50 L/min again no fibres were present after blank correction. The nanotank sampling system with daily sampling (n=15), was much more effective at collecting fibres with 47.1% of identified particles as fragment, and 52.9% of particles as fibres. This ratio was consistent across the 1 L/min, 10 L/min and 25 L/min pumping rates with approximately 47% fragment to 52% fibre. The 50 L/min displayed a slightly larger distribution of fibres (54%) to fragment (45.8%). Although the nanotank sampling system was not as effective in terms of average MP collection it is interesting to observe that it appears to be more effective at collecting a wider range of particle characteristics, and the direct air filtration method may be more biased at collecting fragments. This may be due to the fibres being entrained in a liquid medium in the nanotank but they may be re-entrained with the direct air filtration device as it has a wider inlet than the nanotank.

The weekly sampling duration (n=9) showed a similar distribution of fragment to fibre as the daily direct air filtration with 1% of MPs being identified as fibres. It also shows similar trends across the pumping rates with a small percentage of particles being identified as fibres with the 1 L/min, 10 L/min and 25 L/min rates displaying $<\approx 1\%$ of particles as fibres. When the pumping rate is increased to 50 L/min for the weekly sampling duration the proportion of fibres increases to 1.5% which may correspond to this pumping rate collecting the highest average MP particle count per filter for the weekly sampling duration.

By increasing to a monthly sampling duration there is again a similar distribution of fibres to fragment with 2.17% of MP particles classified as fibres (n=2). There is a slight increase in the proportion of fibres as the pumping rate increases from 10 L/min (1%) to 25 L/min (2%). As the other monthly samples were analysed with μRaman

which did not have the capacity to report on shape and size, it is not known if the smaller or higher pumping rate showed similar patterns of shape distribution. It is interesting to note that the 10 L/min pumping rate collected more particulates than the 25 L/min, but collected less fibres, which makes the difference in fragment and fibre composition surprising. It should also be noted that by increasing the sampling duration from weekly to monthly, there is a similar composition of fibre (2%) to fragment (98%), despite less MP particles being collected with a monthly sampling duration.

4.3.4 Polymer Composition for Pumping Rate and Sampling Duration

From the μRaman analysis, the polymer composition of 58% of the samples was examined. Of the polymers identified, the predominant polymers were Polymethyl methacrylate (PMMA, 16.9%), Polysulfone (PLS, 14.5%), Acrylic (14.2%), and Polyethersulfone (PES, 11.7%). PMMA is often found in windows, automotive lighting and road signage given its durability. PLS is used commonly for medical and laboratory applications as it can withstand repeated sterilisation, and is also used in the food industry as its resistance to chemicals make it appropriate for food processing and microwave-safe dishes. Acrylic is a versatile polymer and is used in construction, for medical, electronic and transport applications. Finally, PES is used for its stability under high temperatures so it is used for filtration membranes, industrial and aerospace applications and electrical equipment. High proportions of these polymers would be expected in an urban environment in which the samples were taken. Each parameter displayed fairly similar polymer composition, as can be observed from **Figure 4.7.**

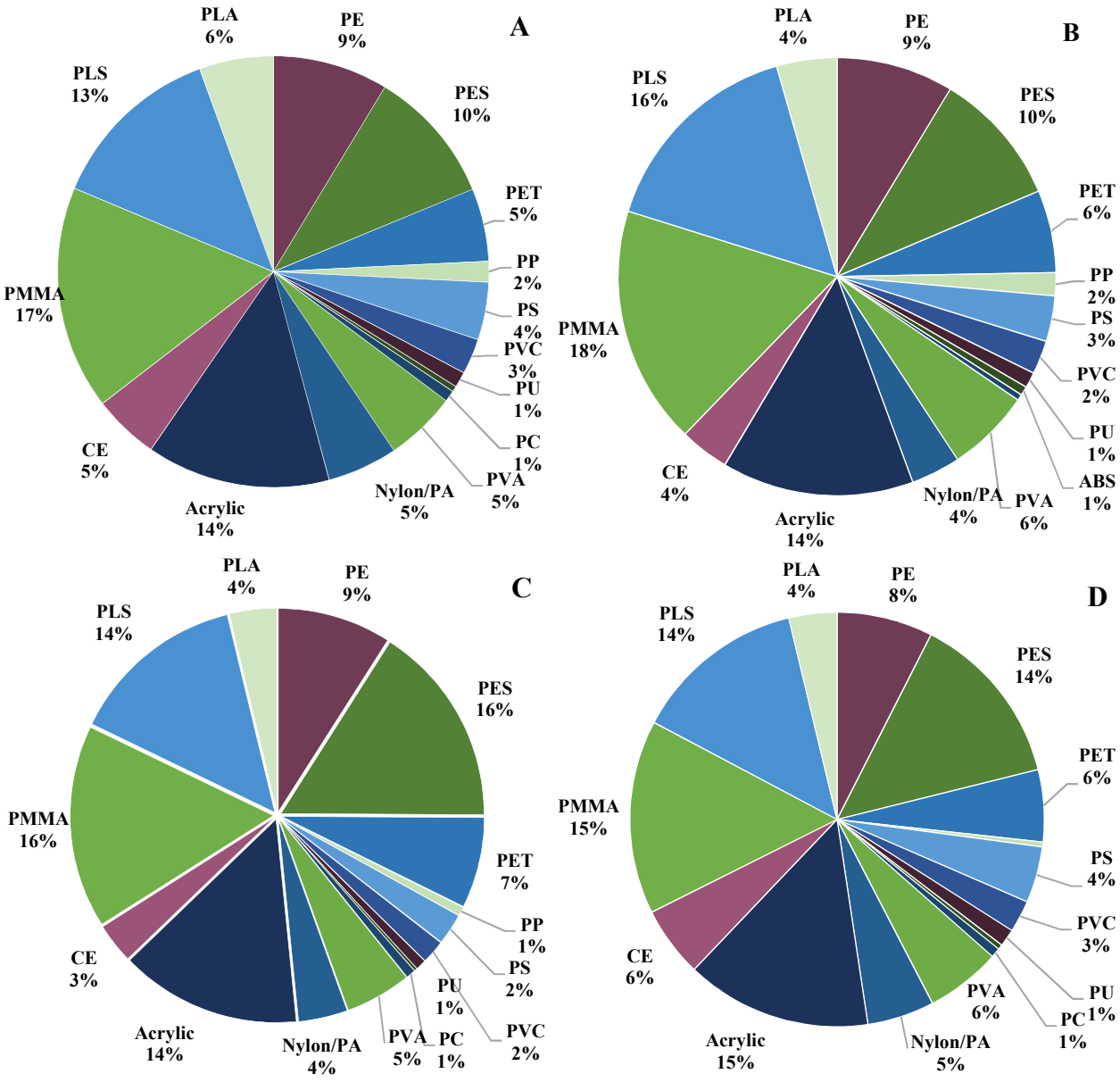


Figure 4. 7 Pie Charts Showing Polymer Composition of Each Sampling Duration as Percentage of Polymers Identified n= 9196 A. Daily Sampling Duration Polymer Composition (Direct Air Filtration) B. Nanotank Daily Sampling Duration Polymer Composition C. Weekly Sampling Duration Polymer Composition D. Monthly Sampling Duration Polymer Composition (Appendix Table V.6)

Daily sampling displayed slightly more Polycarbonate (PC, 1%) and Polylactic acid (PLA, 6%) than other samples. Nanotank sampling displayed slightly more Polypropylene (PP, 2%) than others. Weekly samples appear to have collected slightly

more Polyethylene terephthalate (PET,7%), Polyethersulfone (PES 16%), Polymethyl methacrylate (PMMA, 16%) and monthly samples collected more Polyvinyl chloride (PVC, 3%), Cellulose (CE, 6%) and Acrylic (15%). These slight differences could be due to the changing wind patterns over the month period or other localised influences. However, these are slight differences and overall polymer composition is similar over the pumping rates and sampling durations which indicates that pumping rate and sampling duration are not selective for polymer composition.

4.3.5 Thresholds and Recommendation for Future Research

Overall considerations need to be made when choosing the sampling duration and pumping rate for an active sampling campaign for atmospheric MPs. Although it is helpful to have definitive thresholds for effective particle collection to prevent under-reporting particle concentrations, the most effective parameters for collecting the perfect sample will be different depending on the environment in which the sample is collected, and the research question that is being asked. It is clear that for all samples, apart from the weekly sampling duration, the highest parameter of 50 L/min (or 40 L/min for nanotank samples) is the upper threshold, where the sampler is no longer effectively collecting particulates. But there is nuance in the most effective pumping rate and sampling duration beneath that threshold. From **Table 4.4** it can be observed that by increasing the pumping rate, there is not necessarily an increase in the ratio of MP per m^3 to MP per Filter, which may be expected if you are sampling a higher volume of air. It would be fair to assume the longer sampling durations would collect a concentration of MP particulates that is cumulative of the daily sampling regimes, but it is evident from the numbers presented above that this is not the case. Therefore, sampling a smaller volume of air may result in a higher payoff when it comes to choosing the most effective duration and pumping rate for your research question.

Table 4.4 Ratio of MP per m^3 to MP per Filter for Each Sampling Duration and Pumping Rate

Sample Name		Average MP/m^3	Average MP/Filter	Ratio of MP/m^3 to MP/ Filter
Daily	**1 L/min**	9435.8	13686.9	0.7
	10 L/min	1498.4	21427.5	0.1
	25 L/min	649.3	23196.0	0.0
	50 L/min	939.6	67184.4	0.0
Nanotank	**1 L/min**	2012.3	2892.3	0.7
	10 L/min	246.7	3528.8	0.1
	25 L/min	96.8	3461.8	0.0
	40 L/min	31.8	1821.4	0.0
Weekly	**1 L/min**	1219.5	12470.9	0.1
	10 L/min	572.1	57626.5	0.0
	25 L/min	60.9	15530.6	0.00
	50 L/min	118.1	59498.2	0.00
Monthly	**1 L/min**	23.2	1177.2	0.0
	10 L/min	162.3	65404.3	0.00
	25 L/min	22.3	22509.6	0.00
	50 L/min	0.1	242.1	NA

One of the aims was to examine if a new method of active sampling for atmospheric MP – the nanotank – was more effective than the traditional direct air filtration method. It was assumed that by collecting particulates in a liquid media that there would be a reduced opportunity for particle re-entrainment into the atmosphere. However, these results indicate that the nanotank does not perform better than direct air filtration. The procedural blanks for the nanotank were also higher than the direct air filtration field blanks (see **Appendix V**), which indicates that the opportunity for contamination between samples is more likely with this method. However, it does still collect MP in a cost-effective manner, and although polymer composition was not too dissimilar to the other direct air filtration samples, it does appear to collect a different size fraction to the direct air filtration system. Daily direct air filtration samples collected more particles in the smaller size ranges (<10 μm) and the nanotank sampling system displayed a more varied particle size distribution. It also showed a more even distribution of particle shapes, with more fibres identified than the direct air filtration system. This could be to the larger particle sizes, size distributions, and shapes being

entrained in the liquid media in the nanotank compared to the filter used in the direct air filtration system. Furthermore, the nanotank was only tested with a daily sampling frequency. If the nanotank is to be used, it is evident that the 1L/min pumping rate had the highest average MP count per m^3 and collected a wide range of particle sizes compared to the other parameters tested. The 50 L/min rate tested did collect a slightly higher proportion of fibres than the other parameters, but the difference between the 1 L/min rate is minimal. Therefore a 1L/min rate for the nanotank is optimal in terms of average MP particle collection per m^3 and in terms of collecting a representative particle size and shape range. However, as Glasgow is an industrial city with a high population, a higher pumping rate or longer duration may be necessary in more remote locations. Future research could look to develop the nanotank to improve overall MP collection efficiency.

The direct air filtration system with a daily sampling frequency was more effective on average at collecting particulates across the different pumping rates, than the nanotank system. By utilising a pumping rate of 1 L/min, the highest average MP count per m^3 was achieved. The 25 L/min rate tested collected the widest particle size range despite collecting a much smaller concentration of MP particles per m^3. If the research aim was focused on the size characteristics of atmospheric MP pollution then a 25 L/min rate may be preferable, but in terms of collecting the smallest particles and reporting accurate MP concentrations, the 1 L/min rate was more effective than the higher pumping rates. In terms of shape there was not much difference between the proportion of fibres and fragments between the pumping rates tested. The longer pumping durations are not representative of atmospheric MP concentrations in this area. Therefore, longer sampling durations are not recommended in urban environments.

Sampling duration and pumping rate do not vastly impact the polymer composition found in the samples, which is an important consideration if monitoring polymer composition over time is a key aim. In terms of characteristics, the pumping rate and sampling duration appears to not affect the shape and size of particulate collected. Longer sampling durations with an effective pumping rate may result in a small

increase in the fibres collected which may be of note if fibres are the main focus of a field campaign, but overall the main impact of adjusting the sampling duration and pumping rate is the number of particulates collected and the size distribution.

Overall, sampling duration and pumping rate impact how representative a sample will be in terms of particle collection and size distribution. Future studies should keep these considerations in mind when designing the field sampling campaign. For studies to report on MP concentrations accurately in a similar urban environment, daily direction air filtration with a 1 L/min pumping rate is advised. It is clear that using a longer sampling duration could result in considerably underreporting atmospheric MP concentrations. Studies looking to examine more remote locations with a potentially less polluted environment, should look to increase the sampling duration or pumping rate in order to collect a representative sample.

In order for the field of atmospheric MPs to move towards more harmonious and standardised methods, consideration for the research environment and sampling parameters needs to be the focus. To understand the influence of the sampling environment on the particle collection efficiency this study could be replicated in a range of environments – remote, rural, semi-rural, urban (more densely populated), and megacities – to test how the parameters perform relative to local population and pollution. As the daily sampling frequency was the lowest sampling duration tested in this study and produced the highest MP collection per volume of air, it would be interesting to observe if a more frequent sampling duration, such as twice or three times daily, or slower pumping rate (<1 L/min) would be more effective in more densely populated areas like cities and megacities. Once the thresholds for each environment are understood, practical guidance on how to adjust sampling parameters to produce representative results can be developed and facilitate the standardisation of methods used in the field. This would in turn enable more accurate comparisons across studies and environments.

4.6 Conclusions

This research addressed a key methodological gap in the emerging field of atmospheric MP by examining how sampling duration and pumping rate influence the effectiveness of sample collection. Despite increasing interest in atmospheric MPs, limited guidance exists on optimising these parameters to ensure representative and accurate sample collection. Different sampling durations and pumping rates were tested at a location in Glasgow, Scotland, to examine their outcome on the resulting sample. The sampling durations tested included daily, weekly and monthly direct air filtration sampling, as well as examining the effectiveness of a new sampling system – the nanotank – using a daily sampling duration. Alongside this, four pumping rates were tested including 1 L/min, 10 L/min, 25 L/min and 50L/min (40 L/min for nanotank sampling system).

The µRaman spectrometry results showed that the sampling duration and pumping rate did not vastly impact the polymer composition, which would be of interest if polymer composition was a main research outcome. Results from both the µRaman and Nile Red analysis, showed that MP concentration and size distribution were influenced by sampling parameters. The daily direct air filtration collected the most MP particulates per m^3 across the dataset.. Although the nanotank system was more effective at collecting fibres compared to direct air filtration, it is clear this system needs more development to ensure representative MP collection. The monthly sampling duration collected the largest particle size range, and showed a similar distribution of fibre to fragment to the weekly sampling duration, despite a decrease in overall particle collection. At 10 L/min monthly sampling achieved similar MP particle concentrations to the weekly sampling duration. However, after the data was normalised it is clear that a longer sampling duration is not collecting representative MP concentrations and the daily sampling duration is more effective in this urban environment.

For all the durations tested the upper failure point was to 50 L/min, likely due to filter overloading. The lower failure point was not reached, as the 1 L/min rate consistently collected more MP. Importantly, increasing the pumping rate or sampling duration,

did not result in a proportional increase in particle collection. The opposite was observed. Future work should examine pumping rates <1 L/min to find the lower failure point. As Glasgow is an urban and fairly polluted city, pumping rates and durations may need to be adjusted for research in more polluted or remote locations.

Overall, these findings emphasise that thought and care needs to be taken when planning an active sampling field campaign for atmospheric MPs. Future research should consider these parameters as early as possible in research planning, in order to avoid underestimating particle concentrations and to ensure representative sampling. Further research could examine these parameters in a controlled laboratory setting with a set quantity and type of MP to examine if this impacts the outcome of collection efficiencies. Research examining these parameters in a range of environments is also warranted to develop technical guidance and standardised methods. As the field of atmospheric MP expands and evolves, efforts should be made to improve the consistency of methods used to sample atmospheric MP levels so that the true extent of this pollutant can be known.

Chapter 5 – Remote Atmospheric Microplastic Pollution – Svalbard, Norway

This chapter presents research to answer the second research question (RQ2): "What are the concentrations and main characteristics (polymer composition, particle concentration, shape, and size) of atmospheric microplastics in a remote location (Svalbard, Norway), and how do these relate to weather conditions and potential transport pathways?". The manuscript version of this chapter which can be found in **Appendix VI.** The manuscript has been submitted to the journal *Nature: Earth & Science Communications* on the 5th of September 2025 pending peer-review.

5.1 Introduction

MPs have been reported in every environmental compartment in locations all over the world, from remote mountain catchments (Allen et al., 2019) to megacities (Liu et al., 2019b). MPs have been considered by some to be one of the most pressing concerns of this generation (Thomson et al., 2024) due to the extent of MP pollution, the associated risks to ecosystem function (Akdogan & Guven, 2019), human health (Jenner et al., 2022) and the climate system (Aeschlimann et al., 2022; Revell et al., 2021). MPs have been examined in marine and freshwater systems (Kye et al., 2023), but despite a recent increase in attention of the role of atmospheric transport of MPs (Zhang et al., 2019), there remain notable knowledge gaps. This is especially true in relation to atmospheric transport processes and the weather patterns that contribute to MP dispersion, suspension and deposition. Furthermore, given the nature of this transboundary pollutant, source appointment relies on particle modelling to trace transport patterns.

It is thought that atmospheric pathways are crucial in the transport of MPs to the world's remote regions such as the Arctic (Evangeliou et al., 2020) and Antarctica (Aves et al., 2022). The Arctic region has been described by some as relatively pristine due to its remote location and small population, and act as sentinels with regards to

pollution due to the unique environmental characteristics and ecosystems (Irrgang et al., 2022). The geographic location and distinctive climate make it an important indicator of global environmental health. It is also thought that the Arctic acts as a sink for global pollutants, primarily because of its cold climate and the prevalent atmospheric circulation patterns that transport pollutants from lower latitudes (Zhang et al., 2023b). Due to 'Arctic amplification' it is hypothesised that the Arctic region is warming up to four times faster than the rest of the world, which can affect weather patterns (Rantenten et al. 2022) and the vertical atmospheric transport of pollutants like MPs (Revell et al., 2021). Furthermore, the extensive and seasonally changing ice cover within the Arctic and seasonal variations in temperature and precipitation facilitate the accumulation and release of pollutants (Obbard et al., 2014), which can impact local ecosystems and the global climate system.

The deposition of atmospheric pollutants, including MPs, in the Arctic is facilitated by long-range atmospheric transport mechanisms that can transport contaminants and particulate matter thousands of kilometres away from their source (Zhang et al., 2020a). When suspended in the atmospheric compartment, MP can be transported by prevailing winds to the Artic region where they can accumulate in snow and ice. These precipitously detained MPs can then be transported via ice melt into the Arctic Ocean and impact wildlife and ecosystem functions (Emberson-Marl et al., 2023). MP contamination in the Arctic has been studied in the marine environment (Ramasamy et al., 2021) and has been reported in all levels of the Arctic food web (Bergmann et al., 2022).

While atmospheric MP deposition in the Arctic has been studied through snow sampling (Bergmann et al., 2019), measurement of suspended MPs has yet to be undertaken. Moreover, deposited and suspended particulates have not been measured in conjunction in the Arctic to date. It has been recommended that both forms of atmospheric measurements be conducted in order to create a more complete and comprehensive understanding of total atmospheric content and transport (Zhang et al., 2020a). This study aims to fill this gap by conducting a continuous 28-day sampling

campaign consisting of both active and passive measurements in the Arctic to quantify and collecting deposited and suspended atmospheric MPs. By examining both forms of particulates, it is hoped to gain a better understanding of how particle deposition and suspension influences atmospheric MP concentrations in this region and how this could be influenced by weather patterns and transport processes.

5.2 Methods

5.2.1 Sample location and collection

Ny-Ålesund is located on Svalbard and Jan Mayen, Norway, (**Figure 5.1A**) and hosts a number of research stations and activities supporting Arctic research. The station is located at 78.9237° N, 11.9227° E, and is considered as one of the most northern inhabited civilizations in the world. A former mining village, the site is now run by Kings Bay and hosts a range of international research stations (Kings Bay AS, 2021). The Ny-Ålesund research stations are defined and established, through past research and actions, as a primary Arctic research frontier and one of few truly high latitude Arctic research locations. From 17 May to 14 June 2022, a continuous 28-day atmospheric sampling campaign was conducted at Ny-Ålesund consisting of daily active and passive measurements, with the support of the Norwegian Polar Institute (NPI).

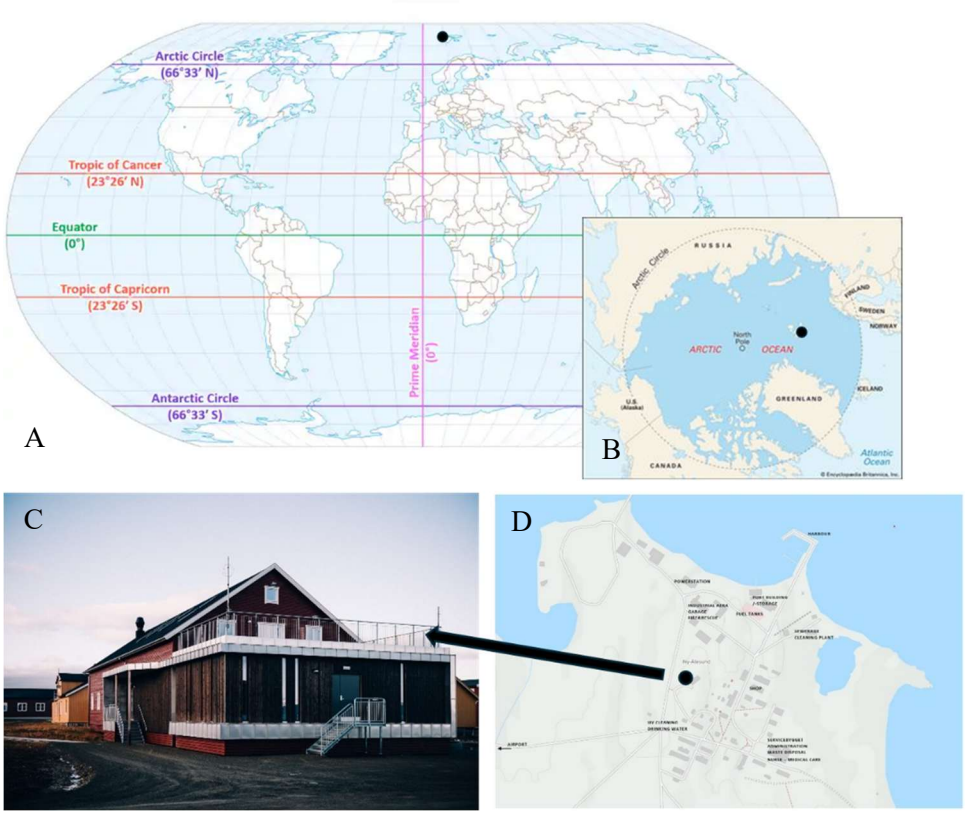


Figure 5. 1 Black points indicate Ny-Ålesund and the location of the research. (A) indicates the sample location relative to the extreme latitudes, (B) highlights the sample location within the more detailed visualisation of the Arctic circle. (C) indicates that actual building location where the sampling was undertaken (D) building and balcony used for sampling

The sampling equipment was placed on the roof of the Veksthuset research station at Ny-Ålesund (see **Figure 5.1D**) at ~4.5m above ground elevation (AGL). The equipment was mounted on a rail, away from the passing footfall of station staff, researchers and any possible tourists, and in an area where access was limited to minimise local contamination.

Passive deposition samples were collected using a deposition chamber (see **Figure 2A**) filled with a solution of 500ml of milli-Q water and 50ml of ethanol (20%) to collect deposited particulates and prevent the liquid from freezing at low temperatures. Quartz filters (Whatmann, QMA, 1.6µm pore size; 25mm) and replaced with a new solution daily.

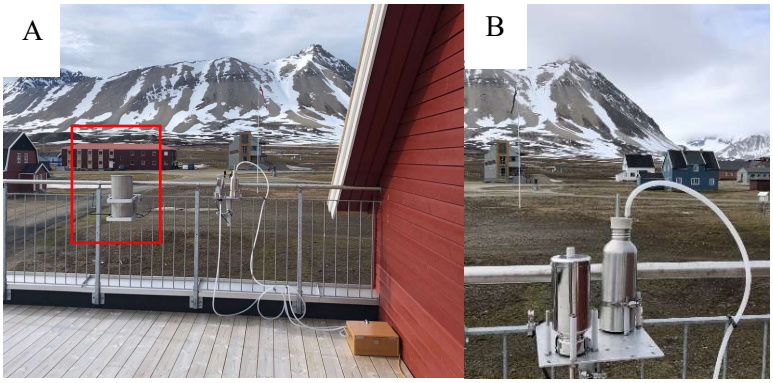


Figure 5. 2 (A) Passive (red box) and active equipment set-up on Veksthuset station roof; (B) Active equipment set-up at the Veksthuset station (air filter and nanotank samplers)

Active suspended atmospheric samples were collected using two comparative methods in order to capture a wider size range of particulates. The first method uses a pump to draw air into a sealed chamber and through 500 mL of sample collection solution (the same 10% ethanol/milli-Q water); this method is identified as the nanotank. The pumping rate was set at 15 L/min, and the nanotank collection solution was collected daily and vacuum filtered onto QMA filters (same porosity and make as used for the deposition samples). The second and commonly used suspended atmospheric sampling method employed was a standard direct air filtration sampler. Using a pumping rate of 20L/min, monitored with air flow measurer, air was drawn through the stainless-steel chamber where particulates were collected on the same QMA filters (see **Figure 5.2B)**. The filters were then switched every 3 days. All samples were stored in pre-treated aluminium tins prior to analysis.

5.2.2 Micro-Raman (µRaman) spectroscopy

Micro-Raman (µRaman) spectroscopy was used to provide polymer characterisation, specifically identification of the types of plastic polymers within the different sample sets. µRaman uses a laser to excite molecules within the selected particle, causing the release of photons and the resulting signal provides information on the chemical structure and molecular interactions. This fingerprint or signal dataset, incorporating both the chemical makeup and types of bonds, create a vibrational spectrum that is unique to individual plastic polymer types. Individual particles can be characterised

through comparison of these μRaman spectra and established libraries of known plastic polymers (Enyoh et al., 2019).

A selection of the samples were analysed with μRaman spectroscopy (23% of samples, 15 unique individual samples completed in triplicate) in order to gain a picture of the polymer composition of the dataset. While it would be ideal to undertake analysis of the totality of all filters using μRaman, the resource (both financial and time) required to achieve this with a sample set of 65 sample types and timesteps (n = 195 including triplicate assessments) make this unviable. Therefore, five days of deposition samples, five days of nanotank samples, and three active direct air filtration samples were randomly selected across the 28-day period and analysed using the μRaman. The μRaman spectrometer (WiTec Alpha 300 RA, Helmholtz Association, Leipzig) used employed a 532nm laser with a 1200mm^{-1} grating and 50μm split settings. The spectrometer was set to collect spectra between 200-2000 cm^{-1} Raman shift for all particles down to 1.6 μm, with an acquisition time of 10 seconds and 2 accumulations and with power at 35 mW. Each sample was analysed in triplicate across three areas (≈1% of the filter in each sub-sample window, 1x1mm). There was no bias in the particle selection for analysis based on colour, shape, or size (all particles were analysed irrespective of appearance), and the filter was also analysed for background spectra analysis. There were >100 particles analysed per subsample. This sub-sample area selection was used to provide a representative sample (>100 particles) (Zhao and Dahal, 2020; Cowger et al., 2024) within a sensible and achievable time frame.

The resulting spectra were saved as SPC files and analysed using Spectragryph (version 1.2.15) (Menges, 2022). Multivariate analysis of each spectra was completed and reference libraries were used to confirm polymer identification (SIMPLE, SLOPP and SLOPPE databases and the laboratory reference plastics spectral database (Jin et al., 2022; Levermore et al., 2020; Xu et al., 2020b). Particles were only confirmed as plastic if a HIT (hit quality index) rate of ≥80% was achieved (Cowger et al., 2020; Levermore et al., 2020), and those below the <80% threshold discounted as non-plastic particles.

5.2.3 Nile Red staining

In order to gain information on the size and shape of the MP particles and a comprehensive particle count, samples were also analysed with Nile Red fluorescence microscopy. Fibres were identified using the standard 1:3 width ratio as used frequently within MP studies (Na et al., 2024; Li et al., 2020), and the rest are classified as fragments. A 1% (0.1µg mL^{-1}) Nile Red solution was used to stain the samples, which were then oven dried at 30°C overnight and then stored in a fridge 4°C in sealed aluminium containers to rest before they are imaged with the fluorescent microscope. It has been reported that this process of drying, cooling and de-energizing (in the dark) can aid with the MP staining, fluorescence efficiency and minimise staining of organics resulting in false-positives (Galvão et al., 2023).

All samples that were not subject to µRaman analysis were imaged with a fluorescence microscope (Nikon Eclipse LV100ND), using a x10 objective and fluorescence mode (with QMA Whatmann with 1.6µm pore size), and a 470nm wavelength lamp. A transect of images (1.4 x 0.94 mm each) were taken from the top to the bottom of the filters resulting in 20% of the filter being analysed (taking into consideration the sub-sample method findings of Huppertsberg and Knepper (2018)). The software FIJI/ImageJ (Schindelin, et al., 2012) enabled automated particle count, shape and size. Resulting MP counts were then calculated relative to the total area of the area analysed and extrapolated for the total area of the filter.

5.2.4 Microplastic contamination prevention

Multiple steps were taken to ensure that contamination of MPs was minimised at each step of the data collection and analysis process. In the field, the equipment was set-up away from any potential interference or contamination from visitors and station staff . In addition to this, only natural materials were worn during the collection of samples (wool, cotton) and blanks were taken during sample collection, in the processing laboratories in Svalbard and in Glasgow. The University of Strathclyde, where sample preparation and all Nile Red staining and images were produced, has a MPs clean lab

where only natural materials are permitted to be worn, cotton lab coats are used, an air filter is used, cleaning with ethanol and milli-Q is conducted regularly and access is limited in order to minimise contamination. In addition, the filters used to collect samples and the stainless-steel containers used to store and transport the samples were heat treated before use (~450̊ C oven for 15 minutes). The ethanol used for field sampling was vacuum filtered before use (Whatmann QMA filters with 1.6 µm pore size) and blanks of the milli-Q, ethanol and the milli-Q/ethanol solution were taken. All blanks were treated in the same way as the samples, with one being analysed with µRaman spectroscopy to gain an understanding of polymer contamination, and the rest stained and imaged with Nile Red to understand the particle size, shape and number of particulates from contamination. All results have been adjusted to account for the contamination found in these field and procedural blanks based on their particle size distribution from the Nile Red staining of blanks (<30% of total plastic particle count), as there were no identified polymers in the blank subjected to µRaman analysis.

5.2.5 Statistical analysis

To calculate the amount of MPs in each deposited and suspended sample, the following sets of equations were used.

To calculate the number of MPs per sample (all samples):

$$\mu P = (P_s/A_s) \times A_f$$

µP = MP per total sample

Ps = MP particles in the subsampled area (count)

A_s = area subsampled (mm^2)

A_f = area of total filter (mm^2)

For individual suspended samples (direct air filtration and nanotank), to calculate the volume of air per sample, following equation was used:

$$V = (t_s \times f_s)/1000$$

t_s = time (mins) for the total sample

f_s = flow rate (L/min) for the sample

V = air volume sampled (m^3)

For the suspended air samples (nanotank and direct active air samples), the total representative MP per m^3 is calculated as:

Total suspended MP = µP/V (MP/m^3) , which in long had is:

$$MP = ((Ps/A_s) \times A_f)/ ((t_s \times f_s)/1000)$$

For total deposition samples

$$MP = \mu P/ A_d \ (MP/m^2)$$

$$V= (Ps/A\ s) \times A_f)/A_d$$

Where A_d = area of the deposition collector open to the atmosphere (m^2) (i.e. the deposition bucket base area).

Filters were generally 47mm diameter for active air samples, 25 mm diameter for nanotank samples and deposition samples. Sample durations ranged from ≈ 1430 mins for 24 hour (nanotank and deposition samples) or ≈ 4305 mins for 3 day set sampling durations (direct air filtration samples). Sample flow rates for active samples were 15 L/min for the nanotank and 20 L/min for the direct air filtration samples.

5.2.6 Relationship with Weather Parameters

One of the main research questions was to identify potential drivers of atmospheric MP pollution in this region and if there was a possible relationship between MP concentrations and weather parameters. Weather data collected at the Ny-Ålesund research station was collated from the Norwegian Centre for Climate Change repository (Maturilli et al., 2022a, 2022b; Norwegian Centre for Climate Services,

2022) for the sampling period May-June 2022. Due to the difference physical processes represented by the deposition vs the nanotank and active air samples, correlation analysis was undertaken for each sample type and atmospheric variable separately. The main weather parameters assessed were precipitation (mm), atmospheric pressure (hPa), humidity (mean dew point, mixing ratio), snow depth (cm), snow cover (%), wind speed (m/s), wind direction (and as an extension of this, whether the wind was land or sea-based). Pearsons correlation coefficient (r) was calculated for each variable and MP dataset along with the corresponding p-value.

5.2.7 Atmospheric dispersion modelling

The transport of MP to the sampling sites (receptor) was simulated using the Lagrangian particle dispersion model FLEXPART version 11 (Bakels et al., 2024). The model was driven by ERA5 assimilated meteorological analyses (Hersbach et al., 2020 with 137 vertical levels and a spatiotemporal resolution of 0.5°x 0.5° and one hour. FLEXPART treats gravitational settling (Tatsii et al., 2024), dry and wet deposition of aerosols (Grythe et al., 2018), turbulence (Cassiani et al., 2018), unresolved mesoscale motions (Stohl et al., 2015), and deep convection (Foster et al., 2007). FLEXPARTv11 uses a new feature that simulates non-spherical shapes (Tatsii et al., 2024), which makes it unique for MP considering that MP are usually in the shape of fragments or fibres.

Surface concentrations were simulated by releasing computational particles at heights 0–100 m from the receptor in the classic “retroplume” mode. Wet and dry deposition at the receptor was simulated separately (Eckhardt et al., 2017). Specifically, wet deposition was reconstructed after releasing computational particles at the sampling site (receptor) at altitudes of 0–20 km above sea level and wet removal was calculated using different coefficients for in-cloud and below-cloud scavenging. For dry deposition, computational particles were released at 0–30 m at the same receptor point, as this shallow layer is equal to the height of the layer in which, in forward mode, particles are subject to dry deposition. All released particles represent a unity

deposition amount, which was converted immediately (i.e. upon release of a particle) to atmospheric concentrations using the deposition intensity as characterized by either the dry deposition velocity or wet scavenging rate (Grythe et al., 2018).

The model output consists of a footprint emission sensitivity that expresses the probability of any emission occurring in each grid-cell to reach and/or deposit at the receptor. It is converted to modelled concentrations or deposition rates, when coupled with gridded emissions. Modelled concentrations or deposition rates can be calculated as a function of the time elapsed since the emission has occurred namely "age spectrum", for specific regions/continents ("continent spectrum"), and for different source categories ("source spectrum"). Here, we coupled footprints with updated emissions from Evangeliou et al. (2022) that were derived with top-down approach.

5.3 Results

5.3.1 Microplastic Concentrations: Suspended and Deposited Particulates

From the μRaman and Nile Red fluorescence particle analysis, the average deposition rate of MP particles during this period was 37.3 $\pm$ 30.2 MP/m^2. The highest reported deposition sample was taken on 26 May 2022 with 127.5 MP/m^2 (Deposition sample number 9), and the lowest (8.20 MP/m^2) was taken on 06 June (Deposition sample number 20). MP concentrations for each timestep (for deposition) and sample type are displayed in **Figure 5.3** (see **Appendix VII** for supplementary data).

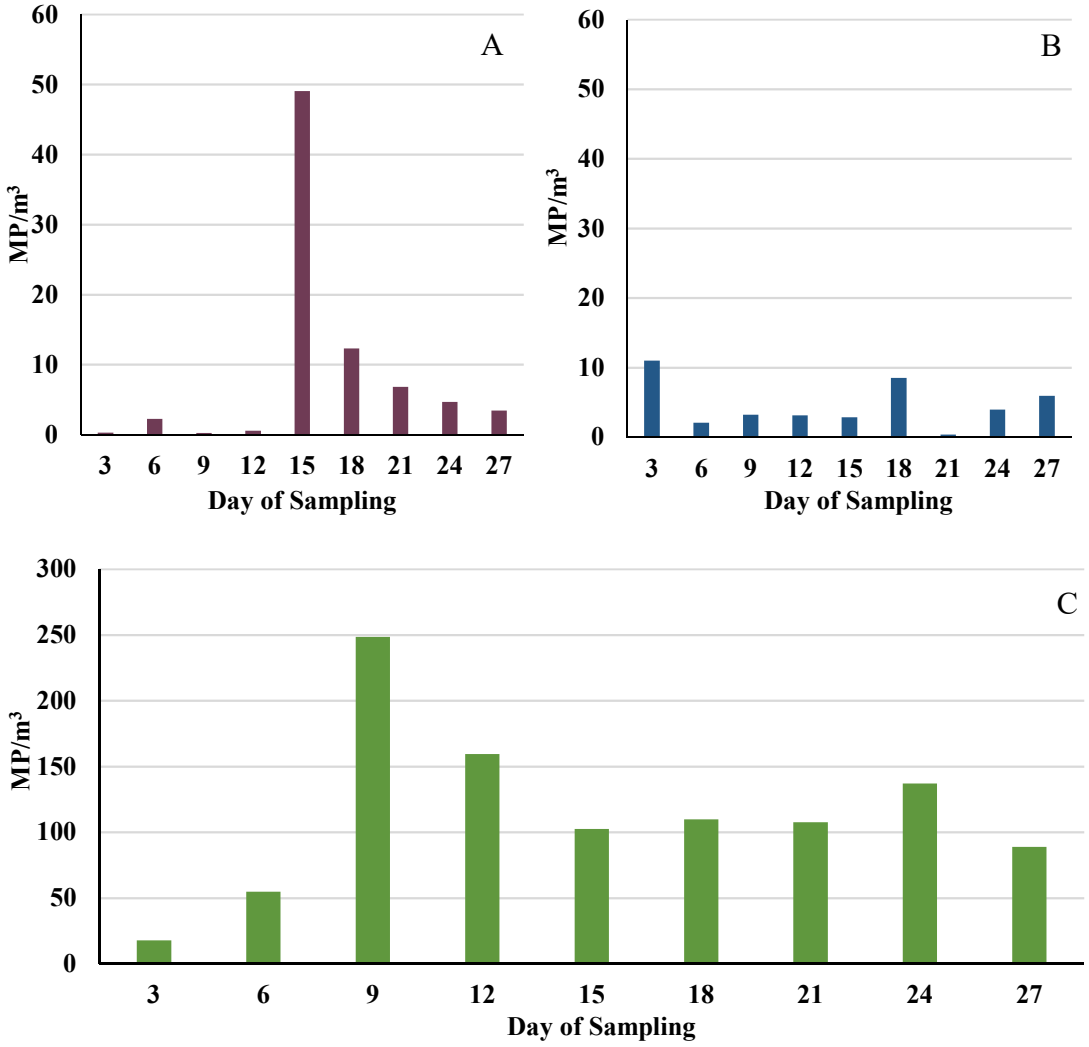


Figure 5. 3 MP concentrations for active direct air filtration samples (MP/m^3); b) MP concentrations for active nanotank samples MP/m^3 c) MP concentrations for passive (deposition) samples (MP/m^2); error bars indicate standard deviation. Nanotank and Deposition samples represent daily sampling, while each direct air filtration sample was collected for three days (Appendix Table VII.1).

The average MP concentration for suspended particulates was 4.2 $\pm$ 9.4 MP/m^3 (with nanotank samples 1.5 $\pm$1.8 MP/m^3 and direct air filtration samples at 8.9 at 8.9 $\pm$ 15.6 MP/m^3). The highest concentration of suspended particulates was 49.06 MP/m^3, taken with a direct air filtration sampler between 29 May and 01 June (direct air filtration sample number 5, **Figure 5.4**), and the lowest concentration from direct air filtration samples from 20-23 May with 2.3 MP/m^3 (direct air filtration sample number 2, **Figure 5.4**).

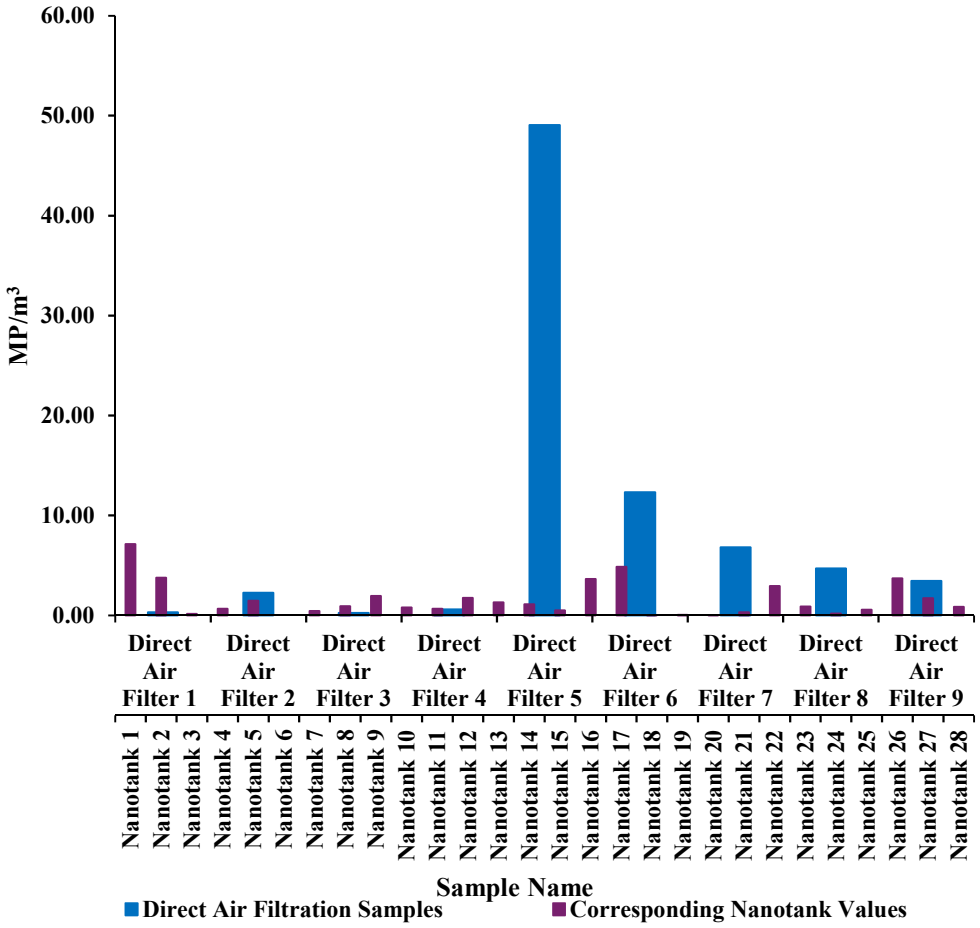


Figure 5. 4 MP Concentrations for Active/Suspended Samples; Direct Air Filtration with Corresponding Nanotank Values (Appendix Table VII.I)

For the nanotank samples, the procedural blanks were fairly contaminated, which was likely due to the milli-Q supply (see Appendix VII). The highest nanotank concentrations were found on 18 May with 7.1 MP/m^3 (Nanotank sample number 1), with the lowest day with no particles present after blank correction on 23 May'21 (Nanotank sample number 6). This lower concentration is in line with comparative lower direct air filtration concentrations on the same day (Air sample number 2) which could indicate low levels of suspended pollution on this day. After reviewing the

nanotank MP results, further method development is recommended in order to collect a representative dataset in a more pristine environment. Furthermore, due the tendency of Nile Red to stain organic material (Chatterjee et al., 2023), a more conservative approach was taken to analyse the dataset which may have resulted in a lower particle count but this was preferred to an over-estimation of results.

It is acknowledged that both nanotank and active air samplers collect particles suspended and transported in the lower atmosphere. The samplers collect particles in different media (water vs directly onto a 1.6 µm filter respectively) and it is recognised through past published research that different sampling methods can result in variation in sample results, especially in the field

With the µRaman analysis, there was a notable difference in the number of MP particles identified in both the active samples and deposition samples (**Table 5.1**). The average MP particle count for all samples identified by µRaman analysis was 1 MP/m^3 ($\pm$ 0.6 MP/m^3 and deposition 12.1 MP/m^2 ($\pm$ 16.6 MP/m^2) (**Table 5.1**). There is also approximately x 3 to an order of magnitude more particles (all particulate matter, not just microplastic) in the deposition samples compared to the air samples and approximately twice as many MP particles in the deposition samples compared to air samples.

Table 5. 1 Average MP for suspended and deposited particulates (µRaman)

	% particles that are plastic	Standard Deviation	Total particles/m^3	MP/m^3	Standard Deviation
Suspended Particulates - Active Air Filter Samples	1%	0.1%	34.5	0.4	0.2
Suspended Particulates - Active Nanotank Samples	1%	0%	118.2	1.2	0.5
Deposited Particulates – Passive Samples	2%	2%	613.5 (m^2)	12.1	16.6

5.3.2 Microplastic Characteristics

The majority of MP particles (72%) were <20µm in size (**Table 5.2**). The largest particle (a fibre) identified was 250µm (found in a deposition sample) and the smallest particle identified was 1.6µm (given the lower limit of the 1.6µm pore size used on the filters). The suspended particulates displayed slightly larger particle size distributions with more particles above >20µm than deposition samples (see **Figure 5.5**).

Table 5. 2 Size ranges of atmospheric MP as a percentage of particles identified for both suspended (air filter and nanotank) and deposited particulates (Appendix Table VII.2-4)

Particle Size Range (µm)	Suspended				Deposited	
	Nanotank Samples (%)	Nanotank Samples (MP count)	Air Filter Samples (%)	Air Filter Samples (MP count)	Deposition Samples (%)	Deposition Samples (MP count)
1.6-5µm	22.0	183.3	48	783	27.1	1214
5-10µm	26.1	217	45.9	749	39.2	1755.7
10-20µm	34.6	288	5.5	89	25	1120
20-30µm	12.6	105	0.1	1.7	5.2	232.3
30-40µm	0.8	6.7	0.1	1.7	16	70
40-50µm	1.5	12.3	0		06	25
50-100µm	1	8.3	0.3	4	1.2	53
100-150µm	0.8	7	0.1	1	0.1	
150-200µm	0.2	2	0.1	1	0	1
200-250µm	0.1	1	0.0			0
250-300µm	0.24	2.00	0	0	0.00	0.00

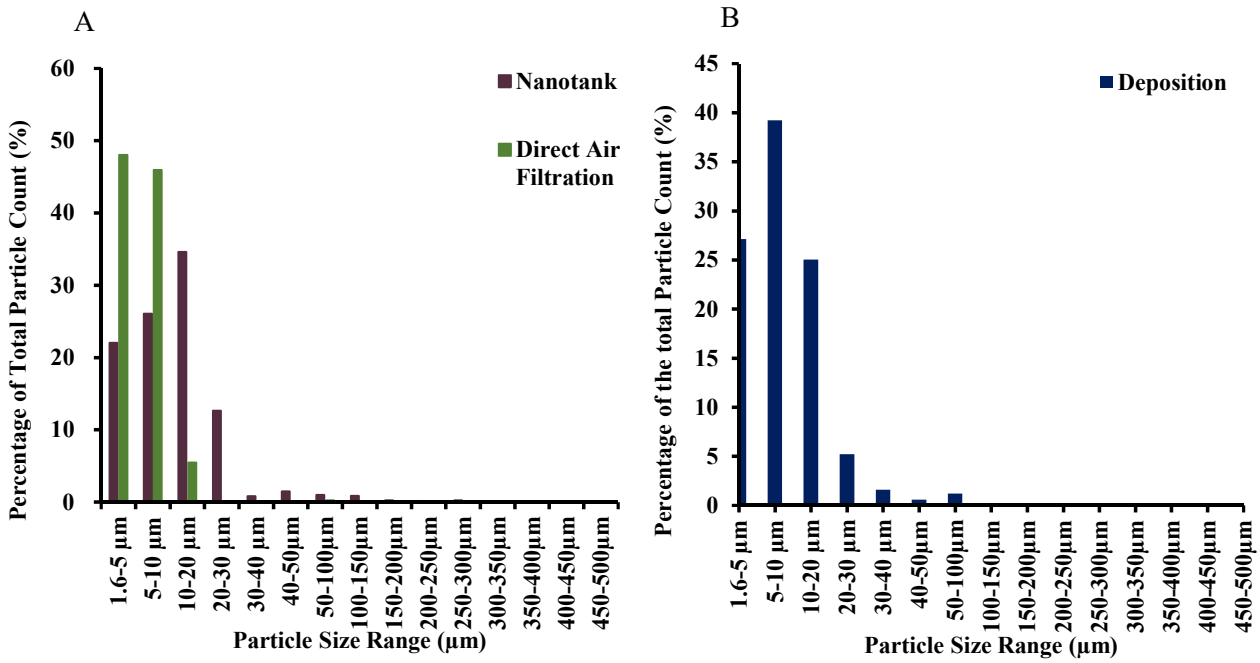


Figure 5. 5 (A) Particle size distribution for suspended particulates (direct air filtration and nanotank samples) as a percentage of the total particle count; (B) Particle size distribution for deposition particulates (deposition samples) as a percentage of the total particle count (Appendix Table VII.2-4)

Fragment and fibre were the two categories chosen for the analysis of particle shape given the difficultly in defining films (Borah et al., 2024; Allen et al., 2019). The most common shape found was fragment with only 2% of the particles analysed being identified as a fibre (**Figure 5.6**). Both the suspended and deposited particulates displayed similar percentages of fragment and fibres (both < ~2% identified as fibres).

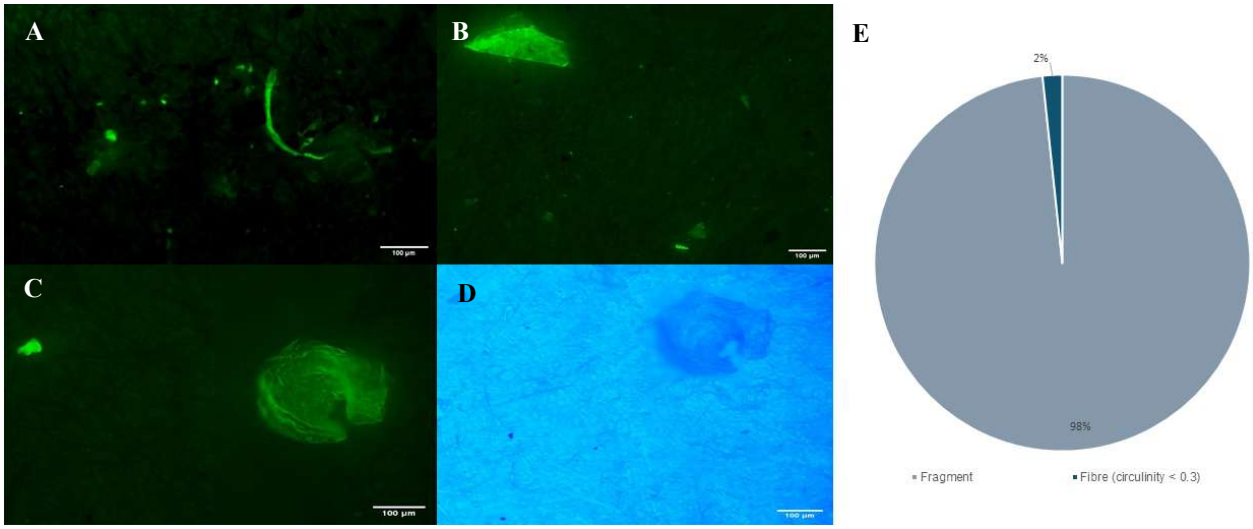


Figure 5. 6 (A) Example Nile Red image of fibre found in a nanotank sample on 19 May 2021; (B) Example Nile Red image of fragment found in a deposition sample on 04 June 2021; (C) Example Nile Red image of fragments found in an air filter sample from 04-07 June 2021; (D) Bright field image of the same fragment (figure 6.c) from air filter sample 04-07 June 2021 (x10 objective for all microscope images); (E) Percentage of particles analysed that are fragments or fibres (<0.3m circularity; n=9229)

5.3.3 Polymer composition (µRaman)

MP particles were identified in all samples (n=15) for both active (suspended) and deposition samples. The predominant polymers were Acrylic (16%), PLS (Polysulfone) (14%); PES (Polyethersulfone) and PVA (Polyvinyl alcohol) (both 11%) (**Figure 5.7**). Both deposited and suspended particulates had similar polymer compositions, however PLS, PU, Rbr, PLA, SBR and SAN were more prevalent in deposition samples.

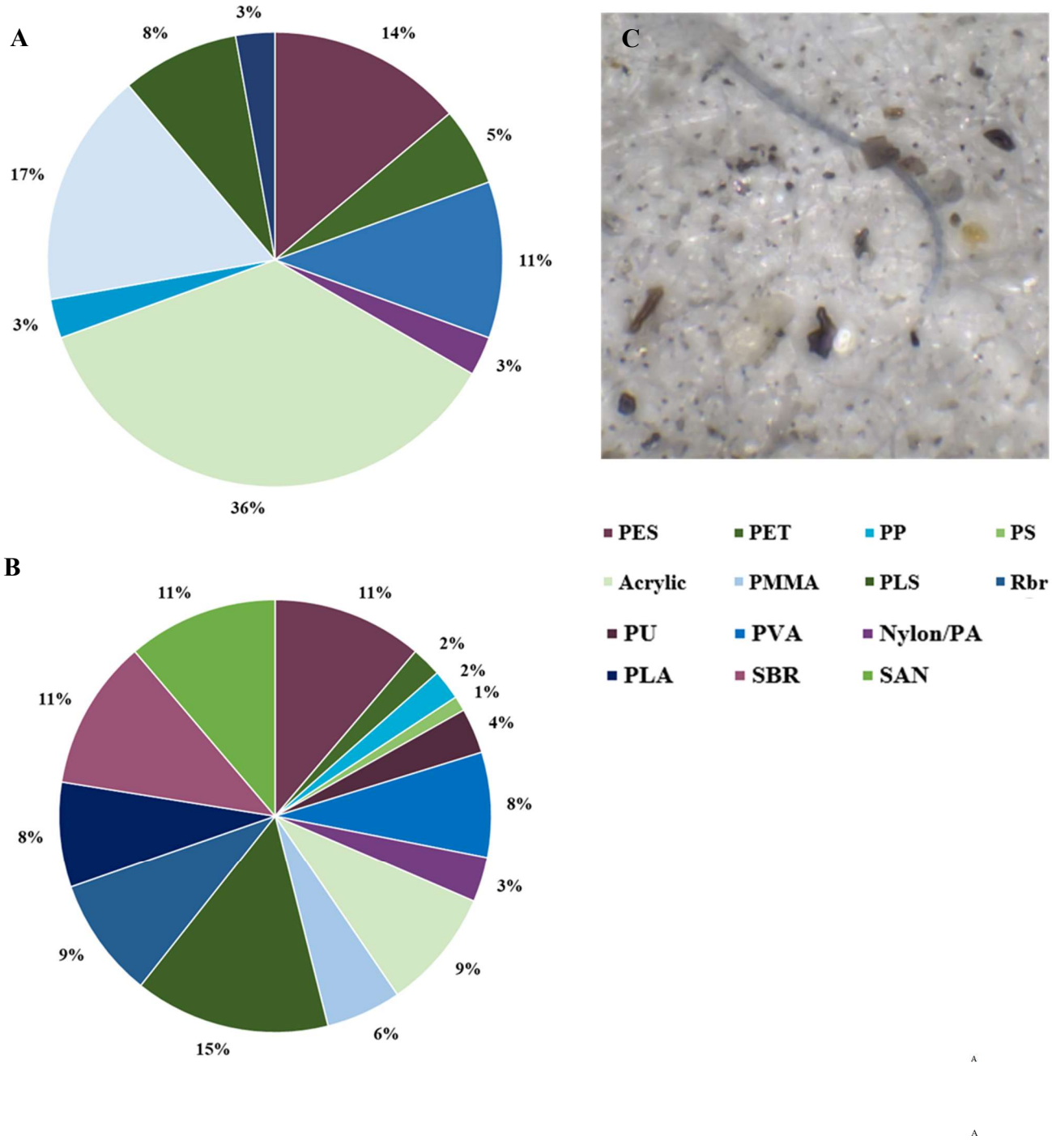


Figure 5. 7 (A) Polymer composition direct air filtration samples; (B) polymer composition of deposition samples; (all expressed as total percentage of polymers identified using µRaman); (C) Image of deposition filter from micro-Raman spectrometer (QMA Whatmann 25mm, 1.6µm; x10 objective)(see Appendix Table VII.5)

Although it is unusual to not see PE, PET, and PVC in the polymer composition of these samples, this could be due to the small particle size at this location, or the influence of different local and distal sources. There could have been a lack of localised PE, PET, and PVC during the sampling period, or due to the degradation and weathering of plastics, they may not have been identified with this spectral technique with the 80% HIT index specified.

5.3.4 Atmospheric MP pollution and weather parameters at Ny-Ålesund, Svalbard

No significant correlation was found between MP concentration and precipitation, and other meteorological variables such as wind speed, wind direction, atmospheric pressure, snow cover and snow depth, for both suspended and deposited particulates. For MP concentration and cloud cover, there was also a moderate positive correlation with deposition ($r=0.454$, Pearson Correlation $p=0.02$), but not with suspended samples, indicating that deposition of atmospheric MP pollution could be influenced by cloud cover. A positive relationship between direct air filtration samples and the mixing ratio (measure of quantity of water vapour in air relative to dry air was identified ($p=0.0001$). However, overall, the absence of a strong correlations between MP numbers and individual local meteorological conditions suggests transport and deposition of MPs at the local level is complex with a number of contributing factors.

When correlations between MP concentration and the weather patterns were not strong, the MP concentrations were split into two size categories >20µm and <20 µm. Given that more than 80% of both deposited and suspended particulates identified were below 20 µm, it was thought that this could be a determining factor in the transport of atmospheric microplastic via weather processes. For snow depth, there was a stronger correlation for particles <20µm than >20µm, for direct air filtration (suspended) particulates ($r=0.939$, $p < 0.001$) and deposition particulates ($r=0.432$, $p= 0.0216$), but a non-significant positive correlation for nanotank samples (suspended) ($r=0.183$, $p= 0.351$). This suggests that snow could be driving the deposition and suspension of atmospheric MP particles below <20µm. The depth of snow in this context is the height of accumulated snow, while precipitation refers to total moisture from the sky

(including rain, snow, sleet and freezing rain) (Norwegian Centre for Climate Services, 2025). As it is considered that snow is a more effective scavenger of airborne pollutants than rain, due to its higher porosity (Nazarenko et al., 2017) this could indicate that Arctic environments are particularly susceptible to being a sink for MPs as they have more snow.

For precipitation there was a stronger negative relationship with particles >20µm ($p=0.040$) than the other samples which is consistent with findings that larger particles are more easily scoured from the atmosphere via rain than smaller particles (Parashar and Hait, 2023). There may be less MP removal efficiency from rain due to the hydrophobic nature of MPs (Revell et al., 2021), which could also explain why the weaker relationship between precipitation and MP concentrations for all sample types. For both active sampling methods, there was a positive relationship between particles <20µm and wind direction ($p<0.01$), but not deposition, which indicates a possible trend with wind direction and suspension of smaller particulates. There was a statistically supported higher concentration when wind direction was on-shore, from sea to land, for nanotank particulates >20µm but no trend with deposition. For direct air filtration samples <20µm there was a statistically significant positive relationship with mixing ratio and the mean dew point average ($p=0.02$), suggesting that the suspension of smaller particulates is influenced by water vapour present in the atmosphere. Overall, even when particles are split into size fractions, it is evident there are numerous complex processes affecting the transport, deposition and suspension of MP particulates in Ny-Ålesund.

5.3.5 Potential contributing sources of MP in Svalbard

The source contribution to modelled atmospheric concentrations or deposition rates is shown in **Figure 5.8** For this, the calculated source-receptor relationships (footprints) for the exact sampling dates and times are coupled with updated emissions from Evangeliou et al. (2022), which are shown in **Appendix Figure VII.1**. Active, nanotank and passive observations are represented by the green line. In general, we

see that modelled concentrations are overestimated. This points out the general problem of efficient atmospheric dispersion modelling of MPs, which is associated with the uncertainty of the current source emissions, both in terms of emission intensity, but also with the accurate geolocation of the main sources. However, especially for the observed concentrations, the model represents well the timing of the highest levels measured (end of May for both passive and nanotank samples).

As regards to the contributing sources to surface concentrations, the prevailing sector is oceanic MPs, though the concentrations are low. Oceanic macroplastics decompose over time to smaller MPs, due to photodegradation, and are often remobilised, when breaking waves cause bubbles of trapped air to rise and burst (Allen et al., 2020). They are then subject to long-range transport and may deposit on the marine or terrestrial environment, somewhat similar to the well-known grasshopper effect for persistent organic pollutants (Gouin, 2021). The peaks of oceanic MPs that coincide with high observed surface concentrations in **Figure 5.8A** originate from North Atlantic on June 1st (see **Appendix Figure VII.2**). Today, there is an ongoing debate about whether the ocean is just a sink for atmospheric MPs or a significant source with many researchers supporting one or the other approach (Evangeliou et al., 2022; Brahney et al., 2021; Yang et al., 2025; Bucci et al., 2024). Observations combined with dispersion models suggest that there is high probability that MP are resuspended from the ocean and transported over long distances for their source. For instance, Goßmann, et al. (2023) reported surface concentration of over 30 ng m^{-3} during a ship campaign over the Norwegian coasts, when air was originating directly from the ocean (west). Ferrero et al (2022) reported concentrations of 24 ± 9 and 45 ± 20 items m^{-3} in the open Baltic Sea and to the Gotland Island, very close to those measured in the sea (79 ± 18 items m^{-3}). Caracci et al. (2023) showed that samples largely influenced by sea-spray and air masses originating from coastal South America and the north Atlantic subtropical gyre were more contaminated by MNPLs along the transect from Vigo (Spain) to Punta Arenas (Chile).

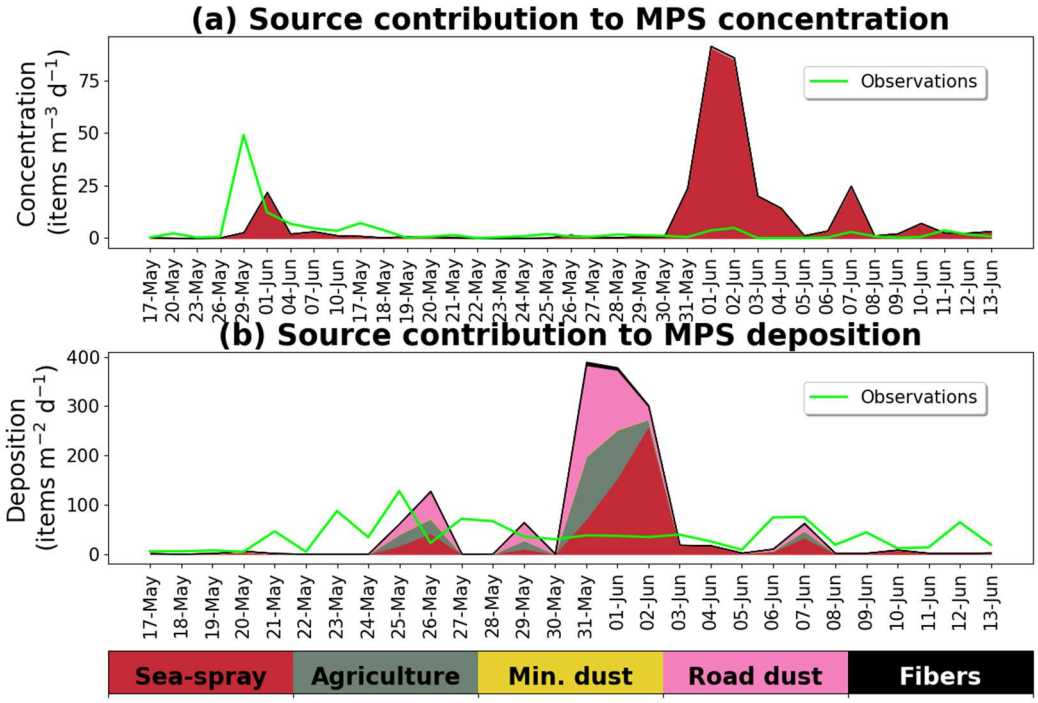


Figure 5. 8 Source contribution to modelled MP at Ny-Ålesund for (A) active and nanotank samples (surface concentrations and (B) passive samples (deposition rates). Five different emission sectors were considered, namely MP suspended from the ocean (sea-spray), agricultural activity (e.g., agricultural nets), soil (mineral dust), road dust (tire wear particles) and microfibers (releases from clothes of the population), adopted from an updated version of the MP emission dataset from Evangeliou et al. (2022). (Figure created by Nikos Evangeliou)

The modelled results for passive samples deviated more from the respective observations (**Figure 7B**), although the highest modelled deposition rates were obtained for observations that were 50 items m^{-2} d^{-1} or higher. However, there were observations, for which model showed zero deposition (e.g., 21 – 24 May). Although in the same order of magnitude, modelled deposition rates are again overestimated; they also show contributions from other emission sectors, such as road dust and agricultural activity (nets). The largest contribution is again achieved for the same dates as in the active and nanotank samples (30 May – 4 June). During this period, the footprint covered not only oceanic domain, but also parts of the United Kingdom and Europe, which denotes that MP can also originate from there too (Figure **Appendix**

VII.3). Following findings from Brahney et al. (2020) who reported that wet deposition constitutes around 20% of total deposited MP (wet + dry) after measuring MP with special buckets that could separate precipitation and settling, we have assumed that wet scavenging contributes about 20% of total deposition by adjusting the scavenging coefficients in the model. This is a realistic approach considering that MP consist of macromolecular polymers that are largely hydrophobic.

5.4 Discussion

5.4.1 Comparison of deposited and suspended particulates

One of the main research aims was to establish if there were differences between deposited and suspended particulates in the Arctic region. However, there was no correlation between the highest and lowest reported concentrations for each type of sample. One of the main research aims was to establish if there were differences between deposited and suspended particulates in the Arctic region. However, there was no correlation between the highest and lowest reported MP concentrations for each type of sample, suggesting that each sample had relative efficiencies at collecting particulates. In terms of the Nile Red results, the average deposition rate during this period was 37.3 $\pm$ 30.2 MP/m^2, and the average suspended particulate concentration was 4.2 $\pm$ 9.4 MP/m^3 (with nanotank samples 1.5 $\pm$ 1.8 MP/m^3 and air filter samples at 8.9 $\pm$ 15.6 MP/m^3). This highlights the difference in reported concentrations of both methods, and how this can make comparison between studies and countries difficult. From the μRaman analysis, the deposition rate was reported at 12.1 MP/m^2 and MP concentration for suspended particulates was 0.95 MP/m^3. This comparison highlights the effect method of analysis can have on the particulates identified and the need for more than one method of particle analysis. In terms of polymer composition, the deposition and suspended particulates displayed similar results. However, the deposited samples had a slightly higher proportion of some polymers such as PLS

(**Figure 5.7A**). It is difficult to pinpoint why this could have occurred due to the complex relationship between weather parameters and transport identified here.

5.4.2 Potential Relationships with Weather Parameters

When examining the influence of weather parameters with the MPs identified in this study, it was evident there were multiple parameters and processes driving suspension and deposition here. There may be a trend with humidity, wind direction and cloud over here but examining these complex relationships over a longer period of time would be beneficial to determine their relative significance. Although the studies examining the relationship with MP and humidity are limited, some have reported increased MP concentrations with increased humidity (Allen et al., 2020; Szewc et al., 2021). Furthermore, it has been reported that humidity can accelerate the photoaging process and lead to increased fragmentation in MP, which could in turn influence MP concentrations and transport (Wang et al., 2023). Wind direction has been found to be an important factor for marine-sourced microplastic pollution (Ryan et al., 2023; Collins and Norton 2024), and given the potential sources of the MP pollution found in Ny-Ålesund, this could be an important factor to monitor and understand. Snowfall is also regarded as one of the main carriers of atmospheric MPs, transporting them to remote regions from the Alps (Jurkschat et al., 2025), and Antarctica (Aves et al., 2022). Studies examining the relationship between snow, microplastics and its resulting climate impacts are limited, but suggest that MP could affect cloud formation and accelerate ice melt (Revell et al 2021.; Aeschlimann et al., 2022), therefore understanding this relationship will be crucial for MP research in the Artic region going forward.

5.4.3 Potential transport of Atmospheric MP pollution in Svalbard

To further elucidate potential transport from hot-spot regions, from where atmospheric MP were resuspended before being transported and deposed in the High Arctic (Svalbard), the average footprint emission sensitivity (FES) was calculated by Dr

Nikos Evangeliou, for those observations that are below and above a certain threshold. Here, the 25th and 85th percentiles of the measured samples were used. The basis of this method is that if a source is located at a given grid cell of the spatial domain, an air parcel passing through this location indicates that material from the source can be collected and transported along the trajectory to the receptor site. **Figure 5.9** shows the average FES for the observations that were lower (left) and higher (right) than the 25% of the samples collected in Svalbard.

It is reported that when observed concentrations in Svalbard are low (< 25th percentile), the source regions of MP to remote high latitude areas of Norway include the North Atlantic Ocean, Northern Greenland and the High Arctic (**Figure 5.9A**). Although these regions present very significant MP emissions, (see **Appendix Figure VII.1**), both the FES and MP emissions are weak in the Northwestern Atlantic. On the contrary, higher MP were measured when long-range transport occurred from the Northeastern Atlantic, the Norwegian coasts and the United Kingdom (Figure 8b), while the FES is stronger towards the eastern part of the North Atlantic. As seen in **Figure 5.9**, this region corresponds to the main oceanic MP emissions. This shows that despite that the geographic location of the oceanic sources is likely correct, their intensity is highly uncertain, causing higher modelled concentrations. While constraining MP emissions in remote regions requires a large number of robust observations (the current analytical methodologies have several limitations), the existing predicted oceanic MP emissions are probably too high in the North Atlantic Ocean.

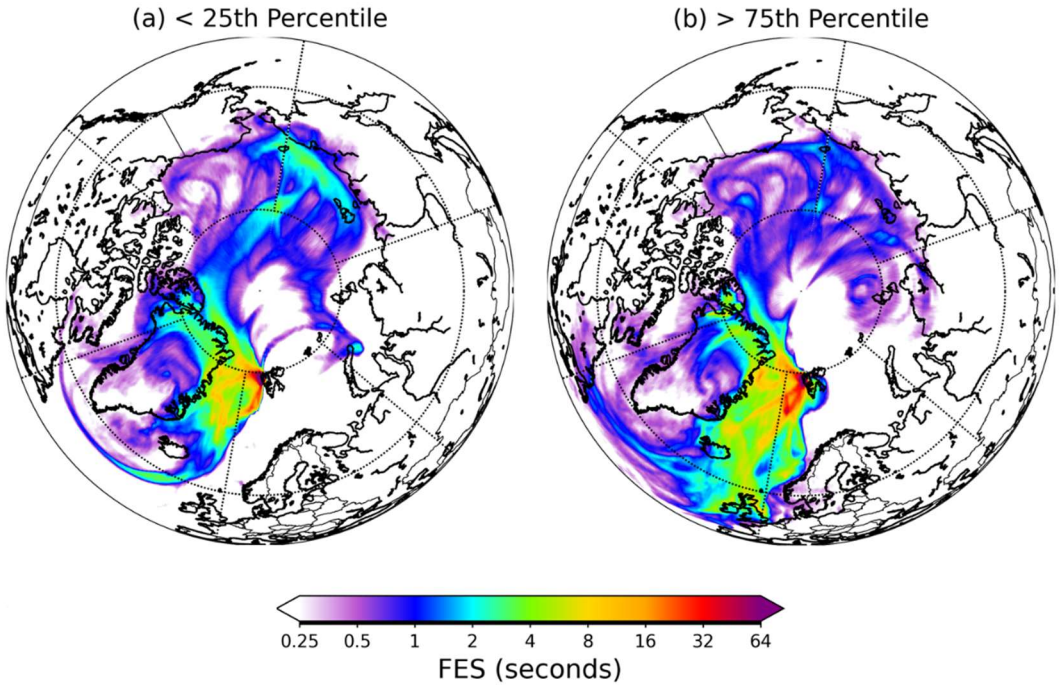


Figure 5. 9 Average footprint emissions sensitivity for the (a) lowest (left) and the (b) highest 25% (right) measured surface concentration (active and nanotank samples) and deposition rates (passive samples) of MP in Ny-Ålesund. (Figure produced by Dr Nikos Evangeliou

5.4.3 Microplastic pollution in the Arctic region

The Bergmann et al. (2019) study of atmospheric fallout in the Arctic region is the most directly comparable study as it is the only other study reporting atmospheric MP pollution in this region. While there are some similarities with the present study, different methods were used, which consisted of snow deposition samples and μFTIR as their main method of analysis (thus different analytical windows prevent direct comparison of the results). The dominance in the present study of Acrylic, PLS, PES and PVA (is consistent with Bergmann et al. (2019), which compared Arctic and European snow (deposition) samples, and identified acrylates and polyurethane, rubber, polyamide and polyvinyl chloride (PVC) as predominant polymer types for Arctic snow. The high proportion of acrylics in the polymer composition here, could be due to its common use in marine fishing equipment and outdoor clothing. PLS is

commonly used industrial membranes and PES is often used for electric insulation, whereas PVA is also common with artificial textiles as well as food packaging. However, due to the small size ranges of the particles sampled it is likely that the MPs identified at Ny-Ålesund originated from distal sources and could have travelled from a range of locations.

Similar to the present study, Bergmann and colleagues (2019) also reported small particle size ranges with particles identified in the 11µm and 475µm size range, and 80% of MPs <25µm and 98% <100µm (Bergmann et al., 2019). This study also reported much smaller fibres found in Arctic snow, compared to European snow, which is similar to the small number of identified fibres in the present study (Chapter 3.2). The distal sources of this pollution in the Arctic region could result in the weathering and fragmentation of particles whilst in transit, and particles here could have a long residency time in the environment. This could cause fibres to breakdown into smaller fragments, or it could be a result of fibres having different transport properties to fragments in the atmosphere (Chen et al., 2023; Evangeliou et al., 2020). The differences in polymer composition between the present study and the previous Arctic study could be due to a number of factors including the methods of sampling, the differences in analytical equipment, time of year and location of sampling. Bergmann et al. (2019) reports MP deposition per litres of snow, which makes comparison to the volumetric data presented in the present study difficult.

Rosso et al. (2024) analysed MP content of the glaciers on Svalbard, again using µFTIR to analyse material composition. This study reported different polymer compositions to the present study, but also found small particle size distributions and the reported concentrations to be in a similar range to the deposition found in the present study (37.31 ± 30.19 MP/m^2) (**Table 5.3**). Rosso et al. (2024) also reported that the Ny-Ålesund station could be a localised source of MP pollution in this region. Another recent study analysed wastewater effluent as a potential source of MP pollution in the Arctic (Bach et al., 2024), highlighting that both localised and distal MP pollution is affecting the region and that both need attention to protect this remote

environment. Whilst the methods used for sample collection and analysis and the reported polymer compositions may be different across the existing Arctic MP studies (Table 3), it is evident that MP are prevalent in this area and are mostly reported in the smaller size fraction <100µm. This highlights the need for harmonisation in methodology and the reporting of MP concentrations where possible, and the need for long-term monitoring of the pollutant.

Table 5. 3 Comparison of MP studies in the Arctic, Antarctica, remote and urban regions (non-exhaustive)

Location	Sampling – Method, Frequency, Duration	Method of Analysis	Principal Shape	Principal Size	LOD	Principal Polymers	Deposition Flux/ Reported Concentration	Weather	Reference
Arctic (Remote)	Active and passive air sampling over 28 day period	Nile Red and µRaman	Fragment	<20µm	1.6µm	Acrylic, PLS, PES, PVA	37.31±30.19 MP/m^2/day; 4.15 ±9.42 MP/m^3/day	Correlation with wind direction	Present study
Arctic (Remote)	Surface snow sampled on 5 ice floes; 2015-2017	Microscope and µFTIR	Fragment	<25µm	11µm	PS, PVC, PC, PLA, PI	0 to 14.4 × 103 N $liter^{-1}$	NA	Bergmann et al., (2019)
Arctic (Remote)	Bulk and surface glacial snow samples; April 2021; multiple sites	Microscope and µFTIR	NA	<100µm	5µm	PTFE, PU, PARA (Polyamide) ABS	49.4 ± 7 mg m^{-2} - 227.2 ± 15 mg m^{-2} (no average reported)	NA	Rosso et al., (2024)
Arctic (Remote)	Raw wastewater samples	Microscope and µFTIR	Fragment	<100µm	20µm	PP, PE, PES	217 L^{-1}	NA	Bach et al., 2024
Antarctica (Remote)	Snow sampling – 19 samples from different locations Nov-Dec 2019	Microscope and µFTIR	Fibre	200-1000µm	50µm	PET, PMMA, PVC, PA	294 ± 4.7 L^{-1}	NA	Aves et al., 2022
Antarctica (Remote)	Bulk atmospheric deposition samples; Jan-	µRaman	Fragment	5–10 µm	5µm	PP, PE, PC	1.7 MP m^{-2} d^{-1}	NA	Illuminiati et al., 2024

Location	Sampling – Method, Frequency, Duration	Method of Analysis	Principal Shape	Principal Size	LOD	Principal Polymers	Deposition Flux/ Reported Concentration	Weather	Reference
	Dec 2020, 7 samples from different sites								
Tibetan Plateau (Remote)	Snow pit sampling; 21st May 2020; 16 samples 10cm intervals	Microscope, Raman and SEM	Fibre	<200µm (43.33%)	48µm	PVC, PPO (Poly(2,6-dimethyl-1,4-phenylene oxide)) Hydroxypropyl cellulose (HPC) (13.33%) and Hydroxypropyl methyl cellulose (HPMC); PVA, PB	9.55 ± 0.9 L^{-1}	Monsoon season affected size, shape, colour and polymer composition	Wang et al., 2022
Pyrenees (Remote)	Deposition sampling; Nov 2017-March 2018; 12-34days	Microscope and µRaman	Fragment	≤50µm	10µm	PS, then PE and PP	365 ±69 $m^{-2}d^{-1}$	No meteorological mechanism driving MP deposition	Allen et al., 2019
London (Urban)	Total atmospheric deposition; Jan-Feb 2019; samples collected 2 per week for 4 weeks	Microscope and µFTIR	Fibre	<100µm	5µm	PAN, PET, PA	712 ± 162 m^2 /d	Wind direction and wind speed influence	Wright et al., 2020
Shanghai (Urban)	Particulate sampler (active); 100 ± 0.1 L/min, sampling in triplicate over	µFTIR	Fibre	<1000µm	23µm	PET, PE, PES, PAN, PAA	1.42 ± 1.42 n/m^3	Strong correlation with wind direction and SAMPs distribution	Liu et al., 2019b

Location	Sampling – Method, Frequency, Duration	Method of Analysis	Principal Shape	Principal Size	LOD	Principal Polymers	Deposition Flux/ Reported Concentration	Weather	Reference
	1 h and ≈6 m^3 of air per sample.								

In other remote regions such as Antarctica, the polymer composition and more common identification of fibres can be highlighted as a main difference (Aves et al., 2019; Illuminati et al., 2024). Again, with different methods of sampling used and differences in reporting, direct comparison is challenging, but values reported are much lower for Antarctic deposition with 1.7 MP m^{-2} d^{-1} compared to 37.3 $\pm$ 30.2 MP/m^2 in the present study (Illuminiati et al., 2024). However, this could be due to the reasons highlighted above. In the Pyrenees mountains, a higher deposition rate was reported (365 ± 69 $m^{-2}d^{-1}$). This study also looked into the relationship with weather and found that there was no single meteorological variable that was strongly influencing MP deposition in this region (Allen et al., 2019).

Even in more urban locations, it is unusual to find a study that has simultaneously measured deposition and total particulates. Wright et al. (2020) reported much higher concentrations for deposition samples in London, United Kingdom (712 ± 162 m^2 /d) as well as fibre being the most common particle shape. A study in Shanghai reported lower values (1.42 ± 1.42 n/m^3 (here the unit n/m^3 is the number of plastic items per m^3) (Liu et al., 2019b), than the values reported in this study (4.2 $\pm$ 9.4 MP/m^3), which is similar to the concentrations reported in the present study. This could be due to the smaller LOD of 23µm for the Shanghai study, which could have resulted in missing the smaller size fraction in this region. Nonetheless, this is concerning given the remote location of the sampling site in this study, and the stark contrast in the populations in each of these regions.

5.5 Conclusions

To answer the research question (RQ2) of examining the concentrations and main characteristics (polymer composition, particle concentration, shape, and size) of atmospheric microplastics in a remote location (Svalbard, Norway), the MP content of the PBL atmosphere in Svalbard was measured over 28-day period. With the use of μRaman spectrometry and Nile Red fluorescence, the size, shape and polymer composition of deposited and suspended particulates were investigated. MPs were found in every sample, and although the differences in methods and reporting make comparison difficult, results are consistent with other remote locations. The polymer composition was examined by μRaman spectroscopy and showed higher levels of Acrylic, PLS, PES, and PVA. This could be due to local contamination from clothing and fishing gear, or distal sources from food packaging or industrial applications. Using Nile Red staining coupled with fluorescence microscopy, the characteristics of this pollutant were examined. Fragment was the most prominent particle shape, which is consistent with other Arctic studies, and could be due to the small size of the particles found there, or their transport mechanisms. Most of the particles found here were <20μm (80%) highlighting the importance of researching this pollutant. Its small size poses a high risk for ingestion, transport and other ecosystem impacts. Furthermore, it shows the need to examine the small fraction of atmospheric content, as this is where a large part of the microplastic concentrations lie, and missing this could result in considerable under-reporting.

In terms of the second part of the research question, which is related to how atmospheric MP pollution in remote environments relate to weather conditions, and potential transport pathways, it is evident that the role of weather parameters on the suspension and deposition of atmospheric MP in this region is complex. There were significant relationships with humidity, wind direction and cloud cover. Humidity appears to be correlated with increased MP suspension, and has been found to encourage the degradation of MPs. Snow also appears to show trends with MP suspension, and the relationship between snow, MP transport and its influence on

climate will become an important focus for the field as climate change progresses. Studying these relationships over a longer time period is recommended to examine the complex relationship between weather parameters and MP pollution in the Artic region. Dispersion modelling suggests that the main sources of the MP measured at this location include the North Atlantic Ocean, Northern Greenland and the High Arctic. However, higher MP were measured when long-range transport occurred not only from the ocean, but also from land-based sources (e.g., road dust). There was no correlation between the highest and lowest reported concentrations for each type of sample, suggesting the particles behave differently depending on deposition or suspension and highlights the need to measure both particles in conjunction.

This study confirmed that atmospheric MP pollution is present and ubiquitous in the Arctic PBL. To date, this is the first time both suspended and deposited particulates have been studied simultaneously in this region highlighting the importance of measuring both particulates simultaneously to gain a better understanding of total atmospheric content. Furthermore, the differences in the outcomes from μRaman analysis and Nile Red staining demonstrate the need for more than one method of analysis in MP research, and methods that are complimentary. Gaining accurate information on both polymer composition and particle morphology and concentration are needed to fully understand the extent of this pollution. It is essential that more consistent methodologies are used to sample, analyse and report MP concentrations in this region and beyond. As more is learned about the risks of MP pollution, it is essential that the pollutant is monitored and reported effectively in order to understand the scale of the problem and mitigate its potential impacts on ecosystem function, human health, and climate processes.

Chapter 6 – Urban Atmospheric Microplastic Pollution – Glasgow

The third research question (RQ3) of this thesis was to investigate the characteristics and extent of atmospheric MP pollution in an urban environment . This chapter focuses on a central residential location in the city of Glasgow, Scotland. Atmospheric MP pollution at this location was measured during a field sampling campaign from November to December 2021, and the pollution has been reported in terms of atmospheric MP concentration (particle count) and the main characteristics identified (including polymer composition, and particle shape and size). As per the remote location, relationships between this pollutant and weather parameters are examined and atmospheric models are used to examine potential sources of this pollutant. In this chapter it was also possible to use forward trajectory modelling to examine where this pollutant could potentially be transported to.

6.1 Introduction

The study of atmospheric MP first occurred in an urban location, in Paris, France by Dris and colleagues (2015). This study was the first to measure atmospheric deposition for MP content and identified MP in samples in the 100-5000 μm range, with a concentration of 29–280 particles m^{-2} day^{-1} (Dris et al., 2015). Since then there have been numerous studies examining atmospheric MP content in urban environments all over the world including in Beijing (Li et al., 2020), Kochi (Kannakai et al., 2024), London (Wright et al., 2020), Mexico City (Shruti et al., 2022a), Auckland (Fan et al., 2022) and Iran (Abassi et al., 2023). It was not until 2025 that an urban location in Africa was examined, in a study which reported on atmospheric MP deposition in Thohoyandou, South Africa (Mutshekwa et al., 2025). This represented a large gap in the knowledge of the geographical extent of atmospheric MP pollution across the globe. As mentioned previously, the different methods used to sample and examine atmospheric MPs makes comparisons between different studies and different locations

difficult. It is therefore not considered an exact science to compare the concentrations from different studies and locations as differences in data collection can impact results in considerable ways (Azari et al., 2023). However, it is important to still examine atmospheric MP content and report concentrations in order to monitor this emerging pollutant and maintain datasets in order to monitor this emerging pollutant long-term. This thesis has used the same methods in both a remote and urban environment in order to facilitate a more accurate comparison.

Measurements of atmospheric MP concentrations have taken place in the UK – in London (Wright et al., 2020) and the Humber region (Jenner et al., 2022) – but there have been no studies to date on the atmospheric MP content in Scotland. Given the influence of local human and industrial activities (clothes drying, waste management, and industrial activities) which can contribute to atmospheric MP pollution, examining atmospheric MP concentrations in urban locations is crucial to add to understanding the extent of atmospheric MP pollution in environments where localised sources are more prevalent. Furthermore, the risk to human health may be higher due to increased population in urban areas (see **Chapter 2**). Daily and weekly active sampling measurements were taken in November until December 2021. μRaman and Nile Red staining coupled with fluorescence microscopy was used to report MP concentrations and characteristics present in the urban atmospheric environment in Glasgow.

As per the chapter that covered remote atmospheric microplastic pollution, it was of interest to observe if there was a potential relationship between atmospheric MP pollution and local weather parameters. As discussed in **Chapter 2**, previous studies on atmospheric MPs have found both negative and positive, as well as insignificant relationships with weather parameters. Therefore this chapter compares atmospheric MP concentrations to local weather data, to examine how weather influences the concentrations of this pollutant in the Glasgow atmospheric environment. Furthermore, given the presence of increased human and industrial activity at this location, it was of interest to observe potential relationships with conventional air pollutants. Local air pollution data was compared with field observations to examine

if there is a connection between the various types of atmospheric pollutants present in this urban environment. Finally, as mentioned previously, there are still considerable gaps in knowledge and understanding of potential sources and pathways of atmospheric MP pollution in urban environments. Although more local sources are expected to play a role in the concentrations observed in an urban environment, particle modelling is employed to observe other sources and potential long-range transport. Forward trajectory modelling is then used to observe where this pollutant could be transported to, in order to gain a fuller picture of atmospheric transport and extent of atmospheric MP pollution. As well as air mass modelling, individual particles with characteristics associated with field observations, are modelled to observe if these characteristics influence transport and dispersion of this pollutant.

6.2 Methods

6.2.1 Field Sampling

As discussed in **Chapter 4**, Glasgow in Scotland is an industrial city with a population of 633,100 (as of 2019) (Glasgow City Council, 2021) and is still known for its commercial and industrial economy (IFSDG, 2021). At the time of field collection in November and December 2021, Covid-19 restrictions were easing in this area but working in offices and laboratories was still limited. To allow for these restrictions' samples were collected at the researcher's house, at a suburban location near Glasgow (**Figure 6.1**). This was chosen to minimise the risks of Covid-19 and due to the location being easy to access but with limited interference from the public. The samples were collected whilst examining the relative collection efficiencies of active sampling equipment in **Chapter 4** but only the samples that displayed the most effective particle collection over the 28-day sampling period have been chosen for detailed analysis.

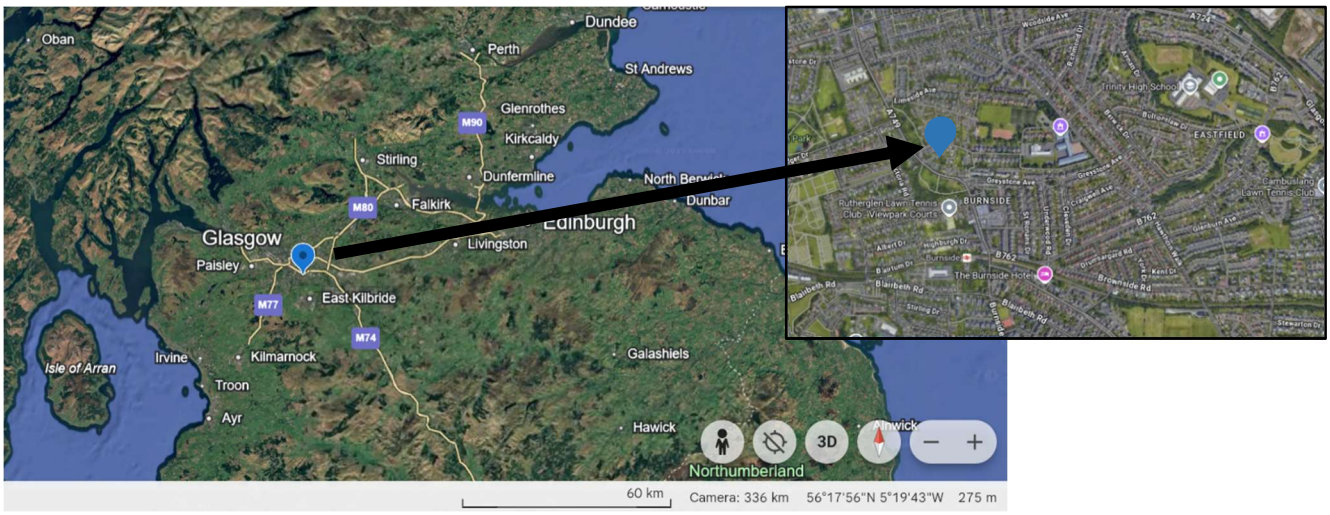


Figure 6. 1 Map of Scotland with Sampling Location (Blue) *(Google Earth, 2025)*

All samples were taken over the same period and same location to ensure there are no spatial or temporal variances. Sixteen samplers were set up at ≈0.75m height, each with one stainless steel filter holder and a silicone hose attached to a calibrated pump to draw air through the chamber to the filter (QMA Whatmann 1.6 µm pore size) (see **Figure 6.2**).

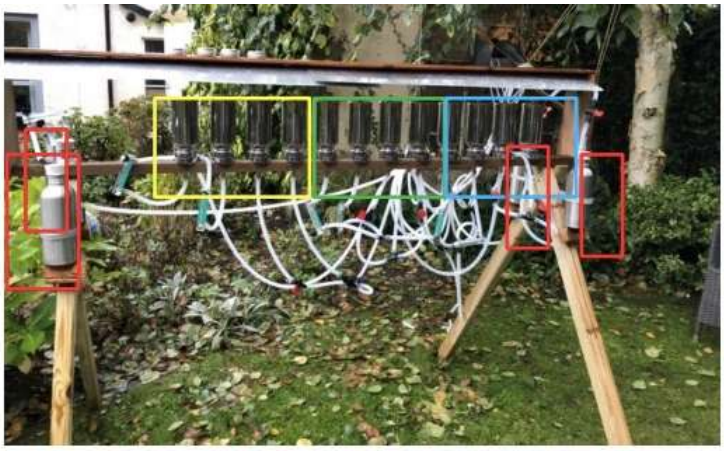


Figure 6. 2 Image of Experimental Set-Up in Glasgow, the nanotank samplers can be seen in the red box; the daily sampling duration direct air filtration samplers are in the yellow box; the weekly sampling duration direct air filtration samplers are in the green box; the monthly sampling duration direct air filtration samplers are pictured in the blue box

Given the information on the relative efficiencies of the direct air filtration and nanotank active air sampling systems, the following flow rates for each sample type were chosen (**Table 6.1**):

Table 6. 1 Sample type and respective flow rate chosen for Glasgow Atmospheric MP content

Sample Type	**Flow Rate**
Daily direct air filtration samples	1 L/min
Weekly direct air filtration samples	1 L/min
Nanotank samples	1 L/min

6.2.2 µRaman and Nile Red Staining with Fluorescence Microscopy

The analysis of field samples was conducted following the methodology detailed in Chapter **4.**

Micro-Raman (µRaman) spectroscopy was used to provide polymer characterisation, specifically identification of the types of plastic polymers within the different sample sets. This enables individual particles to be characterised through comparison of their µRaman spectra with established libraries of known plastic polymers (Enyoh et al., 2019). Given the number of samples in the dataset in Chapter 4, selection of the of daily direct air filtration samples, nanotank daily samples, weekly and monthly direct air filtration samples, were selected for µRaman analysis. The µRaman spectrometer (Horiba Scientific, XPlora Plus, University of Strathclyde) employed a 785nm laser with a 1200mm^{-1} grating and 50 µm split settings. The spectrometer was set to collect spectra between 200-2000 cm^{-1} Raman shift for all particles down to 1.6 µm, with an acquisition time of 10 seconds and 2 accumulations and with power at 35mW. Each sample was analysed in triplicate across three areas (≈1% of the filter in each sub-sample window, 1x1mm). There was no bias in the particle selection for analysis based on colour, shape, or size (all particles were analysed irrespective of appearance), and the filter was also analysed for background spectra analysis. There were >100 particles analysed per subsample. This sub-sample area selection was used to provide a

representative sample (>100 particles) (Zhao, Dahal, & Marfil-Vega, 2020; Cowger et al., 2024) within a sensible and achievable time frame. The resulting spectra were saved as SPC files and analysed using Spectragryph (Version 1.2.15) (Menges, 2022). Multivariate analysis of each spectra was completed and reference libraries were used to confirm polymer identification (SIMPLE, SLOPP and SLOPPE databases and the laboratory reference plastics spectral database (Jin et al., 2022; Levermore et al., 2020; Xu et al., 2020b). Particles were only confirmed as plastic if a HIT (hit quality index) rate of ≥80% was achieved (Cowger et al., 2020; Levermore et al., 2020), and those below the <80% threshold discounted as non-plastic particles.

In order to gain information on the size and shape of the MP particles and a comprehensive particle count, samples were also analysed with Nile Red fluorescence microscopy. Fibres were identified using the standard 1:3 width ratio as used frequently within MP studies (Na et al., 2024; Li et al., 2020), and the rest classified as fragments. A 1% (0.1µg mL^{-1}) Nile Red solution was used to stain the samples, which were then oven dried at 30°C overnight and then stored in a fridge 4^{o}C in sealed aluminium containers to rest before being imaged with the fluorescent microscope. It has been reported that this process of drying, cooling and de-energizing (in the dark) can aid with the MP staining, fluorescence efficiency and minimise staining of organics resulting in false-positives (Galvão et al., 2023). All samples that were not subject to µRaman analysis were imaged with a fluorescence microscope (Nikon Eclipse LV100ND), using a x10 objective and fluorescence mode (with QMA Whatmann with 1.6 µm pore size), and a 470nm wavelength lamp. A transect of images (1.4 x 0.94 mm each) were taken from the top to the bottom of the filters resulting in 20% of the filter being analysed (taking into consideration the sub-sample method findings of (Huppertsberg and Knepper 2018). The software FIJI/ImageJ (Schindelin, et al., 2012) enabled automated particle count, shape and size. Resulting MP counts were then calculated relative to the total area of the area analysed and extrapolated for the total area of the filter.

6.2.3 Microplastic contamination prevention

Multiple steps were taken to ensure that contamination of MPs was minimised at each step of the data collection and analysis process. In the field, the equipment was set-up away from any potential interference from the public. In addition to this, only natural materials (wool, cotton) were worn during the collection of samples and in the processing laboratories in Glasgow. Blanks were taken during sample collection and in the processing laboratories. The University of Strathclyde, where sample preparation and all Nile Red staining and images were produced, has a microplastics clean lab where only natural materials are permitted to be worn, cotton lab coats are used. The air is filtered using a HEPA filter and access to the lab is controlled, with regular thorough cleaning with ethanol and milli-Q conducted regularly and access limited to minimise contamination. In addition, the filters used to collect samples and the stainless-steel containers used to store and transport the samples were heat treated before use (~450°C oven for 15 minutes). The ethanol used for field sampling was vacuum filtered before use (Whatmann QMA filters with 1.6 μm pore size) and blanks of the milli-Q, ethanol and the milli-Q/ethanol solution were taken. Field blanks were conducted by exposing a clean filter to the sampling environment while samples were being changed to account for potential deposition during exposure. Procedural blanks were conducted by leaving a clean filter exposed in the laboratory environment while samples were being processed to account for procedural contamination. All blanks were treated in the same way as the samples, with one field blank and one procedural blank being analysed with μRaman spectroscopy to gain an understanding of polymer contamination, and the rest stained and imaged with Nile Red to understand the particle size, shape and number of particulates from contamination. All results have been adjusted to account for the contamination found in these field and procedural blanks based on their particle size distribution from the Nile Red staining of blanks, and all samples blank corrected based on the polymers presence in the field and procedural blanks.

6.2.4 Statistical analysis

To calculate the amount of MPs in each sample, the following sets of equations for used.

To calculate the number of MPs per sample (all samples):

$$\mu P = (P_s/A_s) \times A_f$$

μP = MP per total sample

P_s = MP particles in the subsampled area (count)

A_s = area subsampled (mm^2)

A_f = area of total filter (mm^2)

For individual suspended samples (direct air filter and nanotank), to calculate the volume of air per sample, following equation was used:

$$V = (t_s \times f_s)/1000$$

t_s = time (mins) for the total sample

f_s = flow rate (L/min) for the sample

V = air volume sampled (m^3)

For the suspended air samples (nanotank and direct active air samples), the total representative MP per m^3 is calculated as:

Total suspended MP = $\mu P/V$ (MP/m^3) , which in long had is:

$$= ((P_s/A_s) \times A_f)/ ((t_s \times f_s)/1000)$$

Filters were 47mm diameter for direct air filtration samples, and 25mm diameter for nanotank samples.

6.2.3 Meteorological Data

One of the main research questions was to identify potential drivers of atmospheric MP pollution in remote and urban locations, and if there is a relationship between MP concentrations and weather parameters.

Correlation analysis was completed for both the direct air filtration samples and the nanotank samples in order to examine potential differences between the two methods of active sampling. The main parameters assessed were precipitation (mm), sea level pressure (hPa), dew (%), wind speed (m/s) and wind direction (Visual Crossing, 2021) (**Appendix Table VII.1**). Pearson's correlation coefficient (r) was calculated for each variable and MP dataset along with corresponding p-value.

6.2.5 Air Quality Data

It was also of interest to observe if there was a potential relationship between atmospheric MP concentration at this urban location, and other air pollutants. Given that Glasgow is an industrial city with some of the highest air pollution levels in Scotland (The Royal Environmental Health Institute of Scotland, 2016), it was hypothesised that there could be a potential correlation or comparable trends between MP and other commonly monitored air pollutants. The location where field sampling took place is located between two air quality sampling stations (Cambuslang, 55.818802°N, -4.167073°W (Air Quality in Scotland, 2025a) 2.3 miles from sampling location; and Rutherglen, 55.828408°N, -4.218786° W (UK AIR, 2025b) 1.3 miles from sampling location). Air quality data is published by Ricardo Group for the Scottish Government for public via Scottish Air Quality (Scottish Air Quality, 2021). These stations measure coarse particulate matter (PM_{10} = 10 µm), fine particulate matter ($PM_{2.5}$ = 2.5 µm) and ultrafine particulate matter (PM_1 = 1 µm). Particulate

matter (PM), is defined as solid or liquid particles added to the atmosphere (European Environment Agency, 2025) and is made up of a range of chemicals and compounds (DEFRA, 2025). It is one of the most researched air pollutants and poses risks to human health and is associated with asthma, cardiovascular disease and lung cancer (DEFRA, 2025). The air pollutant particulates are broken into the different size fractions (1 µm, 2.5 µm, or 10 µmin size) due to the effects the different sizes can have on human health, especially the respiratory system and epithelial boundary transfer (Gunasingam et al., 2024) and absorption by the lungs and into the blood stream (Air Quality Expert Group, 2005). There are a variety of emission sources of this pollutant including industrial and domestic contribution (e.g. soot, dust, wood burning).

These stations also measure nitrogen oxide (NO_x ; consisting of nitrogen dioxide (NO_2) and nitrogen oxide (NO)), NO_2, and nitrogen as nitrogen dioxide (NO_s; consisting of NO predominantly and NO_2). NO_s and NO_2 are measured via chemiluminescence and NO_x is calculated from these values. These pollutants are important given their contribution to GHG and climate change, and damage to ecosystem function (European Environment Agency, 2019). To date these pollutants have not been compared to atmospheric MPs therefore it was interest to observe any potential relationship.

Another station located approx. 4 miles from the sampling location also measures black carbon (BC) (Glasgow Townhead site, 55.865782°N, 4.243631°W (UK AIR, 2025)). Although this is not an accurate measurement of BC at this sampling location, it is used as an approximation of BC levels in the urban atmosphere of Glasgow at the time of sampling. Black carbon is a type of particulate matter, which is mostly elemental carbon formed by the incomplete combustion of fuels such as diesel, petrol, coal and biomass. It is considered carcinogenic and is thought to accelerate ice melt when present on snow or ice (European Environment Agency, 2013), similar to atmospheric MP (Revell et al., 2021). Again, to date these pollutants have not been directly compared or analysed, therefore it was of interest to observe potential relationships between these pollutants in the urban environment of Glasgow

(**Appendix Table VII.2**). Pearson's correlation coefficient was calculated for each variable and MP dataset along with corresponding p-value.

6.2.6 Particle Modelling – HYSPLIT Trajectory Analysis

The transport and dispersion of atmospheric MP at this location were modelled using the Hybrid Single-Particle Lagrangian Integrated Trajectory (HYSPLIT) model created by the National Oceanic and Atmospheric Administration (NOAA) (Version 5.3.0; Stein et al., 2015, Rolph et al., 2017). HYSPLIT was used in both forward and backward modes to simulate potential transport pathways and origins of MP particles present in the urban atmosphere in Glasgow. Meteorological data from the Global Data Assimilation System (GDAS) with 1-degree resolution (NOAA, 2021). Using 0.5-degree resolution would have been preferred but data was only available until 2019, before the field sampling used in this study took place. This data provides accurate inputs for wind, temperature and pressure fields during the time of sampling. KML files were generated for each model and images created using Google Earth (Google Earth, 2025) to visualise spatial and temporal dispersion. Simulations of air mass trajectories were carried out for 48 hrs to get a general overview of the atmospheric transport of particles to Glasgow. This was carried out for three elevations - 10m (the lowest possible elevation possible in the model, and calculated for above sea-level as defined by model), 50m, and 100m. Modelling different elevations helps capture the variability in how particles behave in the lower atmosphere where wind speed, turbulence and vertical mixing may vary with height. As atmospheric MP can be emitted, suspended and transported through the various levels of the atmospheric boundary layer (ABL) (Allen et al., 2019, Evangeliou et al., 2020) it is important to consider this dispersion when modelling transport, sources and pathways.

In order to gain a more accurate picture of particle transport based on the characteristics of atmospheric MPs found in the urban environment in Glasgow, individual particle models were created. Different atmospheric MP size ranges and polymer densities were modelled using their relative settling velocities. A total of 84

scenarios were modelled for each day of sampling with three different polymer size classes (10 µm, 20 µm, 100 µm, based on the particle size distribution of the samples taken at this location) and two different polymer densities (1g density which is an average polymer density (Stride et al., 2024), and 0.625g which is the polymer density of PMMA, the most commonly identified polymer at this location). The results of each of these scenarios can be found in **Appendix IX.**

Settling velocities were calculated following Allen and colleagues (2019) but relative to the particle size and density of the particles identified during field observations (see **Table 6.2**). This was done using Stokes law which denotes the force and motion of spherical particles through gas (Tsuda et al., 2013) and given the dataset used in this chapter was predominantly fragments (see **Chapter 4**), a spherical shape was assumed for the purposes of this modelling. Stokes law is as follows:

$$V = \frac{gr^2(\rho_p - \rho_m)}{18\mu}$$

Where g is the acceleration due to gravity (9.80665 m/s^2); r is the particle diameter (m) ; ρ_p is particle density (kg/m^3); ρ_m is medium density (kg/m^3); and µ is medium viscosity ($N.s/m^2$).

Table 6. 2 Particle Characteristics and Parameters used to Calculate Velocity for HYSPLIT Model Inputs

Particle Diameter (µm)	**Polymer Density (g)**	**Temperature (°C)**	**Density of medium of air (ρ_m, kg/m^3)**	**Medium viscosity (µ)**	**Velocity (VT) m/s**
10 µm	1 g (average)	5°C	1.2696	1.74E-05	0.0031
10 µm	0.625 g (PMMA)	5°C	1.2696	1.74E-05	0.0020
20 µm	1 g (average)	5°C	1.2696	1.74E-05	0.0125
2 0µm	0.625 g (PMMA)	5°C	1.2696	1.74E-05	0.0078
100 µm	1 g (average)	5°C	1.2696	1.74E-05	0.3127

Particle Diameter (µm)	Polymer Density (g)	Temperature (°C)	Density of medium of air (ρ_m, kg/m^3)	Medium viscosity (µ)	Velocity (VT) m/s
100 µm	0.625 g (PMMA)	5°C	1.2696	1.74E-05	0.1953

As dynamic velocity is influenced by temperature (Speed, 2021), the same temperature was used for this dataset. A 5°C temperature was chosen given the average temperature during the time of sampling (Visual Crossing, 2021). A generic emission factor for particles was chosen rather than using the concentration of particles found at this location. Due to the complexity of particle modelling and the current lack of knowledge on atmospheric MP release and transport behaviours (Liu et al., 2025), modelling individual particle release for each day would have been complex. Therefore, the release factor preconfigured in the model was chosen and settling velocity adjusted based on the table above. The outputs of these scenarios can be found in **Appendix IX**.

6.3 Results and Discussion

6.3.1 Particle Concentration, Shape and Size

The general trend in concentration over the sample period presented a high MP/m^3 concentration at the beginning of the sampling period for both methods of daily sampling (direct air filtration and nanotank) (see **Figure 6.3**).

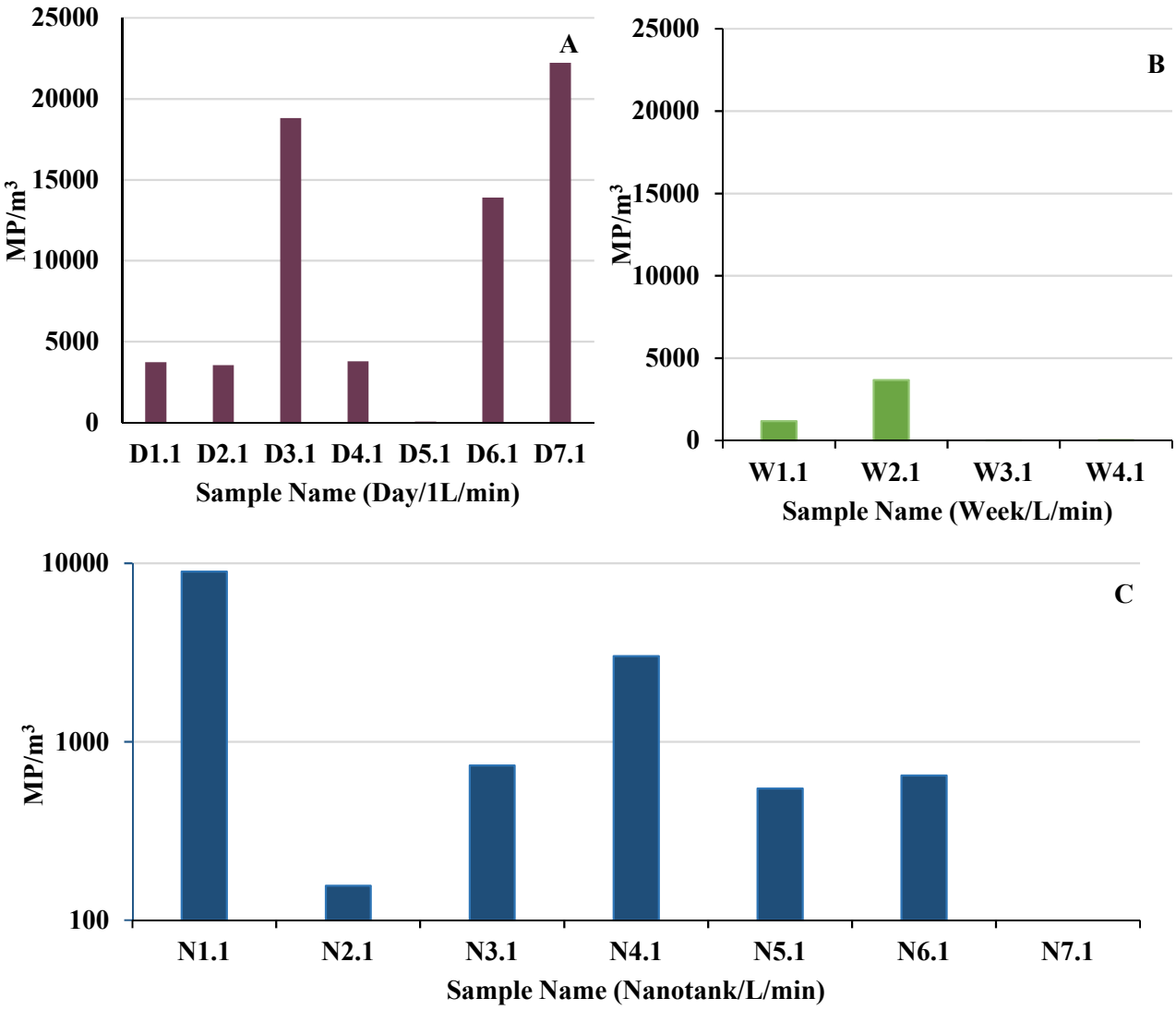


Figure 6. 3 (A) Bar Graph showing concentrations of atmospheric MPs via direct air filtration with a daily sampling frequency from 17th Nov-23rd Nov'21 (n=6, D6.10* presented as an average of other daily measurements due to data loss); (B) Bar Graph showing distribution of atmospheric MP concentrations of weekly measurements via direct air filtration from the 3rd Nov-1st Dec'21 (n=4); (C) Bar Graph showing distribution of atmospheric MP concentrations via nanotank sampling system with daily sampling frequency from the 17th-23rd Nov'21 (n=7) (Appendix Table V.1)

The average MP concentration for daily air filtration measurements over the week was 9435.8 $\pm$ 7318.7 MP/m^3. The lowest reported value was 58.4 MP/m^3 on the 5th day final day of sampling of sampling (21st of Nov) and the highest reported value was

22200 MP/m^3 on the final day of sampling (23rd of Nov) This is considerably higher than results reported by Tunahan Kaya and colleagues (2018) which took samples in urban Sakarya province in Turkey (Tunahan Kaya et al., 2018) . The study reported MP concentrations in the range of 116-3424 MP/m^2 However, their LOD was 50µm so, the smaller size fraction of MP has not been reported and only reported deposition so comparison between concentrations is difficult. A study examining megacities in China reported MP in the range of between 104-650 MP/m^3 (Zhu et al., 2021). This is especially concerning considering the study by Zhu and colleagues (2021) managed to report on concentrations with a LOD of 5.9 µm, meaning the smaller particle size fraction has been included in these results. Wright and colleagues' study in London reported an average concentration of 771 $\pm$ 167 MP/m^2 and reported a range of 510 of 925 MP/m^2 of fibrous MP and 12 to 99 MP/m^2 non-fibrous MPs. Again this study had a low LOD with particles down to 5µm being identified which indicates the smaller particle size fraction is included. Methodology differences have significant influences (**Chapter 4**) and may have influenced the differences in these findings. In Glasgow, weekly direct air measurements were also taken over the course of a month and had an average concentration of 1,730 MP/m^3 $\pm$ 1,220 MP/m^3. During the first week of measurements the concentration of atmospheric MP was 1,170 MP/m3. The highest concentrations were found in the second week, spanning the 10th-17th of November with 3,680 MP/m^3. This was followed by a drop the following week with an average of 0.69 MP/m^3. This sample was analysed with solely µRaman which could explain the lower particle concentrations as the same measurement using a higher pumping rate of 10 L/min (from **Chapter 4**) produced a concentration of 1430 MP/m^3. This was also the week in which daily measurements were made and the reported concentrations were considerably higher than the value for this sample, suggesting that the concentrations may have been underestimated due to the analysis type. As can be observed in **Figure 6.3B**, the following week there is an increase to 27.50 MP/m^3 which is lower than the first two weeks, but again a measurement taken on the same week with a higher pumping rate of 10L/min produced concentrations of 284.45 MP/m^3.

In order for this sample set to be directly comparable to the measurements taken in the remote environment of Svalbard and in the interest of gaining more data about the atmospheric MP content of this urban location, the nanotank measurements have been included in this research alongside the direct air filtration sampling. The nanotank sampling system did not perform as well overall (less representative compared to direct air filtration, **Chapters 4 and 5**). The average concentration for daily nanotank measurements was 2010 $\pm$ 3230 MP/m^3. This concentration drops over the next two days, and there is an increase to 3,020 MP/m^3 on the 20th of November 2021. The concentration of atmospheric MP then drops again to 547 MP/m^3 on the 21st of November and increases again before the lowest concentration is found on the final day of nanotank sampling, on the 23rd of November, again consistent with results from direct air filtration sampling.

The predominant shape found via Nile Red staining was fragment, with only 17.1% of particles identified as fibres (n=11). In terms of the direct air filtration system with a daily sampling frequency, there were the smallest number of fibres identified with 100% of particulates being identified as a fragment (n=6) after blank correction. The weekly samples collected via direct air filtration showed a similar distribution of fibre to fragment, with 99% of particles identified as fragments (n=2). The nanotank sampling system showed the most variation in the proportion of fibre to fragment and displayed a significantly higher proportion of fibres (52%) to fragment (47%), compared to direct air filtration samples. Fibres present in the field blanks reduced the overall number of reported fibres (see **Appendix V**). In terms of other studies in the UK, Wright and colleagues found mostly fibres (2020), whereas the study in the Humber region identified more films and fragments (Jenner et al., 2022). This highlights that the characteristics of atmospheric MP can vary greatly between different urban environments, even within the same country.

The size range of the particles identified via Nile Red staining were 1-214 μm, with 46% of particles identified < 10μm. In **Figure 6.4A**, the daily direct air filtration samples over the course of the week of sampling show a similar particle size

distribution, with the majority of particles <20 μm (98%). This sampling regime also displays the least variance in particle size distribution across the dataset. It is also clear from **Figure 6.4B** that the samples taken using a weekly sampling duration over the course of a month show a similar particle size distribution. During the first week of sampling there are more larger particles found (>100 μm), and overall across the weekly samples there are more particles >20 μm than using a daily sampling frequency. However, again there is a bias towards smaller particles, with the majority of particles <20 μm (90%).

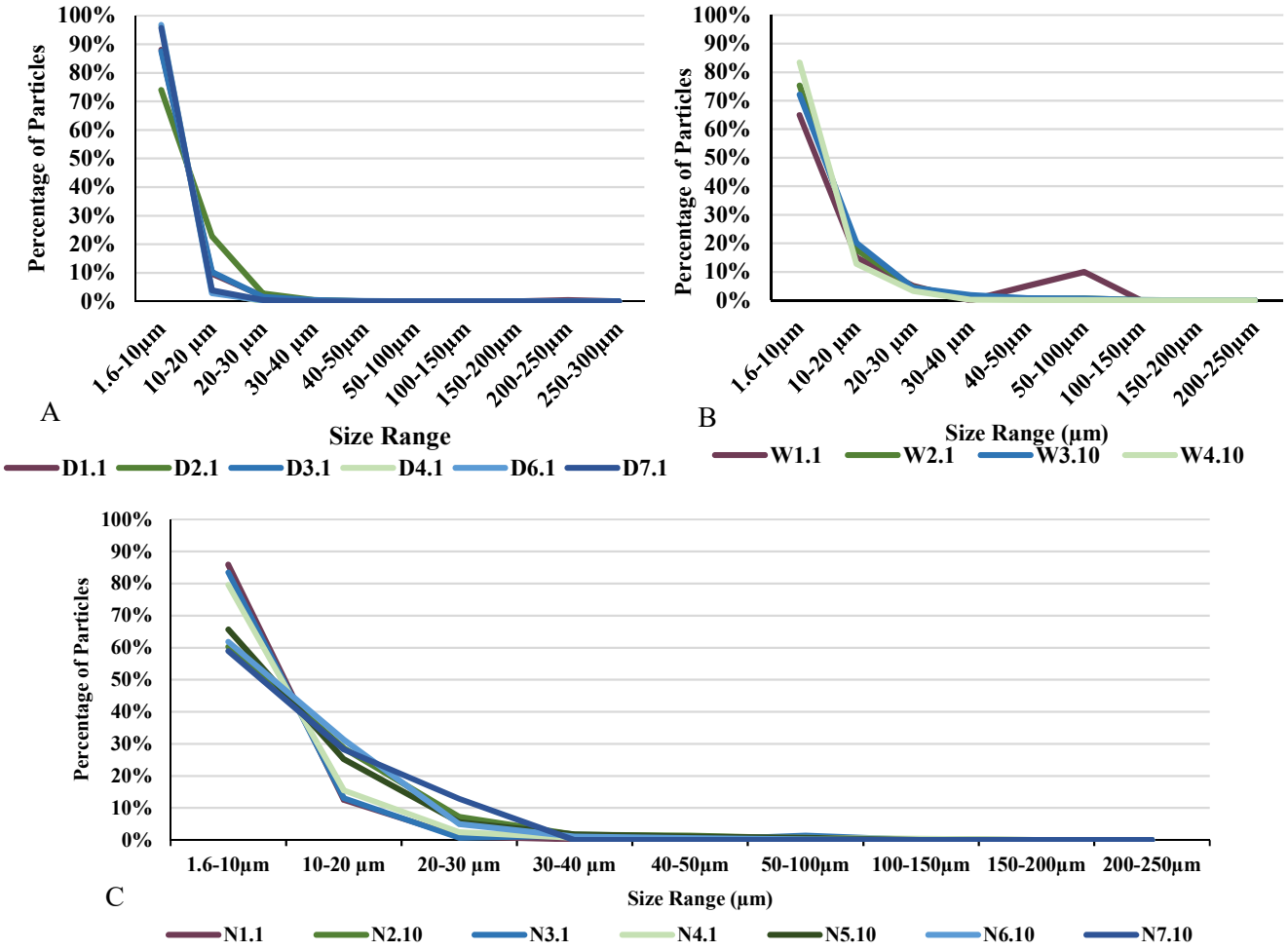


Figure 6. 4 (A) Line Graph showing particle size distribution of daily direct air filtration samples 17th Nov-23rd Nov'21 (n=7); (B) Line Graph showing particle size distribution of weekly direct air filtration samples taken from 3rd Nov-1st Dec'21 (n=7), (C) Line Graph showing particle size distribution of daily nanotank samples taken from the 17th-23rd Nov'2 1(n-7) (Appendix Table V2-5)

The daily nanotank samples showed the most varied particle size distribution as can be observed in **Figure 6.3C**. The majority of particles identified were <20 µm (85%), but it can be observed that on the third and fourth day of sampling there were slightly less particles in the 10-20 µm range. There were as many particles in the >100 µm range as there were with the weekly direct air filtration samples. This could be due to the difference in sampler design not allowing for larger particles to be collected, or

this could be due to the daily sampling frequency, as the direct air filtration daily samples had less range in the larger particle size ranges.

6.3.2 Polymer Composition

Across the four weeks of sampling the polymer composition remains fairly consistent, with Polyethersulfone (PES), Polymethyl methacrylate (PMMA) and Polysulfone (PLS) being the main polymers identified (see **Figure 6.5A**). The second week of sampling was the only week to display Polycarbonate (PC, 1% of polymers) and the final week was the only week to display Polylactic acid (PLA), nylon, and Polypropylene (PP) (all 2% of polymers for that week). Furthermore, in the first two weeks there is some Cellulose (CE) present (3% and 6% respectively), but in week 3 and 4 there is no CE identified. Furthermore, it can be observed that the proportion of PET increases gradually from each week, beginning at 4% and increasing to 8% in week 2 and 3, and reaching 15% in week four.

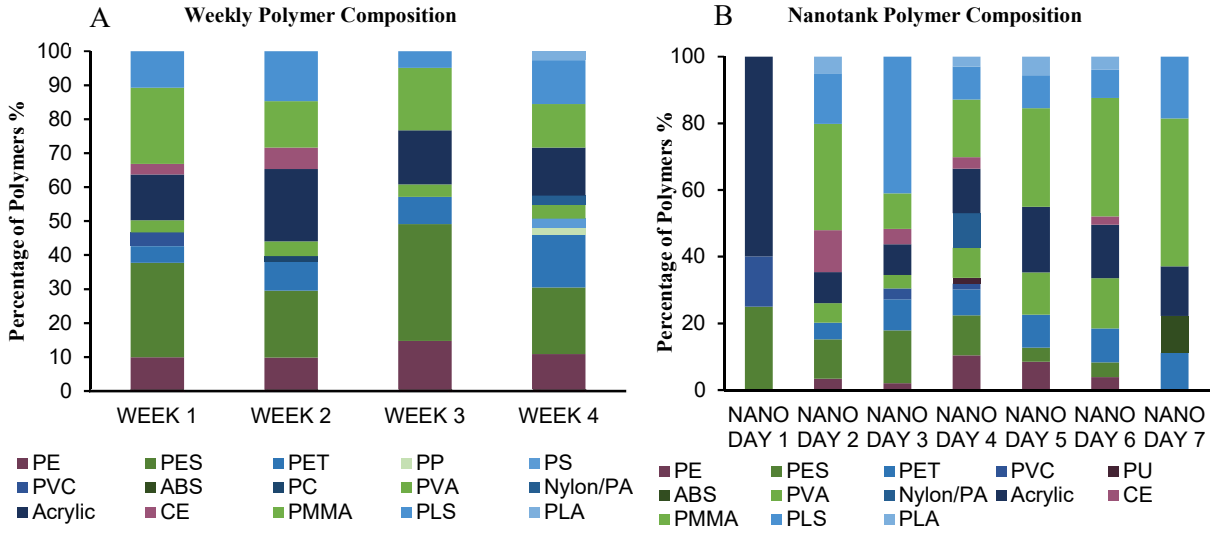


Figure 6. 5 (A) Stacked Column Graph Showing Percentage of Polymers Identified by µRaman spectroscopy for Weekly Direct Air Filtration Samples (n=4); (B) Stacked Column Graph Showing Percentage of Polymers Identified by µRaman spectroscopy for Daily Nanotank Samples (n=7) (due to resource restraints daily direct air filtration samples were mostly analysed with Nile Red staining and there was not a consistent number of daily direct air filtration samples with polymer composition data in order to present consistent dataset)

In terms of daily measurements, the nanotank samples contained the most consistent data from the results of μRaman analysis and have therefore been used in this chapter to discuss polymer composition over the seven days of daily measurements (See **Appendix Figure VII.1**) for overview of daily polymer composition). As can be observed in **Figure 6.5B**, the first day of daily sampling with the nanotank system displayed the least variation in polymer composition with only three polymers making up the proportion of polymers identified, these being acrylic (60%), PES (25%) and Polyvinyl chloride (PVC, 15%). The rest of the samples taken during daily sampling display a more varied polymer composition. PMMA, PLS and Acrylic were found in all the nanotank samples from day 2 to day 7, with PMMA or PLS being the predominant polymer component across these sampling days. CE was noted in only 4 of the samples at a proportion no greater than 13% of any of the samples. PU and ABS were found only in one sample (PU: day 4, 2%, and ABS: day 7, 11%).

6.3.3 Relationship with Meteorological Variables

To examine whether there are weather parameters that could be influencing atmospheric MP pollution in this urban location, local weather data for the same time period was compared to MP concentrations for the dataset of samples taken over the 28-day period. There was no significant relationship between MP concentrations and atmospheric pressure, precipitation, humidity, dew and temperature. There was a significant positive relationship between MP concentrations and cloud cover for weekly samples taken ($r = 0.97$; $p=0.03$). This suggests that cloud cover positively influences concentrations of atmospheric MP pollution over longer sampling periods. There is also significant negative correlation between MP concentrations and wind direction for weekly samples ($r = -0.97$; $p=0.03$), which suggests MP concentration at this location (within the southern area of high-density urban Glasgow residential area) is influenced by wind direction potentially also that suggesting a local and or distal source associated with specific wind directions. The negative relationship between

wind direction is consistent with that found that MP concentrations were significantly influenced by wind direction in Porto (Logvina et al., 2019.

Taking into consideration the predominantly <20 µm particle size distribution for the atmospheric MP pollution at this location, it was of interest to consider if size was a determining factor in the transport of atmospheric MP pollution due to weather processes. After splitting the MP concentrations into <20 µm and >20 µm classes, the concentrations were compared with the weather dataset. There were no significant correlations specifically linked to these two size differentiated MP concentrations with regards to cloud cover or humidity. There were no statistically significant relationships with particles <20 or >20 µm for any of the sample sets taken, which suggests that there is no clear pattern between weather paraments in the Glasgow environment. There have been a range of reported relationships between atmospheric MP concentrations and weather in the literature and the effect of weather on MP concentration is still a gap in the field (Zhao et al., 2020). The lack of correlation with daily direct air filtration measurements may be due to the temporal resolution being too low as they only represent 7 days of sampling in total. There could also be a stronger influence from local sources of atmospheric MP pollution rather than weather parameters. However, longer temporal measurements might identify stronger relationships with weather in future research.

6.3.4 Relationship between Air Pollutants at Urban Location

No statistically significant relationships were found between atmospheric MP levels and black carbon, PM_{10}, $PM_{2.5}$, PM_1, NO_x, NO_2, or NO_s. The dataset was again divided into <20 µm and >20 µm size classes to observe if local air pollution could be influencing specific particle sizes. There were no statistically significant relationships between BC and any of the datasets from Glasgow. Both BC and MP can originate from the burning of synthetic materials and tyre wear (Mayer et al., 2024; Evangeliou et al., 2020) and both pollutants are known to have high concentrations in industrial and urban zones (Zhao et al., 2020; Park et al., 2025). However, there does not seem

to be a strong relationship here. Future research could look into longer temporal measurements of both pollutants and measure the pollutants directly rather than relying on regional air pollution data.

There were no significant relationships with any of the datasets taken and PM_{10} ,PM_{1} $PM_{2.5}$ which is interesting given the particle size for this dataset. These forms of pollution are co-located and share potential local and distal sources (Akhbarizadeh et al., 2021) Future research could look to measure both pollutants over a longer period and again using direct measurements rather than using estimates from regional air quality data.

When compared to the different forms of nitrogen again there were no statistically significant relationships. Similarly to BC, there are no published studies to date that compare concentrations of these two groups of atmospheric pollutants. They could also share similar sources in an urban location such as vehicle traffic and waste burning. It would be interesting to observe any long-term relationships between the two pollutants and collect more local primary data. This could be particularly relevant to the seasonal variations of the pollutant, as both have been found to have higher levels in winter (Liu et al., 2025; Britton et al., 2022), and this study was carried out in the winter season in Glasgow. Future research could measure both pollutants in conjunction over a winter and summer season, to observe potential patterns and gain a more accurate picture of the occurrence of these two pollutants.

Given the public health, environmental and climate risks posed by both atmospheric MP pollution and more traditional air pollutants, and their potential co-occurrence, future research should focus on the potential relationships between these two groups. Measuring both groups of pollutants in the same location over a longer period could give more detail on how they interact and help identify potential drivers. Furthermore, studies on potential chemical interactions between polymers and additives used in their production, and compounds such as PM, BC and NOs could provide more information on the transport properties and the environmental and health risk factors associated with the co-location of these pollutants.

6.3.5 Results of HYSPLIT Backward Trajectory Modelling and Possible Sources

Modelling of both air mass movement and particle dispersion were undertaken to investigate how air masses transport atmospheric MP to and from the sampling point, and also how different particle sizes and densities may be transported in different ways. In order to gain more detail on the transport of the pollutant to and from the site, the week of daily sampling was chosen to observe daily movement of air masses and particles.

From the air mass modelling, it can be observed in **Figure 6.6** the three elevations modelled can be observed (10 m, 50 m, 100 m), which were chosen in order to observe changes in wind patterns at different heights and in order to gain a realistic picture of transport pathways.

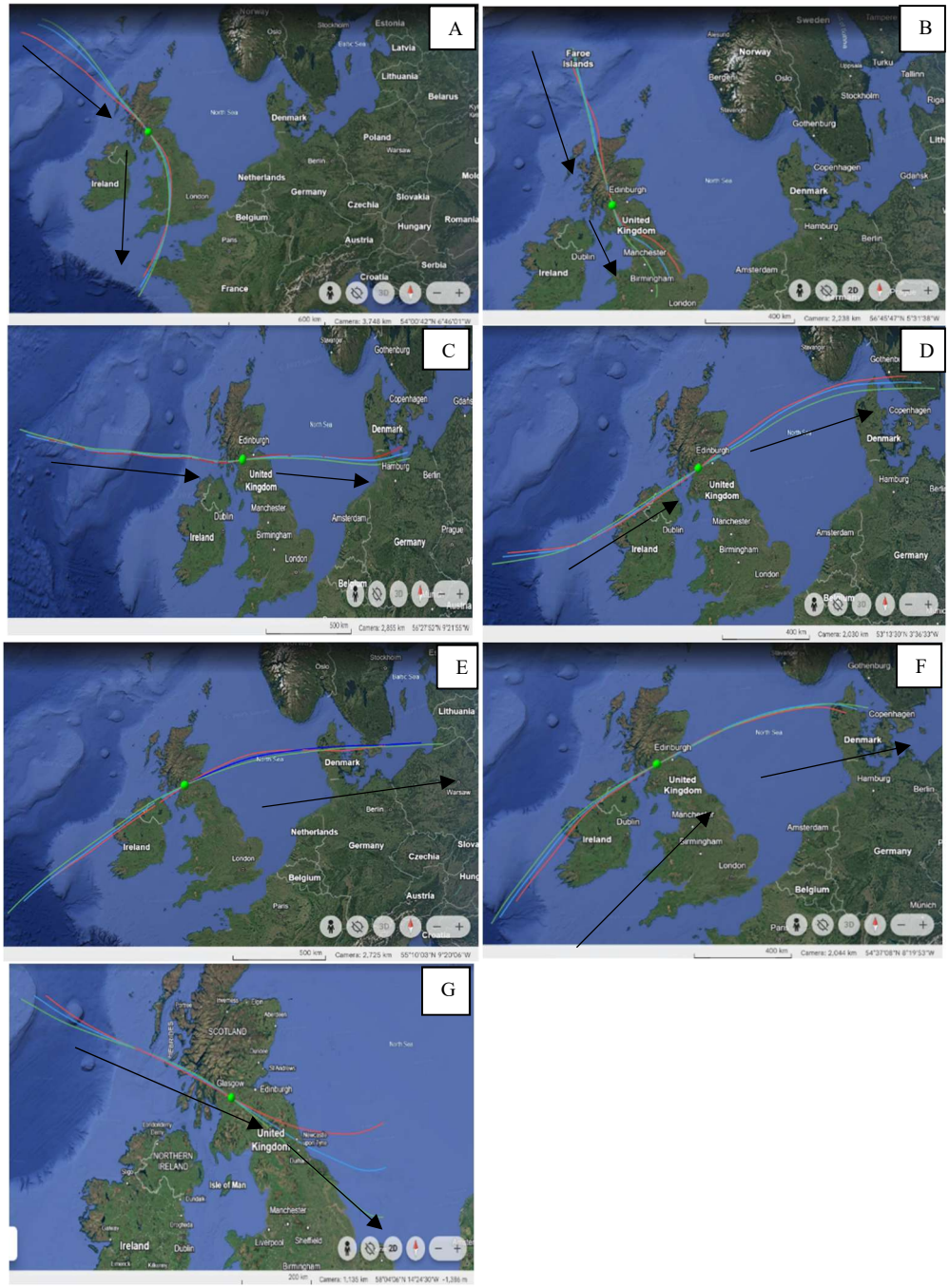


Figure 6. 6 (A) Results from HYSPLIT Back and Forward Trajectory Modelling for the 17th Nov'21; (B) Results from HYSPLIT Back and Forward Trajectory Modelling for the 17*8h* Nov'21; (C) Results from HYSPLIT Back and Forward Trajectory Modelling for the 19th Nov'21; (D) Results from HYSPLIT Back and Forward Trajectory Modelling for the 20th Nov'21 ; (E) Results from HYSPLIT Back and Forward Trajectory Modelling for the 21st Nov'21; (F) Results from HYSPLIT Back and Forward Trajectory Modelling for the 22nd Nov'21; (G) Results from HYSPLIT Back and Forward Trajectory Modelling for the 23rd Nov'21; Different Elevations Depicted by Red – 10 m; Blue – 50 m; Green – 100 m
(Google Earth, 2025)

As can be observed in **Figure 6.6**., there are similarities across the sampling period with a trend of air masses originating in the North Atlantic before travelling east towards Glasgow. There was some variability in the precise origins of the air masses with some originating near the Celtic Sea (see **Figure 6.6 A,C,D,F**), and others originating further north near Iceland and the Faroe Islands (**Figure 6.6.B**), but the dominant trend was long-range transport from the North Atlantic. At all three elevations modelled (10m, 50m, 100m), the air mass trajectories were broadly similar, with minor differences in latitudinal position and higher trajectories originating further north and lower trajectories moving further southward. In general the air masses frequently passed over Ireland, Northern Ireland or the Hebrides before reaching Glasgow, highlighting the influence of both transboundary marine sources and regional land-based inputs.

6.3.7 Results of HYSPLIT Back Trajectory Particle Modelling – Influence of Particle Size and Polymer Density

Of the 42 backward trajectory modelling scenarios for the different particle characteristics, there are some key similarities and differences between MP size classes and polymer types. In terms of source appointment, for the majority of scenarios, there appears to be an influence from the Atlantic Ocean, with trajectories carrying particles from the North Atlantic east towards the sampling location. Furthermore, although there are some scenarios where the lower trajectories originate in the North Atlantic, the majority of the lower trajectories appear to be more local in origin which suggests more of an influence from local urban or industrial sources. The higher trajectories indicate more long-range transport originating in the North Atlantic Ocean, but also remote regions such as Greenland and Southern Iceland. This suggests that there are both long-range marine sources as well as local sources of the atmospheric MP pollution found at this sampling location.

On the day where atmospheric MP concentrations were highest – the 17th of November for both direct air filtration and nanotank sampling systems – for the 10 μm MP size,

there is further long-range transport originating on the south west coast of Greenland (see **Figure 6.7**). Despite its remote location Greenland has high levels of plastic pollution and a recent report has suggested this area of Greenland to have numerous active local sources of plastic pollution such as commercial fishing, hunting and municipal waste (Strietman et al. 2021).

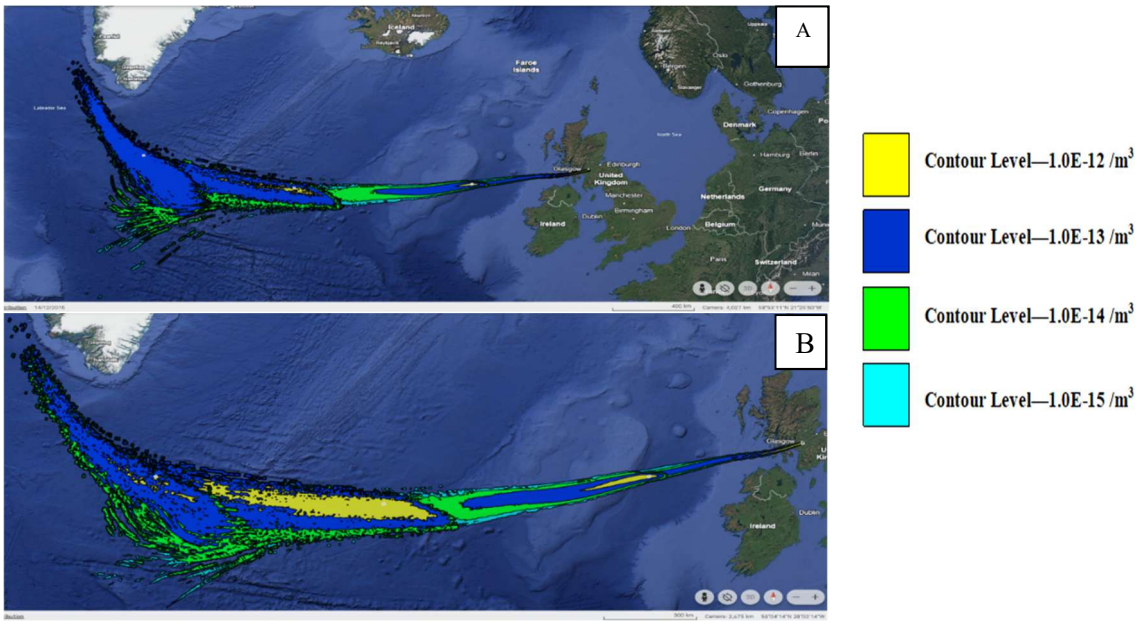


Figure 6. 7 (A) Results from Backward Trajectory Modelling for 48hrs for 10 µm particles with 1 g density 17th of Nov'21; (B) Results from Backward Trajectory Modelling for 48hrs for 10 µm particles with 0.625 g density for the 17th of Nov Backward 0.625g density *(Google Earth, 2025)*

The second highest concentration for direct air filtration sampling occurred on the 19th of November. The model of atmospheric particle transport indicates there is a strong influence from higher trajectories over the Republic of Ireland and Northern Ireland and the west coast of Scotland (**Figure 6.8**) suggesting that the lower trajectories could be picking up pollution from more populated areas and transporting them east towards the sampling location.

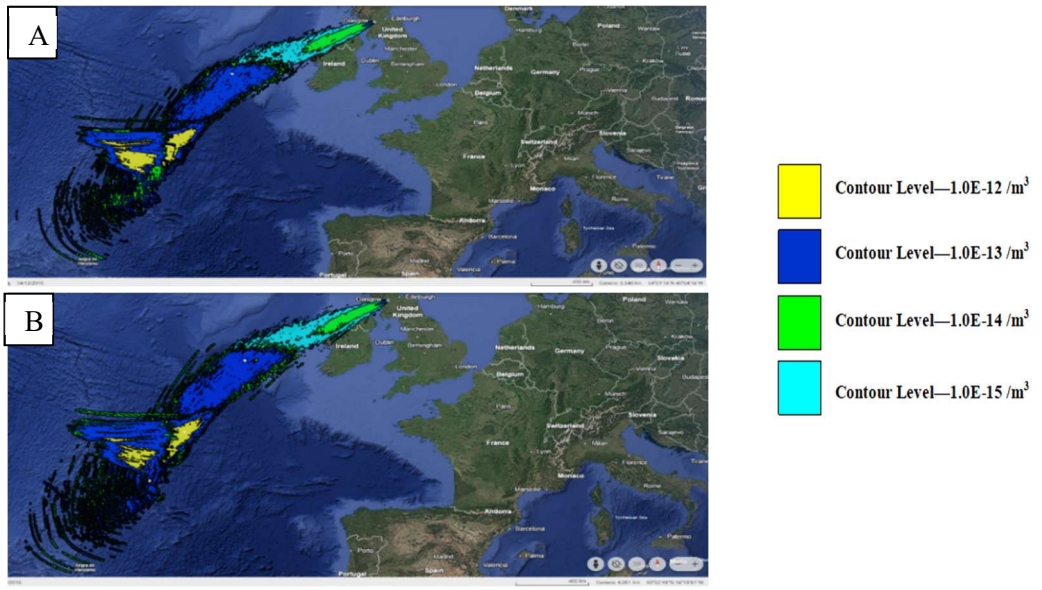


Figure 6. 8 (A) Results from Backward Trajectory Modelling for 48hrs for 10 µm particles with 1 g density 19th of Nov'21; (B) Results from Backward Trajectory Modelling for 48hrs for 10 µm particles with 0.625g density for the 19th of Nov Backward 0.625 g density *(Google Earth, 2025)*

On the second highest day of daily nanotank sampling – the 22nd of November – the higher trajectories originate as far away as the east coast of America and passing over Greenland again before converging over with lower trajectories over the north Atlantic as particles move east to the sampling location (see **Figure 6.9**). This indicates that long-range transport of atmospheric MP from the east coast of North America and the North Atlantic played a strong influence in atmospheric MP pollution at this urban location on this day.

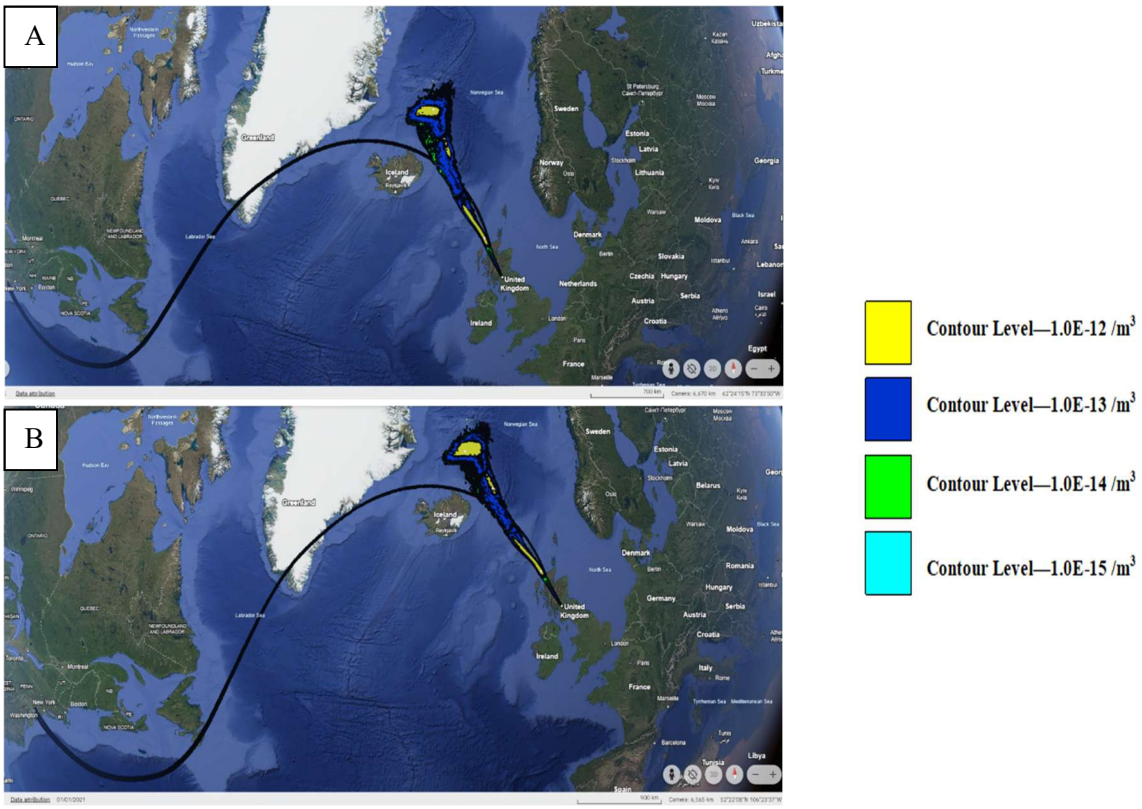


Figure 6. 9 (A) Results from Backward Trajectory Modelling for 48hrs for 10 µm particles with 1 g density 22nd of Nov'21; (B) Results from Backward Trajectory Modelling for 48hrs for 10 µm particles with 0.625g density for the 22nd of Nov Backward 0.625g density *(Google Earth, 2025)*

The lowest reported concentrations were on the final day of sampling for both the direct air filtration and nanotank sampling systems, and on this day, particles may have originated from a couple of areas in the North Atlantic before converging and travelling east to the sampling location. It can be observed in **Figure 6.10** that the trajectories are not as clear and do not follow the typical lateral transport that the other days of modelled particles followed. This could indicate that wind patterns could be dispersing particles in a different manner compared to days with higher concentrations. It can be observed that the trajectories did not pass over land masses before reaching the sampling location, compared to the other days. This could indicate that smaller particles are being transported from distal land masses, as well as marine sources, before reaching the sampling location.

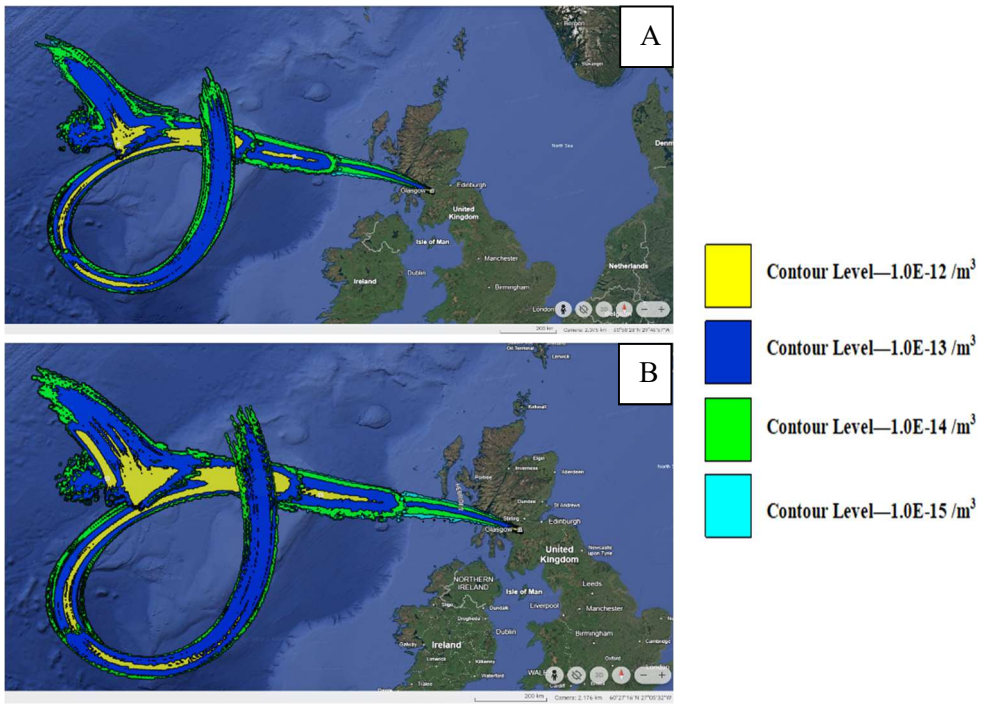


Figure 6. 10 (A) Results from Backward Trajectory Modelling for 48hrs for 10 µm particles with 1 g density 23rd of Nov'21; (B) Results from Backward Trajectory Modelling for 48hrs for 10 µm particles with 0.625 g density for the 23rd of Nov Backward 0.625g density *(Google Earth, 2025)*

The 10 µm particle modelling results also display more scattering and less defined trajectories suggesting there could be more vertical mixing and smaller particles could be more influenced by boundary layer turbulence and convective mixing. This is especially true for the lighter polymer density modelled (0.625 g density). The models where a heavier polymer density was used (1 g) also display more influence from the higher trajectories, suggesting that once particles of this density are suspended they remain within their trajectory air masses for longer, compared to the 0.625g density which was more concentrated in the lower trajectories.

The modelled 20 µm MP particulates displayed less scattering and had more clearly defined trajectories (see **Appendix IX**), when compared to the smaller 10 µm modelled trajectories. This is especially true for the higher particle density (see **Figure 6.11**). On the highest day of reported concentrations there was also a wider spatial

distribution from the lower trajectories compared to the smaller particle size (indicated by the yellow area on the particle model image).

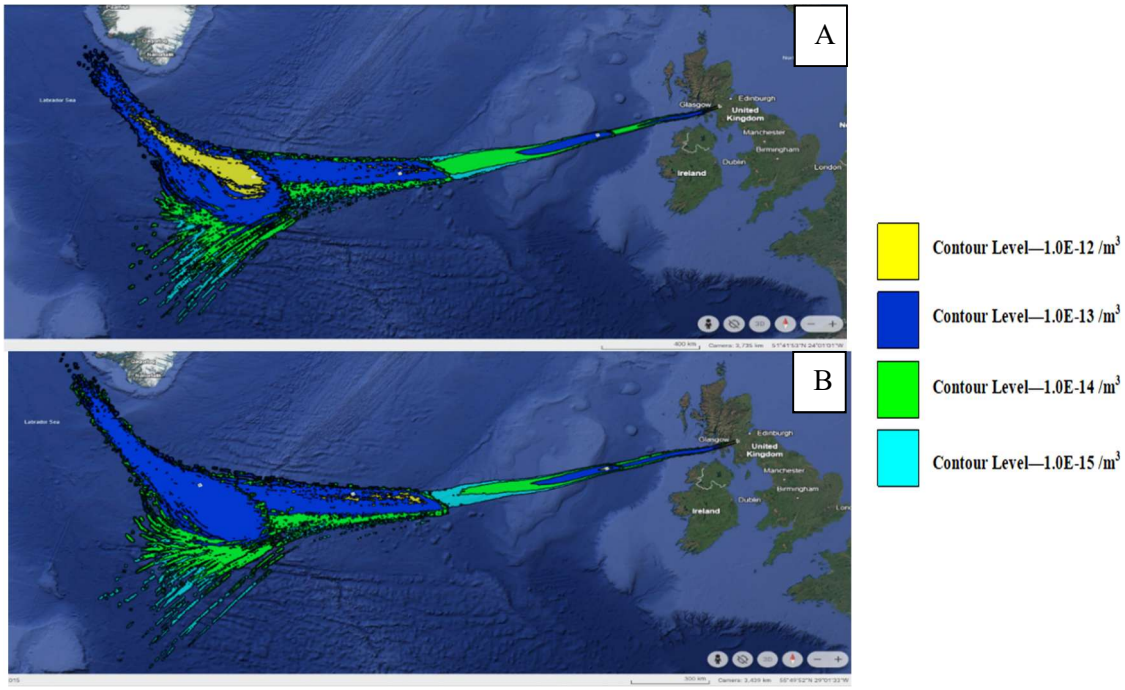


Figure 6. 11 (A) Results from Backward Trajectory Modelling for 48hrs for 20µm particles with 1 g density 23rd of Nov'21; (B) Results from Backward Trajectory Modelling for 48hrs for 20µm particles with 0.625g density for the 23rd of Nov Backward 0.625 g density *(Google Earth, 2025)*

The same is true for the 19th of November, the second highest recorded day for direct air filtration, where the lower trajectories display a higher concentration, especially for the higher particle density which has higher concentrations from lower trajectories over the Atlantic Ocean (**Figure 6.12**). This suggests particles of 20 µm with a 1g density are concentrated from marine sources. On the same day the 0.625 g density is more concentrated in the higher trajectories over the Republic of Ireland and Northern Ireland and there is more scattering where particles originate in the North Atlantic. This suggests that particles of a lighter density with a larger particle size remain in the higher trajectories but are more easily influenced by atmospheric processes, compared to the higher density particles.

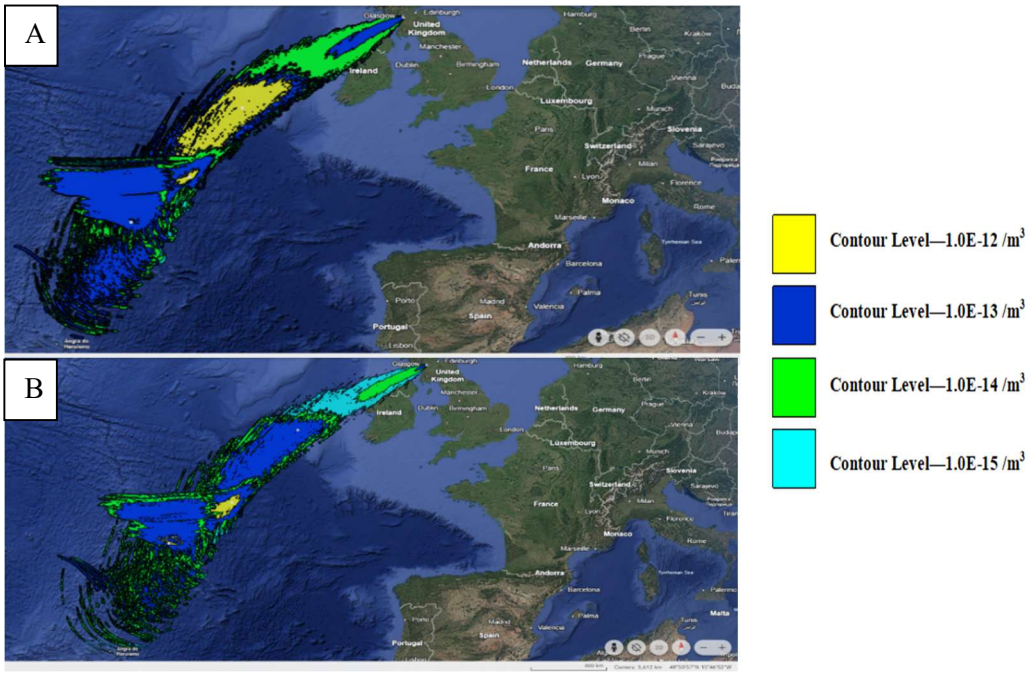


Figure 6. 12 (A) Results from Backward Trajectory Modelling for 20µm particles, 1 g density, for the 19th of Nov' 21; (B) Results from Backward Trajectory Modelling for 20µm particles, 0.625 g density for the 19th of Nov'21 *(Google Earth, 2025)*

On the second highest day of nanotank sampling, for the 20 µm modelled particle trajectory, the lighter density particles can also be observed to have two higher trajectories coming into play on the east coast of North America (**Figure 6.13B**), compared to just one with the higher density particles (**Figure 6.13A**). This indicates that the lighter particle densities originating from distal sources, are more easily transported over a wider spatial distribution.

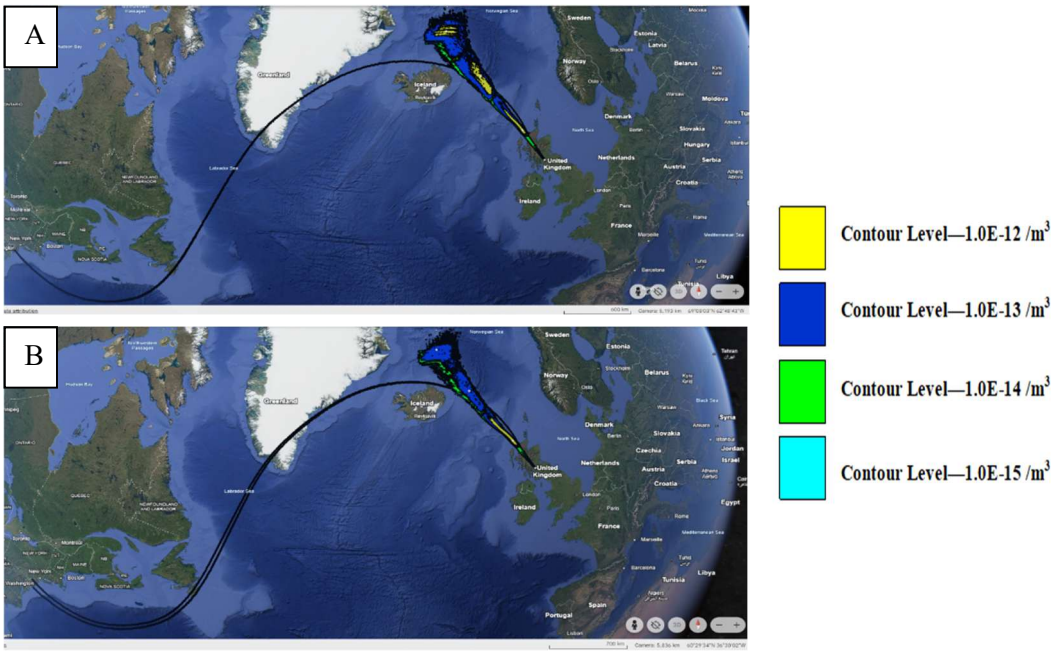


Figure 6. 13 (A) Results from Backward Trajectory Modelling for 20 µm particles, 1 g density, for the 22nd of Nov' 21; (B) Results from Backward Trajectory Modelling for 20 µm particles, 0.625 g density for the 22nd of Nov' 21 (Google Earth, 2025)

On the final day of sampling where the lowest reported concentrations were found, there is a wider spatial distribution from particles originating in the North Atlantic in the higher trajectories compared to 10 µm. There are also more defined trajectories and less scattering compared to the smaller particle size, especially for the higher particle density (**Figure 6.14)**. This could indicate that 20 µm particles originating in the North Atlantic on this day where less influenced by atmospheric processes.

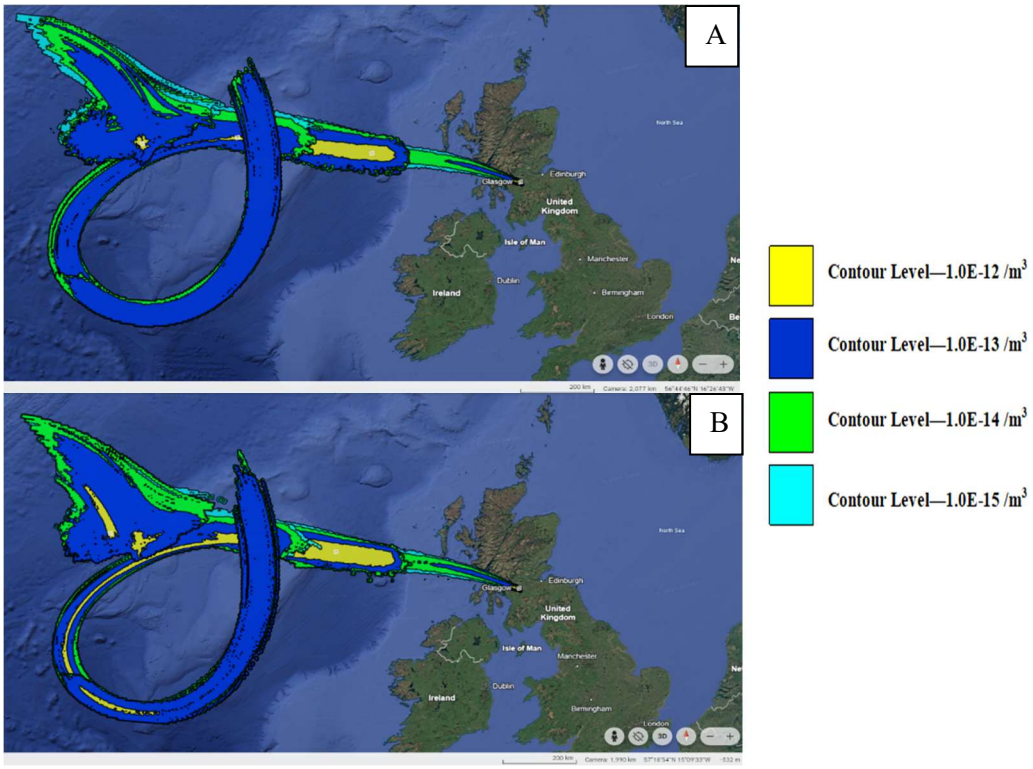


Figure 6. 14 (A) Results from Back Trajectory Modelling for 20 µm 1 g density for the 23rd of Nov'21; (B) Results from Back Trajectory Modelling for 20 µm 0.625 g density for the 23rd of Nov'21 *(Google Earth, 2025)*

The modelled 100 µm particle size displayed the biggest differences when compared to the 20 µm and 10 µm sizes. The trajectories where much clearer and there is a clear pattern of higher trajectories being more concentrated where they originate and then moving to the lower trajectories closer to the sampling location. There was also very little scattering suggesting that the particles of this size were less influenced by vertical mixing and turbulence. Furthermore, there were clear differences between the two polymer densities in terms of source appointment and particle dispersion.

As can be observed in **Figure 4.15B**, the lower particle density has a larger lateral spatial distribution for the lower particle density on the 17th of Nov'21, when concentrations were highest, with the higher trajectories originating further east on the west coast of Scotland before travelling east to the sampling site. Whereas the higher

density (**Figure 4.15A**), the particles originate much closer to the sampling location, on the mainland in the east of Glasgow.

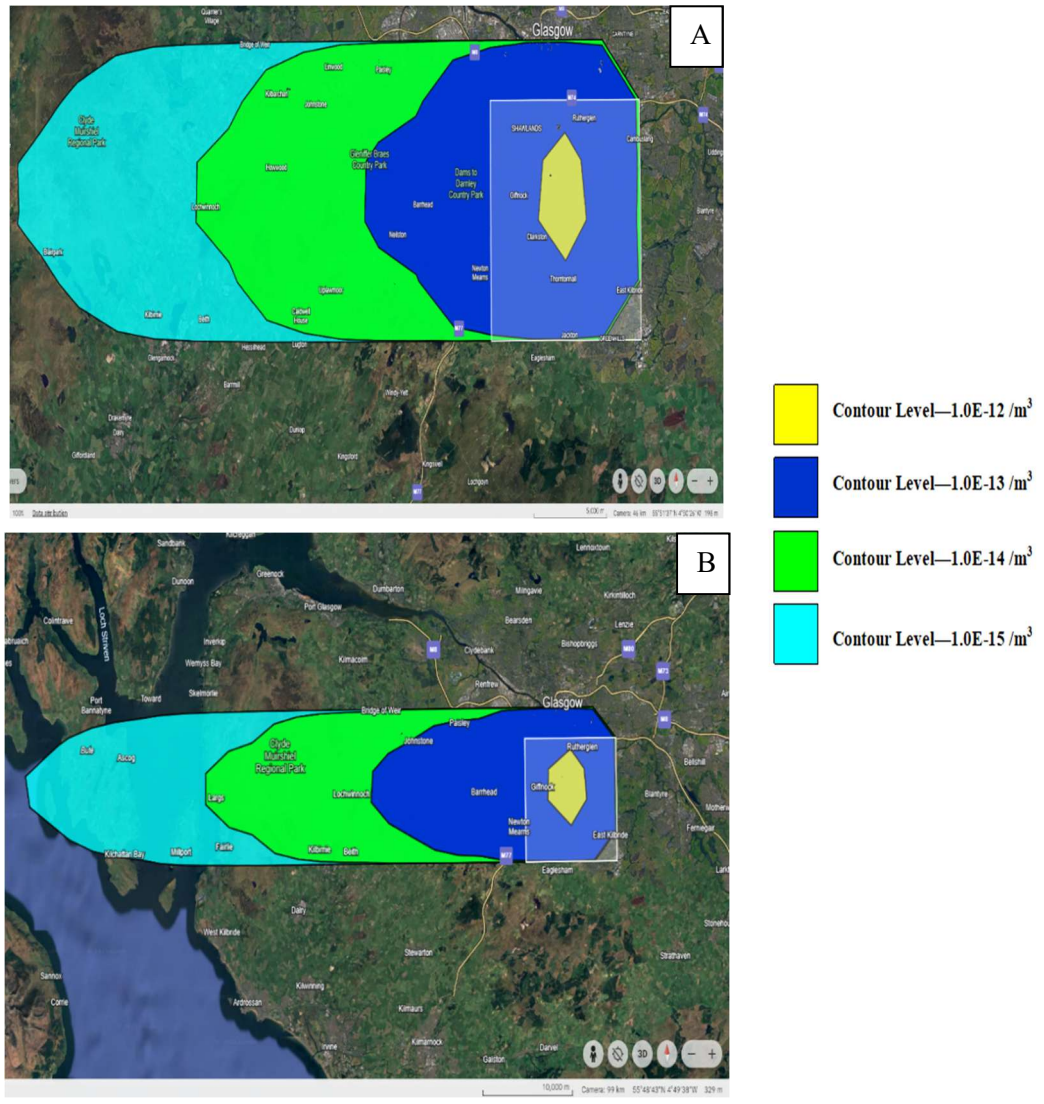


Figure 6. 15 (A) Results from Back Trajectory Modelling for 100 µm 1 g density for 48hrs for the 17th of Nov' 21; (B) Results from Back Trajectory Modelling for 100 µm 0.625 g density for 48hrs for the 17th of Nov' 21 *(Google Earth, 2025)*

On the second highest reported day, the difference between the two densities is more defined, with the higher trajectories for the 1 g density originating over the north coast of Northern Ireland and with clearly defined trajectories moving east to the sampling location (**Figure 4.16A**). The 0.625 g density has higher trajectories originating further

south in the North Atlantic off the coast of the Republic of Ireland near the Celtic shelf and then particles are not depositing again until reaching the sampling location (**Figure 4.16B**). It can also be observed that there is more scattering and less defined trajectories for the lighter polymer density. This could be due to the role of waves and sea spray in this area of the Atlantic, which could influence the lighter polymer density compared to the higher density.

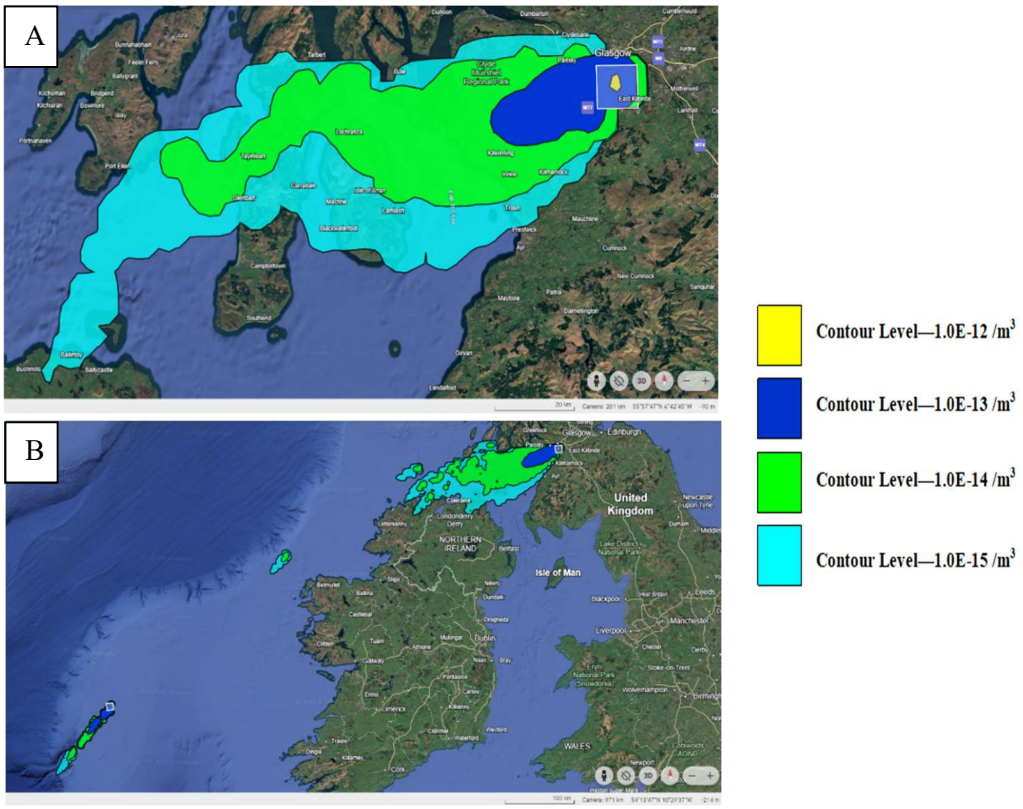


Figure 6. 16 (A) Results from Back Trajectory Modelling for 100 µm 1 g density for 48hrs for the 19th of Nov' 21; (B) Results from Back Trajectory Modelling for 100 µm 0.625 g density for 48hrs for the 19th of Nov' 21 *(Google Earth, 2025)*

A similar trend can also be observed on the 21st of November'21, whereby the higher particle density has higher trajectories originating in the north Atlantic north east of the Outer Hebrides islands in Scotland, with some scattering and a break until the sampling location (see **Figure 6.17A**). Whereas the lower particle density has a much stronger influence from the higher trajectories which originate further north in the North Atlantic to the south east of the Faroe Islands (see **Figure 6.17B**). These trajectories also have a much wider spatial distribution and there is more scattering.

This could indicate that the lighter density is more easily transported from long-range and marine sources, and is more influenced by processes such as waves and sea spray in areas of the Atlantic where they are more prevalent, such as near continental shelfs like the Celtic shelf. This due to a process called wave shoaling with causes the ocean to swell in the shift from deeper to shallower water over the continental shelf, causing waves to become steeper and therefore causing more sea spray. It has been reported that atmospheric MP are transported via waves and sea spray processes (Allen et al., 2020), which could explain the results of the back-trajectory modelling for this period. Although this day of sampling did not produce significantly different concentrations compared to other days (see above), it is interesting to observe the different transport behaviours of particles of different polymer densities in the 100 µm size.

.

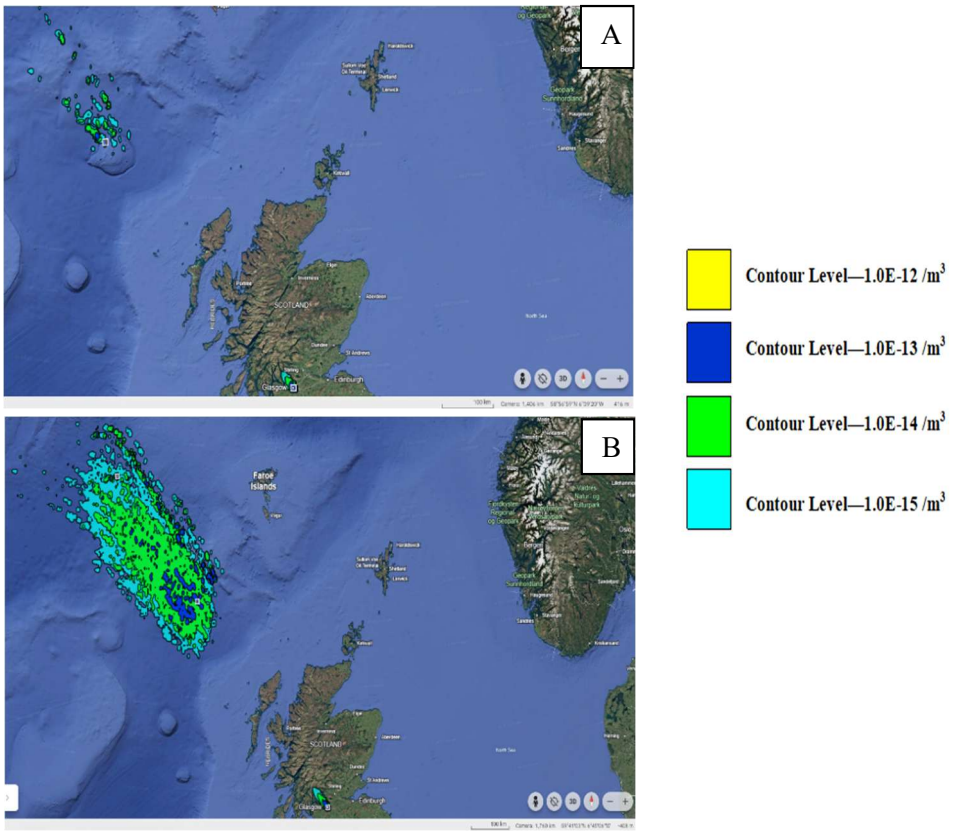


Figure 6. 17 (A) Results from Back Trajectory Modelling for 10 0µm 1 g density for 48hrs for the 21st of Nov' 21;)B) Results from Back Trajectory Modelling for 10 0µm 0.625 g density for 48hrs for the 21st of Nov' 21*(Google Earth, 2025)*

Again on the 23rd of November when the lowest concentrations were reported there is a clear difference between the polymer densities. The higher density displays higher trajectories originating closer to the sampling location north east of Glasgow and there is a clear definition between trajectories which follow a similar pattern of the lower trajectories becoming more concentrated closer to the sampling location (**Figure 6.18**). The lower density on the other hand, has a mixture of higher and lower trajectories originating and concentrated in the North Atlantic off the east coast of the Outer Hebrides, with scattering and a mixing of trajectories. There is a clear gap where these trajectories originate until there are some higher trajectories that originate north east of Glasgow which then follows the same pattern of lower trajectories being more concentrated closer to the sampling location. Again this indicates the lighter polymer

is more influenced by marine and atmospheric processes. The lack of clear lateral transport from marine or local sources could have resulted in a lower MP count on this day, but the modelled smaller particle sizes also indicate a lack of influence from other populated long-range areas on this day.

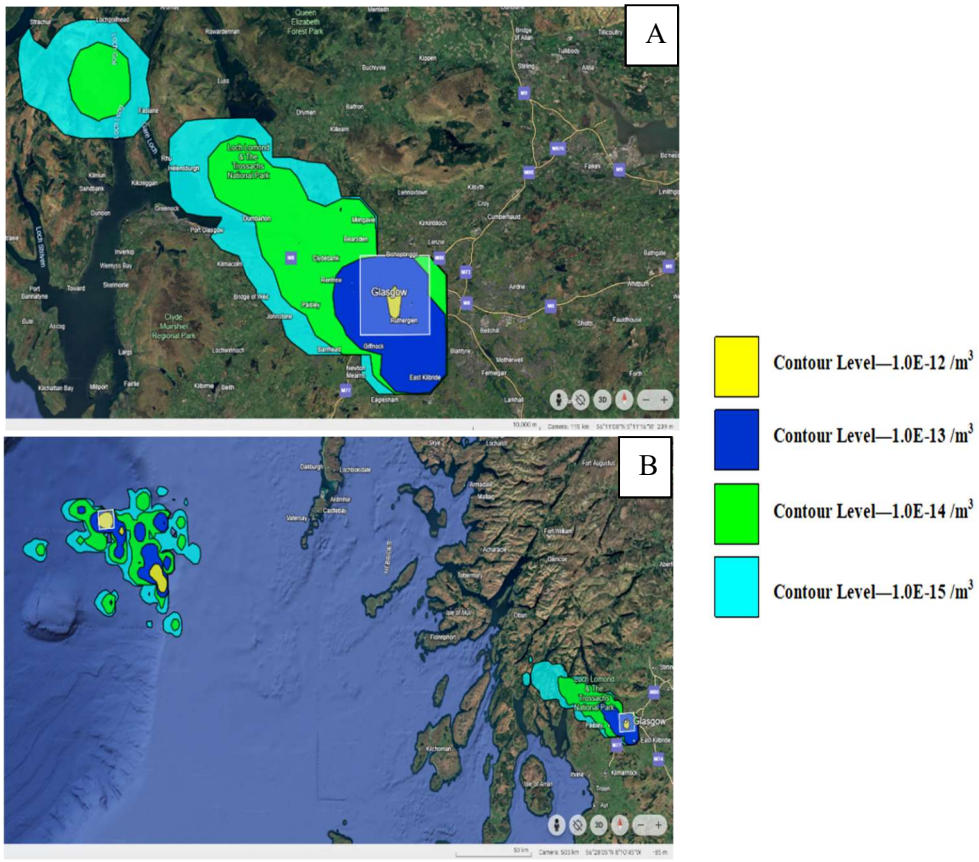


Figure 6. 18 (A) Results from Back Trajectory Modelling for 100 µm 1 g density for 48hrs for the 23rd of Nov' 21; (B) Results from Back Trajectory Modelling for 100 µm 0.625 g density for 48hrs for the 23rd of Nov' 21 (Google Earth, 2025)

Overall there are clear differences for each particle size and polymer density in terms of where they originate and possible sources which suggest both long-range transport and marine influence, as well as more localised influence from urban and industrial sources, especially for the larger particle densities. This highlights the differences in atmospheric transport for this pollutant and the complexity of source appointment and understanding their transport as there is so much nuance in how the particles

behave in the atmospheric compartment and the different processes that could affect their transport.

6.3.7 Results of HYSPLIT Forward Trajectory Modelling and Potential End Point

In **Figure 6.6** it is also possible to observe the forward trajectory air mass modelling for the daily sampling period 17th-23rd of Nov'21. Here it is possible to see the different air mass trajectories for the different elevations examined as they follow slightly different transport pathways after leaving the sampling location. Modelling indicates that after leaving Glasgow, air masses generally travelled eastwards towards the North Sea, with many continuing into northern and central Europe, including the Netherlands, Germany, Denmark, Sweden and occasionally as far as Russia (**Figure 6.6C, D, E, F**). Across the three elevations modelled (10m, 50m, 100m), the overall transport pathways were similar, though higher elevations generally extended further east and south, whereas lower trajectories generally extended further north. In some cases, air masses followed more southerly or south westerly pathways reaching southern England, France (**Figure 6.6A, B, G**) or returning to the North Atlantic (**Figure 6.6A**), highlighting the potential for MPs to both originate from and be redeposited into marine environments. Overall, modelling demonstrates the capacity for atmospheric MPs to be transported both locally and long-distance, with the potential to reach remote environments and populated regions across Europe within 48hrs.

6.3.8 Results of HYSPLIT Forward Trajectory Particle Modelling – Influence of Particle Size and Polymer Density

When examining the effect of different particle sizes and polymer densities on the potential forward trajectory transport, it is evident that the same trends can be observed in relation to the transport properties of each particle type. These parameters also play

a role in the end points of atmospheric MP particles present in this urban environment, as they did with the potential sources.

On the first day of sampling with the highest reported concentrations, particles from higher trajectories can reach as far as east Russia, Estonia and south into Romania and Kosovo. The lower trajectories indicate transport south west into Germany and southern Europe covering Monaco, the south of France and into Northern Spain and Portugal before reaching the Atlantic Ocean. The results from the modelling from the second highest reported concentrations, the 19th of Nov'21 indicate that there is not a clear transport pathway to Europe as noted the previous day. Results show a wider spatial distribution covering Eastern Europe and scattering reaching as far south as Romania and the Black Sea. The nanotank sampling system also had higher concentrations on the 22nd of November and particle modelling indicates that MP particles on this day could be transported further south into England, across the English Channel and reach as far south as southern Italy and the Mediterranean. Finally on the last day of sampling, the 23rd of Nov'21, modelling indicates a wider spatial distribution of particles across England and particles scattering east into northern Europe, and south to Guernsey. However, results indicate that there is less long-range particle transport on this date which could be due to the reduced influence of atmospheric processes or weather on this day. See **Appendix IX** for more detailed images of all forward trajectory models ran for this period.

The modelled 10µm size range displays further long-range transport and more scattering and less defined trajectories than other size classes. This is similar to the back-trajectory scenarios and again suggests the smaller particle sizes may be more influenced by turbulence and wind patterns. With the different polymer densities, there are some clear differences between the heavier and lighter densities modelled. For example, on the 17th of Nov'21 where concentrations were highest, it can be observed in **Figure 6.19B**, that the lighter density (0.625 g) has further long-range transport in the lower trajectories, and similar to the back-trajectory modelling there is more scattering and less defined trajectories with the lighter density. The 1 g density is also

more concentrated in the lower trajectories over Eastern Europe reaching further East into Russia, whereas the lighter density reaches further south into Italy and the Mediterranean in the higher trajectories. This suggests the lighter particles are more easily influenced by wind patterns and can be transported further in the higher trajectories. It can also be observed that both densities diverge over Eastern Germany which could be differences in atmospheric pressure systems in the region during this time, or particle settling over this area.

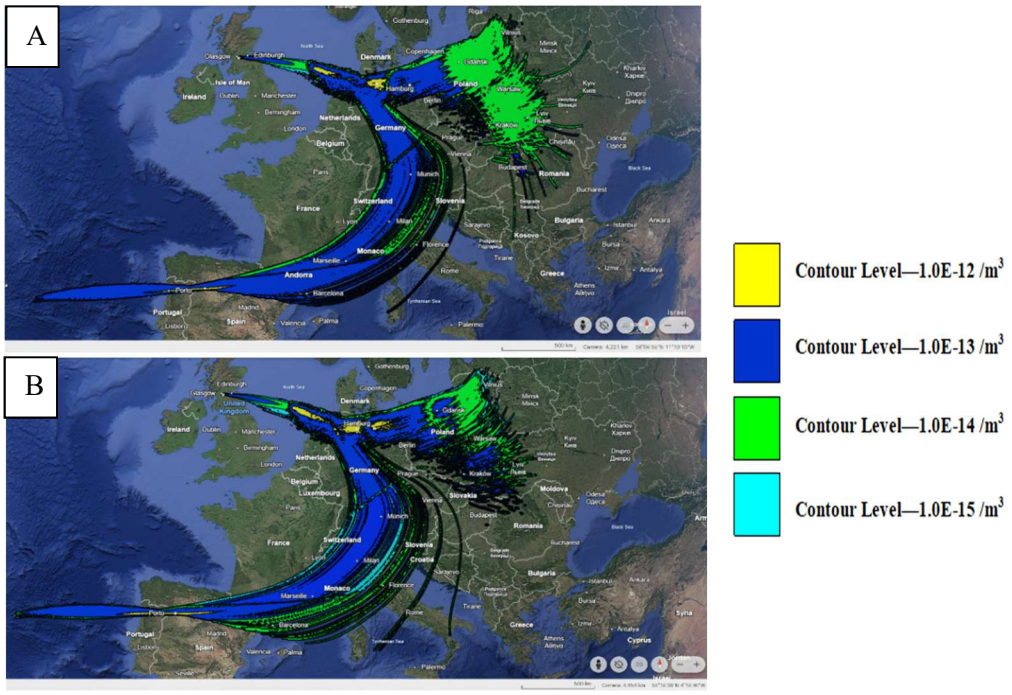


Figure 6. 19 (A) Results from Forward Trajectory Modelling of 10 µm 1 g density for 48hrs on the 17th of Nov'21; (B) Results from Forward Trajectory Modelling of 10 µm 0.625 g density for 48hrs on the 17th of Nov'21 *(Google Earth, 2025)*

On the 19th of Nov'21 when concentrations were high, the 1 g density is more concentrated in the higher trajectories and the 0.625 g density can be observed to be more concentrated in the lower trajectories, especially over Denmark and Eastern Europe (**Figure 6.20**). The lighter density also has more scattering, especially as the trajectories reach their endpoint in the Black Sea and the higher trajectories reach further east into Russia compared to the higher density.

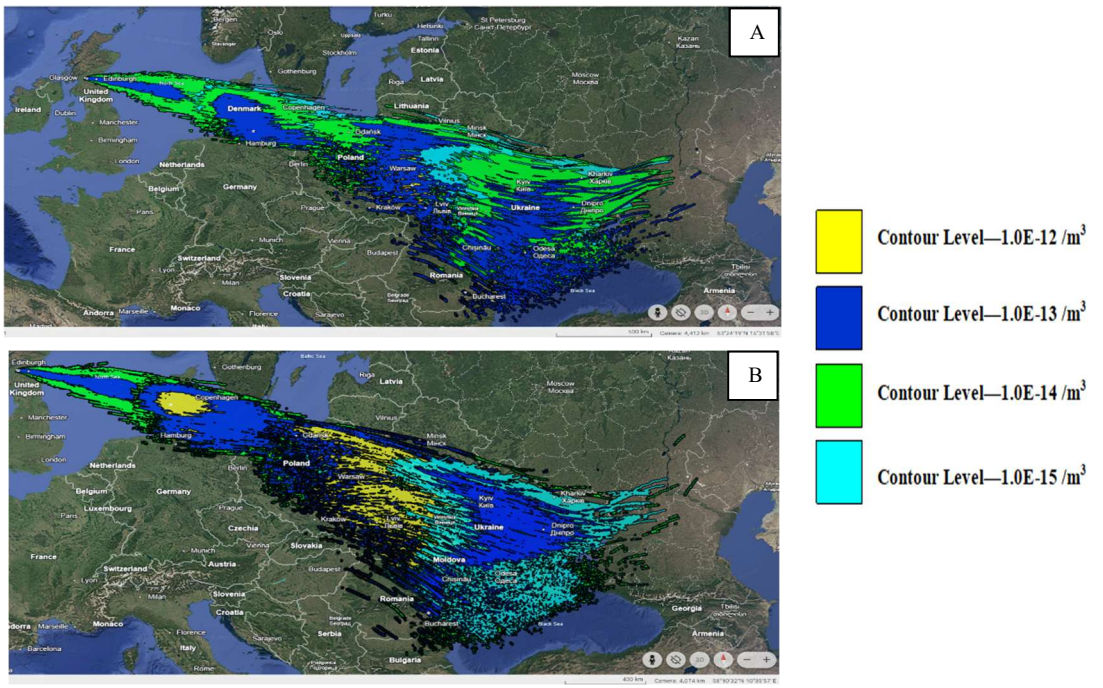


Figure 6. 20 (A) Results from Forward Trajectory Modelling of 10 µm 1 g density for 48hrs on the 19th of Nov'21; (B) Results from Forward Trajectory Modelling of 10 µm 0.625 g density for 48hrs on the 19th of Nov'21 *(Google Earth, 2025)*

On the 22nd of Nov'21, it can be observed the 1g density is more concentrated in lower trajectories, especially over populated areas in England such as Manchester and Birmingham, and again over the Atlantic Ocean and west of France (**Figure 6.21A**). There are also two offshoots in the lower trajectories reaching further south into southern Portugal and Spain and travelling east into Italy and the Mediterranean Sea. The lighter density is more concentrated in the lower trajectories over the English Channel (**Figure 6.21B**), and there is unusually less spatial distribution of the trajectories which does not follow the trend of previous scenarios. This could be due to the role of wet and dry deposition on this day, or increased particle settling over the lower trajectories.

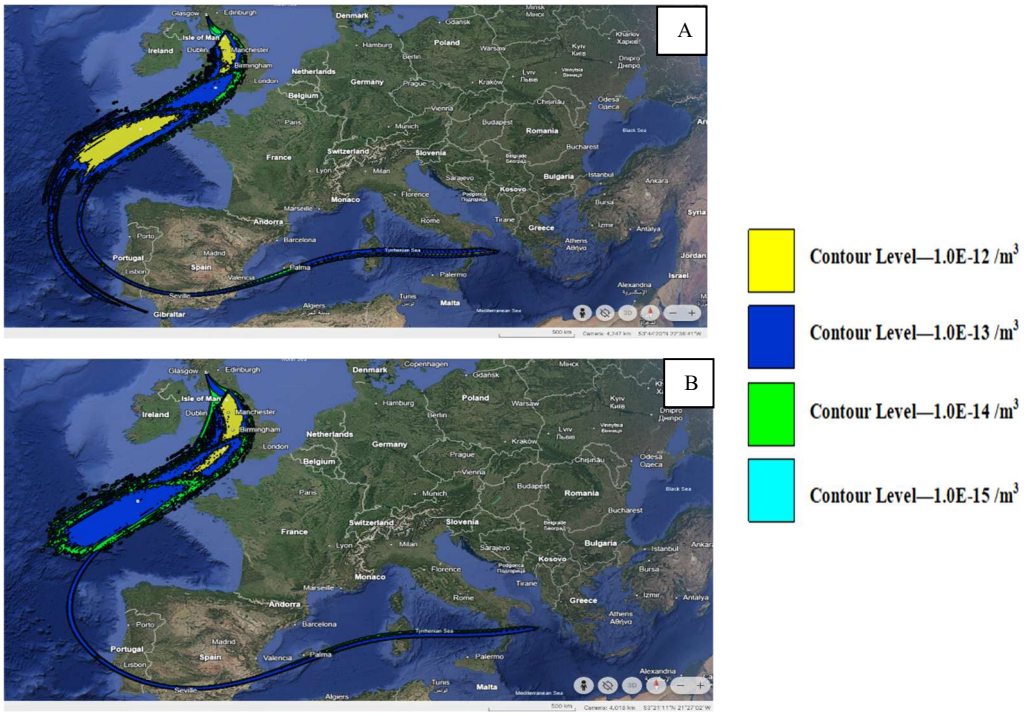


Figure 6. 21 (A) Results from Forward Trajectory Modelling of 10 µm 1 g density for 48hrs on the 22nd of Nov'21; (B) Results from Forward Trajectory Modelling of 10 µm 0.625 g density for 48hrs on the 22nd of Nov'21 *(Google Earth, 2025)*

On the final day of sampling, where concentrations were lowest, there is reduced long-range transport for the 10µm size range for both densities, compared to the other days modelled. The 1 g density again is more concentrated in the lower trajectories, especially over populated areas such as Newcastle, and as particles move further south there is more scattering and wider spatial distribution within the higher trajectories travelling east over the North Sea and Denmark (**Figure 6.22**). The lighter density is more concentrated in the higher trajectories close to the sampling location but as particles travel south they are more concentrated in the higher trajectories, with the lighter density reaching further east into southern Sweden and further south west into northern France when compared to the higher density.

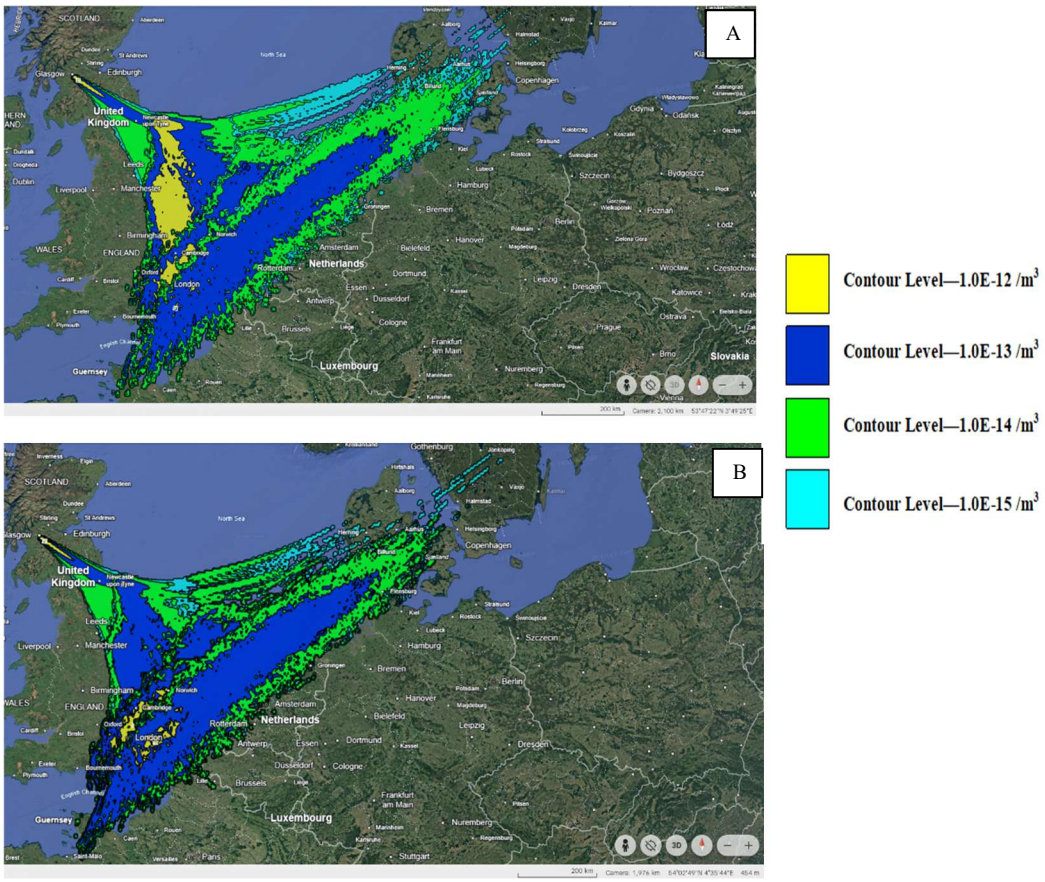


Figure 6. 22 (A) Results from Forward Trajectory Modelling of 10 µm 1 g density for 48hrs on the 23rd of Nov'21; (B) Results from Forward Trajectory Modelling of 10 µm 0.625 g density for 48hrs on the 23rd of Nov'21 *(Google Earth, 2025)*

Overall for the 10 µm particle size it is evident that there is long-range transport possible in lower and higher trajectories, with particles higher trajectories more susceptible to atmospheric processes and long-range transport.

The modelled 20 µm particles surprisingly appear to be more concentrated in the higher trajectories for the 1g density. On the 17th of Nov'21 it can be observed that there are greater concentrations in the higher trajectories and more offshoots which reach further south into Italy and the lower trajectories covering a wider area east in Romania than the 10 µm transport (**Figure 4.23A**). The lighter density is more concentrated in the lower trajectories, and there is more definition between trajectories and less scattering when compared to the 10 µm size (**Figure 4.23B**).

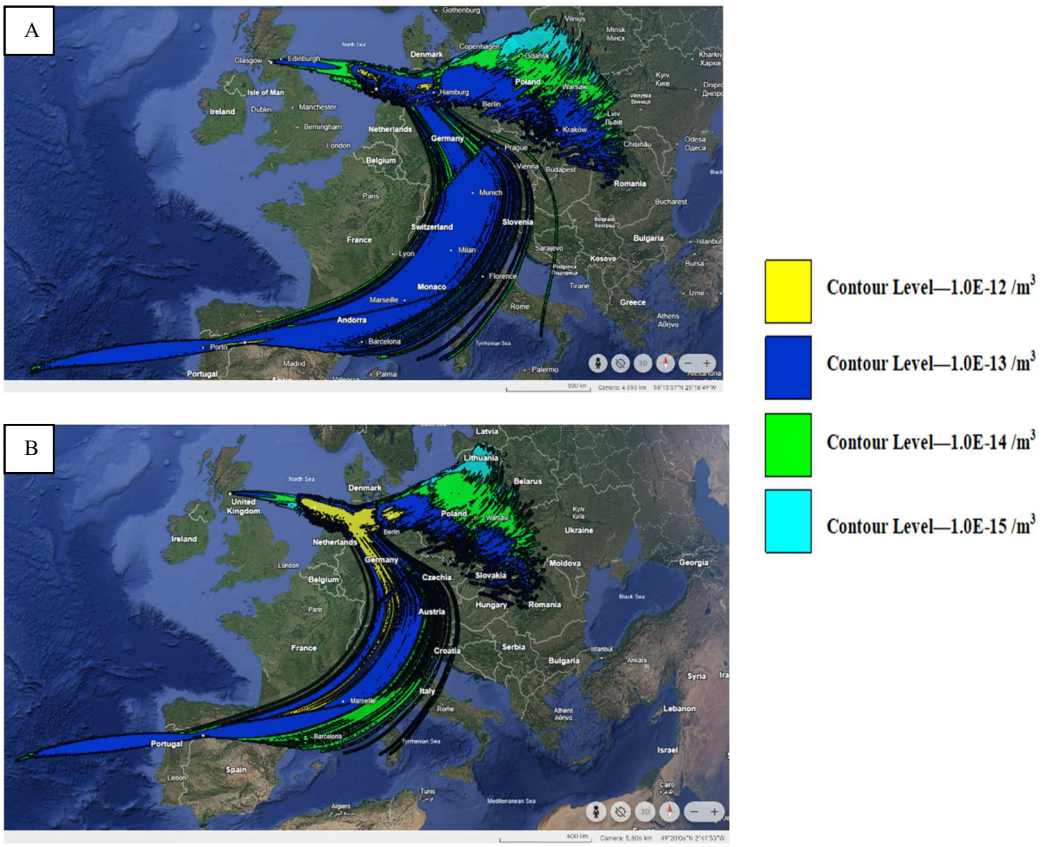


Figure 6. 23 (A) Results from Forward Trajectory Modelling of 20 µm 1 g density for 48hrs on the 17th of Nov'21; (B) Results from Forward Trajectory Modelling of 20 µm 0.625 g density for 48hrs on the 17th of Nov'21 *(Google Earth, 2025)*

Again on the 19th of Nov'21, the 1 g density is more concentrated in the higher trajectories especially as particles move east (**Figure 4.24A**). Although there is some scattering and trajectories are more defined than the 10 µm, which suggests that the larger particle size is less influenced by vertical mixing or wind patterns compared to the smaller size. The lighter density is more concentrated in the lower trajectories when compared to the higher density, especially as particles move east into Poland and travel north east into Lithuania, Belarus and Ukraine and south to the Black Sea (**Figure 4.24B)**. Compared to the 10 µm lower density, there is still some scattering the trajectories are more defined again indicating that the larger size class is less influenced by atmospheric processes.

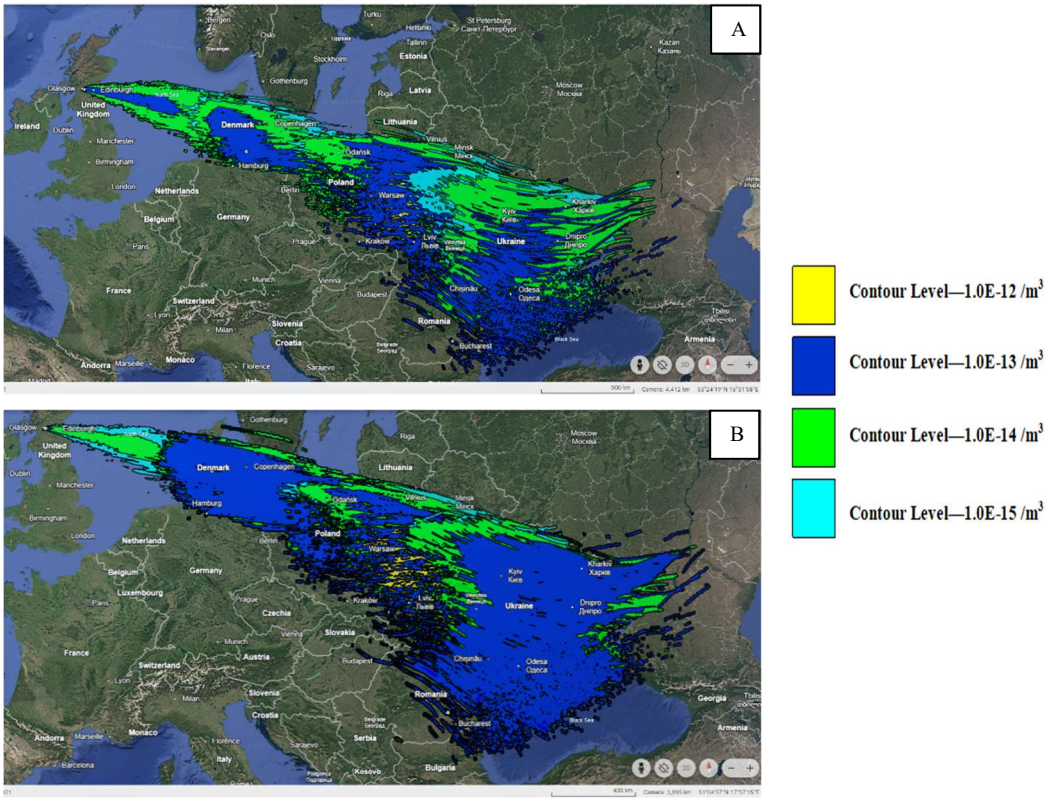


Figure 6. 24 (A) Results from Forward Trajectory Modelling of 20 µm 1g density for 48hrs on the 19th of Nov'21; (B) Results from Forward Trajectory Modelling of 20 µm 0.625 g density for 48hrs on the 19th of Nov'21 *(Google Earth, 2025)*

On the 22nd of Nov'21 when nanotank sampling systems collected high levels of MPs, the 20 µm modelled particles, when compared to the 10 µm modelling, are more concentrated in the higher trajectories and the trajectories are more defined, but there is less long-range transport into the Mediterranean which would be expected from particles with a larger size (**Figure 4.25A**). The lighter density is more concentrated in the higher trajectories compared to the lower density, especially over north west England (**Figure 4.25B**). There is also more scattering as particles are transported south, however with the larger particle size there is an inverse situation with the two polymer densities when compared to the 10µm. In this scenario the lighter particle density as two offshoots reaching further south east into Italy and the Mediterranean, compared to just one with the higher density. This implies that particles that are larger

in size but lighter in density are transported via different mechanisms than 20µm particles with a heavier density.

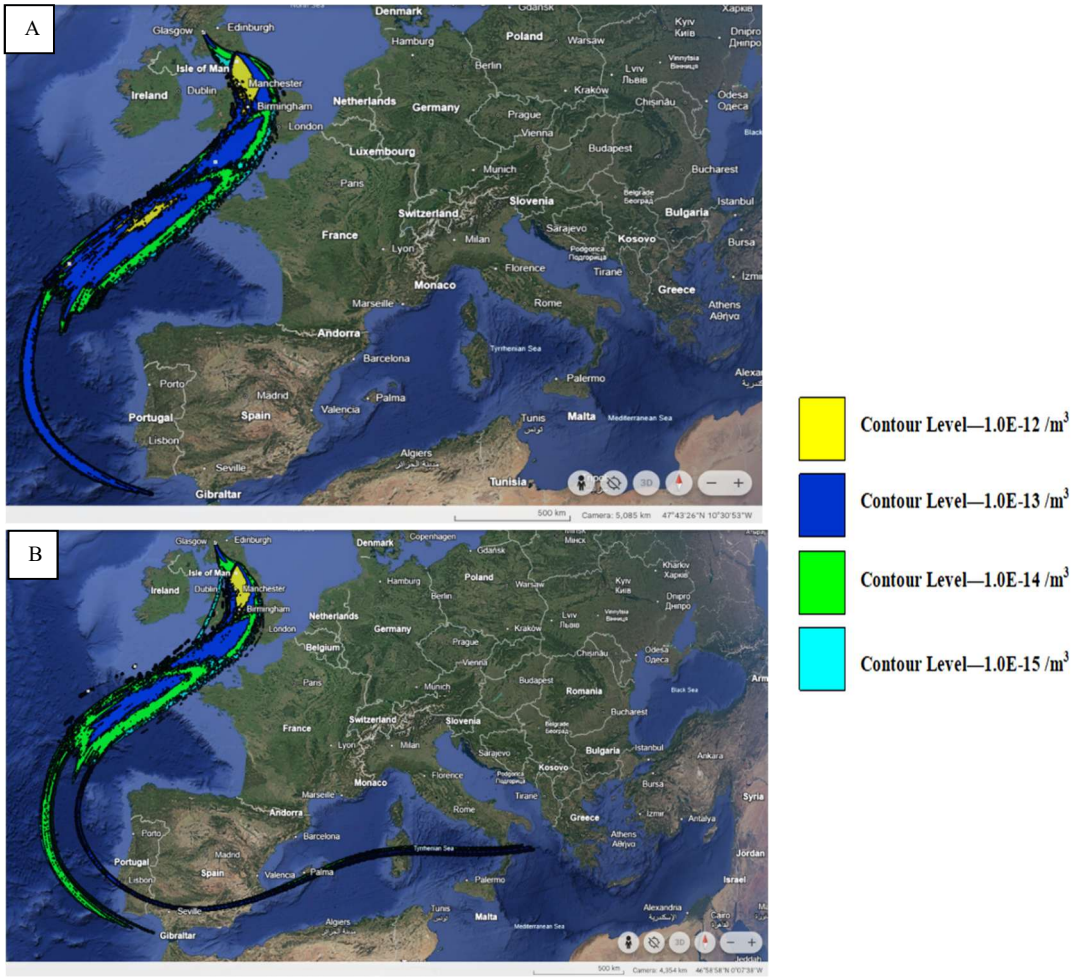


Figure 6. 25 (A) Results from Forward Trajectory Modelling of 20 µm 1 g density for 48hrs on the 22nd of Nov'21; (B) Results from Forward Trajectory Modelling of 20 µm 0.625 g density for 48hrs on the 22nd of Nov'21 *(Google Earth, 2025)*

The final day of sampling when concentrations were low, the 20 µm 1g density can be observed to be more concentrated in the higher trajectories, especially as particles travel south. It can also be observed that there is less long-range transport on this day for the 20 µm size for both densities (**Figure 4.26**). When compared to 10 µm there is less scattering and more defined trajectories, but the higher trajectories appear to have a wider spatial distribution over Denmark (**Figure 4.26A**). This suggests that once suspended, particles of this size may have a more concentrated wider spatial

distribution. The lighter density has higher concentrations in the lower trajectories compared to the heavier density, especially over populated areas in England such as London. This indicates that there could be local urban and industrial pollution being concentrated in these areas. The lighter density is more scattered and trajectories are less defined but the higher trajectories appear to travel further north into Sweden compared to the higher density (**Figure 4.26B**). When compared to 10 µm with the same density, there is more spatial distribution in the lower trajectories over populated areas in England and southern Denmark, suggesting that particles of a 20 µm size are more concentrated in the lower trajectories and travel further in this elevation. It can also be observed that there is less long-range transport on this day compared to other scenarios for the 20 µm size for both densities.

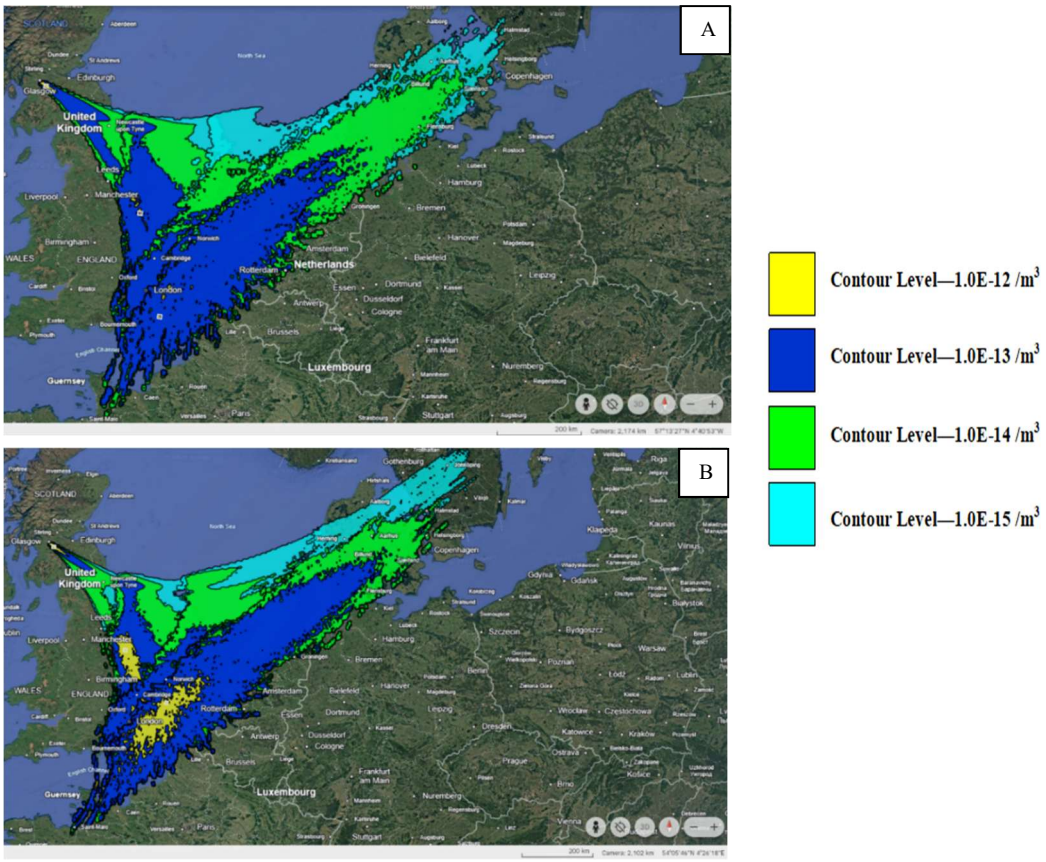


Figure 6. 26 (A) Results from Forward Trajectory Modelling of 20 µm 1 g density for 48hrs on the 23rd of Nov'21; (B) Results from Forward Trajectory Modelling of 20 µm 0.625 g density for 48hrs on the 23rd of Nov'21 *(Google Earth, 2025)*

As with the back-trajectory modelling, the 100µm particle sizes have less spatial distribution and are more concentrated in local areas. On the 17th of Nov'21 the higher density is more concentrated in the lower trajectories close to the sampling site and then becomes more concentrated in the higher trajectories as particles travel further east (**Figure 4.27A**), suggesting vertical transport of particles. It can also be observed that there is no scattering on this day and the trajectories are clearly defined suggesting that the larger particle size is less easily influenced in vertical transport by atmospheric processes. The lighter polymer density can be observed to have a further spatial distribution, highlighting that the lighter polymer density for the larger size classes results in further transport compared to the higher density (**Figure 4.27B**).

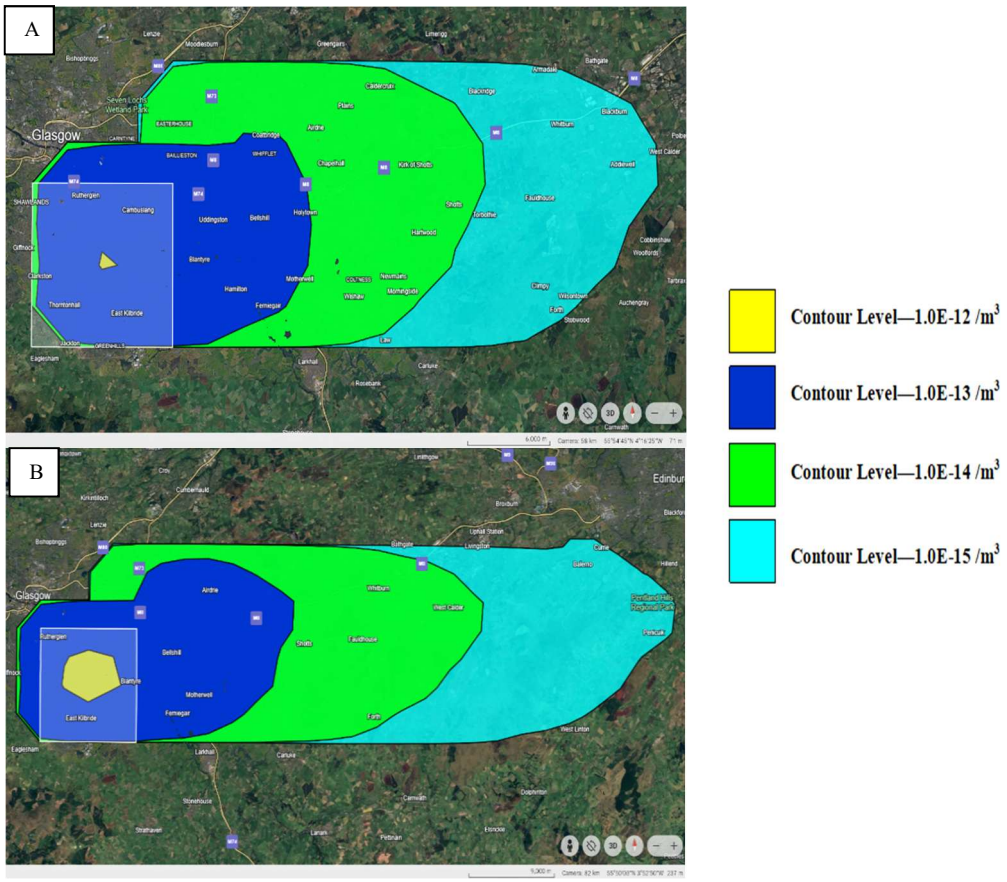


Figure 6. 27 (A) Results from Forward Trajectory Modelling of 100 µm 1 g density for 48hrs on the 17th of Nov'21; (B) Results from Forward Trajectory Modelling of 100 µm 0.625 g density for 48hrs on the 17th of Nov'21 *(Google Earth, 2025)*

On the second highest day, there is more scattering and less defined trajectories compared to the previous scenario for both densities in the 100 µm size class, which could indicate more vertical mixing or turbulence on this day. The higher density is more concentrated in the lower trajectories near the sampling location but again becomes more concentrated in the higher trajectories as particles move east from the site (**Figure 4.28A)**. Again it can be observed that the lighter density has further spatial distribution and long-range transport, with the higher trajectories travelling further east over the North Sea, and the lower trajectories being concentrated again in Denmark (**Figure 4.28B)**. This indicates that the lighter density for the larger size range has a strong influence on transport and potential pathways of atmospheric MP.

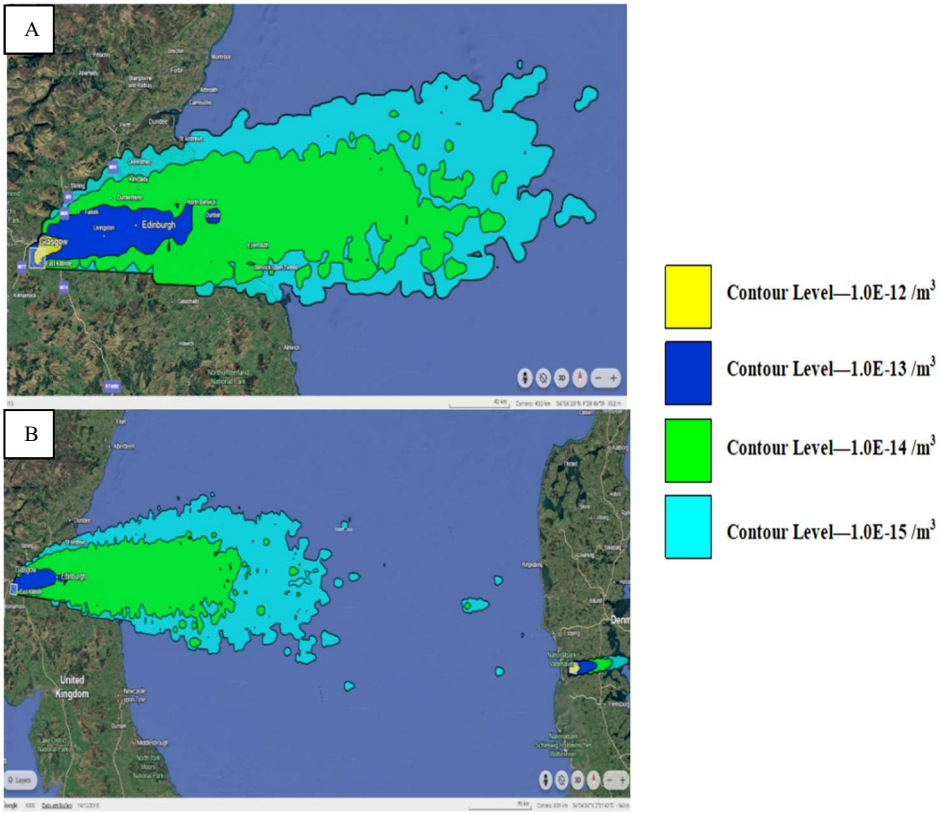


Figure 6. 28 (A) Results from Forward Trajectory Modelling of 100 µm 1g density for 48hrs on the 19th of Nov'21; (B) Results from Forward Trajectory Modelling of 100 µm 0.625g density for 48hrs on the 19th of Nov'21 *(Google Earth, 2025)*

Then on the 22nd of Nov'21 when nanotank sampling systems collected high levels of atmospheric MP, there is reduced forward transport for the 100 µm size. The higher density is concentrated in the lower trajectories close to the sampling location and there is more definition on this day compared to the 19th (**Figure 6.29A**). This difference could be due to reduced wind or turbulence on this day. Again the lighter density has a further spatial distribution concentrated in the higher trajectories as particles move further south, but there is less scattering than the previous scenario. This suggests that for both densities there is reduced influence from atmospheric processes on this day.

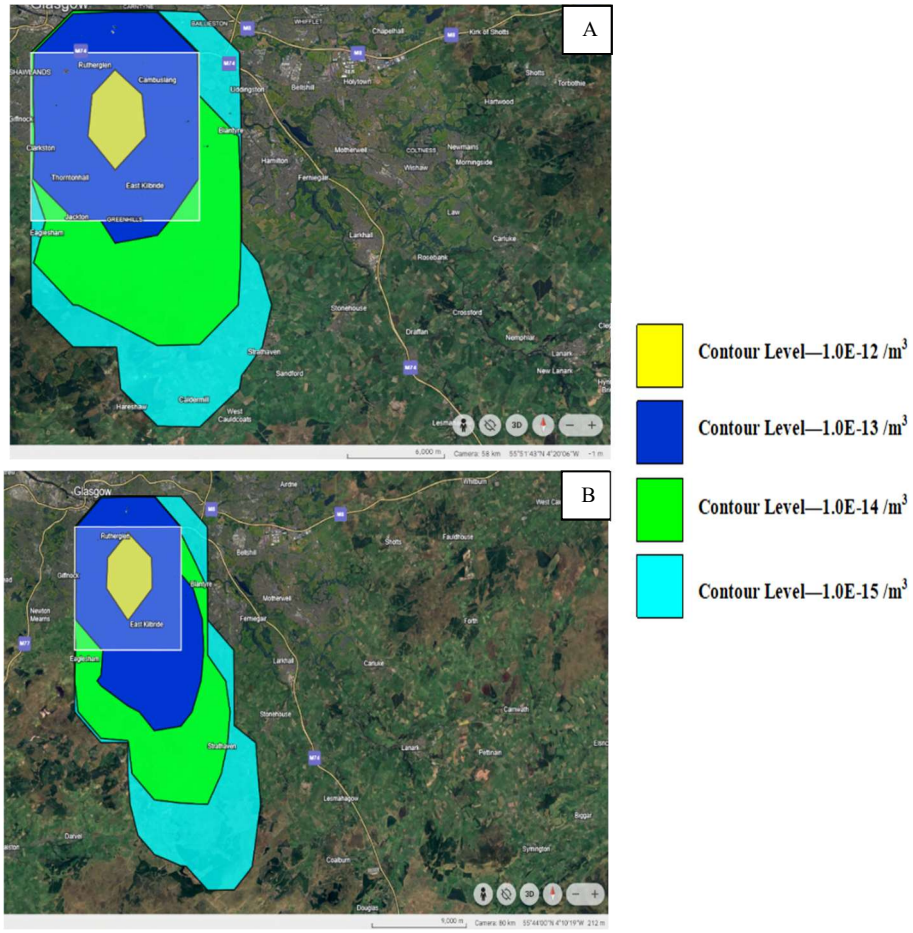


Figure 6. 29 (A) Results from Forward Trajectory Modelling of 100 µm 1 g density for 48hrs on the 22nd of Nov'21; B. Results from Forward Trajectory Modelling of 100 µm 0.625 g density for 48hrs on the 22nd of Nov'21 *(Google Earth, 2025)*

Finally on the 23rd of Nov'21, again there is reduced long-range transport on this day for both polymer densities. For the higher density the lower trajectories are concentrated close to the sampling site and there is some transport to the north but the particles are mostly concentrated in the higher trajectories as they are transported south (**Figure 6.30A**). The lighter density again shows further spatial distribution, with some mixing of trajectories but overall, they are defined and there is no scattering, again indicating the particles were less influenced by vertical mixing and atmospheric processes on this day (**Figure 6.30B**).

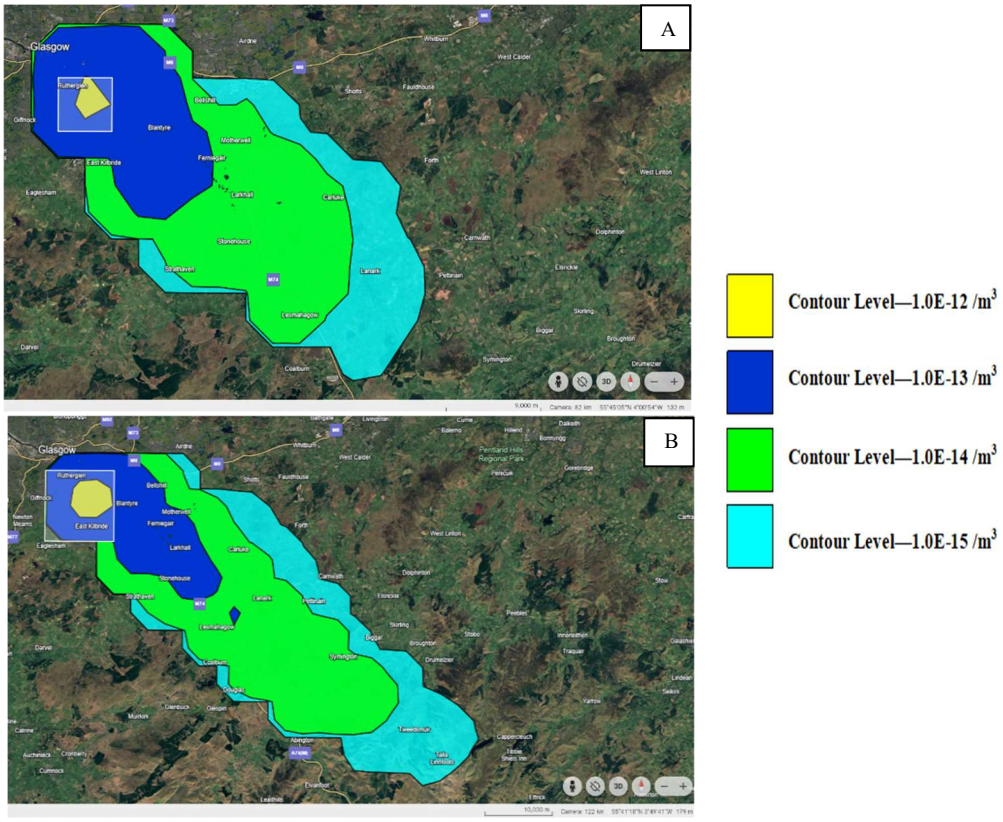


Figure 6. 30 (A) Results from Forward Trajectory Modelling of 100 µm 1 g density for 48hrs on the 23rd of Nov'21; (B) Results from Forward Trajectory Modelling of 100 µm 0.625 g density for 48hrs on the 23rd of Nov'21 *(Google Earth, 2025)*

Overall, from the 42 forward trajectory modelling scenarios, it is evident that there is more local transport in the lower trajectories to other areas in the UK, especially for the larger particle sizes of a higher density. There is further long-range transport by lighter and smaller particles into southern Europe and into other marine environments

such as the Black Sea, the Mediterranean Sea and back into the Atlantic. This highlights the need to understand the 'Plastic Cycle' and how MP particles can be transported from their original source to other urban and remote environments via weather processes.

6.3.9 Limitations of HYSPLIT Dispersion Modelling

Although the HYSPLIT model used here can give an indication of potential transport pathways of atmospheric MPs, it has limitations. The parameters used here assumed that particles were fragments due to their predominance in the urban environment in Glasgow. However, a variety of shapes are actually present (Chapter 4). Whilst this present study models different size categories and polymer densities, environmental concentrations are still likely to be more varied and complex. Uniform behaviour is assumed across all particles (Kaydi et al., 2024). Shape, size, and polymer density clearly affect particle transport. Further model development should evaluate these influences.

HYSPLIT also cannot include interactions between atmospheric chemistry and complex terrain (NOAA, 2024b). These interactions can influence particle deposition processes and may yield critical differences in MP concentrations in specific areas, particularly in densely populated or forested areas (Kaydi et al., 2024).

The results of this chapter highlight the transport mechanism between the marine and atmospheric compartments as source of atmospheric MP pollution; however current dispersion models like HYSPLIT cannot incorporate the complex dynamics driving this transport, such as bubble formation, ascent and aerosolisation (Jiang et al., 2025). Its limitations in depicting interactions between multiple factors such as wind speed, wave activity and temperature all affect the variability of MP emissions and transport (Jiang et al., 2025).

Furthermore, HYSPLIT cannot currently incorporate detail and MP physics into its outputs. Processes like fragmentation, aggregation and surface charge effects could alter particle mass, shape and therefore how it is transported. However, due to the lack

of studies on MP aging and their impact on atmospheric dynamics, this aspect of MP transport will require more research. Due to the assumptions and oversimplification of MP particle behaviour and atmospheric processes, the outputs of the model in this chapter are a generalisation of the reality of atmospheric MP transport which is complex and remains a considerable knowledge gap in the field. However, it can give an indication of the source, dispersion and transport of atmospheric MP in absence of empirical certainties.

6.4 Conclusion

The MP content of the urban atmospheric environment in Glasgow was measured in November-December 2021. Samples were analysed with μRaman spectroscopy and Nile Red staining coupled with fluorescence microscopy. From this atmospheric MP concentration, as well as particle characteristics (size, shape), and polymer composition of suspended particles are reported. MPs were found in the majority of samples and although differences in methodology make comparison between studies difficult, concentrations at this location are higher than other urban studies, and other UK locations. Results from μRaman spectroscopy showed higher levels of PMMA, PES, PLS, as well as Acrylic, PET and PLA. Given that polymers such as PMMA, PLS and PES are often used for automotive and industrial applications this suggests there may be some local influence from industrial activity. PET is often used in food packaging and textiles, as is Acrylic which suggests degradation of clothing and clothes washing and drying could influence concentrations at this location. It is concerning to observe concentrations of PLA which is often seen as a more environmentally friendly alternative to fossil-fuel based polymers used in food packaging. However, has been shown to be toxic in laboratory-based studies, and given its presence in the atmosphere it is evident that it is still contributing to MP pollution in urban environments.

Nile Red staining showed that the majority of atmospheric MP particles found in Glasgow were predominantly fragments, but the nanotank sampling system collected

more fibres during the same period. This is different from atmospheric MP concentrations in London, however this indicates that perhaps there is more localised influence from fragments, rather than fibres which are more easily transported long-range. Furthermore, the majority of particles were <20 µm, and 65% of particles were below 10 µm. The first week of sampling collected more particles >100 µm but overall there is a bias towards the smaller particle size range at this location. This highlights the need to identify the smaller size fraction of MP particles in the atmosphere, as it is evident that as particle size decreases there is an increase in MP, which is consistent with other field observations to date.

One of the aims of this research was to observe potential relationships between atmospheric MP concentrations and local weather parameters during the sampling period. There was a significant positive relationship for weekly samples and cloud cover, and a significant negative relationship with wind direction. However, there were no statistically significant relationships between other weather parameters and the other datasets tested. This suggests that cloud cover positively influences atmospheric MP concentrations over longer sampling periods. It also indicates that MP concentrations at this location are influenced by wind direction. When the datasets were split into <20 µm and >20 µm size fractions and compared with weather data no further statistically significant relationships between the pollutant and weather were observed. This could be due to the small temporal range of this data set or could be related to the ongoing gap in the literature on the influence of weather on atmospheric MP dispersion and deposition. It could also be due to the influence of more local sources of atmospheric MP pollution. Future research could examine the relationship with weather over longer time periods and throughout different seasons to observe if there is a more complex influence of weather on atmospheric MP pollution in urban areas. .

Given the influence of local industrial and human activity, it was also of interest to observe if there were possible relationships with other air pollutants present in the Glasgow atmosphere. There were no statistically significant relationships with overall

atmospheric MP concentrations and any of the air pollutants examined. Even when the MP concentrations were split into the <20 µm and >20 µm size fractions, there were no correlations noted. The lack of relationship with PM_1, PM_{10} or $PM_{2.5}$ given the particle characteristics of atmospheric MPs at this location may be due to comparing local samples with regional data. There has only been one study to date that examines this relationship. Future research could examine long-term and simultaneous measurements of both pollutants during summer and winter seasons to observe potential trends between the pollutants. To date, there have been no studies that have measured or compared atmospheric MP and BC or NOs, therefore a study measuring both pollutants at the same time over a longer period would be beneficial, to understand trends in their concentration and dispersion. Considering the environmental, climate and health implications of both atmospheric MP pollution and the other air pollutants, it is crucial that their interactions be understood and monitored, in order to understand their true extent and potential risk factors.

When examining back-trajectory transport via air masses using particle modelling, on days where there were higher concentrations of atmospheric MP pollution, there appears to be long-range influence from the North Atlantic, as well as local influence from the west coast of Scotland. Additionally, when different particle sizes and densities were modelled , there were clear differences in their transport and dispersion properties. The smaller particles with lighter polymer densities originated further east, and were more susceptible to vertical mixing and dispersion. On days where concentrations were higher, long-range transport of particles from the west of Greenland and the east coast of North America was evident in the higher trajectories, as well as localised influence concentrated in the lower trajectories. On the final day of sampling when concentrations were low, trajectories that originated closer to the site in the North Atlantic, and did not pass over any land masses before reaching the sampling location, which could indicate that there was less localised influence from nearby populated areas on this day. The 20 µm size still displayed long-range transport and were susceptible but trajectories were more defined, suggesting that particles of this size, once suspended, remain within their trajectories for longer. There was a clear

difference in the transport and dispersion of the 100 µm size, which was significantly reduced and more concentrated in the lower trajectories, suggesting particles of this size are more localised in origin. There were also more defined differences between the polymer densities in the larger particle size, with the lighter density originating further away in the higher trajectories, indicating that density is an important characteristic to consider when modelling atmospheric transport, especially in the larger size classes.

When the potential pathways of atmospheric MP pollution in Glasgow were modelled using forward trajectory air mass modelling, it was evident that both local and long-range transport into Europe was possible within just 48hrs. Again, there were clear differences in the transport and dispersion properties of the different size ranges and polymer densities modelled. The 10 µm size displayed further long-range transport and was more vulnerable to atmospheric processes and vertical mixing, especially with the lighter polymer density. The lighter density, which was the predominant density found at this location, travelled further into Europe and into the Mediterranean in the higher trajectories, which indicates that once suspended these particles can be transported long distances within a short period of time. This again highlights the need to examine and report on the small particle size ranges, as this will produce a more accurate picture of the extent and transport of atmospheric MPs. The 20 µm size had reduced long-range transport compared to the 10 µm size, but particles were still able to reach far south into Europe within the 48hrs, especially with the lighter polymer density. Again the spatial distribution and susceptibility to atmospheric processes was significantly reduced for the 100 µm particle size which suggests larger particles are less likely to be transported further away from their source. However, there were clear differences with the lighter density which still displayed transport into northern Europe in the higher trajectory within 48hrs, which again indicates that once suspended, the lighter polymers can be transported to locations far away from their origin.

Overall, this study confirmed the presence of atmospheric MP pollution in Glasgow, Scotland and it is evident that concentrations of atmospheric MP pollution at this urban

location in Glasgow are considerable. It is also clear that this pollutant can be transported to and from local and distal sources. Although basic assumptions are made about the emission rate, size and transport properties of these particles in order to model their transport, it can provide an estimate on where this pollutant could be originating, and potential pathways. As the field develops and more is learned about MP's physical properties and transport properties, models can be adjusted to gain a more accurate picture of the extent of this pollutant and the role of the 'Plastic Cycle' in its transport and potential sources and sinks. It is also evident that the smaller size range of atmospheric MP is important in terms of accurately reporting concentrations and in terms of gaining accurate information on transport. Given the relationship with other hazardous air pollutants, it is essential that both forms of air pollution are monitored and reported effectively in order to understand the makeup of pollution in urban environments, and the potential human, environmental and climate risk factors associated with their presence and transport.

Chapter 7 – Discussion of Urban and Remote Atmospheric Microplastic Pollution

This thesis has examined key topics related to important research gaps in the field of atmospheric MPs. The efficiencies of active sampling have been examined with recommendations made to improve future field studies. The characteristics of atmospheric MP pollution in a remote location – Svalbard, Norway - have been reported and with the use of modelling, key transport pathways to this remote location have been examined. Parallel research has been completed for an urban location - Glasgow, Scotland – and modelling used to examine transport and dispersion of this pollutant using field observations. This chapter will summarise and discuss key findings from these studies, and compare the characteristics of atmospheric MP pollution in remote and urban locations. From this key remaining research gaps are highlighted, and future recommendations for research and policy discussed.

7.1 Summary and Discussion of Key Findings

7.1.1 Guidance for Active Sampling Measurements of Atmospheric Microplastics

For the first time, the effectiveness of active sampling parameters was assessed for the measurement of atmospheric MPs. Technical guidance exists for adjusting active sampling parameters for traditionally measured air pollutants (e.g. PM), but not for atmospheric MP given the novelty of the field. It was established that studies to date have used a variety of different pumping rates and sampling durations in field campaigns, usually designed on an ad-hoc basis. Therefore the aim for the first study of this thesis (RQ1), was to establish if there is an effective pumping rate and sampling duration to be utilised relative to the sampling environment. This was assessed by examining the number of atmosphere MPs collected, as well as shape, size and polymer composition, of three sampling durations and four pumping rates.

It was found that pumping rates and sampling durations were not selective for polymer composition which is beneficial to note if polymer composition is the main aim of a study. However, it was established that the pumping rate and sampling duration used does impact the number of atmospheric MP collected. Furthermore results showed that by increasing the pumping rate, there was no increase in the ratio of MP per filter to MP/m^3. Instead, the opposite trend was observed.

A novel method was also tested, termed the nanotank, which draws particulates into a liquid media instead of a filter. This method did not perform as well as the direct air filtration, however it did collect more fibres in comparison; therefore, more development is needed. Weekly and monthly sampling durations via direct air filtration provided a wider particle size distribution of MPs identified however, the longer sampling durations were not as effective in terms of MP collection and are therefore not recommended for collective representative samples.

In order to gain a representative atmospheric MP sample using active sampling equipment, it is recommended that the environment in which the sample is collected and the parameters that are to be used are considered early in research planning to avoid under-reporting concentrations representative and necessary to address the specific research question. It is hoped this novel guidance can provide a foundation for future research to plan and collect effective atmospheric MP measurements.

7.1.2 Remote Atmospheric Microplastic Pollution: Svalbard, Norway

Atmospheric MP pollution has been reported in the Arctic previously, however this study was the first to measure both suspended and deposited atmospheric MP within the planetary boundary layer (PBL). This research confirmed that atmospheric MPs are present and ubiquitous in the Arctic PBL. With the aim of quantifying and characterising atmospheric MP concentrations (RQ2), a 28-day sampling campaign using both deposition and active sampling, was conducted at the research station Ny-Ålesund, in Svalbard, Norway. The average deposition rate was found to be to be 37.3

± 30.2 MP/m^2, with an average suspended particulate concentration of 4.2 ± 9.4 MP/m^3 which is comparable with other remote studies but had higher deposition rates than studies in the Antarctic and Shanghai. Differences in the methods used and the units reported make comparison difficult, however given the remote location of this site, it is concerning to observe the prevalence of atmospheric MP in this study.

The MPs identified by Nile Red staining were predominantly <20 μm (72%), which highlights the importance of identifying the smaller size fraction of atmospheric MP content and improving the LOD when reporting atmospheric concentrations. As per other studies, the number of MPs increase with the decrease in particle size, therefore improving methods to accurately identify MPs <20 μm is crucial in order to gain an accurate picture of MP content in the atmosphere. Nile Red staining also identified fragment as the primary particle shape which is not in line with previous studies, but this could be due to the small particle size distribution found in this study. μRaman identified Acrylic (16%), PLS (14%), PES (11%), and PVA (11%) as the most prevalent polymers. This suggests local contamination from clothing and fishing gear, or distal sources from food packaging or industrial applications.

A key objective of this study was to examine if there were differences between deposited and suspended particulates. Deposited samples on average had 1% greater plastic content and displayed higher levels of PLS than suspended samples. This highlights the importance of examining both particulates in order to gain a more detailed picture of total atmospheric content. Another objective of the study was to examine potential relationships with local weather conditions. Deposited particulates had a significant positive correlation with cloud cover, suggesting cloud cover could be influencing MP deposition in this area. There was a significant positive correlation with suspended MP <20μm, humidity and dew point, suggesting that humidity is more influential on smaller, suspended particulates. Furthermore, there was an increase in suspended MP concentrations when wind direction was onshore, suggesting a marine influence on atmospheric MP pollution.

Particle modelling was used to observe potential sources and transport of atmospheric MP to the Arctic region. The FLEXPART model established that oceanic sources were a main contributor via sea spray and bubble bursting. It also identified European and UK coastlines as a source during higher atmospheric MP pollution periods in early June. Synthetic fibres and road dust (local sources) were also suggested as potential sources at this remote location. The model also suggests that the High Arctic could be a sink for marine and land-based pollutants, as well as a potential source. This highlights the importance of understanding atmospheric MP transport mechanisms and monitoring pollution at this remote location given its vulnerable geographic location.

7.1.3 Urban Atmospheric Microplastic Pollution: Glasgow, Scotland

This study aimed to quantify and characterise atmospheric MP pollution in Glasgow, Scotland, for the first time (RQ3). To achieve this suspended atmospheric MPs were measured over a 28-day period from November to December 2021. μRaman and Nile Red staining was used to identify the shape, size and polymer composition, as well as overall particle count. Concentrations for daily direction air filtration were on average 9440 $\pm$ 7320 MP/m^3 and 1,730 MP/m^3 $\pm$ 1,220 MP/m^3 for weekly direct air filtration measurements, with fragment being the dominant shape. The nanotank sampling system on average collected 2010 $\pm$ 3230 MP/m^3, with more fibres being identified than in the air filtration samples. The majority of particles were <20μm with over 65% being <10μm, again highlighting the importance of identifying the smaller size fraction of atmospheric MP pollution.

There was some variance in polymer composition over the sampling period but the main polymers identified were PES, PMMA, and PLS, as well as some PLA, PET and Acrylic. PES and PMMA are commonly used in automotive, construction, and electrical appliances which indicates an influence from local industrial activities. Acrylic is used in coatings, paints and adhesives and also commonly used in textiles. PET is one of the most versatile and commonly identified polymers used in food packaging and textiles which also indicates that there is an influence from local human

activity and waste management processes. PLA on the other hand is often used as a 'sustainable' alternative to fossil-fuel based polymers for food packaging and single-use plastic products. Given that it has also been identified as toxic, its presence in the atmosphere is concerning. This again indicates local human activity and waste management as potential sources of this pollutant.

As with the remote location, this urban focused study examined the potential relationship between atmospheric MP pollution and local weather conditions. There was a significant positive correlation with MP concentration and cloud cover, and a significant negative relationship with wind direction for MPs of all sizes for weekly samples. When divided into <20 µm and >20 µm size classes, there were no significant relationships with the weather parameters tested. This could be due to the small temporal range of this data set or could be related to the ongoing gap in the literature on the influence of weather on atmospheric MP dispersion and deposition. It could also be due to the influence of more local sources of atmospheric MP pollution. Future research could examine the relationship with weather over longer time periods and throughout different seasons to observe if there is a more complex influence of weather on atmospheric MP pollution in urban areas.

Given the urban location of the study, one of the research objectives was to examine potential relationships with other monitored air pollutants in the area. There were no significant correlations with MP concentrations and local air pollution, even when divided into <20 µm and >20 µm categories. This could be due to the short temporal range of the data or due to the data being local air pollution data rather than primary data collected alongside atmospheric MP measurements which could provide more accurate comparison. As comparative analysis between MP and BC, and NO_x, NO_2, and NO_s, has not been carried out before future to understand their co-existence is needed.

Utilising the HYSPLIT model it was possible to observe air mass trajectories, as well as individual particle transport based on the characteristics of the MPs identified at the sampling location. This implicated both long-range marine sources from the North-

Atlantic, Greenland, Northern Ireland and the Republic of Ireland, as well as local urban sources on the Scottish mainland. The smaller particle sizes and lighter polymer densities modelled showed more scattering suggesting greater vertical mixing and influence from atmospheric processes. They also displayed a greater potential for long-range transport and dispersion.

It was also possible to use forward trajectory modelling to observe pathways and where this pollutant might be transported to. This indicates that MPs could be transported south east to Germany, Russia and the Baltic Sea, and south to Spain, Italy and the Mediterranean within 48hrs. The smaller and lighter particles presented further long-range transport in the more elevated trajectories suggesting that once these small, lighter plastics are suspended, they have a high potential for long-range transport. The larger particles had a potential for local deposition and the lighter polymers modelled travelled further into the North Sea and Europe, even with the larger particle size. This highlights the transboundary nature of the pollutant, and the speed in which MP can contaminate locations thousands of miles from its original source in a short time frame.

7.2 Comparison of Urban and Remote Atmospheric Microplastics

An overarching research aim of this thesis was to compare atmospheric MP pollution from remote and urban locations (RQ4). No deposition measurements were taken at the Glasgow location, however both studies utilised direct air filtration and the nanotank sampling system to take measurements of suspended particulates over a 28-day period. The two locations examined in this thesis, Glasgow and Svalbard, are vastly different in their geographic location, population, and industrial activity. Due to its remote location in the Arctic Sea it was posited that the remote location would be more vulnerable to long-range pollution and it was hoped that concentrations would be significantly lower than the urban location. It is promising to observe that average daily direct air filtration concentrations for Svalbard (8.9 ± 15.6 MP/m³) are orders of magnitude lower than the Glasgow location (9440 $\pm$ 7320MP/m^3). The same is also true for nanotank measurements which for Svalbard were 1.5 ± 1.8 MP/m³, compared to 2010 $\pm$ 3230 MP/m^3 for Glasgow. However, presence of atmospheric MP in the PBL

atmosphere in Svalbard is concerning due to the unique ecosystems present and the potential for accelerated ice melt due to MPs present on snow and ice. Both locations used the same analytical methods to report on concentration, shape, size and polymer composition. It is evident that for both datasets there were differences in the numbers reported from μRaman analysis and Nile Red staining. This highlights the importance of using complementary methods when analysing atmospheric MPs, in order to gain information on characteristics and chemical composition, and report concentrations accurately.

In terms of shape, both locations displayed a higher proportion of fragment to fibre but Glasgow results displayed a much higher proportion of fibres (17 %) with nanotank MP particulates displaying a composition of 52 % fibres. The higher proportion of fibres in the urban location could be due to localised influence form textiles and clothes drying. The size of MP particles identified at each location displayed a particle size distribution skewed to the smaller size ranges. In the Svalbard samples, 72 % of particles were found to be <20 μm and 57 % <10 μm. It is surprising to observe that 90 % of the particles found in Glasgow were <20 μm and 46% of particles were <10 μm, compared to the Svalbard samples. As Svalbard is more influenced by distal sources of atmospheric MP pollution, it was thought that the MPs identified there would be smaller than at the urban location, as smaller particles may be more easily transported via atmospheric processes.

Samples taken at both locations were analysed using μRaman spectrometry to identify polymer composition and as discussed in **Chapter 3** due to equipment failures, two μRaman spectrometers were used in this thesis. Although efforts were made to make μRaman analysis consistent by sampling three randomised areas, and to keep the spectra treatment consistent, the different lasers used and resulting fluorescence meant different parameters used (see **Chapter 3**). Therefore there is a possibility that there were differences in the results from using two different μRaman spectrometers. It would have been desirable to keep the analysis as harmonious as possible across the dataset used in this thesis, however due to time and resource constraints, utilising two

spectrometers was the best option to obtain polymer composition data for both locations. This also reflects the current field of atmospheric MP which is calling for more harmonised methodologies. But access to equipment such as μRaman spectrometers is limited and their operation can be challenging. This is one of the reasons why comparison across studies and geographic locations is difficult in the field, however until this challenge is overcome it is still important to gain as much information as possible on atmospheric MP pollution, in order to monitor its presence and advance knowledge in the field.

That being said there were some similarities between the two locations in terms of polymer composition. For example, for both locations PLS and Acrylic were two of the main polymers identified. PLS is often used in medical devices, food processing and aerospace components and Acrylic is often found in textile fibres and used in paints and varnish. Therefore, both polymers could be found in local sources in an industrial and populated like Glasgow, and will also be used in remote locations in Svalbard, but could also be transported from distal sources. Glasgow displayed higher levels of PES, PMMA, and some concentrations of PLA and PET, which were absent from the Svalbard samples. These polymers are used in industrial and automotive applications and also in single-use food packaging which will be used frequently in an urban location, and this waste will also be managed local to the urban location in Glasgow which could be a potential source. Svalbard also displayed high levels of PES and PVA, which were identified in the Glasgow samples but not in high concentrations. PES is also used in automotive applications and used in electrical insulation and water filtration which may be used more locally to the Svalbard location. PVA is also found in adhesives, textiles and food packaging which could also be found closer to the sampling location. However, as is highlighted by the particle modelling used for both locations, and given the small size ranges of particles at both locations, these could be transported from distal sources.

Atmospheric MP concentrations were compared to local weather data at both locations to observe potential relationships. Both locations displayed significant correlations

between cloud cover, wind direction and atmospheric MP concentrations. Although cloud cover only influenced deposited particles in Svalbard, and in Glasgow it correlated with weekly direct air filtration, it is interesting to observe the potential role of cloud cover in the levels of atmospheric MP concentration. For both locations the concentrations were divided into <20 µm and >20 µm size classes to observe if weather parameters were bias to a certain size of particle. It is interesting to observe that at the urban location there were no significant correlations with weather parameters which suggests that local weather conditions were less influential on measurements There were significant relationships with particles <20 µm from daily direct air filtration and weather parameters in Svalbard. This was the case for mixing ratio, wind direction and dew point at this location. However, daily nanotank samples >20 µm had a statistically significant positive relationship with atmospheric MP concentrations indicating that weather parameters at the remote location were more influential on atmospheric MP concentrations in the smaller particle size range, than in the urban location. It also highlights that there is clearly a complex relationship between atmospheric MP concentrations and weather parameters at both locations. Long-term monitoring in both urban and remote locations may reveal more detailed answers about the potential influence of weather on the presence of this pollutant.

The final research objective aimed to compare the transport pathways of atmospheric MP pollution from urban and remote locations. Back trajectory modelling for the Svalbard sampling period suggested that marine sources heavily influenced atmospheric MP concentrations at the site, especially from the North Atlantic. This is linked to the ongoing debate whether the ocean is a sink of atmospheric MP but observations support that MPs are resuspended from the ocean, potentially via sea spray and bubble bursting, and transported long-range. The model used also suggested that the Arctic could be a possible sink for atmospheric MP pollution from distal sources which again highlights the need to monitor pollution at this remote location. Back trajectory modelling for the Glasgow atmospheric MP concentrations suggest marine influences from the North Atlantic, and the role of distal sources near Greenland and North America, especially for the smaller, lighter particles. However,

there were also localised concentrations in the lower trajectories on the Scottish mainland. This indicates that both remote and urban locations are influenced by long-range marine sources, again showing that MPs have the potential to be transported to distal end-points via atmospheric transport. Although the models have their relative advantages and disadvantages, the output of both models are clear in their indication that the marine environment is a main source of atmospheric MP contamination. Given that little is known about the plastic cycle and how this pollutant moves between the different compartments, it appears that the marine-atmospheric pathways are a main contributor to long-range MP pollution and this could inform future research on the transport of MP between matrices.

7.3 Recommendations for Future Research and Policy

7.3.1 Recommendations for Future Research

This thesis aimed to fill key research gaps in the field of atmospheric MPs, but in doing so there have also been some new avenues of research which have become apparent. The first study in this thesis aimed to provide guidance on the accurate measurement of atmospheric MPs using active sampling techniques, which have not been examined to date. This is in line with the current demand in the literature to improve MP measurement and use more harmonious methods to improve accuracy and make comparison more precise. It is evident that sampling duration and pumping rate do not appear to influence polymer composition, but can influence the quantity, size and shape of particles collected. Due to the samplers being evaluated in the field environment, variation is to be expected. However, future research could evaluate the effect of pumping rate and sampling duration in a controlled laboratory setting with a set concentration of MPs in order to account for this variation and potentially provide more accurate guidance. Furthermore, this study only evaluated two methods of active sampling (direct air filtration and the nanotank sampling system), but future research

could examine how this influences the other main devices used in the field (e.g. TISCH high volume sampler, TSP middle-flow sampler). Further research in a range of environments could help improve understanding of these parameters relative to the sampling environment and move towards standardisation of methods. This could expand the guidance provided by this thesis and ensure it is adaptable for a wide range of studies.

Another theme that has occurred in this thesis in relation to the measurement of atmospheric MP, is the advantage of measuring both deposited and suspended particulates in order to gain a more accurate picture of total atmospheric content. This thesis did not examine the relevance of sampling duration on deposition sampling. The effectiveness of different deposition chambers has been evaluated (Knobloch et al., 2022), but sampling duration could also influence the effectiveness of particle retention within the chamber used. Although liquid is used to prevent re-entrainment, it could be helpful to examine the effectiveness of a range of sampling durations to observe if there is some particle loss or gain by adjusting this parameter. This could indicate if this form of measurement could also be improved and provide technical guidance for future studies that wish to implement it.

The number of particles in atmospheric (and all other environmental) samples is known to increase with the decrease in particle size. This highlights the need to improve the LOD in studies and ensure the smaller size fraction (<20 μm) is identified, in order to report concentrations accurately. Further to this, due to the differences in capabilities with μRaman spectroscopy and Nile Red staining, it is evident that complimentary methods are needed to provide accurate information on both polymer composition and particle count, shape and size. Future research should aim to improve the LOD reported and use methods that can provide a full picture on the quantity and characteristics of atmospheric MP pollution.

This study reported on suspended and deposited atmospheric MP in the Arctic PBL for the first time. Although this novel dataset is helpful at providing information on the extent of atmospheric MP pollution in remote environments, there is also space for

further research. The higher pumping rates used for both direct air filtration and the nanotank sampling system may have caused an under-estimation of MP concentrations in this location. Furthermore, observations indicate that there are complex interactions with weather parameters at this location, especially in relation to how it influences deposited and suspended particulates in different ways. Given the presence and small particle size of atmospheric MP concentrations at this location, long-term monitoring with an improved sampling regime, may prove useful to monitor the pollutant in this remote and vulnerable environment. By also monitoring how long-term measurements interact with weather parameters, it may be possible to gain more information on how this pollutant is interacting with local meteorology. Humidity appears to be correlated with increased MP suspension, and has been found to encourage the degradation of MPs. Snow depth also appears to show trends with MP suspension, which will be of increasing interest as more is learned about the influence of MP on ice and snow melt. Given the unique ecosystems present in the Arctic, and that observations suggest that the Arctic could be a sink for atmospheric MPs, understanding the environmental impact of this pollutant is crucial. Therefore, long-term monitoring should also seek to include ecological impacts.

This study reported on atmospheric MP concentrations in Glasgow for the first time and it is clear that MP pollution is ubiquitous in the urban environment in Glasgow. This is also the first time that MP concentrations were compared to BC and NO, NO_2, and NO_x. Despite the lack of statistically significant relationships, it may be beneficial to measure these pollutants in conjunction in order to gain a more accurate picture of their co-occurrence. Both MPs and NO_x have been found to have increased concentrations in winter due to the reduced temperature reducing the height of the lower atmospheric boundary layer, which reduces vertical transport. Therefore, monitoring both groups of air pollutants in a summer and winter season may also provide more detailed information about how these pollutants interact, and how weather influences their occurrence. Given the health and environmental risk factors associated with both groups of pollutants it is important to understand how they, and other pollutants, are interacting and their extent in our urban environments. This

research could provide important information on the risk-factors associated with the co-location of pollutants.

The study in Glasgow also highlighted the high concentrations of atmospheric MP present in the urban environment. Given the high population of people living in this environment, and the high levels of MPs <10 μm, the human exposure risk is considerable. Particles <10 μm are more likely to be inhaled and transported throughout the body. Understanding the toxicity of this pollution when present in the body should be a focus of human health studies. This study only reported concentrations at a single residential location in Glasgow, it would be of interest to measure concentrations at more industrial and rural locations to observe if there are differences due to local influences. This could also indicate if individual human activity patterns could increase exposure to atmospheric MP.

In terms of transport, it was interesting to observe the influence of particle size and polymer density in terms of transport and dispersion. This highlighted the role of the 'Plastic Cycle' as particles from oceanic and distal sources could be transported thousands of miles in a matter of days. It was also observed that particles could be transported back to their original source in the North Atlantic or to other marine sources such as the Black Sea or the Mediterranean, as well as to other populated environments. Although it has previously been identified that atmospheric MPs can be transported via waves and bubble bursting, further monitoring of this interaction would be beneficial to help understand the transport mechanisms and extent of MP pollution in marine, atmospheric and terrestrial environments.

Overall, the field of atmospheric MP is still relatively novel and there are still research gaps regarding its measurement, transport and extent in our environment. There are also gaps in understanding of how much of a threat this pollutant poses to our ecosystems, human health and climate. Although the measurement of this pollutant is not standardised and harmonious as of yet, efforts to measure and monitor this pollutant are crucial to examine this pollutant as the field emerges.

7.3.2 Recommendations for Future Policy

From the observations made in this thesis, atmospheric MP pollution is ubiquitous in remote and urban environments, and there is potential for transboundary and long-range transport. Marine sources have been highlighted as a main contributor. Although marine MP pollution has been the focus of the field of microplastics, it is clear that the marine-atmospheric interactions present a gap in knowledge. It is thought that in 2019 global plastic leakage to the environment (aquatic and terrestrial) was 22 Mt (OECD, 2022) and given the nature of this pollutant to be transported to various environments, preventing this leakage should be a policy priority. Given the potential for waste management activities such as recycling, to cause MP leakage to the environment (see **Chapter 2**), it is evident that recycling is not an effective solution to the plastic problem. Preventing the production and demand for plastic should be the first line of defence for preventing further MP contamination in our environment. The circular economy approach where reduction of waste is at the top of the waste management hierarchy, should be a focus of environmental policy.

As plastic is part of our everyday life, a systems approach would be needed to change the habits and systems in place that make plastic the easiest and cheapest option. Although this top-down approach is necessary, it would also be beneficial to understand the individual drivers of human behaviour related to plastic usage. **Appendix III presents** a systemic review that examines existing literature on behaviour change theory and plastic use. From this review it is clear that there is not enough research or policy on the individual motivations and habits that are associated with single-use plastic use. Although attitudes to plastic are changing as the field of MPs gains more public attention, more needs to be done to alter individual behaviour away to reduce plastic use. That being said, this needs to be accompanied with producer accountability, and better waste management policies in order to reduce plastic use and leakage into our environment.

Although research into the effects of MP on climate are still emerging, there are links to MP contamination and increased GHG emissions, and accelerated snow and ice

melt. Therefore, these considerations need to be taken into account when making plans to limit global warming. If countries are to meet the current Paris Agreement goals to limit warming to 1.5ºC above pre-industrial levels, plastic usage and its presence in our environment should be a focus of environmental policy.

Chapter 8 – Conclusion

This thesis aimed to improve understanding of atmospheric MPs, by assessing their measurement, comparing their presence in remote and urban environments and exploring potential long-range transport pathways. To achieve this, four overarching research questions (RQ1-4; see **Chapter 1**) were posed, each addressing key knowledge gaps in the field of atmospheric MP pollution.

The first research question (RQ1) asked how the parameters used in active atmospheric MP sampling influence measured particle concentrations relative to the sampling environment. Results of this comparative study showed that pumping rate and sampling duration strongly influence collection efficiency, shape and size distribution, but not polymer composition Results showed that by increasing the pumping rate and sampling duration, there was no increase in MP collection per volume of sampled air. This comparative study took place in an environmental setting where atmospheric MP concentrations vary over time. A range of environmental conditions could be used to establish more definitive thresholds. This study highlighted the need to consider the parameters used in active sampling early in research planning, in order to avoid under-reporting concentrations and to gain a representative sample.

The second research question (RQ2) investigated atmospheric MPs in remote locations, using a case study of Svalbard, Norway, and to examine how this pollution related to weather conditions and potential transport pathways. Results showed, for the first time, that atmospheric MP pollution is present and ubiquitous in the Arctic environment in both suspended and deposited samples. Nile Red staining showed that MPs were predominantly fragments and <20μm in size. This highlights the need to improve the LOD when reporting atmospheric MP concentrations. As is consistent with other atmospheric MP studies, the number of MPs increase with the decrease in particle size which emphasises the need to report on the smaller size fraction in order to gain a representative picture of atmospheric MP content. μRaman analysis identified

Acrylic (16%), PLS (14%), PES (11%), and PVA (11%) as the most prevalent polymers. This suggests local contamination from clothing and fishing gear, or distal sources from food packaging or industrial applications.

This study showed that there are key differences between deposited and suspended particulates including their polymer composition and relationships with weather parameters. This highlights the benefit of reporting on both suspended and deposited atmospheric MP concentrations, as it is evident the two different forms of atmospheric MP pollution are subject to different influences. Dispersion modelling used to identify the main transport pathways for atmospheric MP pollution, highlighted the role of long-range transport from the North Atlantic and marine influence via sea spray. This indicates the capacity of MPs to be transported from distal sources and reach remote environments. When higher concentrations of atmospheric MP were recorded, air masses originated from continental Europe which shows the potential of urban atmospheric MP pollution to be transported long-range to remote environments.

RQ3 investigated atmospheric MP pollution in an urban location, using Glasgow, Scotland as a case study. Results from the same Nile Red staining and μRaman methods used for the Svalbard case study showed that atmospheric MPs were again ubiquitous in the Glasgow PBL and concentrations were several orders of magnitude higher than in the remote Arctic environment. Atmospheric MP pollution in the urban environment was again characterised predominantly by particles <20 μm, with fragments being the most common shape identified. Results from the μRaman analysis indicate in terms of polymer composition PLS and acrylic were prevalent polymers, as well as PES and PMMA implicating textiles and industrial applications as possible sources. The relationship with weather was also complex and different weather parameters appear to be influential on atmospheric MP pollution in the urban environment. This study also investigated relationships with other atmospheric pollutants, but further long-term monitoring is needed to understand this relationship. Particle modelling highlighted the role of both local industrial sources and long-range marine sources, again predominantly over the North Atlantic. This highlights the need

for more monitoring of atmospheric MP pollution generally using consistent methods to enable further investigation into transport behaviour and relationships with other anthropogenic pollutants.

The final research question, RQ4, compared the atmospheric MP pollution characteristics, relationships with weather, and transport mechanisms, between urban and remote locations. Atmospheric MP concentrations were orders of magnitude higher in the urban location, compared to the remote. Given the increased anthropogenic activity in the urban location, an increased concentration of atmospheric MPs would be expected. However, given the remote location and vulnerable ecosystems present in the Arctic, and the potential for accelerated ice melt due to MPs present on snow and ice, the ability for this remote location to be polluted from long-range sources is still concerning. It is evident that for both datasets there were differences in the numbers reported from μRaman analysis and Nile Red staining, underscoring the importance of using complementary methods when analysing atmospheric MPs to gain information on characteristics and chemical composition, and report concentrations accurately.

Results from both case studies showed that although fragments were the predominant shape in both locations, the urban Glasgow location displayed a higher proportion of fibres, possibly implicating localised influence from textiles and clothes drying. Both locations also displayed small particle size distributions with the majority of particles characterised <20 μm. This again highlights the need for studies in the field to improve the LOD to report on MP concentrations <20 μm in order to report on concentrations accurately. Differences between the two μRaman spectrometers used for the respective locations made comparisons on polymer composition challenging. However, this reflects the current field of atmospheric MP research which is restrained by access to analytical methods and the need for more harmonised methodologies. Despite this, some similarities in polymer composition between the two locations can be observed. For both locations PLS and Acrylic were two of the main polymers identified which indicate the role of industrial applications, food processing and textiles.

Both locations displayed significant correlations between cloud cover, wind direction and atmospheric MP concentrations. For both locations the concentrations were divided into <20 μm and >20 μm size classes to observe if weather parameters were bias to a certain size of particle. The urban location displayed no significant correlations with atmospheric MP concentrations and weather parameters. Alternatively the remote location displayed significant relationships with particles <20μm and local weather parameters. This highlights that there is clearly a complex relationship between atmospheric MP concentrations and weather parameters at both locations and that particle size can play a role in these relationships. Back trajectory modelling used at both locations indicates that marine sources, particularly the North Atlantic, play a role in influencing atmospheric MP concentrations. The results support the view that MPs can be resuspended from the ocean via sea spray and waves, and that long-transport of atmospheric MPs is possible to both remote and urban locations. While each model has limitations, both suggest that the marine-atmospheric pathway is a key contributor to the global transport of MP pollution. Future research should focus on quantifying the role of this interaction as a major pathway of MP dispersion.

This thesis has addressed current knowledge gaps related to the measurement of atmospheric MP concentrations, underpinning the current calls for more consistent and harmonised methodologies. It is hoped the recommendations made on research design related to active sampling campaigns can provide guidance for future research to improve reporting on accurate atmospheric MP concentrations.

Furthermore, atmospheric MP pollution in both a remote and urban location has been reported using consistent methodologies. This has attempted to provide a more accurate comparison of this emerging pollutant in both environments. However, more research and long-term monitoring of this pollutant is needed to understand how this pollutant varies between environments and its relationship with weather and other anthropogenic pollutants.

The polymer composition of the atmospheric MP samples reported in this thesis has indicated the role of industrial applications, food packaging, and textiles as possible

sources of this pollutant. Therefore, policies that focus on the reduction and limitation of these products are needed in order to reduce the contribution of emissions from these sources which can pollute both local and distal environments. This includes both systematic change and individual behaviour change.

Overall, this thesis demonstrates this emerging transboundary pollutant is ubiquitous in our environment. It requires coordinated and long-term monitoring and immediate mitigation policies to protect both urban and remote ecosystems and human health.

References

Abad López, A. P., Trilleras, J., Arana, V. A., Garcia-Alzate, L. S., & Grande-Tovar, C. D. (2023). Atmospheric microplastics: exposure, toxicity, and detrimental health effects. *RSC Advances*, *13*(11), 7468–7489. https://doi.org/10.1039/D2RA07098G

Abbasi, S., Keshavarzi, B., Moore, F., Turner, A., Kelly, F. J., Dominguez, A. O., & Jaafarzadeh, N. (2019). Distribution and potential health impacts of microplastics and microrubbers in air and street dusts from Asaluyeh County, Iran. *Environmental Pollution*, *244*, 153–164. https://doi.org/10.1016/j.envpol.2018.10.039

Abbasi, S., Rezaei, M., Ahmadi, F., & Turner, A. (2022). Atmospheric transport of microplastics during a dust storm. *Chemosphere*, *292*. https://doi.org/10.1016/j.chemosphere.2021.133456

Abbasi, S., Jaafarzadeh, N., Zahedi, A., Ravanbakhsh, M., Abbaszadeh, S., & Turner, A. (2023). Microplastics in the atmosphere of Ahvaz City, Iran. *Journal of Environmental Sciences*, *126*, 95–102. https://doi.org/10.1016/j.jes.2022.02.044

Abnett, K. (2023, April 28). Germans, Dutch and French call for binding EU microplastic rules | Reuters. *Reuters*. https://www.reuters.com/business/sustainable-business/germans-dutch-french-call-binding-eu-microplastic-rules-2023-04-28/

Aeschlimann, M., Li, G., Kanji, Z. A., & Mitrano, D. M. (2022). Potential impacts of atmospheric microplastics and nanoplastics on cloud formation processes. *Nature Geoscience* , *15*, 967–975. https://doi.org/10.1038/s41561-022-01051-9

Air Quality Expert Group. (2005). Particulate Matter in the United Kingdom. In http://uk-air.defra.gov.uk/assets/documents/reports/cat11/1212141150_AQEG_Fine_Particulate_Matter_in_the_UK.pdf.

Air Quality in Scotland. (2025a). *Site Data South Lanarkshire Cambuslang*. Ricardo. https://www.scottishairquality.scot/latest/site-info/SL07

Air Quality in Scotland. (2025b). *Site Data South Lanarkshire Rutherglen*. Ricardo. https://www.scottishairquality.scot/latest/site-info/SL04

Akdogan, Z., & Guven, B. (2019). Microplastics in the environment: A critical review of current understanding and identification of future research needs. In *Environmental Pollution*. https://doi.org/10.1016/j.envpol.2019.113011

Akhbarizadeh, R., Dobaradaran, S., Amouei Torkmahalleh, M., Saeedi, R., Aibaghi, R., & Faraji Ghasemi, F. (2021). Suspended fine particulate matter (PM2.5), microplastics (MPs), and polycyclic aromatic hydrocarbons (PAHs) in air: Their possible relationships and health implications. *Environmental Research*, *192*(110339), 1–12. https://doi.org/10.1016/j.envres.2020.110339

Allen, S., Allen, D., Phoenix, V. R., Le Roux, G., Durántez Jiménez, P., Simonneau, A., Binet, S., & Galop, D. (2019). Atmospheric transport and deposition of microplastics in a remote mountain catchment. *Nature Geoscience*, *12*(5), 339–344. https://doi.org/10.1038/s41561-019-0335-5

Allen, S., Allen, D., Moss, K., le Roux, G., Phoenix, V. R., & Sonke, J. E. (2020). Examination of the ocean as a source for atmospheric microplastics. *PLoS ONE*, *15*(5). https://doi.org/10.1371/journal.pone.0232746

Allen, S., š an Materi ć, D., Allen, D., MacDonald, A., Holzinger, R., le Roux, G., & Phoenix, V. R. (2022). An early comparison of nano to microplastic mass in a remote catchment's atmospheric deposition. *Journal of Hazardous Materials Advances*, *7*(100104), 1–9. https://doi.org/10.1016/j.hazadv.2022.100104

Ali, M. U., Lin, S., Yousaf, B., Abbas, Q., Munir, M. A. M., Ali, M. U., Rasihd, A., Zheng, C., Kuang, X., & Wong, M. H. (2021). Environmental emission, fate and transformation of microplastics in biotic and abiotic compartments: Global status, recent advances and future perspectives. *Science of The Total Environment*, *791*(148422), 1–16. https://doi.org/10.1016/J.SCITOTENV.2021.148422

Anger, P. M., von der Esch, E., Baumann, T., Elsner, M., Niessner, R., & Ivleva, N. P. (2018). Raman microspectroscopy as a tool for microplastic particle analysis. *TrAC Trends in Analytical Chemistry*, *109*, 1–13. https://doi.org/10.1016/j.trac.2018.10.010

Ankit, Y., Ajay, K., Nischal, S., Kaushal, S., Kataria, V., Dietze, E., & Anoop, A. (2024). Atmospheric deposition of microplastics in an urban conglomerate near to the foothills of Indian Himalayas: Investigating the quantity, chemical character, possible sources and transport mechanisms. *Environmental Pollution*, *361*(124629), 1–10. https://doi.org/doi.org/10.1016/j.envpol.2024.124629Rece

AQI, 2021. *Glasgow Air Pollution: Real-time Air Quality Index (AQI).* The World Air Quality Project. (Online). Available at: https://aqicn.org/map/glasgow/. (Accessed 7.3.21)

Ashley, K., & Connor, P. F. O. (2017). NIOSH Manual of Analytical Methods (NMAM), 5th Edition Foreword. *NIOSH Manual of Analytical Methods - Centre for Disease Prevention and Control*, *5th Edition*. 1-860.

Asrin, N., Dipareza, A., & Rizki, N. (2019). Microplastics in Ambient Air (Case Study: Urip Sumoharjo Street and Mayjend Sungkono Street of Surabaya City, Indonesia). *IAETSD Journal for Advanced Journal for Advanced Research in Applied Sciences*, 54–57. http://dx.doi.org/10.12944/CWE.14.2.13

Araujo, C. F., Nolasco, M. M., Ribeiro, A. M. P., & Ribeiro-Claro, P. J. A. (2018). Identification of microplastics using Raman spectroscopy: Latest developments and future prospects. In *Water Research* (Vol. 142). https://doi.org/10.1016/j.watres.2018.05.060

Aves, A. R., Revell, L. E., Gaw, S., Ruffell, H., Schuddeboom, A., Wotherspoon, N. E., Larue, M., & Mcdonald, A. J. (2022). First evidence of microplastics in Antarctic snow. *Cryosphere*, *16*(6), 2127–2145. https://doi.org/10.5194/TC-16-2127-2022

Azari, A., Vanoirbeek, J. A. J., van Belleghem, F., Vleeschouwers, B., Hoet, P. H. M., & Ghosh, M. (2023). Sampling strategies and analytical techniques for assessment of airborne micro and nano plastics. *Environment International*, *174*, 107885. https://doi.org/10.1016/j.envint.2023.107885

Bach, L., Strand, J., Salame, H., Simon, M., Fritt-Rasmussen, J., & Jensen, P. E. (2024). Wet wipes in untreated wastewater are a source of litter pollution to the arctic marine environment – a case study on the loads of litter and microplastics in wastewater effluents in Greenland. *Environmental Science: Advances*, 1–12. https://doi.org/10.1039/D4VA00233D

Baensch-Baltruschat, B., Kocher, B., Stock, F., & Reifferscheid, G. (2020). Tyre and road wear particles (TRWP) - A review of generation, properties, emissions, human health risk, ecotoxicity, and fate in the environment. In *Science of the Total Environment* (Vol. 733). https://doi.org/10.1016/j.scitotenv.2020.137823

Beaurepaire, M., Gasperi, J., Tassin, B., & Dris, R. (2024). COVID lockdown significantly impacted microplastic bulk atmospheric deposition rates. *Environmental Pollution*, *344*(123354), 1–8. https://doi.org/10.1016/J.ENVPOL.2024.123354

Bai, R., Fan, R., Xie, C., Liu, Q., Liu, Q., Yan, C., Cui, J., & He, W. (2023). Microplastics are overestimated due to poor quality control of reagents. *Journal of Hazardous Materials*, *459*. https://doi.org/10.1016/j.jhazmat.2023.132068

Bakels, L., Tatsii, D., Tipka, A., Thompson, R., Dütsch, M., Blaschek, M., Seibert, P., Baier, K., Bucci, S., Cassiani, M., Eckhardt, S., Groot Zwaaftink, C., Henne, S., Kaufmann, P., Lechner, V., Maurer, C., Mulder, M. D., Pisso, I., Plach, A., … Stohl, A. (2024). FLEXPART version 11: improved accuracy, efficiency, and flexibility. *Geoscientific Model Development*, *17*(21), 7595–7627. https://doi.org/10.5194/gmd-17-7595-2024

Bao, M., Huang, Q., Lu, Z., Collard, F., Cai, M., Huang, P., Yu, Y., Cheng, S., An, L., Wold, A., & Gabrielsen, G. W. (2022). Investigation of microplastic pollution in Arctic fjord water: a case study of Rijpfjorden, Northern Svalbard. *Environmental Science and Pollution Research*, *29*(37). https://doi.org/10.1007/s11356-022-19826-3

Barton, S. J., Ward, T. E., & Hennelly, B. M. (2018). Algorithm for optimal denoising of Raman spectra. *Analytical Methods*, *10*(30). https://doi.org/10.1039/c8ay01089g

BBC News. (2016). *Plastic microbeads to be banned in Scotland*. https://www.bbc.co.uk/news/uk-scotland-scotland-politics-38379921

Bergmann, M., Mützel, S., Primpke, S., Tekman, M. B., Trachsel, J., & Gerdts, G. (2019). White and wonderful? Microplastics prevail in snow from the Alps to the Arctic. *Science Advances*, *5*(8), 1–10. https://doi.org/10.1126/sciadv.aax1157

Bergmann, M., Collard, F., Fabres, J., Gabrielsen, G. W., Provencher, J. F., Rochman, C. M., van Sebille, E., & Tekman, M. B. (2022). Plastic pollution in the Arctic. *Nature Reviews Earth & Environment 2022 3:5*, *3*(5), 323–337. https://doi.org/10.1038/s43017-022-00279-8

Borah, S. J. ;, Gupta, A. K. ;, Kumar, V. ;, Jhajharia, P. ;, Singh, P. P. ;, Kumar, P. ;, Kumar, R. ;, Dubey, K. K. ;, Triantafyllidis, S., Timko, M. T., Borah, S. J., Kumar Gupta, A., Kumar, V., Jhajharia, P., Singh, P. P., Kumar, P., Kumar, R., Dubey, K. K., & Gupta, A. (2024). The Peril of Plastics: Atmospheric Microplastics in Outdoor, Indoor, and Remote Environments. *Sustainable Chemistry 2024, Vol. 5, Pages 149-162*, *5*(2), 149–162. https://doi.org/10.3390/SUSCHEM5020011

Brahney, J., Mahowald, N., Prank, M., Cornwell, G., Klimont, Z., Matsui, H., Prather, K.A., 2021. Constraining the atmospheric limb of the plastic cycle. *Proceedings of the National Academy of Sciences*. 118, 1–10. https://doi.org/10.1073/pnas.2020719118

Brander, S. M., Renick, V. C., Foley, M. M., Steele, C., Woo, M., Lusher, A., Carr, S., Helm, P., Box, C., Cherniak, S., Andrews, R. C., & Rochman, C. M. (2020). Sampling and Quality Assurance and Quality Control: A Guide for Scientists Investigating the Occurrence of Microplastics Across Matrices. *Applied Spectroscopy*, *74*(9). https://doi.org/10.1177/0003702820945713

Britton, A.J., Fielding, D.A. & Pakeman, R.J. (2022) Nitrogen and climate: A review of the interactive effects of nitrogen deposition and climate change on Scottish semi-natural ecosystems. The James Hutton Institute, Aberdeen. Zenodo. https://doi.org/10.5281/zenodo.7547364

Brioude, J., Arnold, D., Stohl, A., Cassiani, M., Morton, D., Seibert, P., Angevine, W., Evan, S., Dingwell, A., Fast, J. D., Easter, R. C., Pisso, I., Burkhart, J., & Wotawa, G. (2013). Geoscientific Model Development The Lagrangian particle dispersion model FLEXPART-WRF version 3.1. *Geoscience Model Development*, *6*, 1889–1904. https://doi.org/10.5194/gmd-6-1889-2013

Brown, E., MacDonald, A., Allen, S., & Allen, D. (2023). The potential for a plastic recycling facility to release microplastic pollution and possible filtration remediation effectiveness. *Journal of Hazardous Materials Advances*, *10*(100309), 1–10. https://doi.org/10.1016/j.hazadv.2023.100309

Bucci, S., Richon, C., & Bakels, L. (2024). Exploring the Transport Path of Oceanic Microplastics in the Atmosphere. *Environmental Science & Technology*, *58*(32), 14338–14347. https://doi.org/10.1021/acs.est.4c03216

Bumbrah, G. S., & Sharma, R. M. (2016). Raman spectroscopy – Basic principle, instrumentation and selected applications for the characterization of drugs of abuse. In *Egyptian Journal of Forensic Sciences* (Vol. 6, Issue 3). https://doi.org/10.1016/j.ejfs.2015.06.001

Cai, H., Chen, M., Chen, Q., Du, F., Liu, J., & Shi, H. (2020). Microplastic quantification affected by structure and pore size of filters. *Chemosphere*, *257*. https://doi.org/10.1016/j.chemosphere.2020.127198

Carruthers, H., Clark, D., Clarke, F. C., Faulds, K., & Graham, D. (2022). Evaluation of laser direct infrared imaging for rapid analysis of pharmaceutical tablets. *Analytical Methods*, *14*(19). https://doi.org/10.1039/d2ay00471b

Caracci, E., Vega-Herrera, A., Dachs, J., Berrojalbiz, N., Buonanno, G., Abad, E., Llorca, M., Moreno, T., & Farré, M. (2023). Micro(nano)plastics in the atmosphere of the Atlantic Ocean. *Journal of Hazardous Materials*, *450*, 131036. https://doi.org/10.1016/J.JHAZMAT.2023.131036

Cassiani, M., Stohl, A., & Brioude, J. (2015). Lagrangian Stochastic Modelling of Dispersion in the Convective Boundary Layer with Skewed Turbulence Conditions and a Vertical Density Gradient: Formulation and Implementation in the FLEXPART Model. *Boundary-Layer Meteorology*, *154*(3), 367–390. https://doi.org/10.1007/s10546-014-9976-5

Catarino, A. I., Kramm, J., Völker, C., Henry, T. B., & Everaert, G. (2021). Risk posed by microplastics: Scientific evidence and public perception. In *Current Opinion in Green and Sustainable Chemistry* (Vol. 29). https://doi.org/10.1016/j.cogsc.2021.100467

Chatterjee, S., Krolis, E., Molenaar, R., Claessens, M. M. A. E., & Blum, C. (2023). Nile Red staining for nanoplastic quantification: Overcoming the challenge of false positive counts due to fluorescent aggregates. *Environmental Challenges*, *13*(100744), 1–7. https://doi.org/10.1016/j.envc.2023.100744

Chen, Y.-C., Wei, C.-H., Hsu, W.-T., Proborini, W. D., Hsiao, T.-C., Liu, Z.-S., Chou, H.-C., Soo, J.-C., Dong, G.-C., & Chen, J.-K. (2024). Impact of seasonal changes and environmental conditions on suspended and inhalable microplastics in urban air. *Environmental Pollution*, *362*(124994), 1–8. https://doi.org/10.1016/j.envpol.2024.124994

Chen, Q., Shi, G., Revell, L. E., Zhang, J., Zuo, C., Wang, D., le Ru, E. C., Wu, G., & Mitrano, D. M. (2023). Long-range atmospheric transport of microplastics across the southern hemisphere. *Nature Communications*, *14*(1), 1–10. https://doi.org/10.1038/s41467-023-43695-0

Chen, C.-Y., Chen, S.-Y., & Liao, C.-M. (2025). Regional and population-scale trends in human inhalation exposure to airborne microplastics: Implications for health risk assessment. *Environmental Pollution*, *371*, 125950. https://doi.org/10.1016/j.envpol.2025.125950

Choi, H., Lee, I., Kim, H., Park, J., Cho, S., Oh, S., Lee, M., & Kim, H. (2022). Comparison of Microplastic Characteristics in the Indoor and Outdoor Air of Urban Areas of South Korea. *Water, Air, & Soil Pollution 2022 233:5*, *233*(5), 1–10. https://doi.org/10.1007/S11270-022-05650-5

Collins, S. F., & Norton, A. (2024). Prevailing wind patterns influence the distribution of plastics in small urban lakes. *Scientific Reports*, *14*(1), 1–11. https://doi.org/10.1038/s41598-024-68516-2

Comerford, R. (2024, April 25). UK cash-for-bottle deposit scheme delayed until 2027. *BBC News*. https://www.bbc.co.uk/news/uk-68898109#:~:text=The%20UK's%20bottle%20deposit%20and%20return%20scheme,Delayed%20*%20**2027**%20Current%20scheduled%20launch%20date

Cowger, W., Booth, A. M., Hamilton, B. M., Thaysen, C., Primpke, S., Munno, K., Lusher, A. L., Dehaut, A., Vaz, V. P., Liboiron, M., Devriese, L. I., Hermabessiere, L., Rochman, C., Athey, S. N., Lynch, J. M., de Frond, H., Gray, A., Jones, O. A. H., Brander, S., … Nel, H. (2020). Reporting Guidelines to Increase the Reproducibility and Comparability of Research on Microplastics. *Applied Spectroscopy*, *74*(9). https://doi.org/10.1177/0003702820930292

Cowger, W., Markley, L. A. T., Moore, S., Gray, A. B., Upadhyay, K., & Koelmans, A. A. (2024). How many microplastics do you need to (sub)sample? *Ecotoxicology and Environmental Safety*, *275*(116243), 1–7. https://doi.org/10.1016/J.ECOENV.2024.116243

DEFRA. (2025). *Emissions of air pollutants in the UK – Particulate matter (PM10 and PM2.5)*. Department for Environment, Food & Rural Affairs. GOV UK. . https://www.gov.uk/government/statistics/emissions-of-air-pollutants/emissions-of-air-pollutants-in-the-uk-particulate-matter-pm10-and-pm25

Dehghani, S., Moore, F., & Akhbarizadeh, R. (2017). Microplastic pollution in deposited urban dust, Tehran metropolis, Iran. *Environmental Science and Pollution Research*, *24*, 20360–20371. https://doi.org/DOI10.1007/s11356-017-9674-1

Ding, Y., Zou, X., Wang, C., Feng, Z., Wang, Y., Fan, Q., & Chen, H. (2021). The abundance and characteristics of atmospheric microplastic deposition in the northwestern South China Sea in the fall. *Atmospheric Environment*, *253*(118389), 1–9. https://doi.org/10.1016/J.ATMOSENV.2021.118389

Draxler, R., Stunder, B., Rolph, G., Stein, A., Taylor, A., Zinn, S., Loughner, C., & Crawford, A. (2025). *HYSPLIT USER's GUIDE*.

Dris, R., Gasperi, J., Rocher, V., Saad, M., Renault, N., & Tassin, B. (2015). Microplastic contamination in an urban area: a case study in Greater Paris. *Environmental Chemistry*, *12*(5), 592–599. https://doi.org/10.1071/EN14167

Dris, R., Gasperi, J., Saad, M., Mirande, C., & Tassin, B. (2016). Synthetic fibers in atmospheric fallout: A source of microplastics in the environment? *Marine Pollution Bulletin*, *104*(1–2), 290–293. https://doi.org/10.1016/j.marpolbul.2016.01.006

Dris, R., Gasperi, J., Mirande, C., Mandin, C., Guerrouache, M., Langlois, V., & Tassin, B. (2017). A first overview of textile fibers, including microplastics, in indoor and outdoor environments. *Environmental Pollution*, *221*, 453–458. https://doi.org/10.1016/j.envpol.2016.12.013

D'Hont, A., Gittenberger, A., Leuven, R. S. E. W., & Hendriks, A. J. (2021). Dropping the microbead: Source and sink related microplastic distribution in the Black Sea and Caspian Sea basins. *Marine Pollution Bulletin*, *173*. https://doi.org/10.1016/j.marpolbul.2021.112982

Dong, H., Wang, X., Niu, X., Zeng, J., Zhou, Y., Suona, Z., Yuan, Y., & Chen, X. (2023). Overview of analytical methods for the determination of microplastics: Current status and trends. In *TrAC - Trends in Analytical Chemistry* (Vol. 167). https://doi.org/10.1016/j.trac.2023.117261

Eales, J., Bethel, A., Galloway, T., Hopkinson, P., Morrissey, K., Short, R. E., & Garside, R. (2022). Human health impacts of exposure to phthalate plasticizers: An overview of reviews. In *Environment International* (Vol. 158). https://doi.org/10.1016/j.envint.2021.106903

Eckhardt, S., Cassiani, M., Evangeliou, N., Sollum, E., Pisso, I., & Stohl, A. (2017). Source–receptor matrix calculation for deposited mass with the Lagrangian particle dispersion model FLEXPART v10.2 in backward mode. *Geoscientific Model Development*, *10*(12), 4605–4618. https://doi.org/10.5194/gmd-10-4605-2017

Edinburgh Instruments. (2021a). *How to Choose your Lasers from Raman spectroscopy*. Retrieved April 13, 2025, from https://www.edinst.com/resource/how-to-choose-your-lasers-for-raman-spectroscopy/#:~:text=The%20most%20commonly%20used%20laser,nm%20laser%20may%20be%20needed. (Accessed: 13/04/25)

Edinburgh Instruments. (2021b). *What is Confocal Raman Microscopy?* What is Confocal Raman Microscopy? https://www.edinst.com/resource/what-is-confocal-raman-microscopy/#:~:text=Confocal%20Raman%20microscopy%20combines%20Raman,pinhole%2C%20spectrograph%2C%20and%20detectors. (Accessed: 13/04/25)

Ellen MacArthur Foundation. (2024, March 1). A UN treaty to end plastic pollution. *Ellen MacArthur Foundation*. https://www.ellenmacarthurfoundation.org/un-plastics-treaty/overview
Ellen MacArthur Foundation. (2023). *The Butterfly Diagram: Visualising the Circular Economy*. Ellen MacArthur Foundation. https://ellenmacarthurfoundation.org/circular-economy-diagram

Emberson-Marl, H., Coppock, R. L., Cole, M., Godley, B. J., Mimpriss, N., Nelms, S. E., & Lindeque, P. K. (2023). Microplastics in the Arctic: a transect through the Barents Sea. *Frontiers in Marine Science*, *10*. https://doi.org/10.3389/fmars.2023.1241829

Environment Agency, U. (2011). *M8 Monitoring Ambient Air Environment Agency - Technical Guidance Note*. www.mcerts.net (Accessed: 25/03/201)

Enyoh, C. E., Verla, A. W., Verla, E. N., Ibe, F. C., & Amaobi, C. E. (2019). Airborne microplastics: a review study on method for analysis, occurrence, movement and risks. *Environmental Monitoring and Assessment*, *191*(668), 1–17. https://doi.org/10.1007/s10661-019-7842-0

Enyoh, C. E., Devi, A., Kadono, H., Wang, Q., & Rabin, M. H. (2023). The Plastic Within: Microplastics Invading Human Organs and Bodily Fluids Systems. *Environments*, *10*(11), 194. https://doi.org/10.3390/environments10110194

European Commission. (2020). *Communication from the Commission to the European Parliament, The Council, the European Economic and Social Committee, and the Committee of the Regions: A new Circular Economy Action Plan, For a cleaner and more competitive Europe*. 1–20. https://eur-lex.europa.eu/resource.html?uri=cellar:9903b325-6388-11ea-b735-01aa75ed71a1.0017.02/DOC_1&format=PDF

European Commission. (2023, April 23). REACH committee votes to restrict intentional microplastics. *European Commission* . https://single-market-economy.ec.europa.eu/news/reach-committee-votes-restrict-intentional-microplastics-2023-04-27_

European Environment Agency. (2013). *Black carbon: Better monitoring needed to assess health and climate change impacts*. https://www.eea.europa.eu/highlights/black-carbon-better-monitoring-needed#:~:text=Health%20and%20climate%20effects,absorbs%20more%20heat%2C%20accelerating%20melting.

European Environment Agency. (2019). *Air quality in Europe — 2019 Report. EEA Report No 10/2019.* https://doi.org/10.2800/822355

European Environment Agency. (2025). *Particulate Matter*. European Environment Agency. http://www.eea.europa.eu/maps/ozone/resources/glossary/particulate-matter

European Parliament. (2023, April 25). *Circular economy: definition, importance and benefits*. https://www.europarl.europa.eu/topics/en/article/20151201STO05603/circular-economy-definition-importance-and-benefits#:~:text=What%20is%20the%20circular%20economy,cycle%20of%20products%20is%20extended.

European Union. (2020, February). *A French act of law against waste and for a circular economy*. Issuing Public Authority: French Government. https://circulareconomy.europa.eu/platform/en/strategies/french-act-law-against-waste-and-circular-economy

Evangeliou, N., Grythe, H., Klimont, Z., Heyes, C., Eckhardt, S., Lopez-Aparicio, S., & Stohl, A. (2020). Atmospheric transport is a major pathway of microplastics to remote regions. *Nature Communications 2020 11:1*, *11*(1), 1–11. https://doi.org/10.1038/s41467-020-17201-9

Evangeliou, N., Tichý, O., Eckhardt, S., Zwaaftink, C. G., & Brahney, J. (2022). Sources and fate of atmospheric microplastics revealed from inverse and dispersion modelling: From global emissions to deposition. *Journal of Hazardous Materials*, *432*, 128585. https://doi.org/10.1016/j.jhazmat.2022.128585

Fan, W., Salmond, J. A., Dirks, K. M., Sanz, P. C., Miskelly, G. M., & Rindelbulb, J. D. (2022). Evidence and Mass Quantification of Atmospheric Microplastics in a Coastal New Zealand City. *Environmental Science & Technology*, *56*, 17557–17568. https://pubs.acs.org/doi/pdf/10.1021/acs.est.2c05850

Felsing, S., Kochleus, C., Buchinger, S., Brennholt, N., Stock, F., & Reifferscheid, G. (2018). A new approach in separating microplastics from environmental samples based on their electrostatic behavior. *Environmental Pollution*, *234*, 20–28. https://doi.org/10.1016/j.envpol.2017.11.013

Fernández-González, V., Andrade-Garda, J. M., López-Mahía, P., & Muniategui-Lorenzo, S. (2021). Impact of weathering on the chemical identification of microplastics from usual packaging polymers in the marine environment. *Analytica Chimica Acta*, *1142*, 179–188. https://doi.org/10.1016/j.aca.2020.11.002

Ferrero, L., Scibetta, L., Markuszewski, P., Mazurkiewicz, M., Drozdowska, V., Makuch, P., Jutrzenka-Trzebiatowska, P., Zaleska-Medynska, A., Andò, S., Saliu, F., Nilsson, E. D., & Bolzacchini, E. (2022). Airborne and marine microplastics from an oceanographic survey at the Baltic Sea: An emerging role of air-sea interaction? *Science of The Total Environment*, *824*, 153709. https://doi.org/10.1016/J.SCITOTENV.2022.153709

Filho, W. L., Barbir, J., Abubakar, I. R., Paço, A., Stasiskiene, Z., Hornbogen, M., Christin Fendt, M. T., Voronova, V., & Klõga, M. (2022). Consumer attitudes and concerns with bioplastics use: An international study. *PLOS ONE*, *17*(4), e0266918. https://doi.org/10.1371/journal.pone.0266918

Forster, C., Stohl, A., & Seibert, P. (2007). Parameterization of Convective Transport in a Lagrangian Particle Dispersion Model and Its Evaluation. *Journal of Applied Meteorology and Climatology*, *46*(4), 403–422. https://doi.org/10.1175/JAM2470.1

Frias, J. P. G. L., & Nash, R. (2019). Microplastics: Finding a consensus on the definition. *Marine Pollution Bulletin*, *138*, 145–147. https://doi.org/10.1016/j.marpolbul.2018.11.022

Frontier Labs. (2020). *Analysis of microplastics using pyrolysis (Py)-GC/MS Part 2: Identification of colored marine microplastics*. Multi-Functional Pyrolyzer® Technical Note. https://www.frontier-lab.com/assets/file/technical-note/PYA1-111E.pdf

Gaga, E. O., Döğeroğlu, T., Özden, Ö., Ari, A., Yay, O. D., Altuğ, H., Akyol, N., Örnektekin, S., & van Doorn, W. (2012). Evaluation of air quality by passive and active sampling in an urban city in Turkey: Current status and spatial analysis of air pollution exposure. *Environmental Science and Pollution Research*, *19*(8), 3579–3596. https://doi.org/10.1007/s11356-012-0924-y

Gao, W., Deng, X. J., Zhang, J., Qi, L., Zhao, X. Q., & Zhang, P. Y. (2023). Assessment of quality control measures in the monitoring of microplastic: a critical review. In *Environmental Pollutants and Bioavailability* (Vol. 35, Issue 1). https://doi.org/10.1080/26395940.2023.2203349

Gaston, E., Woo, M., Steele, C., Sukumaran, S., & Anderson, S. (2020). Microplastics Differ Between Indoor and Outdoor Air Masses: Insights from Multiple Microscopy Methodologies. *Applied Spectroscopy*, *74*(9), 1079–1098. https://doi.org/10.1177/0003702820920652

Galvão, L. S., Ferreira, R. R., Fernandes, E. M. S., Correia, C. A., Valera, T. S., dos Santos Rosa, D., & Wiebeck, H. (2023). Analysis of selective fluorescence for the characterization of microplastic fibers: Use of a Nile Red-based analytical method to compare between natural and synthetic fibers. *Journal of Hazardous Materials*, *443*(130217), 1–10. https://doi.org/10.1016/J.JHAZMAT.2022.130217

Glasgow City Council. (2021, March). *Briefing 1: Population in Glasgow (March 2021) - Glasgow City Council*. https://glasgow.gov.uk/index.aspx?articleid=26906 (Accessed: 25/08/21)

Google Earth. (2025). *Google Earth. Data Attribution 14/12/2015–01/01/2021. Glasgow. 55.818645818589026, -4.205149205698905*. https://mapsplatform.google.com/maps-products/earth/capabilities/?utm_source=google_earth&utm_medium=site&utm_campaign=next-25&utm_content=legacy

Geyer, R., Jambeck, J. R., & Law, K. L. (2017). Production, use, and fate of all plastics ever made. *Science Advances*, *3*(7). https://doi.org/10.1126/sciadv.1700782
Giardina, M., & Buffa, P. (2018). A new approach for modeling dry deposition velocity of particles. *Atmospheric Environment*, *180*, 11–22. https://doi.org/10.1016/J.ATMOSENV.2018.02.038

Gong, J., & Xie, P. (2020). Research progress in sources, analytical methods, eco-environmental effects, and control measures of microplastics. *Chemosphere*, *254*(126790), 1–10. https://doi.org/10.1016/j.chemosphere.2020.126790

Goßmann, I., Herzke, D., Held, A., Schulz, J., Nikiforov, V., Georgi, C., Evangeliou, N., Eckhardt, S., Gerdts, G., Wurl, O., & Scholz-Böttcher, B. M. (2023). Occurrence and backtracking of microplastic mass loads including tire wear particles in northern Atlantic air. *Nature Communications*, *14*(1). https://doi.org/10.1038/s41467-023-39340-5

Gouin, T. (2021). Addressing the importance of microplastic particles as vectors for long-range transport of chemical contaminants: perspective in relation to prioritizing research and regulatory actions. *Microplastics and Nanoplastics*, *1*(1). https://doi.org/10.1186/s43591-021-00016-w

Gregoris, E., Gallo, G., Rosso, B., Piazza, R., Corami, F., & Gambaro, A. (2023). Microplastics analysis: can we carry out a polymeric characterisation of atmospheric aerosol using direct inlet Py-GC/MS? *Journal of Analytical and Applied Pyrolysis*, *170*(105903), 1–8. https://doi.org/10.1016/j.jaap.2023.105903

Grythe, H., Kristiansen, N. I., Groot Zwaaftink, C. D., Eckhardt, S., Ström, J., Tunved, P., Krejci, R., & Stohl, A. (2017). A new aerosol wet removal scheme for the Lagrangian particle model FLEXPART v10. *Geoscientific Model Development*, *10*(4), 1447–1466. https://doi.org/10.5194/gmd-10-1447-2017

Haig, C. W., Mackay, W. G., Walker, J. T., & Williams, C. (2016). Bioaerosol sampling: Sampling mechanisms, bioefficiency and field studies. In *Journal of Hospital Infection* (Vol. 93, Issue 3). https://doi.org/10.1016/j.jhin.2016.03.017

Hailstone, J. (2022). it Return Schemes Are A Win-Win For The Environment, So Why Isn't Everyone Doing Them? *Forbes*. https://www.forbes.com/sites/jamiehailstone/2022/05/16/deposit-return-schemes-are-a-win-win-for-the-environment-so-why-isnt-everyone-doing-them/

Han, I., Lee, C., Belchez, C., Shipper, A. G., & Wiens, K. E. (2024). Microplastics in Urban Ambient Air: A Rapid Review of Active Sampling and Analytical Methods for Human Risk Assessment. *Environments*, *11*(11), 256. https://doi.org/10.3390/environments11110256

Hartmann, C., Lomako, I., Schachner, C., el Said, E., Abert, J., Satrapa, V., Kaiser, A.-M., Walch, H., & Köppel, S. (2024). Assessment of microplastics in human stool: A pilot study investigating the potential impact of diet-associated scenarios on oral microplastics exposure. *Science of The Total Environment*, *951*, 175825. https://doi.org/10.1016/j.scitotenv.2024.175825

Hasan Anik, A., Hossain, S., Alam, M., Binte Sultan, M., Hasnine, M. T., & Rahman, M. M. (2021). Microplastics pollution: A comprehensive review on the sources, fates, effects, and potential remediation. In *Environmental Nanotechnology, Monitoring and Management* (Vol. 16). https://doi.org/10.1016/j.enmm.2021.100530

Hebner, T. S., & Maurer-Jones, M. A. (2020). Characterizing microplastic size and morphology of photodegraded polymers placed in simulated moving water conditions. *Environmental Science: Processes and Impacts*, *22*(2). https://doi.org/10.1039/c9em00475k

Hernandez, L. M., Farner, J. M., Claveau-Mallet, D., Okshevsky, M., Jahandideh, H., Matthews, S., Roy, R., Yaylayan, V., & Tufenkji, N. (2023). Optimizing the Concentration of Nile Red for Screening of Microplastics in Drinking Water. *ACS ES&T*, 1029–1038. https://doi.org/10.1021/acsestwater.2c00503

HM Revenue & Customs. (2021). *Plastic Packaging Tax: steps to take*. HM Revenue & Customs. https://www.gov.uk/guidance/check-if-you-need-to-register-for-plastic-packaging-tax#:~:text=You%20will%20need%20to%20pay,tonne%20from%201%20April%202024

Horiba Scientific. (2023). *Raman Spectroscopy* . https://www.horiba.com/rus/scientific/technologies/raman-imaging-and-spectroscopy/raman-spectroscopy/. (Accessed 28th March 2025)

House of Commons. (2022). *The price of plastic: ending the toll of plastic waste Third Report of Session 2022–23*. Environment, Food and Rural Affairs Committee. 1-22.

Huang, Y., Liu, Q., Jia, W., Yan, C., & Wang, J. (2020a). Agricultural plastic mulching as a source of microplastics in the terrestrial environment. *Environmental Pollution*. https://doi.org/10.1016/j.envpol.2020.114096

Huang, Y., Qing, X., Wang, W., Han, G., & Wang, J. (2020b). Mini-review on current studies of airborne microplastics: Analytical methods, occurrence, sources, fate and potential risk to human beings. *TrAC - Trends in Analytical Chemistry*, *125*(115821), 1–8. https://doi.org/10.1016/j.trac.2020.115821

Huang, Y., Yang, Z., Wang, T., Sun, N., Duan, Z., Wigmosta, M., & Maurer, B. (2024). Quantifying the influence of size, shape, and density of microplastics on their transport modes: A modeling approach. *Marine Pollution Bulletin*, *203*(116461), 1–16. https://doi.org/10.1016/j.marpolbul.2024.116461

Ho, D., Liu, S., Wei, H., & Karthikeyan, K. G. (2024). The glowing potential of Nile red for microplastics Identification: Science and mechanism of fluorescence staining. *Microchemical Journal*, *197*(109708), 1–18. https://doi.org/10.1016/J.MICROC.2023.109708

Hofmann, A. E., Chimiak, L., Dallas, B., Griep-Raming, J., Juchelka, D., Makarov, A., Schwieters, J., & Eiler, J. M. (2020). Using Orbitrap mass spectrometry to assess the isotopic compositions of individual compounds in mixtures. *International Journal of Mass Spectrometry*, *457*. https://doi.org/10.1016/j.ijms.2020.116410

Hollis, D., McCarthy, M., Kendon, M., Legg, T., & Simpson, I. (2019). HadUK-Grid—A new UK dataset of gridded climate observations. *Geoscience Data Journal*, *6*(2), 151–159. https://doi.org/10.1002/gdj3.78

Hurrell, J. W., Holland, M. M., Gent, P. R., Ghan, S., Kay, J. E., Kushner, P. J., Lamarque, J. F., Large, W. G., Lawrence, D., Lindsay, K., Lipscomb, W. H., Long, M. C., Mahowald, N., Marsh, D. R., Neale, R. B., Rasch, P., Vavrus, S., Vertenstein, M., Bader, D., … Marshall, S. (2013). The community earth system model: A framework for collaborative research. *Bulletin of the American Meteorological Society*, *94*(9). https://doi.org/10.1175/BAMS-D-12-00121.1

Huppertsberg, S., & Knepper, T. P. (2018). Instrumental analysis of microplastics—benefits and challenges. *Analytical and Bioanalytical Chemistry*, *410*(25). https://doi.org/10.1007/s00216-018-1210-8

Iannilli, V., Corami, F., Grasso, P., Lecce, F., Buttinelli, M., & Setini, A. (2020). Plastic abundance and seasonal variation on the shorelines of three volcanic lakes in Central Italy: can amphipods help detect contamination? *Environmental Science and Pollution Research*, *27*(13). https://doi.org/10.1007/s11356-020-07954-7

IFSDG. (2021). *Economy - UK commercial centre; finance, retail & tourism - Glasgow*. International Financial Services District Glasgow . http://www.ifsdglasgow.co.uk/about-glasgow/economy- (Accessed: 25/08/21)

Illuminati, S., Notarstefano, V., Tinari, C., Fanelli, M., Girolametti, F., Ajdini, B., Scarchilli, C., Ciardini, V., Iaccarino, A., Giorgini, E., Annibaldi, A., & Truzzi, C. (2024). Microplastics in bulk atmospheric deposition along the coastal region of Victoria Land, Antarctica. *Science of The Total Environment*, 949(175221), 1–12. https://doi.org/10.1016/J.SCITOTENV.2024.175221

Iowa State University. (2025). *Physics of Nondestructive Evaluation: Materials and Processes - Polymer Structure*. Iowa State University: Center for Nondestructive Education. https://www.nde-ed.org/Physics/Materials/Structure/polymer.xhtml (Accessed: 27/08/25)

Irrgang, A. M., Bendixen, M., Farquharson, L. M., Baranskaya, A. V., Erikson, L. H., Gibbs, A. E., Ogorodov, S. A., Overduin, P. P., Lantuit, H., Grigoriev, M. N., & Jones, B. M. (2022). Drivers, dynamics and impacts of changing Arctic coasts. *Nature Reviews Earth & Environment 2022 3:1*, *3*(1), 39–54. https://doi.org/10.1038/s43017-021-00232-1

Isobe, A., Uchida, K., Tokai, T., & Iwasaki, S. (2015). East Asian seas: A hot spot of pelagic microplastics. *Marine Pollution Bulletin*, *101*(2), 618–623. https://doi.org/10.1016/J.MARPOLBUL.2015.10.042

Ivleva, N. P. (2021). Chemical Analysis of Microplastics and Nanoplastics: Challenges, Advanced Methods, and Perspectives. *Chemical Reviews*, *121*(19), 11886–11936. https://doi.org/10.1021/acs.chemrev.1c00178

Jarosz, K., Janus, R., Wądrzyk, M., Wilczyńska-Michalik, W., Natkański, P., & Michalik, M. (2022). Characteristic of Airborne Microplastic in the Atmospheric Deposition in Krakow (Southern Poland): A New Semi-Quantitative Approach by Means of the Py-Gc-Ms Technique. *SSRN Electronic Journal*. https://doi.org/10.2139/ssrn.4034510

Jemec Kokalj, A., Kuehnel, D., Puntar, B., Žgajnar Gotvajn, A., & Kalčikova, G. (2019). An exploratory ecotoxicity study of primary microplastics versus aged in natural waters and wastewaters. *Environmental Pollution*, *254 Part A*(112980), 1–8. https://doi.org/10.1016/j.envpol.2019.112980

Jenner, L. C., Sadofsky, L. R., Danopoulos, E., Chapman, E., White, D., Jenkins, R. L., & Rotchell, J. M. (2022). Outdoor Atmospheric Microplastics within the Humber Region (United Kingdom): Quantification and Chemical Characterisation of Deposited Particles Present. *Atmosphere*, *13*(2), 1–16. https://doi.org/10.3390/ATMOS13020265/S1

Jia, Q., Duan, Y., Han, X., Sun, X., Munyaneza, J., Ma, J., & Xiu, G. (2022). Atmospheric deposition of microplastics in the megalopolis (Shanghai) during rainy season: Characteristics, influence factors, and source. *Science of The Total Environment*, *847*(157609), 1–12. https://doi.org/10.1016/J.SCITOTENV.2022.157609

Jiang, F., Gao, C., Chan, A. W. H., Topping, D. O., Zhang, H., Li, W., Coe, H., Liu, X., Ching, J., & Zheng, Z. (2025). A Review of Atmospheric Micro/Nanoplastics: Insights into Source and Fate for Modelling Studies. *Current Pollution Reports 2025 11:1*, *11*(1), 53-. https://doi.org/10.1007/s40726-025-00375-5

Jin, N., Song, Y., Ma, R., Li, J., Li, G., & Zhang, D. (2022). Characterization and identification of microplastics using Raman spectroscopy coupled with multivariate analysis. *Analytica Chimica Acta*, *1197*(339519), 1–9. https://doi.org/10.1016/J.ACA.2022.339519

Jurkschat, L., Gill, A. J., Milner, R., Holzinger, R., Evangeliou, N., Eckhardt, S., & Materić, D. (2025). Using a citizen science approach to assess nanoplastics pollution in remote high-

altitude glaciers. *Scientific Reports*, *15*(1864), 1–9. https://doi.org/10.1038/s41598-024-84210-9

Kannankai, M. P., & Devipriya, S. P. (2024). Atmospheric microplastic deposition in a coastal city of India: The influence of a landfill source on monsoon winds. *Science of The Total Environment*, *908*(168235), 1–12. https://doi.org/10.1016/J.SCITOTENV.2023.168235

Käppler, A., Fischer, D., Oberbeckmann, S., Schernewski, G., Labrenz, M., Eichhorn, K.-J., & Voit, B. (2016). Analysis of environmental microplastics by vibrational microspectroscopy: FTIR, Raman or both? *Analytical and Bioanalytical Chemistry*, *408*(29), 8377–8391. https://doi.org/10.1007/s00216-016-9956-3

Kau, D., Materić, D., Holzinger, R., Baumann-Stanzer, K., Schauer, G., & Kasper-Giebl, A. (2024). Fine micro- and nanoplastics concentrations in particulate matter samples from the high alpine site Sonnblick, Austria. *Chemosphere*, *352*. https://doi.org/10.1016/j.chemosphere.2024.141410

Kaydi, N., Sahand Jorfi, ·, Takdastan, A., Neamatollah, ·, Haghighifard, J., Morteza, ·, & Khafaie, A. (2024.). Source identification and apportionment of ambient air microplastics: a systematic review. *Discover Applied Sciences*, *7*, 41. https://doi.org/10.1007/s42452-024-06422-y

Kings Bay. (2021. Community Operation. Retrieved December 10, 2024 from *https://kingsbay.no/community-operation/*

Kings Bay AS. (2021b). *Marine Lab & Veksthuset.* Retrieved December 10, 2024, from https://kingsbay.no/

Knobloch, E., Ruffell, H., Aves, A., Pantos, O., Gaw, S., & Revell, L. E. (2021). Comparison of Deposition Sampling Methods to Collect Airborne Microplastics in Christchurch, New Zealand. *Water, Air, and Soil Pollution*, *232*(4), 1–10. https://doi.org/10.1007/S11270-021-05080-9/TABLES/2

Klein, M., Bechtel, B., Brecht, T., & Fischer, E. K. (2023). Spatial distribution of atmospheric microplastics in bulk-deposition of urban and rural environments – A one-year follow-up study in northern Germany. *Science of the Total Environment*, *901*. https://doi.org/10.1016/j.scitotenv.2023.165923

Klein, A., Ravetta, F., Thomas, J. L., Ancellet, G., Augustin, P., Wilson, R., Dieudonné, E., Fourmentin, M., Delbarre, H., & Pelon, J. (2019). Influence of vertical mixing and night time transport on surface ozone variability in the morning in Paris and the surrounding region. *Atmospheric Environment*, *197*, 92–102. https://doi.org/10.1016/j.atmosenv.2018.10.009

Knobloch, E., Ruffell, H., Aves, A., Pantos, O., Gaw, S., & Revell, L. E. (2021). Comparison of Deposition Sampling Methods to Collect Airborne Microplastics in Christchurch, New Zealand. *Water, Air, and Soil Pollution*, *232*(4), 1–10. https://doi.org/10.1007/S11270-021-05080-9/TABLES/2

Kutralam-Muniasamy, G., Shruti, V. C., & Pérez-Guevara, F. (2023). Citizen involvement in reducing end-of-life product waste in Mexico City. *Sustainable Production and Consumption*, *41*. https://doi.org/10.1016/j.spc.2023.08.010

Kye, H., Kim, J., Ju, S., Lee, J., Lim, C., & Yoon, Y. (2023). Microplastics in water systems: A review of their impacts on the environment and their potential hazards. *Heliyon*, 9(3), 1–31. https://doi.org/10.1016/J.HELIYON.2023.E14359

Lee, S.-Y., An, J., & Kwon, J.-H. (2023). Sequential quantification of number and mass of microplastics in municipal wastewater using Fourier-transform infrared spectroscopy and pyrolysis gas chromatography-mass spectrometry. *Environmental Pollution*, *336*, 122452. https://doi.org/10.1016/j.envpol.2023.122452

Lenz, R., Enders, K., Stedmon, C. A., MacKenzie, D. M. A., & Nielsen, T. G. (2015). A critical assessment of visual identification of marine microplastic using Raman spectroscopy for analysis improvement. *Marine Pollution Bulletin*. https://doi.org/10.1016/j.marpolbul.2015.09.026

Leslie, H. A., van Velzen, M. J. M., Brandsma, S. H., Vethaak, A. D., Garcia-Vallejo, J. J., & Lamoree, M. H. (2022). Discovery and quantification of plastic particle pollution in human blood. *Environment International*, *163*(107199), 1–8. https://doi.org/10.1016/J.ENVINT.2022.107199

Levermore, J. M., Smith, T. E. L., Kelly, F. J., & Wright, S. L. (2020). Detection of Microplastics in Ambient Particulate Matter Using Raman Spectral Imaging and Chemometric Analysis. *Analytical Chemistry*, *92*(13). https://doi.org/10.1021/acs.analchem.9b05445

Li, Y., Shao, L., Wang, W., Zhang, M., Feng, X., Li, W., & Zhang, D. (2020). Airborne fiber particles: Types, size and concentration observed in Beijing. *Science of The Total Environment,* 705(135967), 1–9. https://doi.org/10.1016/J.SCITOTENV.2019.135967

Li, K., Du, L., Qin, C., Bolan, N., Wang, H., & Wang, H. (2024). Microplastic pollution as an environmental risk exacerbating the greenhouse effect and climate change: a review. In *Carbon Research* (Vol. 3, Issue 1). https://doi.org/10.1007/s44246-023-00097-7

Liao, Z., Ji, X., Yuan, M., Baoqiang, L., Huang, W., Zhu, X., Fang, M., Wang, Q., Wang, Q., Dahlgren, R., & Shang, X. (2021). Airborne microplastics in indoor and outdoor environments of a coastal city in Eastern China. *Journal of Hazardous Materials*, *417*(126007), 1–9. https://doi.org/10.1016/J.JHAZMAT.2021.126007

Liddle, S. C. R., Atherall, C. A., Chapman, E., Watkins, M., D. J. Calaminus, S., & Rotchell, J. M. (2024). Microplastics in human blood: Polymer types, concentrations and characterisation using μFTIR. *Environment International*, *188*, 108751. https://doi.org/10.1016/j.envint.2024.108751

Liu, K., Wang, X., Wei, N., Song, Z., & Li, D. (2019). Accurate quantification and transport estimation of suspended atmospheric microplastics in megacities: Implications for human health. *Environment International*, *132*(105127), 1–10. https://doi.org/10.1016/j.envint.2019.105127

Liu, K., Wang, X., Fang, T., Xu, P., Zhu, L., & Li, D. (2019a). Source and potential risk assessment of suspended atmospheric microplastics in Shanghai. *Science of the Total Environment*, *675*. https://doi.org/10.1016/j.scitotenv.2019.04.110

Liu, K., Wang, X., Wei, N., Song, Z., & Li, D. (2019b). Accurate quantification and transport estimation of suspended atmospheric microplastics in megacities: Implications for human health. *Environment International*, *132*, 1-1-. https://doi.org/10.1016/j.envint.2019.105127

Liu, K., Wu, T., Wang, X., Song, Z., Zong, C., Wei, N., & Li, D. (2019c). Consistent Transport of Terrestrial Microplastics to the Ocean through Atmosphere. *Environmental Science and Technology*, *53*(18), 10612–10619. https://doi.org/10.1021/acs.est.9b03427

Liu, P., Shao, L., Li, Y., Jones, T., Cao, Y., Yang, C. X., Zhang, M., Santosh, M., Feng, X., & BéruBé, K. (2022). Microplastic atmospheric dustfall pollution in urban environment: Evidence from the types, distribution, and probable sources in Beijing, China. *Science of The Total Environment*, *838*(155989), 1–11. https://doi.org/10.1016/J.SCITOTENV.2022.155989

Liu, P., Shao, L., Zhang, Y., Silvonen, V., Oswin, H., Cao, Y., Guo, Z., Ma, X., & Morawska, L. (2024). Comparative study on physicochemical characteristics of atmospheric microplastics in winter in inland and coastal megacities: A case of Beijing and Shanghai, China. *Science of The Total Environment*, *912*(169308), 1–11. https://doi.org/10.1016/J.SCITOTENV.2023.169308

Liu, Y., Nie, Z., Meng, Y., Liu, G., Chen, Y., & Chai, G. (2025). Influence of meteorological conditions on atmospheric microplastic transport and deposition. *Environmental Research*, *265*, 120460. https://doi.org/10.1016/j.envres.2024.120460

Logvina, Y., Moreira, D. S., Santos, R. P. M., Neves, I. F., Ribeiro, H., Pinto da Silva, L., & Esteves da Silva, J. (2024). Microplastic Aerosol Contamination in Porto (Portugal). *Microplastics*, *3*(4), 696–716. https://doi.org/10.3390/microplastics3040043

Luo, X., Wang, Z., Yang, L., Gao, T., & Zhang, Y. (2022). A review of analytical methods and models used in atmospheric microplastic research. In *Science of the Total Environment* (Vol. 828). https://doi.org/10.1016/j.scitotenv.2022.154487

Luo, D., Chu, X., Wu, Y., Wang, Z., Liao, Z., Ji, X., Ju, J., Yang, B., Chen, Z., Dahlgren, R., Zhang, M., & Shang, X. (2024a). Micro- and nano-plastics in the atmosphere: A review of occurrence, properties and human health risks. *Journal of Hazardous Materials*, *465*(133412), 1–22. https://doi.org/10.1016/J.JHAZMAT.2023.133412

Luo, D., Wang, Z., Liao, Z., Chen, G., Ji, X., Sang, Y., Qu, L., Chen, Z., Wang, Z., Dahlgren, R. A., Zhang, M., & Shang, X. (2024b). Airborne microplastics in urban, rural and wildland environments on the Tibetan Plateau. *Journal of Hazardous Materials*, *465*(133177), 1–8. https://doi.org/10.1016/J.JHAZMAT.2023.133177

Lv, L., Qu, J., Yu, Z., Chen, D., Zhou, C., Hong, P., Sun, S., & Li, C. (2019). A simple method for detecting and quantifying microplastics utilizing fluorescent dyes - Safranine T, fluorescein isophosphate, Nile red based on thermal expansion and contraction property. *Environmental Pollution*, *255*, 113283. https://doi.org/10.1016/j.envpol.2019.113283

MacDonald, A., Allen, D., & João, E. (2021). A Pilot Assessment of a Plastic Free Community Initiative, Respective Community Actions and Residents Behaviour. *Microplastics*, *1*(1), 47–66. https://doi.org/10.3390/MICROPLASTICS1010004

Maes, T., Jessop, R., Wellner, N., Haupt, K., & Mayes, A. G. (2017). A rapid-screening approach to detect and quantify microplastics based on fluorescent tagging with Nile Red. *Scientific Reports*, *7*(1), 1–10. https://doi.org/10.1038/srep44501

Mahon, A. M., O'Connell, B., Healy, M. G., O'Connor, I., Officer, R., Nash, R., & Morrison, L. (2017). Microplastics in sewage sludge: Effects of treatment. *Environmental Science and Technology*, *51*(2), 810–818. https://doi.org/10.1021/acs.est.6b04048

Main, D. (2024, August 21). Microplastics are infiltrating brain tissue, studies show: 'There's nowhere left untouched.' *The Guardian*. Online at : https://www.theguardian.com/environment/article/2024/aug/21/microplastics-brain-pollution-health . Accessed: 15/11/24.

Monikh, A, F., Materić, D., Valsami-Jones, E., Grossart, H. P., Altmann, K., Holzinger, R., Lynch, I., Stubenrauch, J., & Peijnenburg, W. (2025). Challenges in studying microplastics in human brain. In *Nature Medicine* (Vol. 31, Issue 12). https://doi.org/10.1038/s41591-025-04045-3

Mao, X., Xu, Y., Cheng, Z., Yang, Y., Guan, Z., Jiang, L., & Tang, K. (2022). The impact of microplastic pollution on ecological environment: a review. In *Frontiers in Bioscience - Landmark* (Vol. 27, Issue 2). https://doi.org/10.31083/j.fbl2702046

Marine Lab & Veksthuset » Kings Bay AS. (n.d.). Retrieved April 11, 2024. https://kingsbay.no/marine-lab-veksthuset/

Martina, M., & Trini Castelli, S. (2023). Modelling the Potential Long-Range Dispersion of Atmospheric Microplastics Reaching a Remote Site. *Atmospheric Environment*, *312*(120044), 1–16. https://doi.org/10.1016/J.ATMOSENV.2023.120044

Materić, D. ; Ø. N. H. ; M. S. ; H. R. (2022a). TD-PTR-MS for nanoplastics research - high sensitivity and big challenges. *EGU22, the 24th EGU General Assembly, Held 23-27 May, 2022 in Vienna, Austria and Online at https://egu22.eu/, id.EGU22-12098https://egu22.eu/, id.EGU22-12098.*

Materić, D., Holzinger, R., & Niemann, H. (2022b). Nanoplastics and ultrafine microplastic in the Dutch Wadden Sea – The hidden plastics debris? *Science of the Total Environment*, *846*. https://doi.org/10.1016/j.scitotenv.2022.157371

Materić, D., Kasper-Giebl, A., Kau, D., Anten, M., Greilinger, M., Ludewig, E., van Sebille, E., Röckmann, T., & Holzinger, R. (2020). Micro-and Nanoplastics in Alpine Snow: A New Method for Chemical Identification and (Semi)Quantification in the Nanogram Range. *Environmental Science and Technology*, *54*(4). https://doi.org/10.1021/acs.est.9b07540

Maturilli, Marion **(2022a):** Continuous meteorological observations at station Ny-Ålesund (2022-06) [dataset]. *Alfred Wegener Institute - Research Unit Potsdam*, *PANGAEA*, https://doi.org/10.1594/PANGAEA.937247,

Maturilli, Marion (**2022b):** Continuous meteorological observations at station Ny-Ålesund (2022-05) [dataset]. *Alfred Wegener Institute - Research Unit Potsdam*, *PANGAEA*, https://doi.org/10.1594/PANGAEA.937246,

Mayer, P. M., Moran, K. D., Miller, E. L., Brander, S. M., Harper, S., Garcia-Jaramillo, M., Carrasco-Navarro, V., Ho, K. T., Burgess, R. M., Thornton Hampton, L. M., Granek, E. F., McCauley, M., McIntyre, J. K., Kolodziej, E. P., Hu, X., Williams, A. J., Beckingham, B. A., Jackson, M. E., Sanders-Smith, R. D., … Mendez, M. (2024). Where the rubber meets the road: Emerging environmental impacts of tire wear particles and their chemical cocktails. *Science of The Total Environment*, *927*, 171153. https://doi.org/10.1016/j.scitotenv.2024.171153

Mbachu, O., Jenkins, G., Pratt, C., & Kaparaju, P. (2020). A New Contaminant Superhighway? A Review of Sources, Measurement Techniques and Fate of Atmospheric Microplastics. In *Water, Air, and Soil Pollution* (Vol. 231, Issue 2). https://doi.org/10.1007/s11270-020-4459-4

McCammon, C. S., Woebkenberg, M. L., & Ashley, K. (2016). General Considerations for Sampling Airborne Contaminants. In *NOISH Manual of Analytical Methods (NMAM), 5th Edition* (5th ed., pp. 1–23). Centre for Disease Control and Prevention; National Institute for Occupational Safety and Health.

Menges, F. (2022). *Spectragryph - optical spectroscopy software* (Version 1.2.15).

Mizuguchi, H., Takeda, H., Kinoshita, K., Takeuchi, M., Takayanagi, T., Teramae, N., Pipkin, W., Matsui, K., Watanabe, A., & Watanabe, C. (2023). Direct analysis of airborne microplastics collected on quartz filters by pyrolysis-gas chromatography/mass spectrometry. *Journal of Analytical and Applied Pyrolysis*, *171*. https://doi.org/10.1016/j.jaap.2023.105946

Munno, K., Lusher, A. L., Minor, E. C., Gray, A., Ho, K., Hankett, J., T Lee, C. F., Primpke, S., McNeish, R. E., Wong, C. S., & Rochman, C. (2023). Patterns of microparticles in blank samples: A study to inform best practices for microplastic analysis. *Chemosphere*, *333*. https://doi.org/10.1016/j.chemosphere.2023.138883

Munro Instruments. (2024). *Powered Portable Air Sampler - Munro Instruments*. https://www.munroinstruments.com/product/l10b-battery-powered-portable-air-sampler-non-rechargeable/

Morioka, T., Tanaka, S., Yamada, Y., Yukioka, S., & Aiba, F. (2023). Quantification of microplastic by particle size down to 1.1 µm in surface road dust in an urban city, Japan. *Environmental Pollution*, *334*. https://doi.org/10.1016/j.envpol.2023.122198

Mutshekwa, T., Mulaudzi, F., Maiyana, V. P., Mofu, L., Munyai, L. F., & Murungweni, F. M. (2025). Atmospheric deposition of microplastics in urban, rural, forest environments: A case study of Thulamela Local Municipality. *PLOS ONE*, *20*(3), e0313840. https://doi.org/10.1371/journal.pone.0313840

Na, S. H., Kim, M. J., Kim, J., Batool, R., Cho, K., Chung, J., Lee, S., & Kim, E. J. (2024). Fate and potential risks of microplastic fibers and fragments in water and wastewater treatment processes. *Journal of Hazardous Materials*, *463*(132938), 1–10. https://doi.org/10.1016/J.JHAZMAT.2023.132938

Nafea, T. H., Chan, F. K. S., Xu, Y., Wang, C., Wang, X., Zhao, W., Ji, D., Xiao, H., & He, J. (2024). Microplastics Aloft: A comprehensive exploration of sources, transport, variations, interactions and their implications on human health in the atmospheric realm. *Earth-Science Reviews*, *255*(104864), 1–17. https://doi.org/10.1016/J.EARSCIREV.2024.104864

Nava, V., Frezzotti, M. L., & Leoni, B. (2021). Raman Spectroscopy for the Analysis of Microplastics in Aquatic Systems. In Applied Spectroscopy (Vol. 75, Issue 11). https://doi.org/10.1177/00037028211043119

Nazarenko, Y., Fournier, S., Kurien, U., Rangel-Alvarado, R. B., Nepotchatykh, O., Seers, P., & Ariya, P. A. (2017). Role of snow in the fate of gaseous and particulate exhaust pollutants from gasoline-powered vehicles. *Environmental Pollution*, *223*, 665–675. https://doi.org/10.1016/j.envpol.2017.01.082

Nel, H. A., Chetwynd, A. J., Kelleher, L., Lynch, I., Mansfield, I., Margenat, H., Onoja, S., Goldberg Oppenheimer, P., Sambrook Smith, G. H., & Krause, S. (2021). Detection limits are central to improve reporting standards when using Nile red for microplastic quantification. *Chemosphere*, *263*, 127953. https://doi.org/10.1016/j.chemosphere.2020.127953

Nihart, A. J., Garcia, M. A., el Hayek, E., Liu, R., Olewine, M., Kingston, J. D., Castillo, E. F., Gullapalli, R. R., Howard, T., Bleske, B., Scott, J., Gonzalez-Estrella, J., Gross, J. M., Spilde, M., Adolphi, N. L., Gallego, D. F., Jarrell, H. S., Dvorscak, G., Zuluaga-Ruiz, M. E., … Campen, M. J. (2025). Bioaccumulation of microplastics in decedent human brains. *Nature Medicine*, *31*(4), 1114–1119. https://doi.org/10.1038/s41591-024-03453-1

NILU: Ecomeasure. (2022). *Product : Atmospheric microplastic collector - iNNOVATION NILU*. Ecomeasure. https://ecomesure.com/en/scientific-instruments/atmospheric-microplastic-collector-innovation-nilu

NOAA. (2024a). *HYSPLIT Model*. https://www.ready.noaa.gov/HYSPLIT.php

NOAA. (2024b). *HYSPLIT Limitations*. https://www.ready.noaa.gov/hypub/limitations.html

National Oceanic and Atmospheric Administration (NOAA). (2021). *Global Data Assimilation System (GDAS) - Nov-Dec'21*. National Center for Environmental Prediction (NCEP). https://www.ncei.noaa.gov/access/metadata/landing-page/bin/iso?id=gov.noaa.ncdc:C00379

Nøklebye, E., Adam, H. N., Roy-Basu, A., Bharat, G. K., & Steindal, E. H. (2023). Plastic bans in India – Addressing the socio-economic and environmental complexities. *Environmental Science and Policy*, *139*. https://doi.org/10.1016/j.envsci.2022.11.005

Norwegian Centre for Climate Services. (2021). Weather data and statistics. Klima Services Center. https://klimaservicesenter.no/kss/om-oss/nccs?locale=en#weather-data-and-statistics (Accessed: 10/02/2025)

Norwegian Centre for Climate Services. (2025). *Station information*. https://seklima.met.no/stations/ (Accessed: 10/02/2025)

Ny-Alesund, Google Maps. (2022). https://www.google.com/maps/place/Ny-Ålesund+9173,+Svalbard+and+Jan+Mayen/@74.4797502,-3.704962,4z/data=!4m5!3m4!1s0x4582b08bd904d97f:0x1ddeb512ac13a0dc!8m2!3d78.9235381!4d11.9098952

Obbard, R. W., Sadri, S., Wong, Y. Q., Khitun, A. A., Baker, I., & Thompson, R. C. (2014). Global warming releases microplastic legacy frozen in Arctic Sea ice. *Earth's Future*, 2(6), 315–320. https://doi.org/10.1002/2014EF000240

O'Brien, S., Rauert, C., Ribeiro, F., Okoffo, E. D., Burrows, S. D., O'Brien, J. W., Wang, X., Wright, S. L., & Thomas, K. v. (2023). There's something in the air: A review of sources, prevalence and behaviour of microplastics in the atmosphere. In *Science of the Total Environment* (Vol. 874). https://doi.org/10.1016/j.scitotenv.2023.162193

OECD (2022), Global Plastics Outlook: Economic Drivers, Environmental Impacts and Policy Options, OECD Publishing, Paris, https://doi.org/10.1787/de747aef-en.

Okoffo, E. D., O'Brien, S., O'Brien, J. W., Tscharke, B. J., Rauert, C., Rødland, E. S., Ribeiro, F., Burrows, S. D., Toapanta, T., Mueller, J. F., & Thomas, K. v. (2022). Does size matter? Quantification of plastics associated with size fractionated biosolids. *Science of The Total Environment*, *811*, 152382. https://doi.org/10.1016/j.scitotenv.2021.152382

Okoffo, E. D., Tscharke, B. J., O'Brien, J. W., O'Brien, S., Ribeiro, F., Burrows, S. D., Choi, P. M., Wang, X., Mueller, J. F., & Thomas, K. v. (2020). Release of Plastics to Australian Land from Biosolids End-Use. *Environmental Science and Technology*, *54*(23), 15132–15141. https://doi.org/10.1021/acs.est.0c05867

Panko, J. M., Hitchcock, K. M., Fuller, G. W., & Green, D. (2019). Evaluation of tire wear contribution to PM2.5 in urban environments. *Atmosphere*, *10*(2), 1–14. https://doi.org/10.3390/ATMOS10020099

Parashar, N., & Hait, S. (2023). Plastic rain-Atmospheric microplastics deposition in urban and peri-urban areas of Patna City, Bihar, India: Distribution, characteristics, transport, and source analysis. *Journal of Hazardous Materials*, *458*(13183), 1–15. https://doi.org/10.1016/j.jhazmat.2023.131883

Park, S.-J., Lugon, L., Jacquot, O., Kim, Y., Baudic, A., D'Anna, B., di Antonio, L., di Biagio, C., Dugay, F., Favez, O., Ghersi, V., Gratien, A., Kammer, J., Petit, J.-E., Sanchez, O., Valari, M., Vigneron, J., & Sartelet, K. (2025). Population exposure to outdoor NO_2, black carbon, and ultrafine and fine particles over Paris with multi-scale modelling down to the street scale. *Atmospheric Chemistry and Physics*, *25*(6), 3363–3387. https://doi.org/10.5194/acp-25-3363-2025

Pérez-Guevara, F., Roy, P. D., Kutralam-Muniasamy, G., & Shruti, V. C. (2022). Coverage of microplastic data underreporting and progress toward standardization. In *Science of the Total Environment* (Vol. 829). https://doi.org/10.1016/j.scitotenv.2022.154727

Peller, J. R., Eberhardt, L., Clark, R., Nelson, C., Kostelnik, E., & Iceman, C. (2019). Tracking the distribution of microfiber pollution in a southern Lake Michigan watershed through the analysis of water, sediment and air. *Environmental Science: Processes and Impacts*, *21*(9), 1549–1559. https://doi.org/10.1039/c9em00193j

Petersen, F., & Hubbart, J. A. (2021). The occurrence and transport of microplastics: The state of the science. In *Science of the Total Environment* (Vol. 758). https://doi.org/10.1016/j.scitotenv.2020.143936

Pfeiffer, F., & Fischer, E. K. (2020). Various Digestion Protocols Within Microplastic Sample Processing—Evaluating the Resistance of Different Synthetic Polymers and the Efficiency of Biogenic Organic Matter Destruction. *Frontiers in Environmental Science*, *8*. https://doi.org/10.3389/fenvs.2020.572424

Phan, S., Padilla-Gamiño, J. L., & Luscombe, C. K. (2022). The effect of weathering environments on microplastic chemical identification with Raman and IR spectroscopy: Part I. polyethylene and polypropylene. *Polymer Testing*, *116*, 107752. https://doi.org/10.1016/j.polymertesting.2022.107752

Picó, Y., & Barceló, D. (2020). Pyrolysis gas chromatography-mass spectrometry in environmental analysis: Focus on organic matter and microplastics. In *TrAC - Trends in Analytical Chemistry* (Vol. 130). https://doi.org/10.1016/j.trac.2020.115964

Pironti, C., Ricciardi, M., Motta, O., Miele, Y., Proto, A., & Montano, L. (2021). Microplastics in the environment: Intake through the food web, human exposure and toxicological effects. In *Toxics* (Vol. 9, Issue 9). https://doi.org/10.3390/toxics9090224

Pironti, C., Notarstefano, V., Ricciardi, M., Motta, O., Giorgini, E., & Montano, L. (2022). First Evidence of Microplastics in Human Urine, a Preliminary Study of Intake in the Human Body. *Toxics*, *11*(1), 40. https://doi.org/10.3390/toxics11010040

Prata, J. C., Reis, V., da Costa, J. P., Mouneyrac, C., Duarte, A. C., & Rocha-Santos, T. (2021a). Contamination issues as a challenge in quality control and quality assurance in microplastics analytics. *Journal of Hazardous Materials*, *403*. https://doi.org/10.1016/j.jhazmat.2020.123660

Prata, J. C., da Costa, J. P., Fernandes, A. J. S., da Costa, F. M., Duarte, A. C., & Rocha-Santos, T. (2021b). Selection of microplastics by Nile Red staining increases environmental sample throughput by micro-Raman spectroscopy. *Science of The Total Environment*, *783*(146979), 1–7. https://doi.org/10.1016/J.SCITOTENV.2021.146979

Prata, J. C., Reis, V., Matos, J. T. V., da Costa, J. P., Duarte, A. C., & Rocha-Santos, T. (2019). A new approach for routine quantification of microplastics using Nile Red and automated software (MP-VAT). *Science of the Total Environment*, *690*. https://doi.org/10.1016/j.scitotenv.2019.07.060

Primpke, S., Christiansen, S. H., Cowger, W., de Frond, H., Deshpande, A., Fischer, M., Holland, E. B., Meyns, M., O'Donnell, B. A., Ossmann, B. E., Pittroff, M., Sarau, G., Scholz-Böttcher, B. M., & Wiggin, K. J. (2020). Critical Assessment of Analytical Methods for the Harmonized and Cost-Efficient Analysis of Microplastics. *Applied Spectroscopy*, *74*(9), 1012–1047. https://doi.org/10.1177/0003702820921465

Purwiyanto, A. I. S., Prartono, T., Riani, E., Naulita, Y., Cordova, M. R., & Koropitan, A. F. (2022). The deposition of atmospheric microplastics in Jakarta-Indonesia: The coastal urban area. *Marine Pollution Bulletin*, *174*, 113195. https://doi.org/10.1016/j.marpolbul.2021.113195

Ramasamy, E. V., Sruthy, S., Harit, A. K., Mohan, M., & Binish, M. B. (2021). Microplastic pollution in the surface sediment of Kongsfjorden, Svalbard, Arctic. *Marine Pollution Bulletin*, *173*(112986), 1–5. https://doi.org/10.1016/j.marpolbul.2021.112986

Rantanen, M., Karpechko, A. Y., Lipponen, A., Nordling, K., Hyvärinen, O., Ruosteenoja, K., Vihma, T., & Laaksonen, A. (2022). The Arctic has warmed nearly four times faster than the globe since 1979. Communications Earth & Environment 2022 3:1, 3(1), 1–10. https://doi.org/10.1038/s43247-022-00498-3

Ragusa, A., Svelato, A., Santacroce, C., Catalano, P., Notarstefano, V., Carnevali, O., Papa, F., Rongioletti, M. C. A., Baiocco, F., Draghi, S., D'Amore, E., Rinaldo, D., Matta, M., & Giorgini, E. (2021). Plasticenta: First evidence of microplastics in human placenta. *Environment International*, *146*, 1–8. https://doi.org/10.1016/J.ENVINT.2020.106274

Revell, L. E., Kuma, P., le Ru, E. C., Somerville, Woy. R. C., & Gaw, S. (2021). Direct radiative effects of airborne microplastics. *Nature*, *598*(7881), 462–467. https://doi.org/10.1038/s41586-021-03864-x

Rivers, M. L., Gwinnett, C., & Woodall, L. C. (2019). Quantification is more than counting: Actions required to accurately quantify and report isolated marine microplastics. *Marine Pollution Bulletin*, 139, 100–104. https://doi.org/10.1016/J.MARPOLBUL.2018.12.024

Rolph, G., Stein, A., & Stunder, B. (2017). Real-time Environmental Applications and Display sYstem: READY. *Environmental Modelling & Software*, *95*, 210–228. https://doi.org/10.1016/j.envsoft.2017.06.025

Roy, P., Mohanty, A. K., & Misra, M. (2022). Microplastics in ecosystems: their implications and mitigation pathways. *Environmental Science: Advances*, *1*(1). https://doi.org/10.1039/d1va00012h

Rosso, B., Scoto, F., Hallanger, I. G., Larose, C., Gallet, J. C., Spolaor, A., Bravo, B., Barbante, C., Gambaro, A., & Corami, F. (2024). Characteristics and quantification of small microplastics (<100 µm) in seasonal Svalbard snow on glaciers and lands. *Journal of Hazardous Materials*, 467(133723), 1–10. https://doi.org/10.1016/J.JHAZMAT.2024.133723

Rumin, J., Bonnefond, H., Saint-Jean, B., Rouxel, C., Sciandra, A., Bernard, O., Cadoret, J.-P., & Bougaran, G. (2015). The use of fluorescent Nile red and BODIPY for lipid measurement in microalgae. *Biotechnology for Biofuels*, *8*(1), 42. https://doi.org/10.1186/s13068-015-0220-4

Ryan, A. C., Allen, D., Allen, S., Maselli, V., LeBlanc, A., Kelleher, L., Krause, S., Walker, T. R., & Cohen, M. (2023). Transport and deposition of ocean-sourced microplastic particles by a North Atlantic hurricane. *Communications Earth and Environment*, *4*(1). https://doi.org/10.1038/s43247-023-01115-7

Samson. Perry J. (1988). Atmospheric Transport and Dispersion of Air Pollutants Associated with Vehicular Emissions. In A. Y. D. Watson, R. R. Bates, & D. Kennedy (Eds.), *Air Pollution, the Automobile, and Public Health* (pp. 77–99). National Academy Press.

Savitzky, Abraham., & Golay, M. J. E. (1964). Smoothing and Differentiation of Data by Simplified Least Squares Procedures. *Analytical Chemistry*, *36*(8), 1627–1639. https://doi.org/10.1021/ac60214a047

Schindelin, J., Arganda-Carreras, I., Frise, E., Kaynig, V., Longair, M., Pietzsch, T., Preibisch, S., Rueden, C., Saalfeld, S., Schmid, B., Tinevez, J.-Y., White, D. J., Hartenstein, V., Eliceiri, K., Tomancak, P., & Cardona, A. (2012). Fiji: an open-source platform for biological-image analysis. *Nature Methods*, *9*(7), 676–682. https://doi.org/10.1038/nmeth.2019

Schmid, C., Cozzarini, L., & Zambello, E. (2021). Microplastic's story. In *Marine Pollution Bulletin* (Vol. 162). https://doi.org/10.1016/j.marpolbul.2020.111820

Schneider, C. A., Rasband, W. S., & Eliceiri, K. W. (2012). NIH Image to ImageJ: 25 years of image analysis. *Nature Methods* , *9*(7), 671–675. https://doi.org/10.1038/nmeth.2089

Senathirajah, K., Attwood, S., Bhagwat, G., Carbery, M., Wilson, S., & Palanisami, T. (2021). Estimation of the mass of microplastics ingested – A pivotal first step towards human health risk assessment. *Journal of Hazardous Materials*, *404*(Part B. 124004), 1–15. https://doi.org/10.1016/j.jhazmat.2020.124004

Scottish Air Quality. (2021). *Air Quality in Scotland Data & Maps - Cambuslang and Rutherglen Nov-Dec'21*. https://www.scottishairquality.scot/data

Sharaf Din, K., Khokhar, M. F., Butt, S. I., Qadir, A., & Younas, F. (2024). Exploration of microplastic concentration in indoor and outdoor air samples: Morphological, polymeric, and elemental analysis. *Science of the Total Environment*, *908*. https://doi.org/10.1016/j.scitotenv.2023.168398

Sharma, S., Sharma, V., & Chatterjee, S. (2023). Contribution of plastic and microplastic to global climate change and their conjoining impacts on the environment - A review. In *Science of the Total Environment* (Vol. 875). https://doi.org/10.1016/j.scitotenv.2023.162627

Shim, W. J., Song, Y. K., Hong, S. H., & Jang, M. (2016). Identification and quantification of microplastics using Nile Red staining. *Marine Pollution Bulletin*, *113*(1–2), 469–476. https://doi.org/10.1016/J.MARPOLBUL.2016.10.049

Shruti, V. C., Kutralam-Muniasamy, G., Pérez-Guevara, F., Roy, P. D., & Martínez, I. E. (2022a). Occurrence and characteristics of atmospheric microplastics in Mexico City. *Science of The Total Environment*, *847*(157601), 1–12. https://doi.org/10.1016/J.SCITOTENV.2022.157601

Shruti, V. C., Pérez-Guevara, F., Roy, P. D., & Kutralam-Muniasamy, G. (2022b). Analyzing microplastics with Nile Red: Emerging trends, challenges, and prospects. *Journal of Hazardous Materials*, *423*(127171), 1–19. https://doi.org/10.1016/J.JHAZMAT.2021.127171

Sigma Aldrich. (2024). *Nile Red Material Safety Sheet*. Sigma Aldrich . Sigma Aldrich. Online at: https://www.sigmaaldrich.com/GB/en/product/sigma/19123?srsltid=AfmBOooHoDTWS48zY2KZuXP7VlYcZu-W6hQbNZZ7k5AAqUbbFFExaB7R. Accessed: 01/04/25

Sloat, S. (2024). How to Minimize Your Exposure to Microplastics. *The New York Times*. Online at: https://www.nytimes.com/2024/06/07/well/microplastics-health.html . Accessed: 15/11/24.

Smith, M., Love, D. C., Rochman, C. M., & Neff, R. A. (2018). Microplastics in Seafood and the Implications for Human Health. In *Current environmental health reports* (Vol. 5, Issue 3). https://doi.org/10.1007/s40572-018-0206-z

Smyth, G. K. (2014). Polynomial Approximation. In *Wiley StatsRef: Statistics Reference Online*. https://doi.org/10.1002/9781118445112.stat05031

South Lanarkshire Council. (2023). *South Lanarkshire State of the Environment Report 2023*. https://www.southlanarkshire.gov.uk/downloads/download/1169/south_lanarkshire_state_of_the_environment_report_2023

Speed, M. (2024, November 24). Countries remain at loggerheads as UN plastics treaty talks resume. *Financial Times*. https://www.ft.com/content/7f9b3b55-0090-4d71-a78e-853d30c176fe (Online; Accessed 25/11/24).

Speed, D. E. (2021). Environmental aspects of planarization processes. In *Advances in Chemical Mechanical Planarization (CMP)* (pp. 257–320). Elsevier. https://doi.org/10.1016/B978-0-12-821791-7.00002-2

Stallard, E. P. M. (2025). Global plastic talks collapse as countries remain deeply divided. *BBC News*. https://www.bbc.co.uk/news/articles/cvgpddpldleo

Stanton, T., Johnson, M., Nathanail, P., Gomes, R. L., Needham, T., & Burson, A. (2019). Exploring the Efficacy of Nile Red in Microplastic Quantification: A Costaining Approach. *Environmental Science and Technology Letters*, *6*(10), 606–611. https://doi.org/10.1021/acs.estlett.9b00499

Stein, A. F., Draxler, R. R., Rolph, G. D., Stunder, B. J. B., Cohen, M. D., & Ngan, F. (2015). NOAA's HYSPLIT Atmospheric Transport and Dispersion Modeling System. *Bulletin of the American Meteorological Society*, *96*(12), 2059–2077. https://doi.org/10.1175/BAMS-D-14-00110.1

Stohl, A., Forster, C., Frank, A., Seibert, P., & Wotawa, G. (2005). Technical note: The Lagrangian particle dispersion model FLEXPART version 6.2. *Atmospheric Chemistry and Physics*, *5*(9), 2461–2474. https://doi.org/10.5194/acp-5-2461-2005

Strietman, W. J., van den Heuvel-Greve, M. J., van den Brink, A. M., Leemans, E., Strand, J., & Bach, L. (2021). *Beach litter in West Greenland: a source analysis : Kalaallit Nunaata Kitaani sissani eqqakkat: eqqakkat suminngaanneernerinik misissuineq Strandaffald fra Vest Grønland: en kildeanalyse*. https://doi.org/10.18174/541149

Stride, B., Abolfathi, S., Bending, G., & Pearson, J. (2024). Quantifying microplastic dispersion due to density effects. *Journal of Hazardous Materials*, *466*. https://doi.org/10.1016/j.jhazmat.2024.133440

Sturm, M. T., Myers, E., Korzin, A., Polierer, S., Schober, D., & Schuhen, K. (2023a). Fast Forward: Optimized Sample Preparation and Fluorescent Staining for Microplastic Detection. *Microplastics*, *2*(4), 334–349. https://doi.org/10.3390/microplastics2040026

Sturm, M. T., Myers, E., Schober, D., Korzin, A., & Schuhen, K. (2023b). Development of an Inexpensive and Comparable Microplastic Detection Method Using Fluorescent Staining with Novel Nile Red Derivatives. *Analytica*, *4*(1), 27–44. https://doi.org/10.3390/ANALYTICA4010004/S1

de Souza Machado, A. A., Kloas, W., Zarfl, C., Hempel, S., & Rillig, M. C. (2018). Microplastics as an emerging threat to terrestrial ecosystems. In *Global Change Biology* (Vol. 24, Issue 4). https://doi.org/10.1111/gcb.14020

Süssmann, J., Fischer, E. K., Hildebrandt, L., Walz, E., Greiner, R., Rohn, S., & Fritsche, J. (2024). Nile red staining for rapid screening of plastic-suspect particles in edible seafood tissues. *Analytical and Bioanalytical Chemistry*, *416*(14), 1–13. https://doi.org/10.1007/S00216-024-05296-8

Syafei, A. D., Nurasrin, N. R., Assomadi, A. F., & Boedisantoso, R. (2019). Microplastic Pollution in the Ambient Air of Surabaya, Indonesia. *Current World Environment*. https://doi.org/10.12944/cwe.14.2.13

Szewc, K., Graca, B., & Dołęga, A. (2021). Atmospheric deposition of microplastics in the coastal zone: Characteristics and relationship with meteorological factors. *Science of the Total Environment*. https://doi.org/10.1016/j.scitotenv.2020.143272

Tatsii, D., Bucci, S., Bhowmick, T., Guettler, J., Bakels, L., Bagheri, G., & Stohl, A. (2024). Shape Matters: Long-Range Transport of Microplastic Fibers in the Atmosphere. *Environmental Science and Technology*, *58*(1), 671–682. https://doi.org/10.1021/ACS.EST.3C08209

Tian, X., Beén, F., & Bäuerlein, P. S. (2022). Quantum cascade laser imaging (LDIR) and machine learning for the identification of environmentally exposed microplastics and polymers. *Environmental Research*, *212*. https://doi.org/10.1016/j.envres.2022.113569

The Royal Environmental Health Institute of Scotland. (2016). *Glasgow Among UK's Most Pollututed Town and Cities*. https://rehis.com/news/glasgow-among-uks-most-polluted-town-and-cities-in-uk/#:~:text=GLASGOW%20AMONG%20UK'S%20MOST%20POLLUTED%20TOWN%20AND,concentration%20of%2016%20micrograms%20per%20cubic%20metre.

Thinh, T. Q., Sang, T. T. N., Viet, T. Q., Tam, L. T. M., Dan, N. P., Strady, E., & Chung, K. L. T. (2020). Preliminary assessment on the microplastic contamination in the atmospheric fallout in the Phuoc Hiep landfill, Cu Chi, Ho Chi Minh city. *Vietnam Journal of Science, Technology and Engineering*, *62*(3), 83–89. https://doi.org/10.31276/vjste.62(3).83-89

TISCH Environmental. (2024). *Total Suspended Particulate Samplers - Tisch Environmental*. TISCH Environmental. https://tisch-env.com/high-volume-air-sampler/TSP

Thomson, R., Olsen, Y., Mitchell, Richard. P., Daviss, A., Rowland, Steven. J., John, A. W. G., McGonigle, D., & Russel, Andrea. E. (2004). Lost at Sea: Where Is All the Plastic? Chemical Characterization of Produced Water View project. *Science*, *304*, 838. https://doi.org/10.1126/science.1094559

Thompson, R. C., Courtene-Jones, W., Boucher, J., Pahl, S., Raubenheimer, K., & Koelmans, A. A. (2024). Twenty years of microplastic pollution research—what have we learned? *Science*, *386*(6720), 1–13. https://doi.org/10.1126/science.adl2746

Thornton Hampton, L. M., Brander, S. M., Coffin, S., Cole, M., Hermabessiere, L., Koelmans, A. A., & Rochman, C. M. (2022). Characterizing microplastic hazards: which concentration metrics and particle characteristics are most informative for understanding toxicity in aquatic organisms? *Microplastics and Nanoplastics*, *2*(1). https://doi.org/10.1186/s43591-022-00040-4

Torres-Agullo, A., Zuri, G., & Lacorte, S. (2024). Pyr-GC-Orbitrap-MS method for the target/untargeted analysis of microplastics in air. *Journal of Hazardous Materials*, *469*. https://doi.org/10.1016/j.jhazmat.2024.133981

Trainic, M., Flores, J. M., Pinkas, I., Pedrotti, M. L., Lombard, F., Bourdin, G., Gorsky, G., Boss, E., Rudich, Y., Vardi, A., & Koren, I. (2020). Airborne microplastic particles detected in the remote marine atmosphere. *Communications Earth & Environment*, *1*(64), 1–9. https://doi.org/10.1038/s43247-020-00061-y

Truong, T.-N.-S., Strady, E., Kieu-Le, T.-C., Tran, Q.-V., Le, T.-M.-T., Thuong, Q.-T., 2021. Microplastic in atmospheric fallouts of a developing Southeast Asian megacity under tropical climate. *Chemosphere*.

Tsuda, A., Henry, F. S., & Butler, J. P. (2013). Particle transport and deposition: Basic physics of particle kinetics. *Comprehensive Physiology*, *3*(4). https://doi.org/10.1002/cphy.c100085

Tuan Tran, H., Lin, C., Bui, X. T., Ky Nguyen, M., Dan Thanh Cao, N., Mukhtar, H., Giang Hoang, H., Varjani, S., Hao Ngo, H., & Nghiem, L. D. (2022). Phthalates in the environment: characteristics, fate and transport, and advanced wastewater treatment technologies. In *Bioresource Technology* (Vol. 344). https://doi.org/10.1016/j.biortech.2021.126249

Tunahan Kaya, A., Yurtsever, M., & Çiftçi Bayraktar, S. (2018). Ubiquitous exposure to microfiber pollution in the air. *The European Physical Journal Plus*, *133*(11), 488. https://doi.org/10.1140/epjp/i2018-12372-7

UK AIR. (2025). *Site Information for Glasgow Townhead(UKA00576)*. Air Information Resource. https://uk-air.defra.gov.uk/networks/site-info?site_id=GLKP

Umurhan, Y., Songsart-Power, M., Limbu, T. B., & Phan, T. (2025). Applications of Raman spectroscopy for microplastic detection and characterization: a comprehensive spectral reference. *Environmental Science and Pollution Research 2025 32:50*, *32*(50), 28630–28677. https://doi.org/10.1007/s11356-025-37224-3

UNEP. (2016). *Marine Plastic Debris and Microplastics: Global Lessons and Research to Inspire Action and Guide Policy Change* | UNEP - UN Environment Programme. https://www.unep.org/resources/publication/marine-plastic-debris-and-microplastics-global-lessons-and-research-inspire

United Nations Environment Programme (2021). *From Pollution to Solution: A global assessment of marine litter and plastic pollution*. Synthesis. Nairobi. 1-44.

UNEP. (2024). *Pivotal fourth session of negotiations on a global plastics treaty opens in Ottawa*. UNEP. Press Release. Chemical & Pollutions Action. . https://www.unep.org/news-and-stories/press-release/pivotal-fourth-session-negotiations-global-plastics-treaty-opens . (Online; Accessed 25/11/24)

US Environmental Protection Agency. (2011). Exposure Factors Handbook: 2011 Edition. *U.S. Environmental Protection Agency*. https://doi.org/EPA/600/R-090/052F

Van der Does, M., Knippertz, P., Zschenderlein, P., Giles Harrison, R., & Stuut, J.-B. W. (2018). The mysterious long-range transport of giant mineral dust particles. *Science Advances*, *4*(12). https://doi.org/10.1126/sciadv.aau2768

Visual Crossing. (n.d.). *Visual Crossing (Nov-Dec 2021)*. Retrieved April 22, 2025, from https://www.visualcrossing.com/weather-data/

Wang, C., Liang, S., Bai, L., Gu, X., Jin, X., Ok, Y. S., & Gu, C. (2023). Photoaging of Typical Microplastics as Affected by Air Humidity: Mechanistic Insights into the Important Role of Water Molecules. *Environmental Science & Technology*, *57*(14), 5967–5977. https://doi.org/10.1021/acs.est.2c08571

Wang, X., Li, C., Liu, K., Zhu, L., Song, Z., & Li, D. (2020). Atmospheric microplastic over the South China Sea and East Indian Ocean: abundance, distribution and source. *Journal of Hazardous Materials*, *389*(121846), 1–9. https://doi.org/10.1016/j.jhazmat.2019.121846

Wang, C., Zhao, J., & Xing, B. (2021). Environmental source, fate, and toxicity of microplastics. *Journal of Hazardous Materials*, *407*(124357), 1–12. https://doi.org/10.1016/J.JHAZMAT.2020.124357

Wang, Z., Zhang, Y., Kang, S., Yang, L., Luo, X., Chen, P., Guo, J., Hu, Z., Yang, C., Yang, Z., & Gao, T. (2022). Long-range transport of atmospheric microplastics deposited onto glacier in southeast Tibetan Plateau. *Environmental Pollution*, *306*(119415), 1–12. https://doi.org/10.1016/J.ENVPOL.2022.119415

Ward, E., Gordon, M., Hanson, R., & Jantunen, L. M. (2024). Modelling the effect of shape on atmospheric microplastic transport. *Atmospheric Environment*, *326*. https://doi.org/10.1016/j.atmosenv.2024.120458

Wieboldt, D. (2010). Understanding Raman Spectrometer Parameters. *Spectroscopy Supplements*. https://doi.org/https://www.spectroscopyonline.com/view/understanding-raman-spectrometer-parameters

Winijkul, E., Latt, K. Z., Limsiriwong, K., Pussayanavin, T., & Prapaspongsa, T. (2024). Depositions of airborne microplastics during the wet and dry seasons in Pathum Thani, Thailand. *Atmospheric Pollution Research*, *15*(10), 102242. https://doi.org/10.1016/J.APR.2024.102242

Wright, S. L., Levermore, J. M., & Kelly, F. J. (2019). Raman Spectral Imaging for the Detection of Inhalable Microplastics in Ambient Particulate Matter Samples. *Environmental Science and Technology*, *53*(15), 8947–8956. https://doi.org/10.1021/acs.est.8b06663

Wright, S. L., Ulke, J., Font, A., Chan, K. L. A., & Kelly, F. J. (2020). Atmospheric microplastic deposition in an urban environment and an evaluation of transport. *Environment International*, *135*(105411), 1–7. https://doi.org/10.1016/j.envint.2019.105411

Wright, S. L., & Kelly, F. J. (2017). Plastic and Human Health: A Micro Issue? *Environmental Science and Technology*, *51*, 6634–6647.

Wu, Y., Liu, J., Zhai, J., Cong, L., Wang, Y., Ma, W., Zhang, Z., & Li, C. (2018). *Comparison of dry and wet deposition of particulate matter in near-surface waters during summer*. *13*(6), 1–15. https://doi.org/10.1371/journal.pone.0199241

Xu, C., Zhang, B., Gu, C., Shen, C., Yin, S., Aamir, M., & Li, F. (2020a). Are we underestimating the sources of microplastic pollution in terrestrial environment? *Journal of Hazardous Materials*, *400*(123228), 1–12. https://doi.org/10.1016/j.jhazmat.2020.123228

Xu, G., Cheng, H., Jones, R., Feng, Y., Gong, K., Li, K., Fang, X., Tahir, M. A., Valev, K., & Zhang, L. (2020b). Surface-Enhanced Raman Spectroscopy Facilitates the Detection of Microplastics <1 μm in the Environment. *Environmental Science & Technology*, *54*, 15594–15603. https://doi.org/10.1021/acs.est.0c02317

Xu, J. L., Lin, X., Wang, J. J., & Gowen, A. A. (2022). A review of potential human health impacts of micro- and nanoplastics exposure. In *Science of the Total Environment* (Vol. 851). https://doi.org/10.1016/j.scitotenv.2022.158111

Yadav, H., Sethulekshmi, S., & Shriwastav, A. (2022). Estimation of microplastic exposure via the composite sampling of drinking water, respirable air, and cooked food from Mumbai, India. *Environmental Research*, *214*(113735), 1–7. https://doi.org/10.1016/J.ENVRES.2022.113735

Yao, X., Luo, X. S., Fan, J., Zhang, T., Li, H., & Wei, Y. (2022). Ecological and human health risks of atmospheric microplastics (MPs): a review. *Environmental Science: Atmospheres*, 2(5), 921–942. https://doi.org/10.1039/D2EA00041E

Zhang, Y., Gao, T., Kang, S., & Sillanpää, M. (2019). Importance of atmospheric transport for microplastics deposited in remote areas. In *Environmental Pollution* (Vol. 254). https://doi.org/10.1016/j.envpol.2019.07.121

Zhang, Y., Kang, S., Allen, S., Allen, D., Gao, T., & Sillanpää, M. (2020a). Atmospheric microplastics: A review on current status and perspectives. *Earth-Science Reviews*, *203*(103118), 1–15. https://doi.org/10.1016/j.earscirev.2020.103118

Zhang, Y., Gao, T., Kang,S., Allen, S., Luo, X., Allen, D. (2020b). Microplastics in glaciers of the Tibetan Plateau: Evidence for the long-range transport of microplastics. *Science of the Total Environment*, *203* (103118). https://doi.org/https://doi.org/10.1016/j.scitotenv.2020.143634

Zhang, R., Jia, X., Wang, K., Lu, L., Li, F., Li, J., & Xu, L. (2023a). Characteristics, sources and influencing factors of atmospheric deposition of microplastics in three different ecosystems of Beijing, China. *Science of the Total Environment*, *883*. https://doi.org/10.1016/j.scitotenv.2023.163567

Zhang, Y., Gao, T., Kang, S., Allen, D., Wang, Z., Luo, X., Yang, L., Chen, J., Hu, Z., Chen, P., Du, W., & Allen, S. (2023b). Cryosphere as a temporal sink and source of microplastics in the Arctic region. Geoscience Frontiers, 14(4), 1–14. https://doi.org/10.1016/J.GSF.2023.101566

Zhao, L., Dahal, S., & Marfil-Vega, R. (2020). Insights Toward Standardization of the Analysis of Microplastics by Infrared Microscopy. *SPECTROSCOPY*, *35*(3).

Zhao, X., Wang, J., Yee Leung, K. M., & Wu, F. (2022). Color: An Important but Overlooked Factor for Plastic Photoaging and Microplastic Formation. *Environmental Science and Technology*, *56*(13), 9161–9163. https://doi.org/10.1021/ACS.EST.2C02402/ASSET/IMAGES/LARGE/ES2C02402_0005.JPEG

Zhu, X., Huang, W., Fang, M., Liao, Z., Wang, Y., Xu, L., Mu, Q., Shi, C., Lu, C., Deng, H., Dahlgren, R., & Shang, X. (2021). Airborne Microplastic Concentrations in Five Megacities of Northern and Southeast China. Environmental Science & Technology, 55, 12871–12881. https://doi.org/10.1021/acs.est.1c03618

Zeb, A., Liu, W., Ali, N., Shi, R., Wang, Q., Wang, J., Li, J., Yin, C., Liu, J., Yu, M., & Liu, J. (2024). Microplastic pollution in terrestrial ecosystems: Global implications and sustainable solutions. In *Journal of Hazardous Materials* (Vol. 461). https://doi.org/10.1016/j.jhazmat.2023.132636

Ziani, K., Ioniță-Mîndrican, C. B., Mititelu, M., Neacșu, S. M., Negrei, C., Moroșan, E., Drăgănescu, D., & Preda, O. T. (2023). Microplastics: A Real Global Threat for Environment and Food Safety: A State of the Art Review. In *Nutrients* (Vol. 15, Issue 3). https://doi.org/10.3390/nu15030617

Zimmermann, L., Dombrowski, A., Völker, C., & Wagner, M. (2020). Are bioplastics and plant-based materials safer than conventional plastics? In vitro toxicity and chemical composition. *Environment International*, *145*(106066), 1–11. https://doi.org/10.1016/j.envint.2020.106066

Appendices

Appendix I. Table Summary of Atmospheric Microplastics Studies (published up to 22nd of November 2024)

(summary includes location, type of sampling, analytical method, pre-treatment methods, MP concentrations, particle size distribution, predominant shape, predominant polymers and reference)

Location	Type of Sample	Analytical Method	Pre-Treatment Method	MP Concentrations	Particle Size Distribution	Predominant Shape	Predominant Polymers	Reference
Taiwan (low density population, and high density villages)	Active Sampling – 10L/min; 24hr sampling; 3 days in a row in a month Aug-July	Microscope; Raman	De-ionised water; and shaken H_2O_2 (30%) for 6 days; $ZnCl_2$ solution at 1.72 g/cm^3 (98%) for density separation; 0.45µm filter	Average high density - 2.20 ± 2.97 particles/m^3 and average low density - 1.92 ± 2.35 particles/m^3	3-5000µm range; most particles in the 3–25 and 26–50µm categories	Fragment and films	Polytetrafluoroethylene (PTFE) and Polyamide (PA)	Jung et al., 2024 https://doi.org/10.1016/j.envres.2024.119996
Shanghai and Hohhot, China	Active Sampling - daily PM2.5 samples taken with high-volume cyclone sampler	Liquid Chromatography Mass Spectrometry (LC-MS/MS)	20 mL of distilled water and shaken; ultrasonication for 30mins; H_2O_2 (30%); (methanol and potassium hydroxide added to polymerise into monomers; 10ml of acetonitrile – for LCMS/MS)	-	-	-	98 monomers detected; plastic additives and binders, mostly polyethylene glycol (PEG); hydroxyl terminated polyether (HTPE), PET, Poly propylene glycol (PPG), and Nylon	Jia et al., 2024 www.elsevier.com/locate/scitotenv https://doi.org/10.1016/j.scitotenv.2024.176254
Lahore, Pakistan	Passive Sampling – dry deposition; 7 day sampling period	Microscope; FTIR	Fenton's reagent (H_2O_2 and FeSO4 (iron sulphate))and hydrogen peroxide	Average deposition rate of 2340 ± 1392 particles/m^2/day	-	Fibre	Polyester (PS), polyethylene terephthalate (PET), polypropylene (PP),	Naqash et al., 2024 https://doi.org/10.1007/s113

Location	Type of Sample	Analytical Method	Pre-Treatment Method	MP Concentrations	Particle Size Distribution	Predominant Shape	Predominant Polymers	Reference
			(30%) for organic matter removal; sodium chloride for density separation;				polyethylene (PE), and polyurethane (PUR) were the most predominant	56-024-34819-0
Tibetan Plateau	Active Sampling -	Laser Direct Infrared Imaging (LDIR)	Rinsed with 1.7–1.8 kg/L$ZnCl_2$ solution; H_2O_2 (30%) solution for organic matter removal;	7.15 ± 2.46 MPs m^{-3}	20.34 to 297.18µm, 87% <100µm	Fragments	PA, PS, PP, PU and PVC	Guo et al.,2024 https://doi.org/10.1007/s10653-024-02125-w
Himalayas, India	Passive Sampling – 18 weeks, collected every week	Fluorescent microscope; Raman	H_2O_2 (30%) solution for organic matter removal; $ZnCl_2$ (1.6–1.7 g/cm^3) for rinsing	2256 ± 1221 particles/m^2/day	67 to 2320µm; <400µm (30%)	Fragments	PE, PET, PP, PS	Ankit et al., 2024 https://doi.org/10.1016/j.envpol.2024.124629
Xinjiang, China	Active Sampling – comprehensive ambient air sampler 5L0/min 7hr per day; Deposition Sampling; Atmospheric Dust Sampling; March-April 2023	Stereo-microscope and FTIR	Density separation - a $ZnCl_2$ solution (ρ1.6 g/cm^3) 30% H2O2 for organic matter removal	103.21 ± 22.12 particles/m2/day;	83-3919.94µm; TSP >1000µm; deposition >1000µm; dust 200-400µm (LOD 80µm)	Fibres	PP, PE, Celluloid/Cellophane.	Du et al., 2024 https://doi.org/10.1002/etc.5951
Sao Carlos, Brazil	Passive Sampling, one dry and two wet seasons, indoor and outdoor	Microscope, Raman	Ultrapure water, 0.05 mol of $FeSO_4.7H_2O$ and 8 mL of H_2SO_4 (0.1 mol L^{-1};95-97%), 8 mL of H_2O^2 (29%) and stirred; sodium	Outdoor - 168.03 items m^{-2} day^{-1} Indoor - 60.16 items m^{-2} day^{-1}	Outdoor - <60µm; Indoor 500-1000µm	Fragments	Polyester, Ethylene Vinyl Acetate (EVA)	Ferraz et al., 2024 (pre-print) https://ssrn.com/abstract=4885543

Location	Type of Sample	Analytical Method	Pre-Treatment Method	MP Concentrations	Particle Size Distribution	Predominant Shape	Predominant Polymers	Reference
			iodide (NaI; 1.7 g mL^{-1}) and agitated for density separation					
Nanjing, China	Active Sampling - middle flow atmospheric particulate samplers with TSP cut-off; 100/min Passive Sampling – stainless-steel bucket, monthly samples Aug'20-Jul'21	Microscope and FTIR (6.5% of particles n=700)	30 % H_2O_2; density separation using NaCl	DAMPs -302.31 ± 107.40 items/m^2 SAMPs 1.31 ± 0.62 items/m^3 for SAMPs	20-5000µm; most <100µm	DAMPs – Fragments; SAMPs Fragments/Fibres Comparable	DAMPs – PA, PE, PES, EP, PP SAMPs – PA.	Rao et al., 2024 https://doi.org/10.1016/j.jhazmat.2023.132860
Yellow Sea and Bohia Sea, China	Active Sampling – atmospheric sampler 100L/min	Stereo-microscope; LDIR	30 % H_2O_2 for organic matter removal	1.65 to 16.80 items/100 m^3 (summer); 0.38 to 14.58 items/100 m^3 (autumn); average - 7.20 items/100 m^3	32.48 µm to 2971.96 µm; average - 739.13 ± 630.18 µm;	Fibres	Polyamide (PA), Chlorinated (CPE), Polyethylene, PET	Liu, Liang and Liu, 2024 https://doi.org/10.1016/j.scitotenv.2024.171906
Mount Tabai, China (Remote)	Active Sampling – three samplers PM_{100}, PM_{10}, and $PM_{2.5}$ - ; Sept'2020-2021; 100L/min monthly	Stereo-microscope and µRaman	$ZnCl_2$ for density separation and hydrogen peroxide (H_2O_2) for organic removal	0.6−3.1 particles/m^3	Mostly 1.6-10µm	Fibres	PS, PE, PP	Wei et al., 2024 https://doi.org/10.1021/acs.est.4c00296
Beijing (urban, suburban, village)	Sampled leaves May-Sep'22	LDIR	0.01 M sterile phosphate-buffered saline (PBS) and ultrasonic treatment	3.62 ± 1.29 items cm^{-2}.	9-2464µm; mostly <80m; (used 10µm sieve)	Fragments	PA, PE and Rubber	Xu et al., 2024a https://doi.org/10.1016/j.jha

Location	Type of Sample	Analytical Method	Pre-Treatment Method	MP Concentrations	Particle Size Distribution	Predominant Shape	Predominant Polymers	Reference
			and oscillation; DNA extraction; digestion and $CaCl_2$ solution for density separation					zmat.2023.132789
Washington State, US (rural/ agricultural)	Passive Sampling – rainfall gauge; 2 years of sampling, collected 5 times	Microscope and LDIR	Fenton's reaction (H_2O_2 and FeSO4 (iron sulphate)) for organic removal and $ZnCl_2$ for density separation	9 particles/(m^2 day)	(Mass conc. used)	Fibres	PA, PU, PE	Adhikari et al., 2024 https://doi.org/10.1016/j.scitotenv.2023.168883
Beijing, China	Passive Sampling – glass jars; dry and wet deposition; monthly (22-31days) collection, Jul'-Jun'22	µFTIR	Fenton reagent and H_2O_2 added after for digestion; density separation	Deposition rate - 33.23 ±233.76 items·m^{-2}·d^{-1} ; dust - 3.00 ± 1.79 items·mg^{-1}	11.7-1992.3µm; mostly 38.4-48.6µm	Fragment	PES, PET, PE, PA	Xu et al., 2024b https://doi.org/10.1021/acs.est.3c09271
Kochi, India (urban)	Passive Sampling – bulk deposition, stainless steel containers; Oct'-Sep'22; sampling period 100 days	Stereo-microscope and Raman (27 particles)	H_2O_2 for organic removal and $ZnCl_2$ for density separation	21.27 particles m^{-2} d^{-1}.	18.51-491723.23µm; mostly 200–500µm	Fibres	PE, PP	Kannakai and Devipriya, 2024 https://doi.org/10.1016/j.scitotenv.2023.168235
Guangzhou, China	Mangrove leaves – five species, five trees from each species	Stereo-microscope and SEM	Soaked in 200m distilled water; sieved, microplastics selected and water filtered (45µm filter paper); SEM prep	1223 items/m^2/day	<0.5-5mm; Mostly <1mm	Fibres	Cellulose, rayon, polyester	Huang et al., 2024 https://doi.org/10.1016/j.jhazmat.2024.133473

Location	Type of Sample	Analytical Method	Pre-Treatment Method	MP Concentrations	Particle Size Distribution	Predominant Shape	Predominant Polymers	Reference
Wuhan, China	Passive sampling – wet and dry; glass bucket; collected every 3 months Dec'202-Dec'2021	Microscope, µRaman	H_2O_2 (30%) for organic removal and $ZnCl_2$ (ρ = 1.5–1.6 g cm^{-3}) for density separation	82.85 ± 57.66 $n \cdot m^{-2} \cdot day^{-1}$.	<0.5-5mm; Mostly <0.5; 0.5-1mm)	Fibres	PET, PP, PE	Zhu et al., 2024 https://doi.org/10.1016/j.envpol.2023.123012
Wuliangsuhai Lake, China (semi-rural/sub-urban)	Passive Sampling – March – Stainless Steel and Glass containers; dry deposition; monthly sample periods; Mar'-June'21	Microscope and Raman (150 particles)	50µm sieve; potassium formate 1.91 g/cm^3 for density separation and H_2O_2 (30%) for organic removal	3371 ± 1423 $n/d \cdot m^2$	0.05-5mm; mostly - 0.05–0.5 mm	Fibres	PE, PET, PS	Wang et al., 2024a https://doi.org/10.1016/j.scitotenv.2023.168201
Anyang City, South Korea (urban)	TSP, PM_{10}, and $PM_{2.5}$ – medium flow air sampler with 100L/min flow rate for 20hr sampling period over 3 days – low, medium and high AQI	Stereo-microscope and µFTIR	Zinc chloride solution1(.6 g/cm^3) for density separation and H_2O_2 30% and Fenton reagent ($FeSO_4$ solution mixed with H_2O_2 solution) for organic removal	TSP - 0.19 itemchs/m^3 PM_{10} - 0.26 items/m^3 $PM_{2.5}$ - 0.42 items/m^3	0.1->1mm; mostly 0.1-1mm	Fibres	PET, EVA (Ethyl vinyl acetate)	Wang et al., 2024b https://doi.org/10.1007/s10661-024-12493-6
Beijing and Shanghai, China (urban)	TSP-PM_{10}-$PM_{2.5}$ sampler; 100 L/min; 20hr sample period	LDIR, SEM (Scanning Electron Microscopy), EDX (Energy Dispersive X-Ray Spectroscopy)	99.7% ethanol; shaken and rinsed; ethanol 100µL and dried	Beijing - 3.0 items/m^3 Shanghai- 1.7 items/m^3	27.5-250µm; Average Beijing – 25.1µm; Shanghai – 38µm (LOD=20µm)	Fibres	PA, Rubber, OVC, PET	Liu et al., 2024b https://doi.org/10.1016/j.scitotenv.2023.169308
Beijing, China (semi-	Sep'2021-Feb'2022; autumn-winter;	Stereo-microscope; µFTIR	H_2O_2 (30 %) for organic removal	167.09 ± 92.03 $item \cdot m^{-2} \cdot d^{-1}$	<500->4000µ; Mostly <500µm	Fibres	PET, Rayon	Lu et al., 2024 https://doi.org/10.1016/j.scit

Location	Type of Sample	Analytical Method	Pre-Treatment Method	MP Concentrations	Particle Size Distribution	Predominant Shape	Predominant Polymers	Reference
urban/rural farmland)	Passive Sampling – wet and dry deposition; 1 month sampling period over 6 months at 6 sites; airborne particle sampler 2m^3 in 20mins							otenv.2023.168834
Tibetan Plateau (urban, rural, wildland)	Active Sampling – middle flow TSP sampler; 100L/min;	Nile Red staining µFTIR	H_2O_2 and shaken in incubator at 60 rpm and 55 °C for 24 h	2.5–58.8 n/m^3	5,9-1000µm; Mostly <100µm	Fragments	PET, PE, PA, PS	Luo et al., 2024 https://doi.org/10.1016/j.jhazmat.2023.133177
Kassel, Germany (urban)	Passive sampling – wet/dry deposition; monthly sampling period over 8 months May'-Dec'19	µFTIR and Raman	Filtered water and resuspended on Anodiscs	µFTIR - 17 ± 14 MP m^{-2} day^{-1} Raman - 207 MP m^{-2} day^{-1}	11-130µm; (LOD – 11mm µFTIR and Raman 0.5µm); average 50µm	-	PP, PE	Kernchen et al., 2024 https://link.springer.com/article/10.1007/s11869-024-01571-w
Paris (suburban)	Passive Sampling - bulk deposition; April-July 2020; March-July 2021; every 4-11 days	Microscope, µFTIR,	Sodium iodide (NaI) for density separation (1.7 g/cm^3); ultrasonic bath Fenton's for organic removal ($FeSO_4$ solution mixed with H_2O_2 solution)	Lockdown - 5.4 MP m^{-2}.d^{-1} Normal - 29.2 MP m^{-2}.d^{-1}	25->500µm; mostly 75-100µm (2020 less >50µm)	-	PP, PE, PS	Beaurepaire et al., 2024 https://doi.org/10.1016/j.envpol.2024.123354
Kangbao County, Northern	Active sampling – middle flow sampler (AMAE) 100±0.2L/min;	Stereomicroscope, µFTIR	-	0.88-0.26 MP/m^3	50-2000µm; mostly 50-400µm	Fibres	-	Long et al., 2024

Location	Type of Sample	Analytical Method	Pre-Treatment Method	MP Concentrations	Particle Size Distribution	Predominant Shape	Predominant Polymers	Reference
China (remote /farmland)	sampling every 6-18 hrs over one month							https://doi.org/10.1029/2024JD041546
Chengdu, China (urban and suburban)	Deposition sampling – stainless steel bucket; bulk deposition sampling every 2-3 weeks	Microscope, µFTIR	H_2O_2 (30%) for organic removal and NaCl (1.2 g/cm^3) for density separation	207.1–364.0 N/m^2/d (14.17–33.75 µg/m^2/d	22.9–4165.5µm; fibres mostly 50–2000µm Fragments - mostly 20–50µm	Fibre	PP, PE, PET	Chen et al., 2024 https://doi.org/10.1016/j.envpol.2024.124192
A Coruña, Spain (semi-urban)	Deposition sampling – bulk deposition over one month; foliage samples	Stereomicroscope, Quantum cascade IR spectrophotometer	Sodium chloride and H_2O_2 (15%)	73, 67 and 101 items per sample (no deposition rate given); leaf samples - 2735 MP/m^{-2} and 6235 MP/m^{-2}	Fibres mostly 100-500µm; fragments 20-50µm	Fragments	PET, PA, PS	Falkadin et al., 2024 https://doi.org/10.1016/j.envpol.2024.123911
Ranchi, India (urban)	Active sampling – outdoor PM_{10} dust sampler for 24hrs; $PM_{2.5}$ -speciation air sampler for 24hrs; indoor – personal sampler (1m^3/min)	Stereomicroscope, SEM, FESEM-EDX (Field Emission Scanning Electron Microscopy and Energy Dispersive X-ray), FTIR	H_2O_2 (30%) for organic removal and $ZnCl_2$ (1.5 g/cm^3) for density separation	PM_{10} - 465 ± 27 particles/m^2 /day $PM_{2.5}$ - 12104 ± 665 and 13833 ± 1152 MP/m^2 /day Indoor - 98717±4544 MP/m^2/day	2.3µm-47µm; mostly 4.7-12.8µm,	Fibres	Outdoor – PE, PP, PS Indoor - PVC	Nandi et al., 2024 https://doi.org/10.1016/j.envpol.2024.123543
Xiamen, China (urban)	Active sampling – TSP with 100±0.1Lmin^{-1}; 24hr sampling duration,	Stereomicroscope, Raman	-	0–0.062 items m^{-3}, with average 0.010 ± 0.012 items m^{-3}.	<01mm-5mm; mostly <1mm	Fibres	PS, PET, PE	Du et al., 2024 https://doi.org/10.1016/j.jclepro.2024.141145
Yancheng, China (urban)	Active sampling – atmospheric sampler	Microscope, µFTIR, LDIR	-	5-38 MP/m^3; 23.8 items/m3	20 to 271µm; marine – avg 44.9µm;	Fragments	Rubber, PFR (Polytetrafluoroethylene)	Liu et al., 2024c

Location	Type of Sample	Analytical Method	Pre-Treatment Method	MP Concentrations	Particle Size Distribution	Predominant Shape	Predominant Polymers	Reference
	(Minivol); 5L/min; 8hr sampling durations;				terrestrial avg - 47.7µm			https://doi.org/10.1016/j.jes.2023.09.027
Goa, India (remote, coastal)	Active sampling – high volume sampler; 24hr sampling period; March 2016 and Nov'2020	µFTIR	H_2O_2 (20%) for organic removal and NaCl (1.2 g/cm^3) for density separation	1.30 ± 0.14 n/m3 in 2016 and 1.46 ± 0.12 n/m3 in Nov'2020	20µm-5 mm;	Fibres	PVC, PMMA	Kaushik et al., 2024 https://doi.org/10.1016/j.scitotenv.2023.168705
Tibetan Plateau, China (remote)	Snow samples – stainless steel bucket and high volume sampler; taken during April, August, October 2021	Stereomicroscope, µFTIR	H_2O_2 (30%) for organic removal	Air – 0.12 MP/m^3 Glacier - 0.13–19.8 items/L	50-6000µm; mostly <300µm	Fibre and film	PP, PET	Niu et al., 2024 https://doi.org/10.1016/j.apgeochem.2024.106026
Nanjing, China (urban)	Dust sampling – portable vacuum cleaner; Dec'2020-June'2021	Stereomicroscope, µFTIR	H_2O_2 (30%) for organic removal and $ZnCl_2$ solution (1.6–1.65 g/mL) for density separation	143.3 ± 40.8 particles/m^2.	<100-2000µm; mostly <500µm	Fragment	PS, PA, PVDF (polyvinylidene difluoride)	Fan et al., 2024 https://doi.org/10.1016/j.jhazmat.2024.133733
Pathum Thani, Thailand (semi-urban)	Passive sampling – wet and dry deposition; rain sampler; collected every 7 days Sept-Jan'	Stereomicroscope, FTIR	NaCl for density separation	Wet - 285 MP/m^2/day Dry - 199 MP/m^2/day Total - 325 numbers/m^2/day	Wet – 121-4990µm; mostly <600µm Dry – 132-4541µm; mostly <900µm	Fibres	PP, PU. PET, PE	Winijkul et al., 2024 https://doi.org/10.1016/j.apr.2024.102242
Islamabad, Pakistan (urban)	Active sampling – gravimetric sampler; 16L/min; collected every 24hrs; Dec'2022	Microscope, FTIR, µRaman, SEM-EDX	H_2O_2 (30%) for organic removal and $ZnCl_2$ (1.6 g/cm^3) for density separation	Indoor - 4.34 ± 1.93 items/m^3	<50µm-1000µm; mostly <50µm	Fibres	PET, PE, PP, PS	Din et al., 2024 https://doi.org/10.1016/j.scit

Location	Type of Sample	Analytical Method	Pre-Treatment Method	MP Concentrations	Particle Size Distribution	Predominant Shape	Predominant Polymers	Reference
				Outdoor - 0.93 ± 0.32 items/ m^3				otenv.2023.168398
Lhasa City, Tibetan Plateau, China (urban)	Active sampling – middle flow TSP sampler; 100L/min; Feb'23 (Tibetan New Year)	LDIR	H_2O_2 (30%) for organic removal	4.32 to 8.77 MPs m^{-3}; avg - 7.15 ± 2.46 MPs m^{-3}	20.34 to 297.18µm; mostly 100µm	Fragment	PA, PS	Guo et al., 2024 https://doi.org/10.1007/s10653-024-02125-w
Dhaka City, Bangladesh (urban)	Passive sampling – glass petri dish ; dust samples from 15 households; Dec'21-Jan'22	Stereomicroscope, FTIR	-	7.52 × 10^3 MPs/m^2/day to 66.29 × 10^3 MPs/m^2/day; avg - 34 × 10^3 MPs/m^2/day.	50-4000µm; mostly 50-250µm	Fibre	PET, PE, nylon, PP	Islam et al., 2024 https://doi.org/10.1016/j.heliyon.2024.e36449
Thuwal, Saudi Arabia (urban, coastal)	Active sampling – high-volume sampler; 20m^3h^{-1}; sampling 1-7days; Sep'2015-Dec'2017	Stereomicroscope, Raman	-	0.9 ± 0.8 × 10^{-2} MFs m^{-3}	183µm to 11,87µm; mostly <2000µm	Fibre	PET, PE	Martynova et al., 2024 https://doi.org/10.1016/j.scitotenv.2023.167902
Kuala Nerus, Terengganu, Malaysia (urban, coastal)	Passive sampling – glass petri dish; sampling 24hrs; Dec'2019	Stereomicroscope, SEM-EDS; FTIR	-	576 to 15,562 MP/m^2/day; avg - 5476 ± 3796 particles/m^2/day,	-	Fibre	PES, PE, PP	Chenappan et al., 2024 https://doi.org/10.1007/s10661-024-12381-z
Heilongjiang Province, Inner Mongolia and Jilin Province, China (urban and remote)	Snow sampling - surface snow, top 5cm; Dec'2020-Jan'21	Nile Red; µFTIR	H_2O_2 (30%) for organic removal	(4.52 ± 3.05) × 10^4 MPs L^{-1}	20-3500µm; mostly <50µm	Fragment	EVA, PE	Wen et al., 2024 https://doi.org/10.1016/j.scitotenv.2023.167923

Location	Type of Sample	Analytical Method	Pre-Treatment Method	MP Concentrations	Particle Size Distribution	Predominant Shape	Predominant Polymers	Reference
Coimbra, Portugal and Wageningen, the Netherlands (urban)	Leaf sampling – fir and pine needles, eucalyptus and cedar leaves; Feb-March'22	Stereomicroscope, µFTIR	Sodium phosphate (NaH_2PO_4, 1.30–1.40 $g \cdot cm^{-3}$) for density separation	Fir leaves – 2.52 ± 2.14 MP cm^{-2} Pine leaves - 0.5 ± 0.13 MP cm^{-2} Eucalyptus leaves - 0.038 ± 0.003 MP cm^{-2} Cedar leaves - (0.037 ± 0.002 MP cm^{-2}	75-183µm; mostly <250µm		PE, PU, acrylates, rubber	Leitão et al., 2024 https://doi.org/10.1016/j.scitotenv.2024.174907
China, (17cities, urban)	Passive Sampling – 50-60days; stainless steel basins	LDIR and FESEM	Density separation with $ZnCl_2$ (1.7–1.8 $g \cdot cm^{-3}$) and H_2O_2 (30%) for organic removal	5.1 items m^{-2} day^{-1} in Qinhuangdao and 228.7 items m^{-2} day^{-1} in Beijing	32-109µm	Fragment	PP, PA, PU, and PE	Liu et al. 2024 https://doi.org/10.1016/j.jhazmat.2024.134024
Lima, Peru (urban indoor dust)	Passive Sampling – settled dust, organic bristle brush	Stereomicroscope, µFTIR	H_2O_2 (30%) for organic removal and $NaCl_2$ (5M) for density separation	0.01 to 33.90 MPs/mg of dust (11.00–411.0 MPs/m^2); average 3.00 ± 4.98 MPs/mg (150.4 ± 109.3 MPs/m^2)	1µ-5mm; Mostly 500µm – 5 mm (82%)	Fibres	PP, PE, EVA	Gonzales e al., 2024 https://doi.org/10.1016/j.scitotenv.2024.170353
Sonnblick Observatory, Austria (remote)	Active Sampling - PM_{10} samples high volume sampler (DIGITEL DH-77); PM_1 with low-volume sampler; 23 weekly samples	TD-PTR-MS	-	35 and 21 ng m^{-3} with maximum concentrations of 165 and 113 ng m^{-3} for PM10 and PM1	-	-	PET, PE, PP	Kau et al., 2024 https://doi.org/10.1016/j.chemosphere.2024.141410

Location	Type of Sample	Analytical Method	Pre-Treatment Method	MP Concentrations	Particle Size Distribution	Predominant Shape	Predominant Polymers	Reference
Najing, China (urban)	Passive – monthly sampling; Active Sampling – middle-flow atmospheric particulate samplers with the total suspended particulate cut off; 100L/min every 4 hrs;	Stereomicroscope, FTIR	H_2O_2 (30%) for organic removal and $NaCl_2$ for density separation	Deposition - 134.18 to 500.94 MP/m^2/day; annual average of 302.31 ± 107.40 MP/m^2/day Suspended - 0.29–4.88 MP/m^3; annual average of 1.31 ± 0.62 MP/m^3		Deposition – fragments Suspended – fibres	PA, PE, PES	Rao et al., 2024 https://doi.org/10.1016/j.jhazmat.2023.132860
Shiraz, Iran (city)	Passive sampling – dry and wet deposition; stainless steel dish; four sampling sites; Dec'2021-Jan'2022	Stereomicroscope, µRaman	H_2O_2 (30%) for organic removal	Wet deposition – max 130 MP m^{-2} h^{-1} Dry deposition – max 50 MP m^{-2} h^{-1}	<100-1000µm; mostly <250µm	Fibres	PE, PET, PS, PP	Abbasi et al., 2024 https://doi.org/10.1016/j.apr.2023.101977
Espírito Santo, Brazil (semi-urban)	Spider webs – collected March 2023;	Raman	KOH 10 % for digestion	3138 MP (total)	-	Fragment	IPP, PET, PU, Nylon/PA, and DPET.	De Costa et al., 2024 https://doi.org/10.1016/j.jhazmat.2024.135190
Beijing, China (rural)	Passive sampling – total atmospheric deposition (wet and dry); stainless steel sampling bottles; monthly sampling;	Stereomicroscope, µFTIR	H_2O_2 (30%) for organic removal	67.06–461.02 item·m^{-2}·d^{-1}; avg. - 194.38 item·m^{-2}·d^{-1}.	30.45µm-6638.06µm; mostly <500µm	Fibre	PET, RY, PP	Zhang et al., 2023 https://doi.org/10.1016/j.scitotenv.2023.163567

Location	Type of Sample	Analytical Method	Pre-Treatment Method	MP Concentrations	Particle Size Distribution	Predominant Shape	Predominant Polymers	Reference
	Sep'2021-Feb'2022							
Patna, India (urban)	Passive sampling – wet deposition; stainless steel funnel; five month sampling period	Microscope, Nile Red, FESEM-EDX, FTIR	H_2O_2 (30%) for organic removal and $ZnCl^2$ for density separation	Urban - 1959.6 ± 205.0 MPs/m2/day Peri-urban - 1320.4 ± 126.0 MPs/m2/day	1.3 and 4623µm; mostly <50µm	Fibre	PET, PP	Parashar and Hait, 2023 https://doi.org/10.1016/j.jhazmat.2023.131883
Guangzhou, China (urban)	Active sampling – middle flow TSP sampler (KB-6120); 100L/min for 24hrs; Passive sampling – stainless steel funnel, wet and dry deposition; Jan-Dec'2021; samples collected twice a week	Stereomicroscope, µFTIR	-	0.01–0.44 items/m^3 Wet season - 0.19 ± 0.01 items/m3 Dry season - 0.15 ± 0.02 items/m^3	Suspended - 12.96 to 333.62 µm; mostly <30-50µm Deposited - 29.01 to 184.64µm; mostly <50-70µm	Fibre	PET, rayon	Yuan et al., 2023 https://doi.org/10.1016/j.scitotenv.2023.161839
Antarctic expedition cruise 2019-2020, mid-Northern Hemisphere to Antarctica (remote)	Active sampling – high volume sampler (TISCH); 1.2 m^3 min^{-1}; 48 h sampling; Passive sampling – quart fibres; during Chinese Antarctic expedition cruise 2019-2020	Stereomicroscope, µFTIR	-	0.020 to 0.048 n m^{-3}; 0.035 n m^{-3}	Fibres – avg length - 1004.8 ± 823.5µm and width - 49.8 ± 39.5µm. Fragments - lengths were 166.2 ± 88.6µm, and width - 99.3 ± 54.4µm	Fibres	Rayon, PS, PET	Chen et al., 2023 https://doi.org/10.1038/s41467-023-43695-0
Peninsular Malaysia (two urban sites, one remote)	Passive sampling – wet and dry deposition; stainless steel	Nile Red, µFTIR	Potassium hydroxide (KOH, 10 %) for organic removal and	114 to 689 MP/m^2/day	5-5000µm; mostly <5-50µm	Fibre, fragment	HDPE, PES	Hee et al. 20203 https://doi.org/10.1016/j.scit

Location	Type of Sample	Analytical Method	Pre-Treatment Method	MP Concentrations	Particle Size Distribution	Predominant Shape	Predominant Polymers	Reference
	funnel; two week sampling duration; Jan-Feb'22		$ZnCl_2$ (1.37 gcm^{-3}) for density separation					otenv.2023.166153
Quzhou Experiment Station, China (urban)	Passive sampling – wet and dry deposition; customised stainless steel funnel; over all four seasons; Aug'2020-Aug'2021	Nile Red, µFTIR	H_2O_2 (30%) for organic removal	Summer – 892–75,421 MP/m^2/day Spring – 735–9428 MP/m^2/day Autumn - 280–4244 MP/m^2/day Winter - 86–1347 MP/m^2/day	3.23-2645µm ; mostly 3-50µm	Fibres	Rayon, PET, PE	Li et al., 2023 http://dx.doi.org/10.1016/j.scitotenv.2023.162947
Plymouth, England (urban)	Passive sampling – deposition glass funnels; Active sampling – air pump with filter 70-100hr sampling duration; Nov-Dec'2021	Stereomicroscope, FTIR	-	Suspended - 0.016 to 0.238 items m^{-3}. Deposited - 0.47 to 3.30 m^{-2} h^{-1}	Suspended <100µm Deposited >500µm	Fibre	Rayon, PVA, PA	Kyriakoudes and Turner (2023) https://doi.org/10.1016/j.chemosphere.2023.140258
Seoul, South Korea (urban)	Active sampling – PM_{10} sampler; 16.7L/min; (KN-L25P1) 24hr sampling duration; July 2021	µFTIR	Lithium metatungstate (LTM, 1.6 g/mL) solution for density separation Fenton reagent and H_2O_2 (25%) for organic removal	0.33–1.21 MP m^{-3}; avg - 0.72 MP m^{-3}	24.38-2278.04µm; mostly <100µm	Fragment	PP, PET	Chang et al., 2023a https://doi.org/10.1016/j.envpol.2023.121481
Harbin, China (urban)	Active sampling – MiniVol particulate	Stereomicroscope, FTIR, SEM	-	1.76 MP/m^3	1->50µm; mostly <35µm	Fibre	PP, PET, PE	Liu et al., 2023a https://doi.org/10.1016/j.scit

Location	Type of Sample	Analytical Method	Pre-Treatment Method	MP Concentrations	Particle Size Distribution	Predominant Shape	Predominant Polymers	Reference
	sampler; 10±0.1L/min;							otenv.2023.166040
Manila, Philippines (urban)	Active sampling – dust sampler; 1.4 L/min; 12hr sampling duration; multiple sampling stations in Manila district; Dec'2021	Microscope, FTIR	-	9.11 ± 5.46 MP (per sampling station)	159–4807µm; mostly <1000µm	Fibre	PS	Romarate et al., 2023 https://doi.org/10.1007/s11356-023-26117-y
Sarakhs, Iran (rural, arid)	Passive – MWAC sediment catchers; soil samples with stainless steel sieves; July-Sep'2021	Microscope, µRaman, SEM. XRD (X-ray Diffraction)	H_2O_2 (30%) for organic removal and $ZnCl_2$ (1.6–1.8 g cm^{-3}) for density separation	450 g - 2600 MP m^{-2} d^{-1} 2630 MP m^{-2} d^{-1}.	20-1000µm; mostly <250µm	Fibre	PE, nylon, PP	Abbasi et al., 2023 https://doi.org/10.1016/j.chemosphere.2023.138150
Arizona, United States (suburban)	Active sampling – high volume sampler (TISCH); 1.13 m^3/min for 24 h; Oct'2020-Nov'2021	Microscope, µRaman	Fe (II) solution prepared from $FeSO_4$ and H_2O_2 (30%) for organic removal,	0.02 to 1.1 MP/m^3; avg. - 0.2 MP/m^3	5–5000µm; mostly 5-100µm	Fibre	PVC, PES, and PS	Chandrakanthan et al., 2023 https://doi.org/10.1016/j.atmosenv.2023.119617
Lanzhou City, China (urban, 23 sampling sites)	Passive sampling – wet and dry deposition; 11-12 days of sampling each season; four seasons March'21-Feb'22	Stereomicroscope, FTIR	$ZnCl_2$ (1.55 g/mL) for density separation	79.5 to 810.0 MP/(m^2·d)	<100-1000µm; mostly <500µm	Fibre	PA, PE, PET	Liu et al., 2023b https://doi.org/10.1007/s11356-023-27581-2
Ganges River, India and Bangladesh (10 sites)	Passive sampling – plastic funnel; May-June 2019	Microscope, FTIR	$ZnCl_2$ (1.55 g/mL) for density separation	41.12 MP/m^2/day^{-1}	30-1320µm	Fibre	Rayon, acrylic,	Napper et al., 2023 https://doi.org/10.1016/j.scit

Location	Type of Sample	Analytical Method	Pre-Treatment Method	MP Concentrations	Particle Size Distribution	Predominant Shape	Predominant Polymers	Reference
								otenv.2023.166640
Spain and Canary Islands (10 sampling sites, urban, suburban)	Passive sampling – wet and dry deposition; custom metal deposition collectors; monthly sampling duration;	Microscope, µFTIR	H_2O_2 (33%) for organic removal	5.6 to 78.6 MPs/m^{-2}/day^{-1}.	2- 398µm; avg - 71µm	Fibre	PES, acrylic, PP	Edo et al., 2023 https://doi.org/10.1016/j.scitotenv.2023.166923
Ahvaz, Iran (urban)	Active sampling – PM_{10} sampler; 1.3 m^3/min; 24hr sampling duration over four months	Microscope, µRaman	H_2O_2 (30%) for organic removal	0-0.017 MP/m^3	<100-1000µm; mostly <100µm	Fibre	PET, nylon, PP	Abbasi et al., 2023 https://doi.org/10.1016/j.jes.2022.02.044
Japanese coast and New Zealand North Island (urban, remote, coastal)	Active sampling – high volume sampler (V-RW); 1000 L/min; weekly sampling durations	Raman	-	0.14- 0.3 MP/m^3	5µm-100µm; mostly 10-80µm	Fibre, fragment	PE, PP, PS	Nagato et al., 2023 https://doi.org/10.1016/j.envpol.2023.122011
Beijing, China (urban)	Passive sampling – rainfall samplers,	µRaman	H_2O_2 (30%) for organic removal and $ZnCl_2$ (1.2g/mL) for density separation	7590–136,778 MP/m^{-32}	5-500µm; mostly <25µm	Fragment	PS, PE	Chen et al., 2023b https://doi.org/10.1021/acs.est.3c03474
Venice, Italy (urban)	Active sampling – high volume sampler (Air Flow PUF); 0.3 m^3 min^{-1}; 24hr sampling duration; summer and winter 2020	µFTIR	H_2O_2 (30%) for organic removal	15-21 MPs/m^3	7-96µm	Fragment	HDPE, PTFE	Rosso et al., 2023 https://doi.org/10.1016/j.envpol.2022.120889

Location	Type of Sample	Analytical Method	Pre-Treatment Method	MP Concentrations	Particle Size Distribution	Predominant Shape	Predominant Polymers	Reference
Birmingham, UK (indoor air, urban)	Active sampling – low-volume active air sampler; 6L/min^{-1}; Passive sampling – glass petri-dish; ; 24hr sampling duration; May-Sep'23	Stereomicroscope, FTIR	H_2O_2 (30%) for organic removal	Suspended - Homes - 15.6 ± 5.4 MP/m^3 ; Offices - 13.1 ± 6.5 MP/m^3 Deposition – Homes - 3735 ± 1343 MP/ m^2/day; Offices - 3177 ± 1860 MP/ m^2/day	10-100µm; mostly 10–25µm	Fibres	PET, PVC	Khalid Ageel, Harrad and Abdallah, 2023 https://doi.org/10.1016/j.envpol.2024.124960
Pristina, Kosovo (urban)	Passive sampling – wet and dry deposition; glass bottles; March'21	Microscope	H_2O_2 (30%) for organic removal	61.7-107.7 MPs/day	Mostly <2.5mm	Fragments	-	Cakaj et al., 2023 https://doi.org/10.3390/su152316464
Mumbai, India (Urban)	Passive Sampling – ceramic mug with distilled water; 24hr sampling period over 7 days	Nile Red; FTIR	H_2O_2 (20%) for organic removal and $ZnCl_2$ (1.6-1.8g/mL) for density separation	1036 ± 493 MP/person	Mostly <100-300 µm	Fragment	(did not use FTIR on air samples)	Yadav, Sethulekshmi and Shrivastav (2022) https://doi.org/10.1016/J.ENVRES.2022.113735
Bandung, Indonesia (urban)	Active Sampling – TSP high volume sampler3hr sampling duration (68.82 m3/h)	Microscope; Hot Needle Test	-	Urban - 86.52 ± 45.76 µ g/m3 Suburban - 154.30 ± 74.02 µ g/m3	Urban samples - 1000–1400µ; Suburban - 600–1000µ m.	Fibre	-	Syafina et al. (2022) https://doi.org/10.1016/J.CHEMOSPHERE.2022.136194

Location	Type of Sample	Analytical Method	Pre-Treatment Method	MP Concentrations	Particle Size Distribution	Predominant Shape	Predominant Polymers	Reference
Hangzhou City, China (Urban)	Deposition Sampling - Pigtail brush and stainless steel dustpan; 2-5 days	Microscope, FTIR	$ZnCl_2$ (1.7 g/cm^3) for density separation and H_2O_2 (30%) for organic removal	Residential apartments – Offices – Businesses – Dorms -	200-1000µm;	Fibre	PE, PP	Zhu et al. (2022) https://doi.org/10.1016/j.scitotenv.2022.155256
Muskoka-Haliburton, South-central Ontario, Canada (Remote)	Passive Sampling - stainless steel Teflon-coated sampler; Sampling every 3-48days for 13 months	Microscope; Hot Needle Test; µRaman	-	4-9 MP/m^2/day; avg 7 MP/m^2/day	20µm to 4980µm; mostly 200-600µm	Fibre	PA, PET	Welsh et al. (2022) https://doi.org/10.1016/J.SCITOTENV.2022.155426
Beijing, China (Urban)	Passive Sampling -PP, , anti-static brush and dustpan; sampling once a week – taken from different sites on different days	LDIR; FESEM (Field Emission Scanning Electron Microscopy)	ZnCl2 (1.7–1.8g cm^{-3}) for density separation; H_2O_2 (30%)	123.6 items/g (7.2 items/g to 481.39 items/g)	37.7µm to 95.78µm; 66.62µm average	Fragment	PP, PA	Liu et al. (2022) https://doi.org/10.1016/J.SCITOTENV.2022.155989
Mexico City, North America (Urban)	Active Sampling - PM_{10} and $PM_{2.5}$ samplers (BGI PQ200 FRM) ; 16.67 L min^{-1} for dry season (January–March) and wet (July–September)	Microscope; Hot Needle; SEM-EDX;FTIR	-	PM_{10} - 0.205 ± 0.061 MP/ m^{-3} for $PM^{2.5}$ -0.110 ± 0.055 MP/ m^{-3}	39 and 5000µm; mostly 39 and 500µm	Fibre	PE, PA, PET	Shruti et al., (2022) https://doi.org/10.1016/j.scitotenv.2022.157601
Shanghai, China (Urban)	Passive sampling – stainless steel bucket; 24hr	Microscope, µFTIR	-	469-12,611.46 MP/m^{-2}·d$^{-1;}$ avg - 261.22 ± 2847.99 P·m^{-2}·d^{-1}	31.72 to 4960.13µm; mostly <1000µm	Fibre	PAM PET, PP, PVF	Jia et al., (2022) https://doi.org/10.1016/J.SC

Location	Type of Sample	Analytical Method	Pre-Treatment Method	MP Concentrations	Particle Size Distribution	Predominant Shape	Predominant Polymers	Reference
	sampling period; April-July'21							ITOTENV.2022.157609
Tibetan Plateau (Remote)	Snowpit sampling; 21st May 2020; 16 samples 10cm intervals	Microscope, Raman and SEM	-	9.55 ± 0.9 L^{-1}	<200µm (43.33%)	Fibre	PVC, PPO (Poly(2,6-dimethyl-1,4-phenylene oxide)) Hydroxypropyl cellulose (HPC) (13.33%) and Hydroxypropyl methyl cellulose (HPMC); PVA, PB	Wang et al., 2022 https://doi.org/10.1016/J.ENVPOL.2022.119415
Antarctica (Remote)	Snow sampling – 19 samples from different locations Nov-Dec 2019	Microscope and µFTIR	Fenton's reagent for organic removal	294 ± 4.7 L^{-1}	200-1000µm (LOD = 50µm)	Fibre	PET, PMMA, PVC, PA	Aves et al., 2022 https://doi.org/10.5194/TC-16-2127-2022
Pic Du Midi Observatory, France (Remote)	Active Sampling – TISCH High Volume PM_{10} Sampler; sampling weekly over 4 months; f 7880 m^3 per sample	Microscope, µRaman	-	0.23 MP/m^3 (0.09–0.66 MP/m^3)	5-163µm; mostly <50µm	Fragment	PE; PS; PVC; PET	Allen et al., 2021 https://doi.org/10.1038/s41467-021-27454-7
South China Sea (remote, coastal)	Active sampling – atmospheric sampler (TISCH); 12-25hr sampling duration; Passive sampling – dry deposition; Oct-Nov'24	Stereomicroscope, FTIR	-	0.013-0.063 MP/m^3; avg. - 0.035 MP/m^3	50µm-2210µm; mostly - <200µm	Fibre	PES, rayon, PP, PE	Ding et al., 2021 https://doi.org/10.1016/J.ATMOSENV.2021.118389

Location	Type of Sample	Analytical Method	Pre-Treatment Method	MP Concentrations	Particle Size Distribution	Predominant Shape	Predominant Polymers	Reference
Beijing, Tianjin, Shanghai, Nanjing, and Hangzhou, China (urban)	Active sampling – middle flow PM sampler (LB-120F); 100L/min; Aug'-Sep'2019	Nile Red, µFTIR	H_2O_2 (30%) for organic removal;	104 to 650 MP/m^3 ; avg- 282 ± 127 MP/m^3	5.9-1475.3µm; mostly - <100µm	Fragment	PE. PE, PS	Zhu et al., 2021 https://doi.org/10.1021/acs.est.1c03618
Badain Jaran Desert, China (remote)	Sand samples – top 2cm; 12 sampling sites; July 2019	Stereomicroscope, µFTIR	NaCl solution (1.2 g/ml) for density separation	0.7 ± 1.5 to 11.7 ± 15.5 MP/kg, with an average of 6.0 ± 15.4 MP/kg.	40µm-5mm; mostly -50-200µm	Fragment	Epoxy resin, PET, phenoxy resin, PA	Wang et al., 2021a https://doi.org/10.1016/j.scitotenv.2021.149529
Ho Chi Minh City, Vietnam (urban)	Passive sampling – wet and dry deposition; 3-4 day sampling duration; glass funnel; June-May'2019	Stereomicroscope and FTIR	NaCl (1.18 ± 0.02 g cm^{-3}) for density separation and H_2O_2 for organic removal;	71-917 MP/$^{-2}$ d^{-1}	300-5000µm; mostly - ~100µm	Fibre	-	Truong et al., 2021 https://doi.org/10.1016/j.chemosphere.2021.129874
Qaqulluit National Wildlife Area, Nunavut, Canada (remote)	Passive sampling – glass petri dishes; 24-48hr sampling duration;	Stereomicroscope and Raman	-	2433 MP/day/m^2	80-5000µm; mostly >300µm	Fibre	PP, cellulose	Hamilton et al., 2021 https://doi.org/10.1016/j.scitotenv.2021.145536
Gdynia, Poland (urban, coastal)	Passive sampling – wet and dry deposition; glass funnel; weekly sampling duration; 2017-2018	Microscope, µFTIR	-	0-30 MP/m^{-2}·d^{-1} ; avg. e: 10 ± 8 MP/m^{-2}·d^{-1}	5-5000µm; mostly -750-900 µm	Fibre	PS, PP, PE, PVC	Szwec et al., 2021 https://doi.org/10.1016/j.scitotenv.2020.143272

Location	Type of Sample	Analytical Method	Pre-Treatment Method	MP Concentrations	Particle Size Distribution	Predominant Shape	Predominant Polymers	Reference
Mount Derak and Shiraz, Iran (remote and urban)	Passive sampling – wet and dry deposition; customised metal deposition collectors; Oct'-Sept'2020	Microscope, µRaman	H_2O_2 (30%) for organic removal and NaCl (1.6-1.8 cm^{-3}) for density separation	6-19 MP/day/m^2; avg. - 12 MP/day/m^2	<100->1000 µm; mostly <100 µm	Fibre	PP, PE, PS, PET	Abbasi and Turner 2021 https://doi.org/10.1016/j.scitotenv.2021.147358
Sydney, Australia (indoor, urban)	Passive sampling – glass petri dishes; 30 day sampling period; 2019	Stereomicroscope, fluorescence microscope, µFTIR	-	22-6169 MP/day/m^2; avg.-3095 MP/day/m^2	50-5000µm; mostly 200-400µm,	Fibre (only)	PE, PS, PA, acrylic, PS	Soltani et al., 2021 https://doi.org/10.1016/j.envpol.2021.117064
New Jersey, US (urban, indoor and outdoor)	Passive sampling (indoor) – quartz filter in glass petri dish; two-week sampling period; (outdoor) – wet and dry deposition; stainless steel funnels and glass jars; Active sampling (outdoor) – Thermo Air Sampler; PM_{10} - 1.67L/min; $PM_{2.5}$ - 15Lmin; April-May'2019	Stereomicroscope, µRaman, SEM-EDX	H_2O_2 (30%) for organic removal	1.29×10^4 to 2.56×10^4 MP/day/m^2; avg. - 327 ± 19 MP/day/m^2	Mostly 35µm-1000µm	Fragment, fibre	PS, PET, PVC, PE, PP	Yao et al., 2021 https://doi.org/10.1016/j.envres.2021.112142
Guangzhou, China (urban)	Passive sampling – wet and dry deposition;	Stereomicroscope, µFTIR	H_2O_2 (30%) for organic removal	51-178 MP/day/m^2; avg.	50-5000µm; fibres mostly 0.5-2mm;	Fibre	PET, PAN	Huang et al., 2021

Location	Type of Sample	Analytical Method	Pre-Treatment Method	MP Concentrations	Particle Size Distribution	Predominant Shape	Predominant Polymers	Reference
	stainless steel bucket; monthly sampling duration (22-40days) over one year			– 114±40 MP/day/m^2	fragments – 100-200µm; films – 1-2mm			https://doi.org/10.1016/j.jhazmat.2021.126168
Weser River catchment, Germany (urban and rural)	Active sampling – pump and filter system with cascade impactor; 9 L/min^{-1}; Passive sampling – total deposition; stainless steel funnel; 3 hr sampling duration;	µFTIR, µRaman	Fenton's reagent ($FeSO_4$ + H_2O_2), enzymatic digestion, and density separation with $ZnCl_2$.	Deposition - 98±85 MP m^2; Suspended – 91±47MP/m^3	4.1µm-5mm; mostly - 11-20 µm	Fragment	PP, PE, PET, PVC, PS	Kernchen et al, 2021 https://doi.org/10.1016/j.scitotenv.2021.151812
Kavir Desert, Iran (remote)	Soil sampling – top 5cm of soil with metallic trowel; Oct'2019-Aug'2020	Microscope, µRaman, SEM	H_2O_2 (30%) for organic removal and NaCl (1.6-1.8 cm^{-3}) for density separation	39-66 MP/300g of sand; avg-51 MP/300g sand	<100-1000 µm	Fibre	PET, nylon	Abbasi et al., 2021 https://doi.org/10.1021/acs.est.1c00615
Aosta Valley, Italian Alps (remote)	Snow sampling – 2L glass jars; 3 samples per sampling location	Stereomicroscope, µFTIR	NaCl (1.2 cm^{-3}) for density separation and H_2O_2 (30%) for organic removal	0.39-4.91 MP/L; avg - 2.32 MP/L	50-2000µm; avg- 339µm	Fibre	PE, PET, HDPE	Parolini et al., 2021 https://doi.org/10.3390/ijerph18020768
Collins Glacier, Antarctica (remote)	Snow sampling – collected plastic debris from glacier; every 10m; additional sampling every 12	Visual, µFTIR	-	0.17 to 0.33 items m^{-2}	2292-12,628µm	-	PS, PU	Gonzalez-Pleiter et al. 2021 https://doi.org/10.5194/tc-15-2531-2021

Location	Type of Sample	Analytical Method	Pre-Treatment Method	MP Concentrations	Particle Size Distribution	Predominant Shape	Predominant Polymers	Reference
	hours (dry deposition – no precipitation)							
Wenzhou, China (indoor and outdoor, urban and rural)	Active sampling – middle flow TSP sampler; 100L/min; 6 hour sampling duration	Nile red, μFTIR	H_2O_2 (30%) for organic removal	Indoor – avg- (1583 ± 1180 MP/m^3 Outdoor – avg. -- 189 ± 85 MP/m^3	5μm-5mm; mostly <100 μm	Fragment	PE, PA, PP, PS	Liao et al., 2021 10.1016/j.jhazmat.2021.126007
Atlantic Coast, France (Remote/Coastal)	Active Sampling – Vacuum Pump; 50L/min; Cloudwater Collector; 5.8m^3; sampling 24hrs;	μRaman	H_2O_2 (30%) for organic removal; Zinc chloride solution($ZnCl_2$,1.6 g/cm^3) for density separation	Onshore - 2.9 MP/m^3 Offshore – 9.6 MP/m^3 (0.02-19 MP/m^3)	2.5-300μm; mostly 5-10μm	-	LD/HDPE; PET; PS	Allen et al., 2020 https://doi.org/10.1371/journal.pone.0232746
Sonnblick, Austria (remote)	Snow samples – surface snow, 2cm, daily sampling	TD-PTR-MS	TD-PTR-MS treatment	0-220.5 ng/ml/day; 2 × 1011 NP/m^2/year	-	-	PET, PVC, PC	Materic et al., 2020 https://doi.org/10.1021/acs.est.9b07540
Beijing, China (Urban)	Active Sampling – Mini Volume Samplers; 5L/min; sampling 6-8hrs; dust sampling	SEM-EDX	-	5600 MP/m^3 (5600-5700 MP/m^3)	5μm – 2mm; mostly <20μm	Fibres	-	Li et al. 2020 https://doi.org/10.1016/j.scitotenv.2019.135967

Location	Type of Sample	Analytical Method	Pre-Treatment Method	MP Concentrations	Particle Size Distribution	Predominant Shape	Predominant Polymers	Reference
California, USA (Urban; Indoor/outdoor)	Active Sampling – Vacuum filtration; 11.7L/min; sampling 5 days	Microscope; Nile Red; µRaman; FTIR	Digestion and density separation (solutions not listed)	Indoor - 7.9 MP/m^3 (3-17 MP/m^3 fibres;2.7-8.3 MP/m^3 fragments) Outdoor - 8.33 MP/m^3 (fibres - 0.7-2.2 MP/m^3; fragments - 12.5-19.6 MP/m^3)	20->3000µm; Indoor - mostly 100-300µm fibres; <50µm fragments; Outdoor – mostly 100-300µm fibres; 76-100µm fragments	Fibres	PS, PET, PE	Gaston et al. 2020 https://doi.org/10.1177/0003702820920652
North Atlantic Ocean (Marine/Remote)	Active Sampling – Pump System; sampling 10-50hrs; 20 L/min	Microscope; µRaman	-	0.0112 MP/m^3 (0-0.079 MP/m^3)	5µm-5mm; mostly 17-175µm;		PS, PE, PP	Trainic et al. 2020 https://doi.org/10.1038/s43247-020-00061-y
Madrid, Spain (Rural; Sub-rural; Urban)	Active Sampling – Cargo Plane fitted with passive air intake sampling ≈4hrs;	Microscope, FITR	-	Rural - 1.5 MP/m^3 Sub-rural - 3.2 MP/m^3 Urban - 8.8 MP/m^3 (1.5-13.9 MP/m^3)	25µm - 5mm (9.8µm stated in paper but 25µm filter used); Mostly 30-70µm	Rural & Sub-rural – Fibres; Urban - Fragments	Rural & Sub-rural – PE; PA; Acrylic; Urban – PY; PS; PB	González-Pleiter et al. 2020 https://doi.org/10.1016/j.scitotenv.2020.143213
Bushehr port, Iran (Urban)	Active Sampling – TISCH high volume sampler; 1.4-1.6m^3/min; sampling 6 days;	Microscope; Nile Red; µRaman	H_2O_2 (30%) for organic removal and potassium iodide (KI, 1.6 g/cm^3) for density separation	Dusty - 2.1 MP/m^3 Calm - 10.3 MP/m^3 (0-14.2 MP/m^3)	<2.5-9500µm	Fragments	PET, PE, Nylon, PS, PP	Akhbarizadeh et al. 2020 https://doi.org/10.1016/j.eacnvres.2020.110339
London (Urban)	Deposition sampling – rain gauge, samples collected twice a week for 4 weeks	Microscope and µFTIR	H_2O_2 (30%) for organic removal	712 ± 162 m^2 /d	<100 (LOD = 5µm)	Fibre	PAN, PET, PA	Wright et al., 2020 https://doi.org/10.1016/j.env

Location	Type of Sample	Analytical Method	Pre-Treatment Method	MP Concentrations	Particle Size Distribution	Predominant Shape	Predominant Polymers	Reference
								int.2019.105411
Pearl River Estuary, South China Sea, Indian Ocean (Coastal/Remote)	Active Sampling – TSP Middle Flow Sampler; KB-120; 100L/min; sampling 10-48hrs;	Stereomicroscope; FTIR	H_2O_2 (30%) for organic removal	0.01 MP/m^3 (0-0.077 MP/m^3)	58-2252µm; mostly <851µm	Fibre	PET, PP	Wang et al., 2020 https://doi.org/10.1016/j.jhazmat.2019.121846
Shanghai, China (urban, indoor)	Passive sampling – stainless steel basins; 24hr sampling duration; Feb'-May 2019	Stereomicroscope, µFTIR	-	500 -24000 MP/day/m^2; 5880 MP/day/m^2	50-5000µm; mostly 50-2000µm	Fibre	PE, rayon	Zhang et al., 2020 https://doi.org/10.1021/acs.est.0c00087
Ho Chi Minh city landfill, Vietnam	Passive sampling – wet and dry deposition; glass funnel; wet and dry deposition	Microscope, FTIR	$NaCl_2$ (1.8 cm^{-3}) for density separation and H_2O_2 for organic removal	913-1801 MP/day/m^2; avg. - 1356.8 MP/day/m^2	100 - 5000µm; mostly – 100-500µm	Fibre	-	Thinh et al. 2020 https://doi.org/10.31276/vjste.62(3).83-89
North America (remote)	Passive sampling – wet/dry deposition collectors; monthly sampling duration over 14months	Microscope, FTIR	-	48-435 MP/day/m^2; avg. – 132 MP/day/m^2	4-3000µm; mostly - <25µm	Fibre	Polyolefin, PTFE, PE	Brahney et al. 2020 https://doi.org/10.1126/science.aaz5819
Idaho and Vermont, USA (suburban)	Passive sampling – lint traps for electric clothes dryers; snow sampling (top 2cm); stainless	Microscope	-	4344-35,627 MP/m^2 ; avg of sample sites - 404 ± 192 MP	-	Fibre (only)	-	Kapp and Miller 2020 https://doi.org/10.1371/journal.pone.0239165O

Location	Type of Sample	Analytical Method	Pre-Treatment Method	MP Concentrations	Particle Size Distribution	Predominant Shape	Predominant Polymers	Reference
	steel spoon and glass jars; Oct'2018							
Mt Everest, (remote)	Passive samples – snow samples, stainless steel containers; top 5cm of snow; April-May, 2019	Microscope, FTIR	-	3-119 MP/L^{-1}; avg - 30 MP/L^{-1}	18-5000µm	Fibre	PS, acrylic, nylon, PP	Napper et al. 2020 https://doi.org/10.1016/j.oneear.2020.10.020
Antisana glacier, Ecuadorian Andes (remote)	Passive sampling – glacier samples, surface sampling; metal sampler; Feb'2020	Microscope	NaCl (1.2g/m^3) for density separation	270 MP/250 snow 89.7MP/10x10m^2 ; avg. - 0.9 MP/m^2	60-2500µm	Fibre	-	Cabrera et al. 2020 https://doi.org/10.1016/j.cscee.2020.100051
Kusatsu (Japan), Da Nang (Vietnam), and Kathmandu (Nepal)	Passive sampling – street dust samples; vacuum cleaner 1 min each;	Stereo microscope, FTIR	H_2O_2 (30%) for organic removal and NaI (1.6 g/cm^3) for density separation	0.2-39.6 MP/m^2 Kusatsu - 2.0 ± 1.6 MP/m^2 in Da Nang 19.7 ± 13.7 MP/m^2 Kathmandu - 12.5 ± 10.1 MP/m^2	75µm-5mm; Kusatsu - 700-800µm; Da Nang – 400-500µm; Kathmandu – 400-500µm	Fragment	PE, PP, PS, PET	Yukioka et al 2020 https://doi.org/10.1016/j.envpol.2019.113447
Shanghai, China (urban)	Active Sampling - middle flow TSP sampler; 100L/min ;1 hr sampling duration	Microscope, FTIR	None	1.42 MP/m^3 (0-4.18M P/m^3)	23µm-5mm; mostly <1000µm	Fibres	PET, PE, PES	Liu K et al., 2019 http://dx.doi.org/10.1016/j.scitotenv.2019.04.110
Pyrenees (Remote)	Deposition sampling (rain sampler and NILU deposition tank); Nov 2017-	Microscope and µRaman	H_2O_2 (30%) for organic removal and $ZnCl_2$ for density separation	365 ±69 $m^{-2}d^{-1}$	≤50µm	Fragment	PS, then PE and PP	Allen et al., 2019 https://doi.org/10.1038/s415

Location	Type of Sample	Analytical Method	Pre-Treatment Method	MP Concentrations	Particle Size Distribution	Predominant Shape	Predominant Polymers	Reference
	March 2018; 12-34days							61-019-0335-5
Arctic (Remote)	Surface snow sampled on 5 ice floes; 2015-2017	Microscope and µFTIR	-	0 to 14.4 × 103 N liter^{-1}	<25µm (LOD = 11µm)	Fragment	PS, PVC, PC, PLA, PI	Bergmann et al., (2019) https://doi.org/10.1126/sciadv.aax1157
Sakarya Province, Turkey (Urban)	Active Sampling – air pump device; 9 m^3 (0.3m3/min); sampling 1/2hrs	Microscope; FTIR	H_2O_2 (30%) for organic removal and $NaCl_2$ (1.5–1.7g-cm^{-3}) for density separation	116-3424 MP/m^3	50µm-5mm	Fibres	PA, PS	Kaya et al. 2019 https://link.springer.com/article/10.1140/epjp/i2018-12372-7
Surabaya, Indonesia (Urban)	Active Sampling – Vacuum Pumps; 207.38 mL/min (Period I) and 446.93mL (Period II); every 2-3 days, not during rain events	Microscope, FITR	-	153 MP/m^3 (131-174 MP/m^3)	~500µm-5mm; mostly 1000-1500µm	Fibres	PET, Cellophane, PS	Asrin and Dipareza, 2019 http://dx.doi.org/10.12944/CWE.14.2.13
Asaluyeh County, Iran (Urban)	Active Sampling - PM ambient filter sampler; 16.67 L /min; sampling 24hrs; dust sampling	Microscope; SEM/EDS	H_2O_2 (30%) for organic removal and NaI (sodium iodide) for density separation	0.3-1.1 MP/m^3	100µm-1mm; mostly >100µm	Fragments	-	Abbasi et al., 2019 https://doi.org/10.1016/j.envpol.2018.10.039
Surabaya, Indonesia (Urban)	Active Sampling - 207.38 mL/min (for Period I)	Microscope, FITR	-	109 MP/m^3 (55.93-174.94 MP/m^3)	<500-5000µm; mostly 500-1500µm	Fibres	PET, PS	Syafei et al. 2019 https://doi.org/10.12944/cwe.14.2.13

Location	Type of Sample	Analytical Method	Pre-Treatment Method	MP Concentrations	Particle Size Distribution	Predominant Shape	Predominant Polymers	Reference
	446.93 mL/min (for Period II) for 3 days							
Lake Michigan, USA (Urban)	Active Sampling – battery powered pump; 3L/min; sampling 2-3days;	Microscope; FTIR; Raman	Fenton's reagent for organic removal and ZnCl2 (1.4 g mL^{-1}) for density separation	LOD<100µm (did not exceed background due to low LOD)	-	-	-	Peller et al. 2019 https://doi.org/10.1039/c9em00193j
Western Pacific Ocean (Shanghai - Mariana Islands) (coastal/remote)	Active Sampling – TSP Middle Flow Sampler; KB-120; 100L/min; sampling 4-14hrs	Stereomicroscope; µFTIR	-	0.01 MP/m^3 (0-1.37 MP/m^3)	20µm-2mm; mostly/avg.318 µm	Fibre	PET, epoxy-resin (EP), PE, PP	Liu et al., 2019a https://doi.org/10.1021/acs.est.9b03427
Shanghai (Urban)	Active sampling – middle flow sampler (KB-120F); 100L/min; Jan-Feb 2019; samples collected 2 per week for 4 weeks	µFTIR	-	1.42 ± 1.42 n/m^3	<1000µm (LOD = 23µm)	Fibre	PET, PE, PES, PAN, PAA	Wang et al., 2019 https://doi.org/10.1016/j.scitotenv.2019.04.110
Hamburg, Germany (urban, remote, city)	Passive sampling – bulk deposition collectors; sampled twice a week Dec'2017-March 2018	Nile Red, µRaman	Sodium hypochlorite solution (NaClO 6-14%) for organic removal	25-800 MP/day/m^2; forest - 428 MP/day/m^2; rural - 331 MP/day/m^2; city - 215 MP/day/m^2	63µm-5mm; fragments <63µm; fibres – 300-5000µm	Fragment	PE, EVA	Klein & Fischer, 2019 https://doi.org/10.1016/j.scitotenv.2019.05.405
Forni Glacier, Italian Alps (remote)	Passive sampling – supraglacial debris collected in glass jars; July 2018	Visual, µFTIR	NaCl (1.2 g cm^{-3}) for density separation and	37-137 MP/kg^{-1} ; 74 MP/kg^{-1} of sediment	16-1695µm;	Fibre	PS, PAM PE, PP	Ambrosini et al., 2019 https://doi.org/10.1016/j.env

Location	Type of Sample	Analytical Method	Pre-Treatment Method	MP Concentrations	Particle Size Distribution	Predominant Shape	Predominant Polymers	Reference
								pol.2019.07.005
Edinburgh, UK (urban, indoor)	Passive sampling – adhesive pads in petri dishes; 20 min sampling period	Nile Red, FTIR	Digestion and organic removal and NaCl for density separation	2315-23148 MP/m^2; avg. - 6944 MP/m^2	0.2 and > 2 mm length;0.01–0.05 mm thickness.	Fibre (only)	PET, PUR	Catarino et al., 2018 https://doi.org/10.1016/j.envpol.2018.02.069
Paris, France (Indoor and Outdoor, Urban)	Active Sampling –Stand-alone sampling pump GH300,Deltanova; Indoor - 8L/min; sampling 4-10 hours; Outdoor - 5–20 m3 at 8L/min; sampling 4-7 hours	Microscope, FTIR	$ZnCl_2$(1.6 g/cm^3) for density separation and H_2O_2 (30%) for organic removal	Indoor - 5.4 MP/m^3 (0.4-60.0 MP/m^3) Outdoor - 0.9 MP/m^3 (0.3-1.5 MP/m^3)	50µm-5mm ; mostly 50-250µm	Fibres	PA, PP, PP, PE	Dris et al., 2017; https://doi.org/10.1016/j.envpol.2016.12.013
Tehran, Iran (urban)	Passive sampling – street dust samples; anti-static wooden brush; 2 months of sampling;	Fluorescence microscopy, SEM-EDX	H_2O_2 (30%) for organic removal and $ZnCl_2$ solution for density separation	88-605 MP/30g dust; avg. - 276 MP/30g dust	100µm-1mm; mostly 250-500µm	; mostly - 250 to 500µm	-	Dehghani et al., 2017 https://doi.org/10.1007/s11356-017-9674-1
Bushehr, Iran	Passive sampling – road dust samples; plastic pan and brush; Sept'2014	Fluorescence microscopy and polarized light microscopy (PLM)	H_2O_2 (30%) for organic removal and NaI for density separation	210-1658 MP/10g dust; 745 MP/10g dust	<100->1000 µm; mostly 250-500µm	Fibre	-	Abbassi et al., 2017 https://doi.org/10.1007/s12665-017-7137-0
Dongguan, China (urban)	Passive sampling – dry and wet deposition, glass	Microscope, µFTIR, SEM	-	175–313 MP/m^2/day	<200-4200µm	Fibre	PE, PP, PS	Cai et al., 2017

Location	Type of Sample	Analytical Method	Pre-Treatment Method	MP Concentrations	Particle Size Distribution	Predominant Shape	Predominant Polymers	Reference
	bottle; monthly Oct'-Dec'21							https://doi.org/10.1007/s11356-017-0116-x
Paris, France (urban)	Passive sampling – wet and dry deposition; stainless steel funnel; Feb'2014-March 2015	Stereomicroscope, FTIR	-	2.1–355.4 MP/m^2/day	50-600µm; mostly 200-600µm	Fibre	Rayon, PET, PA	Dris et al., 2016 https://doi.org/10.1016/j.marpolbul.2016.01.006

Appendix II. Draft copy of manuscript comparing analytical methods used in microplastic research

(which the author of this thesis co-wrote alongside this research)

Appendix II has been removed from this version of the thesis for copyright reasons.

Appendix II has been removed from this version of the thesis for copyright reasons.

Appendix II has been removed from this version of the thesis for copyright reasons.

Appendix II has been removed from this version of the thesis for copyright reasons.

Appendix II has been removed from this version of the thesis for copyright reasons.

Appendix II has been removed from this version of the thesis for copyright reasons.

Appendix II has been removed from this version of the thesis for copyright reasons.

Appendix II has been removed from this version of the thesis for copyright reasons.

Appendix II has been removed from this version of the thesis for copyright reasons.

Appendix II has been removed from this version of the thesis for copyright reasons.

Appendix II has been removed from this version of the thesis for copyright reasons.

Appendix II has been removed from this version of the thesis for copyright reasons.

Appendix II has been removed from this version of the thesis for copyright reasons.

Appendix II has been removed from this version of the thesis for copyright reasons.

Appendix II has been removed from this version of the thesis for copyright reasons.

Appendix II has been removed from this version of the thesis for copyright reasons.

Appendix II has been removed from this version of the thesis for copyright reasons.

Appendix II has been removed from this version of the thesis for copyright reasons.

Appendix II has been removed from this version of the thesis for copyright reasons.

Appendix III. Manuscript published in Environmental Science: Advances which is a systematic highlighting the need for more research into understanding individual motivation for plastic use which was written by the author of this thesis

Environmental Science Advances

ROYAL SOCIETY OF CHEMISTRY

PERSPECTIVE

View Article Online
View Journal | View Issue

Check for updates

People, plastic, and behaviour change – a comment on drivers of plastic pollution, barriers to change and targeted behaviour change interventions†

Anna MacDonald [a] Deonie Allen Lynn Williams Paul Flowers Tony R. Walker

There are many studies considering the use and waste management of plastics but these are primarily focused on recycling. While studies of human interaction with plastics provide some insight into current waste creation and recycling choices, studies on behaviour change and the human relationship to plastic are limited. In this perspective, we pose that understanding individual and community behaviour change is key to determining effective and sustainable drivers of change in the use of plastics. A review of contemporary literature highlights this as a knowledge gap, with only a few studies undertaken which have primarily focused on the theory of planned behaviour and plastic waste. To help support more sustainable and effective plastic use and waste management policy, it is recommended that future research focus on behavioural aspects of the plastic–people relationship with a focus on the Behaviour Change Wheel and the Capability, Opportunity and Motivation model (COM-B), to advance current understanding of individuals' behaviours relating to plastic use and waste. It is suggested that understanding the behavioural elements of the people–plastic relationship is fundamental to identifying effective and sustainable changes in behaviour and the guidance, policies, opportunities, and restrictions that can help achieve change

Environmental significance

The challenge of addressing the creation of plastic waste and plastic pollution is complex and is routed in people's relationship with plastic. Plastic still follows a linear economy at present; hurdles in shifting to a more sustainable and circular economy include difficulties changing people's behaviour. However, the factors driving people's plastic behaviour are understudied, especially through a human behaviour change lens. This perspective paper presents a focused literature assessment identifying that knowledge gap in plastic pollution and the confrontation of the plastic waste problem using behaviour change theories and tools. Specifically, it identifies the potential beneficial implementation of the behaviour change wheel and COM-B tools in identifying plastic behaviour factors and future targeted intervention design.

Cite this:
Environ. Sci.:
Adv., 2023, 2,

Received 12th October 2022
Accepted 20th February 2023

DOI: 10.1039/d2va00248e

rsc.li/esadvances

© 2023 The Author(s). Published by the Royal Society of Chemistry

Open Access Article. Published on 06 March 2023. Downloaded on 9/4/2025 3:13:06 PM.
This article is licensed under a Creative Commons Attribution 3.0 Unported Licence.

Open Access Article. Published on 06 March 2023. Downloaded on 9/4/2025 3:13:06 PM.
This article is licensed under a Creative Commons Attribution 3.0 Unported Licence

Introduction

Impacts of plastic pollution on environmental and potentially human health are well-reported.[1–3] Both larger items (macroplastics) and smaller plastic particles or microplastics (MPs) are becoming more of a public concern due to increasing media attention and public policy.[4–6] Although systemic change is needed to address the current plastic waste problem and its consequences, complementary individual action is also necessary to reduce waste, prevent pollution and decrease exposure to raising awareness of its impact, or introducing restrictions.[7] The implementation of behaviour change models and methods to date have resulted in only a small step rather than a systematic change or significant individual shift in people's relationship to plastic. The significant changes needed to tackle the growing plastics problem have been slow and increasing awareness of the issue has not been found to result in action. A large shift in a broad range of plastic-related behaviours is needed. To implement individual level behaviour change in relation to plastic use, it is logical to understand the science of behaviour change, an understanding that has been predominantly missing in the plastic pollution discourse.

To simplify the use of behaviour change theories in designing behaviour change interventions, various behaviour change tools have been developed. These tools are used extensively in the context of public health (e.g., to examine the drivers of vaccine hesitancy) and therefore hold promise for potential effective use in addressing the plastic pollution problem. One prominent behaviour change framework is The Behaviour Change Wheel (BCW)[8,9] (see Fig. 1). This model is based on the synthesis of 19 existing behaviour change frameworks and provides a comprehensive and systematic meta approach to designing behaviour change interventions.

At the centre of the BCW is the Capability, Opportunity and Motivation model (COM-B) model[8,9] (see Fig. 2). The COM-B model describes behaviour as the interaction between an individual's capability, opportunity, and motivation to engage in the behaviour with six components that drive behaviour (i.e., physical capability, psychological capability, physical opportunity, social opportunity, reflective motivation, and automatic motivation).

These COM-B components are linked to intervention functions (i.e., education, persuasion, incentivization, coercion, training, enablement, modelling, environmental restructuring, restrictions) through which an intervention can change behaviour, and seven broad policy categories (i.e., guidelines, environmental/social planning, communication/marketing, legislation, service provision, regulation, fiscal measures). Intervention functions are then linked to behaviour change techniques (BCTs), which are the observable, replicable, and irreducible active ingredients of an intervention[9,10] (see Fig. 1). While we know that these tools have been used extensively in the health field to achieve positive and effective behaviour changes towards behavioural health issues

(e.g. language development, rehabilitation participation, behaviour change for disease prevention through exercise and diet change, vaccine acceptance and uptake, see ESI†), the current paper will explore their use within the context of plastic-related behaviours.

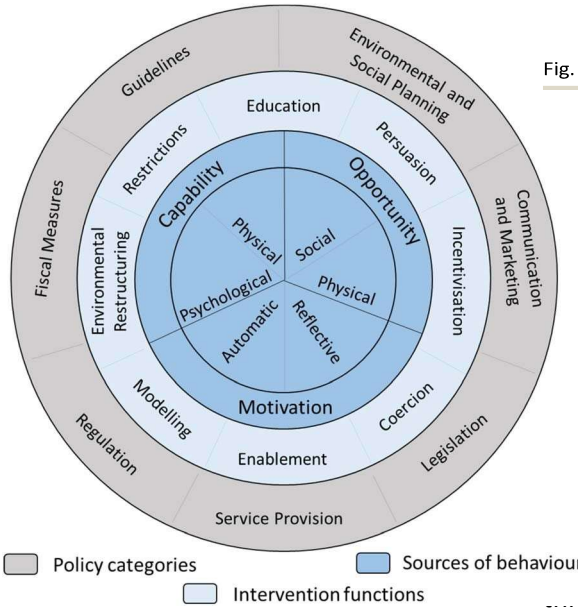


Fig. 1 The Behaviour Change Wheel (modified from Michie et al. 2011).

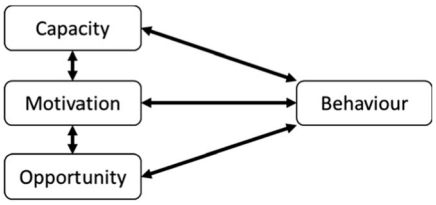


Fig. 2 COM-B System of Behaviour Change (modified from Michie et al. 2011).

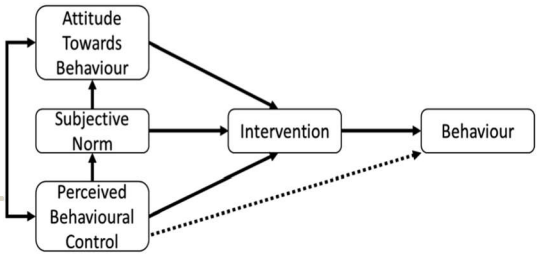


Fig. 3 Ajzen's Theory of Planned Behaviour (Ajzen 1991).

e theory that has been used within the rature on pro-environmental behaviour is en's theory of planned behaviour (TPB).[11] ough this theory and its constructs can ily be subsumed within the BCW and M-B approach it is worth considering it arately because of its predominance hin the field. TPB posits that engaging with ehaviour can be predicted by one's ntion to engage in that behaviour. ntion is determined by interaction of ee variables: attitude; subjective norms; and perceived behavioural control (PBC)[12] (see Fig. 3).

This perspectives paper aims to explore the extent of the contemporary literature on behaviour change and plastic related behaviours and highlight the opportunity to consider behaviour change models such as COM-B, BCW and TPB in addressing the plastic pollution problem. This study makes a tentative step towards identifying what behaviour change concepts and theories have been used to study the use of individual plastic consumption, the use of plastic and waste behaviours. A non-exhaustive literature review was conducted to establish the extent

© 2023 The Author(s). Published by the Royal Society of Chemistry

of the literature that has been published on this matter to-date and to identify gaps in knowledge which could form the basis for future research in this area.

Methodology

A keyword search was completed using SCOPUS, employing a range of terms relating to plastic and behaviour change (Fig. 4). The aim of the high-level scoping literature search was to identify relevant contemporary studies on behaviour change elements, plastic, and general pollution. Results are shown in Table 1, presenting the numbers of papers with titles, abstract or keywords associated with the 'main' and 'sub category' keywords entered into the SCOPUS keyword search. A Scopus search for each individual combination of main and sub

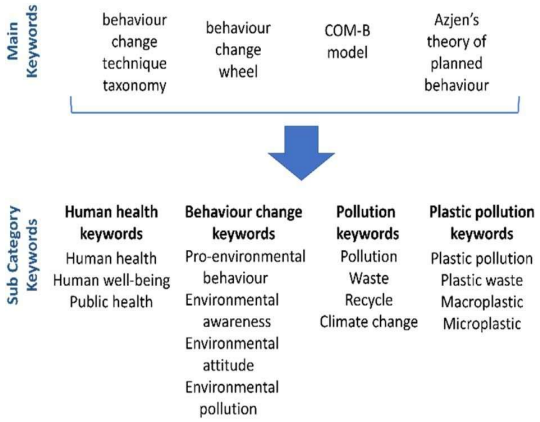


Fig. 4 Flow diagram showing keywords and resulting subcategory words from SCOPUS search.

category keywords was conducted and the resultant papers recorded (see ESI†) to determine the current use of these four main behaviour change models and tools relative to both plastic specific (plastic pollution keywords) and pollution, behaviour and human health research. The search was completed on 16/ 03/2022 and included all results published in peer reviewed journals up to this date. The studies found during this search were checked manually to ensure they were relevant, peer reviewed studies.

As can be observed, most of the literature is biased towards the use of Ajzen's TPB across all subcategories investigated, with only a few papers utilising other behavioural change models and theories, such as COM-B and BCW in relation to plastic, waste management or pollution (**Table 1**). The literature search identifies a knowledge gap and research need for plastic pollution studies to address the human–plastic relationship from a behaviour change lens to identify why people use and waste plastic and what creates or potentially can change this relationship.

		Main key words			
Category Keywords	**Sub category keywords**	**Behaviour change technique taxonomy**	**Behaviour change wheel**	**COM-B model**	**Azjen's theory of planned behaviour**
Plastic pollution	Plastic pollution	0	0	0	9
	Plastic waste	0	6	1	28
	Macroplastic	0	0	0	0
	Microplastic	0	2	0	0
Pollution	Pollution	3	20	7	171
	Waste	5	23	6	389
	Recycle	0	0	69	127
	Climate change	13	37	2	183
Environmental behaviour	Pro-environmental behaviour	0	3	1	275
	Environmental awareness	4	13	12	244
	Environmental attitude	12	37	20	1050
	Environmental pollution	2	9	4	122
Human health	Human health	298	373	317	3474
	Human well-being	12	16	10	78
	Public health	72	104	87	699

© 2023 The Author(s). Published by the Royal Society of Chemistry

There are more papers published that have included behaviour change principles in the context of environmental awareness and pollution (e.g. Barker et al.'s discussion on consumer behaviour change for food waste prevention,[13] Kolodko et al.'s assessment of the BCW method to modify UK littering behaviour,[14] or Lasrado and Zakarina's examination of BCW organisational factors that influence environmental attitudes and self-initiated green behaviour[15]) than directly focus on plastic pollution, and although there will be relevant discussion to plastic-related behaviours within these topics, for the purposes of this initial review, only papers specifically associated with plastic and plastic waste have been included in the plastic pollution publication counts. The general litter and pollution based behaviour change research can provide useful lessons and insight into the potential success of implementing the BCW, COM-B and TPB models to the plastic pollution problem. Potential early translatable findings include the identification that awareness does not translate to action of behaviour change effectively and that incohesive small reward driven interventions do not consistently result in long-term significant behaviour change.

Although the literature on this subject to date is not extensive, there have been interesting observations and findings from the existing studies on behaviour change and plastic related behaviour.

Plastic, waste management and behaviour change

Plastic-related behaviours

It is known that plastic is closely related to many aspects of modern life and therefore there are many behaviours that may encourage or modify the use of plastic. Therefore, plastic related behaviours encompass a range of actions from waste reduction, waste management and responsible consumption through to individual and societal valuation of the product or material. Most of the studies found during this scoping literature search published to date that examine behaviour change in relation to plastic focus on waste management behaviours and recycling. For example, 196 (11 of these with 'recycle' in the title) out of 4932 studies (the total identified through the Scopus search for all main + sub category searches) focused on recycling as the subject of their study (Table S1, ESI†). Although this is an important part of preventing plastic mismanagement, waste management and recycling are only a fragment of the behaviours which need to be addressed to reduce plastic waste, plastic pollution and plastic environmental and human exposure. Behaviours which reduce the production, purchase, use and waste and behaviours which promote the move towards a more circular economy are also to be encouraged. However, there is a large gap in knowledge about what is known about behaviour change and current plastic-related behaviours.

© 2023 The Author(s). Published by the Royal Society of Chemistry

Open Access Article. Published on 06 March 2023. Downloaded on 9/4/2025 3:13:06 PM.
This article is licensed under a Creative Commons Attribution 3.0 Unported Licence

Ajzen's theory of planned behaviour

Ajzen's TPB is one of the most utilized behaviour change theories in relation to plastic and pollution. Despite a general agreement on the applicability of the TPB in predicting plastic elated behaviour change,[16–23] there was is a lack of consensus on which of the elements of TPB – PBC, subjective norms or attitude – have the most influence on plastic-related behaviour change. For some studies the findings suggested PBC was the most important in plastic behaviour change,[24–27] for others it was subjective norms,[28,29] and others it was attitude.[29,30] However, these studies took place in a range of locations with varying cultural approaches to waste management, and varying access to recycling facilities. This cultural and facilities inconsistency could explain the varying degrees of influence of these elements of the TPB, or it could be said that the TPB is too linear in single element focused in its approach. It is expected that different cultural and societal norms will play into plastic related behaviour change, therefore a model with a more variable and flexible approach might be better applied to plastic elated behaviour change research.

Other studies used extended versions of TPB and included elements such as environmental awareness,[22,24,25] habit[17,31] and social norms,[16,31,32] which were all found to be significant in predicting behaviour change. This further emphasises the need for a more extensive model to examine plastic behaviour change. Habit is defined as a "response automatically triggered by the perception of relevant context cues" (Wood, 2017: p. 389).[33] Therefore, relevant social and cultural cues are important for influencing individual behaviour change, especially if the behaviour change is to become more permanent and automatic, and should be factored into considerations on plastic related behaviour change.

COM-B model

The COM-B model consists of three conditions necessary to complete a behaviour. These include capability, which consists of psychological or physical ability; opportunity, which comprises the physical and social environment needed; and motivation, which includes reflective motivation.[8] Only one study was identified during this scoping search that utilised this model to assess plastic-related behaviour, Allison et al. (2021) (Table 1, main keyword = COM-B, category keywords from the plastic pollution list).[34] Allison et al. (2021) surveyed participants on their willingness to purchase bio-degradable compostable plastic packaging (BCPP) to identify barriers and enablers. Survey responses were then organised according to the COM-B model.[34] For example, psychological capability included understanding the terminology of plastics and their labelling and understanding the plastic problem; physical opportunity consisted of access to the correct waste management and shopping environment; and social opportunity included social norms. Finally, automatic motivation and reflective motivation included environmental concerns and believes about the impacts of biodegradable plastics. The focus on

biodegradable and compostable plastic may be inconsistent with current thinking on the importance of the circular economy rather than replacing one waste problem with another, but this paper provides valuable insights. For example, this paper highlights the conditions that affect individual-level behaviour change in relation to plastic. This study identifies the main barriers and enablers in terms of psychological capability are understanding terminology and awareness of the plastic waste problem; within physical opportunity: the shopping environment, access to products, and access to waste management; and within social opportunity: social norms; and finally, within reflective motivation: environmental beliefs and concerns, and beliefs about capability. This tells us that to influence willingness to change behaviour there needs to be access to an environment where alternatives are readily available, the social norms need to be aligned with this change, and their needs to be an environmental awareness and capacity for the individual to make the change.

Perceptions and attitudes towards plastic

Understanding individual perceptions of plastic is a useful starting point in understanding and potentially changing people's relationship and behaviour associated with plastic, as it indicates whether plastic is viewed as a convenient part of modern life or if the increased attention on the environmental impact and human health consequences have altered perceptions. Heidbreger et al. (2019) reviewed 187 studies focused on relevant 'plastic pollution' and 'pollution' and found that the perception of plastic had changed, especially in relation to its impact on health with people becoming more aware of the plastic problem.[35] However, as found in many studies including Heidbreger et al. (2019) behaviour does not always follow awareness and this is definitely true with regards to the plastic pollution problem. It appears most individuals consider the impact of packaging at the point of disposal rather than pre purchase despite education and awareness campaigns.[35] This is consistent with research on consumer preferences for biodegradable packaging.[34] Most recently the COVID-19 pandemic and its associated health and safety concerns have changed the function and perception of many plastic and single-use plastic (SUP) products. The increase in awareness of public health and viral transmission, combined with the many restaurants offering more takeaway services during the international lockdown, and the temporary rejection of reusable items by some retailers due to safety concerns, has resulted in both an increase in use of SUPs and shift in public perception of plastic towards a hygienic and healthy product rather than a pollutant, thus limiting an individual's opportunity to make a change to reduce their use of plastics.[36]

Food hygiene and environmental awareness have been highlighted as important but opposing views influencing plastic behaviour. Studies have identified food hygiene as a priority and an associated willingness to pay for biodegradable alternatives,[37] reflecting the importance of motivation, while other studies suggest environmental concerns are more pertinent and that participants are less willing

© 2023 The Author(s). Published by the Royal Society of Chemistry

Open Access Article. Published on 06 March 2023. Downloaded on 9/4/2025 3:13:06 PM.
This article is licensed under a Creative Commons Attribution 3.0 Unported Licence

to pay for alternatives, but participants would still prefer this to outright bans.[38] Behaviours associated with single-use items are not seen as the focus of SUP reduction but rather the material itself, and that despite a high level of awareness participants are not willing to change their purchasing behaviours to reduce plastic.[39] Similarly, ease of access to recycling information has not been shown to directly relate to appropriate disposal of plastic waste or recycling actions.[40] Awareness and information are not the sole drivers of plastic-related behaviour change, but merely a starting point.

Social patterning

There is a general consensus within published research regarding the influence of sociodemographic factors on the behaviours and attitudes associated with plastic. This consensus identifies that sociodemographic factors such as age, gender, marital status, education and income determine the uptake of anti-plastic behaviours and attitudes, and also the implementation of plastic reduction policies.[41–45] Similarly, the influence of education on plastic and related behaviours suggests individuals of a younger age will have a more effective long-term impact and participate in anti-plastic behaviour, given the importance of socialisation in the attitudes we form.[42]

Many of the studies utilising TPB also investigated the role of gender, but there was no consensus or consistency in inclusion of the gender element. Although it can be argued that examining the differences in gender may lead to a gendered approach to behaviour change,[46] in order to produce targeted behaviour change interventions the role of gender and factors like ethnicity and income may be important to consider. Such targeting logic could also be applied to a wider range of variables (including class, ethnicity, income) to help advance the understanding social patterning, individual or community– plastic interaction and production of targeted interventions. To effectively unpick the influential elements on plastic pollution and use behaviour and identify potential intervention strategies there is a need for individual and multiple factor analysis.

Drivers, obstacles and potentials for research and policy

Convenience culture is one of the main drivers of plastic associated behaviours. This was most apparent in the literature on the perceptions of plastic and in relation to the increase in takeaway culture with COVID-19. Within behaviour change literature, it is known that the ease by which a behaviour can be changed affects the success of interventions. Therefore, successful behaviour change interventions associated with plastic will need to ensure that accessing reusables or sustainable alternatives is just as easy, if not easier than using traditional (single use, SUP) plastic. Ideally, circular approaches (a shift from produce-use-dispose to reduce, reuse, repair, remanufacture, recycle,[47] potentially incorporating elements such as upcycling of plastic waste[48] and implementation of production/waste management policies and regulations[49]) would

be the most accessible and affordable option. Additionally, socio-demographic factors were also identified in the literature, although the degree to which this drives plastic pollution is not established. However, it appears that targeted behaviour change interventions (e.g. by gender, ethnicity, income) are recommended by most studies and this is an interesting avenue for future research.

One of the main obstacles to reducing use of SUP during COVID-19 related to food safety and hygiene concerns, leading to increased SUP use of personal protection equipment (e.g., masks, gloves hand gel, and visors), and food and drinks containers. This is considered an obstacle, as many individuals still perceive a risk with reusable items, and the COVID-19 situation will continue the use of several SUP items for a considerable period. Habit was also identified as an obstacle. This is closely related to our current convenience culture and has been considered as a barrier. Finally, money is another major obstacle in terms of plastic behaviour change, in relation to both the costs associated with behaviour change (by the individual, producers and industry, waste managers and governance bodies) and the policy change required (e.g. the increased cost of plastic construction if regulations require circular economy future reuse/repair/remanufacture to be incorporated in product design; implementation of a plastic levy on plastic use or tax to cover end-of-life costs).[49,50]

However, despite these drivers and obstacles, there are some opportunities for change. COVID-19 could also be an opportunity for change. As the COVID-19 situation continues to evolve, there are opportunities for regime and habit change to be introduced. Also, it is hoped that as the health and safety situation improves this will provide more opportunities for single use items to be reduced. Education is also another theme which arose within the literature. Many of the papers reviewed here recommended education to individuals of all ages. This is especially pertinent as there appears to be situations of misinformation in relation to plastic and the sustainability of biodegradable alternatives. Part of this education could involve de-marketing. This is when a company uses negative messages to discourage demand for a certain product, and has been used for health behaviours, such as tackling obesity.[51] It has also been included in work on behaviour change in relation to antibiotic misuse[52] and sustainable tourism[53] (behaviour changes identified using one of the 3 behaviour models; BCW, COM-B, TPB). Raab et al. (2022) found that it was successful in motivating a reduction in SUP consumption amongst tourists in Canada. This was especially true for those with a stronger recycling attitude, individual commitment, and responsibility.[54] Future research could look to the use of negative messaging within other contexts as it may be more suited to individuals that already have a sense of responsibility for their plastic consumption. Although this review did not focus on pro-environmental behaviour elements of it appeared in the literature, for example, the importance of social norms and locus of control in motivations behind behaviour change.[55] Future research could look at what lessons can be learned from pro-environmental behaviour change for potential

© 2023 The Author(s). Published by the Royal Society of Chemistry

Open Access Article. Published on 06 March 2023. Downloaded on 9/4/2025 3:13:06 PM.
This article is licensed under a Creative Commons Attribution 3.0 Unported Licence

transfer or insight into positive change in the people–plastic relationship and individual plastic behaviour.

Limitations

This paper acknowledges that this review is not systemic or extensive. As stated in the methodology, this search was limited to papers mentioning 'plastic' but this subject area is related to pollution, waste, recycling and litter or specific consideration of 'micro-' or 'macro-' plastic. This may have resulted in some relevant papers being missed or excluded during the search. In addition, only studies published in the English language were included which will have limited the scope of this search and will have caused some bias in the selection of studies covered in this article. A full systemic review is recommended, including an extended selection of terms and investigating papers not directly associated with plastic.

Conclusions

There needs to be multi-level and systemic change to alter our relationship with plastic. Fundamentally this must include individual change. Clarity regarding a range of new behaviours to be adopted must be central moving forwards. Although recycling is important for the public, more focus needs to be placed on specifying, understanding and promoting circular behaviours, detailing waste reduction behaviours, and for manufacturers, providing reusable alternatives, rather than biodegradable ones. The creation of new habits, routines and social norms based around these diverse behaviours will help facilitate a cultural move away from plastic. Previous literature has focused too much on behaviours associated with plastic after it has been purchased and used, rather than behaviours at the beginning of the plastic life cycle. This paper acknowledges that to create individual-level behaviour change individual facing interventions are required. However, it is important to acknowledge that not all individuals are the same and that the barriers and facilitators to individual behaviour change are socially patterned (e.g. by gender, class and ethnicity).

There are many drivers and influences of plastic-related behaviour, including habit, convenience, and culture, and therefore a nuanced approach is necessary (i.e. not considering individual drivers, obstacles or the effectiveness of individual opportunities or actions in isolation). The BCW system with the COM-B model at its core, provides such a nuanced approach and could help identify and guide effective interventions that include mechanisms and policies that could help generate or positively influence behaviour change.

The SCOPUS search shows that there is a lack of research on the BCW in relation to plastic and this needs to be expanded in future research. It is also clear that raising awareness of the plastic problem is not sufficient on its own in instigating behaviour change. Future research should seek to investigate which targeted interventions would work best in different cultural and demographic contexts. Policy also needs to

ensure there is a physical environment where access to reusables, alternatives and waste management is easy, so the convenience of SUP is shifted. A social environment also needs to exist where social norms and culture dictate that reducing plastic waste is a norm to be upheld.

Author contributions

LW, DA and AM: conceptualization, resources, methodology, data curation, investigation, writing – original draft, all authors: writing – review & editing.

Conflicts of interest

There are no conflicts to declare.

Acknowledgements

This research was funded by the UKRI NERC discipline hopping for environmental solutions grant (2022). The authors would like to thank the EPSRC doctoral scholarship EP/T517938/1 for their support of Anna MacDonald, the Natural Sciences and Engineering Research Council of Canada (NSERC), Grant/Award Numbers RGPIN-2018-04119 for support of Tony R. Walker and the Leverhulme Trust, grant ECF-2019-306 for their support of Deonie Allen. This project has received funding from the European Union's Horizon 2020 research and innovation programme under the Marie Skłodowska-Curie grant agreement no. 101023635 for Deonie Allen.

Notes and references

L. C. Jenner, J. M. Rotchell, R. T. Bennett, M. Cowen, V. Tentzeris and L. R. Sadofsky, Sci. Total Environ., 2022, 831, 154907.

M. O. Rodrigues, N. Abrantes, F. J. M. Gonçalves, H. Nogueira, J. C. Marques and A. M. M. Gonçalves,
Environ. Toxicol. Pharmacol., 2019, 72, 103239.

H. A. Leslie, M. J. M. van Velzen, S. H. Brandsma, A. D. Vethaak, J. J. Garcia-Vallejo and M. H. Lamoree,
Environ. Int., 2022, 1–8.

S. Schönbauer and R. Müller, Sci. Commun., 2021, 43, 543– 569.

S. Allen, D. Allen, S. Karbalaei, V. Maselli and T. R. Walker, J. Hazard. Mater. Adv., 2022, 6, 1–12.

J. Kramm, S. Steinhoff, S. Werschmöller, B. Völker and C. Völker, Glob. Environ. Change, 2022, 73, 1–13.

K. Borg, A. Lennox, S. Kaufman, F. Tull, R. Prime, L. Rogers and E. Dunstan, J. Cleaner Prod., 2022, 344, 1–14. 8 S. Michie, M. M. van Stralen and R. West, Implementation Sci., 2011, 6, 1–11.

S. Michie, L. Atkins and R. West, Can. J. Phys. Leadersh., 2014, 2, 1003–1010.

J. Cane, D. O'Connor and S. Michie, Implementation Sci., 2012, 7, 1–17.

I. Ajzen, in Action Control, ed. Kuhl J. and Beckmann J., Springer, Berlin, Heidelberg, 1985, pp. 11–39. 12 I. Ajzen, Organ. Behav. Hum. Decis. Process., 1991, 50, 179– 211.

© 2023 The Author(s). Published by the Royal Society of Chemistry

Open Access Article. Published on 06 March 2023. Downloaded on 9/4/2025 3:13:06 PM.
This article is licensed under a Creative Commons Attribution 3.0 Unported Licence

H. Barker, P. J. Shaw, B. Richards, Z. Clegg and D. Smith, Sustain, 2021, 13, 1–18.

J. Kolodko, K. A. Schmidtke, D. Read and I. Vlaev, PLoS One, 2021, 16, 1–20.

F. Lasrado and N. Zakaria, Asia Pacific J. Manag., 2020, 37, 823–850.

D. Arli, A. Badejo, J. Carlini, C. France, C. Jebarajakirthy, K. Knox, R. Pentecost, H. Perkins, P. Thaichon, T. Sarker and O. Wright, Int. J. Non-profit Volunt. Sect. Mark., 2020, 25, 1–14.

L. Chun T'ing, K. Moorthy, C. Yoon Mei, F. Pik Yin, W. Zhi Ying, C. Wei Khong, G. Zhao Chern and T. Zin Lin,
Heliyon, 2020, 6, 1–11.

W. F. Strydom, Recycling, 2018, 3, 1–20. 19 Y. Sun, S. Wang, J. Li, D. Zhao and J. Fan, Nat. Hazards, 2017, 89, 1327–1342.

S. P. Lam and J. K. Chen, Environ. Behav., 2006, 38, 318–332.

O. Khan, T. Daddi, H. Slabbinck, K. Kleinhans, D. VazquezBrust and S. De Meester, Resour., Conserv. Recycl., 2020, 163, 1–11.

L. Van, N. A. Hamid, M. F. Ahmad, A. N. Aizat Ahmad, R. Ruslan and P. F. Muhamad Tamyez, Emerg. Sci. J., 2021, 5, 269–278.

J. J. B. R. Aruta, Asian J. Soc. Psychol., 2021, 1–15.

D. Asih, M. Setini, M. Soelton, N. Muna, I. G. C. Putra, D. C. Darma and J. A. Judiarni, Manag. Sci. Lett., 2020, 10, 3367–3374.

L. D. Aikowe and J. Mazancov´a, Sustain, 2021, 13, 1–14.

P. Pongpunpurt, N. Navamajiti, K. Sriroongvikrai, M. Onnom, P. Pinitjitsamut, P. Painmanakul,

N. Chawaloesphonsiya and T. Poyai, Eng. J., 2021, 25, 1–11.

S. Vassanadumrongdee, D. Hoontrakool and D. Marks, Appl. Environ. Res., 2020, 42, 27–45.

I. Hameed, K. Khan, I. Waris and B. Zainab, Environ. Qual. Manag., 2021, 1–11.

F. Khan, W. Ahmed and A. Najmi, Resour. Conserv. Recycl., 2019, 142, 49–58.

W. W. M. So, I. N. Y. Cheng, L. T. O. Cheung, Y. Chen, S. C. F. Chow, L. Fok and S. K. Lo, Aust. J. Environ. Educ., 2021, 37, 266–284.

D. Chatterjee and M. R. Barbhuiya, Scand. J. Hosp. Tour., 2021, 21, 531–549.

Y. Liao and Y. Xing, J. Environ. Plan. Manag., 2021, 1–22. 33 W. Wood, Personal. Soc. Psychol. Rev., 2017, 21, 389–403. 34 A. L. Allison, F. Lorencatto, S. Michie and M. Miodownik, Sustain, 2021, 13, 1–15.

L. M. Heidbreder, I. Bablok, S. Drews and C. Menzel, Sci. Total Environ., 2019, 668, 1077–1093.

S. Molloy, P. Varkey and T. R. Walker, Sustain. Prod. Consum., 2022, 30, 1082–1094.

R. Kitz, T. Walker, S. Charlebois and J. Music, Int. J. Consum. Stud., 2021, 1–15.

T. R. Walker, E. McGuinty, S. Charlebois and J. Music, Humanit. Soc. Sci. Commun., 2021, 8, 1–11. 39 M. B. Forleo and L. Romagnoli, Mar. Pollut. Bull., 2021, 165, 1–11.

H. Reijonen, S. Bellman, J. Murphy and H. Kokkonen, Waste Manag., 2021, 131, 88–97.

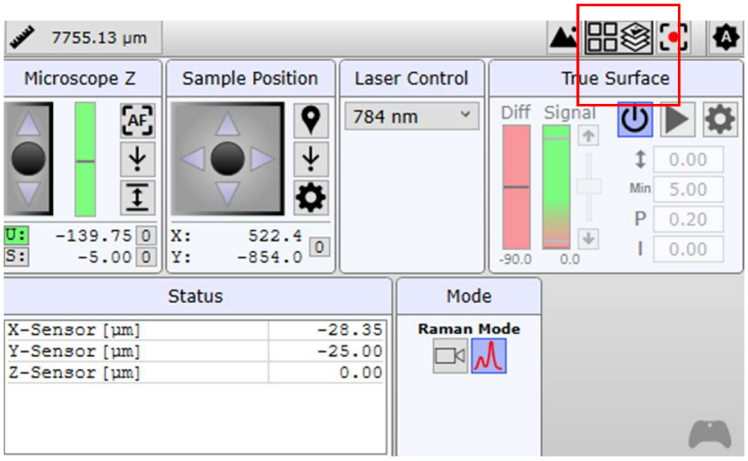
I. Adam, T. R. Walker, C. A. Clayton and J. Carlos Bezerra, Environ. Challenges, 2021, 4, 1–9.
I. Adam, Mar. Pollut. Bull., 2021, 170, 112591.
C. Clayton and A. Bruce, Soc. Sci., 2021, 10(11), 412.
S. M. C. Davison, M. P. White, S. Pahl, T. Taylor, K. Fielding,
B. R. Roberts, T. Economou, O. McMeel, P. Kellett and
L. E. Fleming, Glob. Environ. Chang., 2021, 69, 1–14.
K. A. Willis, B. D. Hardesty and C. Wilcox, J. Environ.
Manage., 2021, 287, 1–8.
J. Pykett, Antipode, 2012, 44, 217–238. 47 A. M. King, S. C. Burgess, W. Ijomah and C. A. McMahon, Sustainable Dev., 2006, 14, 257–267.
X. Zhao, M. Korey, K. Li, K. Copenhaver, H. Tekinalp,
S. Celik, K. Kalaitzidou, R. Ruan, A. J. Ragauskas and
S. Ozcan, Chem. Eng. J., 2022, 428, 131928.
K. Syberg, M. B. Nielsen, L. P. Westergaard Clausen, G. van Calster, A. van Wezel, C. Rochman, A. A. Koelmans, R. Cronin, S. Pahl and S. F. Hansen, Curr. Opin. Green Sustainable Chem., 2021, 29, 100462.
T. Walker, D. Gramlich and A. Dumont-Bergeron, in Sustainability, ed. D. M. Wasieleski and J. Weber, Emeerald Publishing Limited, Bingley, 2020, vol. 4, pp. 185–211. 51 B. Wansink and M. Huckabee, Calif. Manage. Rev., 2005, 47, 1–15.
A. Al-Samydai, M. Jasim AL-Samydai, M. N. Abu Hajleh, I. Ali Qrimea, A. Azez Badir Alindawy, L. Kamal Al-Halaseh and R. Othman Yousif, J. Pure Appl. Microbiol., 2021, 15, 1898– 1906.
D. Eiseman, in Tourism Planning and Destination Marketing, ed. M. Camilleri, Emerald Group Publishing Ltd, 2018, pp. 121–140.
K. Raab, R. Wagner, M. Ertz and M. Salem, J. Ecotourism, 2022, 1–31.
M. Cleveland, J. L. Robertson and V. Volk, J. Cleaner Prod., 2020, 249, 119394.

© 2023 The Author(s). Published by the Royal Society of Chemistry

Appendix IV. Standard Operating Procedure for creating particle mapping ‘mask’ for use on µRaman at Helmholtz Association Leipzig

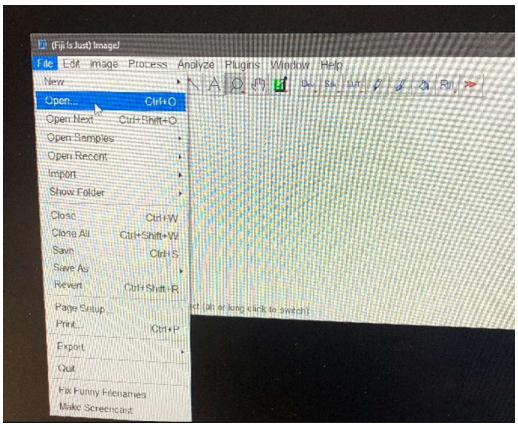
Particle Scout Mask SOP

Once your sample is in place and in focus, create an image using map function in Control 5 and select the ‘Particle Scout’ tab in the menu; select the set centre and set the area you would like to measure

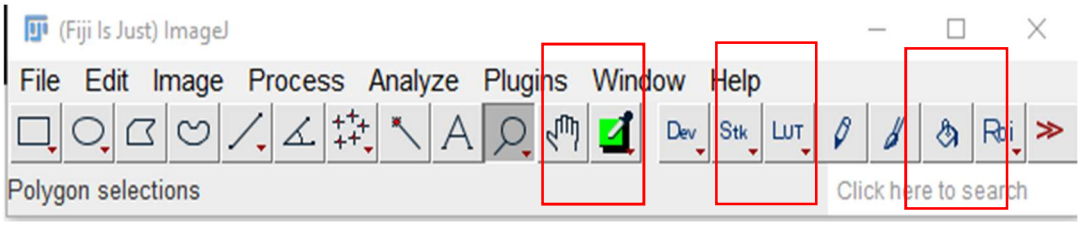


This will then take you to the ‘Particle Scout’ software, with your selected area in an image, then you select the ‘particle scout’ tab and click ‘save image’; then close the map tab; if it is left open it can move where the focus of the microscope is and can be dangerous if there is not enough field of movement for the sample
Then open this image in Fiji by clicking file, then open:

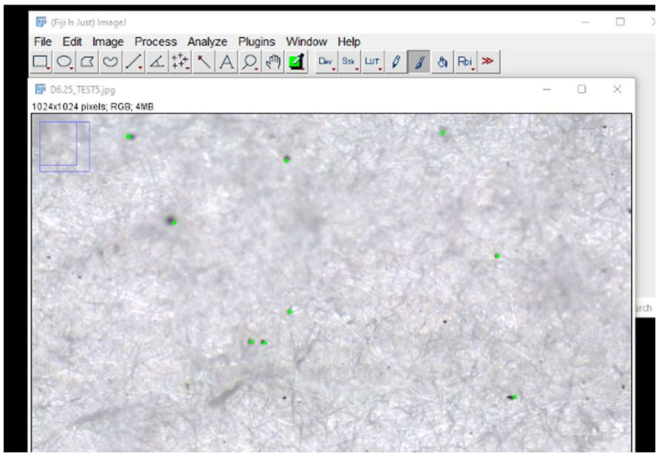




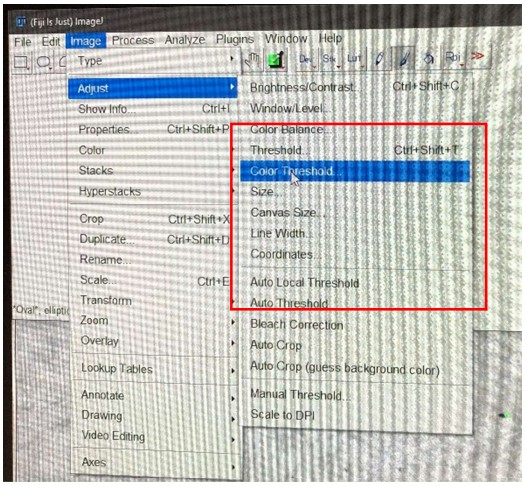
Then, using the paintbrush function, select a brush size that is smaller than your particles, and a green colour – you can change the size by right clicking on the paintbrush; and can change the colour using the dropper button (see below)

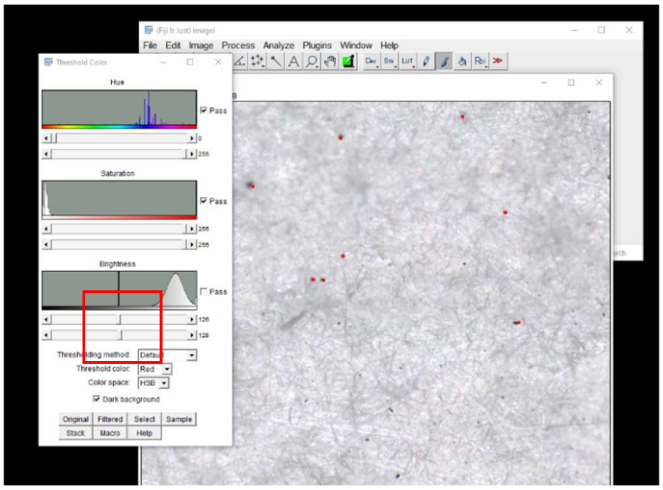


Then select the particles you would like to analyse using the paintbrush – you can also zoom in using the search button (above)



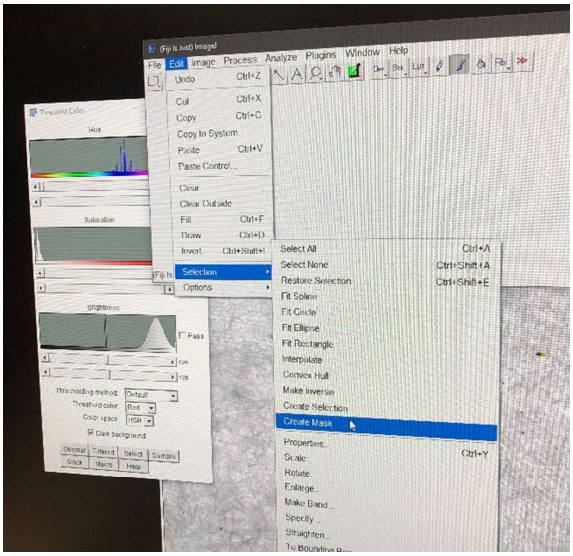
Once you have selected all your particles, you then click image > adjust > colour threshold and a menu will appear



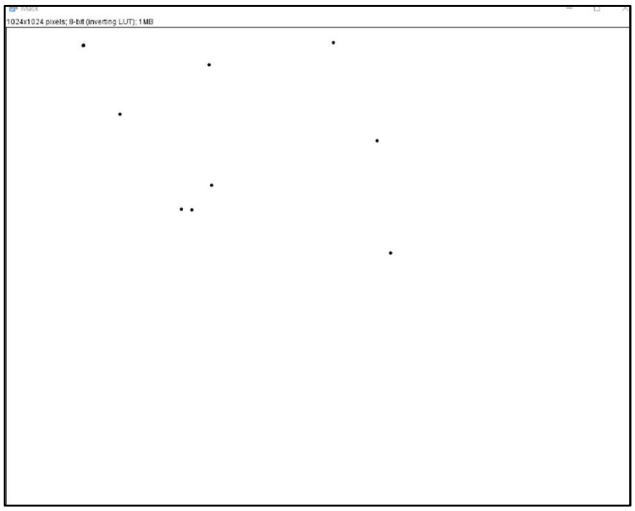


Put the saturation all the way up until the particles selected go from a green to a red colour, then unlick ‘Pass’ in the Brightness section and have this somewhere in the middle, and then click the ‘Select’ button on this menu

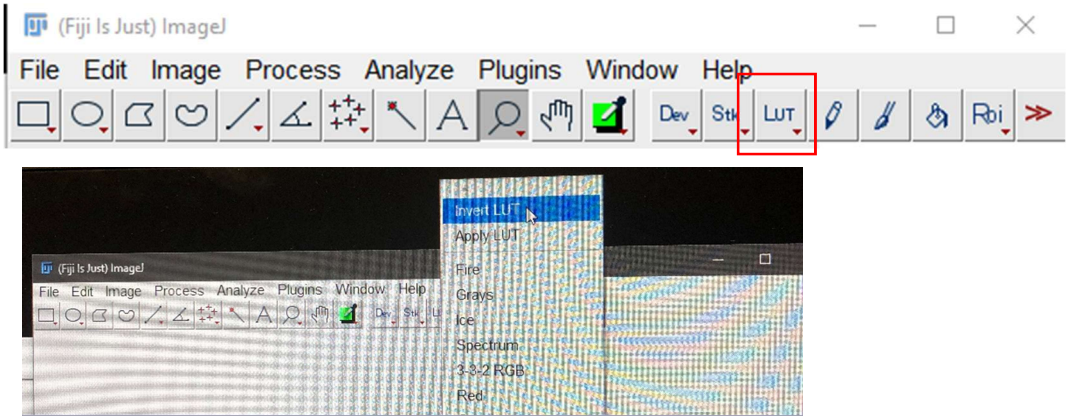
Then click the ‘Edit’ button on the main toolbar > then selection> then click the option ‘Create mask’



This will give you an black and white simple image of the particles you have just selected,



This will then need to be inverted as Particle Cout will want the image to be black with white spots; to do this right click on the ‘LUT’ button on the main toolbar and then click ‘Invert LUT’



This will then give you the same image but with the background as black, and the selected particles as white, this then needs to be saved as a ‘PNG’ file for it to work in Particle Scout; so just click ‘file’ > ‘save as’ > ‘PNG’



Then go back into ‘Particle Scout’, click the particle scout tab and then click the ‘upload mask from file’ button, this will upload the mask into particle scout and it will identify the particles from the mask
Once you are happy with the selection slick the green tick

It is important the sample is not moved from the original spot where the image is taken, otherwise it will not be in alignment with your mask
If you select the ‘autofocus spectrum’ function, this will allow the software to focus on the particle, even if it is a different height to your other particles and will allow for the ‘Z’ focus to move in line with this
Select the parameters you would like to use (integration time; accumulations); make sure the door is shut, open the laser and then press the play button

Appendix V. Supplementary Tables for Research Chapter 4

Table V.1. Particle Counts for each sample expressed as MP per m^3 and MP per Filter

Sample Name	Dates (2021)	MP/m^3	MP/Filter	Analysis Type
D1.1 (Direct Air Filter Day 1, 1L/min)	17.11.21-18.11.21	3729.72	5370.79	Nile Red and Raman
D2.1 (Direct Air Filter Day 2, 1L/min)	18.11.21-19.11.21	3538.80	5060.48	Nile Red
D3.1 (Direct Air Filter Day 3, 1L/min)	19.11.21-20.11.21	18812.38	26901.70	Nile Red
D4.1 (Direct Air Filter Day 4, 1L/min)	20.11.21-21.11.21	3789.18	5418.53	Nile Red
D5.1 (Direct Air Filter Day 5, 1L/min)	22.11.21-23.11.21	58.40	1401.67	Raman
D6.1 (Direct Air Filter Day 6, 1L/min)	23.11.21-24.11.21	13904.80	19883.86	Nile Red
D7.1 (Direct Air Filter Day 7, 1L/min)	24.11.21-25.11.21	22217.63	31771.22	Nile Red
D1.10 (Direct Air Filter Day 1, 10L/min)	17.11.21-18.11.21	2271.84	32487.32	Nile Red
D2.10 (Direct Air Filter Day 2, 10L/min)	18.11.21-19.11.21	1652.55	23631.48	Nile Red
D3.10 (Direct Air Filter Day 3, 10L/min)	20.11.21-21.11.21	1787.76	25564.97	Nile Red
D4.10 (Direct Air Filter Day 4, 10L/min)	20.11.21-21.11.21	1303.68	18642.62	Nile Red
D5.10 (Direct Air Filter Day 5, 10L/min)	22.11.21-23.11.21	1263.62	18069.73	Nile Red
D7.10 (Direct Air Filter Day 7, 10L/min)	24.11.21-25.11.21	711.10	10168.70	Nile Red
D1.25 (Direct Air Filter Day 1, 25L/min)	17.11.21-18.11.21	308.48	11028.03	Nile Red and Raman
D2.25 (Direct Air Filter Day 2, 25L/min)	18.11.21-19.11.21	8.31	167.23	Nile Red and Raman
D3.25 (Direct Air Filter Day 3, 25L/min)	19.11.21-20.11.21	1195.18	42727.63	Nile Red and Raman
D4.25 (Direct Air Filter Day 4, 25L/min)	20.11.21-21.11.21	6.36	228.84	Raman
D5.25 (Direct Air Filter Day 5, 25L/min)	22.11.21-23.11.21	2983.94	106675.86	Nile Red
D6.25 (Direct Air Filter Day 6, 25L/min)	23.11.21-24.11.21	20.17	726.14	Raman
D7.25 (Direct Air Filter Day 7, 25L/min)	24.11.21-25.11.21	22.74	818.56	Raman

Sample Name	Dates (2021)	MP/m^3	MP/Filter	Analysis Type
D1.50 (Direct Air Filter Day 1, 50L/min)	17.11.21-18.11.21	996.87	71276.38	Nile Red
D2.50 (Direct Air Filter Day 2, 50L/min)	18.11.21-19.11.21	2749.24	196570.98	Nile Red and Raman
D3.50 (Direct Air Filter Day 2, 50L/min)	19.11.21-20.11.21	2.66	191.44	Raman
D4.50 (Direct Air Filter Day 4, 50L/min)	20.11.21-21.11.21	1168.14	83521.78	Nile Red and Raman
D5.50 (Direct Air Filter Day 5, 50L/min)	22.11.21-23.11.21	632.64	45234.00	Nile Red
D6.50 (Direct Air Filter Day 6, 50L/min)	23.11.21-24.11.21	471.73	33728.57	Nile Red
D7.50 (Direct Air Filter Day 6, 50L/min)	24.11.21-25.11.21	556.19	39767.73	Nile Red
N1.1 (Nanotank Sample Day 1, 1L/min)	17.11.21-18.11.21	8975.36	12924.51	Raman
N2.1 (Nanotank Sample Day 2, 1L/min)	18.11.21-19.11.21	155.86	224.44	Raman
N3.1 (Nanotank Sample Day 3, 1L/min)	19.11.21-20.11.21	736.72	1053.51	Nile Red
N4.1 (Nanotank Sample Day 4, 1L/min)	20.11.21-21.11.21	3022.83	4322.65	Nile Red and Raman
N5.1 (Nanotank Sample Day 5, 1L/min)	22.11.21-23.11.21	547.05	787.75	Raman
N6.1 (Nanotank Sample Day 6, 1L/min)	23.11.21-24.11.21	647.90	932.98	Raman
N7.1 (Nanotank Sample Day 7, 1L/min)	24.11.21-25.11.21	0.00	0.00	Nile Red
N1.10 (Nanotank Sample Day 1, 10L/min)	17.11.21-18.11.21	1.73	24.95	Raman
N2.10 (Nanotank Sample Day 2, 10L/min)	18.11.21-19.11.21	407.10	5821.46	Nile Red
N3.10 (Nanotank Sample Day 3, 10L/min)	19.11.21-20.11.21	53.18	765.75	Raman
N4.10 (Nanotank Sample Day 4, 10L/min)	20.11.21-21.11.21	66.01	950.58	Raman
N5.10 (Nanotank Sample Day 5, 10L/min)	22.11.21-23.11.21	882.55	12620.41	Nile Red and Raman
N6.10 (Nanotank Sample Day 6, 10L/min)	23.11.21-24.11.21	315.95	4518.15	Nile Red and Raman
N7.10 (Nanotank Sample Day 7, 10L/min)	24.11.21-25.11.21	0.00	0.00	Nile Red
N1.25 (Nanotank Sample Day 1, 25L/min)	17.11.21-18.11.21	2.44	88.02	Raman
N2.25 (Nanotank Sample Day 2, 25L/min)	18.11.21-19.11.21	235.14	8406.36	Nile Red and Raman
N3.25 (Nanotank Sample Day 3, 25L/min)	19.11.21-20.11.21	112.10	4007.68	Nile Red and Raman

Sample Name	Dates (2021)	MP/m^3	MP/Filter	Analysis Type
N4.25 (Nanotank Sample Day 4, 25L/min)	20.11.21-21.11.21	198.99	7113.91	Nile Red and Raman
N5.25 (Nanotank Sample Day 5, 25L/min)	22.11.21-23.11.21	12.35	444.49	Raman
N6.25 (Nanotank Sample Day 6, 25L/min)	23.11.21-24.11.21	13.32	479.69	Raman
N7.25 (Nanotank Sample Day 7, 25L/min)	24.11.21-25.11.21	103.29	3692.72	Nile Red
N1.40 (Nanotank Sample Day 1, 40L/min)	17.11.21-18.11.21	51.46	2943.31	Nile Red
N2.40 (Nanotank Sample Day 2, 40L/min)	18.11.21-19.11.21	53.55	3062.78	Nile Red and Raman
N3.40 (Nanotank Sample Day 3, 40L/min)	19.11.21-20.11.21	11.54	664.53	Raman
N4.40 (Nanotank Sample Day 4, 40L/min)	20.11.21-21.11.21	17.73	1021.00	Raman
N5.40 (Nanotank Sample Day 5, 40L/min)	22.11.21-23.11.21	5.42	312.46	Raman
N6.40 (Nanotank Sample Day 6, 40L/min)	23.11.21-24.11.21	4.89	281.65	Raman
N7.40 (Nanotank Sample Day 7, 40L/min)	24.11.21-25.11.21	78.04	4463.84	Nile Red and Raman
W1.1 (Direct Air Filtration Sample Week 1, 1L/min)	3.11.211-10.11.21	1170.99	11791.87	Nile Red and Raman
W2.1 (Direct Air Filtration Sample Week 2, 1L/min)	10.11.21-17.11.21	3678.90	37046.53	Nile Red
W3.1 (Direct Air Filtration Sample Week 3, 1L/min)	17.11.21-24.11.21	0.69	79.22	Raman
W4.1 (Direct Air Filtration Sample Week 4, 1L/min)	24.11.21-2.12.21	27.50	965.99	Raman
W1.10 (Direct Air Filtration Sample Week 1, 10L/min)	3.11.211-10.11.21			Nile Red
W2.10 (Direct Air Filtration Sample Week 2, 10L/min)	10.11.21-17.11.21	0.00	59.41	Raman
W3.10 (Direct Air Filtration Sample Week 1, 10L/min)	17.11.21-24.11.21	1431.74	144175.92	Nile Red
W4.10 (Direct Air Filtration Sample Week 4, 10L/min)	24.11.21-2.12.21	284.45	28644.22	Nile Red
W1.25 (Direct Air Filtration Sample Week 1, 25L/min)	3.11.211-10.11.21	159.77	40221.26	Nile Red

Sample Name	Dates (2021)	MP/m^3	MP/Filter	Analysis Type
W2.25 (Direct Air Filtration Sample Week 2, 25L/min)	10.11.21-17.11.21	77.94	19621.29	Nile Red
W3.25 (Direct Air Filtration Sample Week 3, 25L/min)	17.11.21-24.11.21	3.50	1397.27	Raman
W4.25 (Direct Air Filtration Sample Week 4, 25L/min)	24.11.21-2.12.21	2.27	882.37	Raman
W1.50 (Direct Air Filtration Sample Week 1, 50L/min)	24.11.21-2.12.21	225.10	113335.64	Nile Red and Raman
W2.50 (Direct Air Filtration Sample Week 2, 50L/min)	10.11.21-17.11.21	146.59	73806.61	Nile Red
W3.50 (Direct Air Filtration Sample Week 3, 50L/min)	17.11.21-24.11.21	99.70	50199.00	Nile Red and Raman
W4.50 (Direct Air Filtration Sample Week 4, 50L/min)	24.11.21-2.12.21	0.94	651.33	Raman
M1.1 (Direct Air Filtration Sample Month 1, 1L//min)	3.11.21-2.12.21	23.17	1177.23	Raman
M1.10 (Direct Air Filtration Sample Month 1, 10L//min)	3.11.21-2.12.21	162.25	65404.31	Nile Red and Raman
M1.25 (Direct Air Filtration Sample Month 1, 25L//min)	3.11.21-2.12.21	22.34	22509.59	Nile Red and Raman
M1.50 (Direct Air Filtration Sample Month 1, 50L//min)	3.11.21-2.12.21	0.10	242.05	Raman

Table V.2. Daily Direct Air Filtration Particle Size Distribution Values (Sample name – D daily direct air filtration and number denoting day (1-7) and pumping rate (1=1 L/min; 10= 10 L/min, 25= 25L/min; 50 = 50L/min); values are blank corrected

Particle size distribution (µm)	D1.1	D1.10	D1.25	D1.50	D2.1	D2.10	D2.50	D3.1	D3.10	D3.25	D4.1	D4.10	D4.50	D5.10	D5.25	D5.50	D6.1	D6.50	D7.1	D7.10	D7.50
1.6-10µm	200	1291	267	2762	162	953	7940	987	1040	1308	225	716	3346	679	4229	1742	809	1367	1276	387	1456
10-20 µm	22	67	146	180	50	32	246	116	27	361	8	60	145	62	203	141	24	40	51	29	180
20-30 µm	4	3	32	36	6	7	46	17	5	90	0	6	9	13	26	13	3	6	6	8	24
30-40 µm	0	1	8	7	1	0	4	5	1	19	0	1	2	2	7	2	0	1	0	2	6
40-50µm	0	0	4	2	0	0	0	2	0	5	0	0	0	2	1	0	0	1	0	0	0
50-100µm	0	0	2	0	0	0	0	0	0	6	0	0	0	0	1	0	0	0	0	0	0
100-150µm	0	0	3	0	0	0	0	0	0	1	0	0	0	0	1	0	0	0	0	0	0
150-200µm	0	1	0	0	0	0	1	0	0	0	0	0	0	0	1	0	0	0	0	0	0
200-250µm	1	0	0	0	0	0	0	0	0	0	0	0	0	0	0	0	0	0	0	0	0
250-300µm	0	0	0	0	0	0	0	0	0	0	0	0	0	0	0	0	0	0	0	0	0
300-350µm	0	0	0	0	0	0	0	0	0	0	0	0	0	0	0	0	0	0	0	0	0
350-400µm	0	0	0	0	0	0	0	0	0	0	0	0	0	0	0	0	0	0	0	0	0
400-450µm	0	0	0	0	0	0	0	0	0	0	0	0	0	0	0	0	0	0	0	0	0
450-500µm	0	0	0	0	0	0	0	0	0	0	0	0	0	0	0	0	0	0	0	0	0
500-550µm	0	0	0	0	0	0	0	0	0	0	0	0	0	0	0	0	0	0	0	0	0
550-600µm	0	0	0	0	0	0	0	0	0	0	0	0	0	0	0	0	0	0	0	0	0
600-650µm	0	0	0	0	0	0	0	0	0	0	0	0	0	0	0	0	0	0	0	0	0
650-700µm	0	0	0	0	0	0	0	0	0	0	0	0	0	0	0	0	0	0	0	0	0
700-750µm	0	0	0	0	0	0	0	0	0	0	0	0	0	0	0	0	0	0	0	0	0
750-800µm	0	0	0	0	0	0	0	0	0	0	0	0	0	0	0	0	0	0	0	0	0

Particle size distribution (µm)	D1.1	D1.10	D1.25	D1.50	D2.1	D2.10	D2.50	D3.1	D3.10	D3.25	D4.1	D4.10	D4.50	D5.10	D5.25	D5.50	D6.1	D6.50	D7.1	D7.10	D7.50
800-850µm	0	0	0	0	0	0	0	0	0	0	0	0	0	0	0	0	0	0	0	0	0
850-900µm	0	0	0	0	0	0	0	0	0	0	0	0	0	0	0	0	0	0	0	0	0
900-950µm	0	0	0	0	0	0	0	0	0	0	0	0	0	0	0	0	0	0	0	0	0
950-1000µm	0	0	0	0	0	0	0	0	0	0	0	0	0	0	0	0	0	0	0	0	0
TOTAL COUNT	427	2654	729	5749	381	1945	16177	2114	2113	3098	458	1499	6848	1437	8698	3640	1645	2782	2609	813	3122

Table V.3. Daily Nanotank Particle Size Distribution Values (Sample name – N nanotank daily and number denoting day (1-7) and pumping rate (1=1 L/min; 10= 10 L/min, 25= 25L/min; 50 = 50L/min); values are blank corrected

Particle Size distribution (µm)	N1.1	N1.40	N2.10	N2.25	N2.40	N3.1	N3.25	N4.1	N4.25	N5.10	N6.10	N7.1	N7.10	N7.25	N7.40
1.6-10µm	1064	160	352	552	220	121	268	355	376	795	287	3	23	272	317
10-20 µm	155	19	167	187	89	19	121	69	209	305	145	0	11	76	92
20-30 µm	13	5	42	51	12	1	16	11	57	67	23	5	5	23	29
30-40 µm	3	1	10	15	5	2	7	3	29	22	5	0	0	8	11
40-50µm	1	0	8	5	2	0	2	3	16	13	3	1	0	5	6
50-100µm	2	1	3	11	2	2	2	3	13	8	1	0	0	4	1
100-150µm	0	0	2	1	0	0	1	2	2	0	0	0	0	0	2
150-200µm	0	0	0	0	0	0	0	0	1	0	0	0	0	0	1
200-250µm	0	1	0	0	0	0	0	0	0	0	0	0	0	0	0
250-300µm	0	0	0	0	0	0	0	0	0	0	0	0	0	0	0
300-350µm	0	0	0	0	0	0	0	0	0	0	0	0	0	0	0
350-400µm	0	0	0	0	0	0	0	0	0	0	0	0	0	0	0
400-450µm	0	0	0	0	0	0	0	0	0	0	0	0	0	0	0
450-500µm	0	0	0	0	0	0	0	0	0	0	0	0	0	0	0
500-550µm	0	0	0	0	0	0	0	0	0	0	0	0	0	0	0
550-600µm	0	0	0	0	0	0	0	0	0	0	0	0	0	0	0
600-650µm	0	0	0	0	0	0	0	0	0	0	0	0	0	0	0
650-700µm	0	0	0	0	0	0	0	0	0	0	0	0	0	0	0
700-750µm	0	0	0	0	0	0	0	0	0	0	0	0	0	0	0
750-800µm	0	0	0	0	0	0	0	0	0	0	0	0	0	0	0

Particle Size distribution (µm)	N1.1	N1.40	N2.10	N2.25	N2.40	N3.1	N3.25	N4.1	N4.25	N5.10	N6.10	N7.1	N7.10	N7.25	N7.40
800-850µm	0	0	0	0	0	0	0	0	0	0	0	0	0	0	0
850-900µm	0	0	0	0	0	0	0	0	0	0	0	0	0	0	0
900-950µm	0	0	0	0	0	0	0	0	0	0	0	0	0	0	0
950-1000µm	0	0	0	0	0	0	0	0	0	0	0	0	0	0	0
TOTAL COUNT	2302	347	936	1374	550	266	685	801	1079	2005	751	12	62	660	776

Table V.4. Weekly Direct Air Filtration Particle Size Distribution Values (Sample name – W weekly direct air filtration; and number denoting week (1-4); and pumping rate (1=1 L/min; 10= 10 L/min, 25= 25L/min; 50 = 50L/min); values are blank corrected

Particle Size Distribution (µm)	W1.1	W1.25	W1.50	W2.1	W2.25	W2.50	W3.10	W3.50	W4.10
1.6-10µm	355	1455	3578	1452	622	2230	5780	1754	998
10-20 µm	107	163	839	86	147	621	221	269	160
20-30 µm	20	43	214	12	30	135	35	69	21
30-40 µm	11	20	57	3	20	57	2	5	12
40-50µm	2	5	24	1	1	25	1	3	0
50-100µm	4	4	31	0	2	20	0	2	3
100-150µm	0	1	3	0	0	3	1	0	5
150-200µm	1	0	0	0	0	1	0	0	1
200-250µm	0	0	1	0	0	0	0	1	1
250-300µm	0	0	0	0	0	0	0	0	0
300-350µm	0	0	0	0	0	0	0	0	0
350-400µm	0	0	1	0	0	0	0	0	0
400-450µm	0	0	0	0	0	0	0	0	0
450-500µm	0	0	0	0	0	0	0	0	0
500-550µm	0	0	0	0	0	0	0	0	0
550-600µm	0	0	0	0	0	0	0	0	0
600-650µm	0	0	0	0	0	0	0	0	0
650-700µm	0	0	0	0	0	0	0	0	0
700-750µm	0	0	0	0	0	0	0	0	0
750-800µm	0	0	0	0	0	0	0	0	0
800-850µm	0	0	0	0	0	0	0	0	0

Particle Size Distribution (µm)	W1.1	W1.25	W1.50	W2.1	W2.25	W2.50	W3.10	W3.50	W4.10
850-900µm	0	0	0	0	0	0	0	0	0
900-950µm	0	0	0	0	0	0	0	0	0
950-1000µm	0	0	0	0	0	0	0	0	0
TOTAL COUNT	855	3146	8326	3006	1444	5322	11820	3857	2199

Table V.5 Monthly Direct Air Filtration Particle Size Distribution Values (Sample name – M monthly direct air filtration; and number denoting month (1-7); and pumping rate (1=1 L/min; 10= 10 L/min, 25= 25L/min; 50 = 50L/min); values are blank corrected

Particle Size distribution (µm)	M1.10	M1.25
<2µm	167	42
2-10 µm	1917	557
1.6-10µm	2084	599
10-20 µm	469	269
20-30 µm	121	49
30-40 µm	30	9
40-50µm	13	7
50-100µm	14	8
100-150µm	5	2
150-200µm	2	0
200-250µm	2	0
250-300µm	0	0
300-350µm	0	0
350-400µm	0	0
400-450µm	0	0
450-500µm	0	0
500-550µm	0	0
550-600µm	0	0
600-650µm	0	0
650-700µm	0	0
700-750µm	0	0
750-800µm	0	0
800-850µm	0	0
850-900µm	0	0
900-950µm	0	0
950-1000µm	0	0
TOTAL COUNT	4824	1542

Table V.6 Daily Direct Air Filtration Particle Shape Characteristics (Sample name – D daily direct air filtration; and number denoting day (1-7) and pumping rate (1=1 L/min; 10= 10 L/min, 25= 25L/min; 50 = 50L/min); values are blank corrected)

Particle Shape	Sample ID																			
	D1.1	D1.10	D1.25	D1.50	D2.1	D2.10	D2.50	D3.1	D3.10	D3.25	D4.1	D4.10	D4.50	D5.10	D5.25	D5.50	D6.1	D6.50	D7.1	D7.10	D7.50
Total number of Particles	225	1361	462	2986	212	990	8235	1127	1071	1790	227	781	3499	757	4469	1895	833	1413	1331	426	1666
Fragment or film	233	1370	465	2992	223	1000	8238	1138	1081	1790	239	789	3509	762	4466	1905	844	1424	1340	422	1670
Fibre	0	0	0	0	0	0	0	0	0	0	0	0	0	0	3	0	0	0	0	4	0

Table V.7 Daily Nanotank Particle Shape Characteristics (Sample name – N nanotank daily and number denoting day (1-7) and pumping rate (1=1 L/min; 10= 10 L/min, 25= 25L/min; 50 = 50L/min); values are blank corrected)

Particle Shape	Sample ID														
	N1.1	N1.40	N2.10	N2.25	N2.40	N3.1	N3.25	N4.1	N4.25	N5.10	N6.10	N7.1	N7.10	N7.25	N7.40
Total number of Particles	1190	271	536	774	282	97	369	398	655	1162	416	0	0	340	411
Fragment or film	1191	272	537	775	283	98	370	399	656	1163	417	0	0	341	412
Fibre	1252	337	592	827	346	160	434	455	719	1220	481	27	58	387	457

Table V.8 Weekly Direct Air Filtration Particle Shape Characteristics (Sample name – W weekly direct air filtration; and number denoting day (1-7) and pumping rate (1=1 L/min; 10= 10 L/min, 25= 25L/min; 50 = 50L/min); values are blank corrected)

Particle Shape	Sample ID								
	W1.1	W1.25	W1.50	W2.1	W2.25	W2.50	W3.10	W3.50	W4.10
Total number of Particles	494	1685	4748	1552	822	3092	6040	2103	1200
Fragment or film	493	1683	4663	1559	829	3027	6039	2101	1187
Fibre	1	2	85	0	0	65	1	2	13

Table V.9 Raman Counts for Glasgow Samples (Research Chapter 4 and 6) (M= monthly; D= daily direct air filtration; N=nanotank daily; W = weekly direct air filtration; number = day (1-7)/week(1-4); number 1 = 1 L/min; 10 = 10 L/min; 25 = 25 L/min; 50 = 50 L/min) and Field Blank and Nano Blank values

	PE	PES	PET	PP	PS	PVC	PU	ABS	PC	PVA	Nylon/ PA	Acrylic	CE	PMMA	PLS	Rbr	PLA	SBR	SAN
M1.1_1	8	14	3	1	6	1	1	1	1	11	6	13	4	17	9	0	4	0	0
M1.1_2	12	15	5	0	1	3	0	0	0	5	3	19	7	14	16	0	8	0	0
M1.1_3	0	16	11	1	10	4	3	0	1	8	13	11	6	14	15	0	6	0	0
Average	10.00	15.00	6.33	0.67	5.67	2.67	1.33	0.33	0.67	8.00	7.33	14.33	5.67	15.00	13.33	0.00	6.00	0.00	0.00
Blank Correction	9.0	13.67	4.50	0.00	3.83	2.50	1.17	0.00	0.00	7.33	4.17	11.00	5.17	12.67	9.33	0.00	4.83	0.00	0.00
M1.10_1	7	8	0	1	1	2	0	0	0	0	0	7	0	6	12	0	1	0	0
M1.10_2	10	13	6	0	1	1	2	0	0	2	2	10	6	10	5	0	4	0	0
Average	8.5	10.5	3	0.5	1	1.5	1	0	0	1	1	8.5	3	8	8.5	0	2.5	0	0
Blank Correction	7.5	9.17	1.17	0	0	1.33	0	0	0	0	0	5.17	2.5	5.67	4.5	0	1.33	0	0
M1.25_2	2	14	4	0	0	1	0	0	0	5	4	8	4	7	13	0	2	0	0
M1.25_3	8	12	3	0	6	4	2	1	3	3	6	19	7	23	13	0	4	0	0
M1.25_4	6	4	1	0	5	1	1	0	0	1	3	12	5	17	7	0	0	0	0
Average	5.33	10	2.67	0	3.67	2	1	0.33	1	3	4.33	13	5.33	15.67	11	0	2	0	0
Blank Correction	4.33	8.67	0	0	1.83	1.83	0	0	1	2.33	1.17	9.67	4.83	13.33	7	0	0	0	0
M1.50_1	5	10	11	0	5	3	2	1	1	10	4	13	4	12	11	0	1	0	0
M1.50_2	3	1	1	0	0	0	0	0	0	0	1	2	0	0	4	0	0	0	0
M1.50_3	2	2	0	0	0	0	0	0	0	2	0	2	1	1	3	0	0	0	0
Average	3.33	4.33	4	0	1.67	1	0.67	0.33	0.33	4	1.67	5.67	1.67	4.33	6	0	0.33	0	0

	PE	PES	PET	PP	PS	PVC	PU	ABS	PC	PVA	Nylon/ PA	Acrylic	CE	PMMA	PLS	Rbr	PLA	SBR	SAN
Blank Correction	2.33	3	2.17	0	0	0	0	0	0	3.33	0	2.33	1.17	2	2	0	0	0	0
W3.1_1	0	0	0	0	0	0	0	0	0	1	1	2	0	2	0	0	0	0	0
W3.1_2	0	3	0	0	0	0	0	0	0	0	0	2	0	0	1	0	0	0	0
Average	0	1.5	0	0	0	0	0	0	0	0.5	0.5	2	0	1	0.5	0	0	0	0
Blank Correction																			
W4.1_1	8	10	7	1	4	3	1	0	0	9	7	10	2	13	12	0	3	0	0
W4.1_2	7	12	5	1	3	1	1	0	2	8	11	12	3	12	15	0	10	0	0
Average	7.5	11	6	1	3.5	2	1	0	1	8.5	9	11	2.5	12.5	13.5	0	6.5	0	0
Blank Correction	6.5	9.67	4.17	0	1.67	1.83	0	0	1	7.83	5.83	7.67	2	10.17	9.5	0	5.33	0	0
W2.10_1	0	0	0	0	0	0	0	0	0	0	1	1	0	0	1	0	0	0	0
W2.10_2	0	1	0	0	0	0	0	0	0	1	0	2	0	0	2	0	0	0	0
Average	0	0.5	0	0	0	0	0	0	0	0.5	0.5	1.5	0	0	1.5	0	0	0	0
Blank Correction																			
W3.10_1	14	23	9	1	2	1	0	0	0	2	1	24	3	32	18	0	8	0	0
W3.10_2	14	23	6	0	5	2	0	0	1	7	6	19	3	17	11	0	4	0	0
Average	14	23	7.5	0.5	3.5	1.5	0	0	0.5	4.5	3.5	21.5	3	24.5	14.5	0	6	0	0
Blank Correction	13	23	5.5	0	1.5	1.5	0	0	0	4.5	1.5	17.5	3	21.5	10.5	0	6	0	0
W1.25_1	3	8	4	0	1	2	0	0	0	2	4	16	4	18	7	0	5	0	0
W1.25_2	3	7	4	1	3	2	0	0	0	1	2	3	2	9	10	0	3	0	0
W1.25_3	11	10	4	0	4	1	2	1	1	7	4	13	4	15	15	0	2	0	0

	PE	PES	PET	PP	PS	PVC	PU	ABS	PC	PVA	Nylon/ PA	Acrylic	CE	PMMA	PLS	Rbr	PLA	SBR	SAN
Average	6	8	4	0	3	2	1	0	0	3	3	11	3	14	11	0	3	0	0
Blank Correction	4.67	7	2.17	0	0	1.5	0	0	0	2.67	0	7.33	2.83	11.67	6.67	0	2.17	0	0
W3.25_1	17	26	14	2	8	3	4	0	0	11	9	15	5	25	16	0	5	0	0
W3.25_2	6	22	10	1	0	5	0	0	1	12	5	14	1	25	18	0	9	0	0
W3.25_3	11	15	3	1	3	1	0	0	2	6	7	12	2	15	16	0	0	0	0
Average	11	21	9	1	4	3	1	0	1	10	7	14	3	22	17	0	5	0	0
Blank Correction	10.33	19.67	7.17	1	1.83	2.83	1.17	0	1	9	3.83	10.33	2.17	19.33	12.67	0	3.5	0	0
W4.25_1	6	17	3	0	2	0	0	0	2	4	7	12	5	16	17	0	4	0	0
W4.25_2	13	14	8	0	3	0	2	0	1	3	3	6	5	15	14	0	1	0	0
W4.25_3	10	5	6	1	4	5	0	0	0	6	2	11	5	11	14	0	7	0	0
Average	10	12	6	0	3	2	1	0	1	4	4	10	5	14	15	0	4	0	0
Blank Correction	8.67	10.67	3.83	0	1.17	1.5	0	0	1	3.67	0	6.33	4.5	11.67	11	0	2.833	0	0
W1.50_1	4	11	3	1	1	0	0	0	0	3	1	7	2	7	12	0	0	0	0
W1.50_2	4	14	3	1	2	2	1	0	0	1	1	8	2	13	8	0	1	0	0
W1.50_3	6	10	5	1	2	3	1	0	0	2	1	10	1	12	4	0	1	0	0
Average	5	12	4	1	2	2	1	0	0	2	1	8	2	11	8	0	1	0	0
Blank Correction	3.67	10.33	1.83	0	0	1.5	0	0	0	1.33	0	5	1.17	8.33	4	0	0	0	0
W2.50_1	6	15	7	0	0	1	1	0	1	7	2	23	5	11	16	0	2	0	0
W2.50_2	7	11	5	0	1	0	0	0	1	1	1	10	3	13	14	0	1	0	0
W2.50_3	8	14	9	0	1	2	2	2	1	2	1	16	5	8	9	0	1	0	0
Average	7	13	7	0	1	1	1	1	1	3	1	16	4	11	13	0	1	0	0

	PE	PES	PET	PP	PS	PVC	PU	ABS	PC	PVA	Nylon/ PA	Acrylic	CE	PMMA	PLS	Rbr	PLA	SBR	SAN
Blank Correction	6	12	5.167	0	0	0	0	0	1	2.67	0	13	3.83	8.33	9	0	0	0	0
W3.50_1	4	13	5	0	0	0	1	0	1	3	1	8	4	4	2	0	2	0	0
W3.50_2	5	12	4	0	0	1	1	0	0	2	2	5	0	6	8	0	2	0	0
W3.50_3	6	7	3	0	0	2	0	0	1	0	0	10	0	12	6	0	2	0	0
Average	5	11	4	0	0	1	1	0	1	2	1	8	1	7	5	0	2	0	0
Blank Correction	4	9.33	2.17	0	0	0	0	0	0	1	0	4.33	0	5	1.33	0	0	0	0
W4.50_1	7	18	20	2	3	1	0	0	0	5	2	11	1	13	11	0	2	0	0
W4.50_2	6	9	3	1	1	0	1	0	1	3	1	14	0	10	12	0	3	0	0
W4.50_3	6	14	3	0	0	2	0	2	0	4	1	14	1	11	11	0	2	0	0
Average	6	14	9	1	1	1	0	1	0	4	1	13	1	11	11	0	2	0	0
Blank Correction	5.33	9.67	7.67	1	1.33	0	0	0	0	2	1.33	7	0	6.33	6.33	0	1.33	0	0
N1.1_1	0	4	2	0	1	0	0	1	0	1	3	7	2	3	7	0	0	0	0
N1.1_2	16	12	5	0	7	6	2	1	0	8	15	14	6	20	20	0	10	0	0
N1.1_3	5	10	3	1	0	2	0	0	1	3	1	10	5	8	4	0	1	0	0
Average	7	9	3	0	3	3	1	1	0	4	6	10	4	10	10	0	4	0	0
Blank Correction	4.33	6.33	2	0	1.33	2.33	0	0	0	4	2.33	6.67	4.33	7	7	0	3.33	0	0
N2.1_1	4	1	1	0	1	0	0	0	0	1	1	6	2	4	6	0	1	0	0
N2.1_2	2	4	2	0	1	0	0	0	0	2	0	11	0	7	10	0	0	0	0
N2.1_3	5	9	1	1	0	1	0	0	0	3	0	9	1	1	11	0	0	0	0
Average	4	5	1	0	1	0	0	0	0	2	0	9	1	4	9	0	0	0	0

	PE	PES	PET	PP	PS	PVC	PU	ABS	PC	PVA	Nylon/ PA	Acrylic	CE	PMMA	PLS	Rbr	PLA	SBR	SAN
Blank Correction	1	2.33	0	0	0	0	0	0	0	2	0	5	1	0	5.67	0	0	0	0
N4.1_1	7	1	3	1	2	2	4	1	0	5	1	4	3	24	10	0	5	0	0
N4.1_2	7	9	4	0	4	1	1	1	0	9	3	14	2	23	5	0	1	0	0
N4.1_3	7	9	5	0	3	2	0	0	0	8	2	12	3	29	11	0	4	0	0
Average	7	6	4	0	3	2	2	1	0	7	2	10	3	25	9	0	3	0	0
Blank Correction	4.33	4	2.67	0	1.67	1.33	1.67	0	0	7.33	0	6.33	2.67	22	5.33	0	3	0	0
N5.1_1	7	4	8	1	2	2	0	0	1	10	2	6	6	10	10	0	8	0	0
N5.1_2	4	7	2	0	2	1	1	1	1	5	1	8	5	24	7	0	4	0	0
N5.1_3	8	8	9	1	4	4	2	0	0	5	5	11	4	18	15	0	4	0	0
Average	6	6	6	1	3	2	1	0	1	7	3	8	5	17	11	0	5	0	0
Blank Correction	3.67	4	5	0	1.33	2	1	0	0	6.67	0	4.67	5	14	7.33	0	5	0	0
N6.1_1	11	8	3	1	2	0	0	0	0	7	2	10	5	11	12	0	5	0	0
N6.1_2	5	7	4	1	0	1	2	0	2	1	0	15	2	15	10	0	3	0	0
N6.1_3	24	12	2	6	10	7	1	2	3	17	2	19	3	4	13	0	12	0	0
Average	13	9	3	3	4	3	1	1	2	8	1	15	3	10	12	0	7	0	0
Blank Correction	10.67	6.67	1.67	0	2.67	2.33	1	0	1.67	8.33	0	11	3.33	6.67	8.33	0	6.33	0	0
N1.10_1	0	0	0	0	0	0	0	0	0	0	0	2	0	0	2	0	0	0	0
N1.10_2	0	2	0	0	0	0	0	0	0	0	0	2	0	0	0	0	0	0	0
N1.10_3	0	0	0	0	0	0	0	0	0	0	0	1	0	0	0	0	0	0	0
Average	0	0.67	0	0	0	0	0	0	0	0	0	1.67	0	0	0.67	0	0	0	0
N3.10_1	8	6	5	1	1	1	1	0	1	2	1	8	3	13	3	0	2	0	0

	PE	PES	PET	PP	PS	PVC	PU	ABS	PC	PVA	Nylon/ PA	Acrylic	CE	PMMA	PLS	Rbr	PLA	SBR	SAN
N3.10_2	3	9	10	1	5	1	3	0	0	7	6	9	4	27	7	0	6	0	0
N3.10_3	5	3	3	4	11	0	2	3	0	7	1	9	7	22	13	0	2	0	0
Average	5	6	6	2	6	1	2	1	0	5	3	9	5	21	8	0	3	0	0
Blank Correction	2.67	3.67	4.67	0	4.33	0	2	1	0	5.33	0	5	4.67	17.33	4.33	0	3	0	0
N4.10_1	6	7	3	1	1	1	3	1	0	8	3	12	5	14	11	0	5	0	0
N4.10_2	9	13	7	1	2	4	1	1	1	4	3	9	1	10	12	0	5	0	0
N4.10_3	9	11	5	1	6	1	1	0	2	13	3	18	5	19	20	0	8	0	0
Average	8	10	5	1	3	2	2	1	1	8	3	13	4	14	14	0	6	0	0
Blank Correction	5.33	8	3.67	0	1.67	1.67	1.67	0	1	8.33	0	9.33	3.67	11	11	0	5.67	0	0
N5.10_1	7	8	3	0	1	1	0	0	0	2	6	8	0	9	7	0	4	0	0
N5.10_2	2	11	1	1	4	1	0	1	0	4	3	7	4	29	17	0	9	0	0
N5.10_3	7	6	5	3	1	5	0	0	1	2	1	13	3	22	9	0	4	0	0
Average	5	8	3	1	2	2	0	0	0	3	3	9	2	20	11	0	6	0	0
Blank Correction	2.67	6	1.67	0	0	2	0	0	0	2.67	0	5.67	2.33	16.67	7.67	0	5.33	0	0
N6.10_1	6	8	2	0	4	4	2	1	0	4	1	9	5	9	42	0	5	0	0
N6.10_2	6	7	2	0	2	0	0	0	0	2	3	5	1	11	5	0	5	0	0
N6.10_3	0	4	7	0	4	6	1	0	0	2	0	8	0	0	63	0	1	0	0
Average	4	6	4	0	3	3	1	0	0	3	1	7	2	7	37	0	4	0	0
Blank Correction	1.333	4	2.33	0	2	3	1	0	0	2.67	0	3.67	2	3.33	33.33	0	3.33	0	0
N1.25_1	0	0	0	0	0	0	0	0	0	0	0	1	0	1	0	0	0	0	0
N1.25_2	2	9	2	4	1	3	0	0	0	0	2	8	1	7	3	0	0	0	0

	PE	PES	PET	PP	PS	PVC	PU	ABS	PC	PVA	Nylon/ PA	Acrylic	CE	PMMA	PLS	Rbr	PLA	SBR	SAN
N1.25_3	2	3	3	3	4	1	0	0	0	0	1	14	1	4	6	0	0	0	0
Average	1	4	2	2	2	1	0	0	0	0	1	8	1	4	3	0	0	0	0
Blank Correction	0	1.67	0	0	0	1	0	0	0	0	0	4	0	0	0	0	0	0	0
N2.25_1	3	9	4	0	1	1	1	0	0	3	4	9	2	7	11	0	5	0	0
N2.25_2	5	2	3	0	0	1	0	0	0	1	4	9	5	9	5	0	2	0	0
N2.25_3	2	4	7	1	0	2	2	0	0	4	0	7	4	11	7	0	3	0	0
Average	3	5	5	0	0	1	1	0	0	3	3	8	4	9	8	0	3	0	0
Blank Correction	0	2.67	3.33	0	0	1	1	0	0	2.67	0	4.67	3.67	5.67	4.33	0	3	0	0
N3.25_1	1	2	3	0	5	0	1	1	0	0	2	1	3	11	4	0	1	0	0
N3.25_2	5	10	6	0	1	1	0	0	0	3	1	7	2	6	9	0	2	0	0
N3.25_3	6	1	3	0	4	1	0	0	0	5	0	7	3	6	4	0	0	0	0
Average	4	4	4	0	3	1	0	0	0	3	1	5	3	8	6	0	1	0	0
Blank Correction	1.33	2	2.67	0	2	0	0	0	0	2.67	0	1.33	2.67	4.33	2.33	0	0	0	0
N4.25_1	4	5	2	1	0	0	0	0	0	2	0	4	2	13	2	0	2	0	0
N4.25_2	1	4	3	5	0	0	1	0	0	3	0	12	0	6	5	0	1	0	0
N4.25_3	4	3	5	6	1	3	0	0	0	1	5	6	0	5	5	0	0	0	0
Average	3	4	3	4	0	1	0	0	0	2	2	7	1	8	4	0	1	0	0
Blank Correction	0	1.67	2	2	0	0	0	0	0	2	0	3.67	0	4.67	0	0	0	0	0
N5.25_1	12	13	4	0	0	0	0	0	0	8	2	17	1	11	5	0	2	0	0
N5.25_2	6	7	5	0	1	0	3	0	0	2	1	8	1	9	6	0	2	0	0
N5.25_3	3	4	4	1	2	1	1	0	0	1	1	7	2	4	3	0	1	0	0

	PE	PES	PET	PP	PS	PVC	PU	ABS	PC	PVA	Nylon/ PA	Acrylic	CE	PMMA	PLS	Rbr	PLA	SBR	SAN
Average	7	8	4	0	1	0	1	0	0	4	1	11	1	8	5	0	2	0	0
Blank Correction	4.33	5.67	3	0	0	0	1.33	0	0	3.67	0	7	1.33	4.67	1.33	0	1.33	0	0
N6.1_1	11	8	3	1	2	0	0	0	0	7	2	10	5	11	12	0	5	0	0
N6.1_2	5	7	4	1	0	1	2	0	2	1	0	15	2	15	10	0	3	0	0
N6.1_3	24	12	2	6	10	7	1	2	3	17	2	19	3	4	13	0	12	0	0
Average	13	9	3	3	4	3	1	1	2	8	1	15	3	10	12	0	7	0	0
Blank Correction	10.67	6.67	1.67	0	2.67	2.33	1	0	1.67	8.33	0	11	3.33	6.67	8.33	0	6.33	0	0
N6.25_1	5	2	10	1	5	0	2	0	0	4	1	12	4	20	9	0	4	0	0
N6.25_2	3	7	1	1	0	2	0	0	0	3	1	1	0	10	4	0	2	0	0
N6.25_3	4	7	3	1	2	3	0	1	0	4	0	11	2	11	8	0	2	0	0
Average	4	5	5	1	2	2	1	0	0	4	1	8	2	14	7	0	3	0	0
Blank Correction	1.33	3	3.33	0	1	1.33	0	0	0	3.67	0	4.33	2	10.33	3.67	0	2.33	0	0
N2.40_1	1	9	5	0	4	0	0	0	0	5	1	9	6	12	10	0	2	0	0
N2.40_2	4	8	2	0	1	1	0	0	0	2	1	7	4	20	12	0	4	0	0
N2.40_3	7	4	3	2	1	0	1	0	0	0	0	6	5	16	6	0	1	0	0
Average	4	7	3	1	2	0	0	0	0	2	1	7	5	16	9	0	2	0	0
Blank Correction	1.33	4.67	2	0	0	0	0	0	0	2.33	0	3.67	5	12.67	6	0	2	0	0
N3.40_1	3	14	5	0	1	3	1	1	0	2	1	9	1	6	62	0	1	0	0
N3.40_2	3	6	7	0	0	2	1	0	0	1	2	9	3	7	8	0	0	0	0
N3.40_3	5	11	6	1	2	1	0	1	0	3	3	7	3	13	2	0	2	0	0
Average	4	10	6	0	1	2	1	1	0	2	2	8	2	9	24	0	1	0	0

	PE	PES	PET	PP	PS	PVC	PU	ABS	PC	PVA	Nylon/ PA	Acrylic	CE	PMMA	PLS	Rbr	PLA	SBR	SAN
Blank Correction	1	8	4.67	0	0	1.67	0	0	0	2	0	4.67	2.33	5.33	20.67	0	0	0	0
N4.40_1	22	24	10	0	2	3	1	0	0	14	28	23	3	27	19	0	5	0	0
N4.40_2	4	2	4	0	2	0	0	1	0	1	0	7	2	10	4	0	3	0	0
N4.40_3	6	9	8	1	0	2	3	1	0	6	8	12	3	13	10	0	0	0	0
Average	11	12	7	0	1	2	1	1	0	7	12	14	3	17	11	0	3	0	0
Blank Correction	8	9.33	6	0	0	1.33	1.33	0	0	7	8	10.33	2.67	13.33	7.67	0	2.33	0	0
N5.40_1	7	5	5	4	3	1	0	0	0	4	1	8	1	6	9	0	2	0	0
N5.40_2	4	3	3	2	0	1	0	0	0	4	2	5	0	16	5	0	1	0	0
N5.40_3	3	2	3	0	2	1	0	0	0	1	0	12	0	9	3	0	2	0	0
Average	5	3	4	2	2	1	0	0	0	3	1	8	0	10	6	0	2	0	0
Blank Correction	2	1	2.33	0	0	0	0	0	0	3	0	4.67	0	7	2.33	0	1.33	0	0
N6.40_1	2	2	3	0	3	1	0	0	0	3	1	5	2	10	5	0	0	0	0
N6.40_2	2	6	3	2	2	2	0	2	0	2	1	5	1	12	5	0	0	0	0
Average	2	4	3	1	3	2	0	1	0	3	1	5	2	11	5	0	0	0	0
Blank Correction	0	1.67	1.67	0	1.17	1.17	0	1	0	2.5	0	1.33	1.5	7.67	1.67	0	0	0	0
N7.40_1	0	2	5	0	1	2	0	1	0	1	3	5	0	5	2	0	0	0	0
N7.40_2	4	1	2	1	0	1	0	2	0	0	0	10	0	17	13	0	3	0	0
N7.40_3	0	0	0	0	0	0	0	0	0	0	1	0	0	0	0	0	0	0	0
Average	1	1	2	0	0	1	0	1	0	0	1	5	0	7	5	0	1	0	0
Blank Correction	0	0	1	0	0	0	0	1	0	0	0	1.33	0	4	1.67	0	0	0	0

	PE	PES	PET	PP	PS	PVC	PU	ABS	PC	PVA	Nylon/ PA	Acrylic	CE	PMMA	PLS	Rbr	PLA	SBR	SAN
D1.1_1	7	4	5	2	9	2	3	1	0	5	1	8	3	19	10	0	4	0	0
D1.1_2	7	15	5	2	10	2	2	0	2	1	2	10	5	8	11	0	5	0	0
D1.1_3	7	8	5	1	2	2	0	0	4	2	3	7	5	13	9	0	8	0	0
Average	7	9	5	2	7	2	2	0	2	3	2	8	4	13	10	0	6	0	0
Blank Correction	6	7.67	3.17	1.33	5.17	1.83	1.5	0	2	2	0	5	3.83	11	6	0	4.5	0	0
D1.25_1	3	0	2	0	1	4	1	0	1	0	6	4	3	7	5	0	2	0	0
Average	5	4	3	1	3	3	1	0	2	1	3	5	3	9	6	0	3	0	0
Blank Correction	3.5	2.5	0	0	1.25	2.75	1.08	0	1.5	0	0	1.17	2.92	6.67	1.5	0	2.08	0	0
D2.25_1	4	5	5	0	1	1	1	0	0	0	4	3	1	9	2	0	1	0	0
D2.25_2	4	5	1	0	1	0	0	0	0	0	2	6	0	8	5	0	3	0	0
D2.25_3	3	5	1	0	2	0	0	0	0	0	2	3	0	9	3	0	2	0	0
Average	4	5	2	0	1	0	0	0	0	0	3	4	0	9	3	0	2	0	0
Blank Correction	2.67	3.67	0	0	0	0	0	0	0	0	0	0	0	6.33	0	0	0	0	0
D2.50_1	9	8	5	0	2	1	0	2	0	8	5	12	4	19	10	0	6	0	0
D2.50_2	6	18	4	2	2	3	1	0	0	4	3	4	4	7	13	0	7	0	0
D2.50_3	3	3	1	0	1	1	0	1	0	3	0	8	3	6	3	0	2	0	0
Average	6	10	3	1	2	2	0	1	0	5	3	8	4	11	9	0	5	0	0
Blank Correction	5	8.33	1.5	0	0	1.5	0	0	0	4.33	0	4.67	3.17	8.33	4.67	0	3.83	0	0
D3.25_5_1	1	0	0	0	0	0	1	0	0	0	1	0	0	1	4	0	0	0	0
D3.25_5_2	2	3	3	0	1	0	0	0	0	0	0	1	0	0	3	0	0	0	0
D3.25_5_3	2	1	0	0	0	0	0	0	0	0	0	0	1	0	2	0	0	0	0

	PE	PES	PET	PP	PS	PVC	PU	ABS	PC	PVA	Nylon/ PA	Acrylic	CE	PMMA	PLS	Rbr	PLA	SBR	SAN
Average	2	1	1	0	0	0	0	0	0	0	0	0	0	0	3	0	0	0	0
Blank Correction	0	0	0	0	0	0	0	0	0	0	0	0	0	0	0	0	0	0	0
D3.50_1	6	6	4	2	5	0	1	0	1	8	1	7	6	10	7	0	3	0	0
D3.50_2	0	0	0	0	0	0	0	0	0	0	0	1	0	0	0	0	0	0	0
D3.50_3	6	5	2	0	3	0	0	0	0	2	3	5	1	2	11	0	1	0	0
Average	4	4	2	1	3	0	0	0	0	3	1	4	2	4	6	0	1	0	0
Blank Correction	3	2.33	0	0	0	0	0	0	0	2.67	0	1	1.83	1.67	2	0	0	0	0
D4.10_1	0	2	3	1	3	1	0	0	0	0	3	6	0	5	9	0	2	0	0
D4.10_2	4	5	3	0	0	0	0	0	0	0	1	6	1	5	3	0	0	0	0
D4.10_3	2	4	3	0	4	0	0	0	0	0	3	3	1	3	1	0	2	0	0
Average	2	4	3	0	2	0	0	0	0	0	2	5	1	4	4	0	1	0	0
Blank Correction	1	2.33	1.17	0	0	0	0	0	0	0	0	1.67	0	2	0	0	0	0	0
D4.25_1	4	5	2	2	3	1	0	1	0	4	0	9	1	6	2	0	3	0	0
D4.25_2	3	2	1	0	0	0	0	0	0	4	1	7	3	9	2	0	3	0	0
D4.25_3	3	3	1	0	0	0	0	0	0	2	2	4	2	4	3	0	2	0	0
Average	3	3	1	1	1	0	0	0	0	3	1	7	2	6	2	0	3	0	0
Blank Correction	2.33	2	0	0	0	0	0	0	0	2.67	0	3.33	1.5	4	0	0	1.5	0	0
D4.50_1	22	15	11	7	5	9	2	0	1	16	16	22	7	36	35	0	10	0	0
D4.50_2	7	12	16	2	3	3	0	0	2	6	5	15	1	12	6	0	5	0	0
D4.50_3	0	0	0	0	0	0	0	0	0	0	0	0	0	0	0	0	0	0	0
Average	10	9	9	3	3	4	1	0	1	7	7	12	3	16	14	0	5	0	0

	PE	PES	PET	PP	PS	PVC	PU	ABS	PC	PVA	Nylon/ PA	Acrylic	CE	PMMA	PLS	Rbr	PLA	SBR	SAN
Blank Correction	8.67	7.67	7.17	2.67	0	3.83	0	0	1	6.67	3.83	9	2.17	13.67	9.67	0	3.83	0	0
D5.1_1	24	21	11	6	4	13	5	1	3	18	28	32	20	25	27	0	19	0	0
D5.1_2	0	2	1	0	1	1	0	0	0	0	2	5	3	4	1	0	1	0	0
D5.1_3	6	14	3	1	5	3	0	0	4	7	8	18	5	17	11	0	5	0	0
Average	10	12	5	2	3	6	2	0	2	8	13	18	9	15	13	0	8	0	0
Blank Correction	9	11	3.17	2	1.5	5.5	1.5	0	2.33	7.67	9.5	15	8.83	13	9	0	7.17	0	0
D5.10_1	5	6	1	2	1	0	1	2	0	0	0	9	0	14	3	0	2	0	0
D5.10_2	8	14	7	1	4	1	0	0	0	10	4	9	3	10	16	0	5	0	0
D5.10_3	6	20	3	1	5	4	3	0	0	2	5	20	4	15	13	0	0	0	0
Average	6	13	4	1	3	2	1	1	0	4	3	13	2	13	11	0	2	0	0
Blank Correction	5.33	12	1.83	1	1.5	1.5	1.17	0	0	3.33	0	9.33	1.83	10.67	6.67	0	1.17	0	0
D5.25_1	5	5	2	0	0	0	1	0	0	1	2	6	2	4	9	0	3	0	0
D5.25_2	13	10	2	2	3	4	0	0	0	6	6	18	6	3	12	0	9	0	0
D5.25_3	1	4	1	0	0	1	0	0	1	2	0	6	2	5	5	0	1	0	0
Average	6	6	2	1	1	2	0	0	0	3	3	10	3	4	9	0	4	0	0
Blank Correction	5.33	5	0	0	0	1.5	0	0	0	2.33	0	6.67	2.83	1.67	4.67	0	3.17	0	0
D6.25_1	5	4	2	2	9	2	1	1	0	4	4	14	10	22	13	0	5	0	0
D6.25_2	5	0	3	1	4	1	0	1	0	8	1	22	6	23	16	0	8	0	0
D6.25_3	1	5	3	0	2	2	2	0	0	0	0	2	1	10	7	0	3	0	0
Average	4	3	3	1	5	2	1	1	0	4	2	13	6	18	12	0	5	0	0
Blank Correction	2.67	1.67	0	0	3.17	1.5	0	0	0	3.33	0	9.33	5.17	16	8	0	4.17	0	0

	PE	PES	PET	PP	PS	PVC	PU	ABS	PC	PVA	Nylon/ PA	Acrylic	CE	PMMA	PLS	Rbr	PLA	SBR	SAN
D7.25_1	12	4	5	1	3	0	1	1	0	2	1	14	2	24	17	0	3	0	0
D7.25_2	6	3	3	1	7	1	2	0	1	5	2	11	2	40	12	0	3	0	0
D7.25_3	5	7	7	0	2	4	1	0	1	4	5	8	6	6	8	0	1	0	0
Average	8	5	5	1	4	2	1	0	1	4	3	11	3	23	12	0	2	0	0
Blank Correction	6.67	3.33	3.17	0	2.17	1.5	1.17	0	0	3	0	7.67	2.83	21	8.33	0	1.17	0	0
Field Blank 1.1	1	3	1	0	2	0	0	0	0	0	2	3	1	2	5	0	3	0	0
Field Blank 1.2	0	0	2	1	2	0	0	0	0	0	2	4	0	3	4	0	0	0	0
Field Blank 1.3	5	3	3	0	1	0	1	0	0	2	5	4	1	2	5	0	1	0	0
Field Blank 2.1	0	0	2	1	2	0	0	0	0	0	2	4	0	3	4	0	0	0	0
Field Blank 2.2	0	2	1	0	3	0	0	1	0	1	0	2	0	1	1	0	2	0	0
Field Blank 2.2	0	0	2	0	1	1	0	0	0	1	8	3	1	3	5	0	1	0	0
Average Field Blank	1.0	1.3	1.8	0.3	1.8	0.2	0.2	0.2	0.0	0.7	3.2	3.3	0.5	2.3	4.0	0.0	1.2	0.0	0.0
Nano Blank 1.1	3	4	0	1	3	0	0	0	0	0	5	5	0	2	3	0	1	0	0
Nano Blank 1.3	2	1	1	3	1	1	0	0	0	0	5	2	0	4	4	0	0	0	0
Nano Blank 1.3	3	2	3	2	0	0	0	0	0	0	2	4	0	4	3	0	0	0	0
Average Nano Blank	2.7	2.3	1.3	2.0	1.3	0.3	0.0	0.0	0.0	0.0	4.0	3.7	0.0	3.3	3.3	0.0	0.3	0.0	0.0

Appendix VI. Manuscript version of research Chapter 5 on Svalbard Atmospheric MP Pollution

(submitted to the journal *Nature: Earth & Science Communications* pending peer review)

Polar Particles: Atmospheric Microplastic Pollution in the Arctic Region – an examination of deposited and suspended microplastics in Ny-Ålesund, Svalbard

Anna MacDonald[1*]; Nikolaos Evangeliou[2]; Sabine Eckhardt[2]; Deonie Castle[3]; Christopher J. White[1]; Vernon R. Phoenix[1]; Dušan Materić[4*],

[1]University of Strathclyde, Department of Civil and Environmental Engineering, Glasgow, UK
[2]Stiftelsen NILU (former Norwegian Institute for Air Research), Department of Atmospheric & Climate Research (ATMOS), Kjeller, Norway
[3] University of Waikato, School of Science, Hamilton, New Zealand
[4]Helmholtz Centre for Environmental Research, UFZ, Department of Environmental Analytical Chemistry, Leipzig, Germany
*correspondence: dusan.materic@ufz.de and anna.macdonald@strath.ac.uk

Abstract

Atmospheric microplastics (MPs) are an emerging environmental concern due to their influence on human, environmental and climate health. MPs have been reported globally, from large urban centres such as Shanghai, to remote regions as far as Antarctica. However, there are still considerable knowledge gaps regarding the presence, characteristics and transport pathways of MPs in remote regions. For the first time, deposition and suspended particulates in the planetary boundary layer in the Arctic are measured over a 28-day at Ny-Ålesund in Svalbard (78.9235° N, 11.9099° E), Norway. By utilising μRaman and Nile Red staining with fluorescence microscopy, the average deposition rate was found to be 37.31 ± 30.19 MP/m^2, with an average suspended particulate concentration of 4.15 ± 9.42 MP/m^3. MP particles were primarily <20 μm (72%) and fragments were the most common shape. Predominant polymers identified are Acrylic (16%), Polysulfone (PLS), (14%), Polyethersulfone (PES) (11%), and Polyvinyl alcohol (PVA) (11%). Deposited particles were in general 1% greater in plastic content and had a higher PLS component than suspended atmospheric samples. Local weather data is used to explore the potential meteorological drivers and transport mechanisms affecting MP concentration. Modelling indicates as potential sources of pollution in Svalbard the North Atlantic Ocean, Northern Greenland and the High Arctic, but highlight that when higher concentrations were measured, the air was coming from continental Europe. This is the first time both suspended and deposited atmospheric MPs have been reported concurrently in the Arctic, providing crucial evidence of MP pollution transport and deposition in the Svalbard PBL. More consistent remote region sampling, analysis and reporting are needed for more effective comparison and monitoring of this pollutant in pristine and vulnerable locations such as the Arctic.

Introduction

Microplastics (MPs) have been reported in every environmental compartment in locations all over the world, from remote mountain catchments (Allen et al., 2019) to megacities (Liu et al., 2019). MPs have been considered by some to be one of the most pressing concerns of this generation (Thomson et al., 2024) due to the extent of MP pollution, the associated risks to ecosystem function (Akdogan & Guven, 2019), human health (Jenner et al., 2022) and the climate system (Aeschlimann et al., 2022; Revell et al., 2021). MPs have been examined in marine and freshwater systems (Kye et al., 2023), but despite a recent increase in attention of the role of atmospheric transport of MPs (Zhang et al., 2019), there remain notable knowledge gaps. This is especially true in relation to atmospheric transport processes and the weather patterns that contribute to MP dispersion, suspension and deposition. Furthermore, given the nature of this transboundary pollutant, source appointment relies on particle modelling to trace transport patterns.

It is thought that atmospheric pathways are crucial in the transport of MPs to the world's remote regions such as the Arctic (Evangeliou et al., 2020) and Antarctica (Aves et al., 2022). The Arctic region has been described by some as relatively pristine due to its remote location and small population, and act as sentinels with regards to pollution due to the unique environmental characteristics and ecosystems (Irrgang et al., 2022). The geographic location and distinctive climate make it an important indicator of global environmental health. It is also thought that the Arctic acts as a sink for global pollutants, primarily because of its cold climate and the prevalent atmospheric circulation patterns that transport pollutants from lower latitudes (Zhang et al., 2023). Due to 'Arctic amplification' it is hypothesised that the Arctic region is warming up to four times faster than the rest of the world, which can affect weather patterns (Rantenten et al. 2022) and the vertical atmospheric transport of pollutants like MPs (Revell et al., 2021). Furthermore, the extensive and seasonally changing ice cover within the Arctic and seasonal variations in temperature and precipitation facilitate the accumulation and release of pollutants (Obbard et al., 2014), which can impact local ecosystems and the global climate system.

The deposition of atmospheric pollutants, including MPs, in the Arctic is facilitated by long-range atmospheric transport mechanisms that can transport contaminants and particulate matter thousands of kilometres away from their source (Zhang et al., 2020). When suspended in the atmospheric compartment, MP can be transported by prevailing winds to the Artic region where they can accumulate in snow and ice. These precipitously detained MPs can then be transported via ice melt into the Arctic Ocean and impact wildlife and ecosystem functions (Emberson-Marl et al., 2023). MP contamination in the Arctic has been studied in the marine environment (Ramasamy et al., 2021) and has been reported in all levels of the Arctic food web (Bergmann et al., 2022). -

While atmospheric MP deposition in the Arctic has been studied through snow sampling (Bergmann et al., 2019), measurement of suspended MPs has yet to be undertaken, Moreover, deposited and suspended particulates have not been measured in conjunction in the Arctic. It has been recommended that both forms of atmospheric measurements be conducted in order to create a more complete and comprehensive understanding of total atmospheric content and

transport (Zhang et al., 2020). This study aims to fill this gap by conducting a continuous 28-day sampling campaign consisting of both active and passive measurements in the Arctic to quantify and collecting deposited and suspended atmospheric MPs. By examining both forms of particulates, it is hoped to gain a better understanding of how particle deposition and suspension influences atmospheric MP concentrations in this region and how this could be influenced by weather patterns and transport processes.

2. Methods

2.1 Sample location and collection

Ny-Ålesund is located on Svalbard and Jan Mayen, Norway, (**Figure 1a**) and hosts a number of research stations and activities supporting Arctic research. The station is located at 78.9237° N, 11.9227° E, and is considered as one of the most northern inhabited civilizations in the world. A former mining village, the site is now run by Kings Bay and hosts a range of international research stations (Kings Bay AS, 2021). The Ny-Ålesund research stations are defined and established, through past research and actions, as a primary Arctic research frontier and one of few truly high latitude Arctic research locations. From 17 May to 14 June 2022, a continuous 28-day atmospheric sampling campaign was conducted at Ny-Ålesund consisting of daily active and passive measurements, with the support of the Norwegian Polar Institute (NPI).

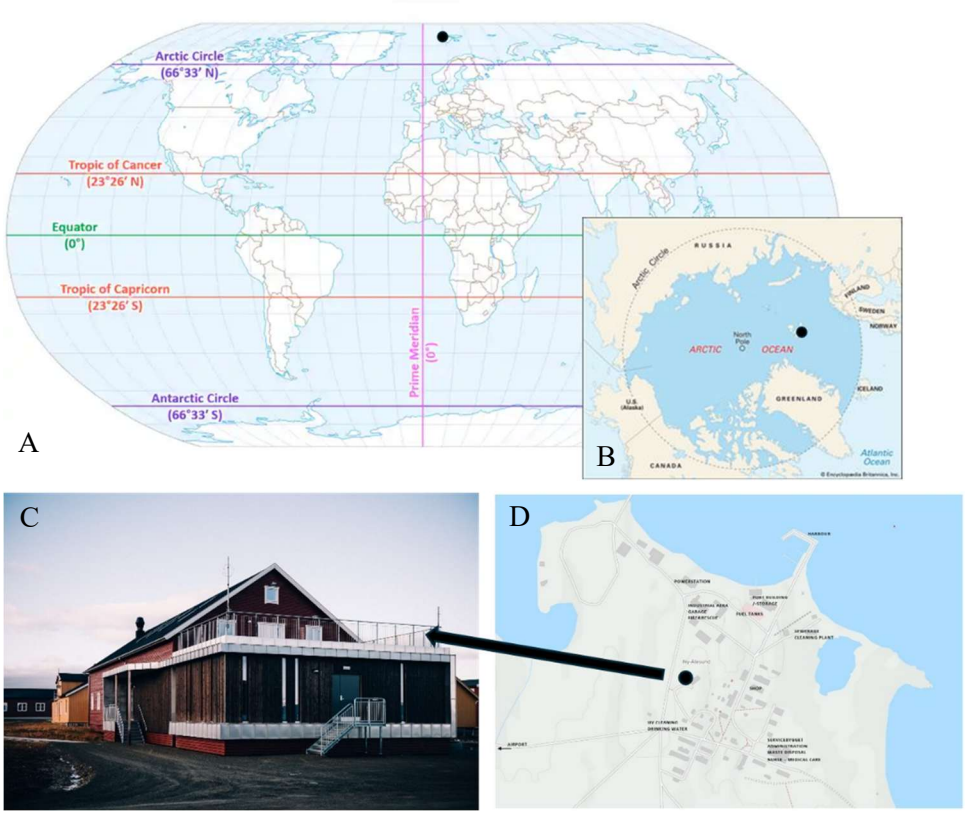


Figure 1. Black points indicate Ny-Ålesund and the location of the research. 1A indicates the sample location relative to the extreme latitudes, 1B highlights the sample location within the more detailed visualisation of the Arctic circle. 1C indicates that actual building location where the sampling was undertaken, building image provided in 1D.

The sampling equipment was placed on the roof of the Veksthuset research station at Ny-Ålesund (see **Figure 1d**) at ~4.5m above ground elevation (AGL). The equipment was mounted on a rail, away from the passing footfall of station staff, researchers and any possible tourists, and in an area where access was limited to minimise local contamination.

Passive deposition samples were collected using a deposition chamber (see **Figure 2a**) filled with a solution of 500ml of milli-Q water and 50ml of ethanol (20%) to collect deposited particulates and prevent the liquid from freezing at low temperatures. Quartz filters (Whatmann, QMA, 1.6µm pore size; 25mm) and replaced with a new solution daily.

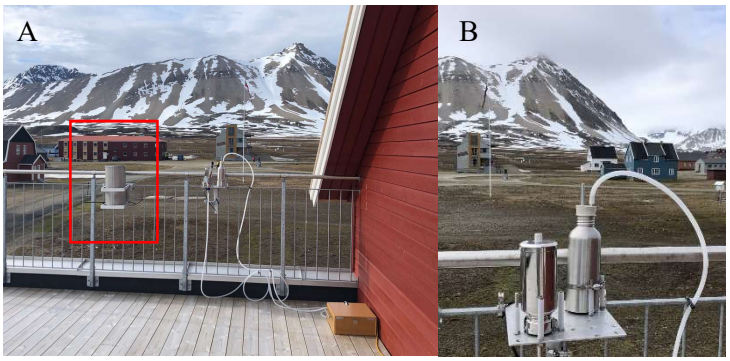


Figure 2. a) Passive (red box) and active equipment set-up on Veksthuset station roof; b) Active equipment set-up at the Veksthuset station (direct air filtration sampler and nanotank samplers)

Active suspended atmospheric samples were collected using two comparative methods in order to capture a wider size range of particulates. The first method uses a pump to draw air into a sealed chamber and through 500 mL of sample collection solution (the same 10% ethanol/milli-Q water); this method is identified as the nanotank. The pumping rate was set at 15 L/min, and the nanotank collection solution was collected daily and vacuum filtered onto QMA filters (same porosity and make as used for the deposition samples). The second and commonly used suspended atmospheric sampling method employed was a standard direct air filtration sampler. Using a pumping rate of 20L/min, monitored with air flow measurer, air was drawn through the stainless-steel chamber where particulates were collected on the same QMA filters (see **Figure 2b)**. The filters were then switched every 3 days. All samples were stored in pre-treated aluminium tins prior to analysis.

2.2 Micro-Raman (µRaman) spectroscopy

Micro-Raman (µRaman) spectroscopy was used to provide polymer characterisation, specifically identification of the types of plastic polymers within the different sample sets. µRaman uses a laser to excite molecules within the selected particle, causing the release of photons and the resulting signal provides information on the chemical structure and molecular interactions. This fingerprint or signal dataset, incorporating both the chemical makeup and types of bonds, create a vibrational spectrum that is unique to individual plastic polymer types. Individual particles can be characterised through comparison of these µRaman spectra and established libraries of known plastic polymers (Enyoh et al., 2019).

A selection of the samples were analysed with µRaman spectroscopy (23% of samples, 15 unique individual samples completed in triplicate) in order to gain a picture of the polymer composition of the dataset. While it would be ideal to undertake analysis of the totality of all filters using µRaman, the resource (both financial and time) required to achieve this with a sample set of 65 sample types and timesteps (n = 195 including triplicate assessments) make this unviable. Therefore, five days of deposition samples, five days of nanotank samples, and three active direct air filtration samples were randomly selected across the 28-day period and analysed using the µRaman. The µRaman spectrometer (WiTec Alpha 300 RA, Helmholtz Association, Leipzig) used employed a 532nm laser with a 1200mm^{-1} grating and 50µm split settings. The spectrometer was set to collect spectra between 200-2000 cm^{-1} Raman shift for

all particles down to 1.6 µm, with an acquisition time of 10 seconds and 2 accumulations and with power at 35 mW. Each sample was analysed in triplicate across three areas (≈1% of the filter in each sub-sample window, 1x1mm). There was no bias in the particle selection for analysis based on colour, shape, or size (all particles were analysed irrespective of appearance), and the filter was also analysed for background spectra analysis. There were >100 particles analysed per subsample. This sub-sample area selection was used to provide a representative sample (>100 particles) (Zhao and Dahal, 2020; Cowger et al., 2024) within a sensible and achievable time frame.

The resulting spectra were saved as SPC files and analysed using Spectragryph (version 1.2.15) (Menges, 2022). Multivariate analysis of each spectra was completed and reference libraries were used to confirm polymer identification (SIMPLE, SLOPP and SLOPPE databases and the laboratory reference plastics spectral database (Jin et al., 2022; Levermore et al., 2020; Xu et al., 2020). Particles were only confirmed as plastic if a HIT (hit quality index) rate of ≥80% was achieved (Cowger et al., 2020; Levermore et al., 2020), and those below the <80% threshold discounted as non-plastic particles.

2.3 Nile Red staining

In order to gain information on the size and shape of the MP particles and a comprehensive particle count, samples were also analysed with Nile Red fluorescence microscopy. Fibres were identified using the standard 1:3 width ratio as used frequently within MP studies (Na et al., 2024; Li et al., 2020), and the rest are classified as fragments. A 1% (0.1µg mL^{-1}) Nile Red solution was used to stain the samples, which were then oven dried at 30°C overnight and then stored in a fridge 4ºC in sealed aluminium containers to rest before they are imaged with the fluorescent microscope. It has been reported that this process of drying, cooling and de-energizing (in the dark) can aid with the MP staining, fluorescence efficiency and minimise staining of organics resulting in false-positives (Galvão et al., 2023).

All samples that were not subject to µRaman analysis were imaged with a fluorescence microscope (Nikon Eclipse LV100ND), using a x10 objective and fluorescence mode (with QMA Whatmann with 1.6µm pore size), and a 470nm wavelength lamp. A transect of images (1.4 x 0.94 mm each) were taken from the top to the bottom of the filters resulting in 20% of the filter being analysed (taking into consideration the sub-sample method findings of Huppertsberg and Knepper (2018)). The software FIJI/ImageJ (Schindelin, et al., 2012) enabled automated particle count, shape and size. Resulting MP counts were then calculated relative to the total area of the area analysed and extrapolated for the total area of the filter.

2.4 Microplastic contamination prevention

Multiple steps were taken to ensure that contamination of MPs was minimised at each step of the data collection and analysis process. In the field, the equipment was set-up away from any potential interference or contamination from visitors and station staff . In addition to this, only natural materials were worn during the collection of samples (wool, cotton) and blanks were

taken during sample collection, in the processing laboratories in Svalbard and in Glasgow. The University of Strathclyde, where sample preparation and all Nile Red staining and images were produced, has a MPs clean lab where only natural materials are permitted to be worn, cotton lab coats are used, an air filter is used, cleaning with ethanol and milli-Q is conducted regularly and access is limited in order to minimise contamination. In addition, the filters used to collect samples and the stainless-steel containers used to store and transport the samples were heat treated before use (~450℃ oven for 15 minutes). The ethanol used for field sampling was vacuum filtered before use (Whatmann QMA filters with 1.6µm pore size) and blanks of the milli-Q, ethanol and the milli-Q/ethanol solution were taken. All blanks were treated in the same way as the samples, with one being analysed with µRaman spectroscopy to gain an understanding of polymer contamination, and the rest stained and imaged with Nile Red to understand the particle size, shape and number of particulates from contamination. All results have been adjusted to account for the contamination found in these field and procedural blanks based on their particle size distribution from the Nile Red staining of blanks (<30% of total plastic particle count), as there were no identified polymers in the blank subjected to µRaman analysis.

2.5 Statistical analysis

To calculate the amount of MPs in each deposited and suspended sample, the following sets of equations for used.

To calculate the number of MPs per sample (all samples):

$$\mu P = (P_s/A_s) \times A_f$$

μP = MP per total sample

P_s = MP particles in the subsampled area (count)

A_s = area subsampled (mm^2)

A_f = area of total filter (mm^2)

For individual suspended samples (direct air filtration and nanotank), to calculate the volume of air per sample, following equation was used:

$$V = (t_s \times f_s)/1000$$

t_s = time (mins) for the total sample

f_s = flow rate (L/min) for the sample

V = air volume sampled (m^3)

For the suspended air samples (nanotank and direct active air samples), the total representative MP per m^3 is calculated as:

Total suspended MP = $\mu P/V$ (MP/m^3) , which in long had is:

$$MP = ((P_s/A_s) \times A_f)/ ((t_s \times f_s)/1000)$$

For total deposition samples

$$MP = \mu P/ A_d \ (MP/m^2)$$

$$V= (P_s/A_s) \times A_f)/A_d$$

Where A_d = area of the deposition collector open to the atmosphere (m^2) (i.e. the deposition bucket base area).

Filters were generally 47mm diameter for active air samples, 25mm diameter for nanotank samples and deposition samples. Sample durations ranged from ≈ 1430mins for 24 hour (nanotank and deposition samples) or ≈ 4305 mins for 3 day set sampling durations (direct air filtration samples). Sample flow rates for active samples were 15 L/min for the nanotank and 20 L/min for the direct air filtration samples.

2.6 Relationship with Weather Parameters

One of the main research questions was to identify potential drivers of atmospheric microplastic pollution in this region and if there was a possible relationship between MP concentrations and weather parameters. Weather data collected at the Ny-Ålesund research station was collated from the Norwegian Centre for Climate Change repository (Maturilli et al., 2022a, 2022b; Norwegian Centre for Climate Services, 2022) for the sampling period May-June 2022. Due to the difference physical processes represented by the deposition vs the nanotank and active air samples, correlation analysis was undertaken for each sample type and atmospheric variable separately. The main weather parameters assessed were precipitation (mm), atmospheric pressure (hPa), humidity (mean dew point, mixing ratio), snow depth (cm), snow cover (%), wind speed (m/s), wind direction (and as an extension of this, whether the wind was land or sea-based). Pearsons correlation coefficient (r) was calculated for each variable and MP dataset along with the corresponding p-value.

2.7 Atmospheric dispersion modelling

The transport of MP to the sampling sites (receptor) was simulated using the Lagrangian particle dispersion model FLEXPART version 11 (Bakels et al., 2024). The model was driven by ERA5 assimilated meteorological analyses (Hersbach et al., 2020 with 137 vertical levels and a spatiotemporal resolution of 0.5°x 0.5° and one hour. FLEXPART treats gravitational settling (Tatsii et al., 2024), dry and wet deposition of aerosols (Grythe et al., 2018), turbulence (Cassiani et al., 2018), unresolved mesoscale motions (Stohl et al., 2015), and deep convection

(Foster et al., 2007). FLEXPARTv11 uses a new feature that simulates non-spherical shapes (Tatsii et al., 2024), which makes it unique for MP considering that MP are usually in the shape of fragments or fibres.

Surface concentrations were simulated by releasing computational particles at heights 0–100 m from the receptor in the classic "retroplume" mode. Wet and dry deposition at the receptor was simulated separately (Eckhardt et al., 2017). Specifically, wet deposition was reconstructed after releasing computational particles at the sampling site (receptor) at altitudes of 0–20 km above sea level and wet removal was calculated using different coefficients for in-cloud and below-cloud scavenging. For dry deposition, computational particles were released at 0–30 m at the same receptor point, as this shallow layer is equal to the height of the layer in which, in forward mode, particles are subject to dry deposition. All released particles represent a unity deposition amount, which was converted immediately (i.e. upon release of a particle) to atmospheric concentrations using the deposition intensity as characterized by either the dry deposition velocity or wet scavenging rate (Grythe et al., 2018).

The model output consists of a footprint emission sensitivity that expresses the probability of any emission occurring in each grid-cell to reach and/or deposit at the receptor. It is converted to modelled concentrations or deposition rates, when coupled with gridded emissions. Modelled concentrations or deposition rates can be calculated as a function of the time elapsed since the emission has occurred namely "age spectrum", for specific regions/continents ("continent spectrum"), and for different source categories ("source spectrum"). Here, we coupled footprints with updated emissions from Evangeliou et al. (2022) that were derived with top-down approach.

3. Results

3.1 Microplastic Concentrations: Suspended and Deposited Particulates

From the μRaman and Nile Red fluorescence particle analysis, the average deposition rate of MP particles during this period was 37.31 $\pm$ 30.19 MP/m^2. The highest reported deposition sample was taken on 26 May 2022 with 127.45 MP/m^2 (Deposition sample number 9), and the lowest with 8.20 MP/m^2 was taken on 06 June (Deposition sample number 20). MP concentrations for each timestep (for deposition) and sample type are displayed in **Figure 3** (SuppInfo Table X5).

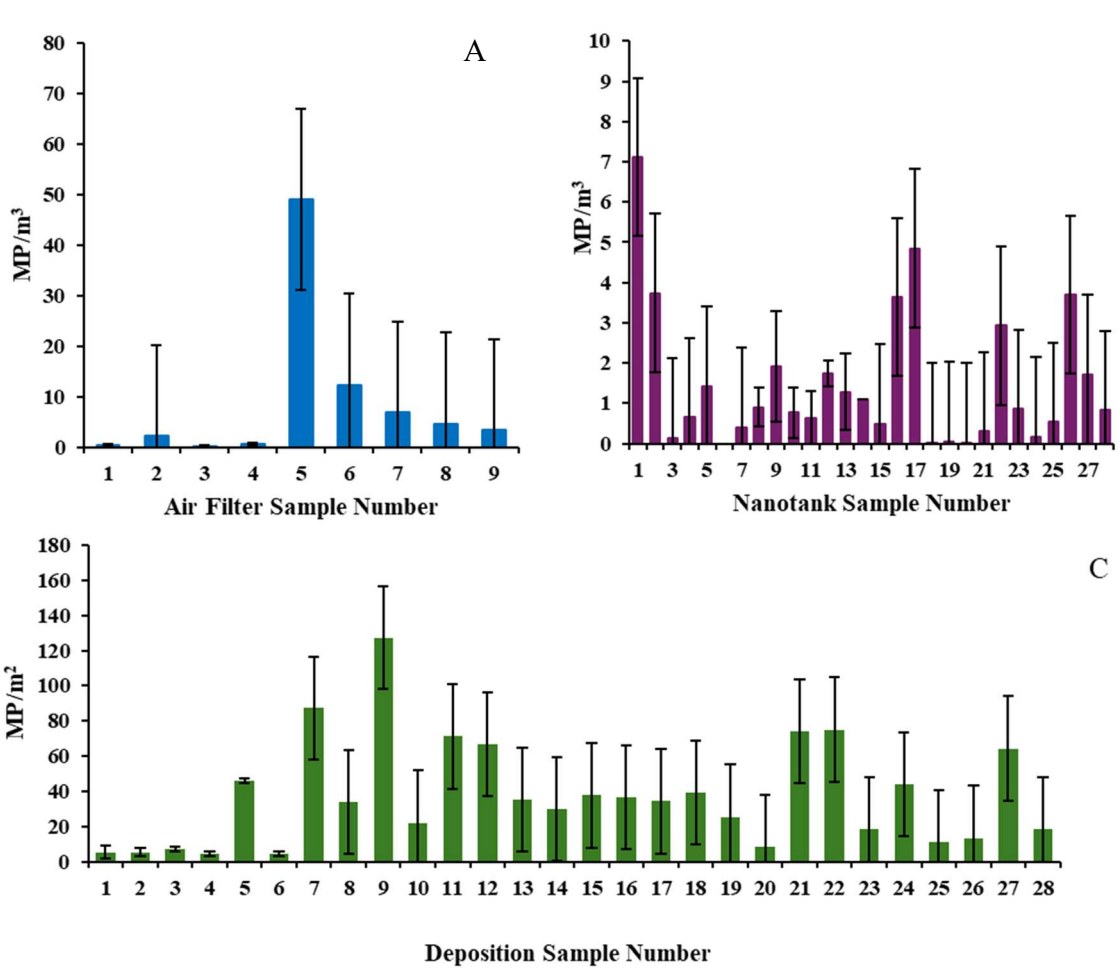


Figure 3. a) MP concentrations for active direct air filtration samples (MP/m^3); b) MP concentrations for active nanotank samples MP/m^3 c) MP concentrations for passive (deposition) samples (MP/m^2); error bars indicate standard deviation. Nanotank and Deposition samples represent daily sampling, while each direct air filtration sample was collected for three days.

The average MP concentration for suspended particulates was 4.15 $\pm$ 9.42 MP/m^3 (with nanotank samples 1.51 $\pm$1.75 MP/m^3 and direct air filtration samples at 8.85 at 8.85 $\pm$ 15.57MP/m^3). The highest concentration of suspended particulates was 49.06 MP/m^3, taken with a direct air filtration sampler between 29 May and 01 June (direct air filtration sample number 5, ***Figure 4***), and the lowest concentration from direct air filtration samples from 20-23 May with 2.26 MP/m^3 (direct air filtration sample number 2, ***Figure 4***).

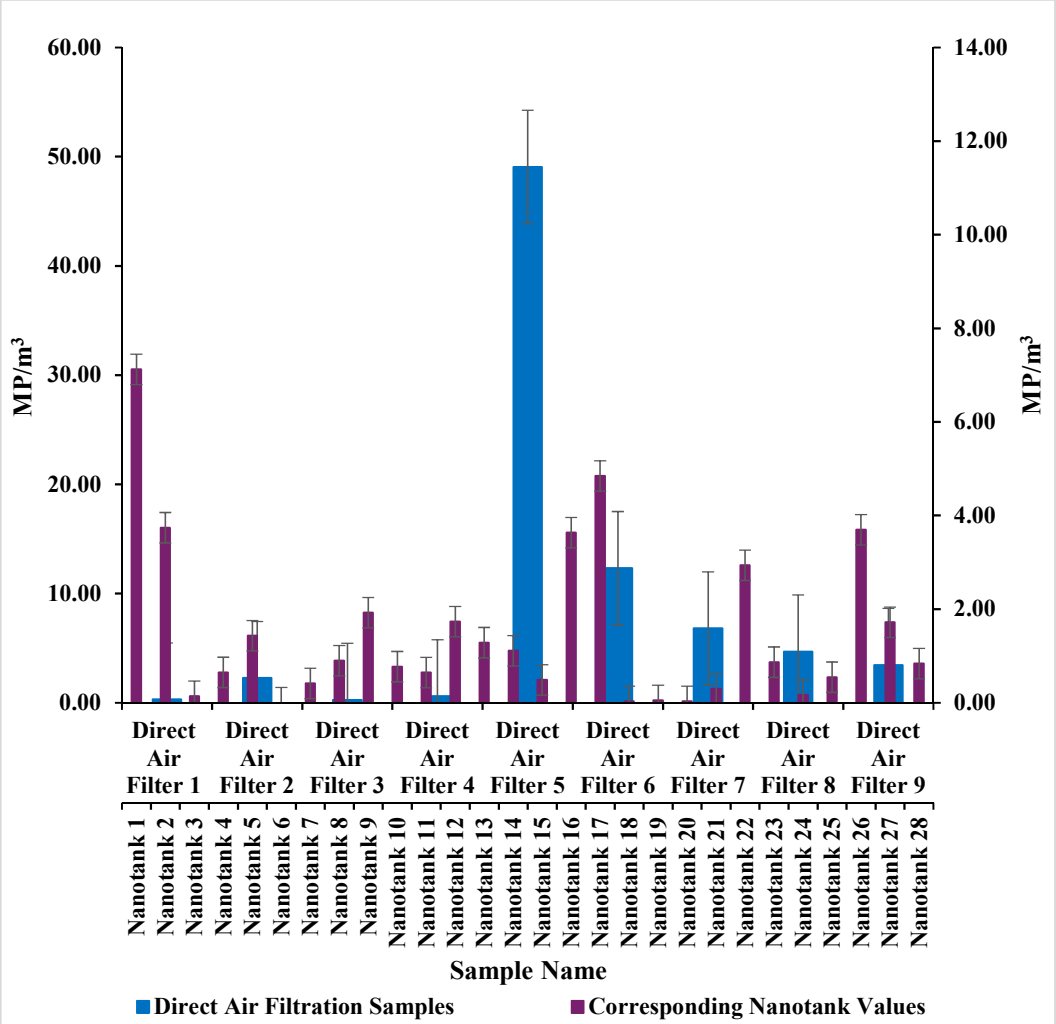


Figure 4. MP Concentrations for Active/Suspended Samples; Direct Air Filtration with Corresponding Nanotank Values (Supp Info Table X5)

For the nanotank samples, the procedural blanks were fairly contaminated, which was likely due to the milli-Q supply (see Supplementary Information). The highest nanotank concentrations were found on 18 May with 7.12 MP/m^3 (Nanotank sample number 1), with the lowest day with no particles present after blank correction on 23 May'21 (Nanotank sample number 6). This lower concentration is in line with comparative lower direct air filtration concentrations on the same day (Air sample number 2) which could indicate low levels of suspended pollution on this day. After reviewing the nanotank MP results, a longer sampling duration or a higher pumping rate is recommended in order to collect a representative dataset in a more pristine environment. Furthermore, due the tendency of Nile Red to stain organic material (Chatterjee et al., 2023), a more conservative approach was taken to analyse the dataset which may have resulted in a lower particle count but this was preferred to an over-estimation of results.

It is acknowledged that both nanotank and active air samplers collect particles suspended and transported in the lower atmosphere. The samplers collect particles in different mediums

(water vs directly onto a 1.6 µm filter respectively) and it is recognised through past published research that different sampling methods can result in variation in sample results, especially in the field.

With the µRaman analysis, there was a notable difference in the number of MP particles identified in both the active samples and deposition samples (Table 1). The average MP particle count for all samples identified by µRaman analysis is 0.95MP/m^3 ($\pm$ 0.57 MP/m^3 and deposition 12.1 MP/m^2 ($\pm$ 16.6 MP/m^2) (**Table 1** and Supp Info). There is also approximately x 3 to an order of magnitude more particles (all particulate matter, not just microplastic) in the deposition samples compared to the air samples and approximately twice as many MP particles in the deposition samples compared to air samples.

Table 1. Average MP for suspended and deposited particulates and Total Particles (all particles highlighted for analysis, including non-polymers) identified using µRaman analysis

	% particles that are plastic	**Standard Deviation**	**Total particles/m^3**	**MP/m^3**	**Standard Deviation**
Suspended Particulates - Active Direct Air Filtration Samples	1%	0.06%	34.49	0.4	0.18
Suspended Particulates - Active Nanotank Samples	1%	0%	118.2	1.2	0.49
Deposited Particulates – Passive Samples	2%	2%	613.5 (m^2)	12.1	16.6

3.2 Microplastic characteristics

The majority of MP particles (72%) were <20µm in size. The largest particle (a fibre) identified was 250µm (found in a deposition sample) and the smallest particle identified was 1.6µm (given the lower limit of the 1.6µm pore size used on the filters). The suspended particulates displayed slightly larger particle size distributions with more particles above >20µm than deposition samples (see **Figure 5A**).

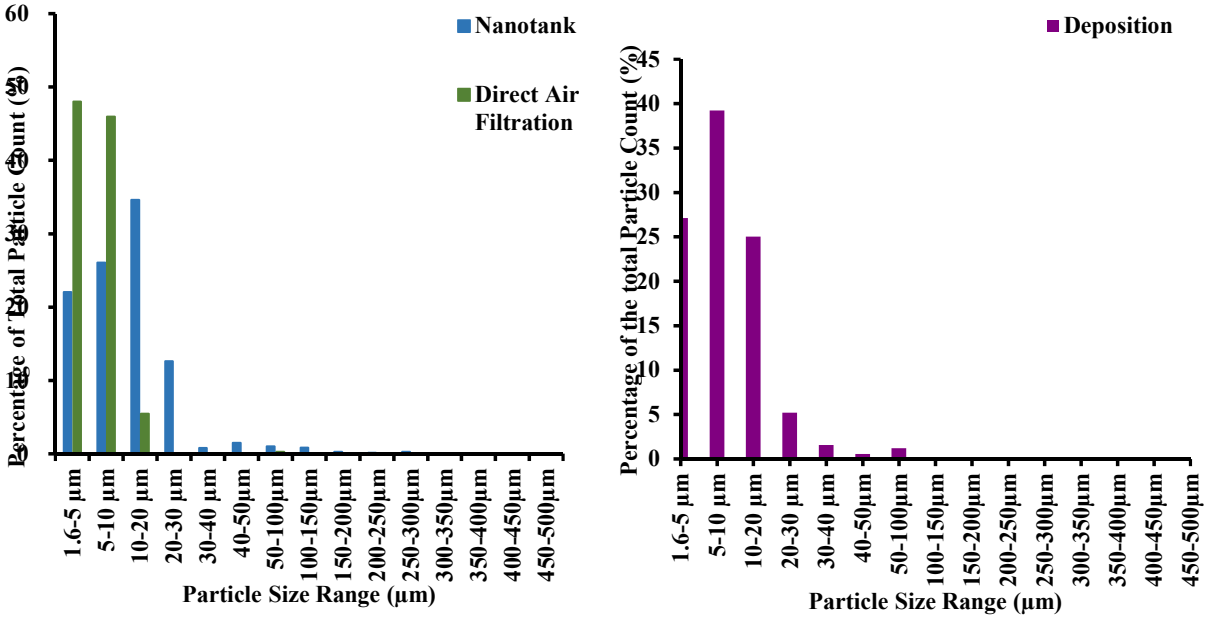


Figure 5. a) Particle size distribution for suspended particulates (direct air filtration and nanotank samples) as a percentage of the total particle count; b) Particle size distribution for deposition particulates (deposition samples) as a percentage of the total particle count (SuppInfo Table X1-3)

Fragment and fibre were the two categories chosen for the analysis of particle shape given the difficultly in defining films (Borah et al., 2024; Allen et al., 2019). The most common shape found was fragment with only 2% of the particles analysed being identified as a fibre (Supplementary Info). Both the suspended and deposited particulates displayed similar percentages of fragment and fibres (both < ~2% identified as fibres).

3.3 Polymer composition (µRaman)

MP particles were identified in all samples (n=15) for both active (suspended) and deposition samples. The predominant polymers were Acrylic (16%), PLS (polysulfone) (14%); PES (Polyethersulfone) and PVA (Polyvinyl alcohol) (both 11%) (**Figure 6**). Both deposited and suspended particulates had similar polymer compositions, however PLS, PU, Rubber, PLA, SBR and SAN was more prevalent in deposition samples.

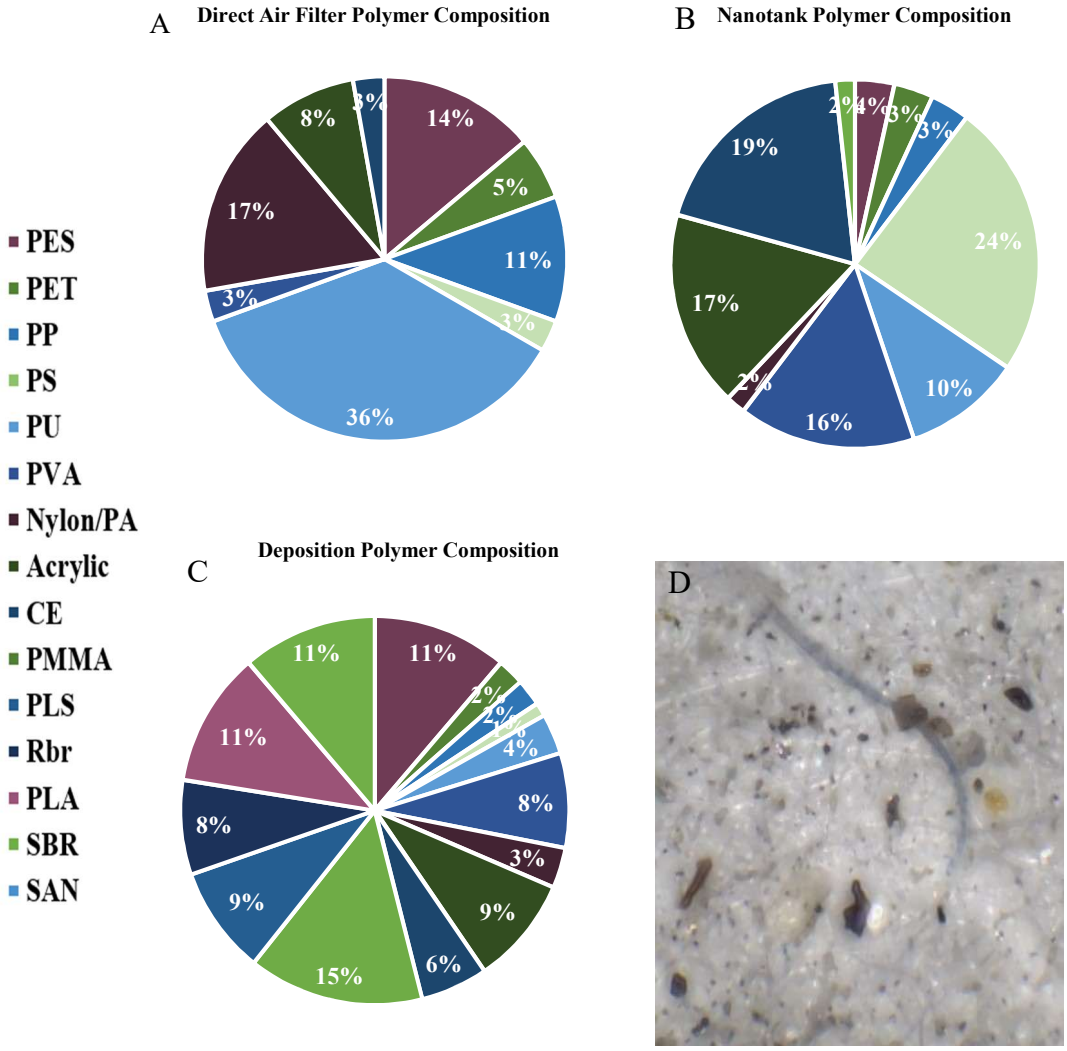


Figure 6. a) Polymer composition direct air filtration samples; b) polymer composition of nanotank air filtration samples; c) polymer composition of deposition samples; (all expressed as total percentage of polymers identified using µRaman); d) Image of deposition filter from micro-Raman spectrometer (QMA Whatmann 25mm, 1.6µm; x10 objective)

Although it is unusual to not see PE, PET, and PVC in the polymer composition of these samples, this could be due to the small particle size at this location, or the influence of different local and distal sources.

3.4 Atmospheric MP pollution and weather parameters at Ny-Ålesund, Svalbard

No significant correlation was found between MP concentration and precipitation, and other meteorological variables such as wind speed, wind direction, atmospheric pressure, snow

cover and snow depth, for both suspended and deposited particulates. For MP concentration and cloud cover, there was also a moderate positive correlation with deposition (r=0.454, Pearson Correlation p=0.02), but not with suspended samples, indicating that deposition of atmospheric MP pollution could be influenced by cloud cover. A positive relationship between direct air filtration samples and the mixing ratio (measure of quantity of water vapour in air relative to dry air was identified (p=0.0001). However, overall, the absence of a strong correlations between MP numbers and individual local meteorological conditions suggests transport and deposition of MPs at the local level is complex with a number of contributing factors.

When correlations between MP concentration and the weather patterns were not strong, the MP concentrations were split into two size categories >20µm and <20 µm. Given that more than 80% of both deposited and suspended particulates identified were below 20 µm, it was thought that this could be a determining factor in the transport of atmospheric microplastic via weather processes. For snow depth, there was a stronger correlation for particles <20µm than >20µm, for direct air filtration (suspended) particulates (r=0.939, p < .001) and deposition particulates (r=0.432, p= 0.0216), but a non-significant positive correlation for nanotank samples (suspended) (r=0.183, p= 0.351). This suggests that snow could be driving the deposition and suspension of atmospheric MP particles below <20µm. The depth of snow in this context is the height of accumulated snow, while precipitation refers to total moisture from the sky (including rain, snow, sleet and freezing rain) (Norwegian Centre for Climate Services, 2025). As it is considered that snow is a more effective scavenger of airborne pollutants than rain, due to its higher porosity (Nazarenko et al., 2017) this could indicate that Arctic environments are particularly susceptible to particularly susceptible to being a sink for MPs as they have more snow.

For precipitation there was a stronger negative relationship with particles >20µm (p=0.040) than the other samples which is consistent with findings that larger particles are more easily scoured from the atmosphere via rain than smaller particles (Parashar and Hait, 2023). There may be less MP removal efficiency from rain due to the hydrophobic nature of MPs (Revell et al., 2021), which could also explain why the weaker relationship between precipitation and MP concentrations for all sample types. For both active sampling methods, there was a positive relationship between particles <20µm and wind direction (p<0.01), but not deposition, which indicates a possible trend with wind direction and suspension of smaller particulates. There was a statistically supported higher concentration when wind direction was on-shore, from sea to land, for nanotank particulates >20µm but no trend with deposition. For direct air filtration samples <20µm there was a statistically significant positive relationship with mixing ratio and the mean dew point average (definitions in Supplementary Information; p=0.02), suggesting that the suspension of smaller particulates are influenced by water vapour present in the atmosphere. Overall, even when particles are split into size fractions, it is evident there are numerous complex processes affecting the transport, deposition and suspension of MP particulates in Ny-Ålesund.

3.5 Potential contributing sources of MP in Svalbard

The source contribution to modelled atmospheric concentrations or deposition rates is shown in **Figure 7.** For this, the calculated source-receptor relationships (footprints) for the exact sampling dates and times are coupled with updated emissions from Evangeliou et al. (2022), which are shown in Supplementary Figure X1. Active, nanotank and passive observations are represented by the green line. In general, we see that modelled concentrations are overestimated. This points out the general problem of efficient atmospheric dispersion modelling of MPs, which is associated with the uncertainty of the current source emissions, both in terms of emission intensity, but also with the accurate geolocation of the main sources. However, especially for the observed concentrations, the model represents well the timing of the highest levels measured (end of May for both passive and nanotank samples).

As regards to the contributing sources to surface concentrations, the prevailing sector is oceanic MPs, though the concentrations are low. Oceanic macroplastics decompose over time to smaller MPs, due to photodegradation, and are often remobilised, when breaking waves cause bubbles of trapped air to rise and burst (Allen et al., 2020). They are then subject to long-range transport and may deposit on the marine or terrestrial environment, somewhat similar to the well-known grasshopper effect for persistent organic pollutants (Gouin, 2021). The peaks of oceanic MPs that coincide with high observed surface concentrations in **Figure 7a** originate from North Atlantic on June 1st (see Fig. X2). Today, there is an ongoing debate about whether the ocean is just a sink for atmospheric MPs or a significant source with many researchers supporting one or the other approach (Evangeliou et al., 2022; Brahney et al., 2021; Yang et al., 2025; Bucci et al., 2024). Observations combined with dispersion models suggest that there is high probability that MP are resuspended from the ocean and transported over long distances for their source. For instance, Goßmann, et al. (2023) reported surface concentration of over 30 ng m^{-3} during a ship campaign over the Norwegian coasts, when air was originating directly from the ocean (west). Ferrero et al (2022) reported concentrations of 24 ± 9 and 45 ± 20 items m^{-3} in the open Baltic Sea and to the Gotland Island, very close to those measured in the sea (79 ± 18 items m^{-3}). Caracci et al. (2023) showed that samples largely influenced by sea-spray and air masses originating from coastal South America and the north Atlantic subtropical gyre were more contaminated by MNPLs along the transect from Vigo (Spain) to Punta Arenas (Chile).

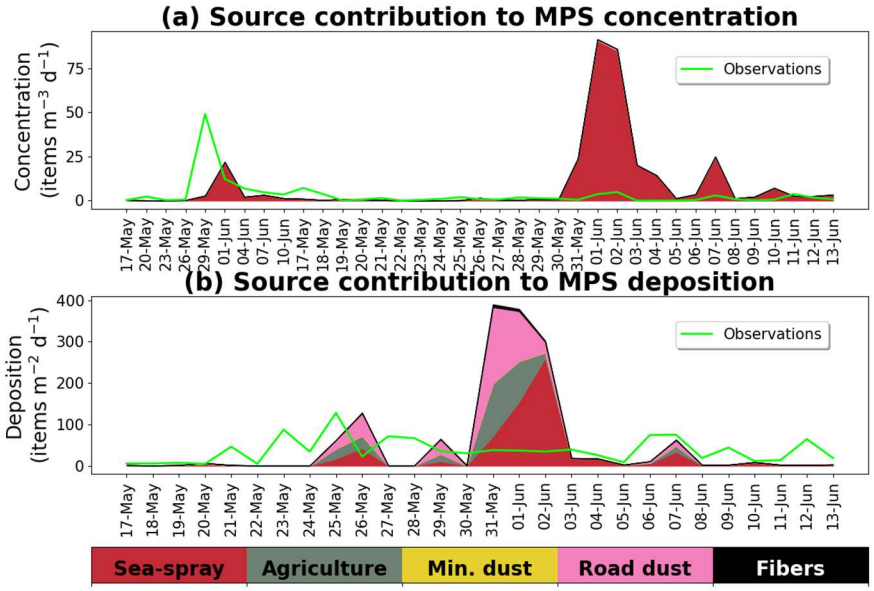


Figure 7. Source contribution to modelled MP at Ny-Ålesund for (a) active and nanotank samples (surface concentrations and (b) passive samples (deposition rates). Five different emission sectors were considered, namely MP suspended from the ocean (sea-spray), agricultural activity (e.g., agricultural nets), soil (mineral dust), road dust (tire wear particles) and microfibers (releases from clothes of the population), adopted from an updated version of the MP emission dataset from Evangeliou et al. (2022).

The modelled results for passive samples deviated more from the respective observations (Figure **7b**), although the highest modelled deposition rates were obtained for observations that were 50 items m-2 d^{-1} or higher. However, there were observations, for which model showed zero deposition (e.g., 21 – 24 May). Although in the same order of magnitude, modelled deposition rates are again overestimated; they also show contributions from other emission sectors, such as road dust and agricultural activity (nets). The largest contribution is again achieved for the same dates as in the active and nanotank samples (30 May – 4 June). During this period, the footprint covered not only oceanic domain, but also parts of the United Kingdom and Europe, which denotes that MP can also originate from there too (Fig. X3). Following findings from Brahney et al. (2020) who reported that wet deposition constitutes around 20% of total deposited MP (wet + dry) after measuring MP with special buckets that could separate precipitation and settling, we have assumed that wet scavenging contributes about 20% of total deposition by adjusting the scavenging coefficients in the model. This is a realistic approach considering that MP consist of macromolecular polymers that are largely hydrophobic.

4. Discussion

One of the main research aims was to establish if there were differences between deposited and suspended particulates in the Arctic region. However, there was no correlation between the highest and lowest reported MP concentrations for each type of sample, suggesting that each sample had relative efficiencies at collecting particulates. In terms of the Nile Red results, the average deposition rate during this period was 37.31 $\pm$ 30.19 MP/m^2, and the average suspended particulate concentration was 4.15 $\pm$ 9.42 MP/m^3 (with nanotank samples 1.51 $\pm$ 1.75 MP/m^3 and air filter samples at 8.85 $\pm$ 15.57MP/m^3). This highlights the difference in reported concentrations of both methods, and how this can make comparison between studies and countries difficult. From the µRaman analysis, the deposition rate was reported at 12.1 MP/m^2 and MP concentration for suspended particulates was 0.95 MP/m^3. This highlights the effect method of analysis can have on the particulates identified and the need for more than one method of particle analysis. In terms of polymer composition, the deposition and suspended particulates displayed similar results. However, the deposited samples had a slightly higher proportion of some polymers such as PLS (see **Figure 7A**). It is difficult to pinpoint why this could have occurred due to the complex relationship between weather parameters and transport identified here.

When examining the influence of weather parameters with the MPs identified in this study, it was evident there were multiple parameters and processes driving suspension and deposition here. There may be a trend with humidity, wind direction and cloud over here but examining these complex relationships over a longer period of time would be beneficial to determine their relative significance. Although the studies examining the relationship with MP and humidity are limited, some have reported increased MP concentrations with increased humidity (Allen et al., 2020; Szewc et al., 2021). Furthermore, it has been reported that humidity can accelerate the photoaging process and lead to increased fragmentation in MP, which could in turn influence MP concentrations and transport (Wang et al., 2023). Wind direction has been found to be an important factor for marine-sourced microplastic pollution (Ryan et al., 2023; Collins and Norton 2024), and given the potential sources of the MP pollution found in Ny-Ålesund, this could be an important factor to monitor and understand. Snowfall is also regarded as one of the main carriers of atmospheric MPs, transporting them to remote regions from the Alps (Jurkschat et al., 2025), and Antarctica (Aves et al., 2022). Studies examining the relationship between snow, microplastics and its resulting climate impacts are limited, but suggest that MP could affect cloud formation and accelerate ice melt (Revell et al 2021.; Aeschlimann et al., 2022), therefore understanding this relationship will be crucial for MP research in the Artic region going forward.

To further elucidate potential transport from hot-spot regions, from where atmospheric MP were resuspended before being transported and deposed in the High Arctic (Svalbard), we calculated the average footprint emission sensitivity (FES) for those observations that are below and above a certain threshold. Here, we use the 25th and 85th percentiles of the measured samples. The basis of this method is that if a source is located at a given grid cell of the spatial domain, an air parcel passing through this location indicates that material from the source can be collected and transported along the trajectory to the receptor site. **Figure 8** shows the average FES for the observations that were lower (left) and higher (right) than the 25% of the samples collected in Svalbard.

We report that when observed concentrations in Svalbard are low (< 25th percentile), the source regions of MP to remote high latitude areas of Norway include the North Atlantic Ocean, Northern Greenland and the High Arctic (**Figure 8a**). Although these regions present very significant MP emissions, (see Figure X1), both the FES and MP emissions are weak in the Northwestern Atlantic. On the contrary, higher MP were measured when long-range transport occurred from the Northeastern Atlantic, the Norwegian coasts and the United Kingdom (Figure 8b), while the FES is stronger towards the eastern part of the North Atlantic. As seen in **Figure 8**, this region corresponds to the main oceanic MP emissions. This shows that despite that the geographic location of the oceanic sources is likely correct, their intensity is highly uncertain, causing higher modelled concentrations. While constraining MP emissions in remote regions requires a large number of robust observations (the current analytical methodologies have several limitations), the existing oceanic MP emissions are probably too high in the North Atlantic Ocean.

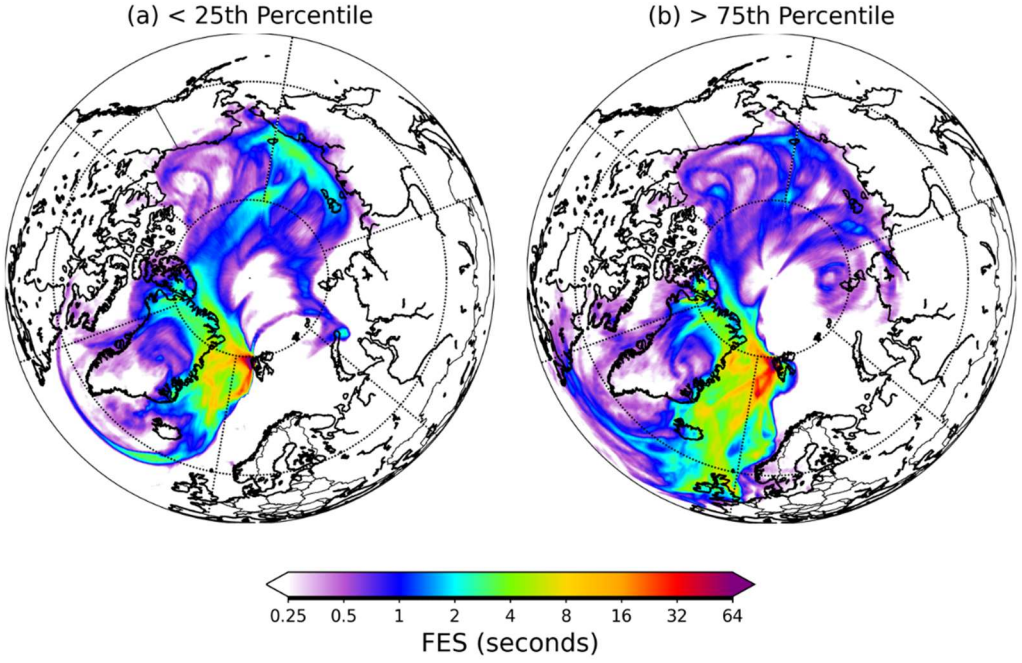


Figure 8. Average footprint emissions sensitivity for the (a) lowest (left) and the (b) highest 25% (right) measured surface concentration (active and nanotank samples) and deposition rates (passive samples) of MP in Ny-Ålesund.

The Bergmann et al. (2019) study of atmospheric fallout in the Arctic region is the most directly comparable study as it is the only other study reporting atmospheric MP pollution in this region. While there are some similarities with the present study, different methods were used, which consisted of snow deposition samples and µFTIR as their main method of analysis (thus different analytical windows prevent direct comparison of the results). The dominance in the present study of Acrylic, PLS, PES and PVA (is consistent with Bergmann et al. (2019), which compared Arctic and European snow (deposition) samples, and identified acrylates and polyurethane, rubber, polyamide and polyvinyl chloride (PVC) as predominant polymer types

for Arctic snow. The high proportion of acrylics in the polymer composition here, could be due to its common use in marine fishing equipment and outdoor clothing. PLS is commonly used industrial membranes and PES is often used for electric insulation, whereas PVA is also common with artificial textiles as well as food packaging. However, due to the small size ranges of the particles sampled it is likely that the MPs identified at Ny-Ålesund originated from distal sources and could have travelled from a range of locations.

Similar to the present study, Bergmann and colleagues (2019) also reported small particle size ranges with particles identified in the 11µm and 475µm size range, and 80% of MPs $\leq$25µm and 98% <100µm (Bergmann et al., 2019). This study also reported much smaller fibres found in Arctic snow, compared to European snow, which is similar to the small number of identified fibres in the present study (**section 3.2**). The distal sources of this pollution in the Arctic region could result in the weathering and fragmentation of particles whilst in transit, and particles here could have a long residency time in the environment. This could cause fibres to breakdown into smaller fragments, or it could be a result of fibres having different transport properties to fragments in the atmosphere (Chen et al., 2023; Evangeliou et al., 2020). The differences in polymer composition between the present study and the previous Arctic study could be due to a number of factors including the methods of sampling, the differences in analytical equipment, time of year and location of sampling. Bergmann et al. (2019) reports MP deposition per litres of snow, which makes comparison to the volumetric data presented in the present study difficult.

Rosso et al. (2024) analysed MP content of the glaciers on Svalbard, again using µFTIR to analyse material composition. This study reported different polymer compositions to the present study, but also found small particle size distributions and the reported concentrations to be in a similar range to the deposition found in the present study (37.31$\pm$30.19 MP/m^2) (**Table 3**). Rosso et al. (2024) also reported that the Ny-Ålesund station could be a localised source of MP pollution in this region. Another recent study analysed wastewater effluent as a potential source of MP pollution in the Arctic (Bach et al., 2024), highlighting that both localised and distal MP pollution is affecting the region and that both need attention to protect this pristine environment. Whilst the methods used for sample collection and analysis and the reported polymer compositions may be different across the existing Arctic MP studies (**Table 3**), it is evident that MP are prevalent in this area and are mostly reported in the smaller size fraction <100µm. This highlights the need for harmonisation in methodology and the reporting of MP concentrations where possible, and the need for long-term monitoring of the pollutant.

Table 3. Comparison of MP studies in the Arctic, Antarctica, remote and urban regions (non-exhaustive)

Location	Sampling – Method, Frequency, Duration	Method of Analysis	Principal Shape	Principal Size	LOD	Principal Polymers	Deposition Flux/ Reported Concentration	Weather	Reference
Arctic (Remote)	Active and passive air sampling over 28-day period	Nile Red and µRaman	Fragment	<20µm	1.6µm	Acrylic, PLS, PES, PVA	37.31±30.19 MP/m^2; 4.15 ±9.42 MP/m^3	Correlation with wind direction	Present study
Arctic (Remote)	Surface snow sampled on 5 ice floes; 2015-2017	Microscope and µFTIR	Fragment	<25µm	11µm	PS, PVC, PC, PLA, PI	0 to 14.4 × 103 N $liter^{-1}$	NA	Bergmann et al., (2019)
Arctic (Remote)	Bulk and surface glacial snow samples; April 2021; multiple sites	Microscope and µFTIR	NA	<100µm	5µm	PTFE, PU, PARA (Polyamide) ABS	49.4 ± 7 mg m^{-2} - 227.2 ± 15 mg m^{-2} (no average reported)	NA	Rosso et al., (2024)
Arctic (Remote)	Raw wastewater samples	Microscope and µFTIR	Fragment	<100µm	20µm	PP, PE, PES	217 L^{-1}	NA	Bach et al., 2024
Antarctica (Remote)	Snow sampling – 19 samples from different locations Nov-Dec 2019	Microscope and µFTIR	Fibre	200-1000µm	50µm	PET, PMMA, PVC, PA	294 ± 4.7 L^{-1}	NA	Aves et al., 2022
Antarctica (Remote)	Bulk atmospheric deposition samples; Jan-Dec 2020, 7 samples from different sites	µRaman	Fragment	5–10 µm	5µm	PP, PE, PC	1.7 MP m^{-2} d^{-1}	NA	Illuminiati et al., 2024
Tibetan Plateau (Remote)	Snowpit sampling; 21st May 2020; 16 samples 10cm intervals	Microscope, Raman and SEM	Fibre	<200µm (43.33%)	48µm	PVC, PPO (Poly(2,6-dimethyl-1,4-phenylene oxide)) Hydroxypropyl cellulose (HPC) (13.33%) and Hydroxypropyl methyl cellulose (HPMC); PVA, PB	9.55 ± 0.9 L^{-1}	Monsoon season affected size, shape, colour and polymer composition	Wang et al., 2022
Pyrenees (Remote)	Deposition sampling; Nov 2017-March 2018; 12-34days	Microscope and µRaman	Fragment	≤50µm	10µm	PS, then PE and PP	365 ±69 $m^{-2}d^{-1}$	No meteorological mechanism driving MP deposition	Allen et al., 2019
London (Urban)	Total atmospheric deposition; Jan-Feb 2019; samples collected 2 per week for 4 weeks	Microscope and µFTIR	Fibre	<100µm	5µm	PAN, PET, PA	712 ± 162 m^2 /d	Wind direction and wind speed influence	Wright et al., 2020
Shanghai (Urban)	Particulate sampler (active); 100 ± 0.1 L/min, sampling in triplicate over 1 h and ≈6 m^3 of air per sample.	µFTIR	Fibre	<1000µm	23µm	PET, PE, PES, PAN, PAA	1.42 ± 1.42 n/m^3	Strong correlation with wind direction and SAMPs distribution	Liu et al., 2019b

In other remote regions such as Antarctica, the polymer composition and more common identification of fibres can be highlighted as a main difference (Aves et al., 2019; Illuminati et al., 2024). Again, with different methods of sampling used and differences in reporting,

direct comparison is challenging, but values reported are much lower for Antarctic deposition with 1.7 MP m^{-2} d^{-1} compared to 37.31±30.19 MP/m^2 compared to the present study (Illuminiati et al., 2024). However, this could be due to the reasons highlighted above. In the Pyrenees mountains, a higher deposition rate was reported (365 ±69 $m^{-2}d^{-1}$). This study also looked into the relationship with weather and found that there was no one simple meteorological variable that was influencing MP deposition in this region (Allen et al., 2019).

Even in more urban locations, it is unusual to find a study that has simultaneously measured deposition and total particulates. Wright et al. (2020) reported much higher concentrations for deposition samples in London, United Kingdom (712 ± 162 m^2 /d) as well as fibre being the most common particle shape. A study in Shanghai reported lower values (1.42 ± 1.42 n/m^3 (Liu et al., 2019b), than the values reported here (4.15±9.42 MP/m^3), which is similar to the concentrations reported in the present study. This could be due to the smaller limit of detection (LOD) of 23µm for the Shanghai study, which could have resulted in missing the smaller size fraction in this region. Nonetheless, this is concerning given the remote location of the sampling site in this study, and the stark contrast in the populations in each of these regions.

5. Conclusions

The MP content of the PBL atmosphere in Svalbard was measured over 28-day period, examining the size, shape and polymer composition of deposited and suspended particulates with the use of µRaman spectrometry and Nile Red fluorescence. MPs were found in every sample, and although the differences in methods and reporting make comparison difficult, results are consistent with other remote locations. The polymer composition was examined by µRaman spectroscopy and showed higher levels of Acrylic, PLS, PES, and PVA. This could be due to local contamination from clothing and fishing gear, or distal sources from food packaging or industrial applications. Using Nile Red staining coupled with microscopy, the characteristics of this pollutant were examined. It was reported that fragment was the most consistent particle shape, which is consistent with other Arctic studies, and could be due to the small size of the particles found here, or their transport mechanisms. Most of the particles found here were <20µm (80%) highlighting the importance of researching this pollutant. Its small size poses a high risk for ingestion, transport and other ecosystem impacts. Furthermore, it shows the need to examine the small fraction of atmospheric content, as this is where a large part of the microplastic concentrations lie, and missing this could result in considerable under-reporting.

It is evident that the role of weather parameters on the suspension and deposition of atmospheric MP in this region is complex. There were significant relationships with humidity, wind direction and cloud cover. Humidity appears to be correlated with increased MP suspension, and has been found to encourage the degradation of MPs. Snow also appears to show trends with MP suspension, and the relationship between snow, MP transport and its influence on climate will become an important focus for the field as climate change progresses. Studying these relationships over a longer time period is recommended to examine the complex relationship between weather parameters and MP pollution in the Artic region.

Dispersion modelling suggests that the main sources of the MP measured at this location include the North Atlantic Ocean, Northern Greenland and the High Arctic. However, higher MP were measured when long-range transport occurred not only from the ocean, but also from land-based sources (e.g., road dust). There was no correlation between the highest and lowest reported concentrations for each type of sample, suggesting the particles behave differently depending on deposition or suspension and highlights the need to measure both particles in conjunction.

This study confirmed that atmospheric MP pollution is present and ubiquitous in the Arctic PBL. To date, this is the first time both suspended and deposited particulates have been studied simultaneously in this region highlighting the importance of measuring both particulates simultaneously to gain a better understanding of total atmospheric content. Furthermore, the differences in the outcomes from μRaman analysis and Nile Red staining demonstrate the need for more than one method of analysis in MP research, and methods that are complimentary. Gaining accurate information on both polymer composition and particle morphology and concentration are needed to fully understand the extent of this pollution. It is essential that more consistent methodologies are used to sample, analyse and report MP concentrations in this region and beyond. As more is learned about the risks of MP pollution, it is essential that the pollutant is monitored and reported effectively in order to understand the scale of the problem and mitigate its potential impacts on ecosystem function, human health, and climate processes.

Acknowledgements

FLEXPART simulations are cross-atmospheric research infrastructure services provided by ATMO-ACCESS (EU grant agreement No 101008004). The computations/simulations/[SIMILAR] were performed on resources provided by Sigma2 - the National Infrastructure for High Performance Computing and Data Storage in Norway. N.E. was funded by the Norwegian Research Council (NFR) project MAGIC (Airborne Microplastic Detection, Origin, Transport and Global Radiative Impact, Project No.: 334086). All modelled results can be seen from https://atmo-access.nilu.no/MPS_ZEPP_AM_2021.py or obtained from Dr. N. Evangeliou (e-mail: ne@nilu.no) upon request. AM, DA and CJW acknowledges that the funding provided through the EPSRC Doctoral Training Partnership (Grant No: EP/T1517938/1).

Data Availability

The data that support the findings of this study can be downloaded from public data repository Zenodo at: https://doi.org.10.5281/zenodo.16967571.

References

Aeschlimann, M., Li, G., Kanji, Z. A., & Mitrano, D. M. (2022). Potential impacts of atmospheric microplastics and nanoplastics on cloud formation processes. *Nature Geoscience* |, *15*, 967–975. https://doi.org/10.1038/s41561-022-01051-9

Akdogan, Z., & Guven, B. (2019). Microplastics in the environment: A critical review of current understanding and identification of future research needs. *Environmental Pollution*, *254*(Part A), 1–24. https://doi.org/10.1016/j.envpol.2019.113011

Allen, S., Allen, D., Phoenix, V. R., Le Roux, G., Durántez Jiménez, P., Simonneau, A., Binet, S., & Galop, D. (2019). Atmospheric transport and deposition of microplastics in a remote mountain catchment. *Nature Geoscience*, *12*(5), 339–344. https://doi.org/10.1038/s41561-019-0335-5

Allen, S., Allen, D., Moss, K., le Roux, G., Phoenix, V. R., & Sonke, J. E. (2020). Examination of the ocean as a source for atmospheric microplastics. *PLoS ONE*, *15*(5). https://doi.org/10.1371/journal.pone.0232746

Aves, A. R., Revell, L. E., Gaw, S., Ruffell, H., Schuddeboom, A., Wotherspoon, N. E., Larue, M., & Mcdonald, A. J. (2022). First evidence of microplastics in Antarctic snow. *Cryosphere*, *16*(6), 2127–2145. https://doi.org/10.5194/TC-16-2127-2022

Bach, L., Strand, J., Salame, H., Simon, M., Fritt-Rasmussen, J., & Jensen, P. E. (2024). Wet wipes in untreated wastewater are a source of litter pollution to the arctic marine environment – a case study on the loads of litter and microplastics in wastewater effluents in Greenland. *Environmental Science: Advances*, 1–12. https://doi.org/10.1039/D4VA00233D]

Bakels, L., Tatsii, D., Tipka, A., Thompson, R., Dütsch, M., Blaschek, M., Seibert, P., Baier, K., Bucci, S., Cassiani, M., Eckhardt, S., Groot Zwaaftink, C., Henne, S., Kaufmann, P., Lechner, V., Maurer, C., Mulder, M. D., Pisso, I., Plach, A., … Stohl, A. (2024). FLEXPART version 11: improved accuracy, efficiency, and flexibility. *Geoscientific Model Development*, *17*(21), 7595–7627. https://doi.org/10.5194/gmd-17-7595-2024

Bergmann, M., Collard, F., Fabres, J., Gabrielsen, G. W., Provencher, J. F., Rochman, C. M., van Sebille, E., & Tekman, M. B. (2022). Plastic pollution in the Arctic. *Nature Reviews Earth & Environment 2022 3:5*, *3*(5), 323–337. https://doi.org/10.1038/s43017-022-00279-8

Bergmann, M., Mützel, S., Primpke, S., Tekman, M. B., Trachsel, J., & Gerdts, G. (2019). White and wonderful? Microplastics prevail in snow from the Alps to the Arctic. *Science Advances*, *5*(8), 1–10. https://doi.org/10.1126/SCIADV.AAX1157

Borah, S. J. ;, Gupta, A. K. ;, Kumar, V. ;, Jhajharia, P. ;, Singh, P. P. ;, Kumar, P. ;, Kumar, R. ;, Dubey, K. K. ;, Triantafyllidis, S., Timko, M. T., Borah, S. J., Kumar Gupta, A., Kumar, V., Jhajharia, P., Singh, P. P., Kumar, P., Kumar, R., Dubey, K. K., & Gupta, A. (2024). The Peril of Plastics: Atmospheric Microplastics in Outdoor, Indoor, and Remote Environments. *Sustainable Chemistry 2024, Vol. 5, Pages 149-162*, *5*(2), 149–162. https://doi.org/10.3390/SUSCHEM5020011

Bucci, S., Richon, C., & Bakels, L. (2024). Exploring the Transport Path of Oceanic Microplastics in the Atmosphere. *Environmental Science & Technology*, *58*(32), 14338–14347. https://doi.org/10.1021/acs.est.4c03216

Caracci, E., Vega-Herrera, A., Dachs, J., Berrojalbiz, N., Buonanno, G., Abad, E., Llorca, M., Moreno, T., & Farré, M. (2023). Micro(nano)plastics in the atmosphere of the Atlantic Ocean. *Journal of Hazardous Materials*, *450*, 131036. https://doi.org/10.1016/J.JHAZMAT.2023.131036

Cassiani, M., Stohl, A., & Brioude, J. (2015). Lagrangian Stochastic Modelling of Dispersion in the Convective Boundary Layer with Skewed Turbulence Conditions and a Vertical Density Gradient: Formulation and Implementation in the FLEXPART Model. *Boundary-Layer Meteorology*, *154*(3), 367–390. https://doi.org/10.1007/s10546-014-9976-5

Chatterjee, S., Krolis, E., Molenaar, R., Claessens, M. M. A. E., & Blum, C. (2023). Nile Red staining for nanoplastic quantification: Overcoming the challenge of false positive counts due to fluorescent aggregates. *Environmental Challenges*, *13*(100744), 1–7. https://doi.org/10.1016/j.envc.2023.100744

Chen, Q., Shi, G., Revell, L. E., Zhang, J., Zuo, C., Wang, D., le Ru, E. C., Wu, G., & Mitrano, D. M. (2023). Long-range atmospheric transport of microplastics across the southern hemisphere. *Nature Communications*, 14(1), 1–10. https://doi.org/10.1038/s41467-023-43695-0

Collins, S. F., & Norton, A. (2024). Prevailing wind patterns influence the distribution of plastics in small urban lakes. *Scientific Reports*, *14*(1), 1–11. https://doi.org/10.1038/s41598-024-68516-2

Cowger, W., Markley, L. A. T., Moore, S., Gray, A. B., Upadhyay, K., & Koelmans, A. A. (2024). How many microplastics do you need to (sub)sample? *Ecotoxicology and Environmental Safety*, *275*(116243), 1–7. https://doi.org/10.1016/J.ECOENV.2024.116243

Eckhardt, S., Cassiani, M., Evangeliou, N., Sollum, E., Pisso, I., & Stohl, A. (2017). Source–receptor matrix calculation for deposited mass with the Lagrangian particle dispersion model FLEXPART v10.2 in backward mode. *Geoscientific Model Development*, *10*(12), 4605–4618. https://doi.org/10.5194/gmd-10-4605-2017

Emberson-Marl, H., Coppock, R. L., Cole, M., Godley, B. J., Mimpriss, N., Nelms, S. E., & Lindeque, P. K. (2023). Microplastics in the Arctic: a transect through the Barents Sea. *Frontiers in Marine Science*, *10*. https://doi.org/10.3389/fmars.2023.1241829

Enyoh, Christian Ebere; Verla, Andrew Wirnkor; Verla, E. N. I. F. C. A. C. E. (2019). Airborne microplastics: a review study on method for analysis, occurrence, movement and risks. *Environmental Monitoring and Assessment*, *191*(668), 1–17.

Evangeliou, N., Grythe, H., Klimont, Z., Heyes, C., Eckhardt, S., Lopez-Aparicio, S., & Stohl, A. (2020). Atmospheric transport is a major pathway of microplastics to remote regions. *Nature Communications 2020 11:1*, *11*(1), 1–11. https://doi.org/10.1038/s41467-020-17201-9

Evangeliou, N., Tichý, O., Eckhardt, S., Zwaaftink, C. G., & Brahney, J. (2022). Sources and fate of atmospheric microplastics revealed from inverse and dispersion modelling: From global emissions to deposition. *Journal of Hazardous Materials*, *432*, 128585. https://doi.org/10.1016/j.jhazmat.2022.128585

Ferrero, L., Scibetta, L., Markuszewski, P., Mazurkiewicz, M., Drozdowska, V., Makuch, P., Jutrzenka-Trzebiatowska, P., Zaleska-Medynska, A., Andò, S., Saliu, F., Nilsson, E. D., & Bolzacchini, E. (2022). Airborne and marine microplastics from an oceanographic survey at the Baltic Sea: An emerging role of air-sea interaction? *Science of The Total Environment*, *824*, 153709. https://doi.org/10.1016/J.SCITOTENV.2022.153709

Forster, C., Stohl, A., & Seibert, P. (2007). Parameterization of Convective Transport in a Lagrangian Particle Dispersion Model and Its Evaluation. *Journal of Applied Meteorology and Climatology*, *46*(4), 403–422. https://doi.org/10.1175/JAM2470.1

Galvão, L. S., Ferreira, R. R., Fernandes, E. M. S., Correia, C. A., Valera, T. S., dos Santos Rosa, D., & Wiebeck, H. (2023). Analysis of selective fluorescence for the characterization of microplastic fibers: Use of a Nile Red-based analytical method to compare between natural and synthetic fibers. *Journal of Hazardous Materials*, *443*(130217), 1–10. https://doi.org/10.1016/J.JHAZMAT.2022.130217

Goßmann, I., Herzke, D., Held, A., Schulz, J., Nikiforov, V., Georgi, C., Evangeliou, N., Eckhardt, S., Gerdts, G., Wurl, O., & Scholz-Böttcher, B. M. (2023). Occurrence and backtracking of microplastic mass loads including tire wear particles in northern Atlantic air. *Nature Communications*, *14*(1). https://doi.org/10.1038/s41467-023-39340-5

Gouin, T. (2021). Addressing the importance of microplastic particles as vectors for long-range transport of chemical contaminants: perspective in relation to prioritizing research and regulatory actions. *Microplastics and Nanoplastics*, *1*(1). https://doi.org/10.1186/s43591-021-00016-w

Grythe, H., Kristiansen, N. I., Groot Zwaaftink, C. D., Eckhardt, S., Ström, J., Tunved, P., Krejci, R., & Stohl, A. (2017). A new aerosol wet removal scheme for the Lagrangian particle model FLEXPART v10. *Geoscientific Model Development*, *10*(4), 1447–1466. https://doi.org/10.5194/gmd-10-1447-2017

Huppertsberg, S., & Knepper, T. P. (2018). Instrumental analysis of microplastics—benefits and challenges. *Analytical and Bioanalytical Chemistry*, *410*(25). https://doi.org/10.1007/s00216-018-1210-8

Illuminati, S., Notarstefano, V., Tinari, C., Fanelli, M., Girolametti, F., Ajdini, B., Scarchilli, C., Ciardini, V., Iaccarino, A., Giorgini, E., Annibaldi, A., & Truzzi, C. (2024). Microplastics in bulk atmospheric deposition along the coastal region of Victoria Land, Antarctica. *Science of The Total Environment*, 949(175221), 1–12. https://doi.org/10.1016/J.SCITOTENV.2024.175221

Irrgang, A. M., Bendixen, M., Farquharson, L. M., Baranskaya, A. V., Erikson, L. H., Gibbs, A. E., Ogorodov, S. A., Overduin, P. P., Lantuit, H., Grigoriev, M. N., & Jones, B. M. (2022). Drivers, dynamics and impacts of changing Arctic coasts. *Nature Reviews Earth & Environment 2022 3:1*, *3*(1), 39–54. https://doi.org/10.1038/s43017-021-00232-1

Jenner, L. C., Rotchell, J. M., Bennett, R. T., Cowen, M., Tentzeris, V., & Sadofsky, L. R. (2022). Detection of microplastics in human lung tissue using μFTIR spectroscopy. *Science of The Total Environment*, *831*(154907), 1–10. https://doi.org/10.1016/J.SCITOTENV.2022.154907

Jurkschat, L., Gill, A. J., Milner, R., Holzinger, R., Evangeliou, N., Eckhardt, S., & Materić, D. (2025). Using a citizen science approach to assess nanoplastics pollution in remote high-altitude glaciers. *Scientific Reports*, *15*(1864), 1–9. https://doi.org/10.1038/s41598-024-84210-9

Kings Bay. (2021. Community Operation. Retrieved December 10, 2024 from *https://kingsbay.no/community-operation/*

Kings Bay AS. (2021b). *Marine Lab & Veksthuset.* Retrieved December 10, 2024, from https://kingsbay.no/

Kye, H., Kim, J., Ju, S., Lee, J., Lim, C., & Yoon, Y. (2023). Microplastics in water systems: A review of their impacts on the environment and their potential hazards. *Heliyon*, 9(3), 1–31. https://doi.org/10.1016/J.HELIYON.2023.E14359

Li, Y., Shao, L., Wang, W., Zhang, M., Feng, X., Li, W., & Zhang, D. (2020). Airborne fiber particles: Types, size and concentration observed in Beijing. *Science of The Total Environment,* 705(135967), 1–9. https://doi.org/10.1016/J.SCITOTENV.2019.135967

Liu, K., Wang, X., Wei, N., Song, Z., & Li, D. (2019a). Accurate quantification and transport estimation of suspended atmospheric microplastics in megacities: Implications for human health. *Environment International*, *132*(105127), 1–10. https://doi.org/10.1016/j.envint.2019.105127

Liu, K., Wang, X., Fang, T., Xu, P., Zhu, L., & Li, D. (2019b). Source and potential risk assessment of suspended atmospheric microplastics in Shanghai. *Science of the Total Environment*, 675. https://doi.org/10.1016/j.scitotenv.2019.04.110

Marine Lab & Veksthuset » Kings Bay AS. (n.d.). Retrieved April 11, 2024. https://kingsbay.no/marine-lab-veksthuset/

Maturilli, Marion **(2022a):** Continuous meteorological observations at station Ny-Ålesund (2022-06) [dataset]. *Alfred Wegener Institute - Research Unit Potsdam*, *PANGAEA*, https://doi.org/10.1594/PANGAEA.937247,

Maturilli, Marion (**2022b):** Continuous meteorological observations at station Ny-Ålesund (2022-05) [dataset]. *Alfred Wegener Institute - Research Unit Potsdam*, *PANGAEA*, https://doi.org/10.1594/PANGAEA.937246,

Menges, F. (2022). *Spectragryph - optical spectroscopy software* (Version 1.2.15).

Na, S. H., Kim, M. J., Kim, J., Batool, R., Cho, K., Chung, J., Lee, S., & Kim, E. J. (2024). Fate and potential risks of microplastic fibers and fragments in water and wastewater treatment processes. *Journal of Hazardous Materials*, *463*(132938), 1–10. https://doi.org/10.1016/J.JHAZMAT.2023.132938

Nazarenko, Y., Fournier, S., Kurien, U., Rangel-Alvarado, R. B., Nepotchatykh, O., Seers, P., & Ariya, P. A. (2017). Role of snow in the fate of gaseous and particulate exhaust pollutants from gasoline-powered vehicles. *Environmental Pollution*, *223*, 665–675. https://doi.org/10.1016/j.envpol.2017.01.082

Norwegian Centre for Climate Services. (2022). Weather data and statistics. Klima Services Center. https://klimaservicesenter.no/kss/om-oss/nccs?locale=en#weather-data-and-statistics (Accessed: 10/02/2025)

Norwegian Centre for Climate Services. (2025). *Station information*. https://seklima.met.no/stations/ (Accessed: 10/02/2025)

Ny-Alesund, Google Maps. (2022). https://www.google.com/maps/place/Ny-Ålesund+9173,+Svalbard+and+Jan+Mayen/@74.4797502,-3.704962,4z/data=!4m5!3m4!1s0x4582b08bd904d97f:0x1ddeb512ac13a0dc!8m2!3d78.9235381!4d11.9098952

Obbard, R. W., Sadri, S., Wong, Y. Q., Khitun, A. A., Baker, I., & Thompson, R. C. (2014). Global warming releases microplastic legacy frozen in Arctic Sea ice. *Earth's Future*, 2(6), 315–320. https://doi.org/10.1002/2014EF000240

Parashar, N., & Hait, S. (2023). Plastic rain-Atmospheric microplastics deposition in urban and peri-urban areas of Patna City, Bihar, India: Distribution, characteristics, transport, and source analysis. *Journal of Hazardous Materials*, *458*(13183), 1–15. https://doi.org/10.1016/j.jhazmat.2023.131883

Phan, S., Padilla-Gamiño, J. L., & Luscombe, C. K. (2022). The effect of weathering environments on microplastic chemical identification with Raman and IR spectroscopy: Part I. polyethylene and polypropylene. *Polymer Testing*, *116*, 107752. https://doi.org/10.1016/j.polymertesting.2022.107752

Ramasamy, E. V., Sruthy, S., Harit, A. K., Mohan, M., & Binish, M. B. (2021). Microplastic pollution in the surface sediment of Kongsfjorden, Svalbard, Arctic. *Marine Pollution Bulletin*, *173*(112986), 1–5. https://doi.org/10.1016/j.marpolbul.2021.112986

Rantanen, M., Karpechko, A. Y., Lipponen, A., Nordling, K., Hyvärinen, O., Ruosteenoja, K., Vihma, T., & Laaksonen, A. (2022). The Arctic has warmed nearly four times faster than the globe since 1979. Communications Earth & Environment 2022 3:1, 3(1), 1–10. https://doi.org/10.1038/s43247-022-00498-3

Revell, L. E., Kuma, P., Le Ru, E. C., Somerville, W. R. C., & Gaw, S. (2021). Direct radiative effects of airborne microplastics. *Nature*, *598*(7881), 462–467. https://doi.org/10.1038/s41586-021-03864-x

Rivers, M. L., Gwinnett, C., & Woodall, L. C. (2019). Quantification is more than counting: Actions required to accurately quantify and report isolated marine microplastics. *Marine Pollution Bulletin*, 139, 100–104. https://doi.org/10.1016/J.MARPOLBUL.2018.12.024

Rosso, B., Scoto, F., Hallanger, I. G., Larose, C., Gallet, J. C., Spolaor, A., Bravo, B., Barbante, C., Gambaro, A., & Corami, F. (2024). Characteristics and quantification of small microplastics (<100 µm) in seasonal svalbard snow on glaciers and lands. *Journal of Hazardous Materials*, 467(133723), 1–10. https://doi.org/10.1016/J.JHAZMAT.2024.133723

Ryan, A. C., Allen, D., Allen, S., Maselli, V., LeBlanc, A., Kelleher, L., Krause, S., Walker, T. R., & Cohen, M. (2023). Transport and deposition of ocean-sourced microplastic particles by a North Atlantic hurricane. *Communications Earth and Environment*, *4*(1). https://doi.org/10.1038/s43247-023-01115-7

Schindelin, J., Arganda-Carreras, I., Frise, E., Kaynig, V., Longair, M., Pietzsch, T., Preibisch, S., Rueden, C., Saalfeld, S., Schmid, B., Tinevez, J.-Y., White, D. J., Hartenstein, V., Eliceiri, K., Tomancak, P., & Cardona, A. (2012). Fiji: an open-source platform for biological-image analysis. *Nature Methods*, *9*(7), 676–682. https://doi.org/10.1038/nmeth.2019

Stohl, A., Forster, C., Frank, A., Seibert, P., & Wotawa, G. (2005). Technical note: The Lagrangian particle dispersion model FLEXPART version 6.2. *Atmospheric Chemistry and Physics*, *5*(9), 2461–2474. https://doi.org/10.5194/acp-5-2461-2005

Szewc, K., Graca, B., & Dołęga, A. (2021). Atmospheric deposition of microplastics in the coastal zone: Characteristics and relationship with meteorological factors. *Science of the Total Environment*. https://doi.org/10.1016/j.scitotenv.2020.143272

Tatsii, D., Bucci, S., Bhowmick, T., Guettler, J., Bakels, L., Bagheri, G., & Stohl, A. (2024). Shape Matters: Long-Range Transport of Microplastic Fibers in the Atmosphere. *Environmental Science & Technology*, *58*(1), 671–682. https://doi.org/10.1021/acs.est.3c08209

Thompson, R. C., Courtene-Jones, W., Boucher, J., Pahl, S., Raubenheimer, K., & Koelmans, A. A. (2024). Twenty years of microplastic pollution research—what have we learned? *Science*, *386*(6720), 1–13. https://doi.org/10.1126/science.adl2746

Van der Does, M., Knippertz, P., Zschenderlein, P., Giles Harrison, R., & Stuut, J.-B. W. (2018). The mysterious long-range transport of giant mineral dust particles. *Science Advances*, *4*(12). https://doi.org/10.1126/sciadv.aau2768

Wang, C., Liang, S., Bai, L., Gu, X., Jin, X., Ok, Y. S., & Gu, C. (2023). Photoaging of Typical Microplastics as Affected by Air Humidity: Mechanistic Insights into the Important Role of Water Molecules. *Environmental Science & Technology*, *57*(14), 5967–5977. https://doi.org/10.1021/acs.est.2c08571

Wang, Z., Zhang, Y., Kang, S., Yang, L., Luo, X., Chen, P., Guo, J., Hu, Z., Yang, C., Yang, Z., & Gao, T. (2022). Long-range transport of atmospheric microplastics deposited onto glacier in southeast Tibetan Plateau. *Environmental Pollution*, 306(119415), 1–12. https://doi.org/10.1016/J.ENVPOL.2022.119415

Yang, S., Brasseur, G., Walters, S., Lichtig, P., & Li, C. W. Y. (2025). Global atmospheric distribution of microplastics with evidence of low oceanic emissions. *Npj Climate and Atmospheric Science*, *8*(1), 81. https://doi.org/10.1038/s41612-025-00914-3

Yao, X., Luo, X. S., Fan, J., Zhang, T., Li, H., & Wei, Y. (2022). Ecological and human health risks of atmospheric microplastics (MPs): a review. *Environmental Science: Atmospheres*, 2(5), 921–942. https://doi.org/10.1039/D2EA00041E

Zhang, Y., Gao, T., Kang,S., Allen, S., Luo, X., Allen, D. (2020). Microplastics in glaciers of the Tibetan Plateau: Evidence for the long-range transport of microplastics. *Science of the Total Environment*, *203* (103118). https://doi.org/https://doi.org/10.1016/j.scitotenv.2020.143634

Zhang, Y., Gao, T., Kang, S., Allen, D., Wang, Z., Luo, X., Yang, L., Chen, J., Hu, Z., Chen, P., Du, W., & Allen, S. (2023). Cryosphere as a temporal sink and source of microplastics in the Arctic region. Geoscience Frontiers, 14(4), 1–14. https://doi.org/10.1016/J.GSF.2023.101566

Zhang, Y., Gao, T., Kang, S., & Sillanpää, M. (2019). Importance of atmospheric transport for microplastics deposited in remote areas. In *Environmental Pollution* (Vol. 254). https://doi.org/10.1016/j.envpol.2019.07.121

Zhang, Y., Kang, S., Allen, S., Allen, D., Gao, T., & Sillanpää, M. (2020). Atmospheric microplastics: A review on current status and perspectives. In *Earth-Science Reviews*. https://doi.org/10.1016/j.earscirev.2020.103118

Zhao, L. D. S. ; M.-V. R. (2020). Insights Toward Standardization of the Analysis of Microplastics by Infrared Microscopy. *Spectroscopy Supplements*, *35*(S3).

Appendix VII. Supplementary Data and Figures for Research Chapter 5

Table VII.1 Svalbard Atmospheric Microplastic Concentrations expressed as MP/m^3

Sample Name	MP/m^3/day	Dates (2022)	Standard Deviation	Analysis Type
Direct Air Filter 1	0.29	17.05-20.05	0.21	Raman
Direct Air Filter 2	2.26	20.05-23.05	17.97	Nile Red
Direct Air Filter 3	0.24	23.05-26.05	0.16	Raman
Direct Air Filter 4	0.58	26.05-29.05	0.18	Raman
Direct Air Filter 5	49.06	29.05-1.06	17.97	Nile Red
Direct Air Filter 6	12.32	1.05-4.06	17.97	Nile Red
Direct Air Filter 7	6.80	4.06-7.06	17.97	Nile Red
Direct Air Filter 8	4.67	07.06-10.06	17.97	Nile Red
Direct Air Filter 9	3.45	10.06-13.06	17.97	Nile Red
Deposition 1	5.29	18.05	3.74	Raman
Deposition 2	5.29	19.05	2.16	Raman
Deposition 3	7.06	20.05	1.25	Raman
Deposition 4	4.41	21.05	1.25	Raman
Deposition 5	45.88	22.05	1.25	Raman
Deposition 6	4.41	23.05	1.25	Raman
Deposition 7	87.24	24.05	29.57	Nile Red
Deposition 8	33.81	25.05	29.57	Nile Red
Deposition 9	127.45	26.05	29.57	Nile Red
Deposition 10	22.11	27.05	29.57	Nile Red
Deposition 11	71.03	28.05	29.57	Nile Red
Deposition 12	66.43	29.05	29.57	Nile Red
Deposition 13	35.01	30.05	29.57	Nile Red
Deposition 14	29.81	31.05	29.57	Nile Red
Deposition 15	37.62	1.06	29.57	Nile Red
Deposition 16	36.61	2.06	29.57	Nile Red
Deposition 17	34.21	3.06	29.57	Nile Red
Deposition 18	39.02	4.06	29.57	Nile Red
Deposition 19	25.41	5.06	29.57	Nile Red
Deposition 20	8.20	6.06	29.57	Nile Red
Deposition 21	74.03	7.06	29.57	Nile Red
Deposition 22	74.83	8.06	29.57	Nile Red
Deposition 23	18.41	9.06	29.57	Nile Red
Deposition 24	43.82	10.06	29.57	Nile Red
Deposition 25	11.20	11.06	29.57	Nile Red
Deposition 26	13.41	12.06	29.57	Nile Red
Deposition 27	64.23	13.06	29.57	Nile Red
Deposition 28	18.41	14.06	29.57	Nile Red
Nanotank 1	7.12	18.05	1.97	Nile Red
Nanotank 2	3.74	19.05	1.97	Nile Red
Nanotank 3	0.14	20.05	1.97	Nile Red
Nanotank 4	0.65	21.05	1.97	Nile Red
Nanotank 5	1.43	22.05	1.97	Nile Red
Nanotank 6	0.00	23.05	0.00	Nile Red
Nanotank 7	0.41	24.05	1.97	Nile Red

Sample Name	MP/m^3/day	Dates (2022)	Standard Deviation	Analysis Type
Nanotank 8	0.90	25.05	0.48	Raman
Nanotank 9	1.92	26.05	1.37	Raman
Nanotank 10	0.77	27.05	0.63	Raman
Nanotank 11	0.64	28.05	0.65	Raman
Nanotank 12	1.73	29.05	0.31	Raman
Nanotank 13	1.28	30.05	0.96	Raman
Nanotank 14	1.1	31.05	0	Raman
Nanotank 15	0.49	1.06	1.97	Nile Red
Nanotank 16	3.64	2.06	1.97	Nile Red
Nanotank 17	4.84	3.06	1.97	Nile Red
Nanotank 18	0.03	4.06	1.97	Nile Red
Nanotank 19	0.05	5.06	1.97	Nile Red
Nanotank 20	0.03	6.06	1.97	Nile Red
Nanotank 21	0.29	7.06	1.97	Nile Red
Nanotank 22	2.93	8.06	1.97	Nile Red
Nanotank 23	0.87	9.06	1.97	Nile Red
Nanotank 24	0.17	10.06	1.97	Nile Red
Nanotank 25	0.54	11.06	1.97	Nile Red
Nanotank 26	3.69	12.06	1.97	Nile Red
Nanotank 27	1.72	13.06	1.97	Nile Red
Nanotank 28	0.83	14.06	1.97	Nile Red

Table VII.2 Svalbard Deposition Particle Size Distribution Values (Sample name – D denoting deposition and number denoting number of sample)

Particle size (count)	Field Blank Values	D7	D8	D9	D10	D11	D12	D13	D14	D5	D16	D17	D18	D19	D20	D21	D22	D23	D24	D25	D26	D27	D28	SUM	%
1.6-5µm	5.33	127	51	211	44	110	93	58	51	46	46	49	60	47	9	91	146	30	33	20	16	89	20	1447	22.05
5-10µm	9.33	179	94	257	45	151	132	52	53	85	72	64	78	57	28	177	131	39	81	21	28	96	41	1961	29.89
10-20µm	7	100	22	151	31	78	92	61	47	50	52	46	56	24	10	93	71	21	91	23	29	101	25	1274	19.42
20-30µm	1.33	27	7	25	0	13	15	11	5	14	14	12	5	5	3	13	26	6	16	0	3	35	4	259	3.95
30-40µm	0.33	9	3	2	1	11	6	3	2	4	4	4	2	2	0	4	8	3	4	2	1	3	1	79	1.20
40-50µm	0.33	4	2	1	0	2	4	1	0	0	1	3	1	0	0	2	1	4	2	0	0	5	1	34	0.52
50-100µm	0	1	2	2	0	2	2	1	3	1	6	5	5	4	1	2	3	1	4	2	2	4	0	53	0.81
100-150µm	0	2	0	1	0	0	0	0	0	0	2	0	0	0	0	0	1	0	0	0	0	0	0	6	0.09
150-200µm	0	1	0	0	0	0	0	0	0	0	0	0	0	0	0	0	0	0	0	0	0	0	0	1	0.02
200-250µm	0	0	0	0	0	0	0	0	0	0	0	0	0	0	0	0	0	0	0	0	0	0	0	0	0.00
250-300µm	0	0	0	0	0	0	0	0	0	0	0	0	0	0	0	0	0	0	0	0	0	0	0	0	0.00
300-350µm	0	0	0	0	0	0	0	0	0	0	0	0	0	0	0	0	0	0	0	0	0	0	0	0	0.00
350-400µm	0	0	0	0	0	0	0	0	0	0	0	0	0	0	0	0	0	0	0	0	0	0	0	0	0.00
400-450µm	0	0	0	0	0	0	0	0	0	0	0	0	0	0	0	0	0	0	0	0	0	0	0	0	0.00
450-500µm	0	0	0	0	0	0	0	0	0	0	0	0	0	0	0	0	0	0	0	0	0	0	0	0	0.00
500-550µm	0	0	0	0	0	0	0	0	0	0	0	0	0	0	0	0	0	0	0	0	0	0	0	0	0.00
550-600µm	0	0	0	0	0	0	0	0	0	0	0	0	0	0	0	0	0	0	0	0	0	0	0	0	0.00
600-650µm	0	0	0	0	0	0	0	0	0	0	0	0	0	0	0	0	0	0	0	0	0	0	0	0	0.00
650-700µm	0	0	0	0	0	0	0	0	0	0	0	0	0	0	0	0	0	0	0	0	0	0	0	0	0.00

Particle size (count)	Field Blank Values	D7	D8	D9	D10	D11	D12	D13	D14	D5	D16	D17	D18	D19	D20	D21	D22	D23	D24	D25	D26	D27	D28	SUM	%
700-750µm	0	0	0	0	0	0	0	0	0	0	0	0	0	0	0	0	0	0	0	0	0	0	0	0	0.00
750-800µm	0	0	0	0	0	0	0	0	0	0	0	0	0	0	0	0	0	0	0	0	0	0	0	0	0.00
800-850µm	0	0	0	0	0	0	0	0	0	0	0	0	0	0	0	0	0	0	0	0	0	0	0	0	0.00
850-900µm	0	0	0	0	0	0	0	0	0	0	0	0	0	0	0	0	0	0	0	0	0	0	0	0	0.00
900-950µm	0	0	0	0	0	0	0	0	0	0	0	0	0	0	0	0	0	0	0	0	0	0	0	0	0.00
950-1000µm	0	0	0	0	0	0	0	0	0	0	0	0	0	0	0	0	0	0	0	0	0	0	0	0	0.00
1000-2000µm	0	0	0	0	0	0	0	0	0	0	0	0	0	0	0	0	0	0	0	0	0	0	0	0	0.00
2000-3000µm	0	0	0	0	0	0	0	0	0	0	0	0	0	0	0	0	0	0	0	0	0	0	0	0	0.00
3000-4000µm	0	0	0	0	0	0	0	0	0	0	0	0	0	0	0	0	0	0	0	0	0	0	0	0	0.00
4000-5000µm	0	0	0	0	0	0	0	0	0	0	0	0	0	0	0	0	0	0	0	0	0	0	0	0	0.00

Table VII.3 Svalbard Nanotank Particle Size Distribution Values (Sample name – D denoting nanotank and number denoting number of sample)

Particle size (count)	Nano blank	N1	N2	N3	N4	N5	N6	N7	N15	N16	N17	N18	N19	N20	N21	N22	N23	N24	N25	N26	N27	N28	SUM	%
1.6-5 µm	13.33	17	17	3	19	20	11	25	11	45	70	4	5	4	9	31	12	5	31	29	21	7	396	17.28
5-10 µm	35.33	37	30	14	35	68	21	23	37	77	96	19	17	19	25	65	38	19	16	85	50	41	832	36.30
10-20 µm	19.33	12	16	15	24	15	8	17	17	62	51	6	16	14	24	50	32	6	14	62	38	27	526	22.95
20-30 µm	2.67	0	4	6	2	1	1	1	5	3	4	2	3	0	2	13	4	6	3	8	5	6	79	3.45
30-40 µm	1.33	1	0	3	0	0	1	0	4	2	5	1	1	0	2	2	0	1	1	3	1	1	29	1.27
40-50µm	0.67	0	2	0	0	0	0	0	0	0	0	0	0	1	1	3	1	1	3	2	0	1	15	0.65
50-100µm	0.00	1	0	0	0	1	0	1	1	0	3	0	0	0	1	1	0	2	1	0	2	0	14	0.61
100-	0.00	0	0	0	0	0	0	0	0	0	0	0	0	0	0	0	0	0	0	0	0	0	0	0.00
150-	0.00	0	0	0	0	0	0	0	0	0	0	0	0	1	0	0	1	0	0	0	0	0	2	0.09
200-	0.00	1	0	0	0	0	0	0	0	0	0	1	0	0	0	1	0	0	0	0	0	0	3	0.13
250-	0.00	0	0	0	0	0	0	0	0	0	0	0	0	0	0	0	0	0	0	0	0	0	0	0.00
300-	0.00	0	0	0	0	0	0	0	0	0	0	0	0	0	0	0	0	0	0	0	0	0	0	0.00
350-	0.00	0	0	0	0	0	0	0	0	0	0	0	0	0	0	0	0	0	0	0	0	0	0	0.00
400-	0.00	0	0	0	0	0	0	0	0	0	0	0	0	0	0	0	0	0	0	0	0	0	0	0.00
450-	0.00	0	0	0	0	0	0	0	0	0	0	0	0	0	0	0	0	0	0	0	0	0	0	0.00
500-	0.00	0	0	0	0	0	0	0	0	0	0	0	0	0	0	0	0	0	0	0	0	0	0	0.00
550-	0.00	0	0	0	0	0	0	0	0	0	0	0	0	0	0	0	0	0	0	0	0	0	0	0.00
600-	0.00	0	0	0	0	0	0	0	0	0	0	0	0	0	0	0	0	0	0	0	0	0	0	0.00
650-	0.00	0	0	0	0	0	0	0	0	0	0	0	0	0	0	0	0	0	0	0	0	0	0	0.00
700-	0.00	0	0	0	0	0	0	0	0	0	0	0	0	0	0	0	0	0	0	0	0	0	0	0.00
750-	0.00	0	0	0	0	0	0	0	0	0	0	0	0	0	0	0	0	0	0	0	0	0	0	0.00
800-	0.00	0	0	0	0	0	0	0	0	0	0	0	0	0	0	0	0	0	0	0	0	0	0	0.00
850-	0.00	0	0	0	0	0	0	0	0	0	0	0	0	0	0	0	0	0	0	0	0	0	0	0.00
900-	0.00	0	0	0	0	0	0	0	0	0	0	0	0	0	0	0	0	0	0	0	0	0	0	0.00
950-	0.00	0	0	0	0	0	0	0	0	0	0	0	0	0	0	0	0	0	0	0	0	0	0	0.00
1000-	0.00	0	0	0	0	0	0	0	0	0	0	0	0	0	0	0	0	0	0	0	0	0	0	0.00
2000-	0.00	0	0	0	0	0	0	0	0	0	0	0	0	0	0	0	0	0	0	0	0	0	0	0.00
3000-	0.00	0	0	0	0	0	0	0	0	0	0	0	0	0	0	0	0	0	0	0	0	0	0	0.00

Particle size (count)	Nano blank	N1	N2	N3	N4	N5	N6	N7	N15	N16	N17	N18	N19	N20	N21	N22	N23	N24	N25	N26	N27	N28	SUM	%
4000-	0.00	0	0	0	0	0	0	0	0	0	0	0	0	0	0	0	0	0	0	0	0	0	0	0.00

Table VII.4 Svalbard Direct Air Filtration Particle Size Distribution Values (Sample name – AF denoting air filtration and number denoting number of sample)

Particle size (count)	Field Blank Values	AF2	AF5	AF6	AF7	AF8	AF9	SUM	%
<2µm	4.67	6	48	42	4	4	5	113.67	4.23
2-5 µm	6	8	393	155	71	62	49	744.00	27.69
1.6-5 µm	10.67	14	441	197	75	66	54	857.67	31.92
5-10 µm	9.33	19	384	113	93	114	82	814.33	30.31
10-20 µm	7	11	59	3	25	13	16	134.00	4.99
20-30 µm	1.33	1	2	0	2	3	2	11.33	0.42
30-40 µm	0.33	0	0	0	1	2	1	4.33	0.16
40-50µm	0.33	1	0	0	0	0	0	1.33	0.05
50-100µm	0	0	1	0	0	0	3	4	0.15
100-150µm	0	0	1	0	0	0	0	1	0.04
150-200µm	0	0	0	0	1	0	0	1	0.04
200-250µm	0	0	0	0	0	0	0	0	0.00
250-300µm	0	0	0	0	0	0	0	0	0.00
300-350µm	0	0	0	0	0	0	0	0	0.00
350-400µm	0	0	0	0	0	0	0	0	0.00
400-450µm	0	0	0	0	0	0	0	0	0.00
450-500µm	0	0	0	0	0	0	0	0	0.00
500-550µm	0	0	0	0	0	0	0	0	0.00
550-600µm	0	0	0	0	0	0	0	0	0.00
600-650µm	0	0	0	0	0	0	0	0	0.00
650-700µm	0	0	0	0	0	0	0	0	0.00
700-750µm	0	0	0	0	0	0	0	0	0.00
750-800µm	0	0	0	0	0	0	0	0	0.00
800-850µm	0	0	0	0	0	0	0	0	0.00
850-900µm	0	0	0	0	0	0	0	0	0.00
900-950µm	0	0	0	0	0	0	0	0	0.00
950-1000µm	0	0	0	0	0	0	0	0	0.00
1000-2000µm	0	0	0	0	0	0	0	0	0.00

Particle size (count)	Field Blank Values	AF2	AF5	AF6	AF7	AF8	AF9	SUM	%
2000-3000µm	0	0	0	0	0	0	0	0	0.00
3000-4000µm	0	0	0	0	0	0	0	0	0.00
4000-5000µm	0	0	0	0	0	0	0	0	0.00

Table VII.5. Table X8. Raman Counts for Svalbard Samples (Research Chapter 5) (Sample Names – AF= Direct Air Filtration; DEPO = Deposition; NANO = Nanotank; number of sample; scan number)

Sample Name	PE	PES	PET	PP	PS	PVC	PU	ABS	PC	PVA	Nylon/PA	Acrylic	CE	PMMA	PLS	Rbr	PLA	SBR	SAN
AF1_SV_1	0	0	0	0	0	0	0	0	0	0	0	1	0	0	0	0	0	0	0
AF1_SV_2	0	0	0	0	0	0	0	0	0	1	0	1	0	0	0	0	0	0	0
AF1_SV_3	0	0	0	0	0	0	0	0	0	0	1	2	0	2	1	0	0	0	0
AF3_SV_1	0	0	0	0	0	0	0	0	0	0	0	4	0	0	0	0	0	0	0
AF3_SV_2	0	0	0	0	0	0	0	0	0	0	0	1	0	0	0	0	0	0	0
AF3_SV_3	0	0	1	0	0	0	0	0	0	0	0	2	0	0	1	0	1	0	0
AF4_SV_1	0	1	1	0	0	0	0	0	0	2	0	0	0	2	0	0	0	0	0
AF4_SV_2	0	1	0	0	0	0	0	0	0	1	0	1	0	2	1	0	0	0	0
AF4_SV_3	0	0	0	0	0	0	0	0	0	0	0	1	1	0	0	0	0	0	0
DEPO1_SV_1	0	0	0	0	0	0	0	0	0	0	0	1	0	2	0	0	0	0	0
DEPO1_SV_2	0	0	0	0	1	0	0	0	0	1	0	0	0	0	1	0	0	0	0
DEPO1_SV_3	0	0	0	0	0	0	0	0	0	0	0	0	0	0	0	0	0	0	0
DEPO2_SV_1	0	2	0	0	0	0	0	0	0	0	0	0	0	1	0	0	0	0	0
DEPO2_SV_2	0	0	0	0	0	0	0	0	0	1	0	1	0	0	0	0	0	0	0
DEPO2_SV_3	0	0	0	0	0	0	0	0	0	0	0	0	0	0	0	0	1	0	0
DEPO3_SV_1	0	0	1	0	0	0	0	0	0	0	0	2	0	0	0	0	0	0	0
DEPO3_SV_2	0	0	1	0	0	0	0	0	0	0	2	0	0	0	0	0	0	0	0
DEPO3_SV_3	0	0	0	0	0	0	0	0	0	1	0	1	0	0	0	0	0	0	0
DEPO4_SV_1	0	0	0	0	0	0	0	0	0	0	1	0	0	1	0	0	0	0	0
DEPO4_SV_2	0	0	0	0	0	0	0	0	0	1	0	0	0	0	0	0	0	0	0

Sample Name	PE	PES	PET	PP	PS	PVC	PU	ABS	PC	PVA	Nylon/PA	Acrylic	CE	PMMA	PLS	Rbr	PLA	SBR	SAN
DEPO4_SV_3	0	0	0	0	0	0	0	0	0	0	0	1	0	1	0	0	0	0	0
DEPO5_SV_1	0	0	0	0	0	0	2	0	0	0	0	0	0	0	4	2	2	4	3
DEPO5_SV_2	0	0	0	1	0	0	1	0	0	0	0	0	0	0	4	4	1	2	4
DEPO5_SV_3	0	1	0	1	0	0	0	0	0	0	0	0	0	0	4	2	3	4	3
DEPO6_SV_1	0	0	0	0	0	0	0	0	0	1	0	1	0	0	0	0	0	0	0
DEPO6_SV_2	0	0	0	0	0	0	0	0	0	1	0	0	0	0	0	0	0	0	0
DEPO6_SV_3	0	0	0	0	0	0	0	0	0	1	0	1	0	0	0	0	0	0	0
NANO8_SV_1	0	0	0	0	0	0	0	0	0	1	0	1	0	0	0	0	0	0	0
NANO8_SV_2	0	0	0	0	0	0	0	0	0	0	0	0	0	0	1	0	0	0	0
NANO8_SV_3	0	0	0	0	0	0	0	0	0	0	1	2	0	0	1	0	0	0	0
NANO9_SV_1	0	0	0	0	0	0	0	0	0	0	1	0	0	0	2	0	0	0	0
NANO9_SV_2	0	0	0	0	0	0	0	0	0	0	0	0	0	1	1	0	0	0	0
NANO9_SV_3	0	1	2	0	0	0	0	0	0	3	1	1	0	1	1	0	0	0	0
NANO10_SV_1	0	0	0	0	0	0	0	0	0	0	0	3	0	0	1	0	0	0	0
NANO10_SV_2	0	0	0	0	0	0	0	0	0	1	1	0	0	0	0	0	0	0	0
NANO10_SV_3	0	0	0	0	0	0	0	0	0	0	0	0	0	1	0	0	0	0	0
NANO11_SV_1	0	0	0	0	0	0	0	0	0	0	0	0	0	0	0	0	0	0	0
NANO11_SV_2	0	0	0	0	0	0	0	0	0	1	0	0	1	2	0	0	0	0	0
NANO11_SV_3	0	0	0	0	0	0	0	0	0	0	0	0	0	1	0	0	0	0	0
NANO12_SV_1	0	0	0	0	0	0	0	0	0	4	0	0	0	0	1	0	0	0	0
NANO12_SV_2	0	0	0	0	0	0	0	0	0	1	1	0	0	1	1	0	0	0	0
NANO12_SV_3	0	0	0	0	0	0	0	0	0	1	0	0	0	1	1	0	0	0	0

Sample Name	PE	PES	PET	PP	PS	PVC	PU	ABS	PC	PVA	Nylon/PA	Acrylic	CE	PMMA	PLS	Rbr	PLA	SBR	SAN
NANO13_SV_1	0	0	0	0	1	0	0	0	0	1	0	2	0	1	1	0	0	0	0
NANO13_SV_2	0	0	0	0	0	0	0	0	0	0	0	0	0	0	0	0	0	0	0
NANO13_SV_3	0	0	0	0	1	0	0	0	0	1	0	0	0	1	0	0	1	0	0
NANO14_SV_1	0	1	0	0	0	0	0	0	0	0	1	0	0	0	0	0	0	0	0
FIELDBLANK2_1	0		0	0	0	0	0	0	0	0	0	0	0	0	0	0	0	0	0
FIELDBLANK2_2	0		0	0	0	0	0	0	0	0	0	0	0	0	0	0	0	0	0
FIELDBLANK2_3	0		0	0	0	0	0	0	0	0	0	0	0	0	0	0	0	0	0

Table VII.6 Svalbard Weather Data used for Correlation (Norwegian Climate Institute)

Sample	Date (2022)	Mean Cloud Cover (24hr)	Average air pressure, sea level (hPa; 24 h)	Average of mean wind speed (m/s; 24 h)	Precipitation (mm)	Snow Cover (%)	Snow Depth (mm)	Wind Direction	Mean Dew Point Temperature (ºC; 24hr)	Maximum Relative Humidity (24 hr)	Mixing Ratio
Direct Air Filter 1	17.05-20.05	5.325	1022.3	2.275	0.25	4	45	SE	-6.525	87.75	2.325
Direct Air Filter 2	20.05-23.05	4	1016.8	4	1.575	4	53	SE	-8.1	81.75	2.075
Direct Air Filter 3	23.05-26.05	6.675	1019.075	3.925	0.05	4	52	NW	-6.125	84.75	2.425
Direct Air Filter 4	26.05-29.05	6.75	1013.15	4.125	0.1	4	47.5	NW	-4.25	87.5	2.8
Direct Air Filter 5	29.05-1.06	5.7	1012.8	2.5	0.05	4	42.25	SE	-2.2	89.5	89.5
Direct Air Filter 6	1.05-4.06	8	1006.5	5.1	3.2	3	26.75	NW	0.475	96.25	3.95
Direct Air Filter 7	4.06-7.06	8	1011.3	2.3	1.125	3	15	NW	-0.275	95.5	3.7
Direct Air Filter 8	07.06-10.06	8	1000.3	4.9	0.65	3	8.75	NW	-1.05	92.5	3.525
Direct Air Filter 9	10.06-13.06	4.3	1005.5	5.6	0.2	3	10	SE	-3.725	-3.725	2.925
Deposition and Nanotank 1	18.05	5	1024.8	2.1	0	4	46	SE	-6.3	85	2.1
Deposition and Nanotank 2	19.05	3.3	1022.8	1.2	0	4	46	SE	-6.5	91	2.3
Deposition and Nanotank 3	20.05	8	1017.9	1.4	0	4	46	SE	-5.2	86	2.3
Deposition and Nanotank 4	21.05	8	1016.3	3	1	4	56	SE	-8.3	89	2.6
Deposition and Nanotank 5	22.05	7.3	1016.1	3.9	4.3	4	56	NW	-10.7	81	2
Deposition and Nanotank 6	23.05	4	1016.8	4	1	4	54	W	-8.2	75	1.7
Deposition and Nanotank 7	24.05	6.7	1020.7	5.2	0	4	52	NW	-7.8	82	2
Deposition and Nanotank 8	25.05	8	1024.6	3.8	0	4	52	W	-6.1	82	2.1

Sample	Date (2022)	Mean Cloud Cover (24hr)	Average air pressure, sea level (hPa; 24 h)	Average of mean wind speed (m/s; 24 h)	Precipitation (mm)	Snow Cover (%)	Snow Depth (mm)	Wind Direction	Mean Dew Point Temperature (ºC; 24hr)	Maximum Relative Humidity (24 hr)	Mixing Ratio
Deposition and Nanotank 9	26.05	8	1014.2	2.7	0	4	50	NW	-2.4	86	2.4
Deposition and Nanotank 10	27.05	4.3	1007.9	7.8	0.2	4	48	NW	-4.3	89	3.2
Deposition and Nanotank 11	28.05	7	1017.4	4.3	0.2	4	47	SE	-6.7	93	2.8
Deposition and Nanotank 12	29.05	7.7	1013.1	1.7	0	4	45	SW	-3.6	79	2.3
Deposition and Nanotank 13	30.05	5.7	1006.5	2.1	0	4	43	SE	-3.1	89	2.9
Deposition and Nanotank 14	31.05	6	1012.1	4.4	0	4	42	SE	-2.8	89	3
Deposition and Nanotank 15	1.06	5.7	1012.8	2.5	0	4	39	SE	0.7	85	3.1
Deposition and Nanotank 16	2.06	8	1004.6	5.7	0.2	3	30	SW	1.7	95	4
Deposition and Nanotank 17	3.06	5.7	1009.4	4.6	0	3	23	SE	-0.8	100	4.3
Deposition and Nanotank 18	4.06	8	1006.5	5.1	10.5	3	15	NW	0.3	92	3.6
Deposition and Nanotank 19	5.06	8	1016.1	4.3	2.1	3	15	NW	-1.1	98	3.9
Deposition and Nanotank 20	6.06	4.3	1020.7	2.2	0.8	3	15	SE	-1.2	92	3.5
Deposition and Nanotank 21	7.06	8	1011.3	2.3	1.6	3	15	NW	0.9	92	3.4
Deposition 22	8.06	7.7	1008.5	2.2	0	3	12	NW	-1.3	100	4
Deposition 23	9.06	4.7	1002.6	2.3	2.4	3	6	NW	-1.8	92	3.5
Deposition 24	10.06	8	1000.3	4.9	0	3	2	NW	-2	88	3.3
Deposition 25	11.06	5	1000.6	3.3	0.2	3	0	NW	-2.8	90	3.3
Deposition 26	12.06	2.7	1002.9	2.3	0.6	3	0	SE	-4.7	85	3.1

Sample	Date (2022)	Mean Cloud Cover (24hr)	Average air pressure, sea level (hPa; 24 h)	Average of mean wind speed (m/s; 24 h)	Precipitation (mm)	Snow Cover (%)	Snow Depth (mm)	Wind Direction	Mean Dew Point Temperature (ºC; 24hr)	Maximum Relative Humidity (24 hr)	Mixing Ratio
Deposition 27	13.06	4.3	1005.5	5.6	0	3	0	SE	-5.4	70	2.7
Deposition 28	14.06	7	999.8	5.5	0	3	0	NW	-5	62	2.6

Supplementary Figures Research Chapter 5

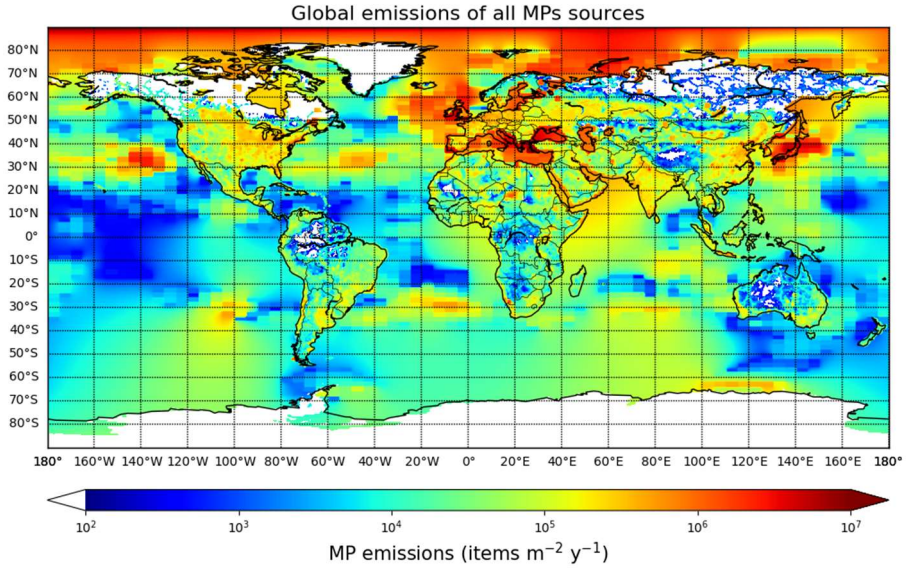


Figure VII.1: Global emissions of MP (5-250 um) updated from Evangeliou et al. (2022). All sources are plotted, namely oceanic, agricultural, soil/mineral dust, road dust and clothing fibers.

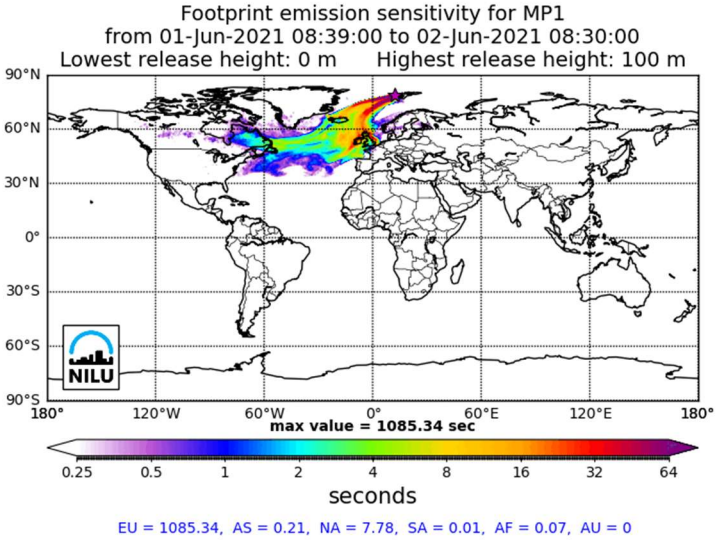


Figure VII.2: Footprint emissions sensitivity of MP arriving at Svalbard on June 1st, 2022, when the largest surface concentrations were detected.

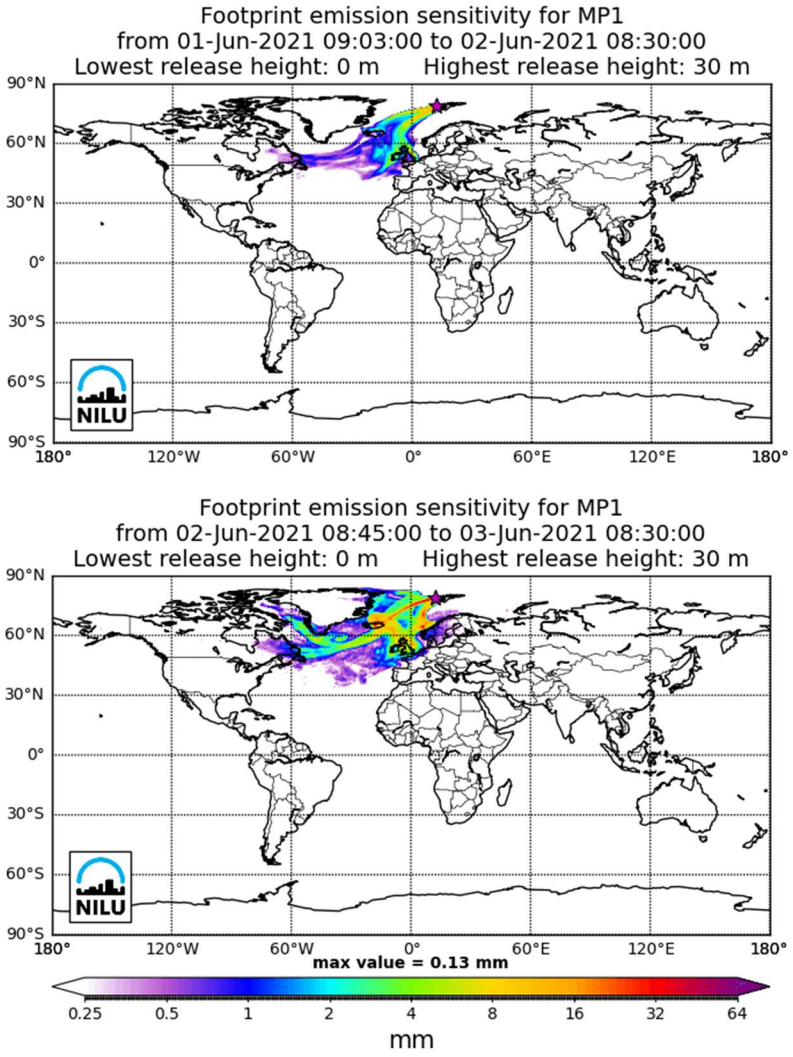


Figure VIII.3: Footprint emissions sensitivity of MP arriving and depositing at Svalbard due to dry deposition. Here, we have assumed that MP are slightly affected by wet deposition (in cloud and below cloud scavenging), as they are macromolecular polymers and therefore highly hydrophobic.

Appendix VII. Supplementary Data used in Research Chapter 6 on Glasgow Atmospheric MP Pollution

Table VII.1 Glasgow Weather Data used for Correlation (Visual Crossing, 2021)

Date	Temp max	Temp min	Temp	Dew	Humidity	Precipitation	Wind speed	Wind direction	Sea level pressure	Cloud cover
02/11/2021	12	2	6.7	4.9	89.1	0	14.8	255.7	995.5	69.7
03/11/2021	11	0	5.3	2.8	85.3	0	16.6	287.8	1008.8	23.8
04/11/2021	9	0	4.5	2	84.7	0	16.6	273.5	1018.7	51.1
05/11/2021	12	6	10	8.3	89.8	2.2	22.3	242.9	1021.8	80.4
06/11/2021	12	8	10.1	7.7	85.3	6	44.6	239.8	1012.5	79.6
07/11/2021	11	5	8.7	3.6	70.6	0	42.5	279.6	1015.8	65.1
08/11/2021	14	3	9.2	8.2	93.8	3.6	37.1	202.4	1015.6	96.9
09/11/2021	13	9	11.1	9.2	88.2	1.1	27.7	232.9	1014.4	78.4
10/11/2021	10	4	7.4	5.3	86.6	0.5	23.4	225.6	1019.8	68.7
11/11/2021	12	8	10.4	7.7	83.3	1.2	27.7	176.6	1015.6	87.4
12/11/2021	13	11	11.4	9.5	88.1	6.9	37.1	214.4	998.6	85.5
13/11/2021	13	5	8	6.4	89.9	0	16.6	269.1	1016.4	61.5
14/11/2021	11	5	8.4	7.6	95.1	0	14	106	1024	97.3
15/11/2021	12	5	9	7.8	92.1	2	14.8	240.2	1024.3	79.4
16/11/2021	11	6	9.1	6.8	85.7	2.9	37.1	220.2	1015.4	83
17/11/2021	11	3	8.1	6.2	87.9	1.2	33.5	236.3	1016.9	77.1
18/11/2021	14	11	12.8	11.3	90.7	1.1	33.5	236.1	1020	98
19/11/2021	13	12	12.8	10.5	86.2	0.9	31.7	233.3	1023.3	97.5

Date	Temp max	Temp min	Temp	Dew	Humidity	Precipitation	Wind speed	Wind direction	Sea level pressure	Cloud cover
20/11/2021	11	4	9	7	87.2	0.9	38.9	244.4	1018.9	64.6
21/11/2021	8	-2	3.6	0.4	80.5	0	22.3	306.1	1025.6	11.8
22/11/2021	9	-3	3.3	1.8	90.5	0	18.4	247.1	1032.9	45.3
23/11/2021	10	4	7.8	5.8	87.9	0	22.3	242.2	1031	85
24/11/2021	9	1	6	3.8	85.6	2	31.7	237.2	1018.6	59.5
25/11/2021	8	2	4.6	1.8	82.3	2.5	29.5	268.9	1016.6	48.6
26/11/2021	9	4	6	1	70.8	5.5	50	309	993.4	70.9
27/11/2021	5	-2	2.6	-4.8	58.9	0	36	341.6	1009.9	49.9
28/11/2021	5	-3	1	-1.6	83.4	1.9	11.2	289.4	1010	55.8
29/11/2021	11	-3	3.3	2	91.8	0.8	24.1	241.4	1010.1	95.1
30/11/2021	12	8	10.2	9.1	92.8	17.1	27.7	247.3	1001.2	86.2
01/12/2021	8	-3	5	1.1	76.9	2.8	25.9	302.7	1000.7	44.2
02/12/2021	4	-1	2.2	-1.7	76.2	2.6	22.3	257.9	1011.4	63.4
03/12/2021	8	4	6.8	4.7	86.6	8.1	31.7	227.4	997.1	79.9

Table VII.2 Glasgow Air Pollution Data used for Correlation (Scottish Air Quality, 2021)

Glasgow Townshead		Cambuslang			Rutherglen		
Date	**Black Carbon (24hr average)**	**PM_{10} (24hr average)**	**$PM_{2.5}$ (24hr average)**	**PM_{1} (24hr average)**	**Nitric oxide (24hr average)**	**Nitrogen dioxide (24hr average)**	**Nitrogen oxides as nitrogen dioxide (24hr average)**
02/11/2021	0.98	10.42	3.46	2.08	61.44	45.42	139.61
03/11/2021	0.89	6.53	2.08	1.39	46.36	41.43	112.53
04/11/2021	0.82	8.59	3.16	1.98	57.28	42.54	130.38
05/11/2021	no data	6.74	4.61	3.93	35.50	31.63	86.07
06/11/2021	no data	7.98	4.56	2.69	12.40	11.43	30.45
07/11/2021	no data	14.84	7.41	3.72	14.91	16.93	39.80
08/11/2021	no data	9.53	4.58	2.90	35.40	33.10	87.37
09/11/2021	no data	8.45	4.06	2.20	23.92	18.70	55.36
10/11/2021	no data	20.32	7.60	4.05	42.82	30.39	96.05
11/11/2021	0.31	10.93	4.28	2.95	24.84	19.45	57.55
12/11/2021	0.24	4.66	2.78	1.77	21.08	18.63	50.95
13/11/2021	1.00	11.61	7.22	5.86	81.63	47.64	172.79
14/11/2021	0.59	8.68	4.65	3.71	28.55	33.44	77.23
15/11/2021	0.50	7.63	2.77	1.54	50.91	39.28	117.32
16/11/2021	0.43	8.73	3.93	2.13	6.41	6.31	16.16
17/11/2021	0.36	8.76	4.67	2.52	no data	no data	no data
18/11/2021	0.23	5.19	2.67	1.57	19.75	18.26	50.31
19/11/2021	0.31	8.90	3.81	2.28	19.28	14.03	43.58
20/11/2021	0.23	5.40	2.80	1.75	24.28	22.45	59.68
21/11/2021	0.23	7.78	3.74	2.83	47.69	43.70	116.81

Glasgow Townshead		Cambuslang			Rutherglen		
Date	**Black Carbon (24hr average)**	**PM_{10} (24hr average)**	**$PM_{2.5}$ (24hr average)**	**PM_{1} (24hr average)**	**Nitric oxide (24hr average)**	**Nitrogen dioxide (24hr average)**	**Nitrogen oxides as nitrogen dioxide (24hr average)**
22/11/2021	2.77	9.28	4.91	3.93	93.50	45.53	188.91
23/11/2021	0.41	4.00	1.73	1.00	35.95	28.47	83.57
24/11/2021	0.37	8.62	3.90	2.17	44.76	37.33	105.96
25/11/2021	0.41	7.90	3.77	2.12	38.65	34.75	94.01
26/11/2021	0.24	7.77	2.78	1.42	22.82	24.66	59.65
27/11/2021	0.19	10.33	4.17	2.57	16.10	26.61	51.30
28/11/2021	0.41	8.22	5.26	4.54	54.52	53.68	137.26
29/11/2021	1.92	7.71	4.50	3.84	59.32	41.35	132.28
30/11/2021	0.34	2.84	1.06	0.66	22.76	19.32	54.23
01/12/2021	0.31	9.98	3.39	1.85	27.18	32.53	74.21
02/12/2021	0.49	22.75	5.32	2.60	63.55	48.95	146.40
03/12/2021	0.46	7.71	4.08	2.51	37.39	33.95	91.27

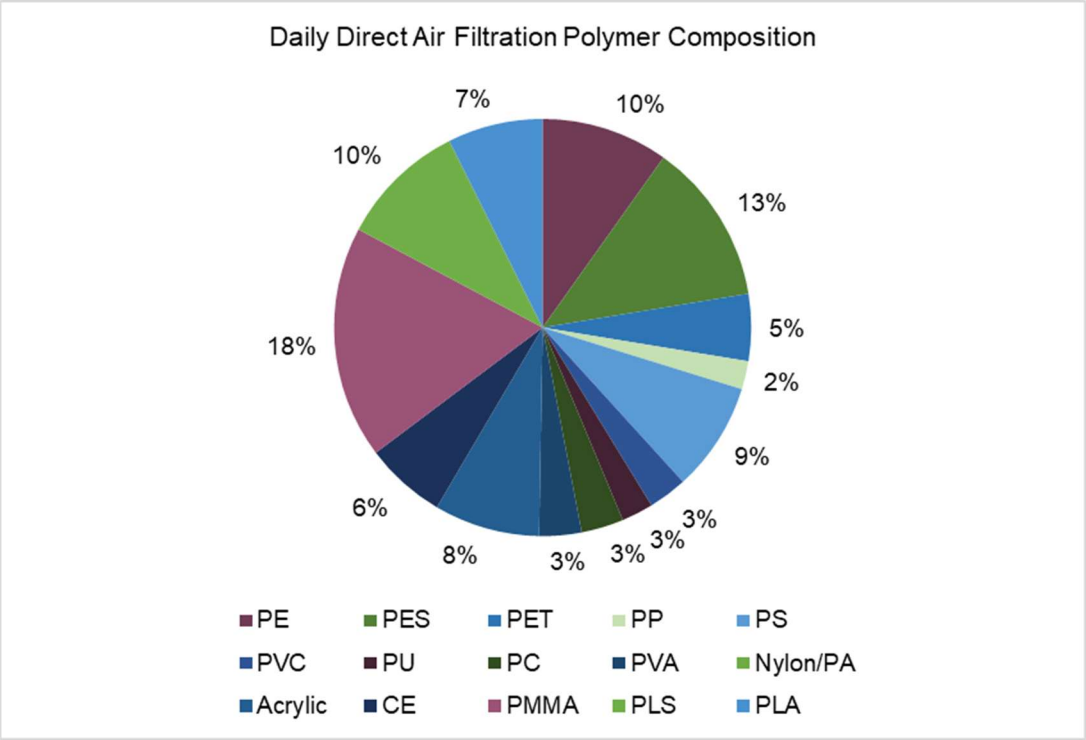


Figure VII.1 Daily Direct Air Filtration Overall Polymer Composition (% of Polymers Identified by µRaman spectroscopy from samples from Glasgow, Scotland)

Appendix IX. Results of Individual HYSPLIT Scenarios Forward and Backward Trajectory

Figure IX.1 10µm 5oC density 1g – Backward 17th Nov'21

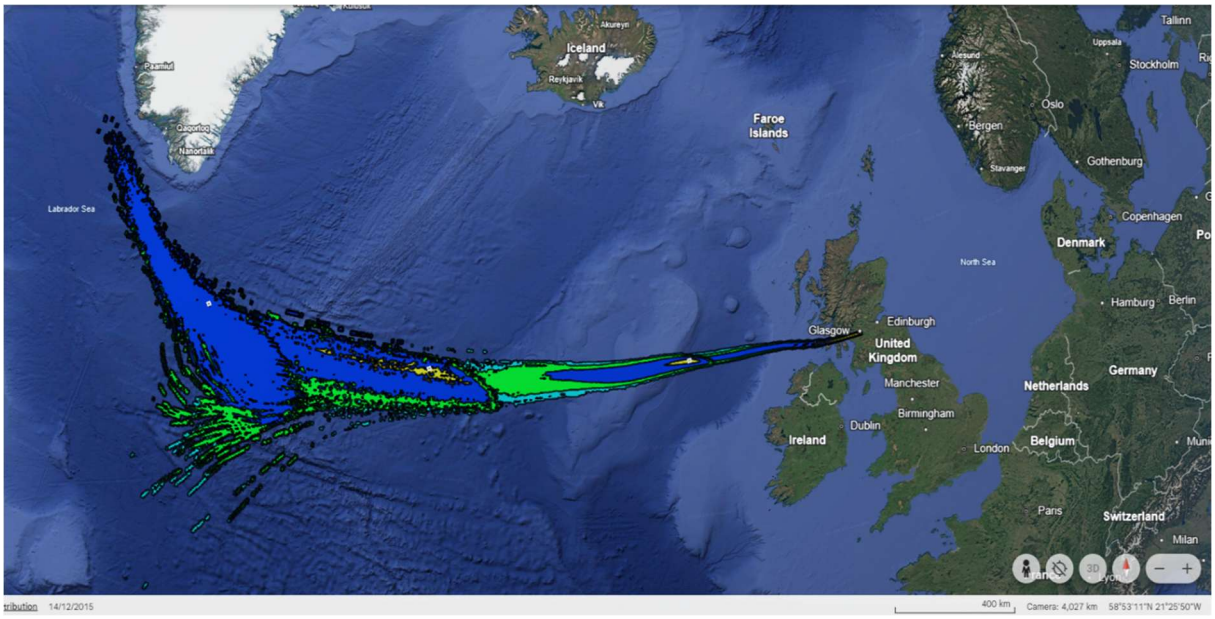


Figure IX.2 10µm 5oC density 1g – Backward 18th Nov'21

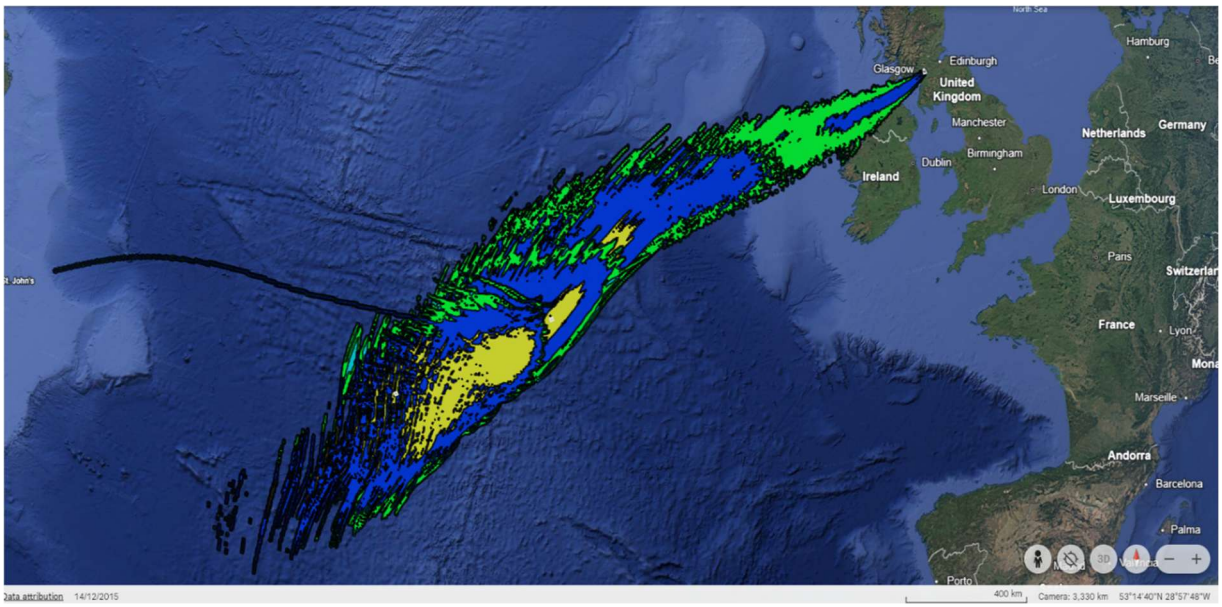


Figure IX.3 10µm 5oC density 1g – Backward 19th Nov'21

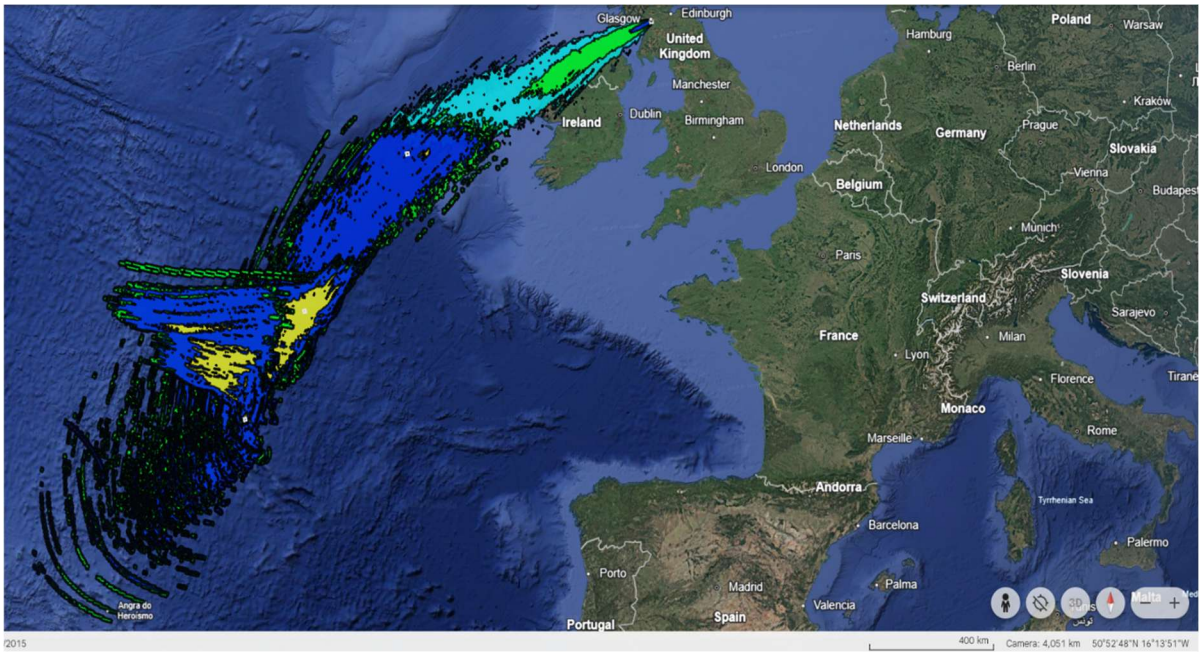


Figure IX.4 10µm 5oC density 1g – Backward 20th Nov'21

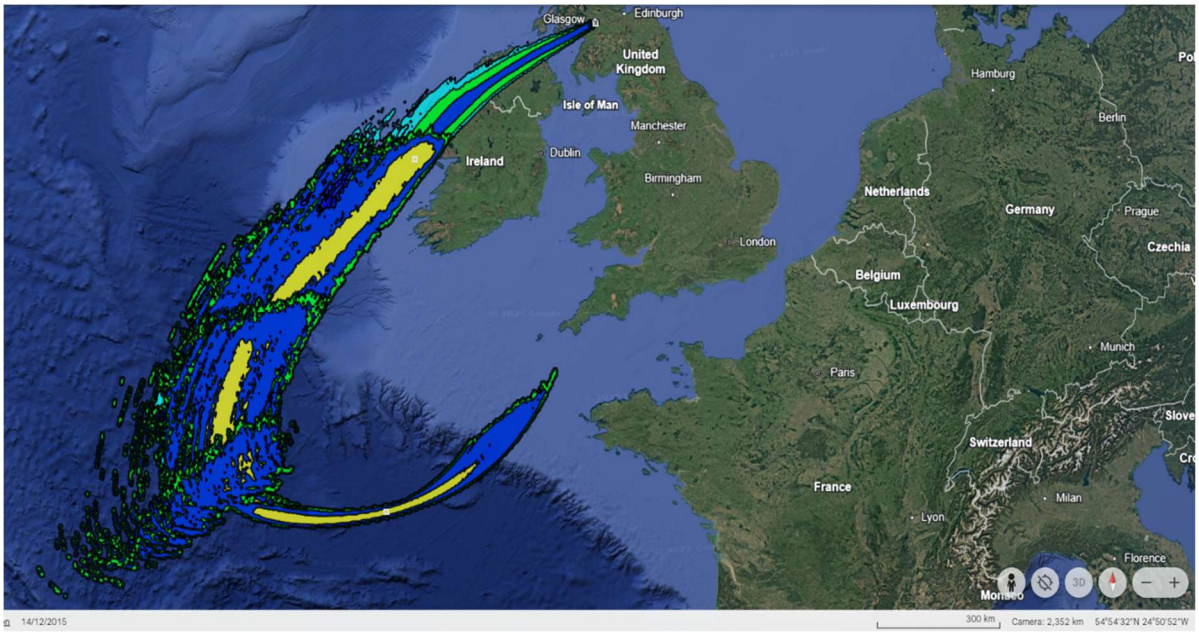


Figure IX.5 10µm 5oC density 1g – Backward 21st Nov'21

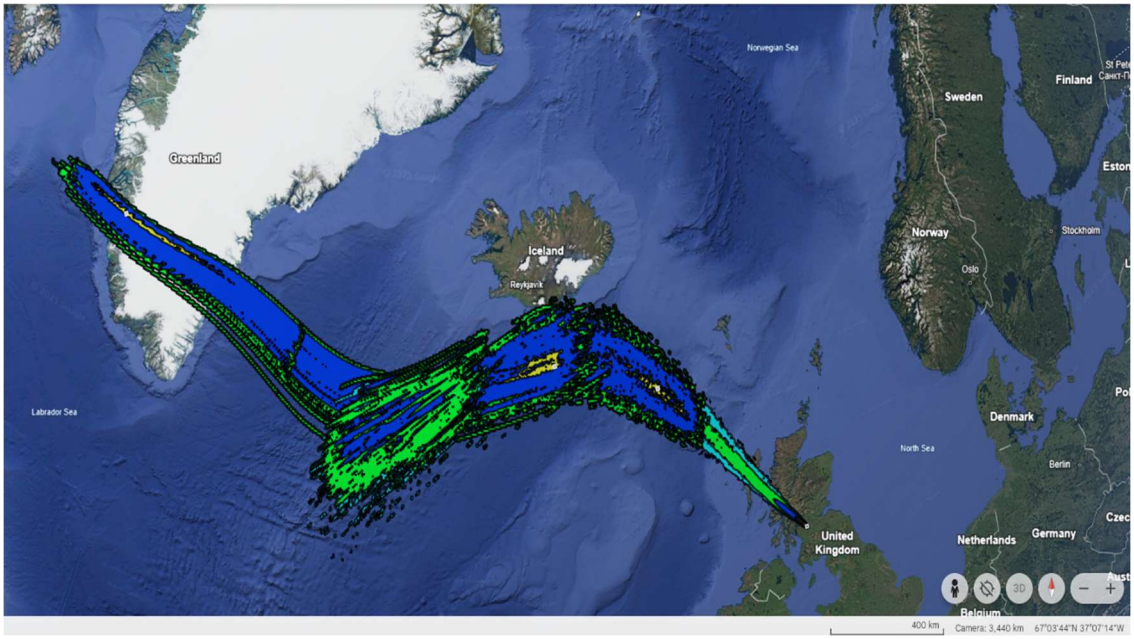


Figure IX.6 10µm 5oC density 1g – Backward 22nd Nov'21

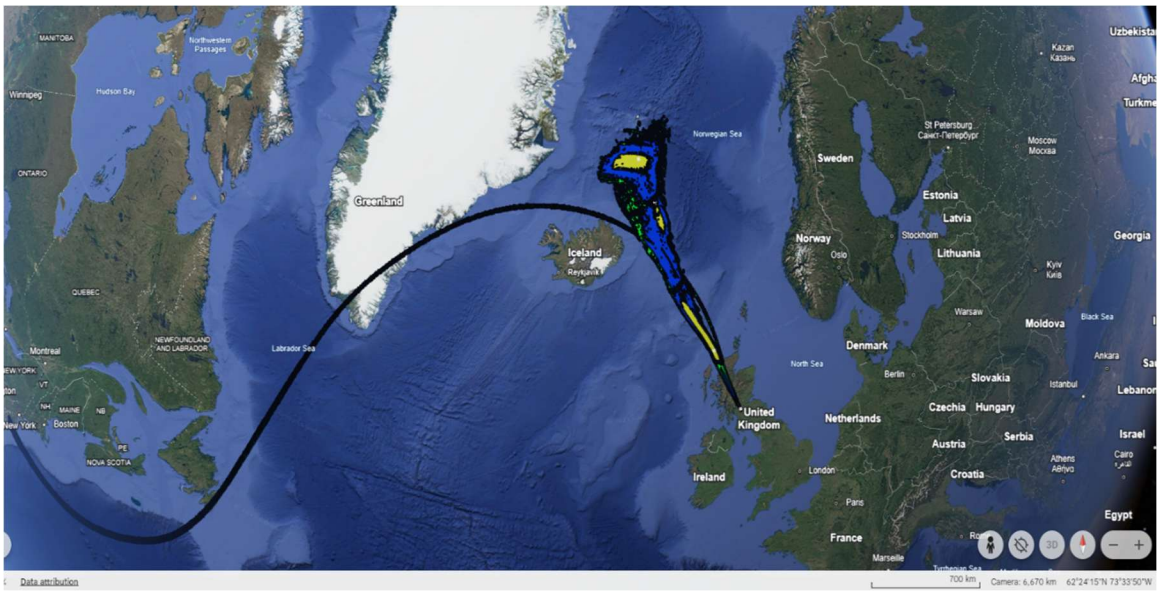


Figure IX.7 10µm 5oC density 1g – Backward 23rd Nov'21

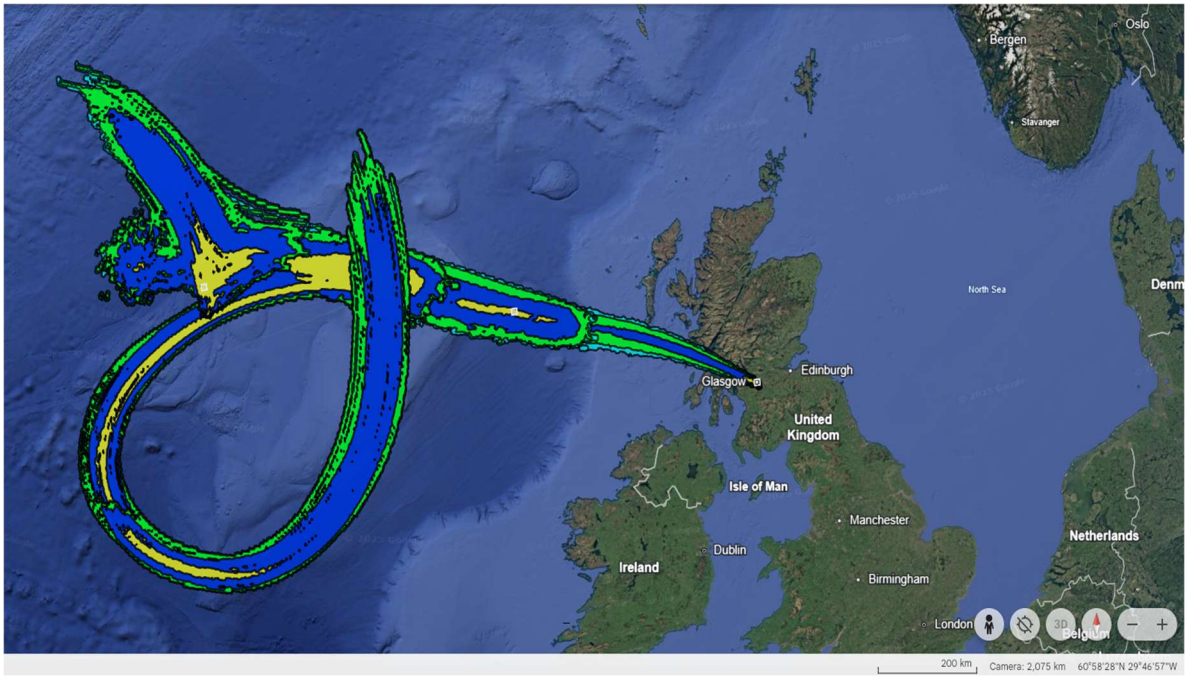


Figure IX.8 10µm 5oC density 1g – Forward 17th Nov'21

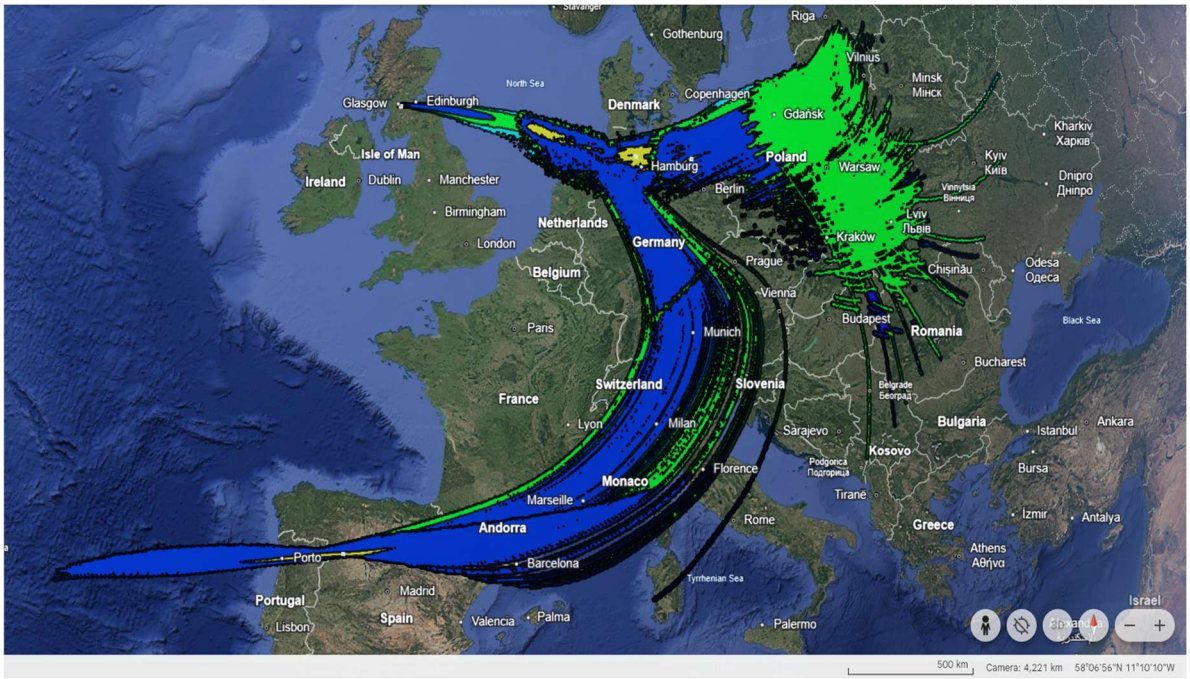


Figure IX.9 10µm 5oC density 1g – Forward 18th Nov'21

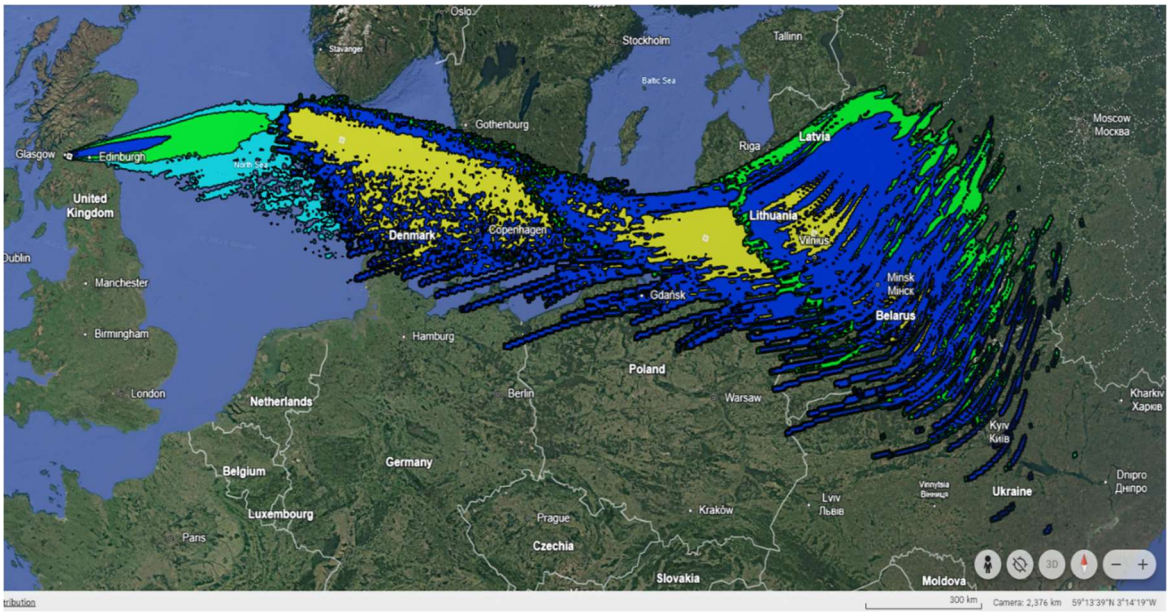


Figure IX.10 10µm 5oC density 1g – Forward 19th Nov'21

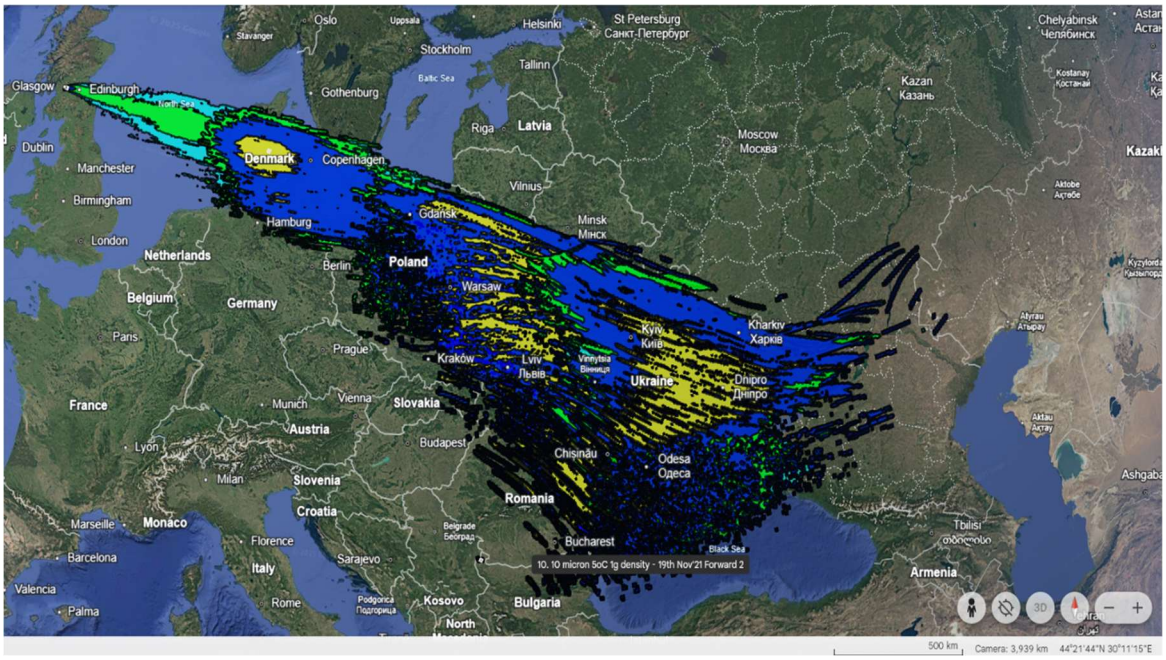


Figure IX.11 10µm 5oC density 1g – Forward 20th Nov'21

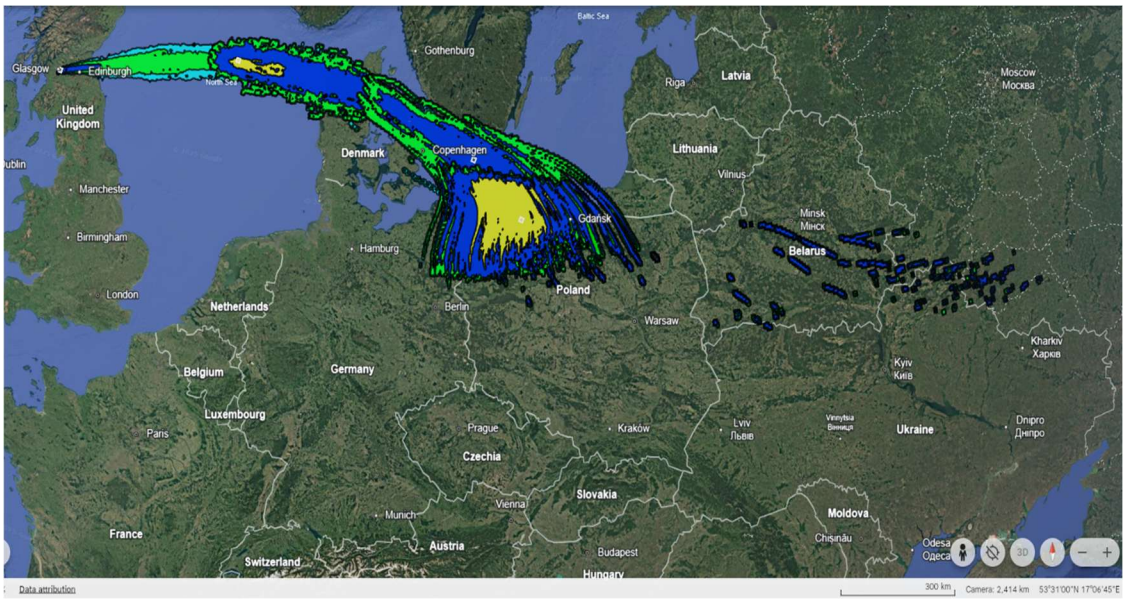


Figure IX.12 10µm 5oC density 1g – Forward 21st Nov'21

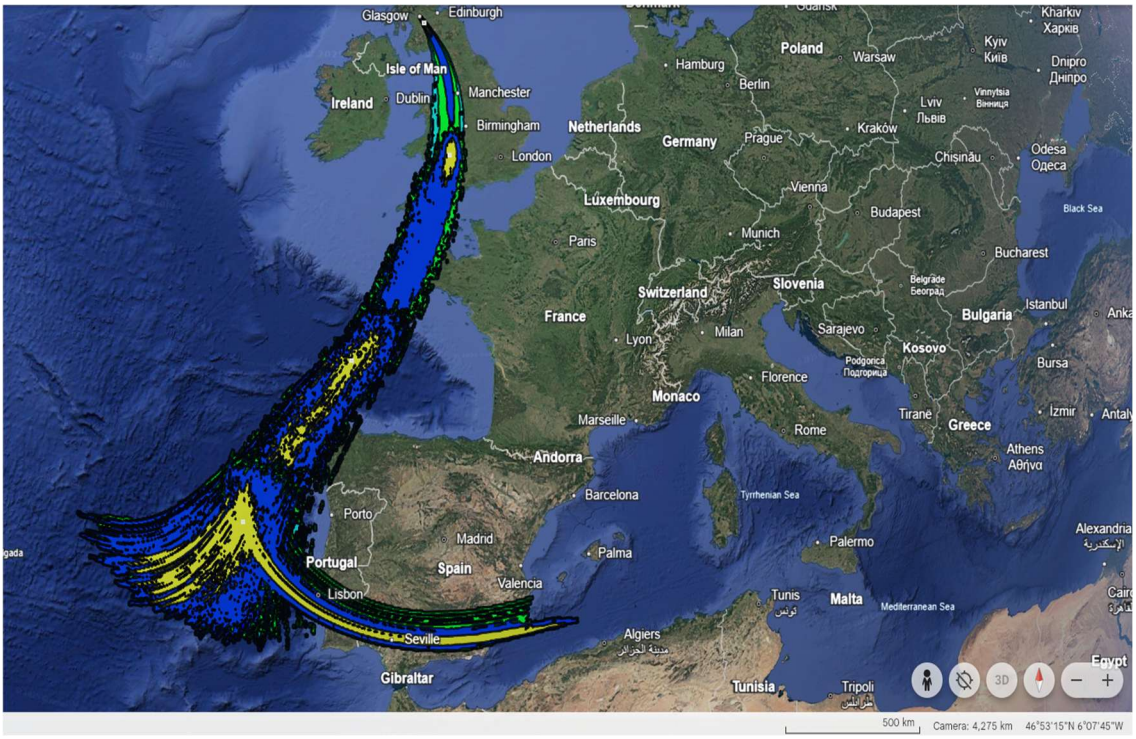


Figure IX.1 13 10µm 5oC density 1g – Forward 22nd Nov'21

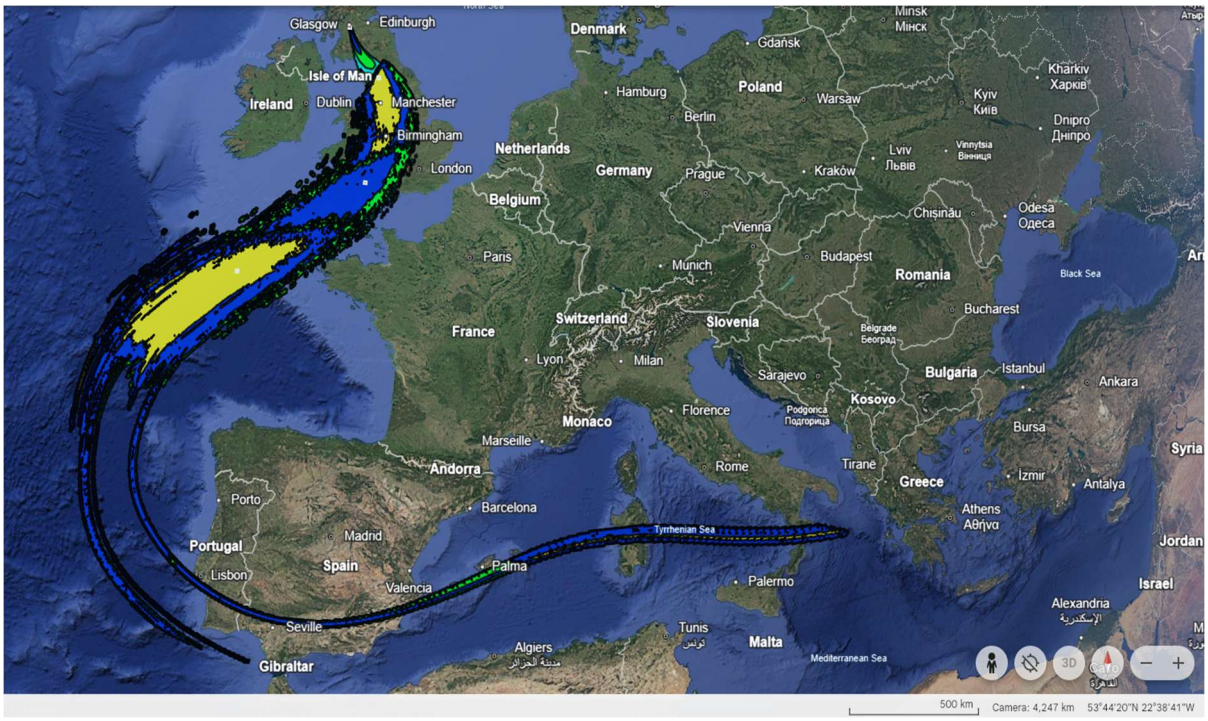


Figure IX.14 10µm 5oC density 1g – Forward 23rd Nov'21

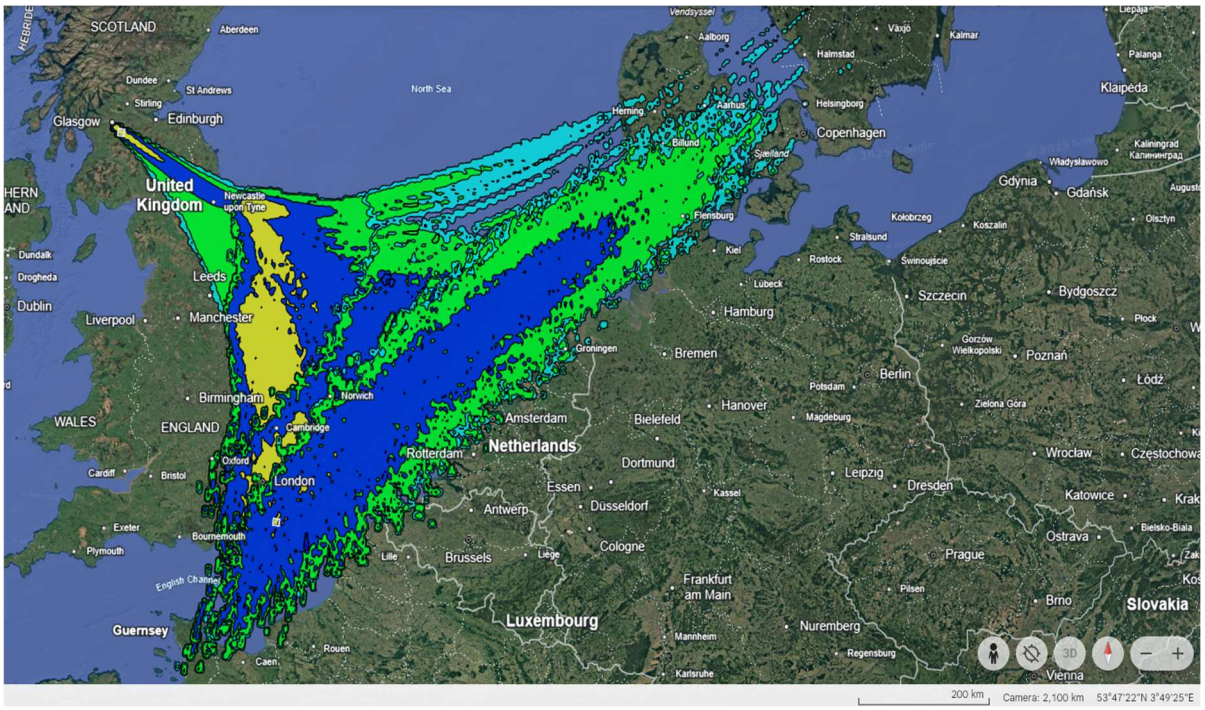


Figure IX.15 20µm 50c 1g density 17th Nov, Backward

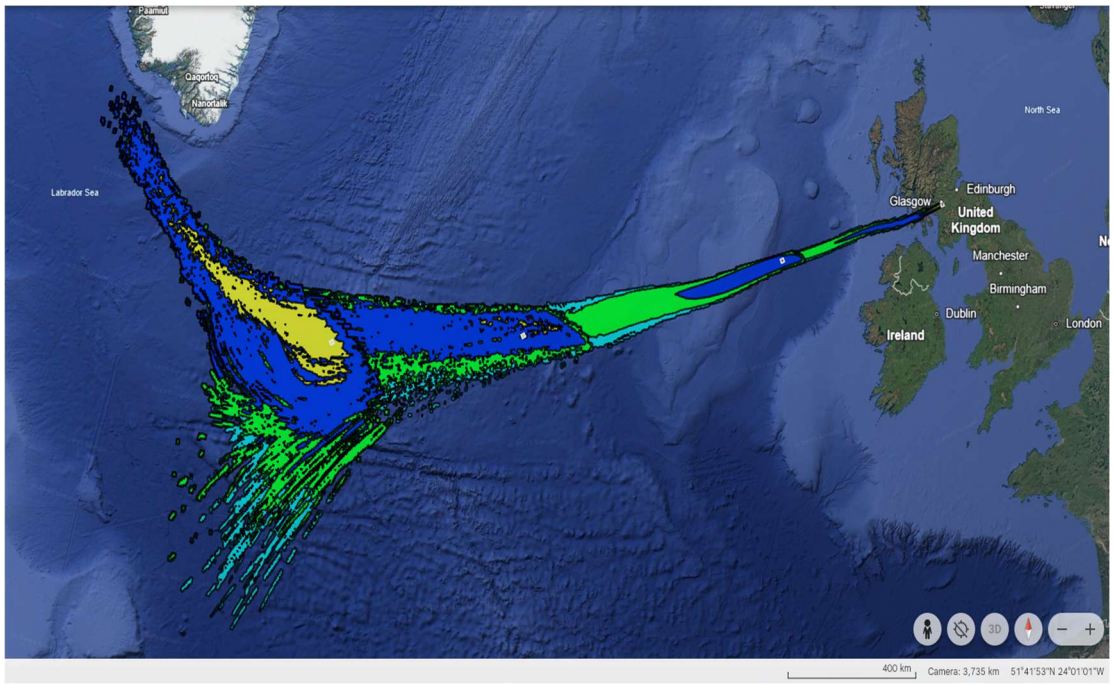


Figure IX.16 20µm 5oC density 1g – Backward 18th Nov'21

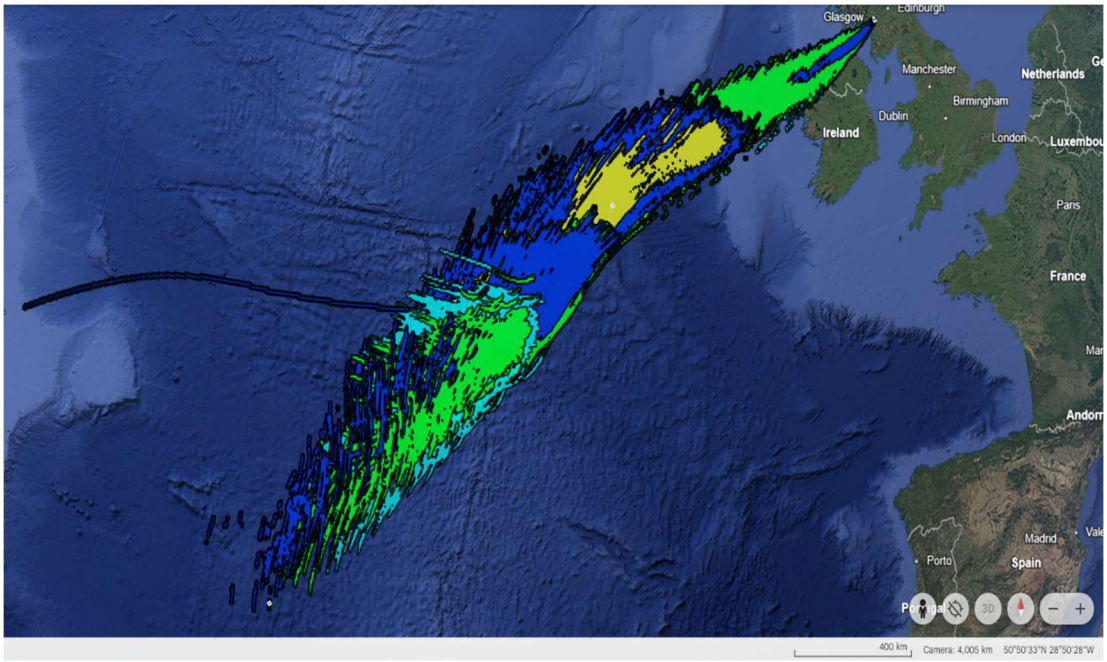


Figure IX.17 20µm 5oC density 1g – Backward 19th Nov'21

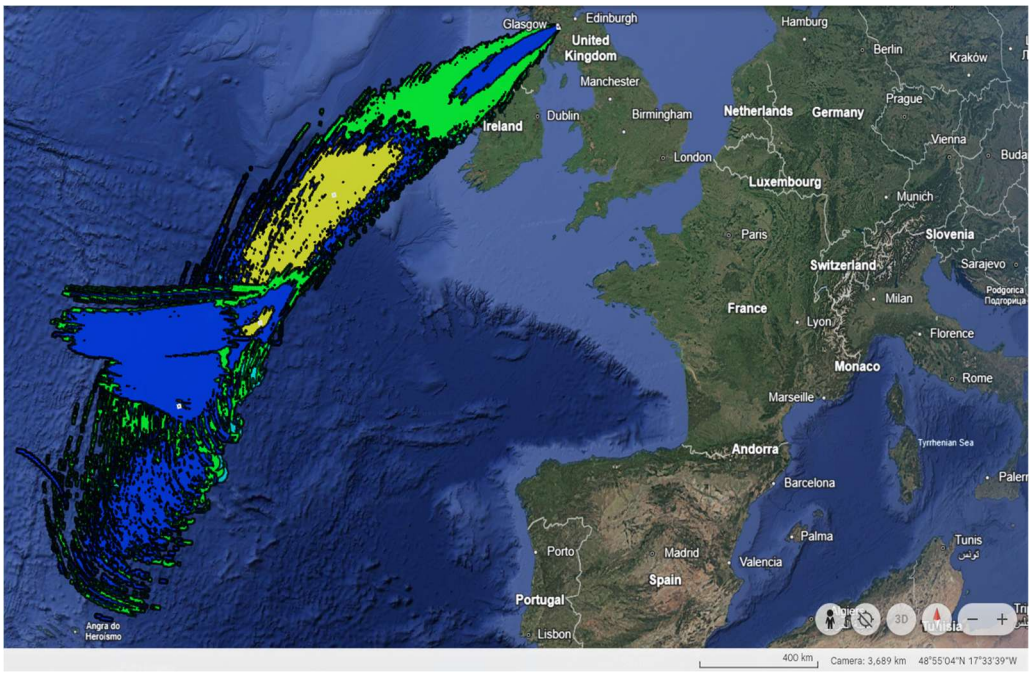


Figure IX.18 20µm 5oC density 1g – Backward 20th Nov'21

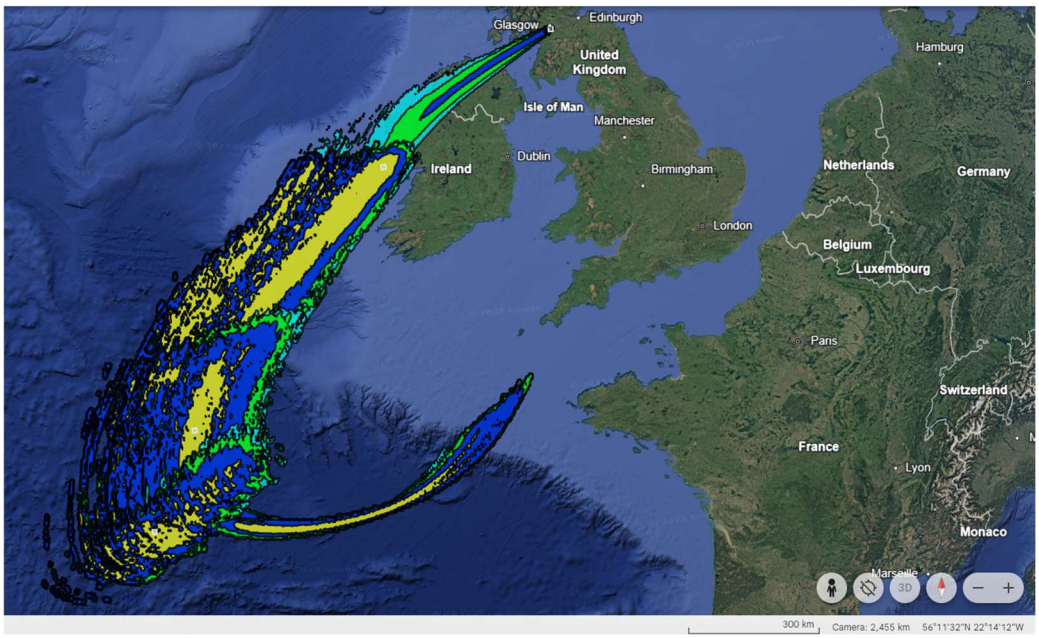


Figure IX.19 20µm 5oC density 1g – Backward 21st Nov'21

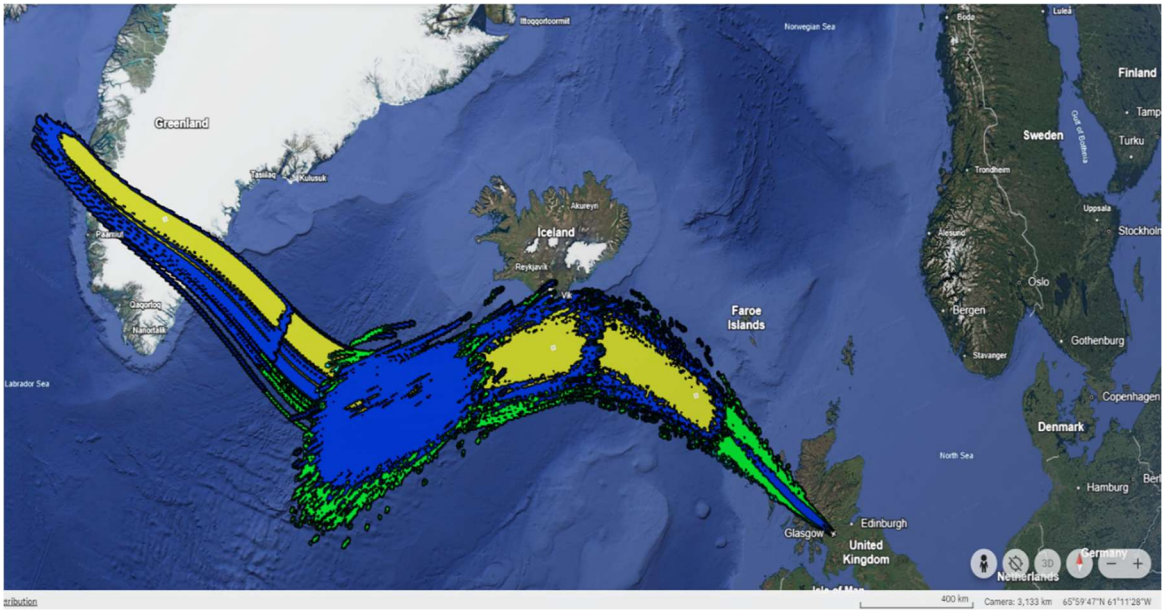


Figure IX.20 20µm 5oC density 1g – Backward 22nd Nov'21 2

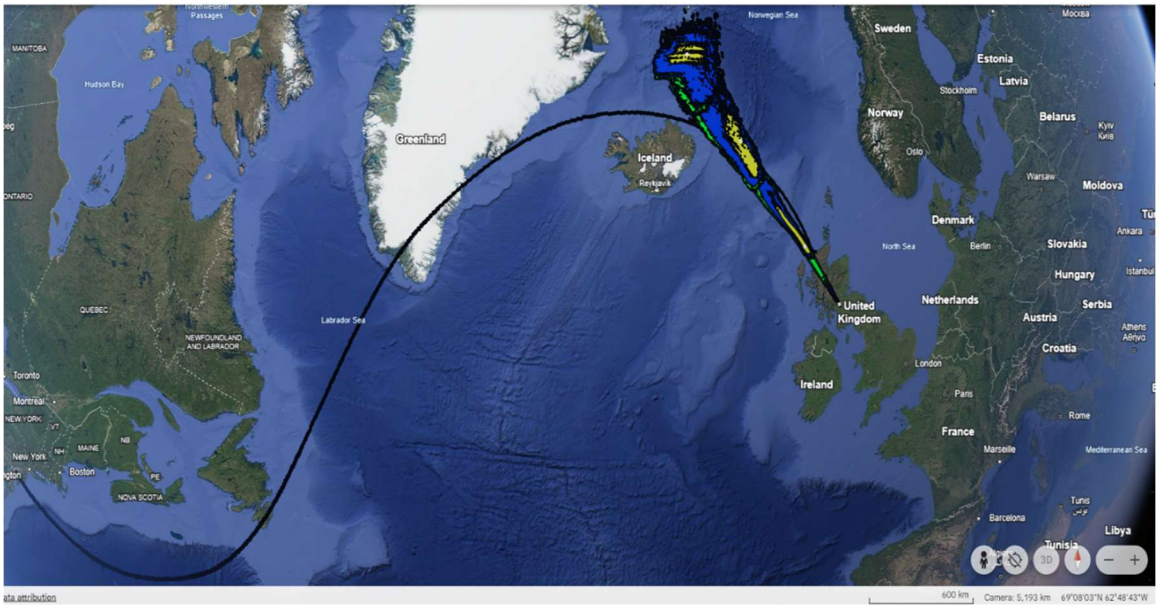


Figure IX.21 20µm 5oC density 1g – Backward 23rd Nov'21

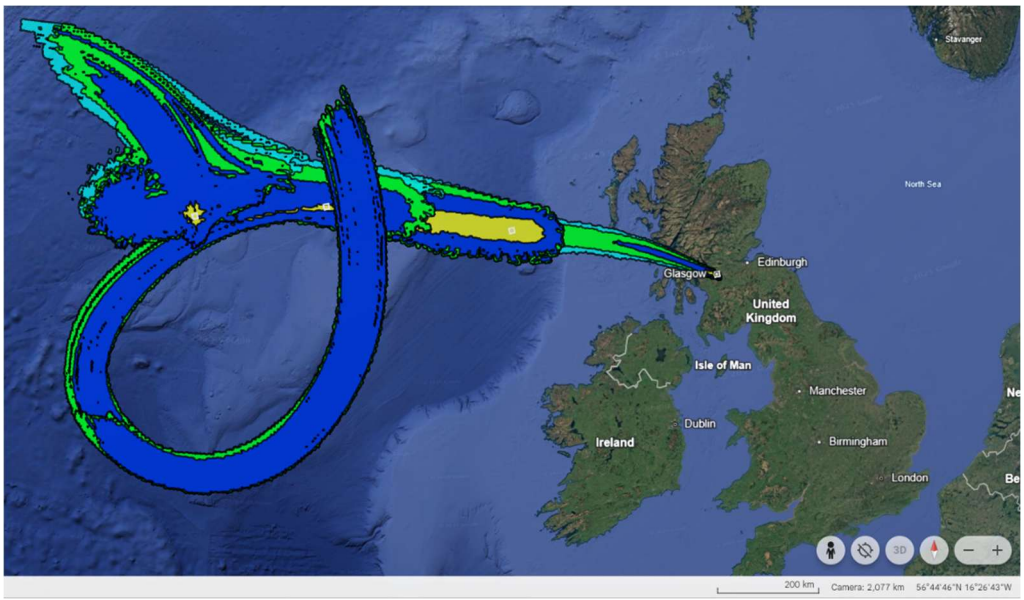


Figure IX.22 20µm 5oC density 1g – Forward 17th Nov'21

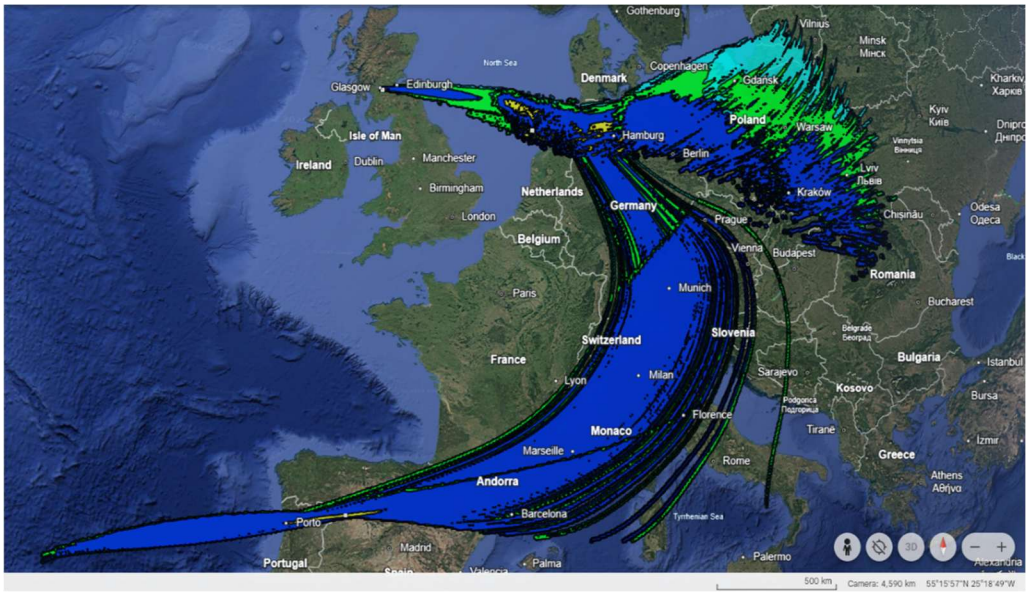


Figure IX.23 20µm 5oC density 1g – Forward 18th Nov'21

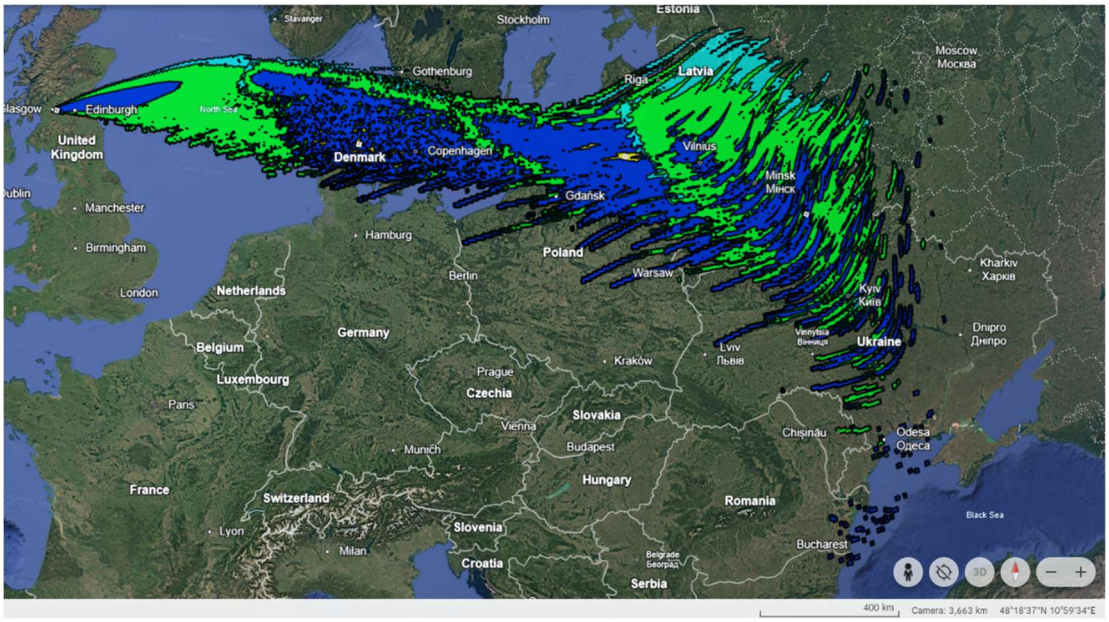


Figure IX.24 20µm 5oC density 1g – Forward 19th Nov'21

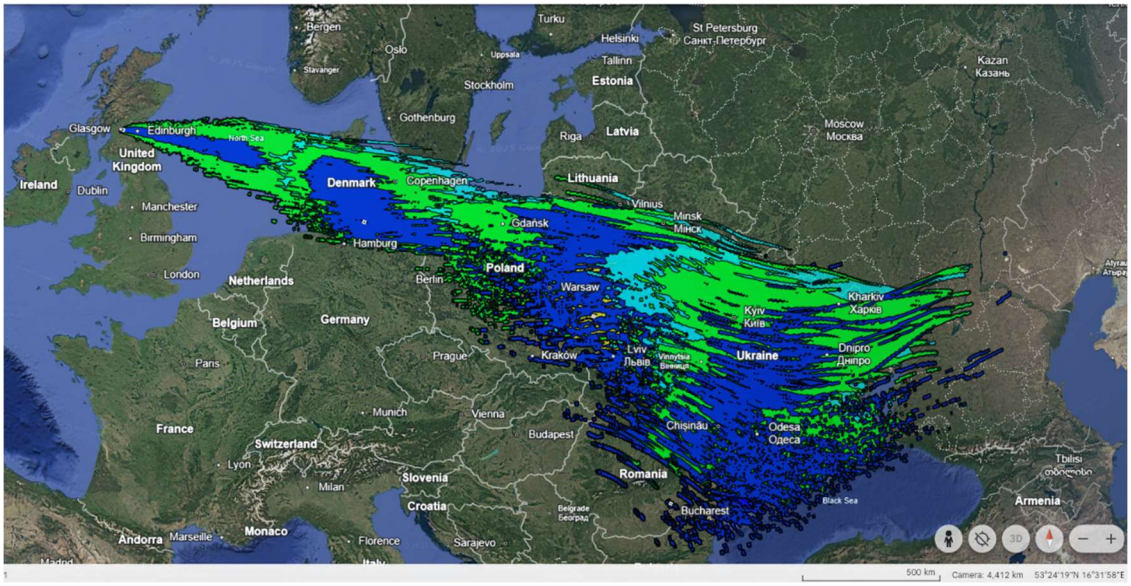


Figure IX.25 20µm 5oC density 1g – Forward 20th Nov'21

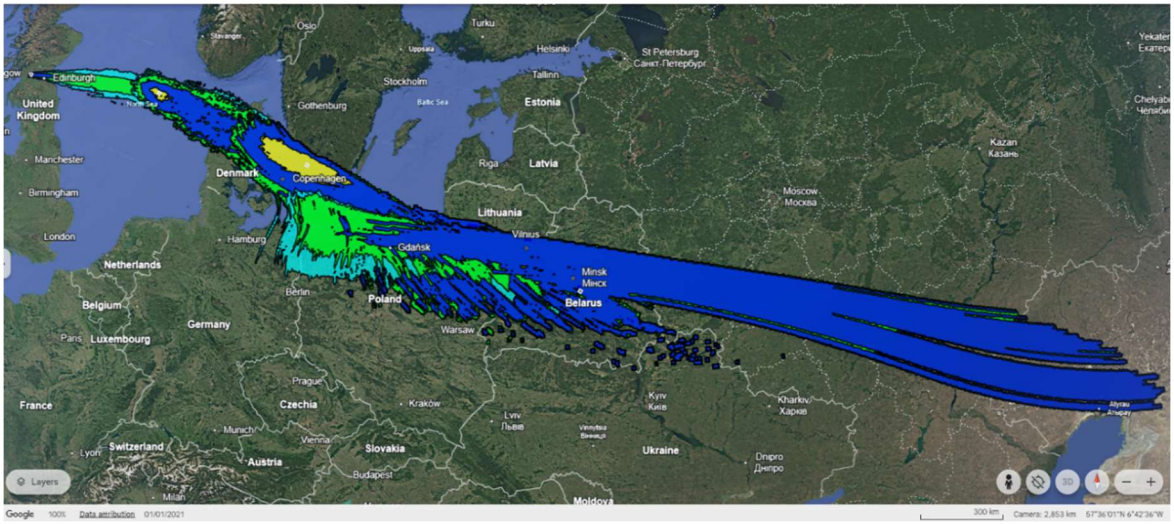


Figure IX.2. 20µm 5oC density 1g – Forward 21st Nov'21

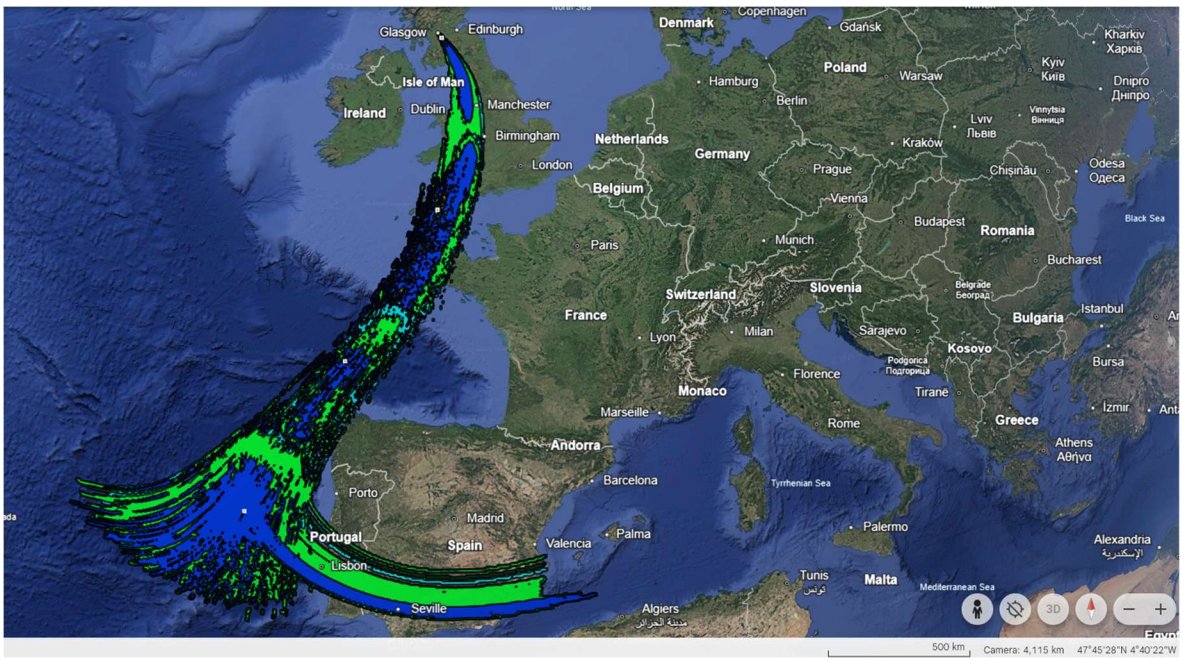


Figure IX.27 20µm 5oC density 1g – Forward 22nd Nov'21



Figure IX.28 20µm 5oC density 1g – Forward 23rd Nov'21

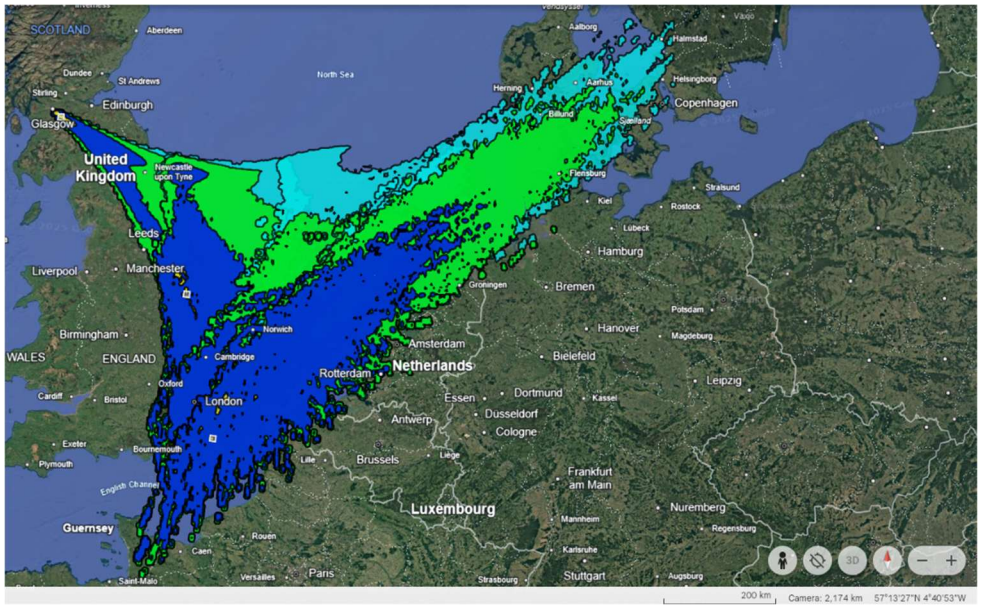


Figure IX.29 100µm 5oC density 1g – Backward 17th Nov'21

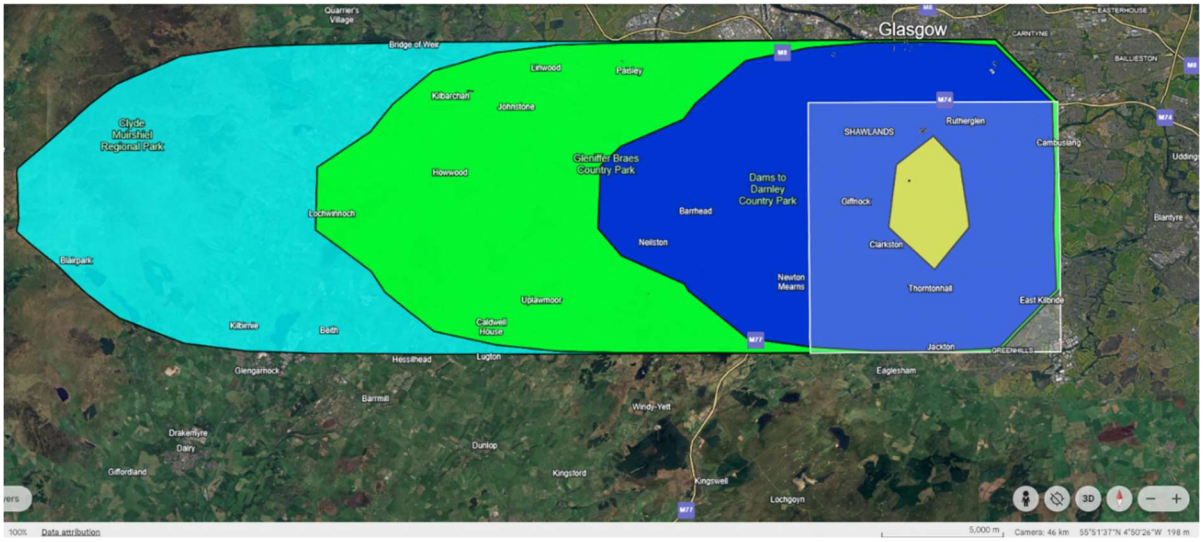


Figure IX.30 100µm 5oC density 1g – Backward 18th Nov'21

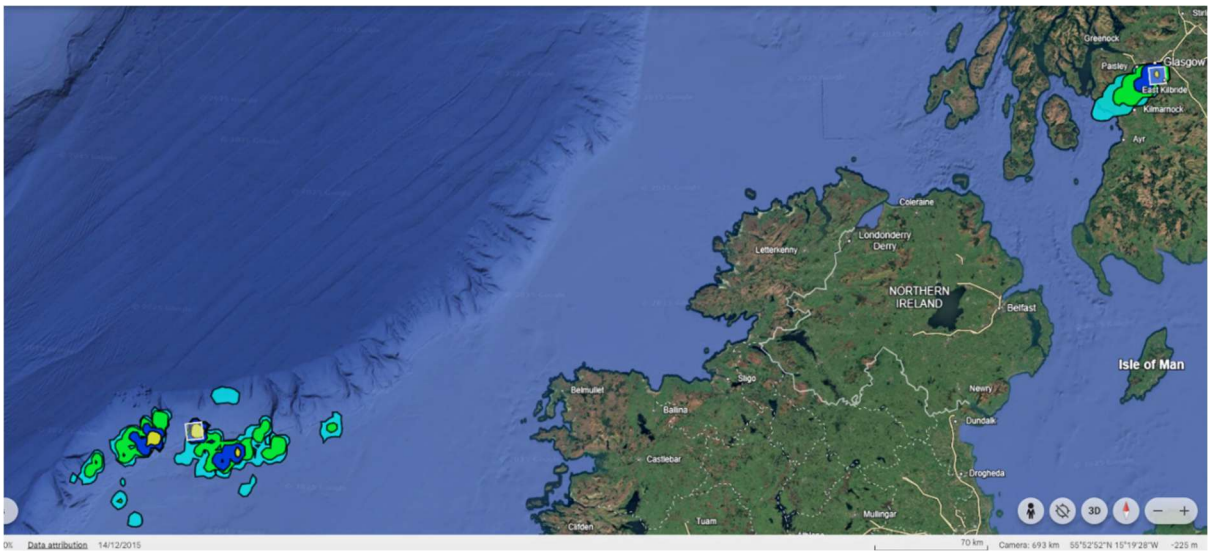


Figure IX.31 100m 5oC density 1g – Backward 19th Nov'21

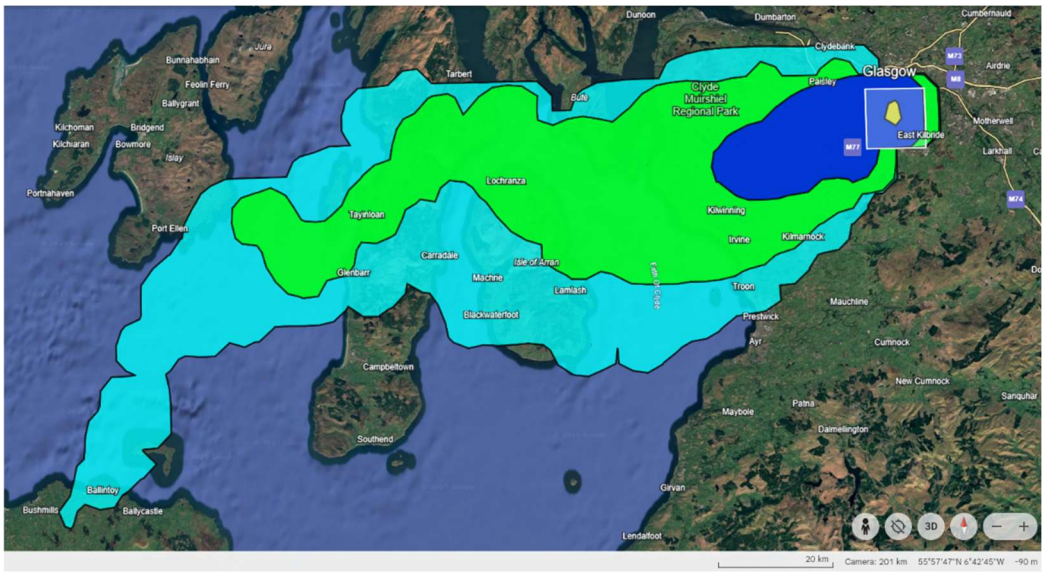


Figure IX.32 100µm 5oC density 1g – Backward 20th Nov'21

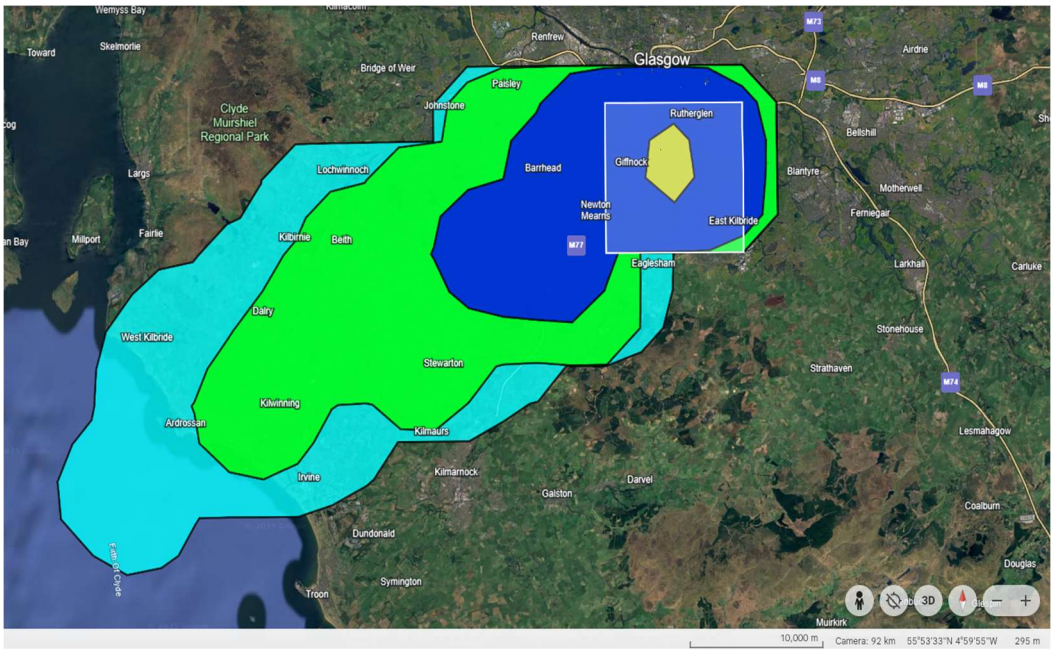


Figure IX.33 100µm 5oC density 1g – Backward 21st Nov'21

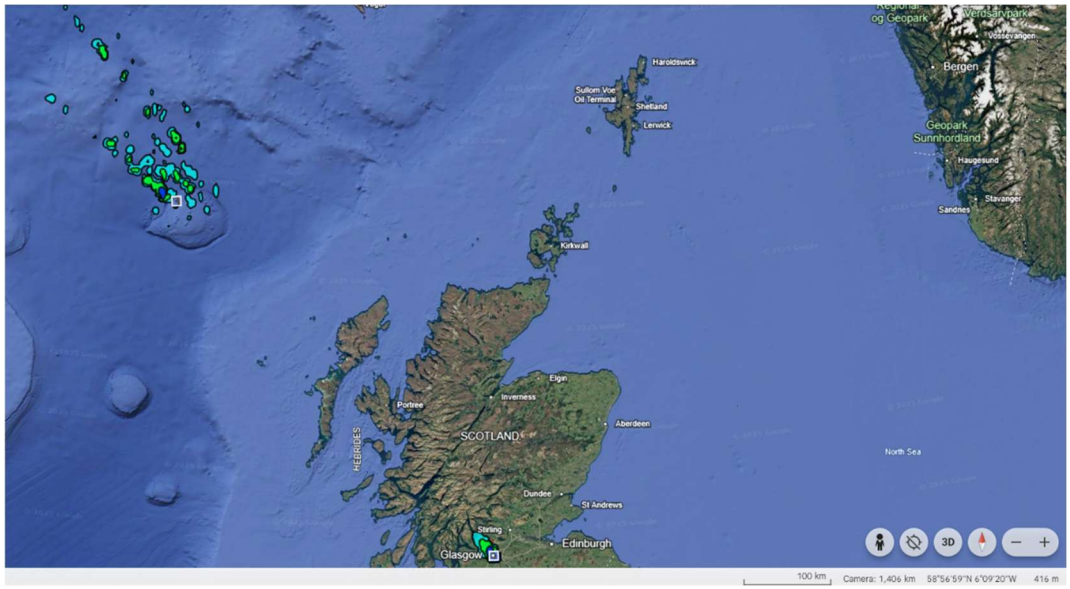


Figure IX.34 100µm 5oC density 1g – Backward 22nd Nov'21

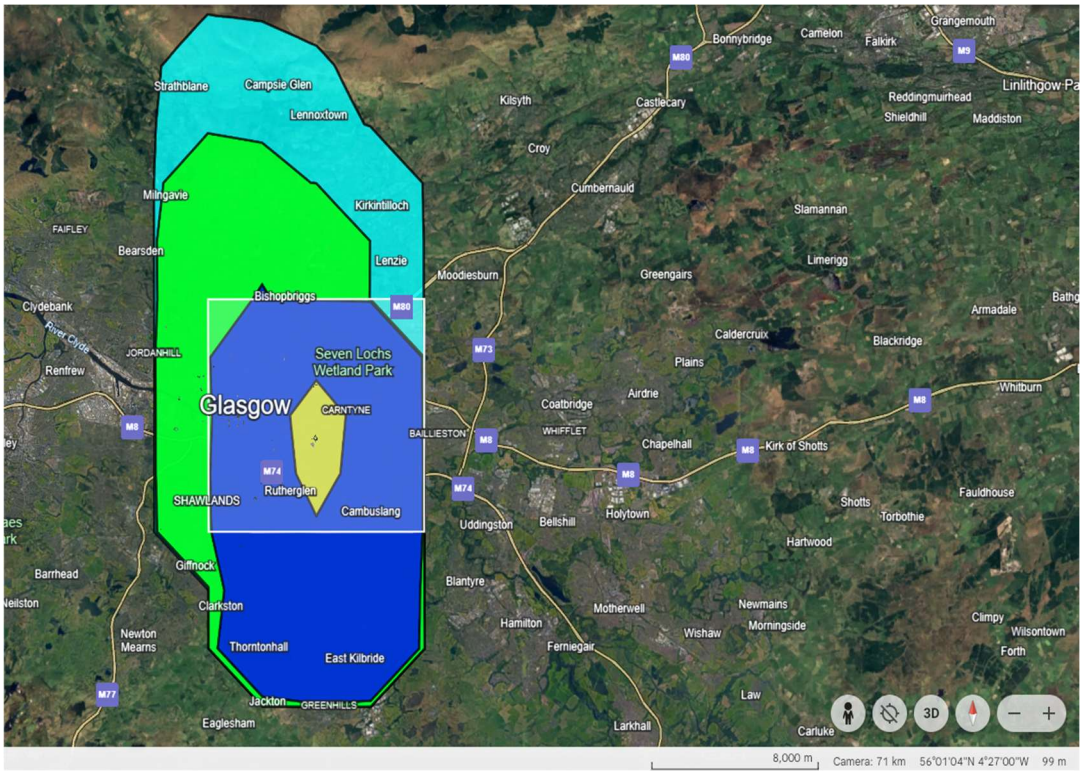


Figure IX.35 100µm 5oC density 1g – Backward 23rd Nov'21

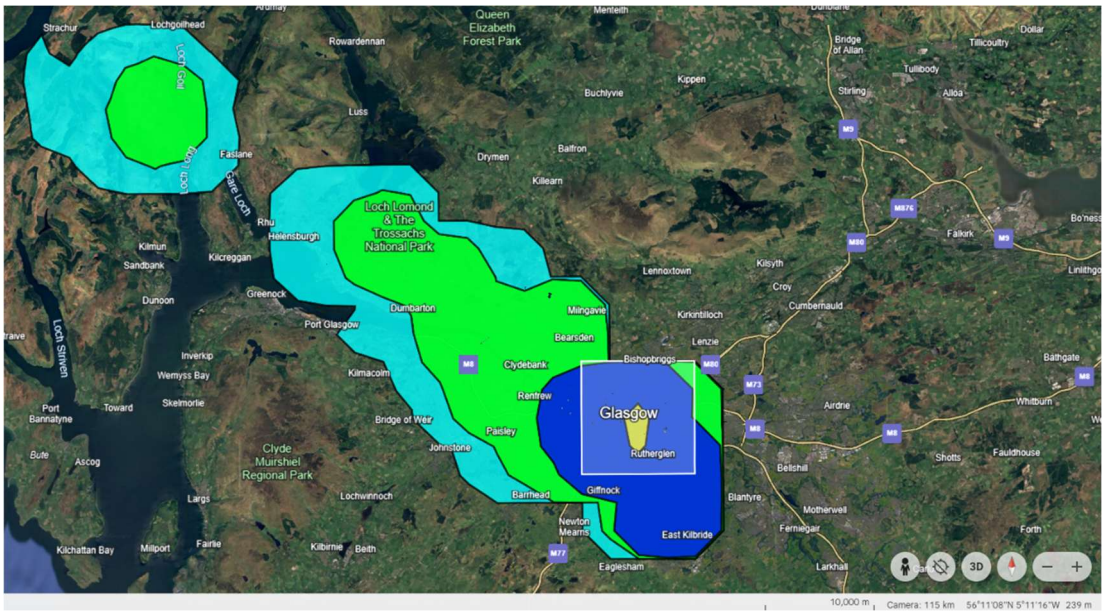


Figure IX.36 100µm 5oC density 1g – Forward 17th Nov'21

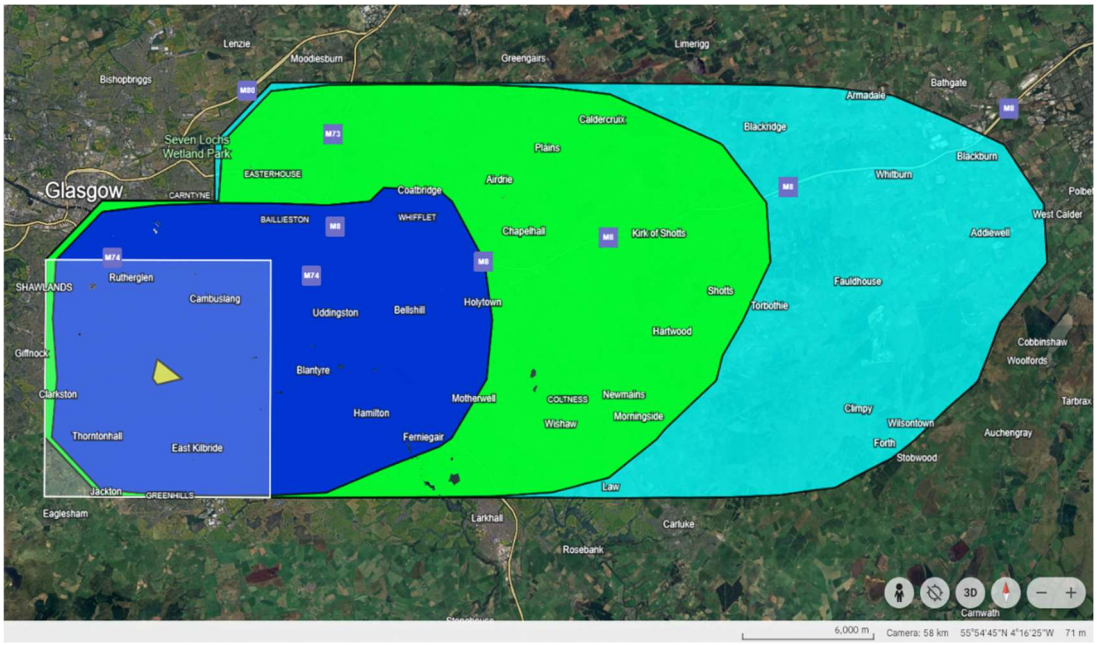


Figure IX.37 100µm 5oC density 1g – Forward 18th Nov'21

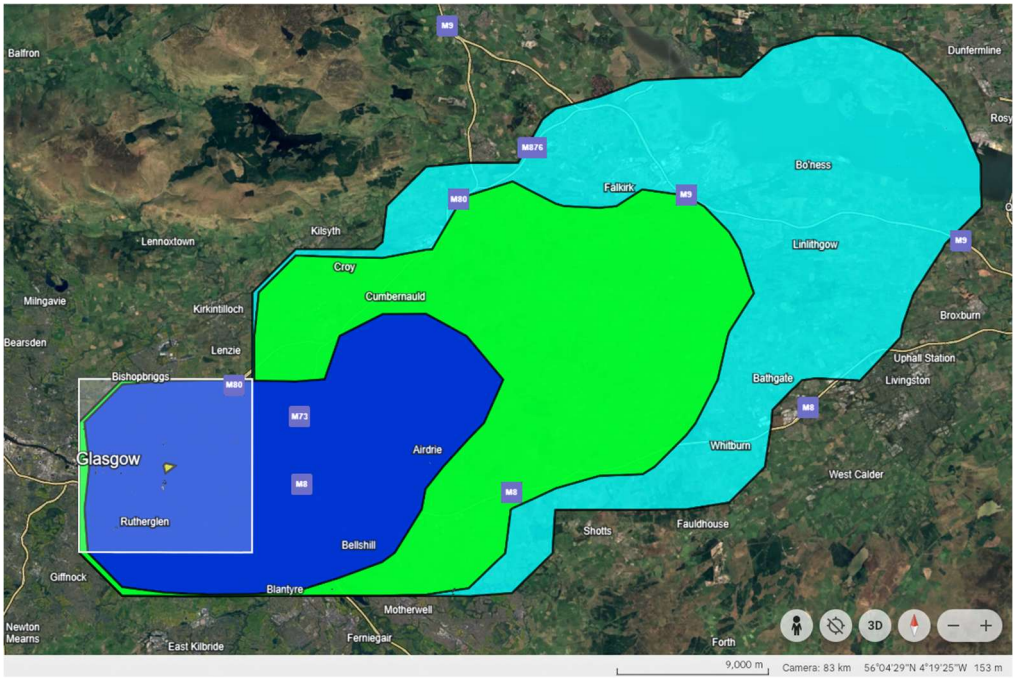


Figure IX.38 100µm 5oC density 1g – Forward 19th Nov'21

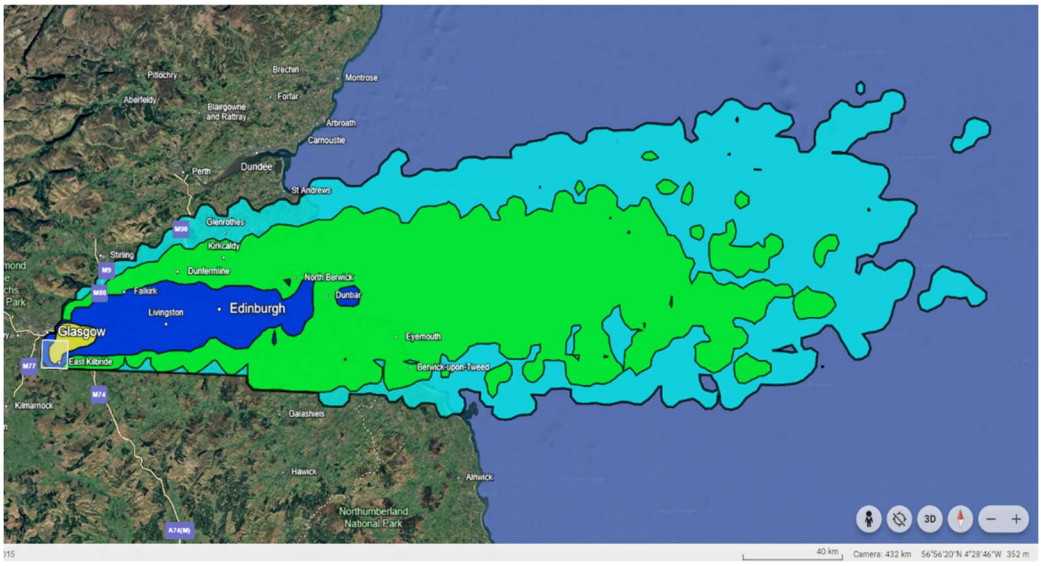


Figure IX.39 100µm 5oC density 1g – Forward 20th Nov'21

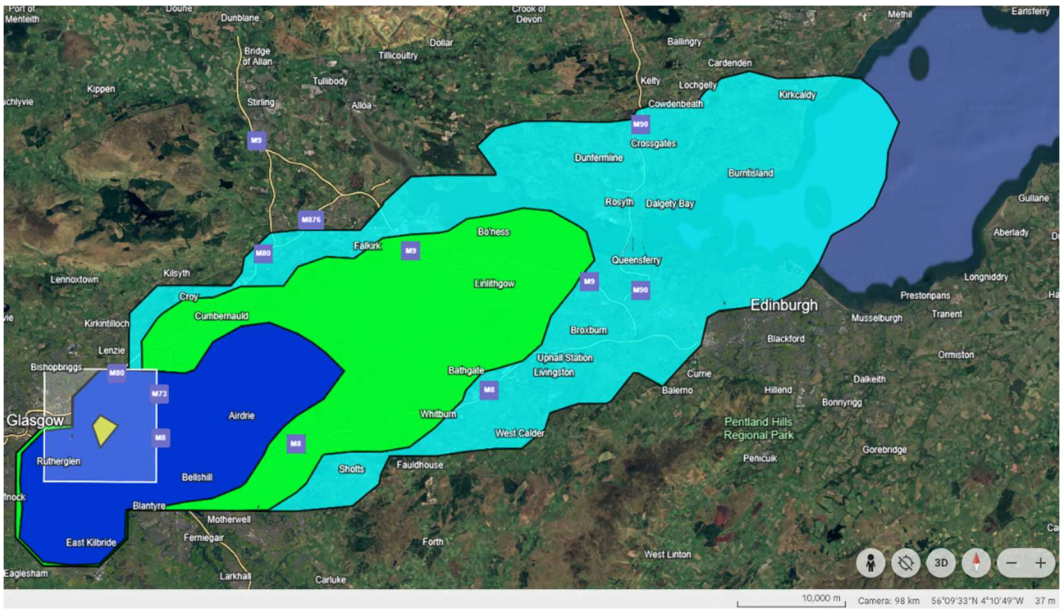


Figure IX.40 100µm 5oC density 1g – Forward 21st Nov'21

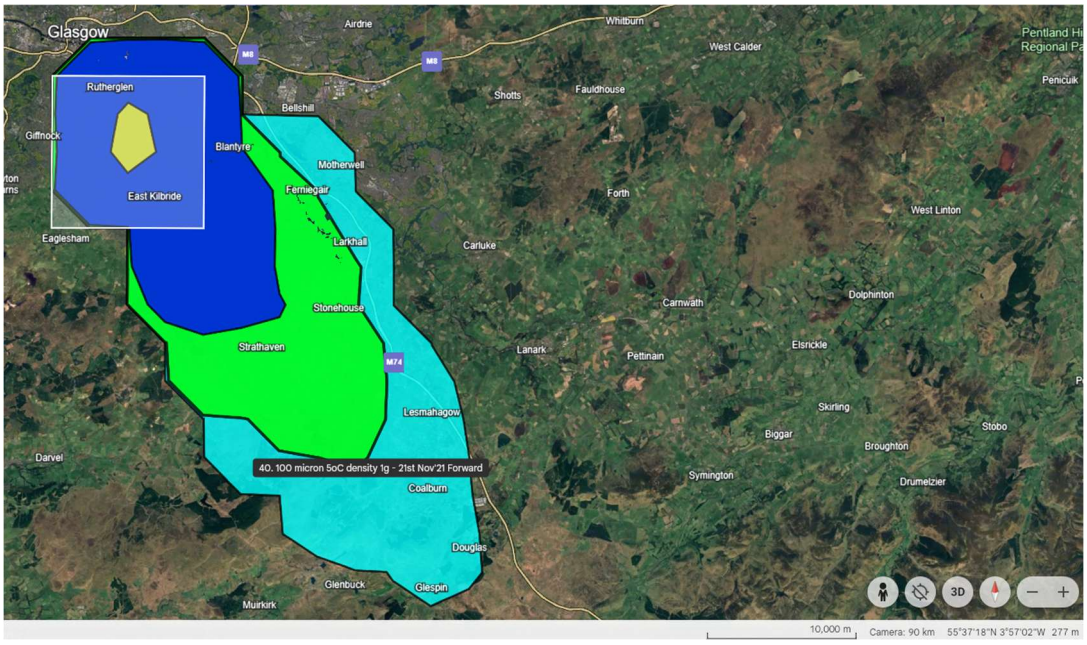


Figure IX.41 100µm 5oC density 1g – Forward 22nd Nov'21

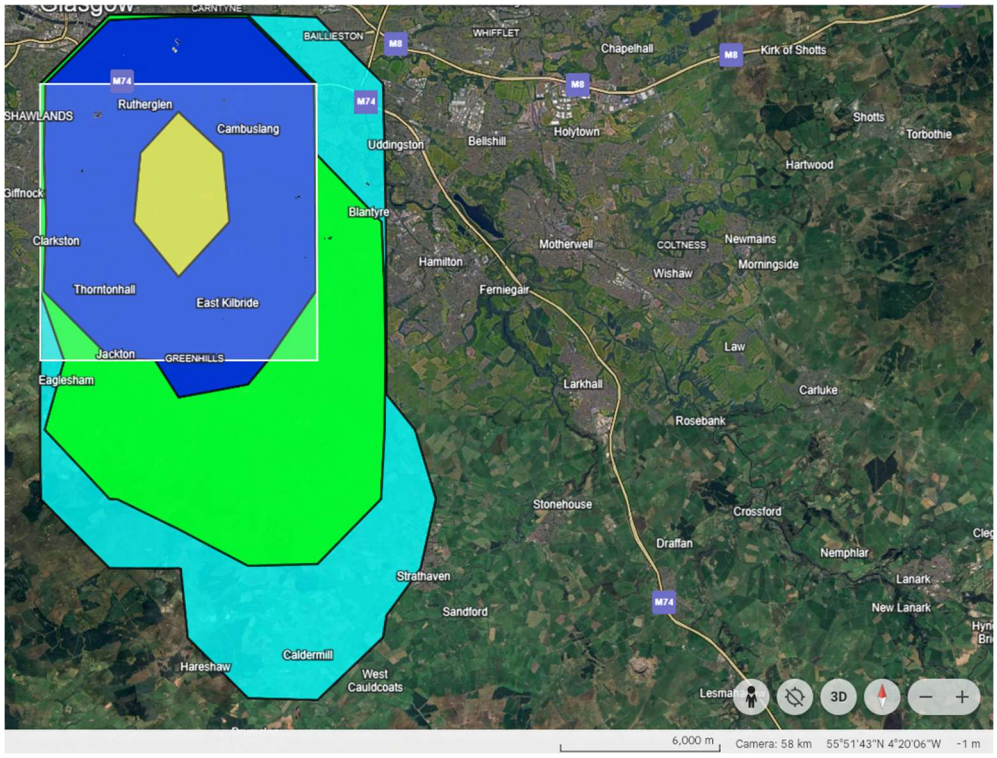


Figure IX.42 100µm 5oC density 1g – Forward 23rd Nov'21

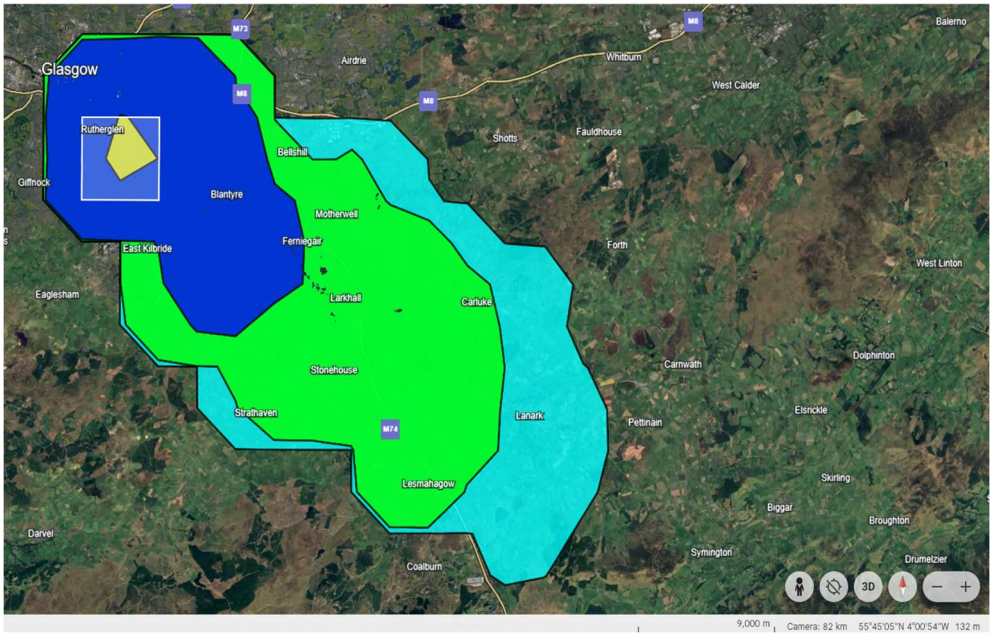


Figure IX.43 10µm 5oC 0.625g density 17th Nov, Backward

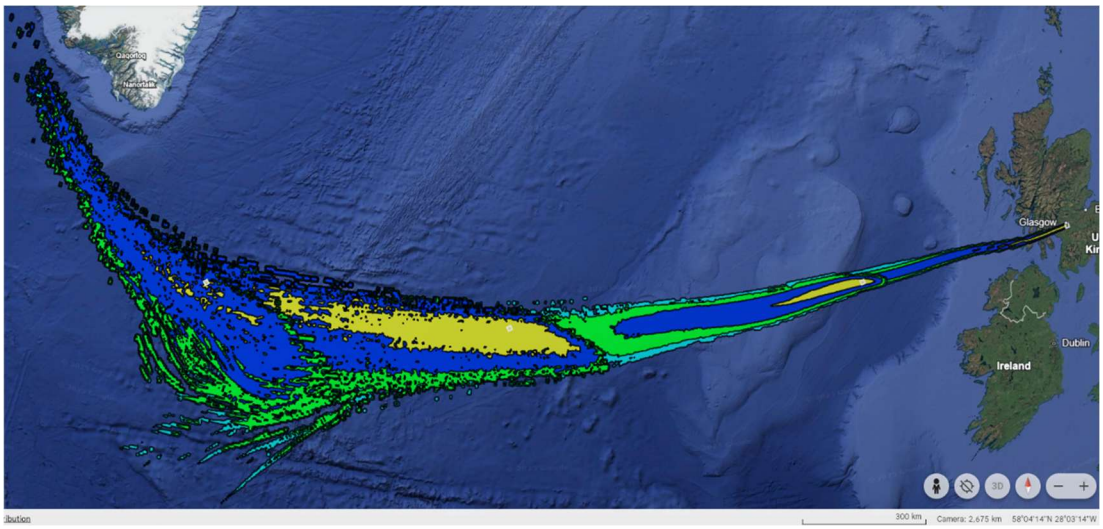


Figure IX.44 10µm 5oC 0.625g density – Backward 18th Nov'21

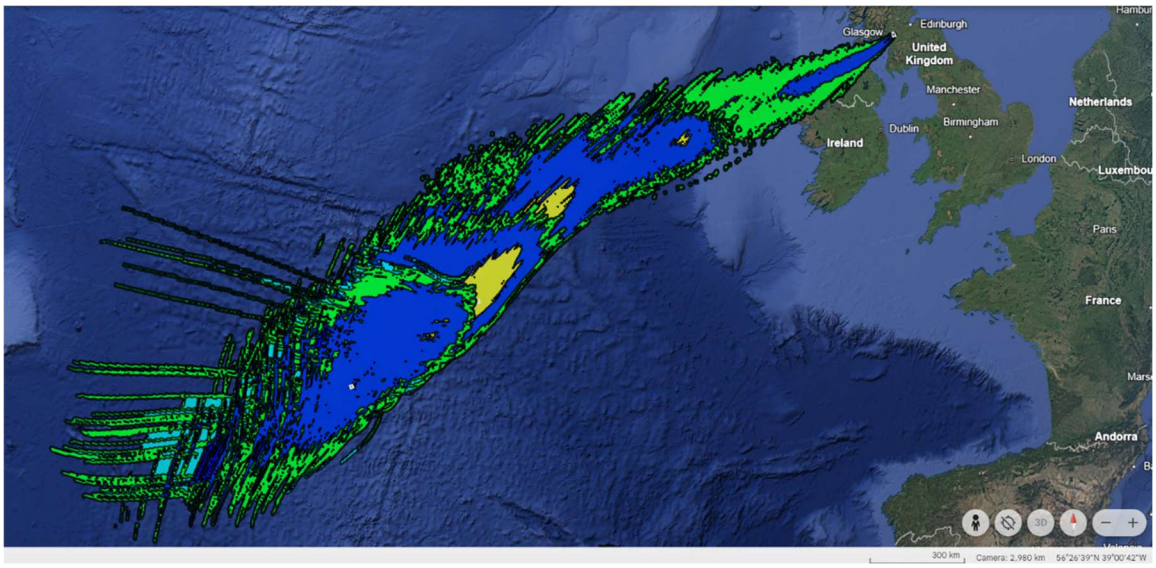


Figure IX.45 10µm 5oC 0.625g density – Backward 19th Nov'21

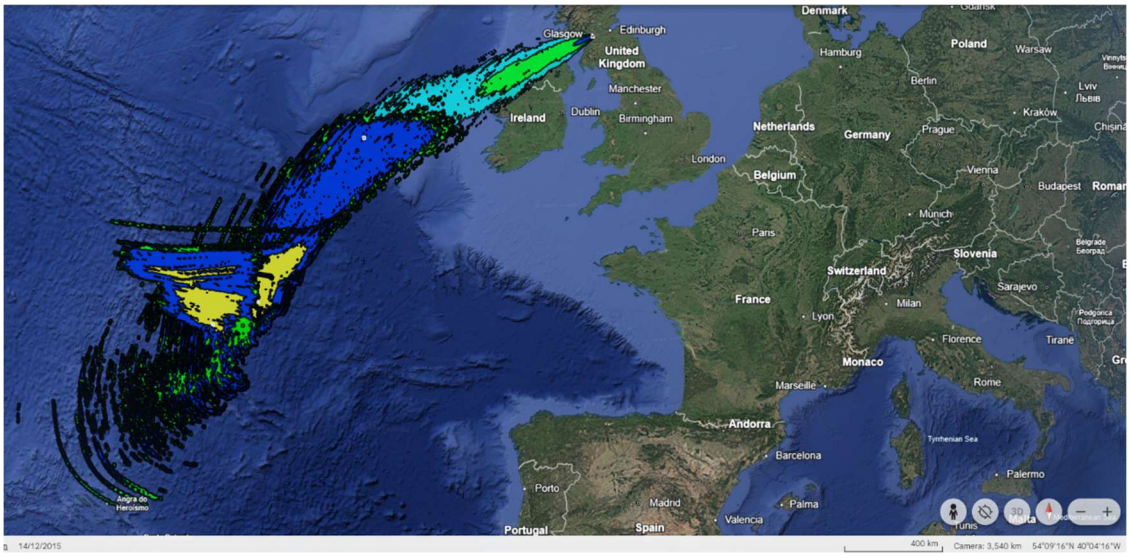


Figure IX.46 10µm 5oC 0.625g density – Backward 20th Nov'21

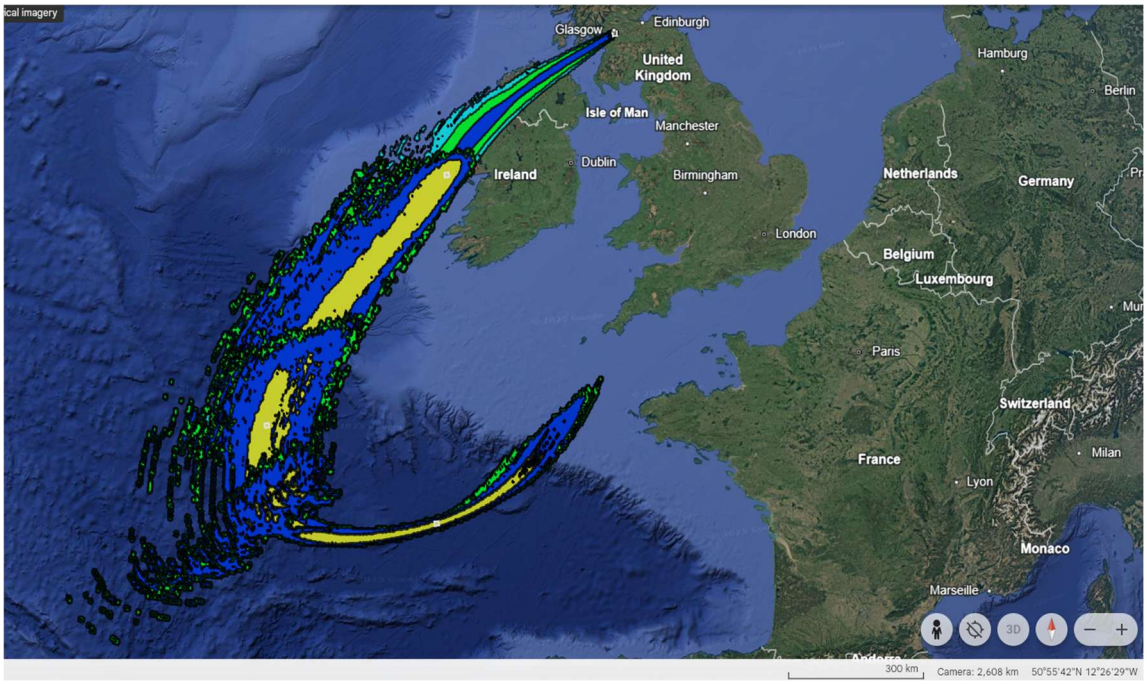


Figure IX.47 10µm 5oC 0.625g density – Backward 21st Nov'21

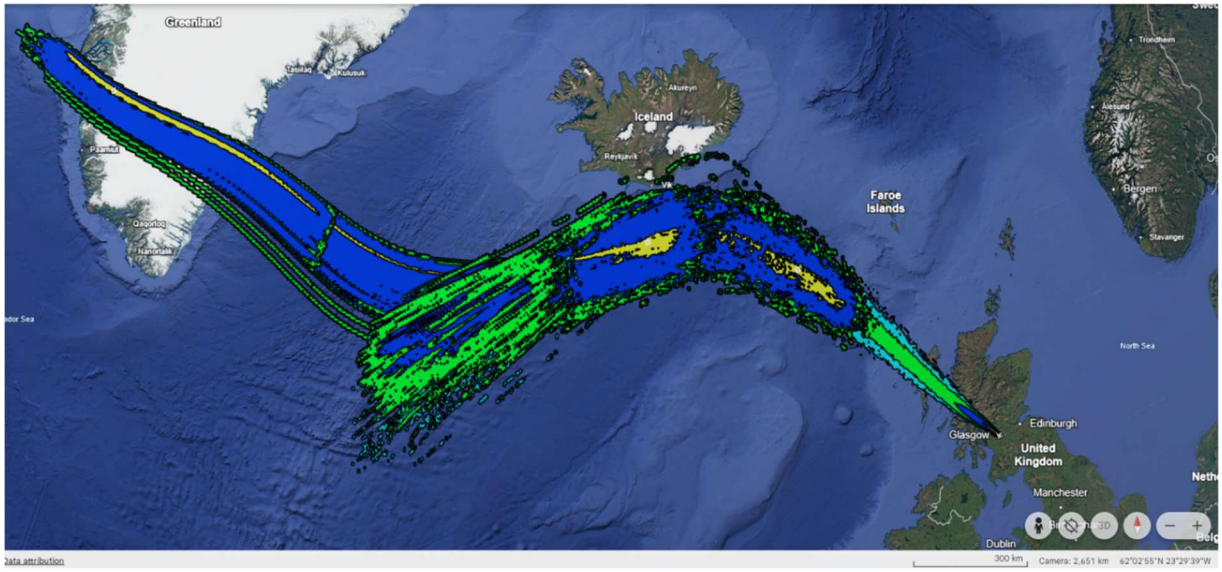


Figure IX.48 10µm 5oC 0.625g density – Backward 22nd Nov'21

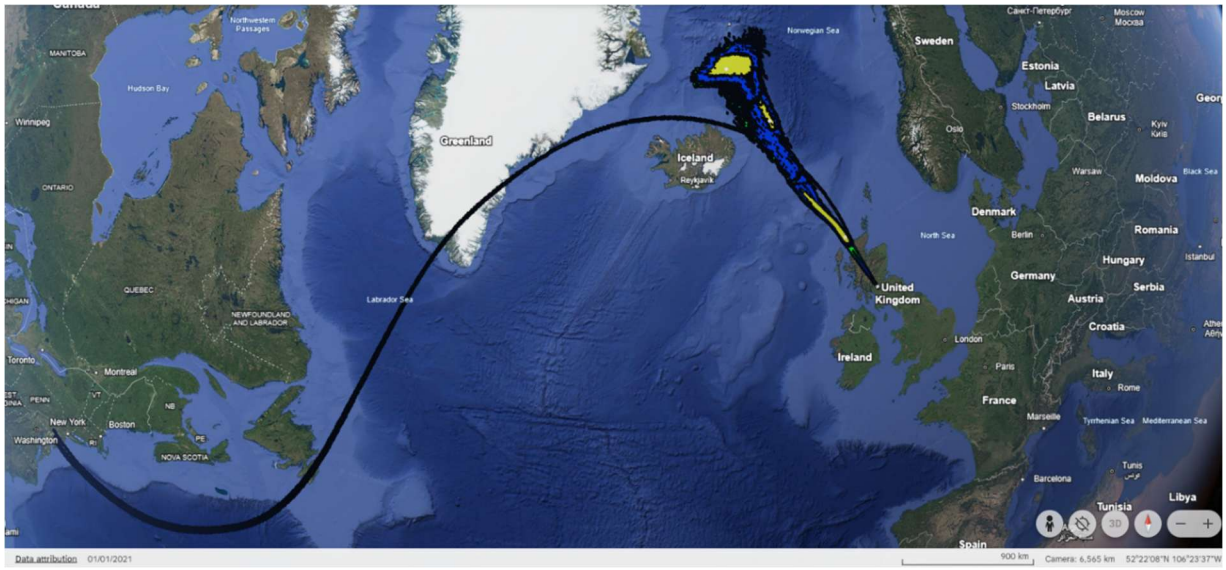


Figure IX.49 10µm 5oC 0.625g density – Backward 23rd Nov'21

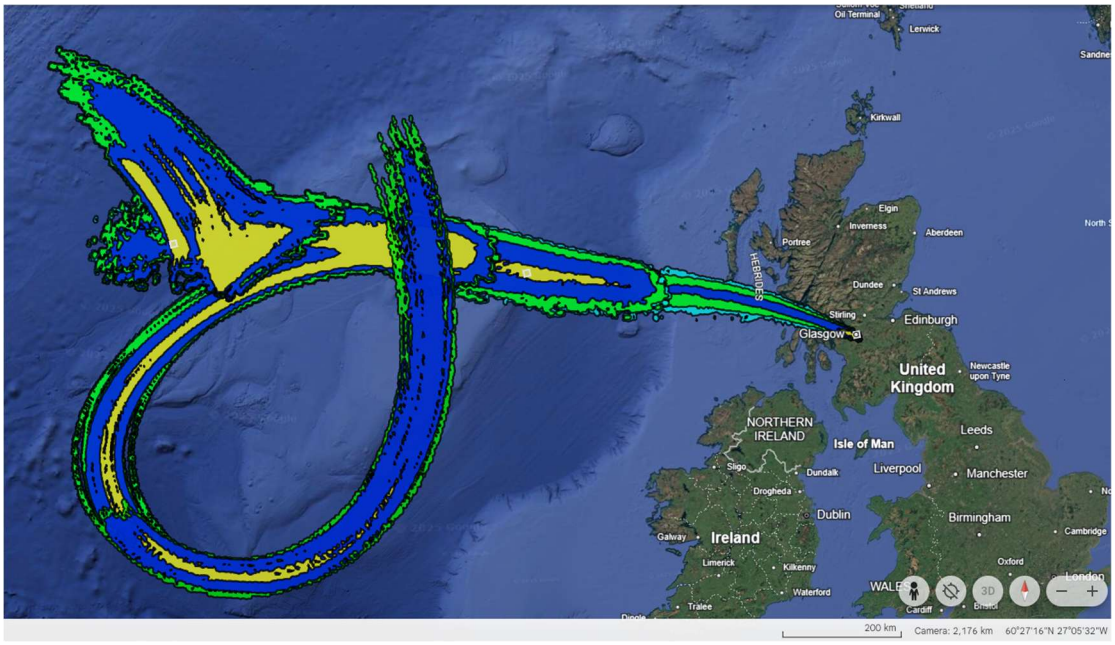


Figure IX.50 10µm 5oC 0.625g density – Forward 17th Nov'21

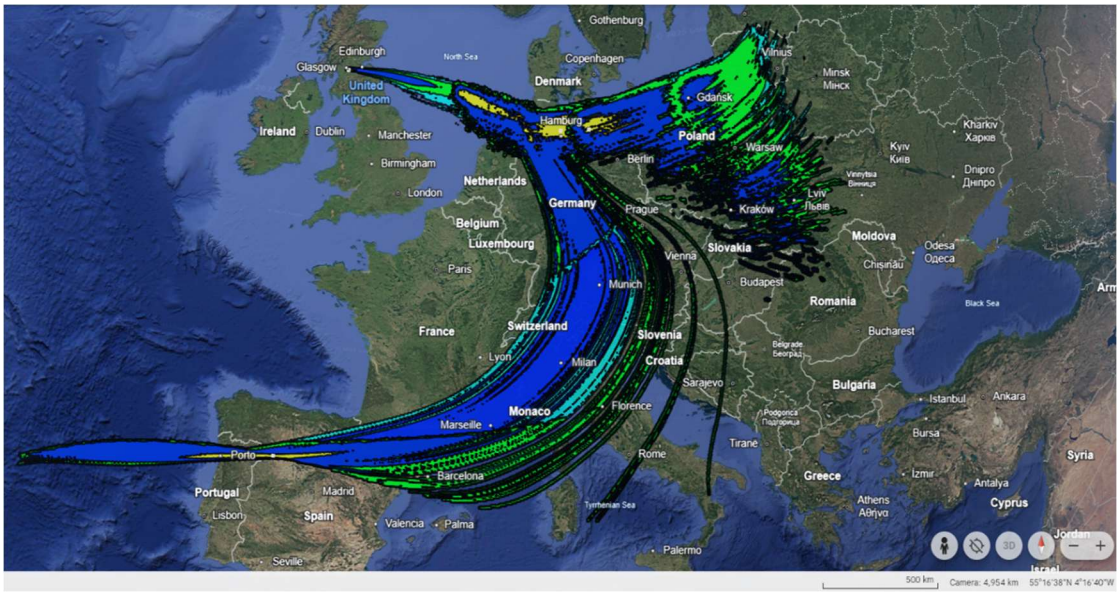


Figure IX.51 10µm 5oC 0.625g density – Forward 18th Nov'21

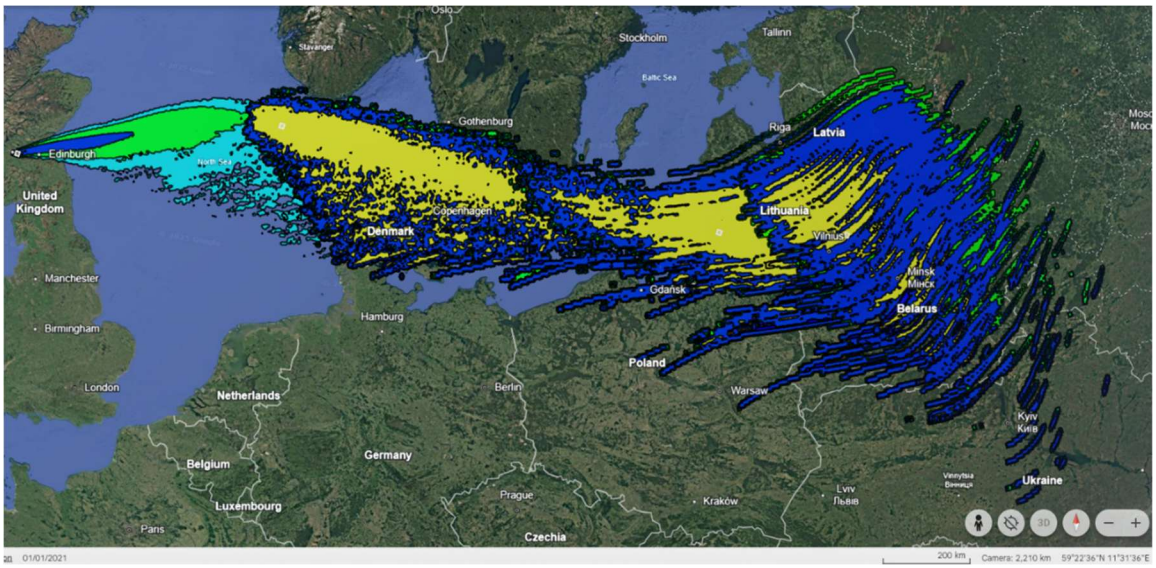


Figure IX.52 10µm 5oC 0.625g density – Forward 19th Nov'21

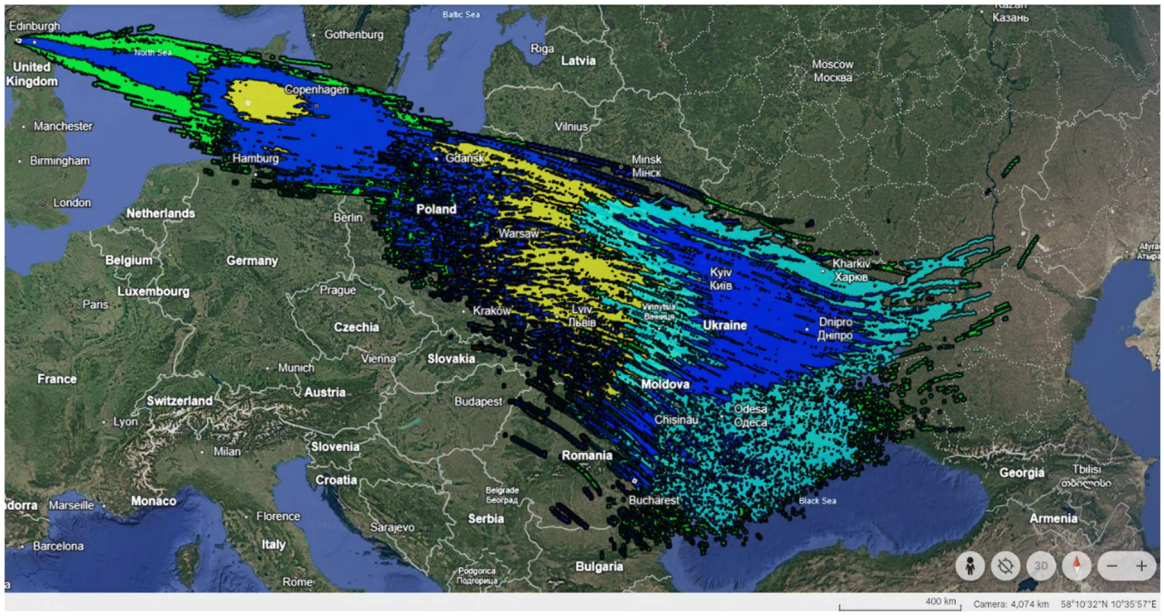


Figure IX.53 10µm 5oC 0.625g density – Forward 20th Nov'21

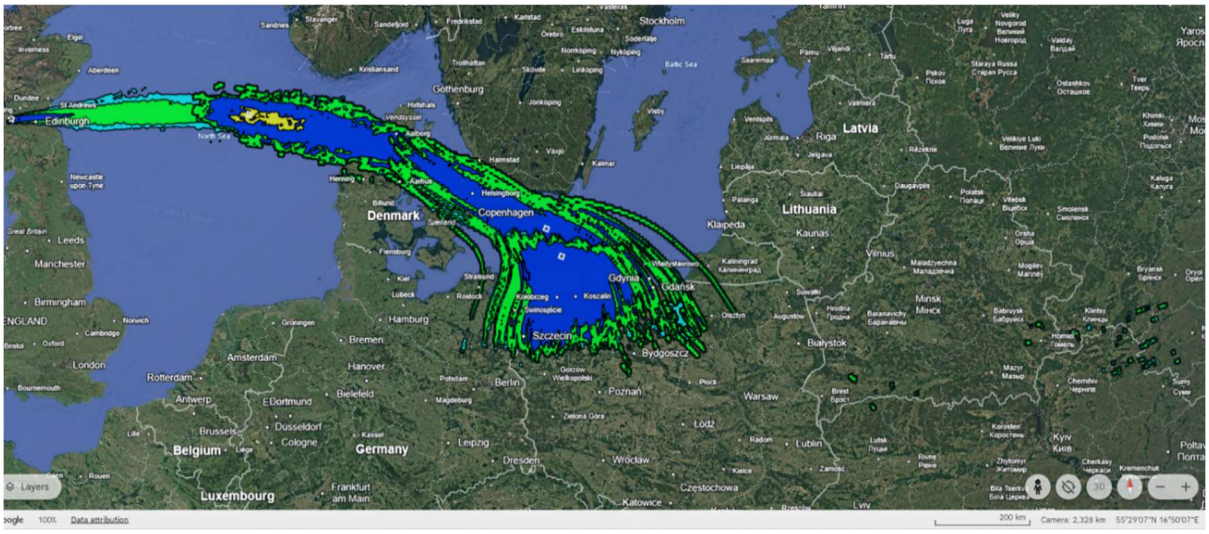


Figure IX.54 10µm 5oC 0.625g density – Forward 21st Nov'21

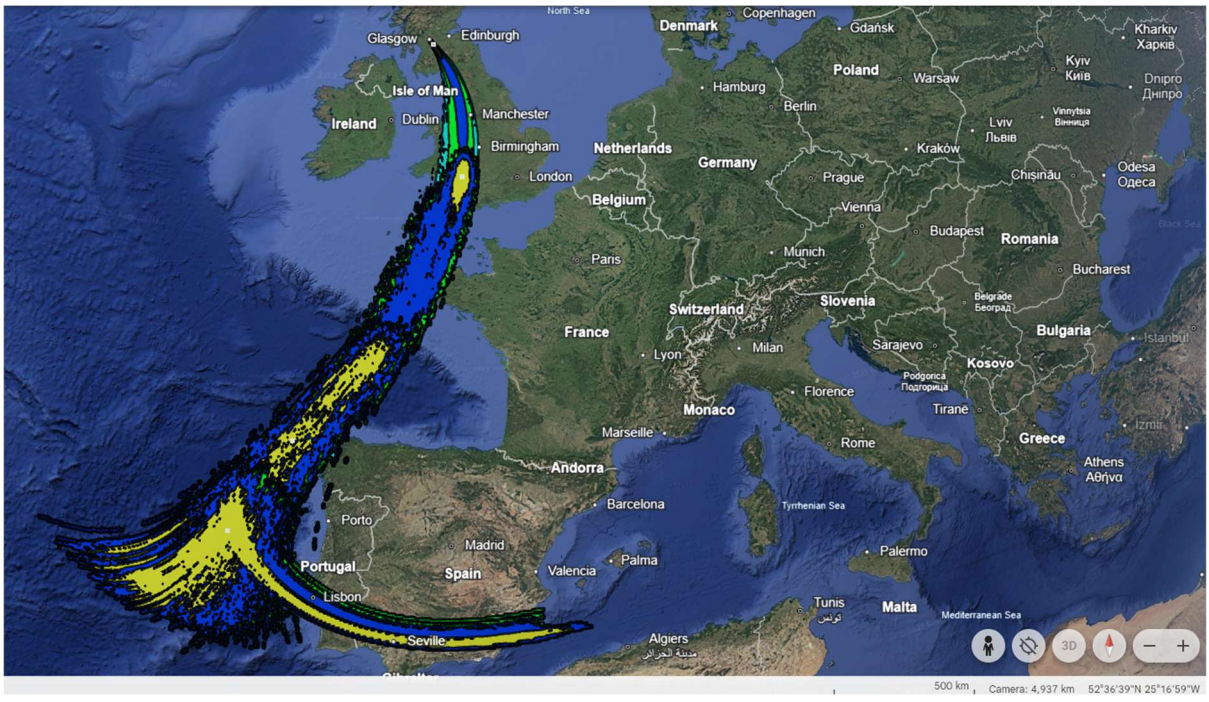


Figure IX.55 10µm 5oC 0.625g density – Forward 22nd Nov'21

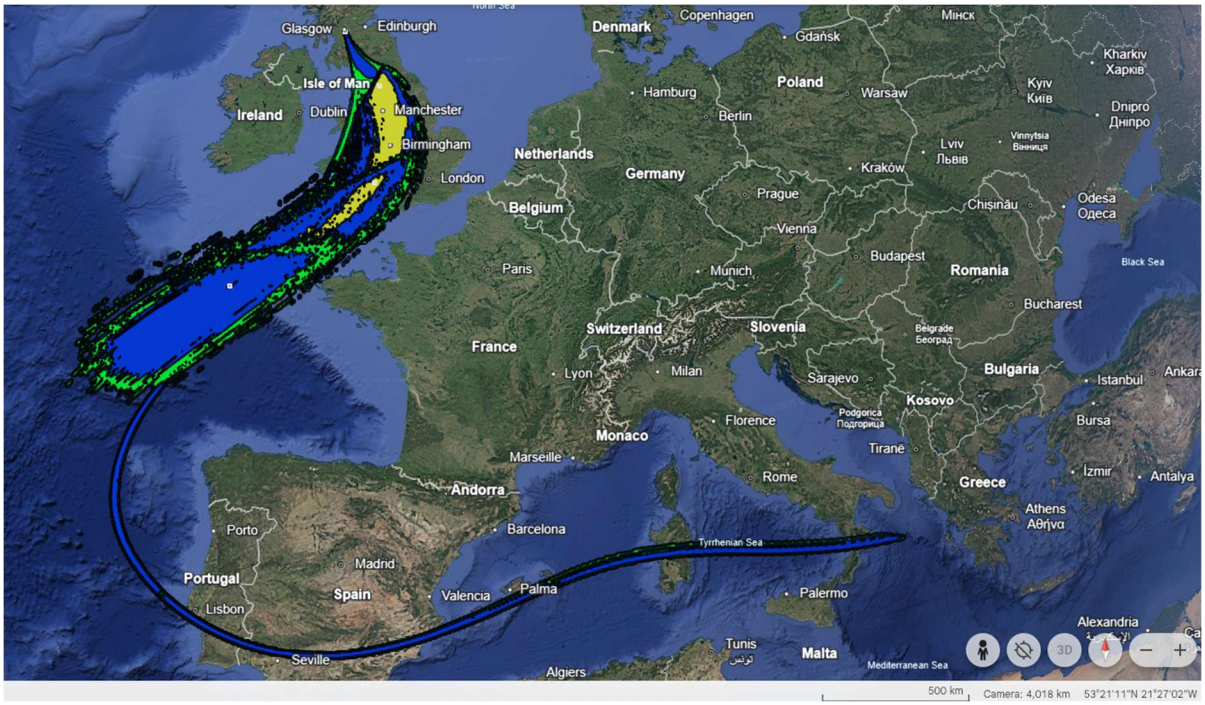


Figure IX.56 10µm 5oC 0.625g density – Forward 23rd Nov'21

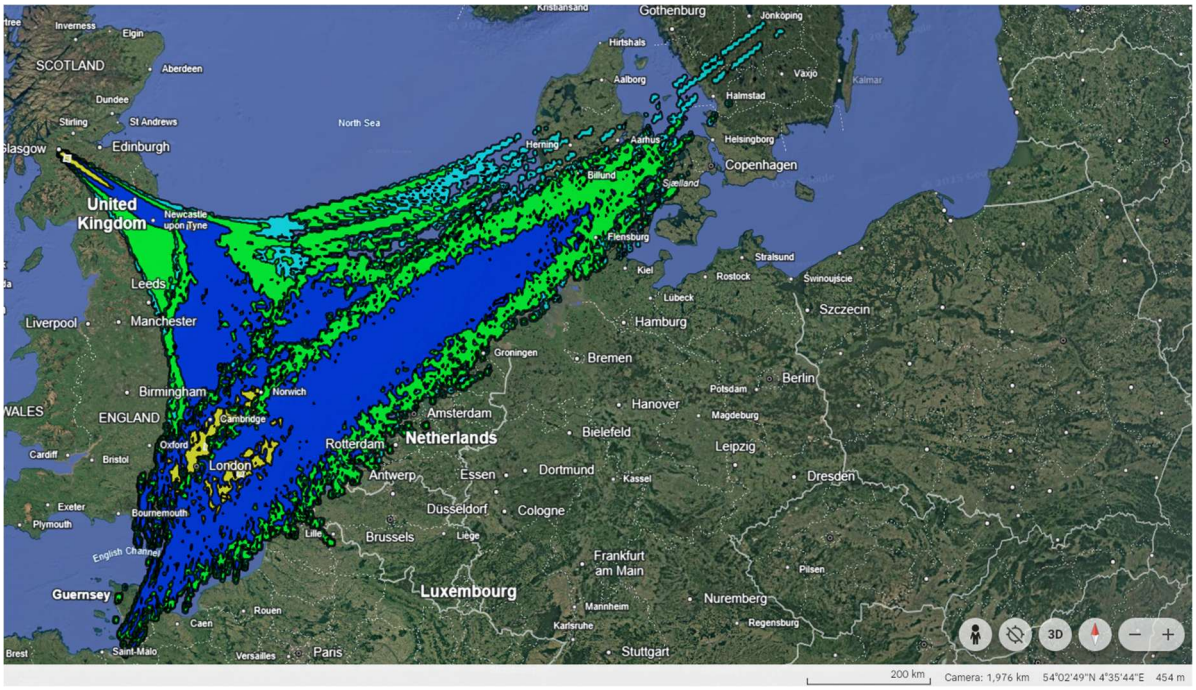


Figure IX.57 20µm 5oC 0.625g density – Backward 17th Nov' 21,

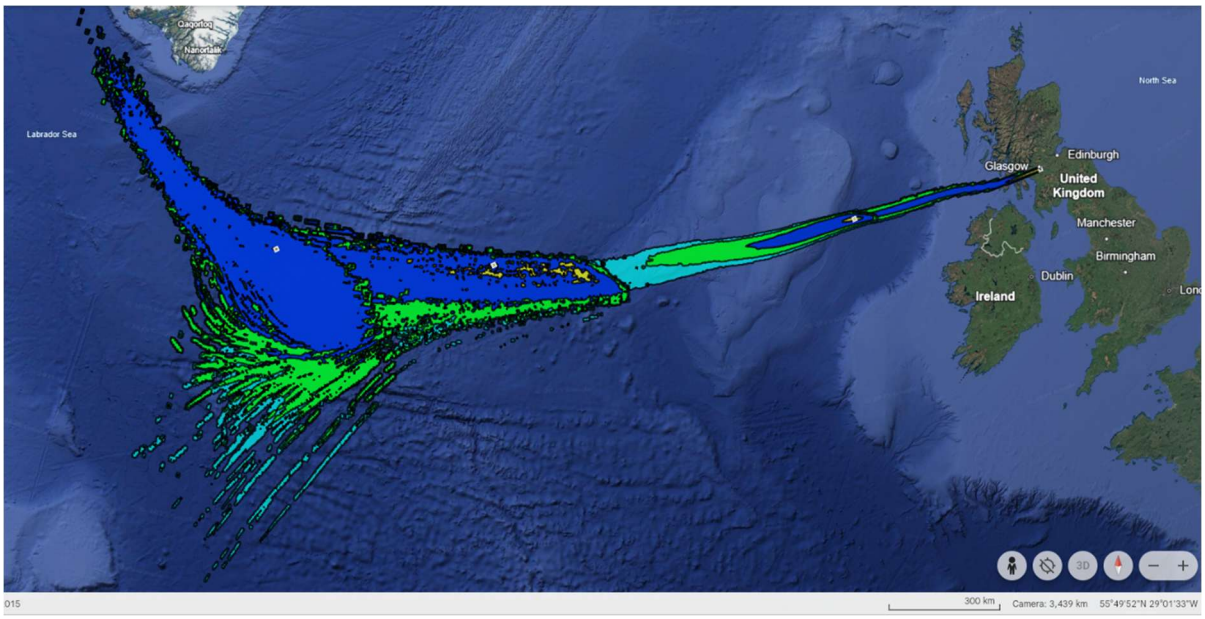


Figure IX.58 20µm 5oC 0.625g density – Backward 18th Nov'21

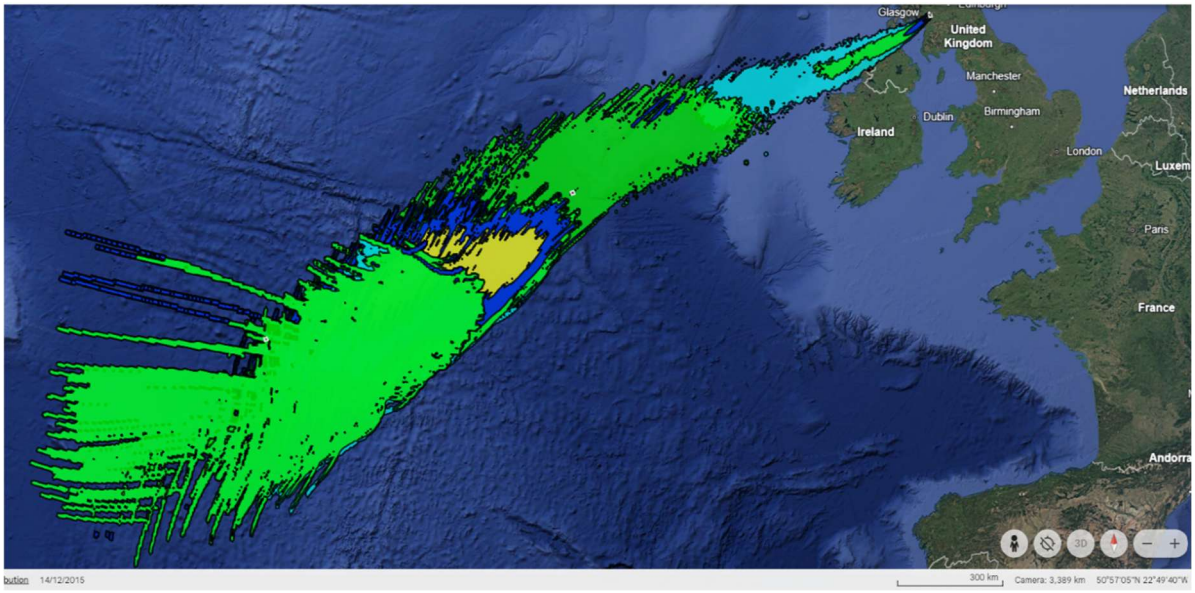


Figure IX.59 20µm 5oC 0.625g density – Backward 19th Nov'21

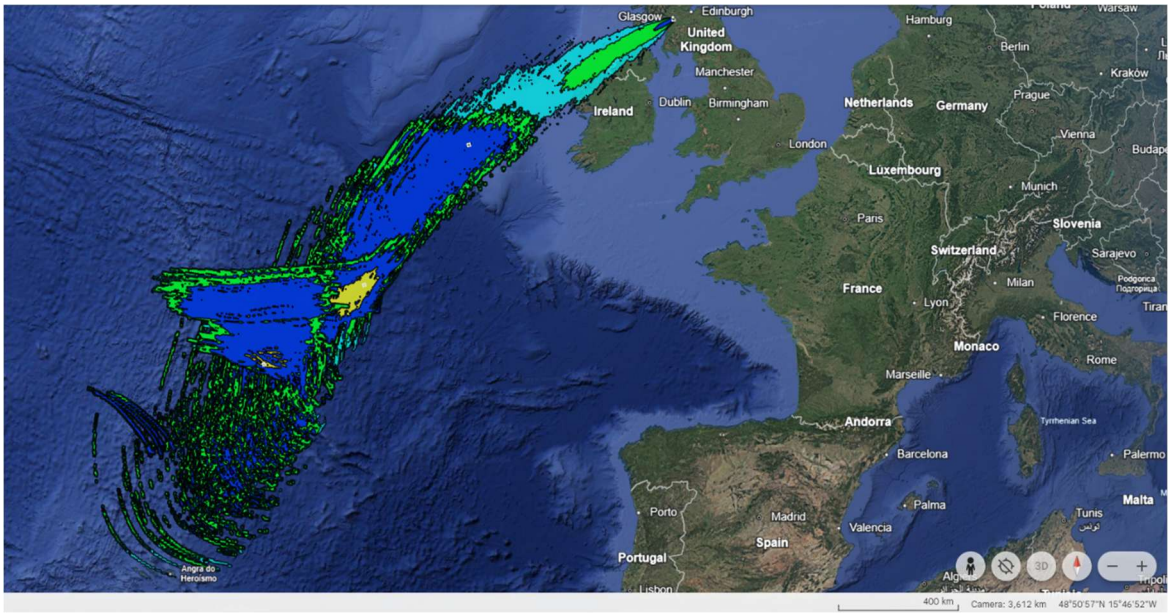


Figure IX.60 20µm 5oC 0.625g density – Backward 20th Nov'21

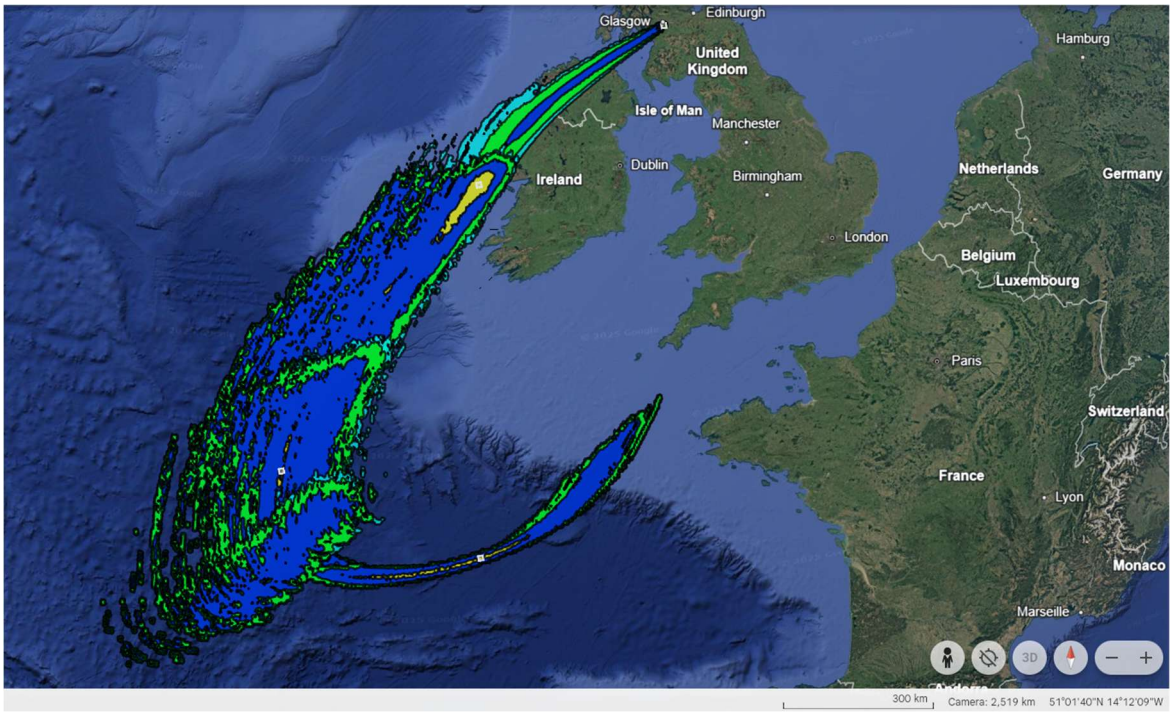


Figure IX.61 20µm 5oC 0.625g density – Backward 21st Nov'21

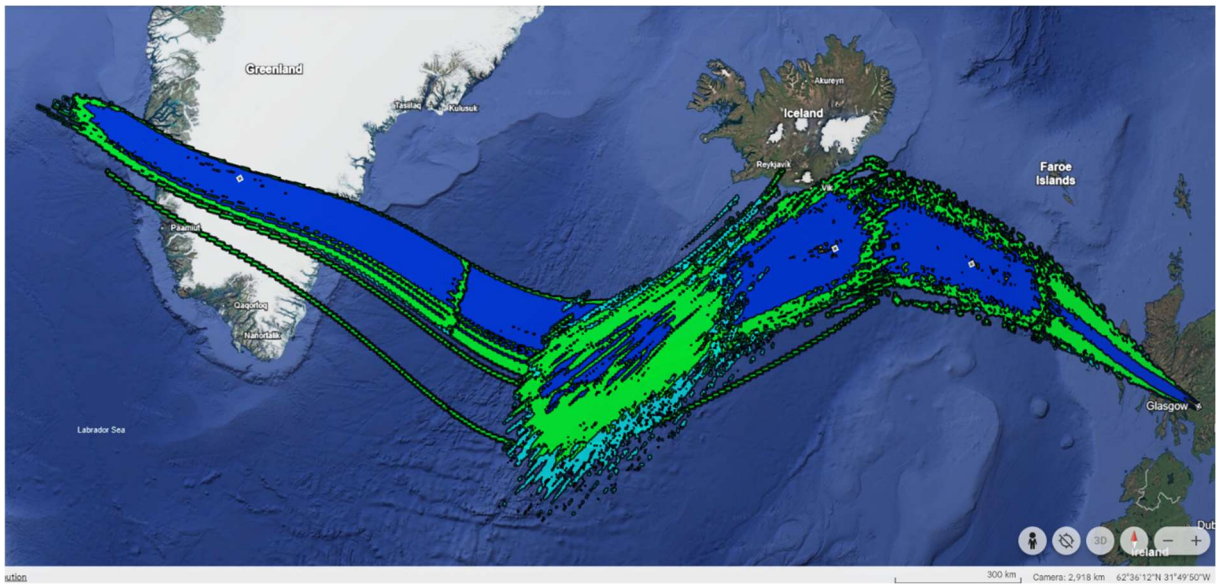


Figure IX.62 20µm 5oC 0.625g density – Backward 22nd Nov'21

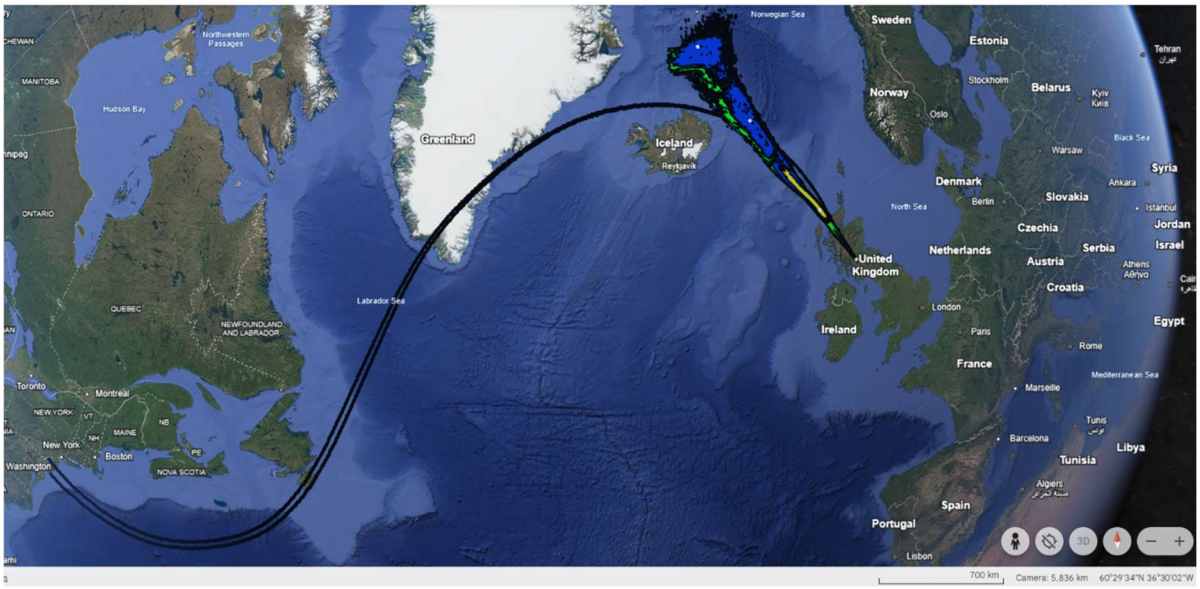


Figure IX.63 20µm 5oC 0.625g density – Backward 23rd Nov'21

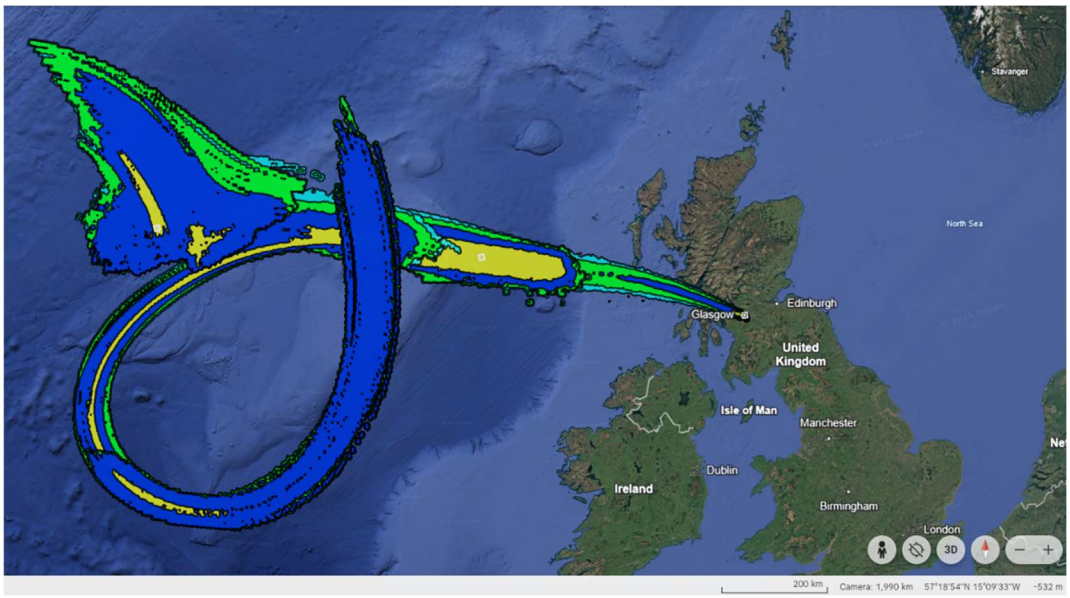


Figure IX.64 20µm 5oC 0.625g density – Forward 17th Nov'21

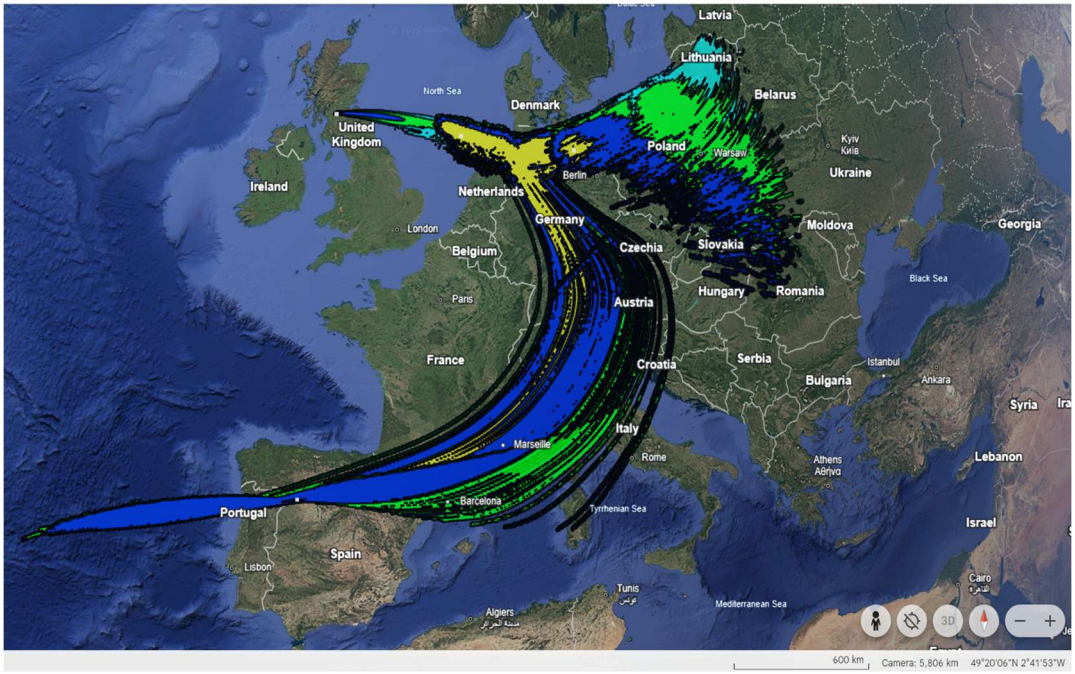


Figure IX.65 20µm 5oC 0.625g density – Forward 18th Nov'21

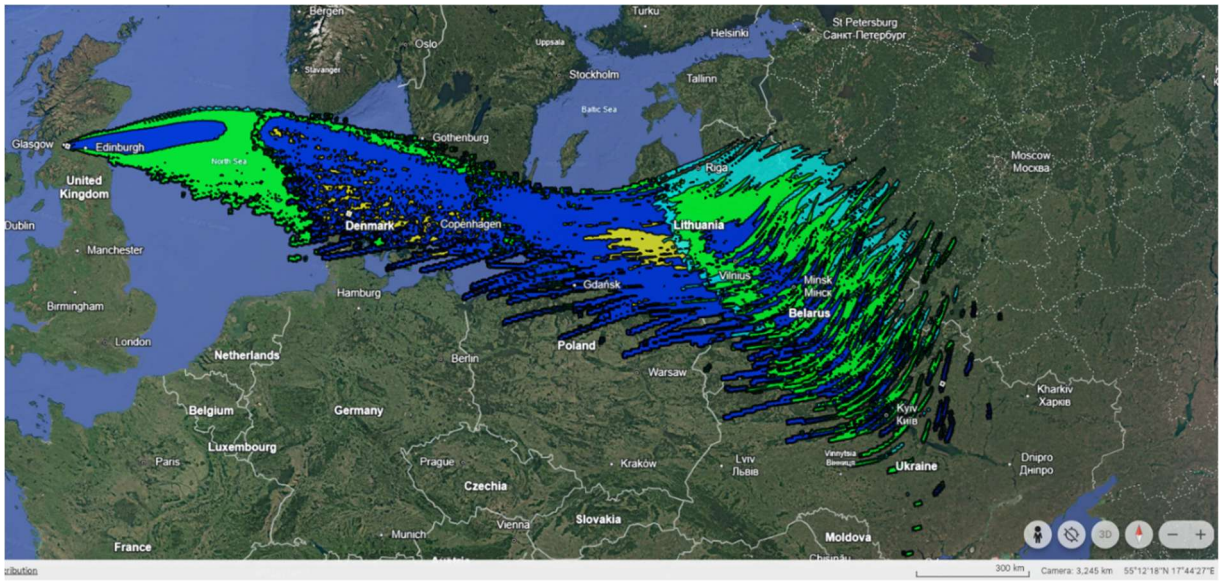


Figure IX.66 20µm 5oC 0.625g density – Forward 19th Nov'21

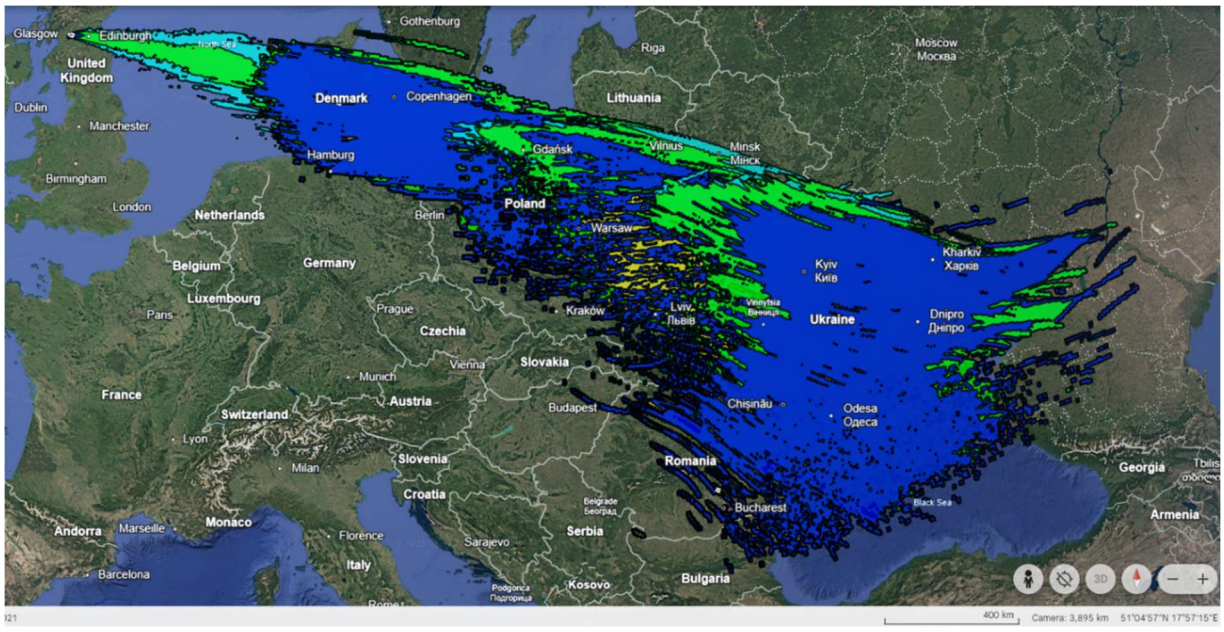


Figure IX.67 20µm 5oC 0.625g density – Forward 20th Nov'21

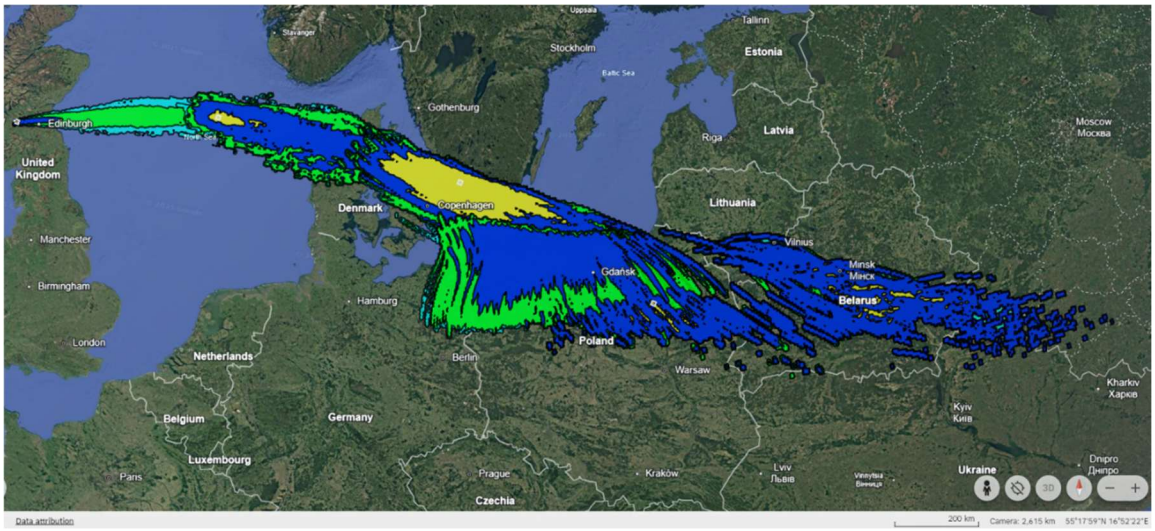


Figure IX.68 20µm 5oC 0.625g density – Forward 21st Nov'21

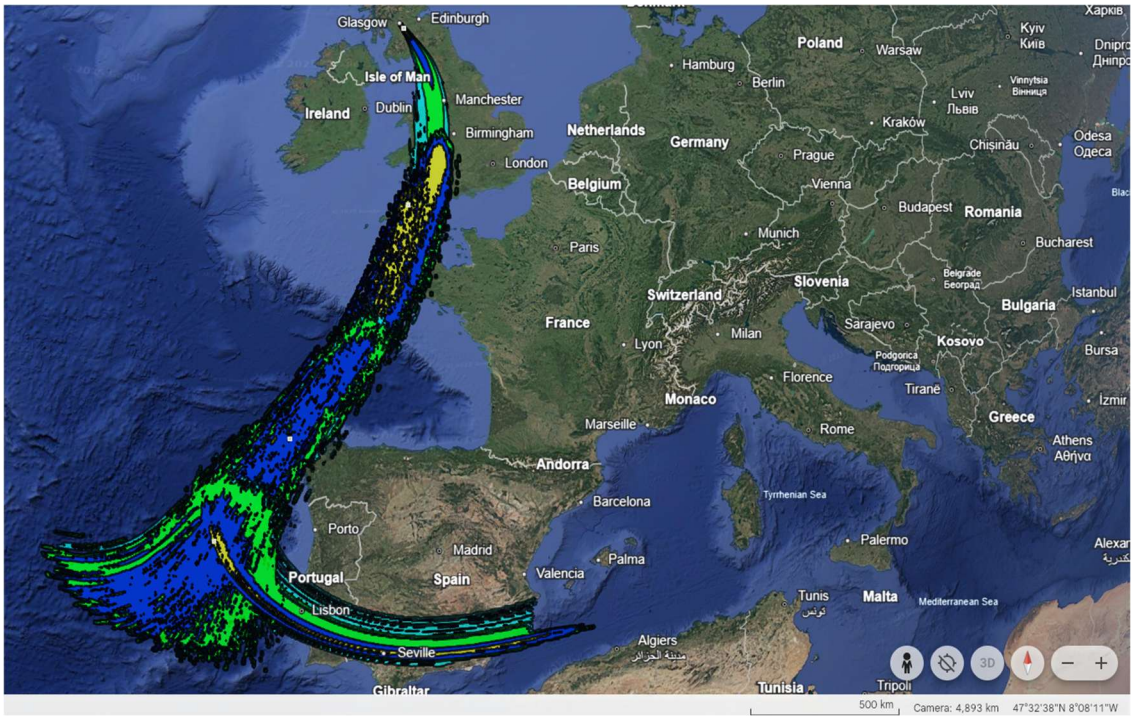


Figure IX.69 20µm 5oC 0.625g density – Forward 22nd Nov'21

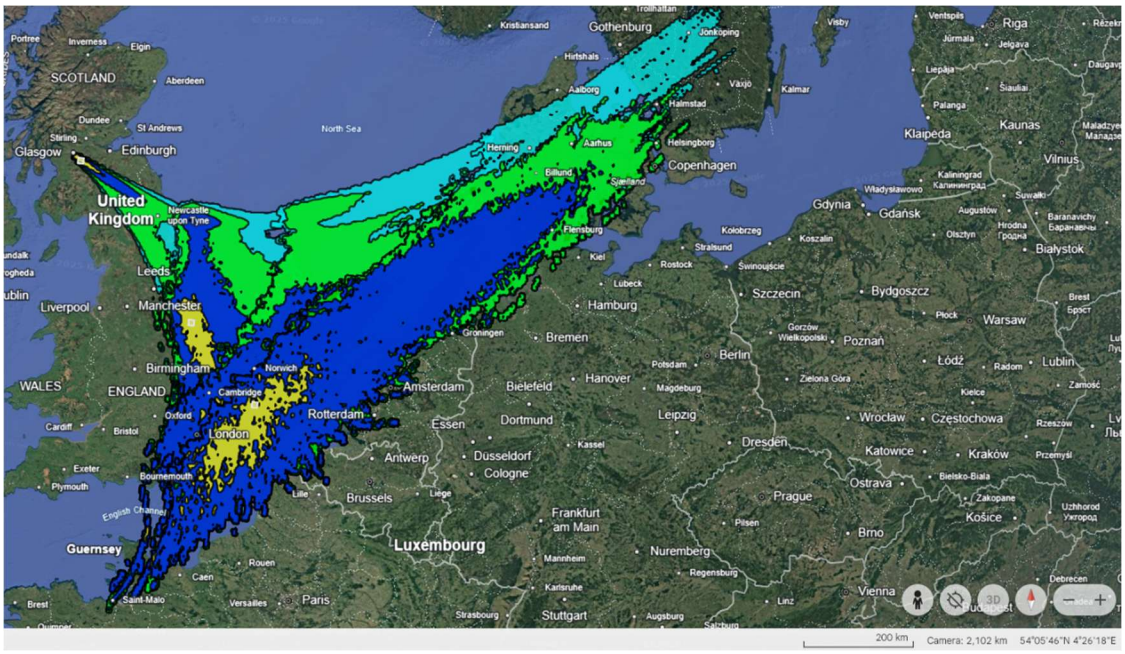


Figure IX.70 20µm 5oC 0.625g density – Forward 23rd Nov'21

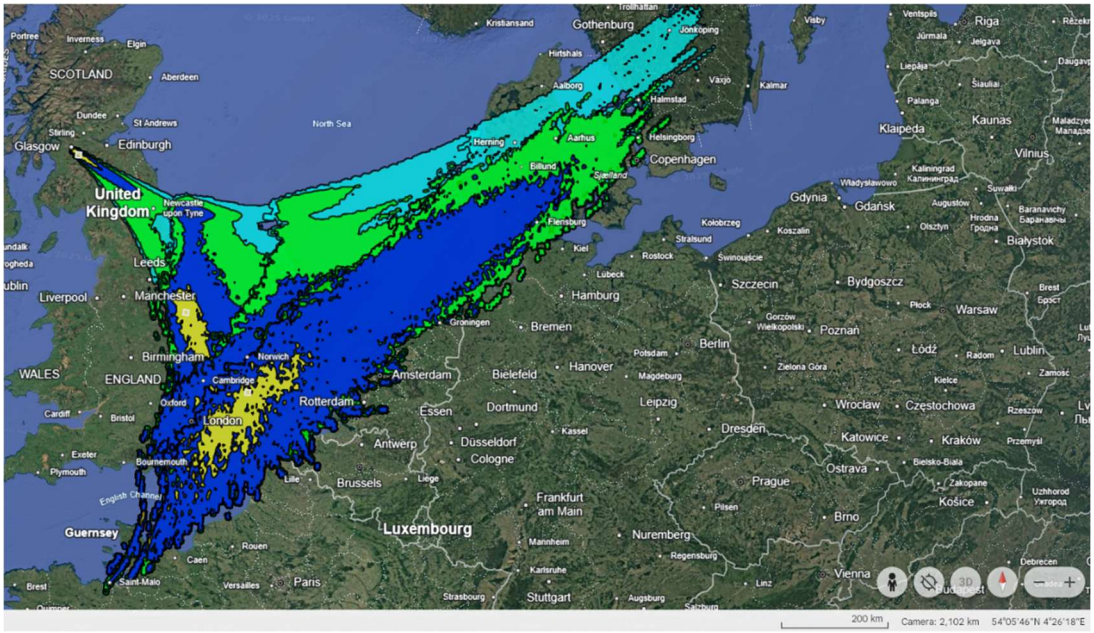


Figure IX.71 100µm 5oC 0.625g density 17th Nov, Backward

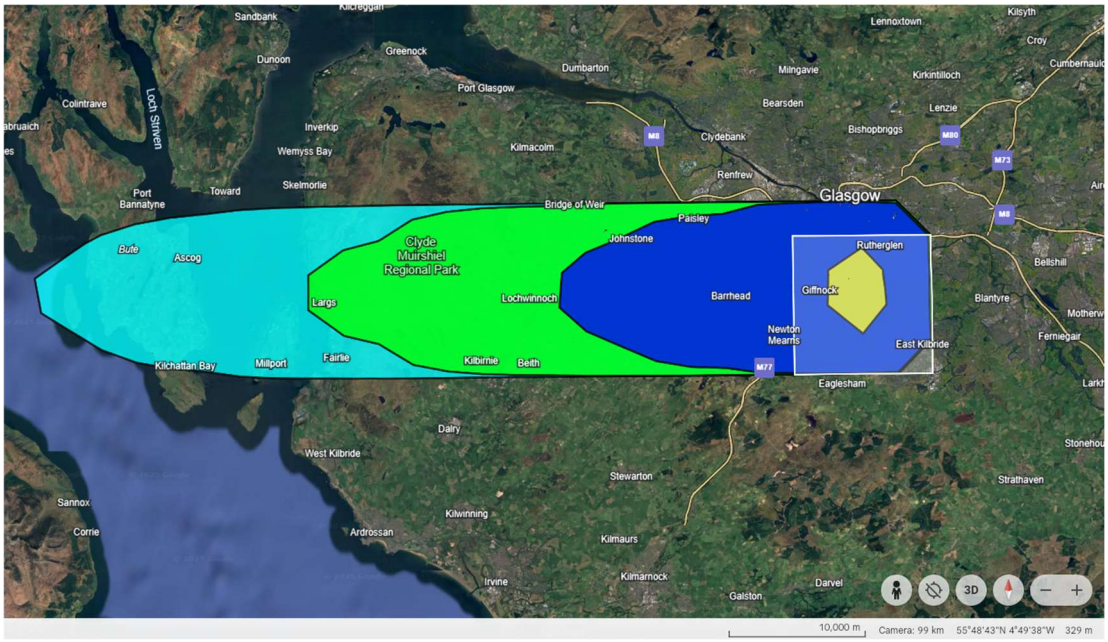


Figure IX.72 100µm 5oC 0.625g density – Backward 18th Nov'21

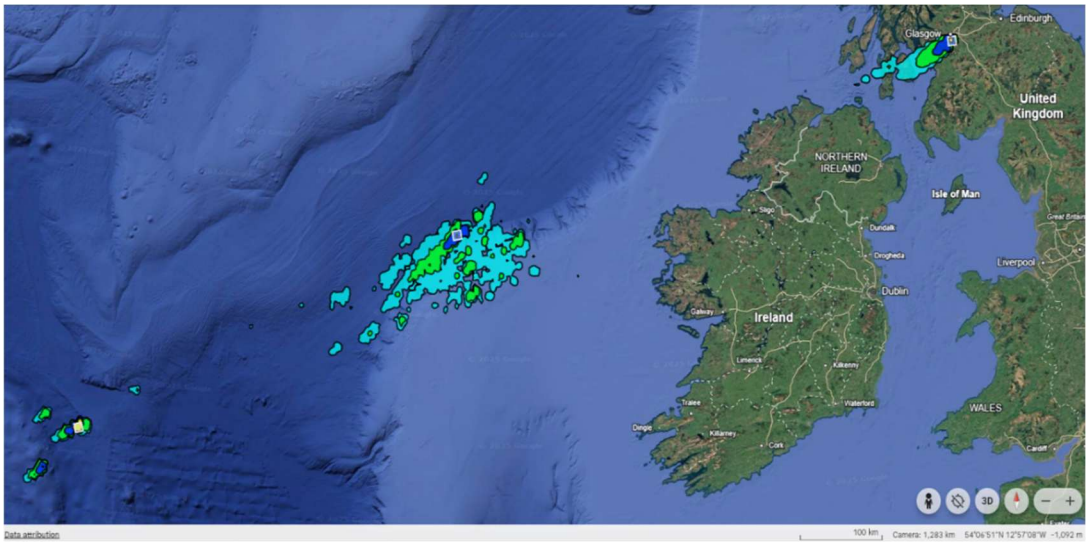


Figure IX.73 100µm 5oC 0.625g density – Backward 19th Nov'21

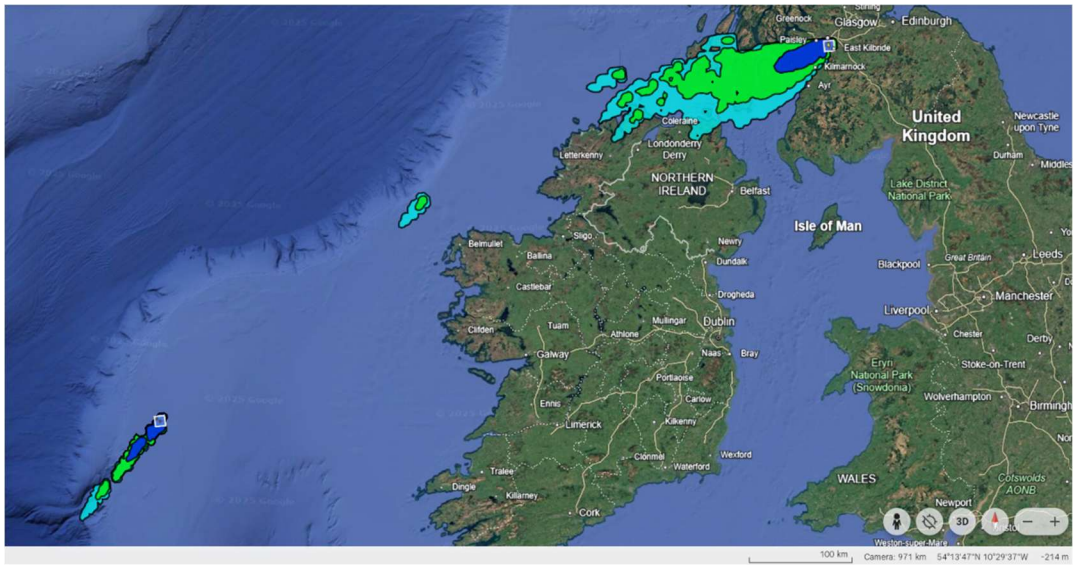


Figure IX.74 100µm 5oC 0.625g density – Backward 20th Nov'21

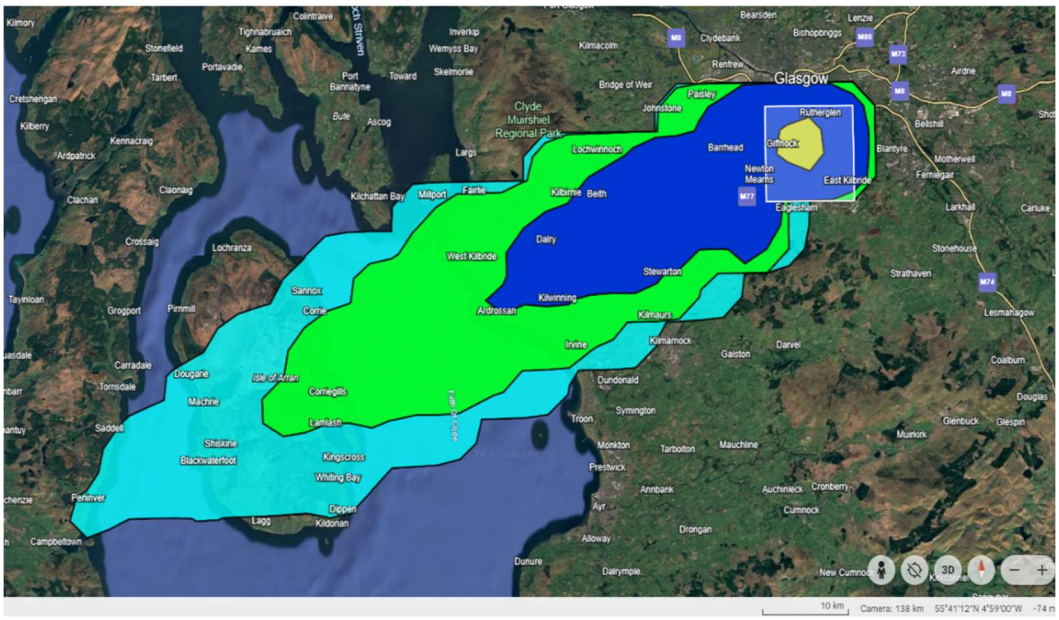


Figure IX.75 100µm 5oC 0.625g density – Backward 21st Nov'21

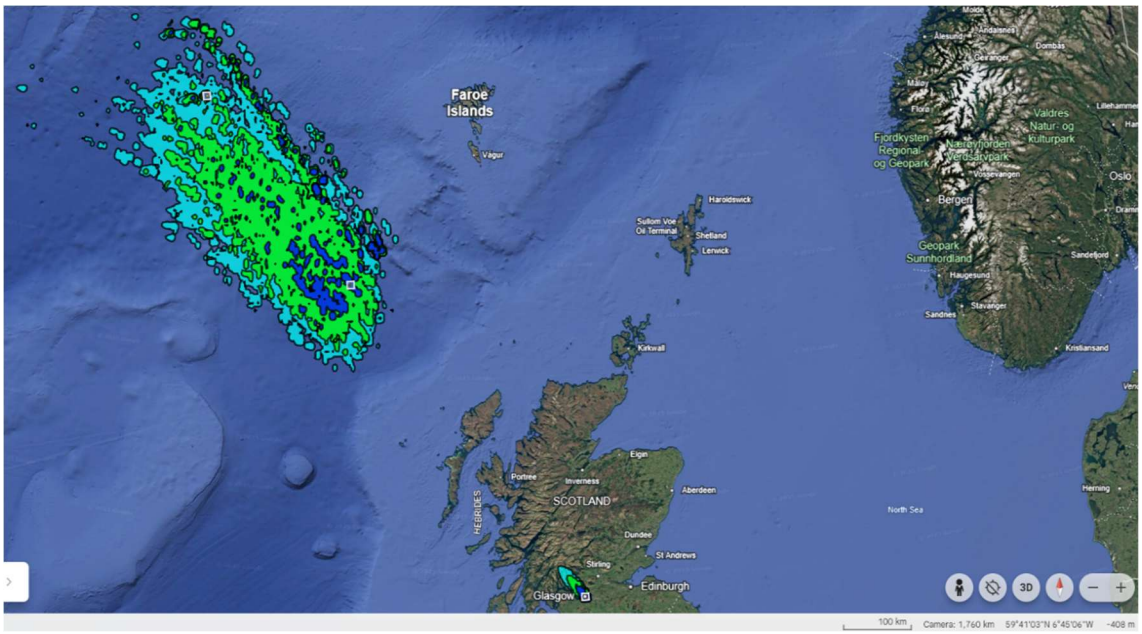


Figure IX.76 100µm 5oC 0.625g density – Backward 22nd Nov'21

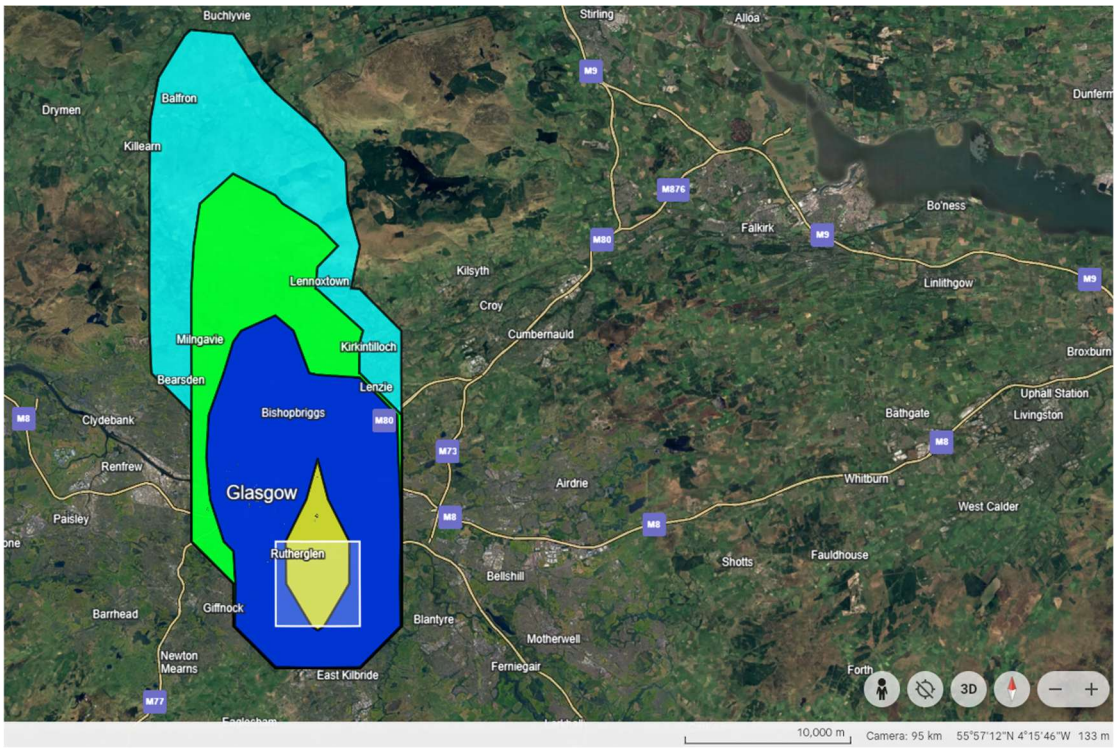


Figure IX.77 100µm 5oC 0.625g density – Backward 23rd Nov'21

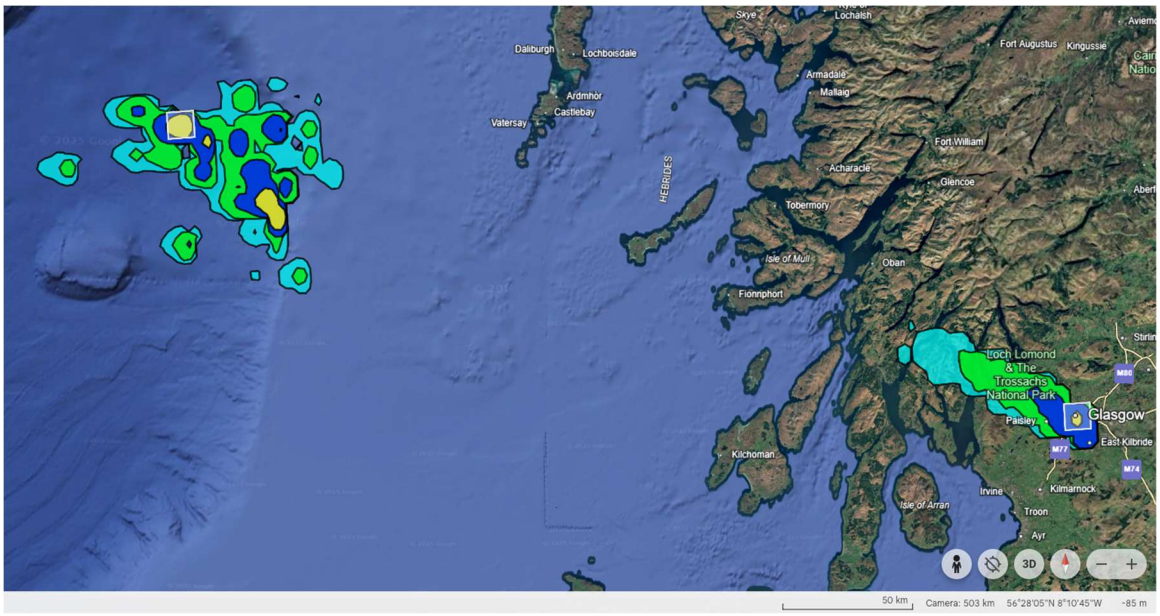


Figure IX.78 100µm 5oC 0.625g density – Forward 17th Nov'21

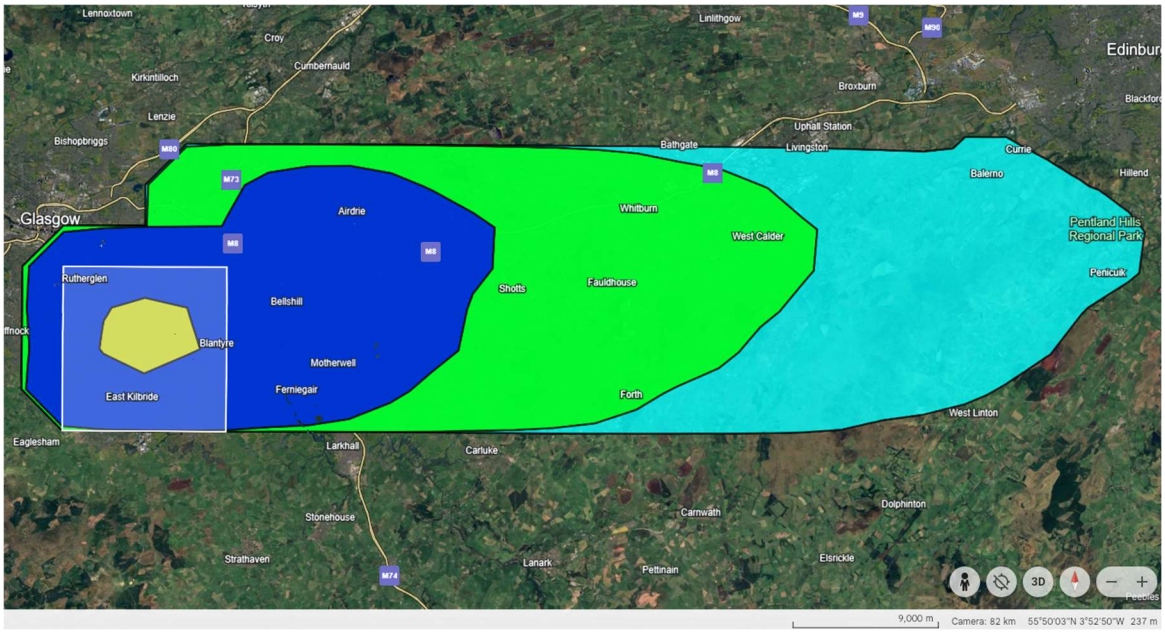


Figure IX.79 100µm 5oC 0.625g density – Forward 18th Nov'21

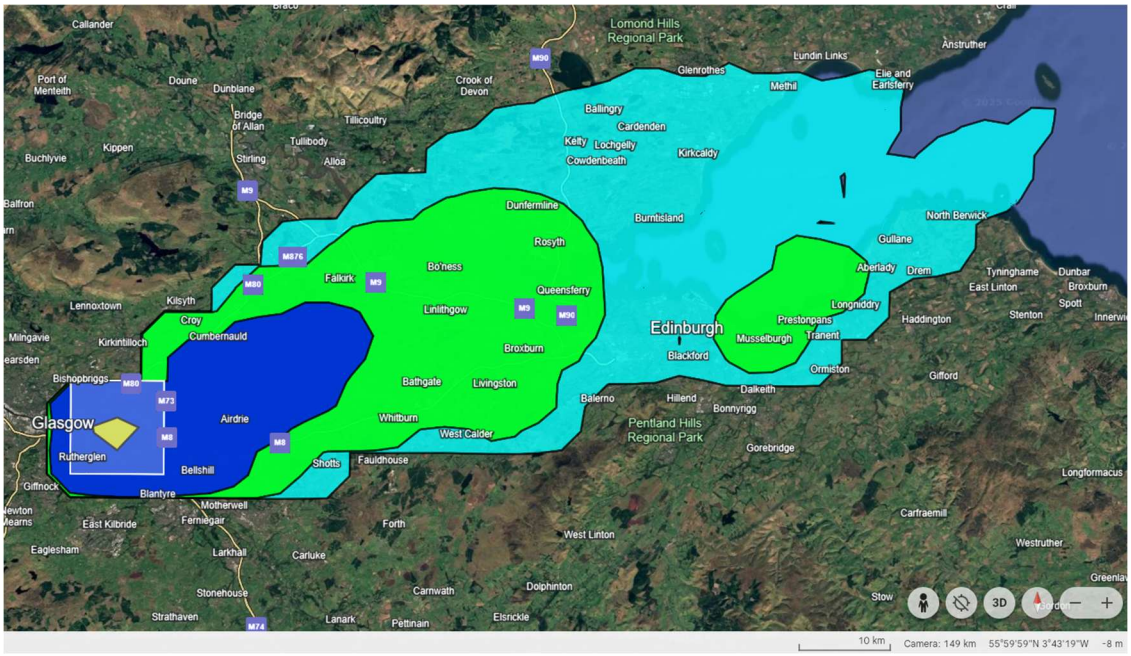


Figure IX.80 100µm 5oC 0.625g density – Forward 19th Nov'21

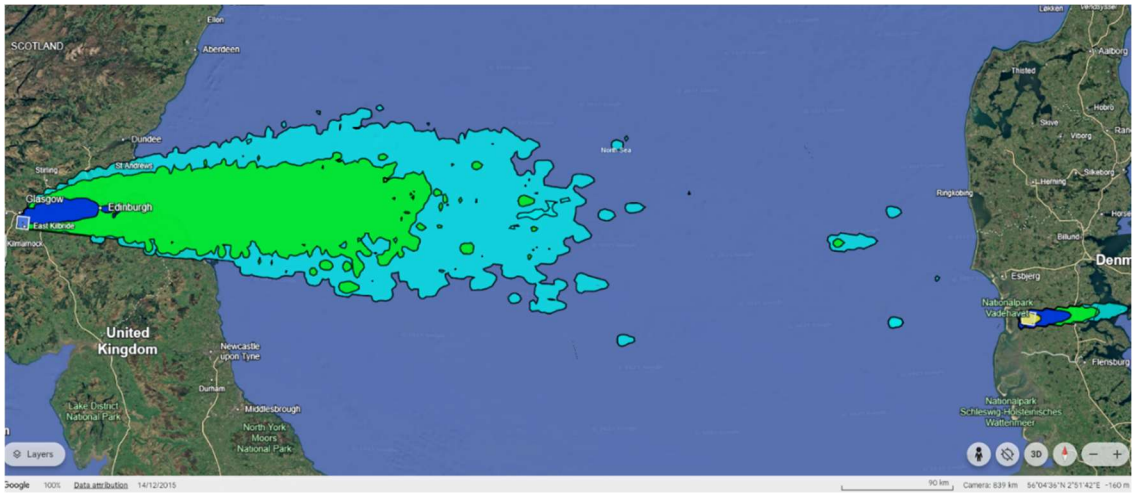


Figure IX.81 100µm 5oC 0.625g density – Forward 20th Nov'21

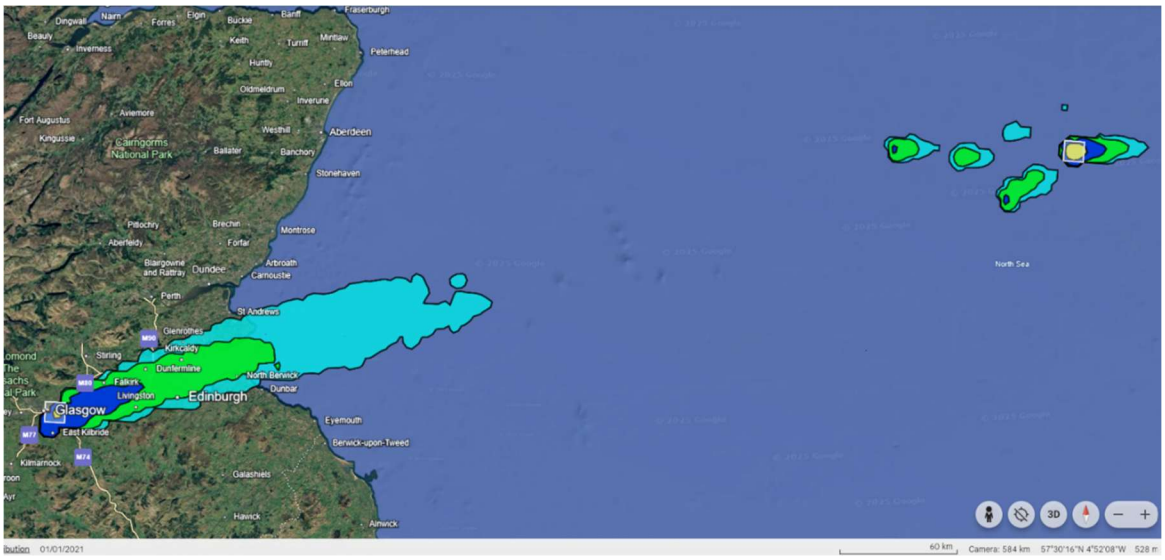


Figure IX.82 100µm 5oC 0.625g density – Forward 21st Nov'21

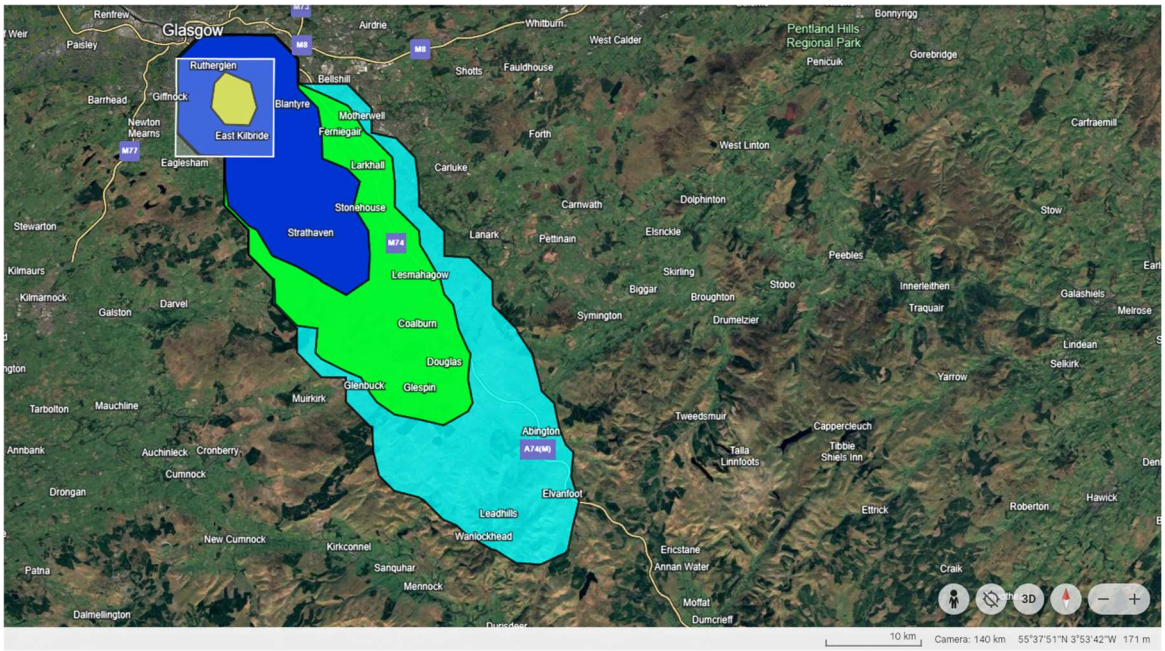


Figure IX.83 100µm 5oC 0.625g density – Forward 22nd Nov'21

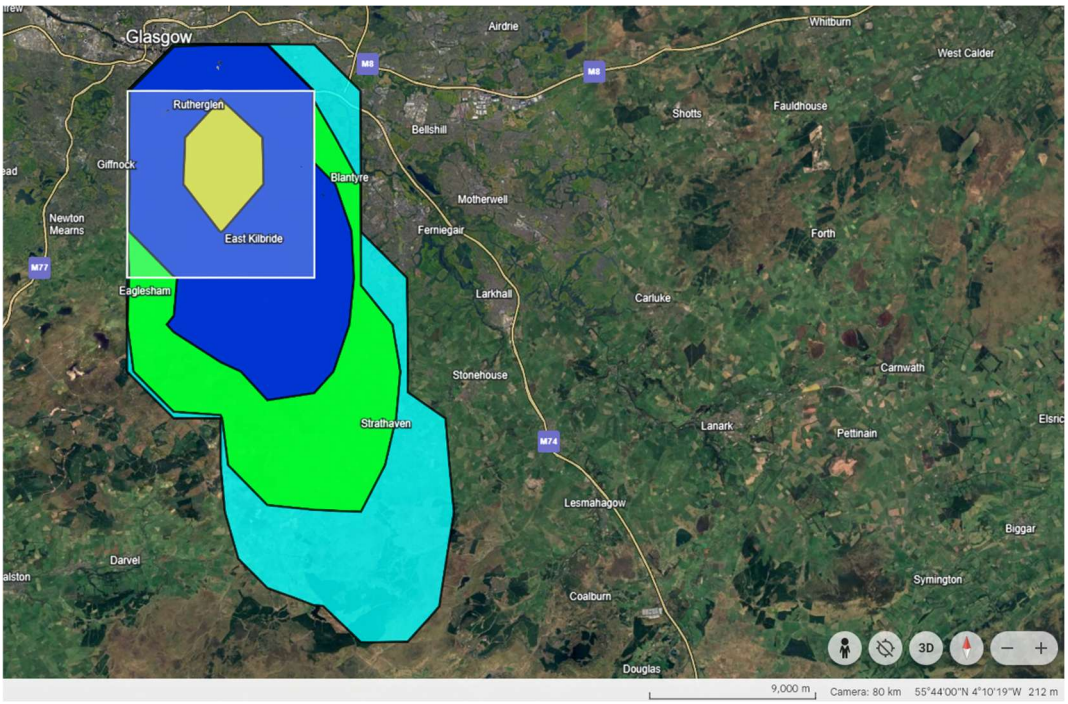


Figure IX.84 100µm 5oC 0.625g density – Forward 23rd Nov'21

